(NASA-CR-165143) A STUDY OF THE TRANSMISSION CHARACTERISTICS OF SUPPRESSOR NOZZLES (Lockheed-Georgia Co., Marietta.) 108 p HC A12/MF A01 CSCL 20A

N80-32186

Unclas
G3/71 28611

A STUDY OF THE ACOUSTIC TRANSMISSION CHARACTERISTICS OF SUPPRESSOR NOZZLES

K. K. Ahuja
M. Salikuddin
R. H. Burrin
H. E. Plumblee, Jr.

CONTRACT NAS3-20797
JUNE 1980

National Aeronautics and Space Administration

Lewis Research Center
Cleveland, Ohio 44135

NASA CR-165133

A STUDY OF THE ACOUSTIC TRANSMISSION CHARACTERISTICS OF SUPPRESSOR NOZZLES

K. K. Ahuja
M. Salikuddin
R. H. Burrin
H. E. Plumblee, Jr.

CONTRACT NAS3-20797
JUNE 1980

National
Aeronautics and
Space
Administration

Lewis Research Center
Cleveland, Ohio 44135

FOREWORD

This report was prepared by the Lockheed-Georgia Company, Marietta, Georgia, for the NASA-Lewis Research Center, Cleveland, Ohio, under Contract NAS3-20797.

Mr. Eugene A. Krejsa was the Project Manager for NASA-Lewis Research Center. Lockheed's Program Manager was Dr. Harry E. Plumblee, Jr.

The authors would like to thank Mr. D. F. Blakney for his help in data processing and Drs. H. K. Tanna, P. D. Dean and R. Ramkrishnan for many helpful discussions. Thanks are also due to Mr. W. H. Brown for his assistance in conducting experiments and Mrs. Shelby Christophers for typing the manuscript.

CONTENTS

SUMMARY

The work described in this report represents a first step in understanding and evaluating how internal noise radiates through multi-element, single as well as dual stream, mechanical suppressors.

The objective of this program was to conduct a series of tests to determine the efficiency of internal noise radiation for two mechanical suppressor nozzles, namely, a single stream 12-lobe 24-tube suppressor nozzle and a dual stream 36-chute suppressor nozzle. An equivalent single round conical nozzle and an equivalent coannular nozzle system were also tested to provide a reference for the two suppressors.

An impulse test technique developed in Phase 1 of this program was used to study the radiation characteristics of these nozzles. This technique utilizes a high voltage spark discharge as a noise source within the test duct and enables one to separate the incident, reflected and transmitted signals in the time domain. These signals are then Fourier transformed to obtain various transmission parameters, in particular, the nozzle transmission coefficient (NTC) and the power transfer function (PTF).

These transmission parameters for the 12-lobe, 24-tube suppressor nozzle and the reference conical nozzle are presented as a function of jet Mach number, duct Mach number, polar angle and temperature. Effects of simulated forward flight are also considered for these nozzles.

For the dual stream, 36-chute suppressor, the NTC and PTF are presented as a function of velocity ratios and temperature ratios. Where possible data for the equivalent coaxial nozzle is also presented.

As a by-product of this work, data on jet-mixing noise and broad-band amplification was also available. Typical results describing the jet noise suppression by these suppressors are, therefore, presented.

A new technique using signal recovery and an electro-acoustic driver, developed to improve the single-shot spark discharge method, has also been discussed.

Many of the results described here are new and are not amenable to immediate explanations. Due to the interesting nature of these results and their usefulness, the transmission data has been included in this report as an appendix.

1. INTRODUCTION

In order for supersonic cruise aircraft to meet at least the FAR-36 (1969) noise rule, the use of variable cycle engines utilizing coannular inverted-velocity-profiles or low by pass (two stream) engines with suppressor nozzles have been advanced in recent years. With the introduction of the FAR-36 (1977) noise goals, and even more stringent goals proposed for the future, all practical current engine cycles being considered will require jet noise suppressor nozzles.

An idea of recent vintage for reducing jet engine noise is to use coannular jet exhaust streams with inverted velocity profiles. Model-scale tests of this concept indicate jet exhaust noise reductions of the order of 6-8 EPNdB. However, before full-scale flight testing of new engines designed to produce such profiles is undertaken, all aspects of engine noise must be understood, including core noise generation, core noise radiation, and flight effects on fan/jet noise generation and radiation [1.1, 1.2].

In an effort to ensure that minimization of the exhaust noise does not give rise to another noise problem (as occurred in the development of the fan jet engine), NASA-Lewis awarded a contract to Lockheed-Georgia Company in 1978 to determine the acoustic radiation characteristics of internal noise for this inverted velocity profile cycle. A number of coannular nozzles were tested as a function of velocity ratio, temperature ratio and nozzle geometry (e.g. L/h, nozzle angle etc.) and the results are described in reference 1.3. The above contract was later extended to determine the transmission characteristics of typical mechanical suppressors.

A number of mechanical suppressors have been developed in the course of trying to minimize the noise of aircraft engines. These suppressors have been tested for a variety of test conditions, both statically and in flight and appear to offer jet n se reductions of as much as 10 PNdB [1.4-1.6]. With this promise offered b, the scale model tests, it is crucial to know if other problems exist that may negate the jet noise suppression noticed in the model tests. One of the potential problems that may contribute to a reduction in the effectiveness of the mechanical suppressors is the radiation of the internal noise. If the radiation efficiency of the mechanical suppressor nozzle increased over other types of suppressor nozzles (for example coaxial nozzles with inverted velocity profiles) or even just simple convergent round nozzles, this would be crucial in the ultimate evaluation of the mechanical suppressor nozzle.

Due to their importance, the radiation characteristics of two mechanical suppressor nozzles, namely the dual stream multi-chute suppressor nozzle and a single stream multi-lobe multi-tube suppressor nozzle were therefore recently studied. The dual stream suppressor was modeled after one of the 36 chute nozzles of G.E. [1.5] and the single stream suppressor after a 12-lobe 24-tube suppressor nozzle tested by Douglas Aircraft Corporation and Rolls-Royce Ltd. [1.6, 1.7]. The program was primarily experimental and was aimed at understanding the acoustic transmission characteristics of internal noise sources for these nozzles. An equivalent coannular nozzle system and a single round conical nozzle were also tested to provide a reference for the multi-chute and the multi-lobe-multi-tube suppressors, respectively.

The above program for the suppressor nozzles is described in this report and represents a first step in understanding and evaluating how internal noise radiates through multi-element, single as well as dual stream, mechanical suppressors.

An impulse test technique developed in Phase 1 of this program [1.3] was used to determine the transmission characteristics of these suppressor nozzles. This technique utilizes a high voltage spark discharge as a noise source within the test duct and enables one to separate the incident , reflected and the transmitted signals in the time domain. These signals are then Fourier transformed to obtain various transmission parameters.

The above method has been calibrated [1.8] against the classical theories such as that by Levine and Schwinger [1.9] for unflanged pipes and against the standard test techniques such as the standing wave tube method.

Facility description, test plan and the method of data acquisition and analysis are described in the next section. This is followed, in Section 3, by the experimental results for the 12-lobe, 24-tube suppressor nozzle. Results for a range of flow conditions are presented and compared with those for an equivalent round conical nozzle of the same exit area. Effects of nozzle geometry, jet Mach number, duct Mach number, jet temperature and flight velocity on the radiation characteristics of these nozzles are discussed.

Results for the 36-chute suppressor nozzle and the reference coannular nozzle (L/h for both nozzles = 3) are then presented in section 4. Effects of velocity and temperature ratios are discussed on the transmission of internal noise from the impulse source located within the secondary plenum.

It is found that for very high levels of jet noise, for example at supersonic Mach numbers, signal to noise ratio is unacceptable at some measurement locations. This problem is particularly severe close to the jet axis where refraction effect reduces the pulse amplitude while the convective amplification increases the jet mixing noise. The traditional solution in this situation is to use the technique of signal averaging. If a sufficient number of individual records are averaged, the stochastic contribution from the jet mixing noise will average out to zero and the pulse time history should be recovered cleanly.

This signal averaging technique to recover incident, reflected and the transmitted pulses was also developed in the present study by injecting pulses through acoustic drivers instead of the spark source. Limited data obtained by using this technique is presented in section 5.

General discussions and the main conclusions are given in section 6.

Finally, the majority of the transmission data is tabulated as an appendix.

2. TEST CONFIGURATIONS AND PROCEDURES

The acoustic measurements for determining the transmission coefficients were carried out in two separate facilities. The daisy lobe nozzle and the reference conical round nozzle were tested in the anechoic free jet facility. The multi-chute suppressor nozzle and the reference coaxial round nozzle, for which no flight simulation data was required, were tested in the anechoic static jet facility. Both of these facilities have been used extensively in our previous work for studying the effects of forward velocity on jet mixing noise, shock noise and internal noise (for example see ref. 2.1 and 2.2) and to study jet mixing noise from single and coaxial model jets (ref. 2.3-2.6).

A description of the facilities is given in section 2.1 below. The details of the anechoic chambers and the air flow systems are given first. This is followed by a description of the nozzles, the source section and the spark circuit used to generate the sparks for the impulse noise. The test plan is described in section 2.2. Finally, details of the data acquisition and analysis system including facility instrumentation, microphone calibrations and definition of various transmission parameters are described in section 2.3.

2.1 FACILITY DESCRIPTION

2.1.1 Anechoic Free Jet Facility

This facility was used to test the effects of forward motion on the transmission characteristics of the daisy lobe suppressor nozzle and the reference round conical nozzle. The facility is powered by a jet ejector and is capable of providing continuous free-jet velocities up to 95 m/s with a circular test section of diameter 0.71 m. A planview schematic of the complete facility is shown in Figure 2.1. Starting from the left, air is drawn into the intake, through the honeycomb and screens to the contraction, across the anechoic room (test section) to the collector, through the diffuser, the two right-angle corners with turning vanes, and through the duct silencers to the transition section. The exhaust and entrainment flows of the jet ejector (diameter = 8.6 cm) are diffused through the 17.1 m long muffler/diffuser section shown on the right of Figure 2.1.

The basic anechoic room surrounding the free-jet test section is 4.3 m long, 4.3 m wide, and 6.1 m high between wedge tips. The interior is lined with polyurethane foam wedges. The chamber is completely isolated from the rest of the acoustics laboratory since it is mounted on massive springs. A spring-tensioned cable floor, suspended from the walls, provides easy access to the interior of the chamber for instrumentation and hardware changes and for calibration purposes.

Because of the high noise levels generated by the jet ejector, being operated at pressure ratios up to 8 to induce flows through the working section of up to 95 m/s, a significant amount of acoustic treatment has been incorporated in the tunnel ducting between the anechoic room and the jet ejector. A detailed description of this treatment is given in reference 2.1.

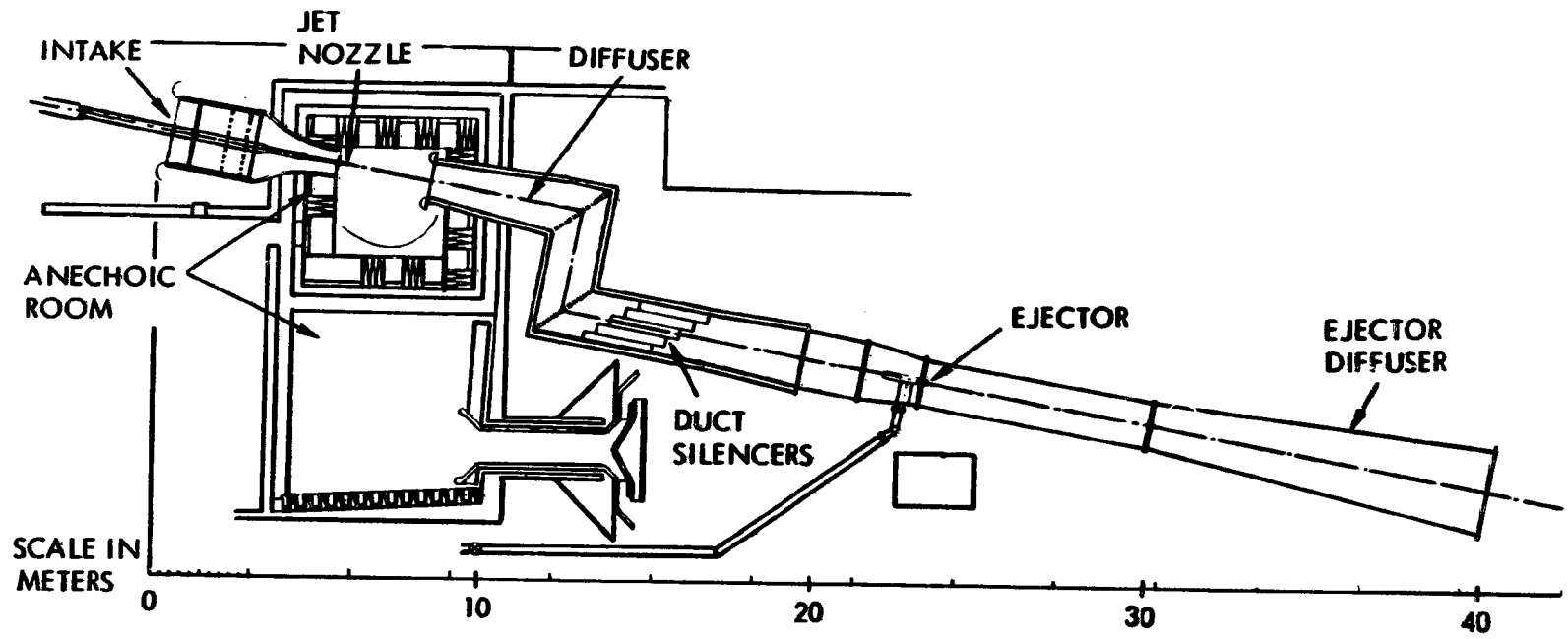

Figure 2.1 Planview schematic of the anechoic free-jet facility.

A series of tests were conducted to determine the anechoic quality of the anechoic chamber with the free jet installed (ref. 2.2). The facility was found anechoic down to a frequency of approximately 160 Hz.

The free jet section is 0.71 m in diameter. A photographic view of the free jet section with the daisy lobe nozzle mounted in place is shown in Figure 2.2. The inlet diameter of the free jet at the upstream section is 1.9 m, and the inner contour is designed to provide a flat velocity profile at the exit plane. The total length of the contraction section is 2.44 m. Other pertinent details about the construction and the aerodynamic performance of the free jet and the free jet intake (Fig. 2.3) can be seen in references 2.2 and 2.1.

The air supply to the jet ejector originates from the main 2.07×10^6 N/m^2 compressor which supplies dry air to all research center facilities. In addition, storage tanks retain approximately 5500 Kgm of air at 2.07×10^6 N/m^2 for higher demands. The ejector air supply ducting and the ejector diffuser section are shown in Figure 2.4.

SINGLE JET AIR SUPPLY. - For minimum blockage (and therefore minimum flow disturbance) in the working section, the air-supply ducting for the primary jet is installed in the intake/contraction section rather than through a swept pylon mounted on the anechoic room wall. The ducting is designed to avoid any flow separation within the accelerating free-jet flow in the contraction section, a totally welded construction being adopted for this purpose. The ducting is aligned by using a low power laser, placed at the end of the collector/diffuser and aimed along the free-jet centerline, ensuring that the model jet would exhaust axially in the free stream.

For heated jet noise tests, the air is first heated to approximately 1000 K by a Marquardt Sudden Expansion (SUE) Propane Burner located outside the laboratory building. The air is then passed through a muffler section which has been previously shown (ref. 2.3) to be highly effective in minimizing upstream internal noise levels. Downstream of this muffler section, the air passes through approximately 30 meters of 10.2 cm diameter Inconel pipe before finally reaching the model-jet nozzle. To compensate for the heat losses from this long length of pipe, a portion of the pipe (approximately 10 m long and located upstream of free-jet intake) is wrapped with commercially available half-circle electric heating units. In order to provide further heat insulation, all bare pipework and outer surfaces of electric heating units are covered with 7.6 cm thick kaowool blanket (see Fig. 2.3). Over the final section of the pipe, just upstream of the model-jet nozzle, the insulation is smoothly tapered to provide a clean free-jet flow.

2.1.2 Anechoic Static Jet Facility

The acoustic measurements to determine the nozzle transmission coefficients and the jet mixing noise of the dual stream multi-chute nozzle and also the reference coaxial nozzle were made in the Anechoic Static Jet Facility located in the Lockheed-Georgia research laboratories. This facility has been used extensively in the past to make measurements of noise from single jets. In 1977, the existing facility was modified to enable

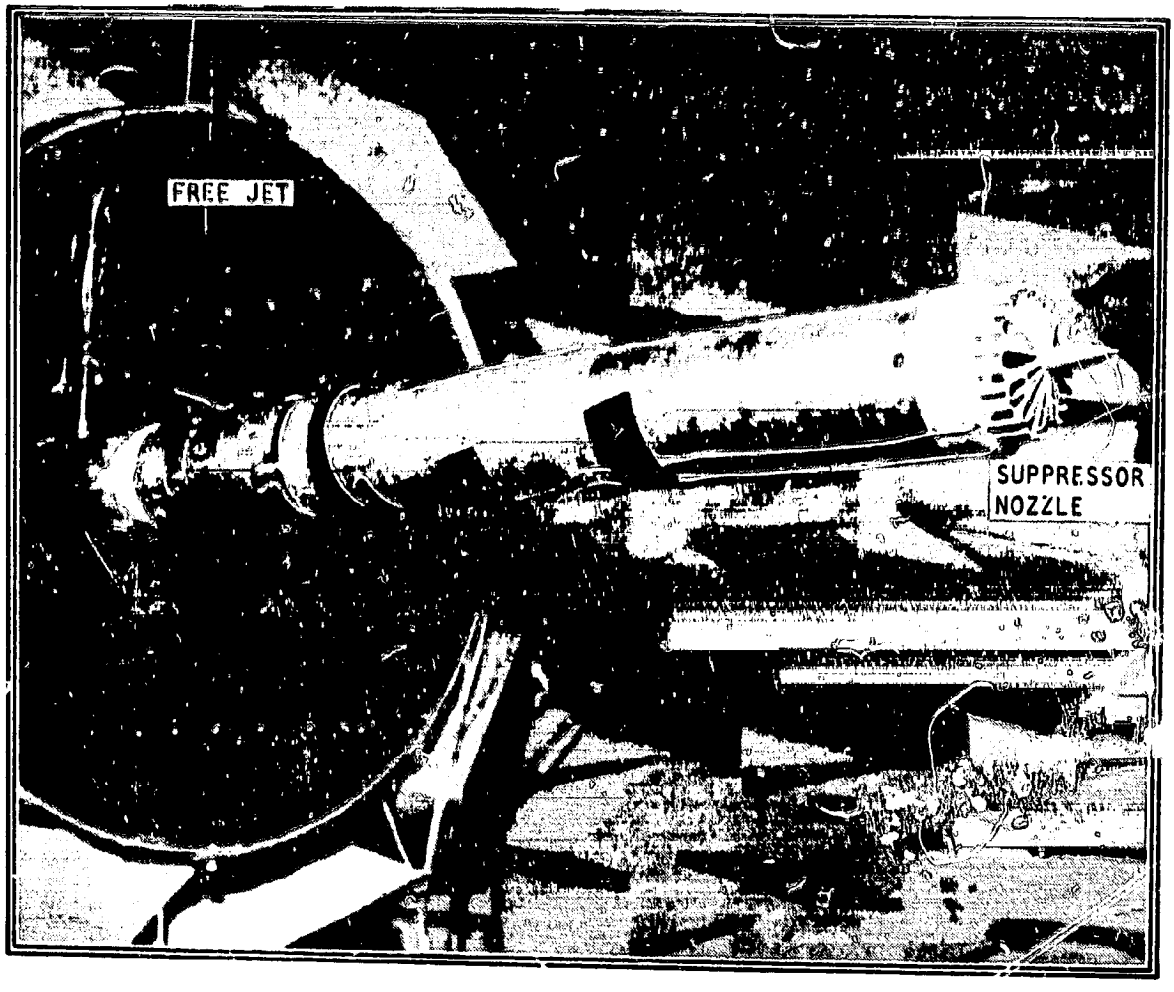

Figure 2.2 A photographic view of the 12-lobe, 24-tube nozzle suppressor mounted in the flight simulation facility.

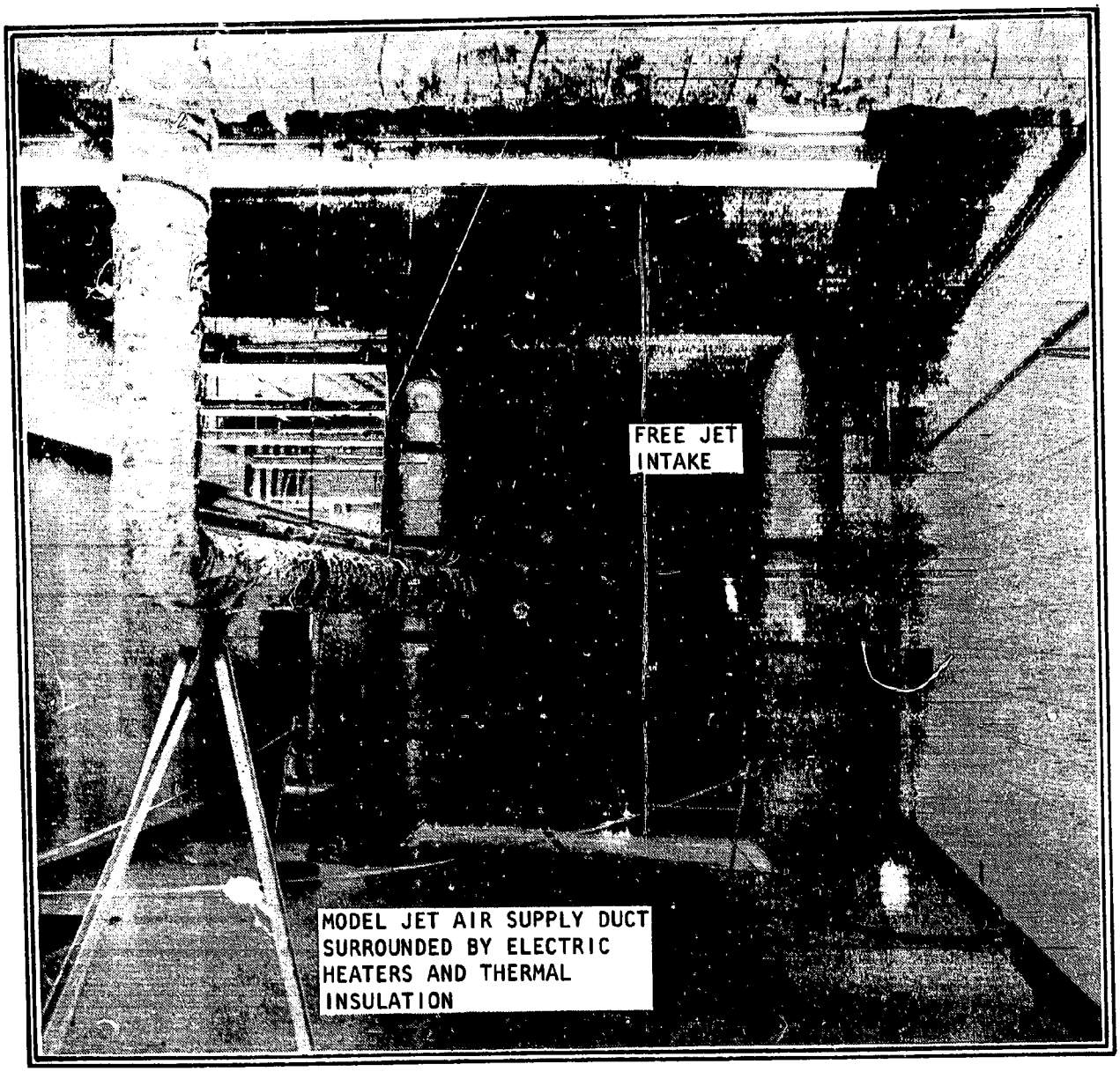

Figure 2.3 Free-jet intake showing model-jet air supply pipework.

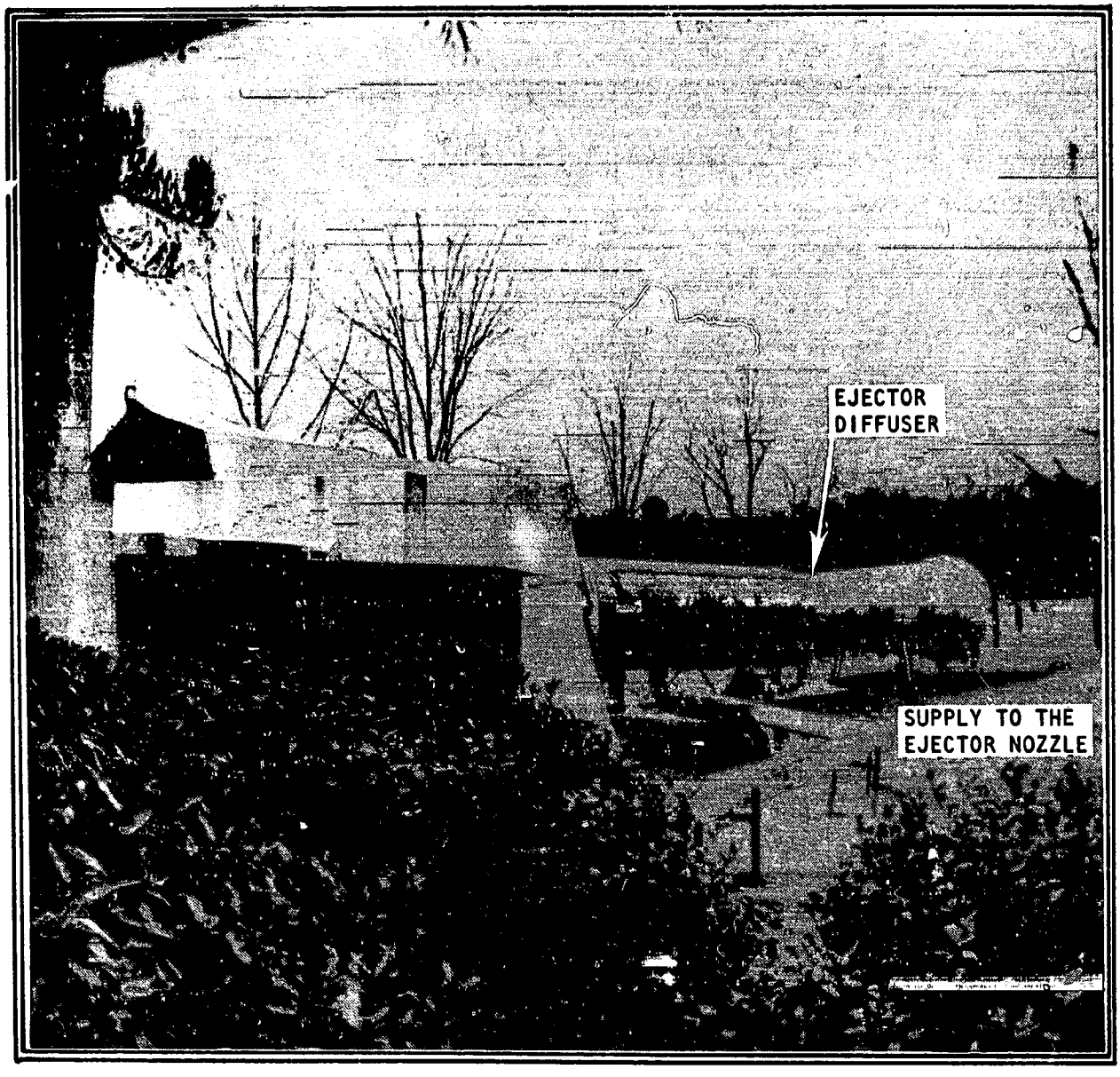

Figure 2.4 Anechoic free-jet facility ejector diffuser and air-supply ducting

measurements of noise from dual flow jets. This modified facility and the calibration tests conducted to check both the acoustic and the aerodynamic cleanliness of the facility are described in detail in references 2.6 and 2.7. The same facility was used to study the transmission characteristics of coaxial nozzles with inverted velocity profiles during the first phase of the present study [2.8].

The anechoic chamber used for these studies provides a free-field environment for all frequencies above 200 Hz, and incorporates a specially-designed exhaust collector/muffler which (1) provides adequate quantities of jet entrainment air, (2) distributes this entrainment air symmetrically around the jet axis, and (3) keeps the air flow circulation velocities in the room to a minimum.

The air for the primary and secondary jets is supplied by the main compressor which provides up to 9 Kg/sec. of clean dry air at 2.07×10^6 Pa. The air is heated by a propane burner to approximately 1000K. The primary and secondary air supplies are controlled independently downstream of the burner. Each supply has a hot and cold valve such that the desired operating conditions can be obtained within the pressure and temperature limitations of the system. Each air stream is then directed through a set of diffuser/muffler systems to minimize internal noise levels. The two streams finally enter their respective plenums which are located upstream of the coannular nozzle section.

In order to insure that the relative axial positions of the exit planes of the two nozzles do not vary, a special expansion coupling has been incorporated in the primary duct work, with a corresponding spacer in the secondary duct work. It provides for expansion or contraction of the inner duct relative to the outer duct of ±4 mm from center which is adequate for the thermal expansion associated with the likely temperature differentials between primary and secondary flows.

2.1.3 Nozzle Description

DAISY LOBE NOZZLE. The multi-lobe multi-tube suppressor has been modeled after a 12-lobe 24-tube suppressor tested by Rolls-Royce Ltd. and McDonnell Douglas Corporation (ref. 2.9, 2.10). Two photographic views of this nozzle are shown in Figures 2.5(a) and 2.5(b). A cross-sectional view of the nozzle with important dimensions is shown in Figure 2.6. The total flow area through the 12-lobes and 24 tubes is 30.21 sq. cm. and is equivalent to that of a round nozzle with a diameter equal to 6.21 cm (2.44 in). Both the tubes and the lobes are attached to a conic section which makes an angle of 50 degrees with the nozzle axis. The 24 tubes are equispaced on a circle of [illegible]ameter 9.59 cm. The tube diameter is 0.409 cm and the tube wall thickness is 0.762 mm. The inlets of these tubes are well rounded for smooth flow entry and the exits are chamfered to minimize flow separation at the lip.

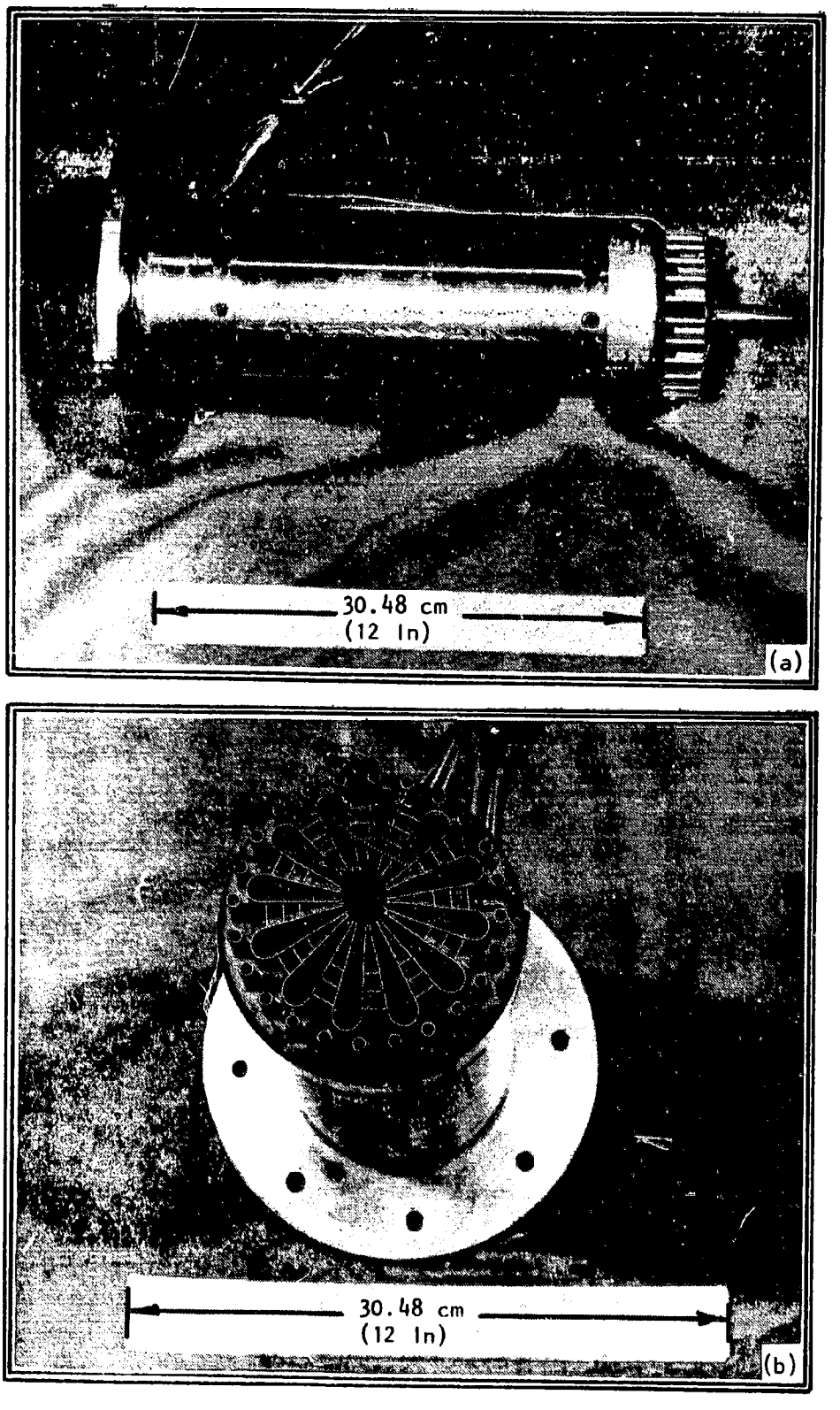

Figure 2.5 The 12-lobe, 24-tube suppressor nozzle.

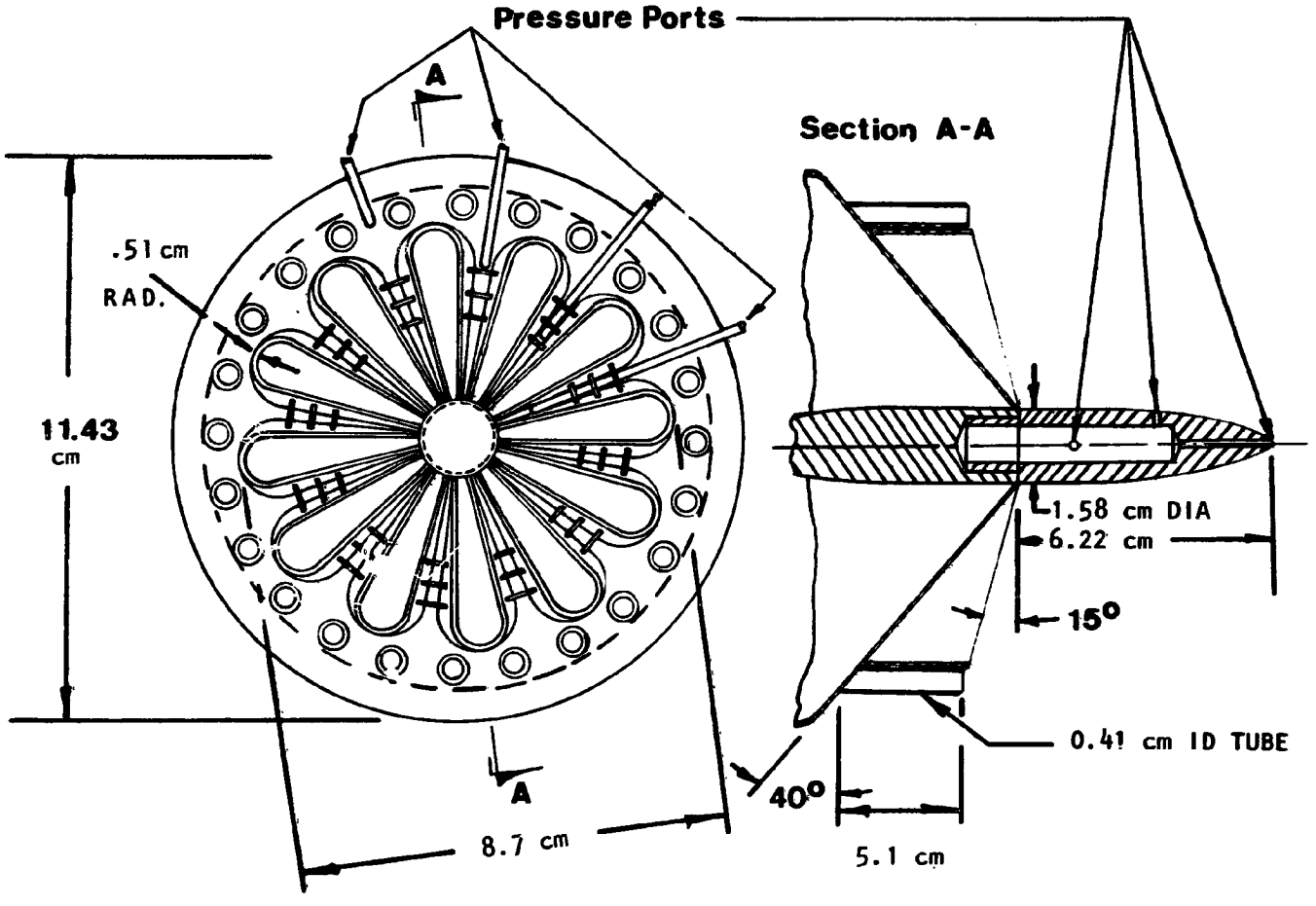

Figure 2.6 A cross-sectional view of the daisy lobe nozzle.

The 12 daisy lobes are also equispaced and each lobe consists of two straight and two rounded walls (see Fig 2.6). The lobe angle is 15 degrees and the flow area of each lobe is 2.26 sq. cm. This provides a ratio of total area of the lobes and that of the tubes equal to 9.6. Three stiffner pins of diameter 0.80 mm are inserted between the adjacent walls of each pair of lobes.

A plug is mounted in the center of the nozzle. It is ogival in shape, has a maximum diameter of 1.58 cm and protrudes beyond the lobe exit by 4.95 cm. It extends upstream into the 10.16 cm diameter test duct by 7.08 cm and has an elliptical leading edge (major axis = 6.34 cm, minor axis = 1.58 cm). The plug is actually detachable from the main body of the nozzle such that tests can be carried out with a different plug or no plug at all, if so required.

To obtain a measure of the drag on this nozzle, seven static pressure sensing ports have been provided, four in the entrainment area between the lobes, and three on the plug itself. Exact locations of these ports are shown in Figure 2.6. The four pressure ports in between the lobes can be seen in a close up shot of the nozzle shown in Figure 2.7 where the plug has been removed.

REFERENCE CONICAL NOZZLE. The reference nozzle is a round conical convergent nozzle of flow area equal to that of the daisy lobe nozzle with an exit diameter = 6.21 cm (2.44 in). Pertinent dimensions of this nozzle are given in Figure 2.8. The nozzle was designed such that when mounted on the 10.16 cm diameter supply duct, the distances of the spark source or the induct transducer from the exit plane remained the same as those from the exit of the daisy lobe nozzle.

MULTI-CHUTE SUPPRESSOR NOZZLE. The multi-chute suppressor is a co-axial 36-chute nozzle and matches that tested by G.E. (reference 2.11) in NASA Contract NAS3-18008. This nozzle is illustrated in Figure 2.9. Relevant dimensions are also given in this figure. Photographic views of the exhaust and also of the inlet are shown in Figure 2.10. This nozzle, while matching the exhaust characteristics of the G.E. nozzle is scaled to be physically as close as possible to one of the coaxial nozzles (described later) tested under Contract NAS3-20797 *(of which the present contract is an extension)* and is constructed such that it will fit the existing coaxial facility. This suppressor is fitted with a 6.7 cm (2.7 in.) diameter plug. Other parameters of interest for this nozzle are as follows:

- Area of primary annulus = 45.6 cm^2 (7.068 $in.^2$)
  [Equivalent round jet dia. = 7.62 cm (3 in.)]
- Flow area through primary/chute flow area = 1.5
- Projected area of secondary annulus/chute flow area = 2.5
- Protrusion of primary exit plane with respect to the secondary exit (L)/height of the annulus (h) = 3

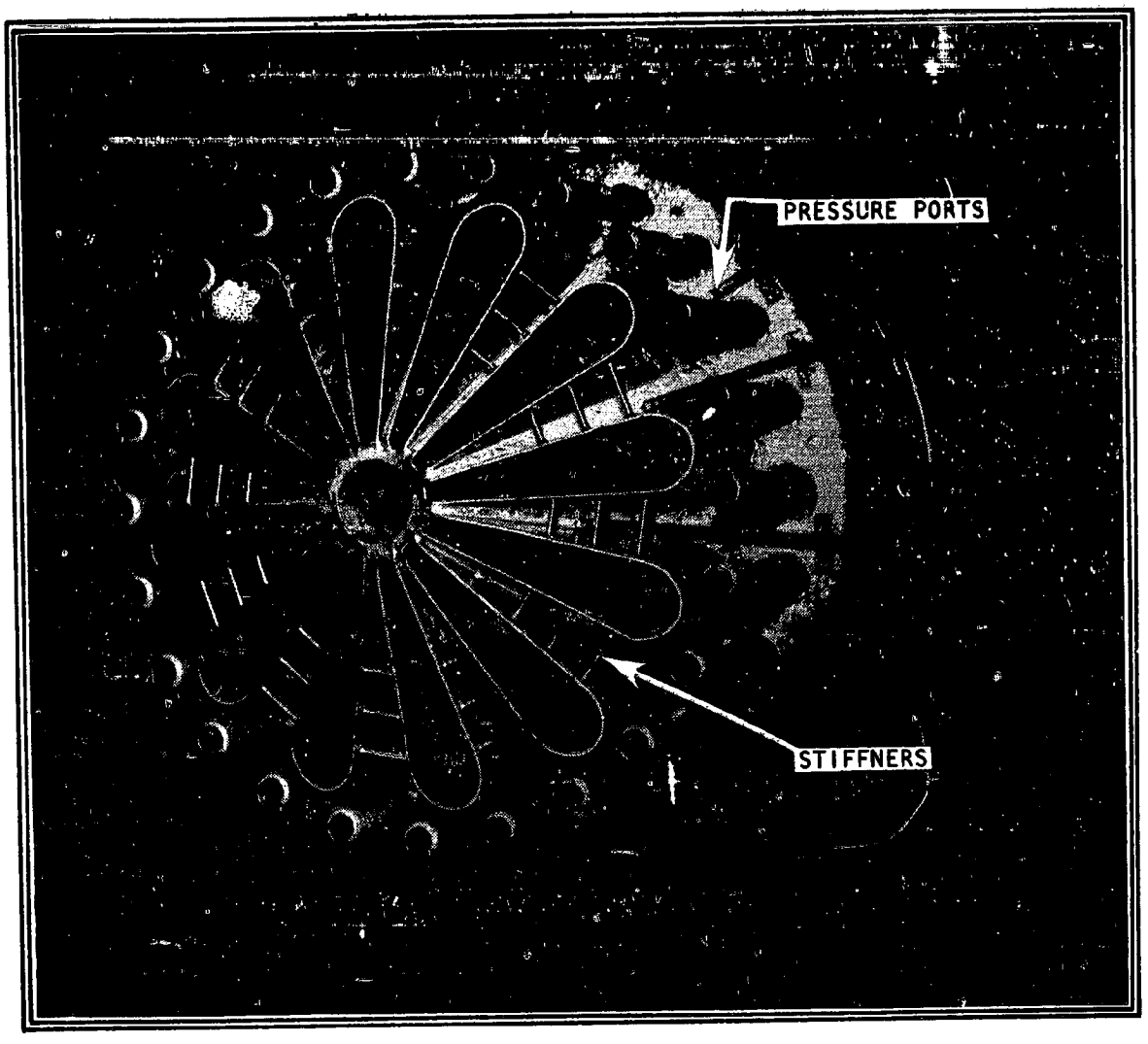

Figure 2.7 A close-up view of the daisy lobe suppressor with the plug removed.

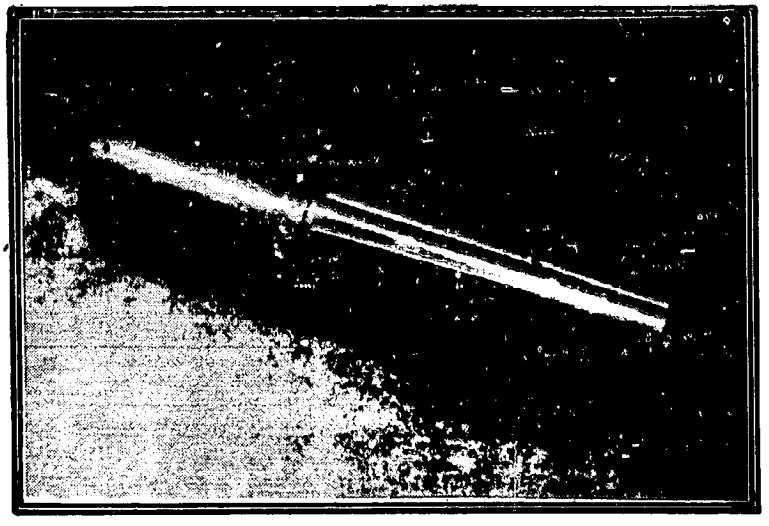

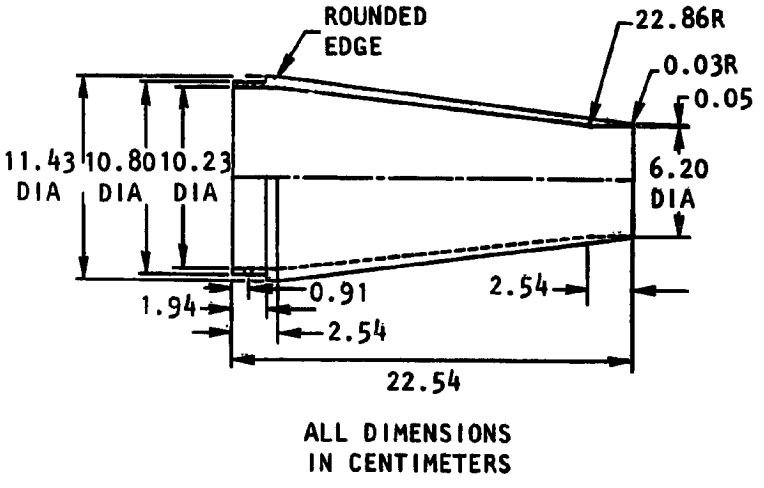

Figure 2.8 The reference conical nozzle (dia = 6.21 cm)

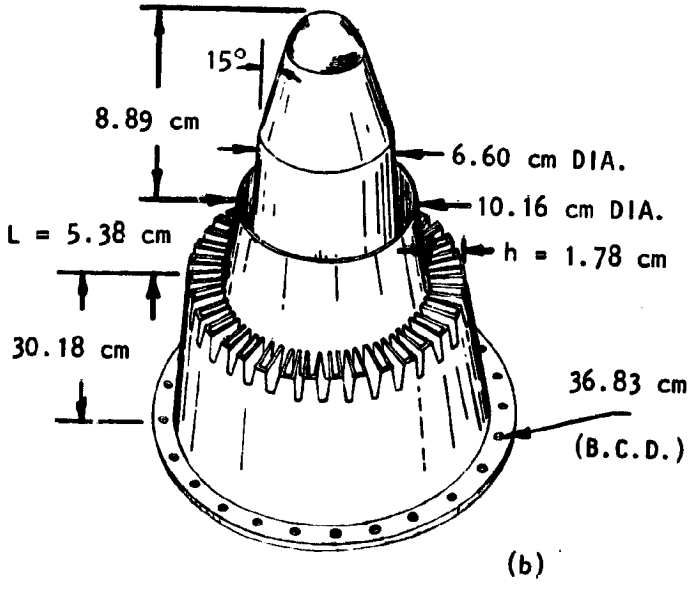

Figure 2.9 The 36-chute dual stream suppressor nozzle (L/h = 3)

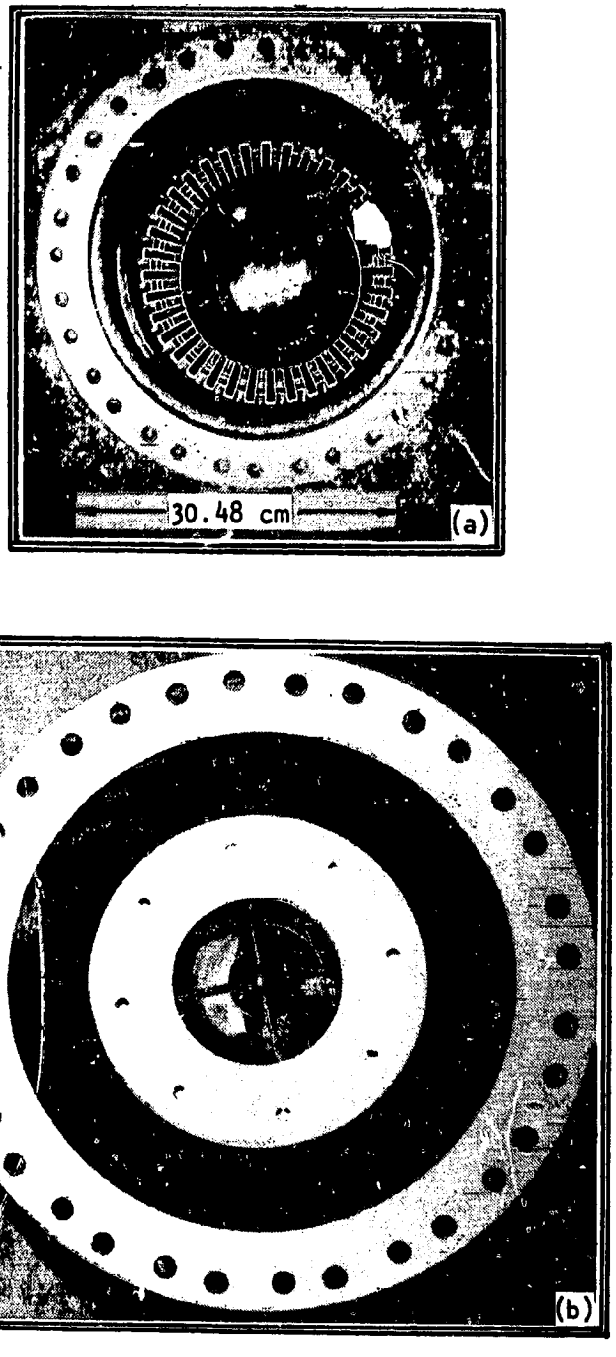

Figure 2.10 Photographic view of (a) the exhaust end and (b) the inlet end of the multi-chute suppressor nozzle.

REFERENCE COAXIAL NOZZLE. The reference coaxial nozzle tested to compare with the results from the multi-chute nozzle is shown in Figure 2.11. It is one of the six coaxial nozzles tested earlier (see ref. 2.8) to study the transmission characteristics of coaxial nozzles with inverted velocity profiles. The area of the primary nozzle (diameter = 7.62 cm) is equal to that of the primary annulus of the multi-chute nozzle, i.e. 45.6 sq. cm. The only other parameter that is the same for the two nozzles is the ratio, L/h which is equal to 3. A comparison of other parameters of interest is made in table 2.1 below:

Table 2.1 Various geometric parameters for the multi-chute suppressor and the reference coaxial nozzle.

	Primary Jet Exit Area, A_P (cm^2)	Secondary Jet Exit Area, A_F (cm^2)	$\frac{A_P}{A_F}$	Height of the Secondary Annulus, h (cm)	L/h	Convergence angle of the Secondary Nozzle ϕ_2
Reference Coaxial Nozzle	45.60	64.14	0.71	1.70	3	20°
Multi-chute Suppressor Nozzle	45.60	30.40	1.50	1.79	3	14.1°

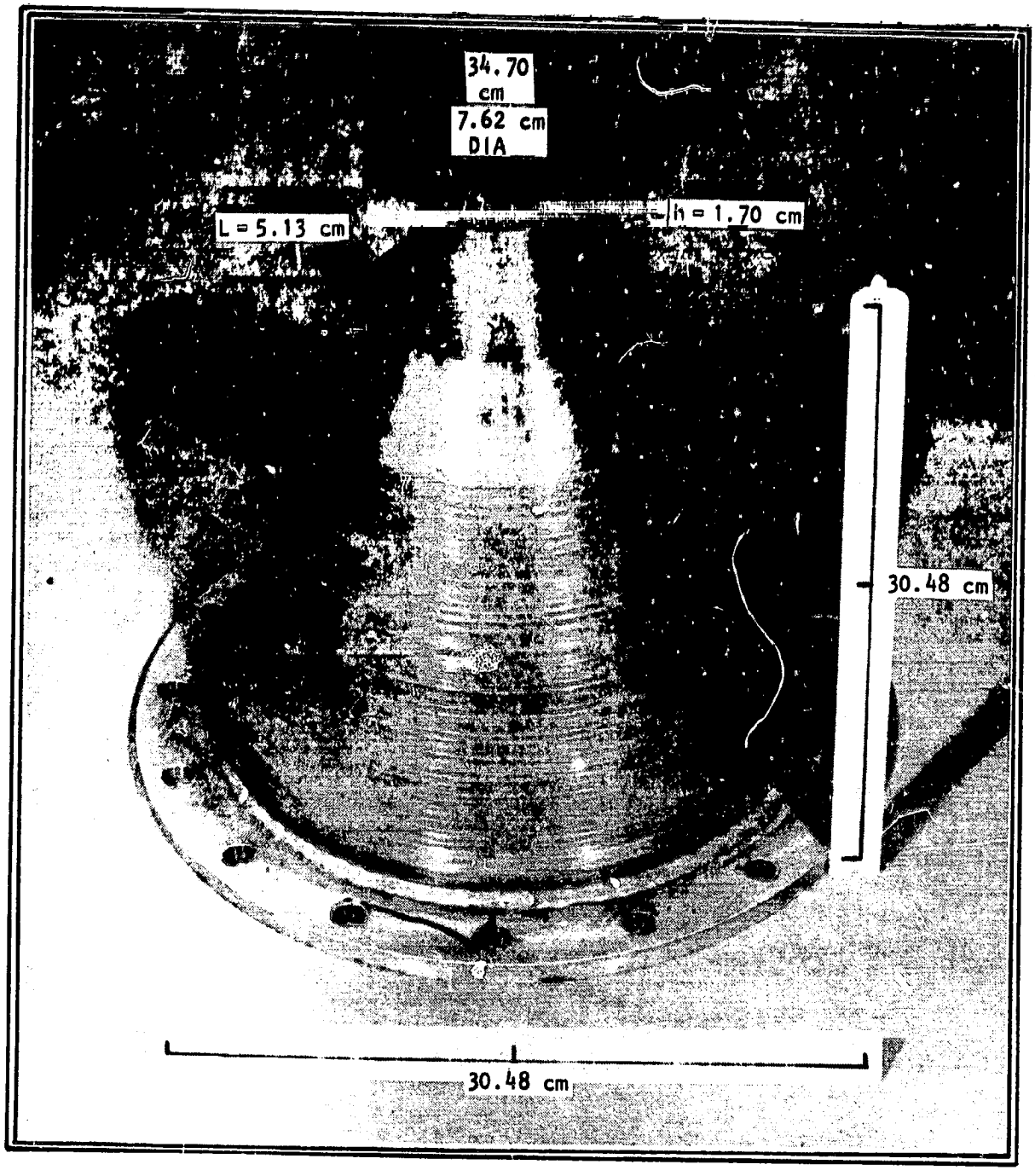

Figure 2.11 Reference coaxial nozzle (L/h = 3)

2.1.4 Source Section

The source section for the single stream nozzle suppressor and the reference conical nozzle was different from that used for the dual stream suppressor and the reference coaxial nozzle. The two types of source sections are described separately below.

SOURCE SECTION FOR THE SINGLE STREAM NOZZLES. The experimental configuration in its basic form is shown in Figure 2.12. It contains the spark source placed on the center line of a 10.16 cm diameter supply duct, about 6 meters upstream of the nozzle exit. Internal noise is generated by inducing sparks across two graphite electrodes (dia. = 0.318 cm) separated by 0.6 mm wide air gap.

SOURCE SECTION FOR THE DUAL STREAM NOZZLE. For the dual stream nozzles, six spark sources, equispaced in the secondary plenum, were used. The source section, which is also a part of the secondary plenum is visible in Figures 2.13 and 2.14 where the reference coaxial nozzle and the multi-chute suppressor respectively are shown mounted downstream of the source section. A schematic view of the source section is shown in Figure 2.15. The source section for the primary plenum is also shown here, although the primary source was not used in the present study.

It is to be noted that unlike the configuration for the single stream nozzle, where the spark source was placed a considerable distance away from the nozzle exit, the source in the dual nozzle configuration was located only 74 cm upstream of the nozzle exit plane. As explained in appendix A a larger travelling distance is desirable so that the spherical wave fronts of an impulsive point source will have such large radius of curvature that it will appear essentially as a plane wave, which is the desired in-duct condition. A very long secondary plenum was not practical with our facility. As shown in Figure 2.15, the spark source (electrode gap) was used in conjunction with a paraboloidal reflector. The spark source itself was placed at the focus of the paraboloid. The effect of the paraboloidal reflector was to increase the impulse energy traveling in the axial direction and to modify the wave front from spherical to essentially plane in nature.

Each of the spark gaps in this configuration was connected in series through high voltage cables such that all of them fired simultaneously. Unlike the electrodes for the single nozzle configuration where the two electrodes actually faced each other, the secondary plenum electrodes in this case had an included angle of 20° as shown in Figure 2.15(b).

Each electrode was removable through a threaded connection and entered the paraboloid through narrow openings drilled on the sides of the reflectors.

2.1.5 Spark Circuit

The essential elements of the spark discharge circuit are shown in Figure 2.16. A high voltage power supply charges a storage capacitor (70 μF) to 5 to 10 KV. The discharge of the capacitor occurs through the air gap between the electrodes, thus producing a powerful, but physically small, acoustic pulse.

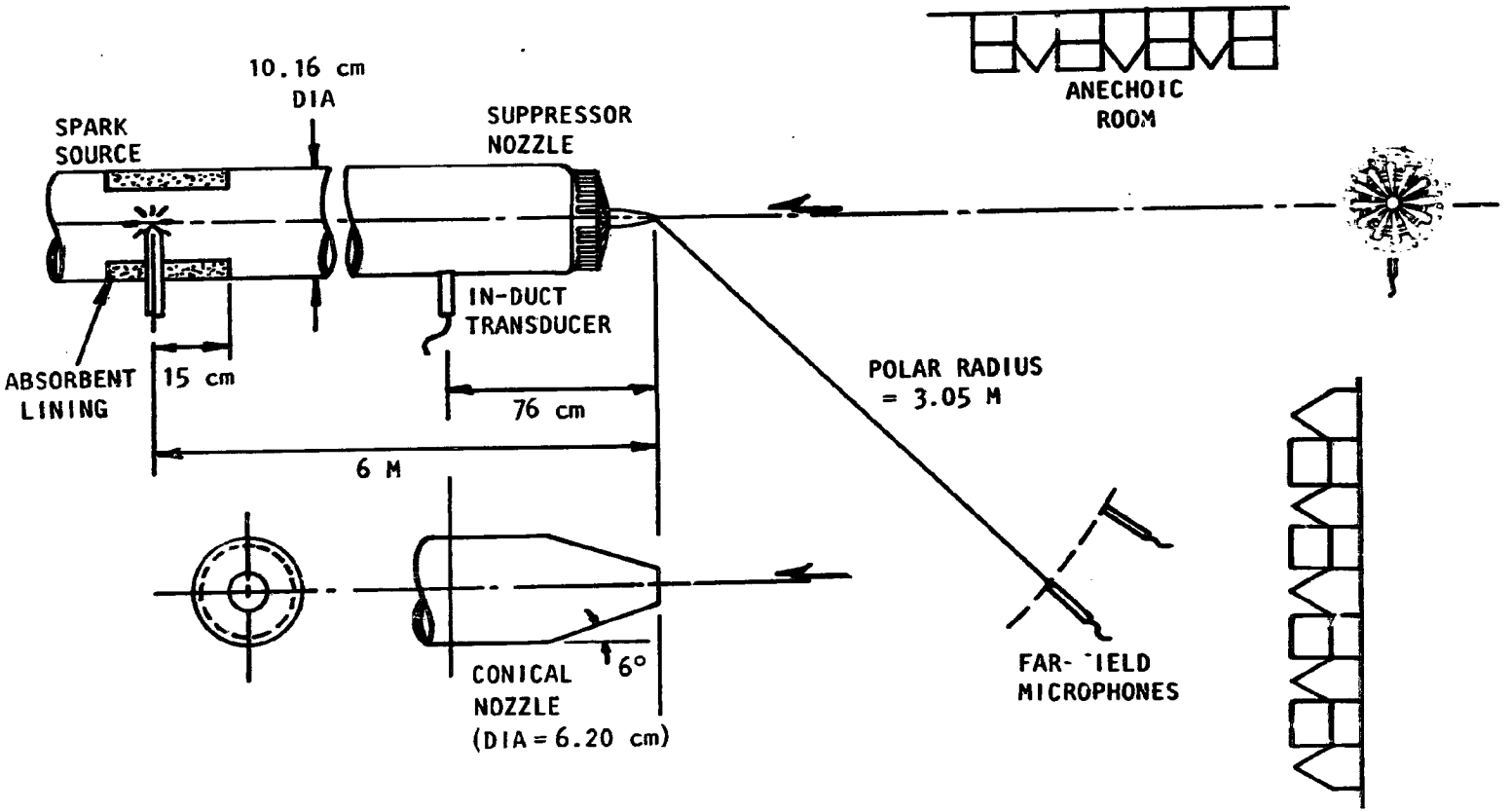

Figure 2.12 The source section for the daisy lobe and the reference conical nozzle and the measurement configuration

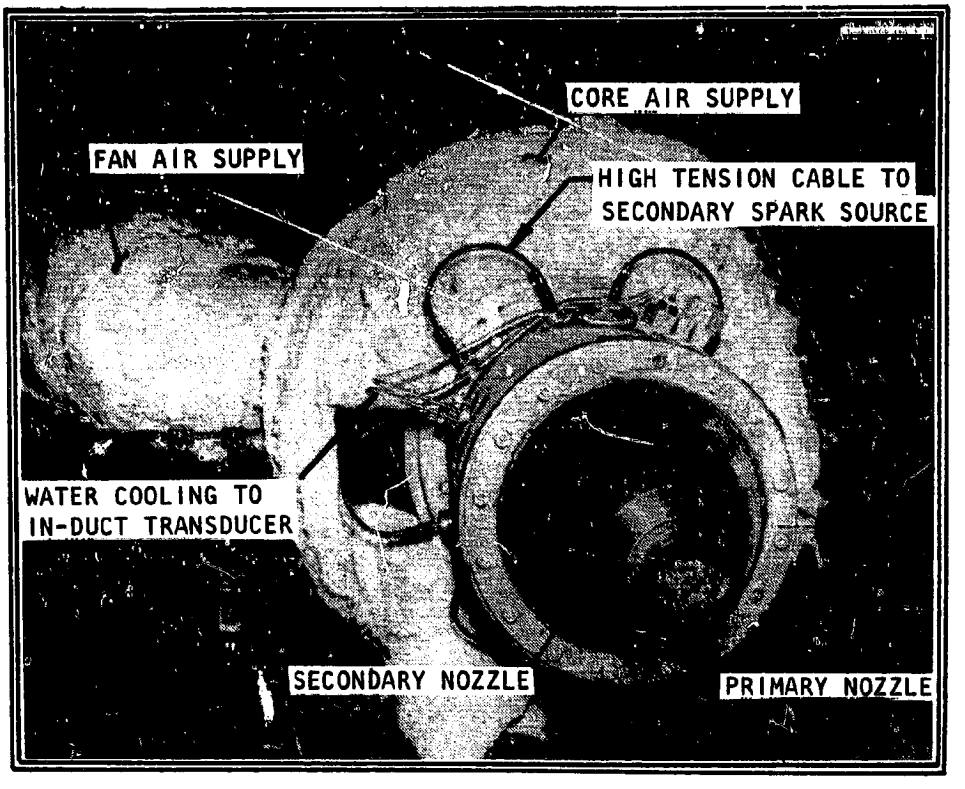

Figure 2.13 The coaxial jet facility

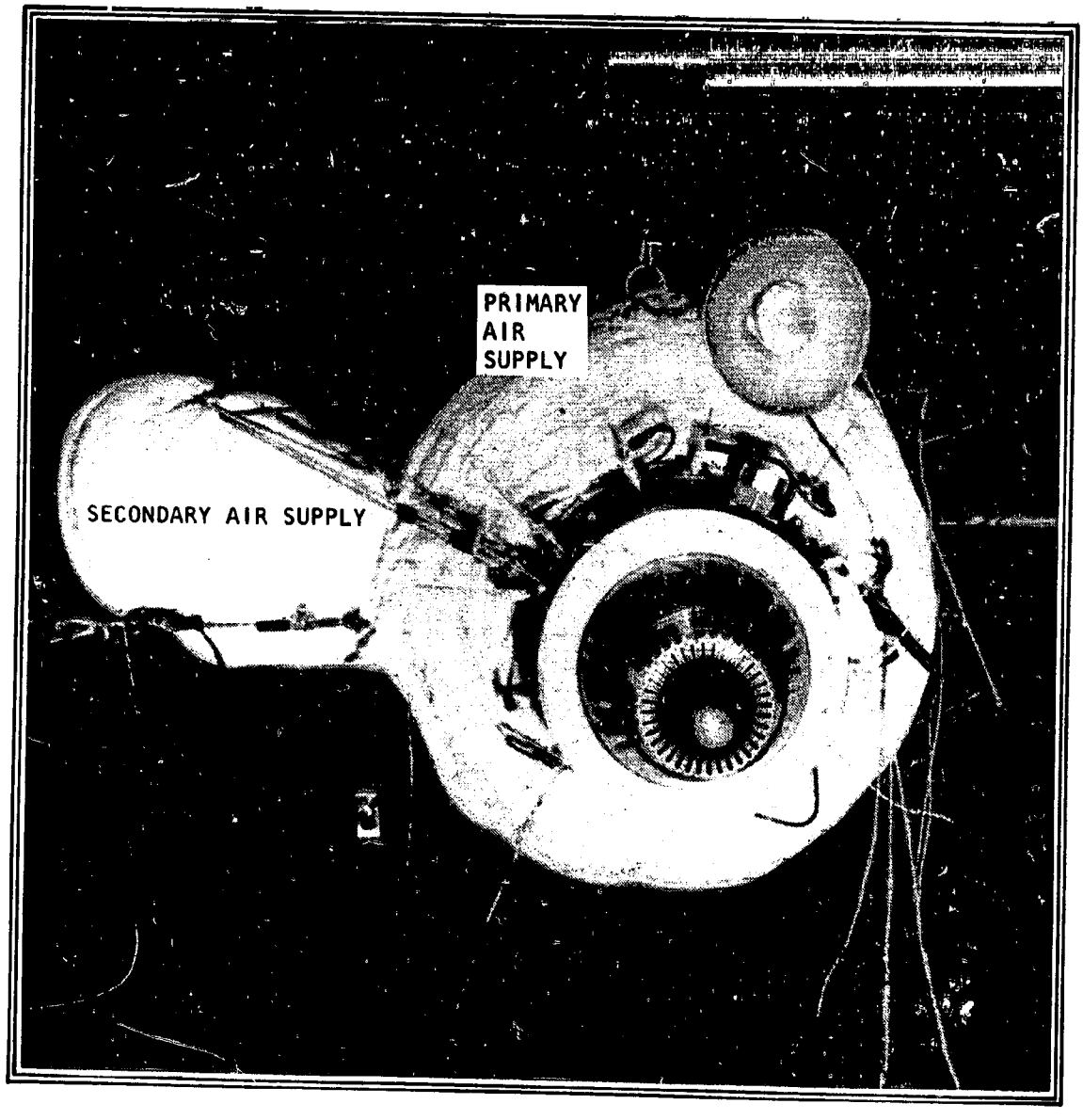

Figure 2.14 The multi-chute suppressor nozzle mounted on the dual flow supply facility

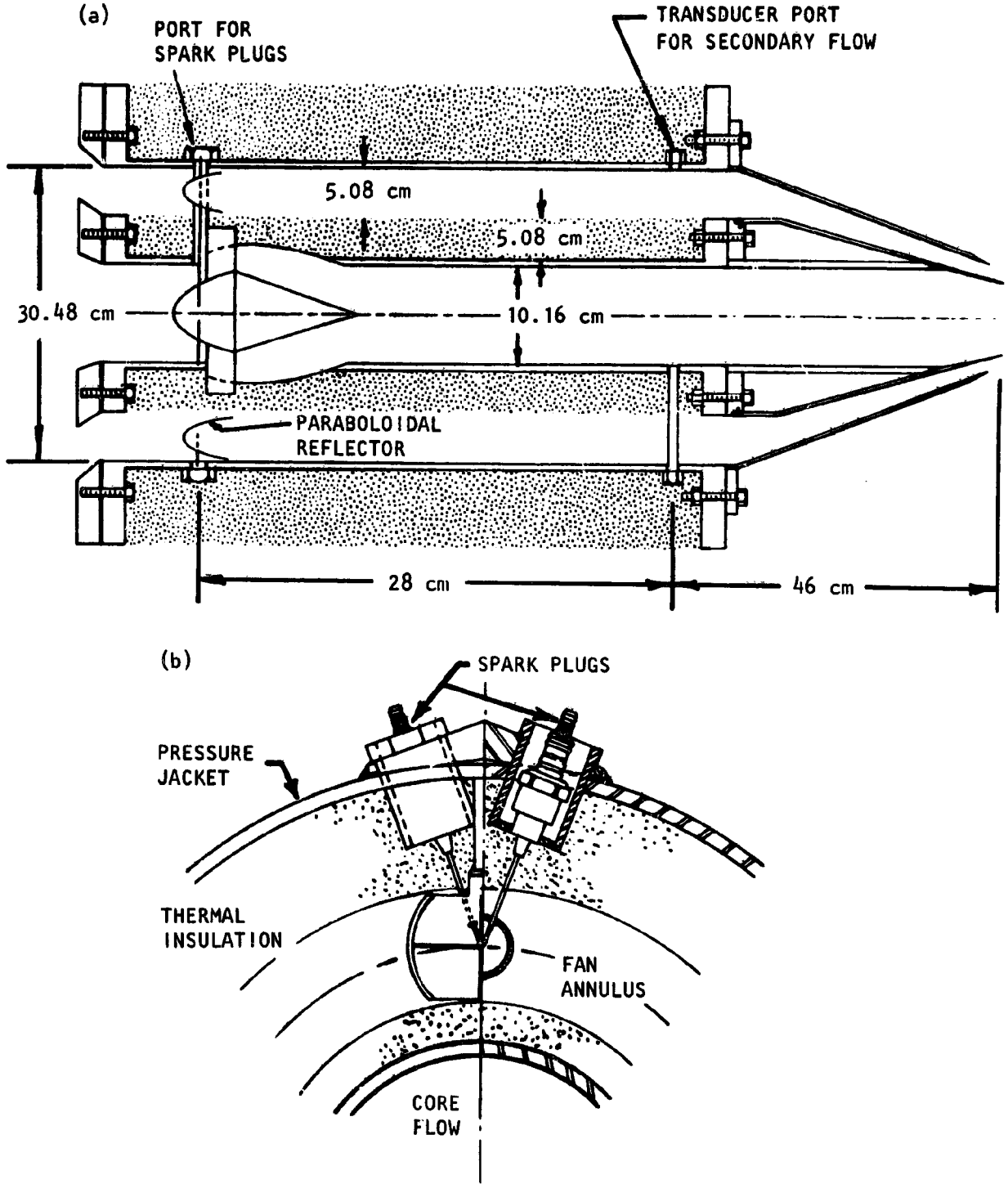

Figure 2.15 Source section for the multichute and the reference coaxial nozzle.
(Not to Scale)

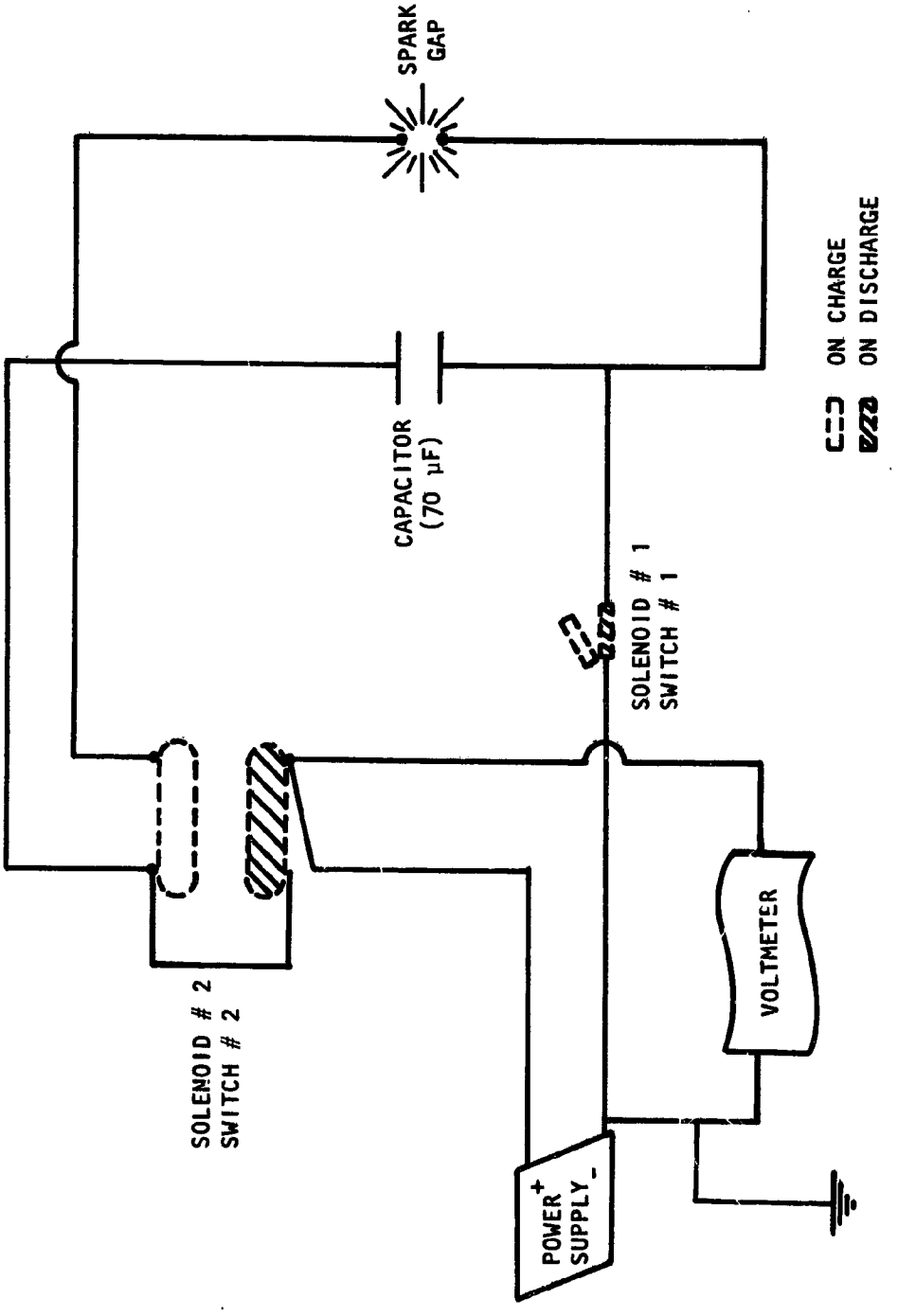

Figure 2.16 The spark discharge circuit

To fire the spark, special vacuum switches were used to prevent current surges back through the power supply. It was found essential to "float" the capacitor from all ground circuits as the discharge currents (~2,000 amp) induced local ground potential shifts, with resultant digital equipment malfunctions.

2.2 TEST PLAN

The flow conditions for which the daisy lobe nozzle and the reference conical nozzle were tested are given in Table 2.2. Thus basically the two single stream nozzles were tested for the no flow case, three subsonic and one supersonic Mach numbers, three tunnel Mach numbers and two temperatures.

The flow conditions at which the multi-chute nozzle and the reference coaxial nozzle were tested are given in Table 2.3.

Table 2.2 Test conditions for the diasy lobe and the reference conical nozzle.

Reservoir Temperature (T_R)	Fully Expanded Jet Mach No. (M_J)	Pressure Ratio P_R/P_0	Tunnel Mach number (M_T)
Ambient	0.0	1.0000	0.0, 0.08, 0.16, 0.24
Ambient	0.4	1.1166	0.0, 0.08, 0.16, 0.24
Ambient	0.6	1.2755	0.0, 0.08, 0.16, 0.24
Ambient	0.8	1.5244	0.0, 0.08, 0.16, 0.24
Ambient	1.2	2.4248	0.0, 0.16, 0.24
600K	0.8	1.5244	0.0, 0.08, 0.16, 0.24
600K	1.2	2.4248	0.0, 0.16, 0.24

Table 2.3 Test conditions for the multi-chute nozzle and the reference coaxial nozzle.

Primary Jet (Core)			Secondary Jet (Fan)		
Reservoir Temperature (T_{R_1})	Fully Expanded Jet Mach No. (M_{J_1})	Pressure Ratio P_{R_1}/P_0	Reservoir Temperature (T_{R_2})	Fully Expanded Jet Mach No. (M_{J_2})	Pressure Ratio (P_{R_2}/P_0)
Ambient	0.0	1.0000	Ambient	0.0	1.0000
Ambient	0.0	1.0000	Ambient	1.2	2.4248
Ambient	0.4	1.1166	Ambient	0.6	1.2755
Ambient	0.8	1.5244	Ambient	0.9	1.6912
Ambient	0.8	1.5244	Ambient	1.2	2.4248
Ambient	0.8	1.5244	600K	0.9	1.6912
Ambient	0.8	1.5244	900K	0.9	1.6912
Ambient	0.8	1.5244	600K	1.2	2.4248
450K	0.8	1.5244	600K	0.9	1.6912
675K	0.8	1.5244	900K	0.9	1.6912

2.3 DATA ACQUISITION AND ANALYSIS

2.3.1 Facility Instrumentation

The in-duct signals were measured by a Model 202 Series Piezotron pressure transducer made by Sundstrand Data Control, Inc. This transducer has a rugged stainless steel mounting with provision for water cooling. The transducer used for the daisy lobe nozzle and the reference conical nozzle was located 6 m downstream of the spark source and 76.2 cm upstream of the nozzle exit plane. Similarly the transducer for the multi-chute nozzle and the reference coaxial nozzle was mounted 28 cm down stream of the spark source and 46 cm upstream of the suppressor nozzle exit plane. The transducers in each facility were mounted in an electrically isolated bushing made from machinable ceramic to avoid ground-induced voltage spikes from the spark discharge electromagnetic radiation.

Far-field signals were measured on a polar arc of 3.05 m radius with 0.635 cm diameter B&K microphones (Type B&K 4135) in conjunction with B&K cathode followers (B&K 2619). Measurements in the far-field were made between 0° and 120° at intervals of 10°.

The basic test procedure consisted of firing the spark at the desired operating flow conditions and simultaneously recording the signals, both in-duct and the far-field, on a 28-channel tape recorder. Subsequent analysis of each pulse was achieved conveniently on a dual-channel transfer function analyzer, while maintaining accurate time interrelationship between the impulse signals. The system schematic is shown in Figure 2.17.

2.3.2 Transient Capture and Editing

Using the transient capture capability of Spectral Dynamics SD360 digital FFT signal analyzer, the in-duct and the far-field signals were first captured on channels A and B. The analyzer has the ability not only of capturing the time histories, but also of data editing and relative time translation (rotation). With the exception of the highest Mach number (i.e. 1.2) where jet noise levels are quite high, the far-field pulse was easily detectable. The in-duct pulse, however, was always strong. Having located the in-duct pulse and the corresponding far-field pulse, all components of the two time histories except these two pulses were edited out. An example of this procedure is shown in Figure 2.18. The two pulses were then Fourier transformed to produce their respective power spectra. The ratio of far-field to in-duct power spectra was then used to compute transfer function as discussed in section 2.3.4. This procedure was repeated for each measurement angle.

The above transfer functions were obtained up to a frequency of 100 KHz. Since atmospheric absorption becomes important at these frequencies, appropriate corrections were made to the far-field data in accordance with the data of reference 2.12.

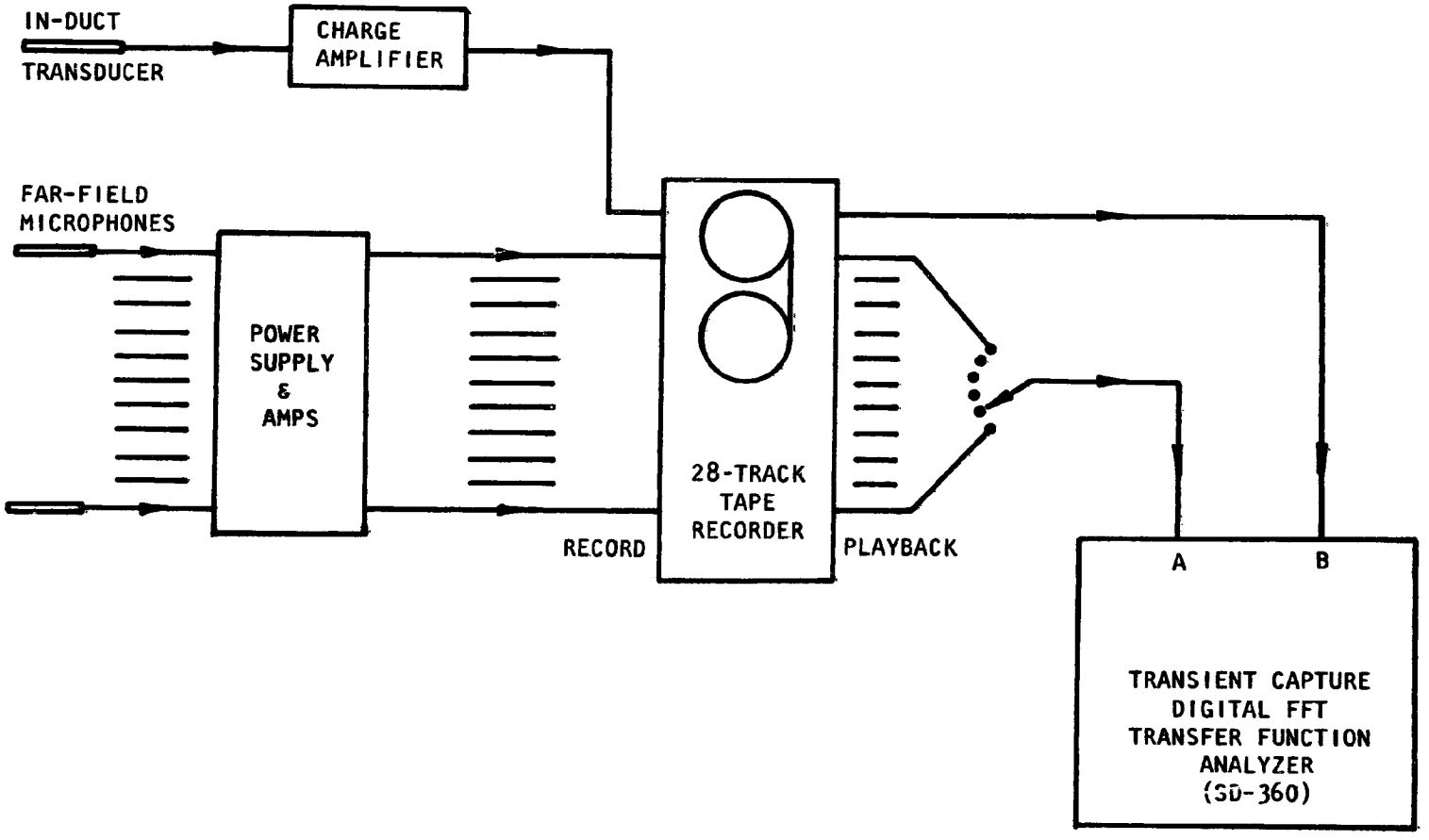

Figure 2.17 Instrumentation layout.

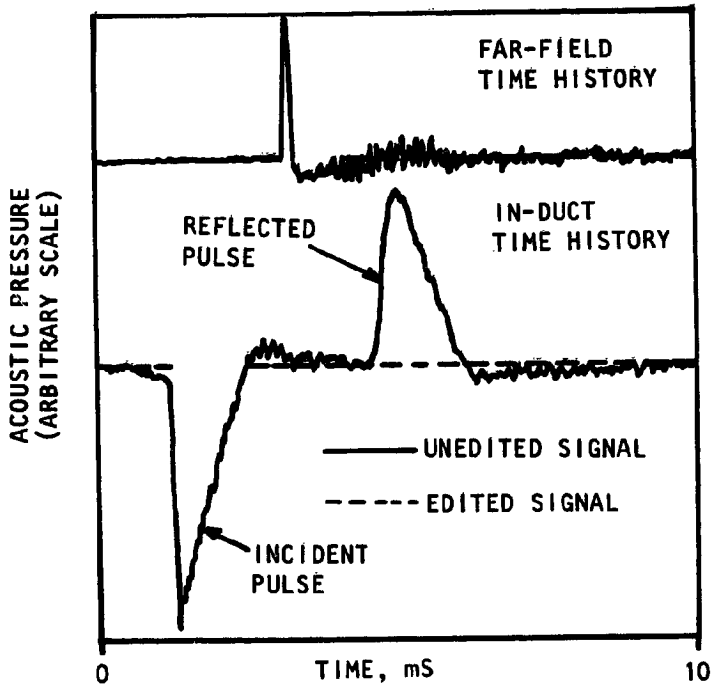

Figure 2.18 An example of the editing process used in the evaluation of incident and transmitted power spectra

2.3.3 Calibrations of Far-field Microphones with Respect to the In-Duct Transducer

In order to obtain a true measure of the transfer function B/A, it was essential to account for the frequency responses of each microphone and the in-duct transducer. This was accomplished by mounting the transducer next to a given microphone as shown in Figure 2.19 and measuring the noise of a pulse generated by a spark source mounted at a location directly in front of the transducer and the microphone. The spark source produced a pulse with high spectral energy up to a frequency of 100 KHz. Since the signals captured by the microphone and the transducer were the same, a transfer function between the two was the calibration of one with respect to the other. Using the in-duct transducer as the reference, the calibration of each microphone was thus obtained and incorporated as a frequency response correction. A typical frequency response is shown in Figure 2.20.

2.3.4 Presentation of Transmission Data

Three basic parameters of interest were calculated from the measurements made in the far-field and inside the duct. These were the Reflection Coefficient (σ), the Nozzle Transfer Function (NTF) and the Power Transfer Function (PTF) respectively. Various reasons for using the above parameters are described in detail in reference 2.8. Expressions for these parameters as used in the present report are given below:

REFLECTION COEFFICIENT (σ). The duct termination reflection coefficient is defined to be the ratio of the squares of the reflected and the incident wave pressure amplitudes as measured by the in-duct transducer.

Thus, σ in dB = $10 \text{ Log}_{10} (p_r^2/p_i^2)$. (2.1)

In the present case the above ratio was obtained by taking the difference between the power spectra of the reflected and the incident signals.

NOZZLE TRANSFER FUNCTION (NTF) OR NOZZLE TRANSMISSION COEFFICIENT (NTC). NTF (also referred as NTC) in essence relates the measured sound pressures at any fixed polar angle to that produced in the free field by a point source of power equal to that of the incident pulse. The derivation of the expression for the NTC in terms of the measured quantities is given below:

If p_i^2 is the mean square of the incident pressure at the in-duct transducer location, then the in-duct intensity will be given by:

$$I_D = \frac{p_i^2 \, (1 + M_D)^2}{\rho_D c_D} \tag{2.2}$$

where M_D is the flow Mach number in the duct and $\rho_D c_D$ is characteristic in-duct impedance.

Figure 2.19 Illustration of microphone/pressure transducer calibration using the spark source.

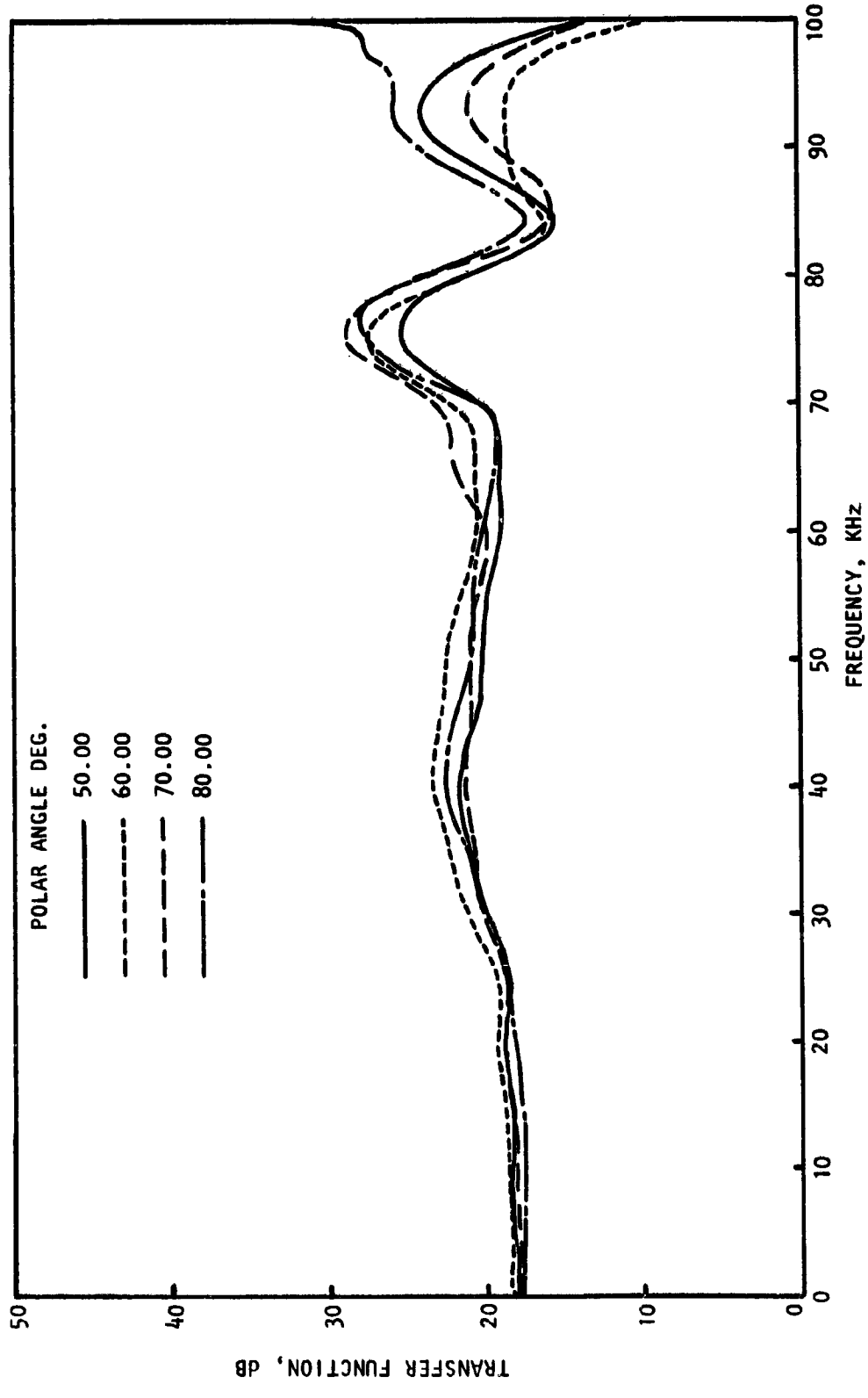

Figure 2.20 Typical frequency response calibrations between the in-duct transducer and the microphone used in the far field. ($\Delta f = 200$ Hz)

Therefore the total in-duct incident power $W_i = \frac{p_i^2 (1 + M_D)^2}{\rho_D c_D} A_D$ (2.3)

where A_D = duct area at the measured location.

If we assume that a point source of power equal to W_i is now radiating in the far-field from the nozzle exit the intensity at the measurement location at a distance R_m from the nozzle exit due to this source will be

$$I_p = W_i / 4\pi R_m^2 \tag{2.4}$$

Nozzle Transmission Coefficient is simply the ratio of the measured intensity $I_f(\theta)$ and I_p can be expressed in the following form:

$$(NTC)dB = 10 \log_{10} \left\{ \frac{p_f^2(\theta)}{p_i^2} \right\} + 10 \log_{10} \left\{ \frac{4\pi R_m^2}{A_D} \cdot \sqrt{\frac{T_o}{T_D}} \cdot \frac{P_D}{P_o} \cdot \frac{1}{(1+M_D)^2} \right\} \tag{2.5}$$

where,

$p_f^2(\theta)$ = mean square pressure in the far-field at angle θ at a distance R_m from the nozzle exit.

P_D = static pressure in the duct

P_o = ambient pressure

T_D = static temperature in the duct

T_o = ambient temperature

The details of the NTC calculation from the measured data are shown in appendix B.

It should be noted that the data was analyzed at a bandwidth of 200Hz but has been converted into 1/3-octave values as described in appendix B. The data is presented up to 63 KHz.

Of course as described in detail in reference 2.8 the following three basic characteristics are implicit in this definition:

(1) A single-point in-duct measurement is representative of the average mean square pressure over the duct cross-section.

(2) The far-field mean square pressure is azimuthally axisymmetric.

(3) Below the first higher-mode cut-on frequency the incident plane mode will be transmitted as plane-mode radiation to the far-field.

Above this frequency, higher modes will be reflected from the nozzle and will also contribute to the far-field pressures even though the incident wave may be plane. Thus, nozzle reflection and transmission coefficients cannot *rigorously* be ascribed to any one mode or combination of in-duct modes. In this work, however, it is tacitly assumed that the *dominant* mode component reflected inside the duct and transmitted out of the duct is a plane wave.

POWER TRANSFER FUNCTION (PTF). Power Transfer Function (PTF) is the ratio of the far-field acoustic power (W_f) and that transmitted through the duct. The acoustic power (W_t) transmitted through the duct was corrected according to Blokhintsev (Ref. 2.13) to eliminate the influence of the flow velocity in the duct by using the following expression

$$W_T = \frac{A_D}{\rho_D c_D} \left[p_i^2 (1+M_D)^2 - p_r^2 (1-M_D)^2\right] \tag{2.6}$$

The radiated sound power (W_f) in the far-field was determined by

$$W_f = \oint I_f(\theta)\, ds \tag{2.7}$$

where ds is the elemental strip shown in Figure 2.21. The far-field acoustic intensity can be expressed as

$$I_f = \frac{p_f^2}{\rho_o c_o} \tag{2.8}$$

where $\rho_o c_o$ is the ambient acoustic impedance. Since only a finite number of far-field measurements were possible, it is assumed that the far-field intensity in the angular strip between angles $\theta + (\Delta\theta/2)$ remains constant and equal to that measured at polar angle θ. Here $\Delta\theta$ is the interval between successive measurement locations and was equal to 10° in the present work. Thus, the integral for W_f can be approximated by a finite sum and is given by:

$$W_f = \frac{1}{\rho_o c_o} \sum_i p_f^2 \, \Delta s_i \tag{2.9}$$

where p_f^2 over the elemental surface area Δs_i has been assumed to be a constant. Typical elemental surface areas can be written as

$$\Delta s_i = 4\pi R_m^2 \sin(i\Delta\theta) \sin(\Delta\theta/2) \quad 0 < i\Delta\theta < \pi. \tag{2.10}$$

At $i\Delta\theta = 0, \pi$

$$\Delta s_o = \Delta s_\pi = 2\pi R_m^2 \left[1 - \cos(\Delta\theta/2)\right]. \tag{2.11}$$

Owing to the refraction effects on the sound waves by the jet stream, the directional pattern of the measurements in presence of flow shows dips in sound pressure levels close to the jet axis. In addition, if $\Delta\theta$ is small,

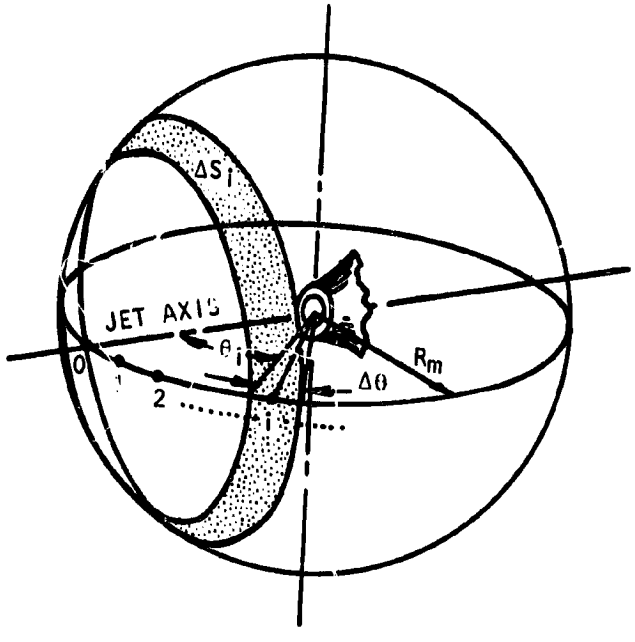

Figure 2.21 Schematic of acoustic power calculations

the contribution to acoustic power by Δs_o is insignificant. Also, accurate measurements at $\theta = 0°$ in the presence of flow were difficult to make. Therefore, except for zero flow velocity, the contribution due to $\theta = 0°$ in the far-field acoustic power calculations has been ignored. Similarly, since no measurements were available beyond $\theta = 120°$, the calculations stop at $125°$ [$=120° + (\Delta\theta/2)$]. The exclusion of energy for those angles beyond 120° is expected to have little effect at high frequencies *(which dominate in the rear arc)* but may have pronounced effect for low frequencies at which the directivity is almost omnidirectional. In such a case the calculated acoustic powers will be about 3 dB lower than the true values.

The power transfer function in dB with respect to transmitted power is given by:

$$PTF_t = 10 \text{ Log}_{10} \frac{W_f}{W_t} \tag{2.12}$$

To be consistent with the NTF where the normalizing parameter is the incident sound wave amplitude, far-field acoustic power was also normalized with respect to incident power and is given by

$$PTF_i = 10 \text{ Log}_{10} \frac{W_f}{W_i} \tag{2.13}$$

where

$$W_i = \frac{A_D}{\rho_D c_D} [p_i^2 (1+M_D)^2] \tag{2.14}$$

For data obtained under flight simulation, the measured far-field sound pressure levels were converted to those under ideal wind tunnel conditions where the shear layer between the noise source and the microphone is not present. Shear layer correction procedure developed at Lockheed and described in reference 2.2 was used.

3. TRANSMISSION RESULTS FOR MULTI-LOBE MULTI-TUBE SUPPRESSOR

Characteristics of internal noise radiation from the 12-lobe 24-tube suppressor nozzle tested statically and under flight simulation for both unheated and heated jets are presented here. Effect of *jet-Mach number* on the in-duct and far-field time histories, reflection coefficients, nozzle transmission coefficients and power transfer functions are first described in section 3.1. Results showing the effects of *heating* (section 3.2) and *flight simulation* (section 3.3) on the same transmission parameters are then described. A summary of the studied effects is given at the end of each section and the general conclusions are presented in section 3.4.

3.1 MACH NUMBER EFFECTS

Experimental results showing the effects of jet Mach number on the transmission characteristics of the daisy lobe suppressor are presented in this section. This is done by first presenting both the in-duct and the far-field time histories as a function of the jet Mach number. Frequency spectra for the reflection coefficient amplitudes and also for the Nozzle Transmission Coefficients (NTC) are then presented in subsections 3.1.2 and 3.1.3. This is followed by a comparison of the transmitted acoustic power with that measured in the far-field. A summary of the Mach number effects is presented in subsection 3.1.5.

3.1.1 In-Duct Time Histories

WHAT DOES AN IN-DUCT TIME HISTORY LOOK LIKE? In order to obtain a better insight into the acoustic behavior inside the duct with the suppressor nozzle as a termination, a short discussion on the in-duct time history when the suppressor is not present is given first. Figure 3.1(a) gives an example of the time history, with no flow, measured by the in-duct transducer located in the 10.16 cm diameter straight duct (unflanged) on to which the suppressor nozzle or the reference conical nozzle will be mounted later. The time history clearly shows the incident wave and its reflection from the open end of the duct. This reflected wave is 180° out of phase with respect to the incident wave. Had the open end been blocked off with a hard termination the reflection would have been in phase with the incident signal, a phenomenon well known in underwater acoustics and gas dynamics.

Figure 3.1(b) shows the history when the daisy lobe nozzle is attached to the supply duct. Besides the incident signal, two more pulses are seen, the first, being in phase with the incident, is the reflection from the solid parts (hard termination) on to which the lobes and the tubes of the suppressor are attached. The second reflection, 180° out of phase with the incident signal, is the reflection from the flow areas (soft termination) of the suppressor nozzle, namely the exits of the 12-lobes and the 24-tubes.

The time histories shown in the above two Figures (3.1(a) and 3.1(b)) are for a no flow condition. The reflection from the solid part is typical of that from the shoulders of convergent nozzles and takes place before the exit reflection. This is illustrated in Figure 3.1(c) where a typical time history with the daisy lobe nozzle replaced by the reference conical nozzle is shown.

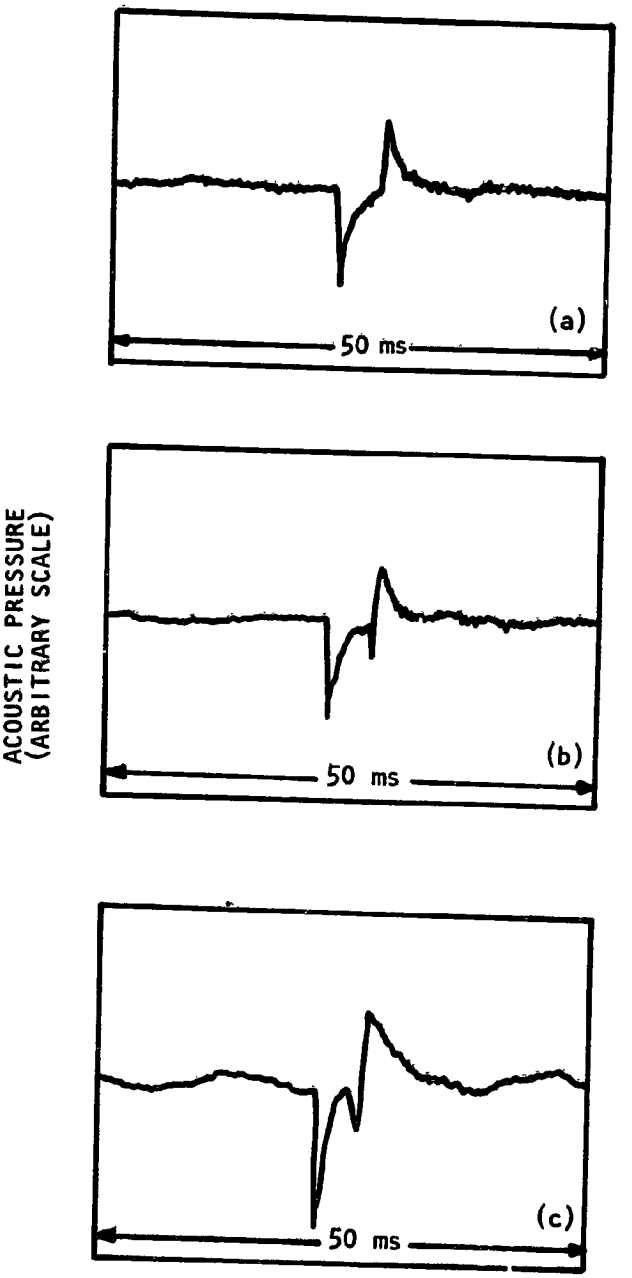

Figure 3.1 In-duct time histories at $M_J = 0$ for (a) 10.16 cm diameter straight duct, (b) daisy lobe suppressor nozzle and (c) 6.20 cm diameter conical nozzle.

VARIATION OF IN-DUCT REFLECTION WITH MACH NUMBER. Figure 3.2(a) and (b) show the effect of jet Mach number (M_J = 0.2 and M_J = 0.3) on the relative levels of the incident and the reflected components of the in-duct signal for the daisy lobe nozzle. Clearly, the reflection from the open end decreases with increasing Mach number. A dramatic change in the time histories is noticed as the jet Mach number is increased beyond 0.4. This is shown in Figure 3.3 for fully-expanded Mach numbers (M_J) of 0.4, 0.6, 0.8, and 1.2, respectively. There is little sign of reflection from the open end but that from the hard (or solid) part of the nozzle termination increases considerably until at M_J = 1.2 the incident and the reflected signals appear to be of the same amplitude.

The implication of these results is that if there was considerable internal noise generated upstream of the suppressor nozzle exit, much of it should be reflected back at higher Mach numbers.

Similar qualitative results were obtained for the 6.20 cm diameter reference conical nozzle. This is shown in Figure 3.4

The behavior depicted in Figures 3.2-3.4 can be better seen when plotted in the form of reflection factors as shown in Figure 3.5. Data for 6.20 cm reference round nozzle are also shown. If, in the peak sound pressure amplitudes in the time histories, we use symbols A for the incident waves, B_1 for the reflection from the hard part of the nozzle exit and B_2 for the reflection from the soft part (or flow area) then we can introduce *reflection* factors B_1/A and B_2/A to provide a measure of the reflection from the hard and soft parts of the nozzle termination, respectively. A comparison of B_1/A values for the suppressor nozzle and the reference conical nozzle indicates that the suppressor nozzle may be a less efficient radiator of internal noise compared to the round nozzle. Both of these reflection factors are plotted in Figure 3.5 as a function of fully expanded jet Mach number for both nozzles. Clearly they follow the same trend, that is, beyond $M_j \approx 0.4$ the amplitude of the reflection from the open end is negligible and that from the solid parts of the nozzle termination keeps increasing with Jet Mach number (i.e. with duct Mach number).

In order to understand how the reflection factors behave in the frequency domain as a function of jet Mach number, the reflection coefficients as defined in section 2.3.4 were obtained. Both components of reflection, i.e. the soft and the hard termination reflections were retained. The results are described in the next section.

3.1.2 Reflection Coefficients

Reflection coefficients for the daisy lobe (σ_{DL}) nozzle for four jet Mach numbers (M_J = 0, 0.4, 0.8 and 1.2) are presented in Figure 3.6 as a function of 1/3-octave frequencies. For comparison, the data for the reference conical nozzle(σ_c)is also superimposed in this figure.These results are further cross plotted as shown in Figures 3.7 and 3.8, where reflection coefficients for various frequencies are plotted as a function of the duct Mach number at the measurement location.

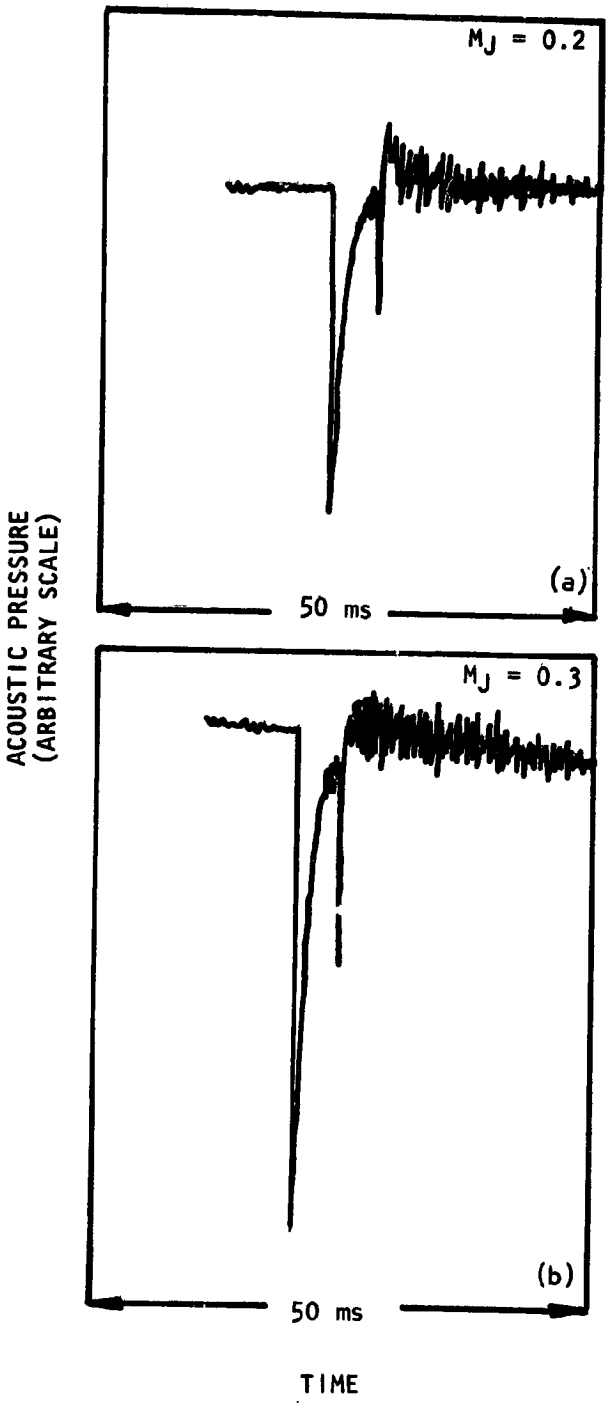

Figure 3.2 In-duct time histories for the daisy lobe nozzle at various jet Mach numbers.
M_J: (a) 0.2 and (b) 0.3

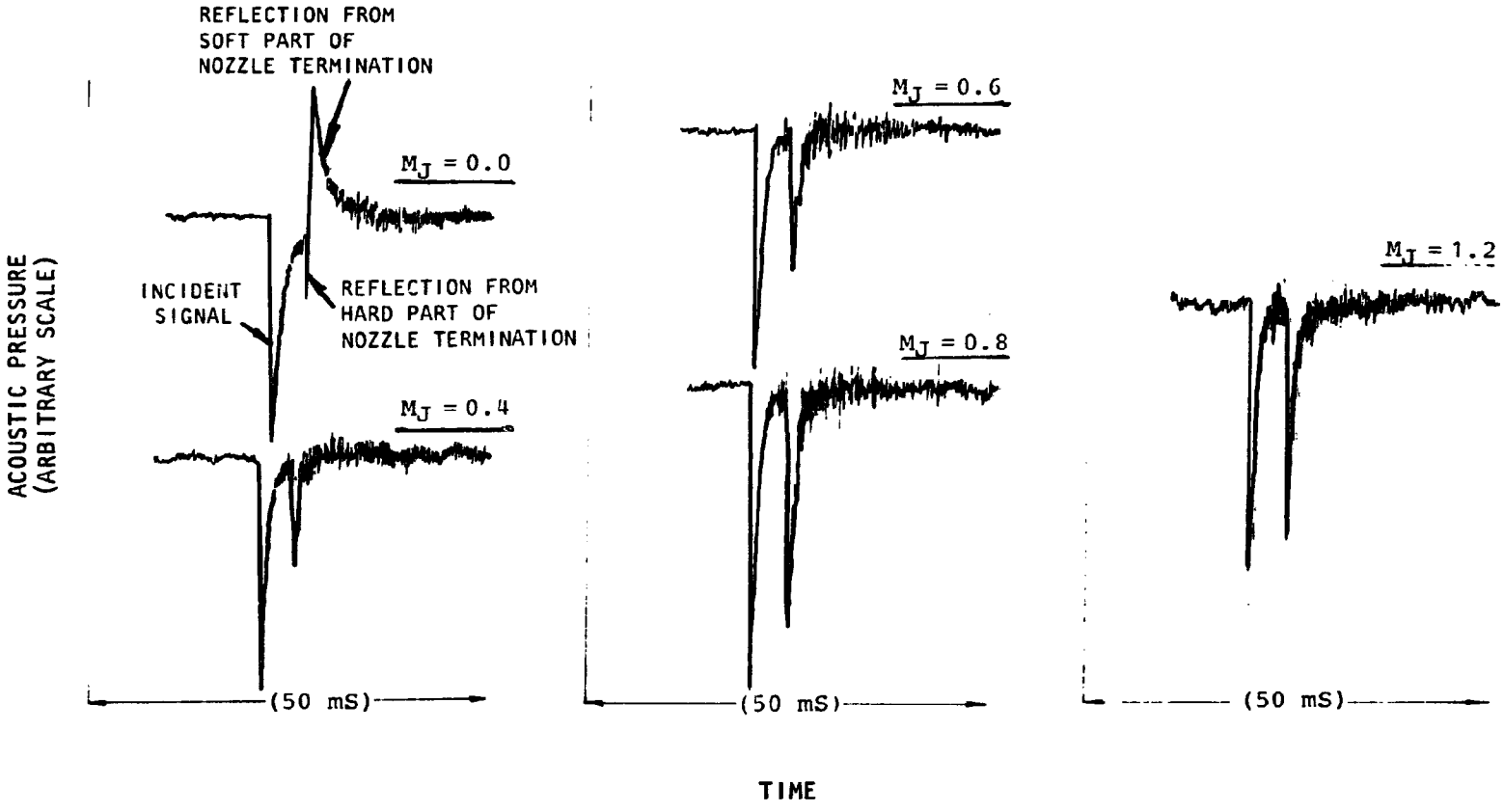

Figure 3.3 In-duct time histories for the daisy lobe nozzle at various jet Mach numbers.

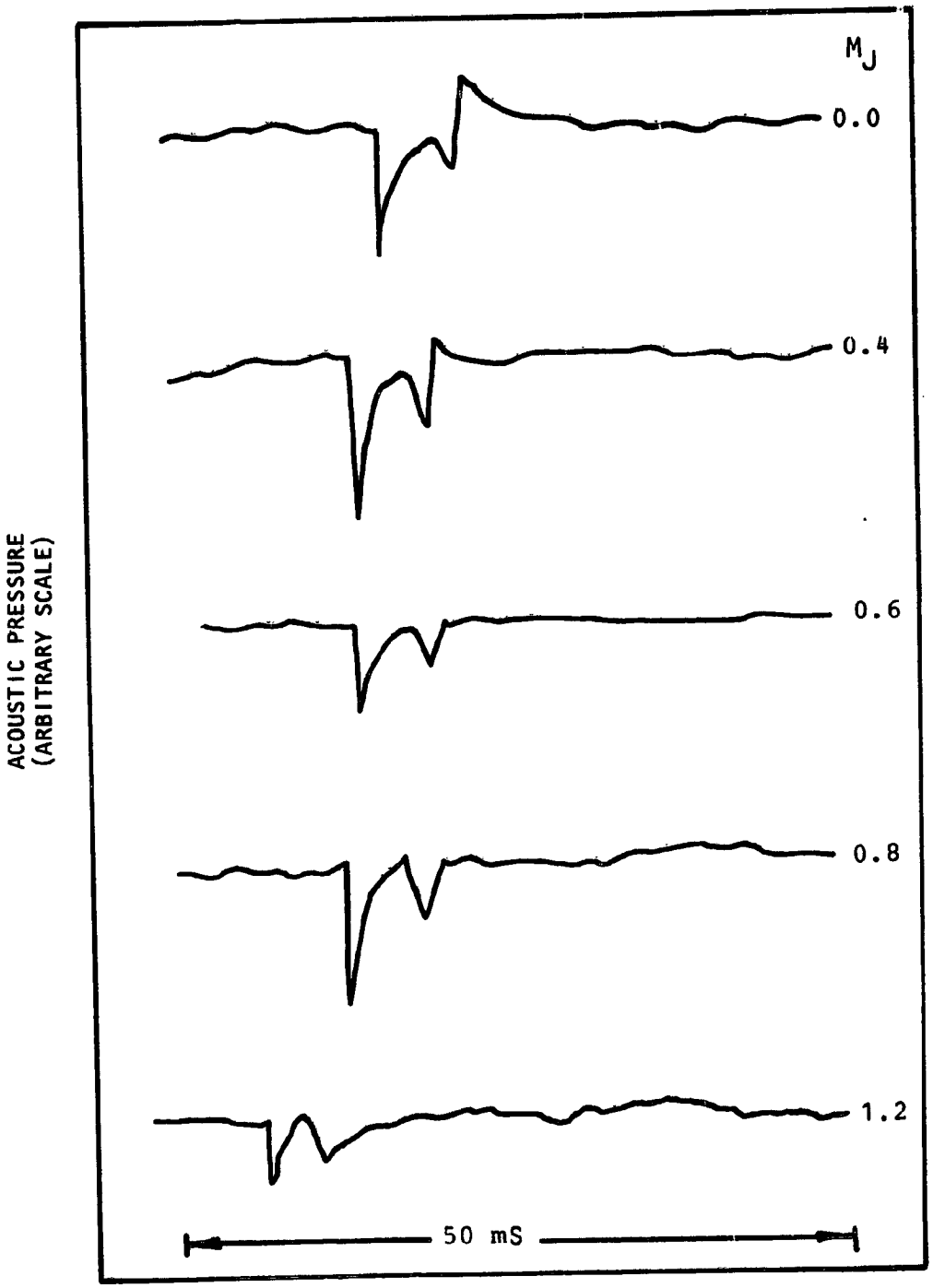

Figure 3.4 In-duct time histories for the 6.20 cm diameter reference conical nozzle at various jet Mach numbers (unheated).

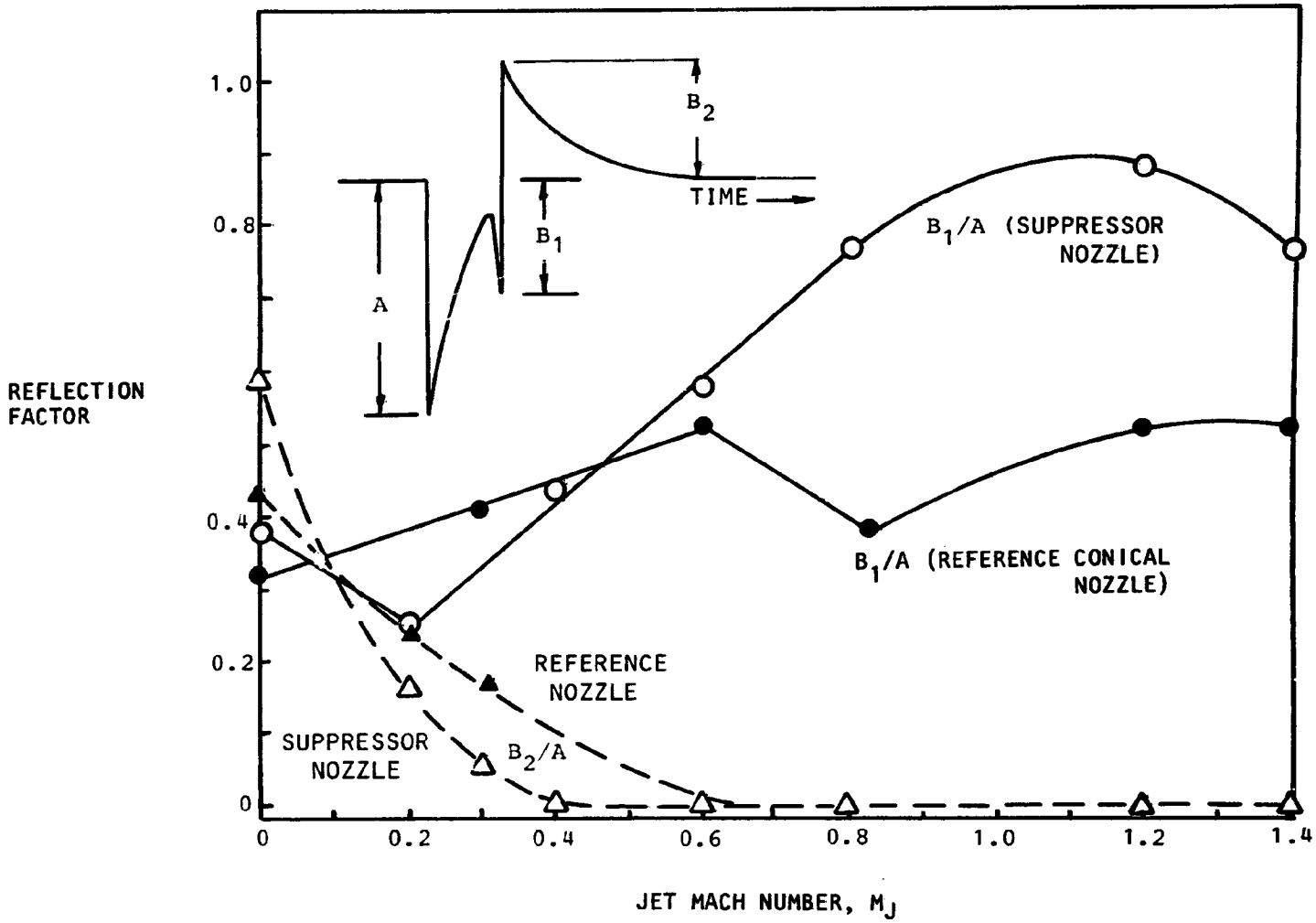

Figure 3.5 Reflection factors for the daisy lobe nozzle and the reference conical nozzle as a function of jet Mach number.

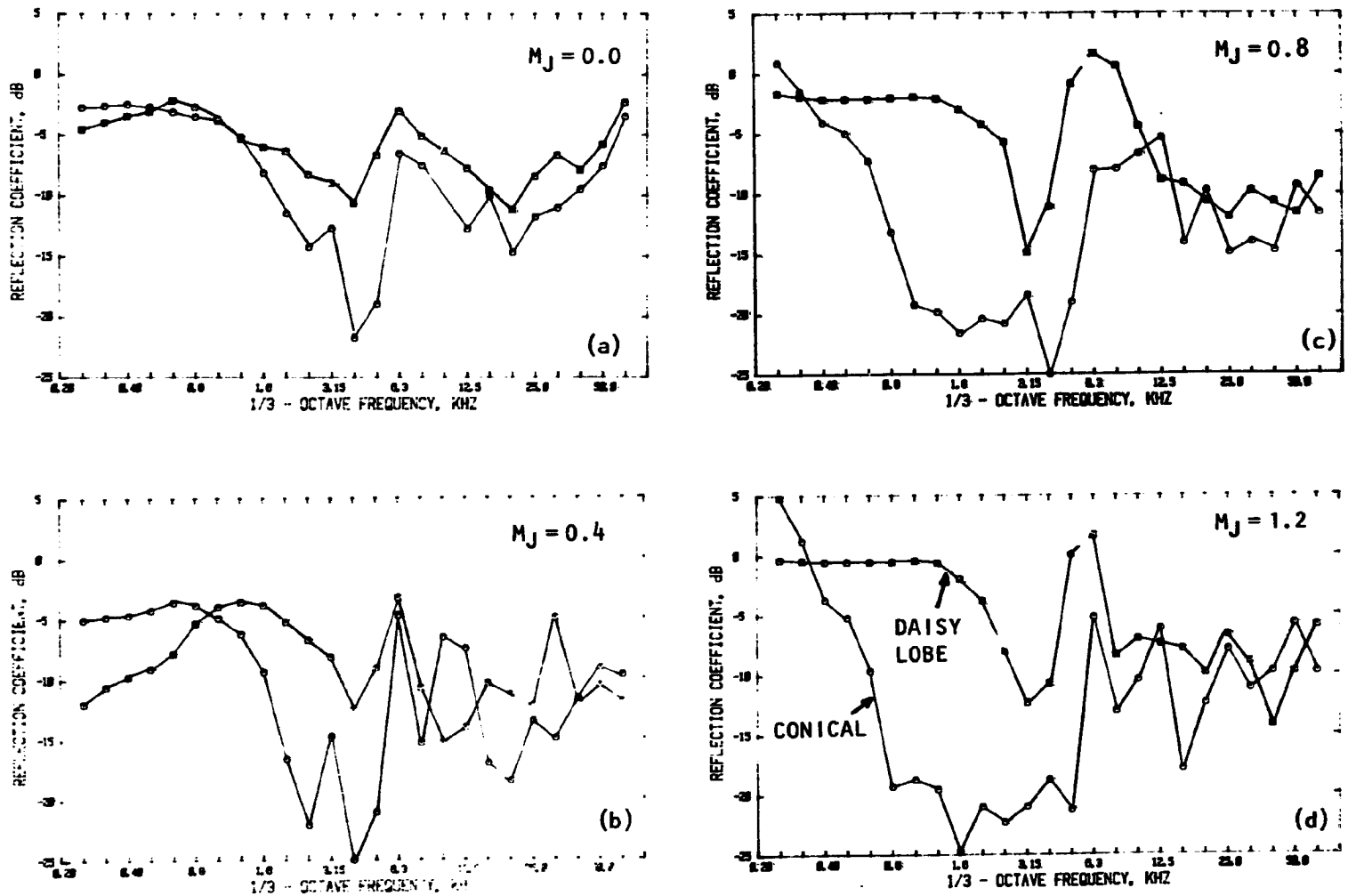

Figure 3.6 Effect of nozzle geometry on reflection coefficient spectra for various jet exit Mach numbers (unheated). (a) $M_J = 0$, (b) $M_J = 0.4$ (c) $M_J = 0.8$ and (d) $M_J = 1.2$
⊡ daisy lobe nozzle; ⊙ reference conical nozzle

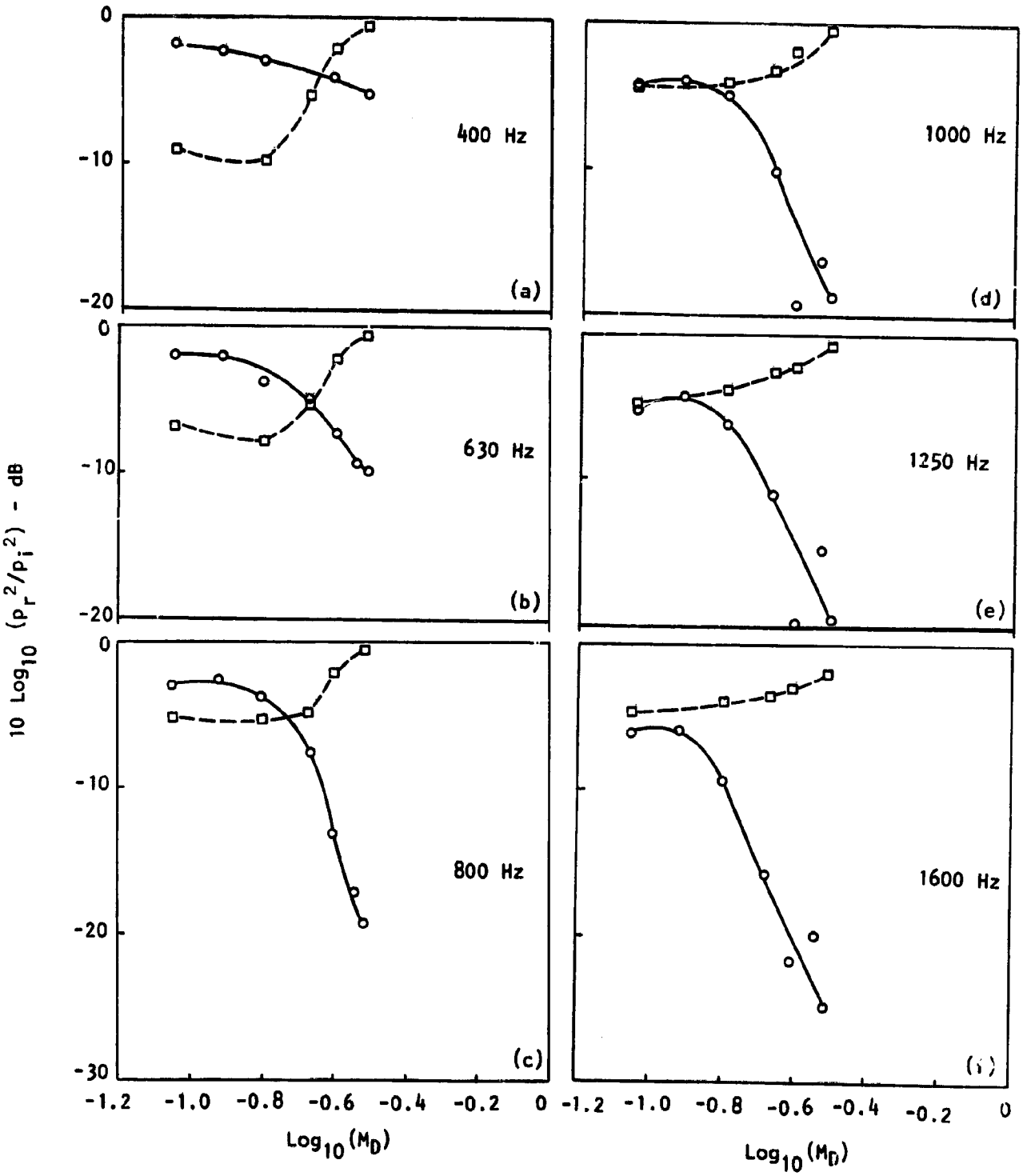

Figure 3.7 Effect of duct Mach number on the reflection coefficients of the daisy lobe nozzle and the reference conical nozzle at various 1/3-octave frequencies.

LEGEND: -⊟-DAISY LOBE NOZZLE. —⊖— REFERENCE CONICAL NOZZLE.

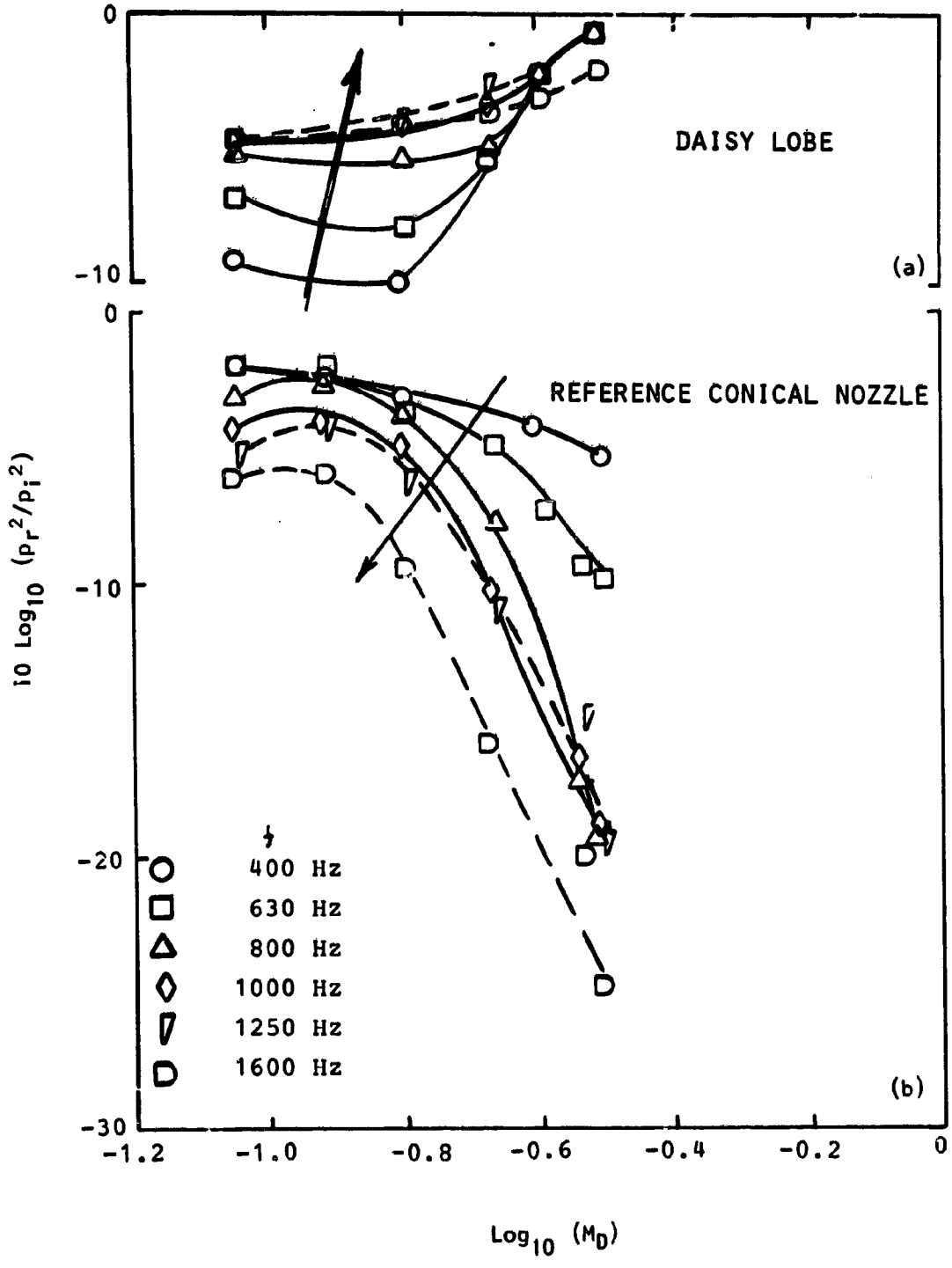

Figure 3.8 Effect of duct Mach number on the reflection coefficients of (a) daisy lobe nozzle and (b) conical nozzle at various frequencies.

Both σ_{DL} and σ_c at f = 400, 630, 800, 1000, 1250 and 1600 Hz are plotted against $Log_{10}(M_D)$ for both the nozzles. Results follow a very consistent trend with change in frequency and the duct Mach number M_D. After careful examination of Figures 3.6, 3.7 and 3.8 the following observations, particularly for the plane wave regime, can be made about the reflection coefficients:

(1) Variation with duct Mach number (M_D). As the jet Mach number (and so the duct Mach number) is increased, the reflection coefficients for the conical nozzle decrease while those for the daisy lobe suppressor nozzle increase at all frequencies. At supersonic jet Mach numbers, σ_{DL} appears to approach 0 dB (linear value 1).

(2) Variation with frequency. The trends in variation of σ with frequency are exactly opposite for the two nozzles. This is shown in Figure 3.8. The daisy lobe reflection coefficients increase with frequency while those for the conical nozzle decrease with frequency at almost all Mach numbers.

(3) Reflection Coefficient (σ_c) higher than 0 dB at low frequency and high Mach numbers for the conical nozzle. At high jet Mach numbers (e.g. see Figures 3. 6(c) and (d)) and low frequencies the reflection coefficients appear to be higher than unity for the conical nozzle.

The behavior of σ_{DL} is difficult to explain without considerable theoretical and further experimental work. This is certainly related to the complicated geometry and the flow conditions encountered by the incident wave in travelling from upstream to the multi-jet exits and back. For example, the daisy lobe has a sharp shoulder with convergence angle of 50° (see Fig. 2.6). The tubes and the daisy lobes are attached to this shoulder, the inlets of which do not all lie in the same plane. The tubes are straight while the lobes are convergent and have different widths at different radial locations. The exits of all tubes lie in the same plane (which is also normal to the nozzle axis) while those for the lobes lie in a conic (Fig. 2.6). This also means that for a given axial location the flow Mach numbers will be different at various radial positions.

Undoubtedly, the reflection will depend upon all these features. The current understanding on the effect of the simple conical nozzle itself on duct acoustics is far from well developed let alone a complicated nozzle like the daisy lobe nozzle. It is therefore not attempted to explain the daisy lobe reflection coefficients in detail. The results described here will, however, be borne in mind to correlate and understand the far-field data, described later.

3.1.3 Far-Field Time Histories

Typical far-field time histories for the daisy lobe nozzle and the reference conical nozzle are shown in Figures 3.9 and 3.10 respectively. Data for zero, subsonic (M_J = 0.6) and supersonic (M_J = 1.2) jet Mach numbers are shown at θ = 30°, 60°, 90°and 120°. The time histories shown here have fixed time scale but have arbitrary amplitude scale. The main purpose of

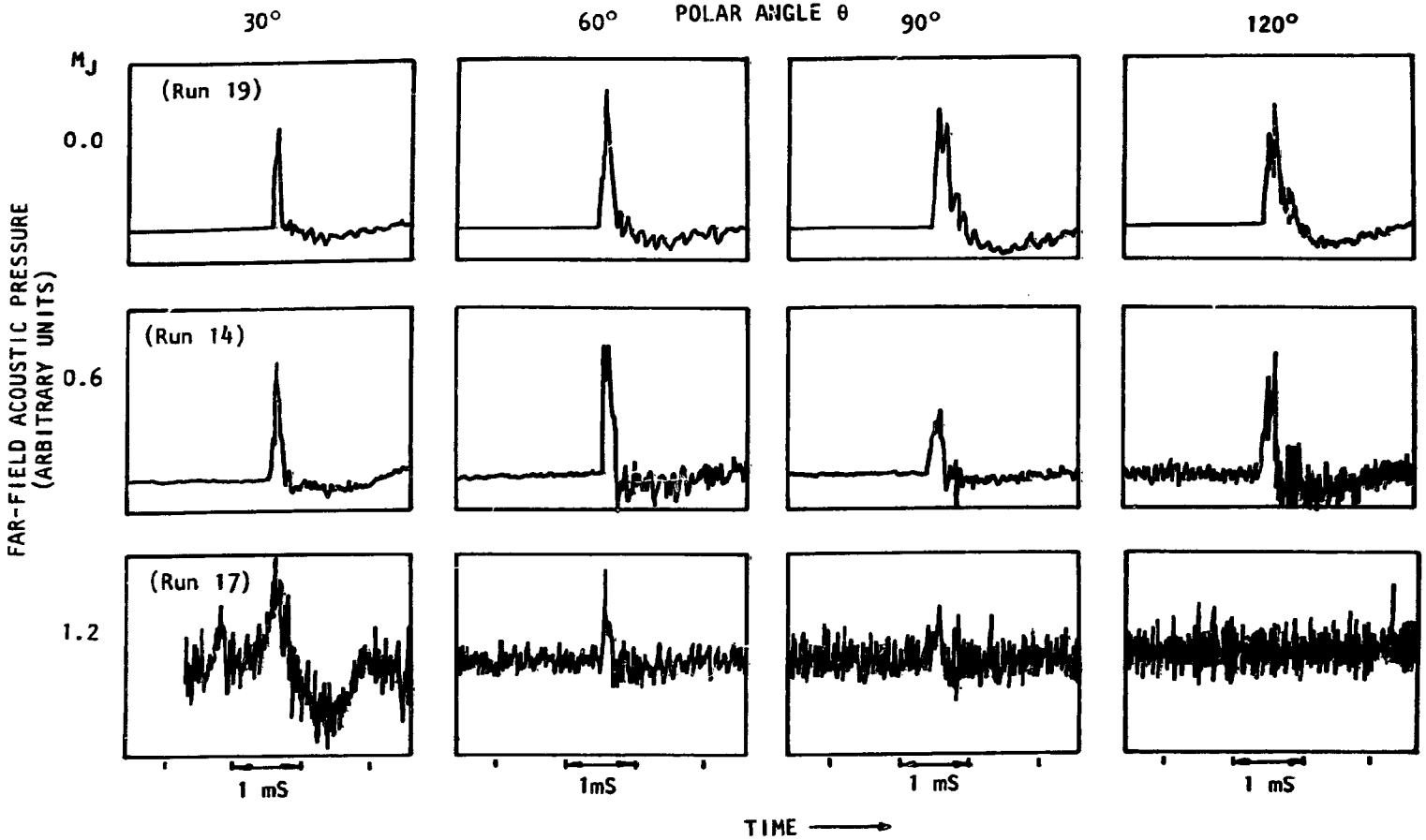

Figure 3.9 Far-field time histories for the daisy lobe nozzle as a function of jet Mach number and measurement angle (jet unheated)

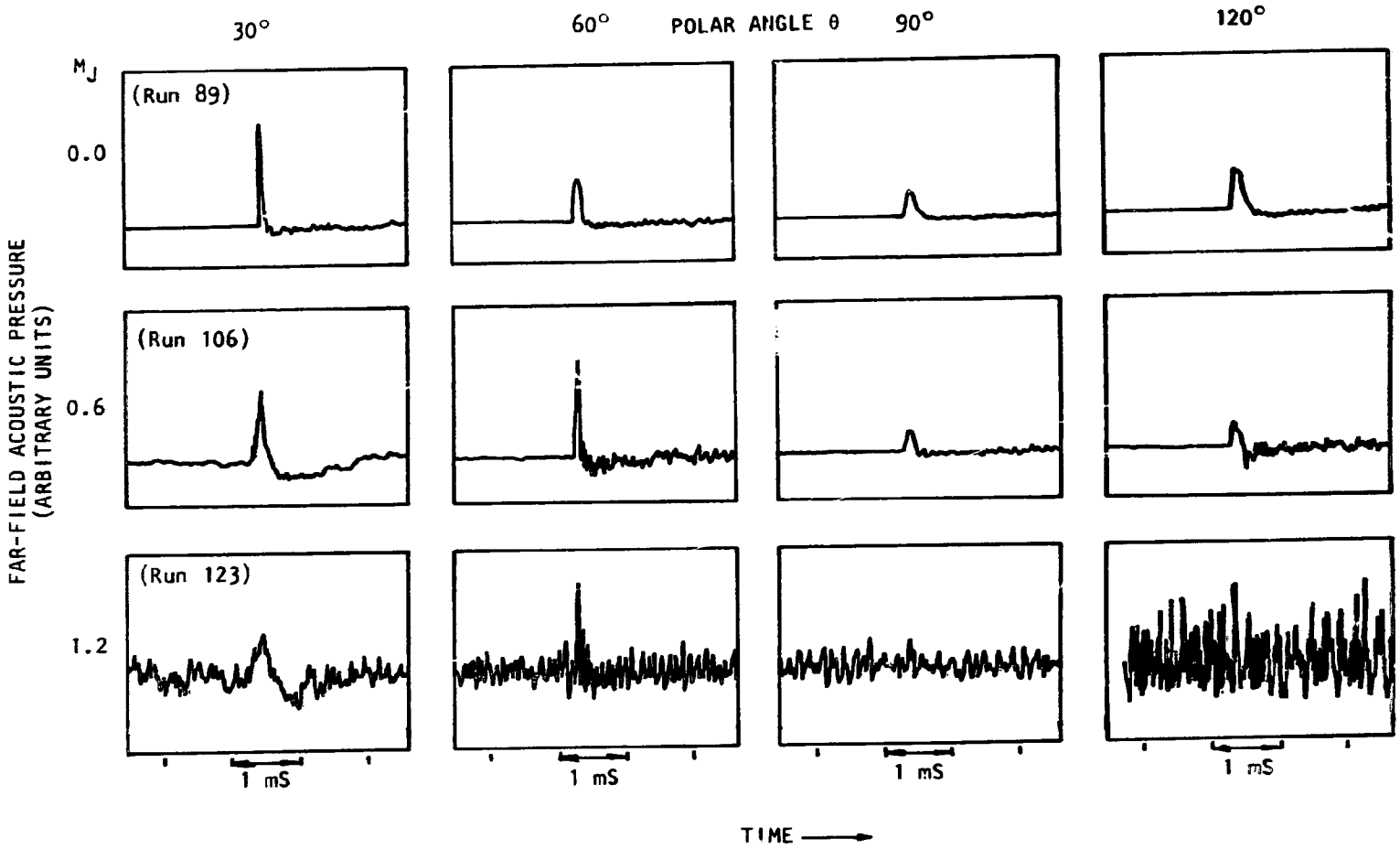

Figure 3.10 Far-field time histories for the reference conical nozzle as a function of jet Mach number and measurement angle.

these figures, however, is to examine the narrowing or widening of the pulses as a function of angle and jet Mach number.

In fact, there are only minor differences in the far-field signals for the two nozzles. For zero flow, both nozzles display narrower pulses at small angles compared to the large angles indicating more high frequency radiation at small angles. As the jet Mach number is increased, effect of refraction becomes obvious in that the pulse at small angles (e.g., $\theta = 30°$) becomes wider indicating depletion of high frequency sound which apparently has been refracted to larger angles as seen by the narrowing of the pulse at larger angles (e.g. 60°). This effect becomes stronger as the jet Mach number is increased from $M_J = 0.6$ to 1.2.

Other notable differences are the number of peaks in the time histories for the two nozzles. The daisy lobe time histories at large angles ($\theta = 90°$, 120°) show dual peaks in the far-field time histories while those for the conical nozzle do not. These peaks are about 0.1mS apart. This could be due to the difference in path lengths travelled by the radiation through the tubes, and that through the lobes whose exits are not coplaner with those of the tubes (the lobes have a slope of 15°). The path difference will become larger at angles close to 90°.

The pulses for larger angles at $M_J = 1.2$ show considerable contamination by the jet mixing and shock associated noise. Such data points were not analyzed further.

NTC data obtained from these time histories will now be presented

3.1.4 One Third Octave NTC

TYPICAL NTC SPECTRA. Typical 1/3 octave NTC spectra for the daisy lobe nozzle at $\theta = 30°$, 60°, 90° and 120° for $M_J = 0$, 0.4, 0.6 and 1.2 are presented in Figure 3.11(a), (b), (c) and (d) respectively. These figures show that at zero flow condition the radiation is predominantly towards the jet axis for both the low as well as the high frequencies. Effect of flow is to widen the difference between the radiation at small angles and that at larger angles with the jet axis.

As noticed earlier in the far-field time histories, the effect of refraction at high frequencies is noticeable here also as the jet Mach number is increased. This is reflected as a high frequency decrease at $\theta = 30°$ and a corresponding increase at $\theta = 60°$. These refraction effects are best described by examining the radiation directivities at various frequencies and jet Mach numbers as shown in Figure 3.12. Directivities for $M_J = 0$, 0.4 and 0.8 are plotted for four frequencies, namely 4KHz, 8KHz, 16KHz and 31.5KHz in this figure. These results show quite clearly that as the jet Mach number is increased the refraction effect becomes more important. This is indicated by the fact that the NTC values at small angles to the jet axis decrease with increasing Mach number and more so at high frequencies. A shift in the peak in directivity with increasing Mach number is also quite obvious. For example the peak radiation at f = 8KHz

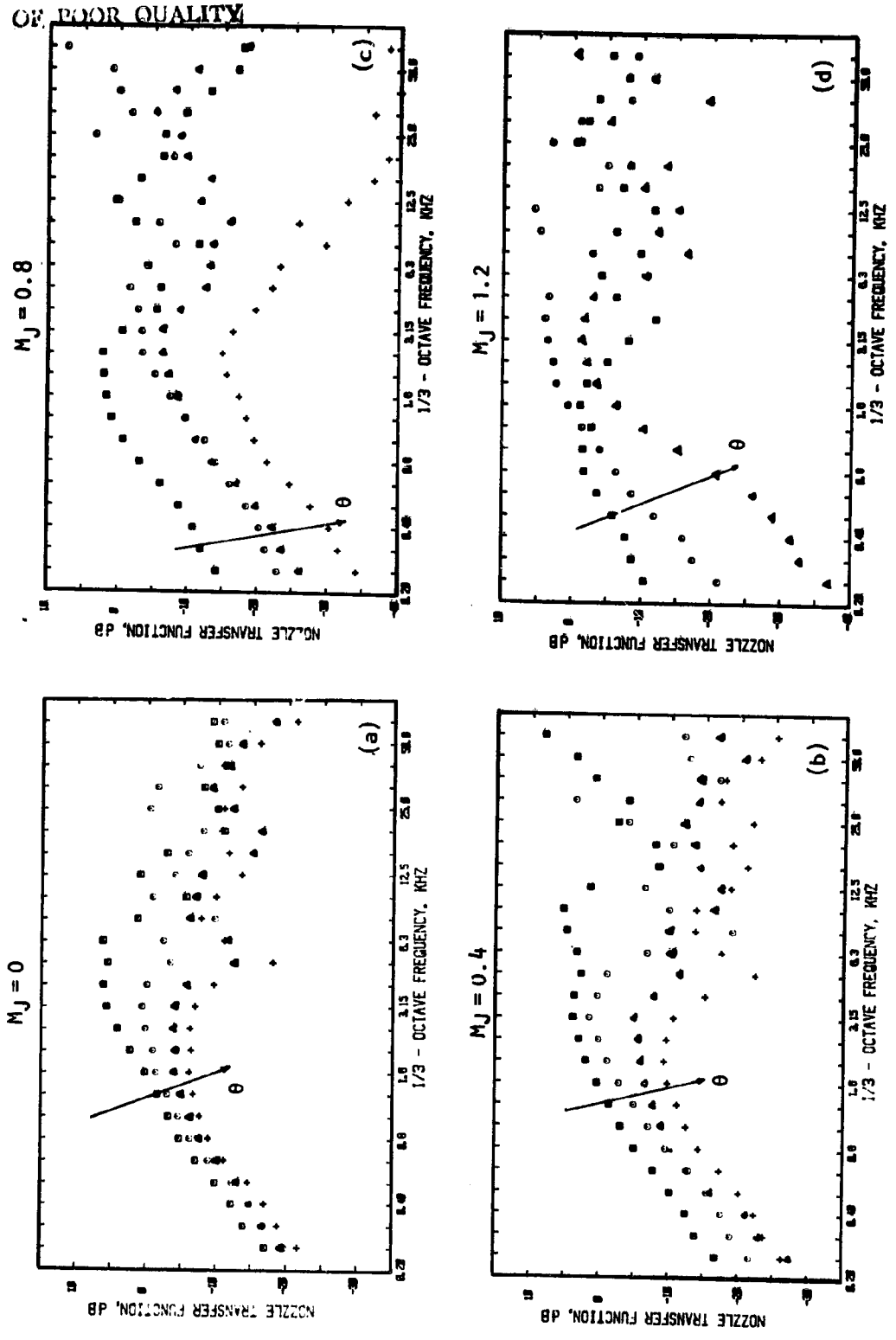

Figure 3.11 Variation of NTC spectra with angle and jet Mach number for daisy lobe nozzle.
M_J: (a) 0.0, (b) 0.4, (c) 0.8 and (d) 1.2
θ: ⊡ 30°, ⊙ 60°, △ 90° and +, 120°

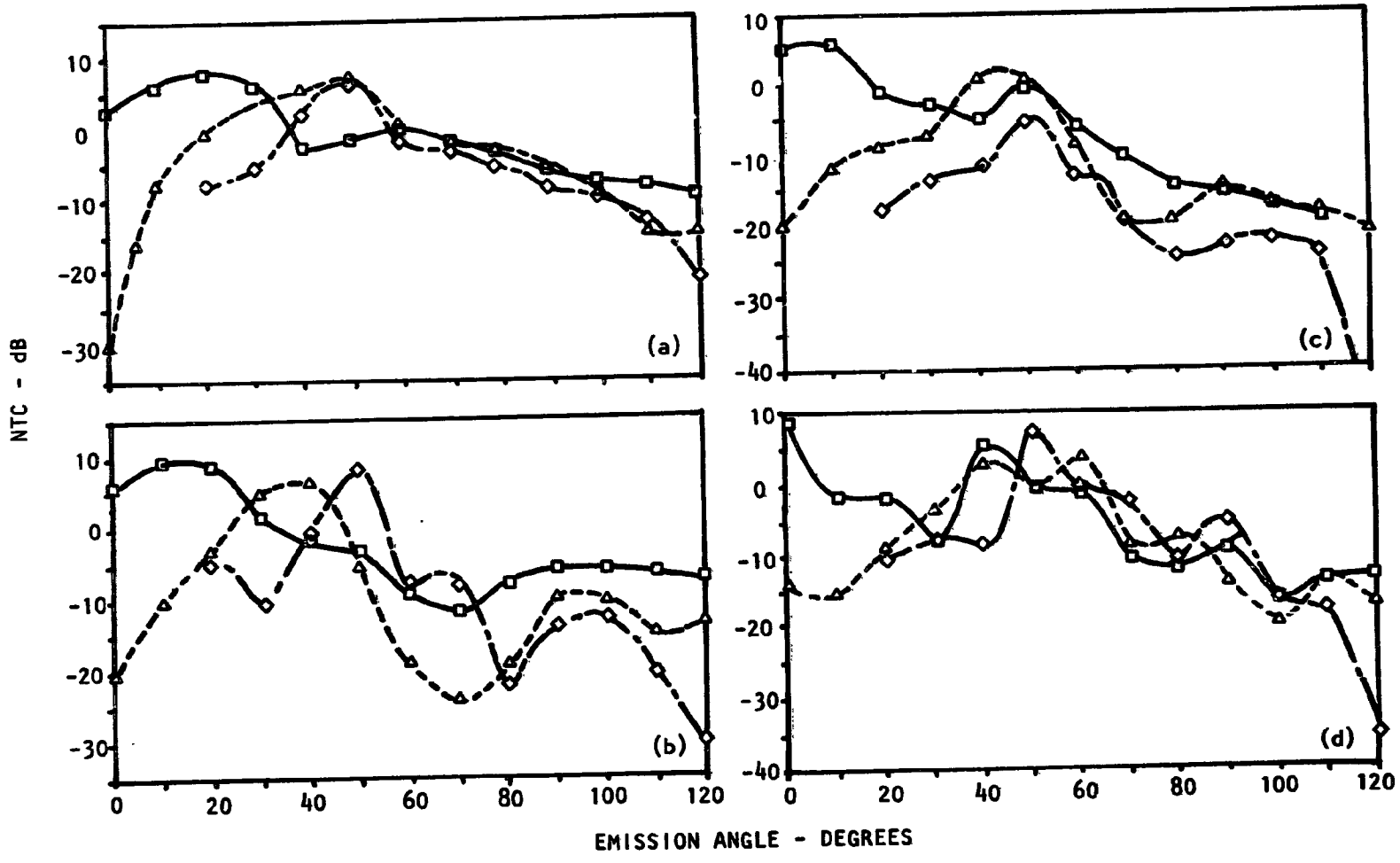

Figure 3.12 Effect of Jet Mach number on the 1/3 octave NTC directivities
f (KHz): (a) 4 KHz, (b) 8 KHz, (c) 16 KHz and (d) 31.5 KHz
Legend for M_j: □ , 0.0; △ , 0.4 and ◇ 0.8

is at $\theta = 10°$ for $M_J = 0$, at $\theta = 40°$ for $M_J = 0.4$ and at $\theta = 50°$ for $M_J = 0.8$ (see Figure 3.12(b)).

How do the radiation characteristics of the daisy lobe nozzle differ from those of the reference conical nozzle? Can the fact that the reflection coefficients for the two nozzles were different be accounted for in the far-field measurements? Results to address some of these questions will now be presented.

COMPARISON WITH THE REFERENCE CONICAL NOZZLE. A comparison of the 1/3-octave NTC spectra for the two nozzles at $\theta = 30°$, 60°, 90° and 110° is made for $M_J = 0$, 0.4 and 1.2 in Figures 3.13, 3.14 and 3.15. It is interesting that for $M_J = 0$ and 0.4 the NTC values over almost the whole frequency range have the same shape. Other data at subsonic jet Mach numbers (not shown here) had the same trend also. The same was true of the directivities as shown in Figure 3.16 for $M_J = 0$ and in Figure 3.17 for $M_J = 0.4$ where the NTC directivities at 1, 4, 8 and 16KHz are compared for the two nozzles. With a few exceptions (e.g. Figures 3.16(d) and 3.17(c)) even the NTC directivities for the two nozzles have the same shapes and nearly the same levels at zero flow and subsonic jet Mach numbers. This behavior is surprising in that the geometry of the two nozzles is so different but is encouraging in that it indicates that the equivalent diameter could be used in normalizing the frequency scale for a complicated nozzle (*both nozzles have the same equivalent diameter of 6.20 cm*).

This "area equivalence" has also been verified by Imelmann [3.1] who tested different nozzle shapes as well as perforated plates and apertures and more recently by Salikuddin and Plumblee [3.2]. Bechert [3.3] also derived an equation to show that only the nozzle exit area determines the shape of the radiation spectra.

The far-field data at subsonic jet Mach numbers, in general, does not tie-in with the in-duct reflection coefficient data (see Figures 3.5 - 3.8). Based upon the reflection coefficient data it was expected that little radiation would be observed in the far-field for the daisy lobe nozzle. It was, however, not found to be so for subsonic Mach numbers as shown by a remarkable collapse of the NTC data of the two nozzles in Figures 3.13 and 3.14. At supercritical conditions (Figure 3.15), however, there was some correlation between the far-field data and the reflection coefficient data. This effect is demonstrated in the 1/3-octave NTC directivities for the two nozzles also (Figures 3.16 - 3.18).

Because of inadequate signal to noise ratio at many angles for the conical nozzle, only limited data at $M_J = 1.2$ is plotted (Figure 3.18). Nevertheless, the results show that, for this Mach number, the daisy lobe nozzle radiates less efficiently but only at small angles to the jet axis.

Of course, a more accurate way to determine which of the two nozzles radiates more efficiently is to compare the far-field acoustic powers radiated by each nozzle for the same incident power. Such a comparison is discussed in the next subsection.

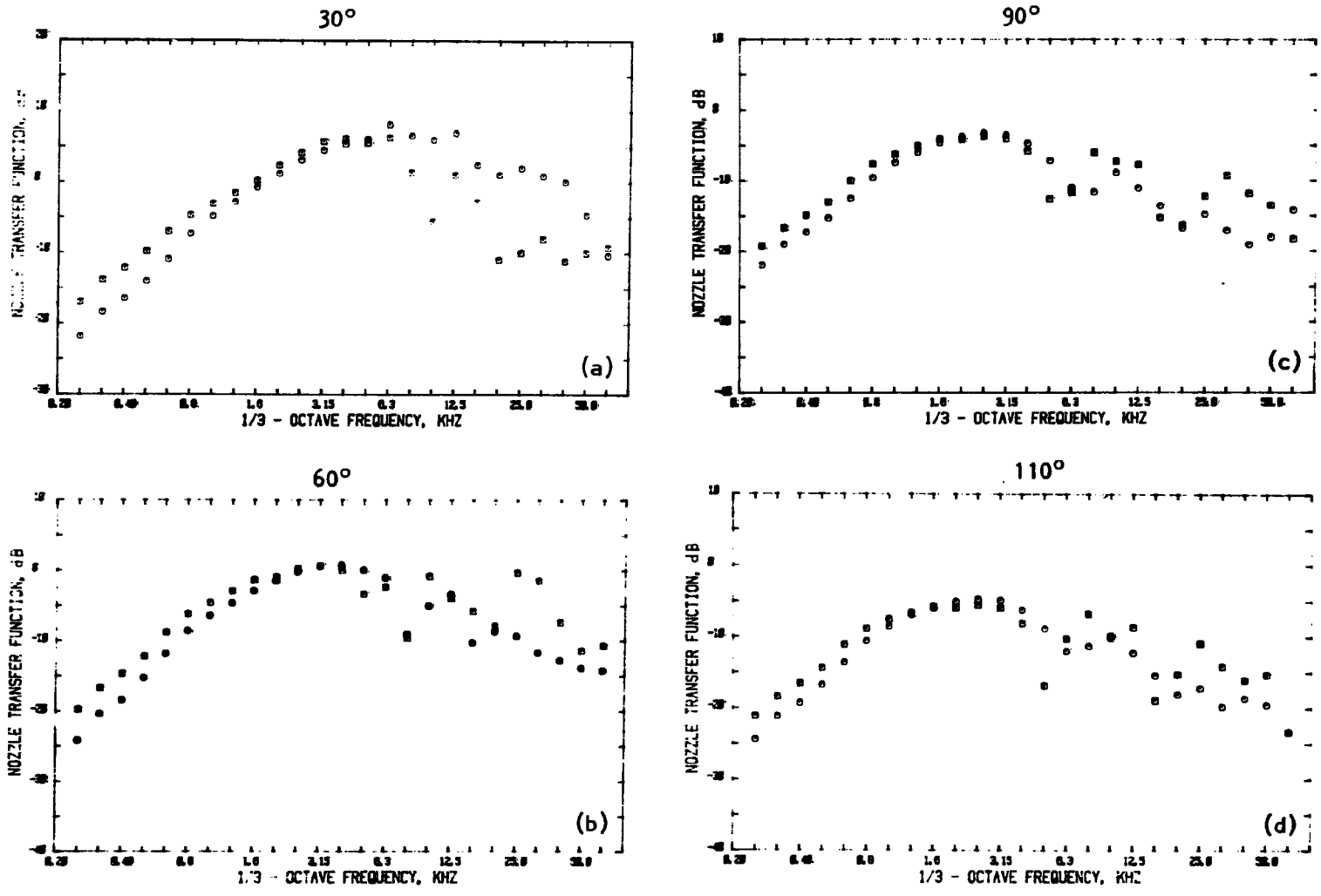

Figure 3.13 Effect of nozzle geometry on NTC spectra
at $M_J = 0$
θ_T: (a) 30°, (b) 60°, (c) 90° and (d) 110°
⊡ daisy lobe nozzle; ⊙ , conical nozzle

ORIGINAL PAGE IS
OF POOR QUALITY

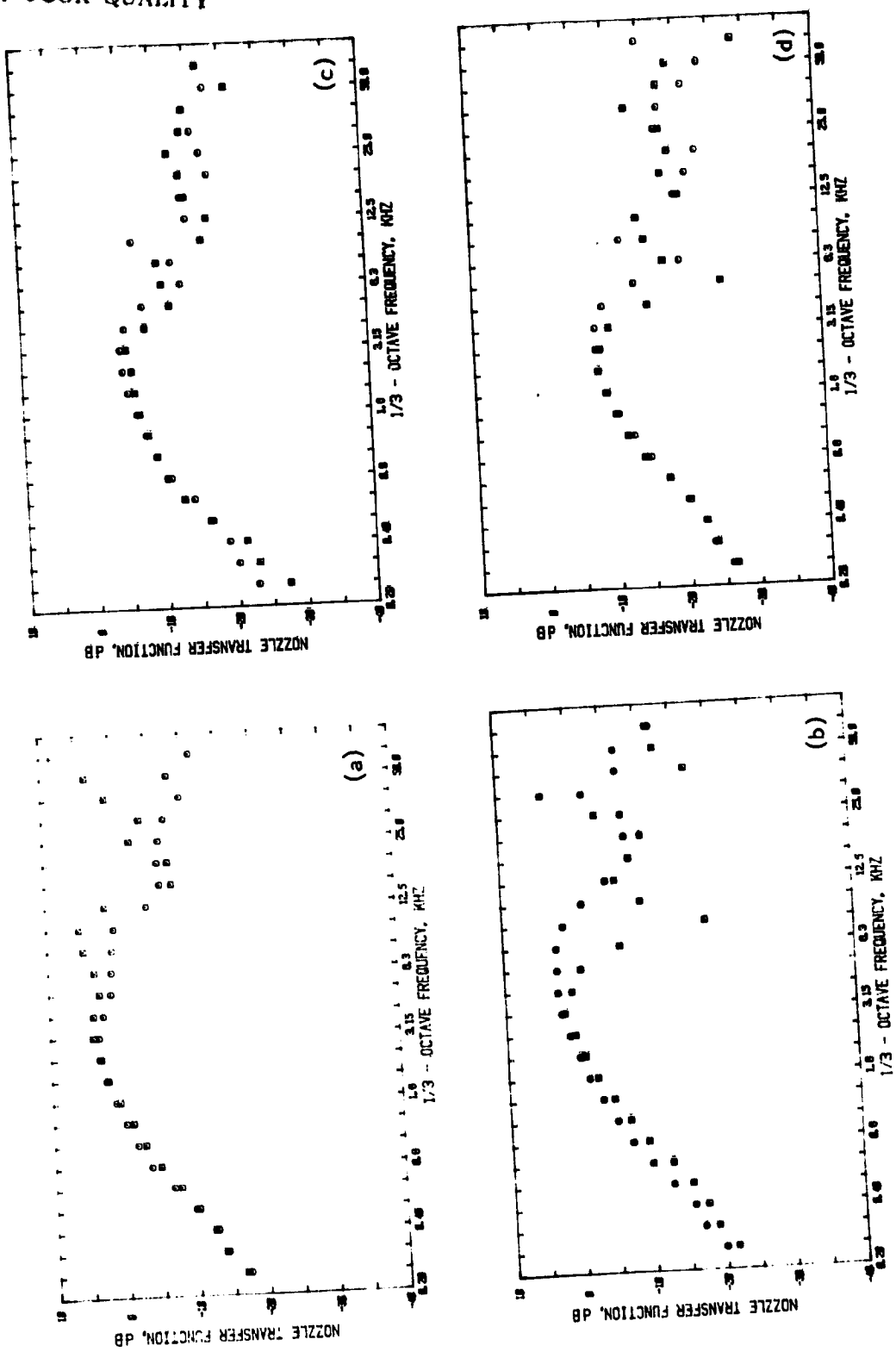

Figure 3.14 Effect of nozzle geometry on NTC spectra at $M_j = 0.4$
θ_T: (a) 30°, (b) 60°, (c) 90° and (d) 110°
Legend: ⊡ daisy lobe nozzle, ⊙ conical nozzle

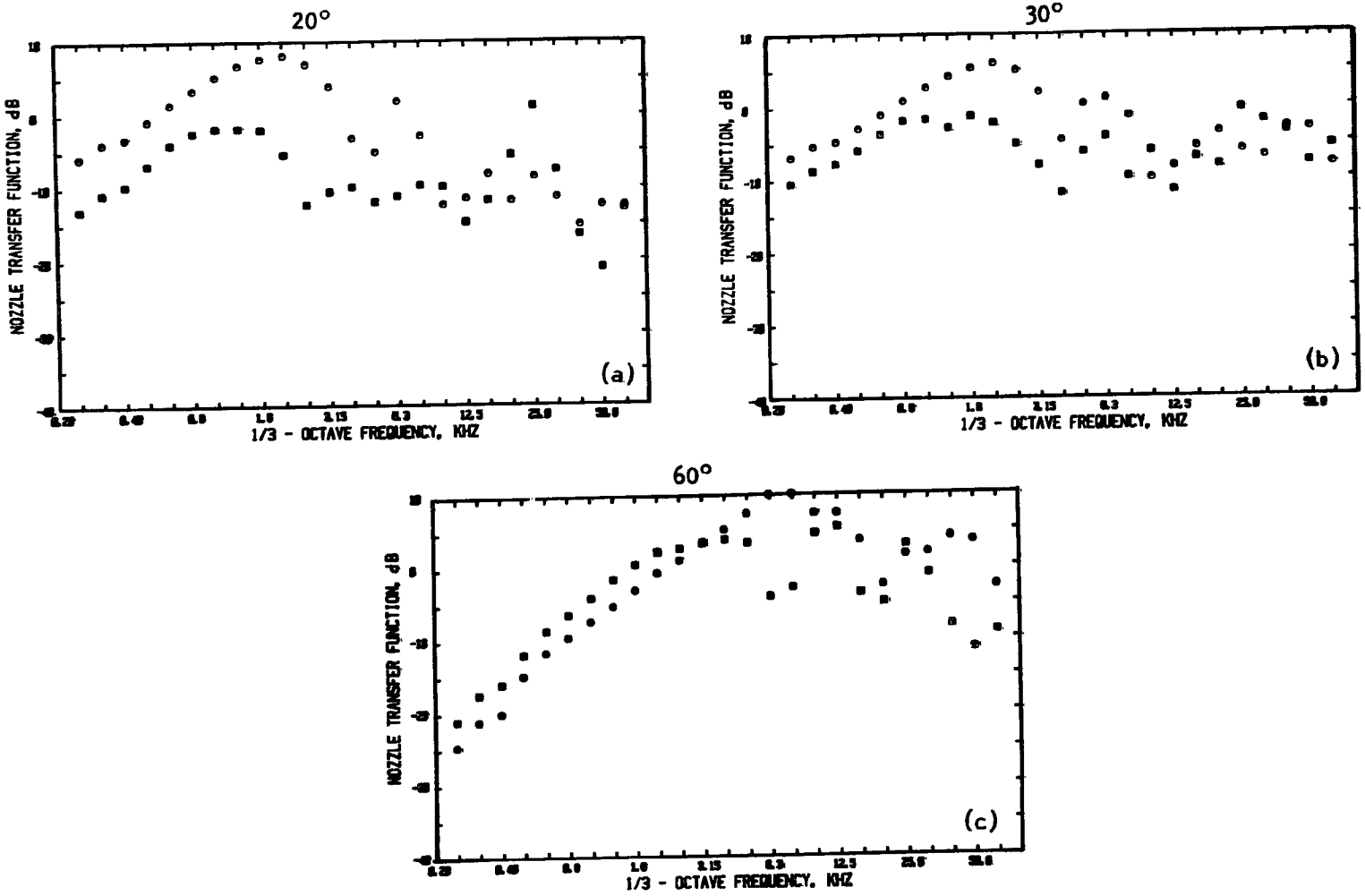

Figure 3.15 Effect of nozzle geometry on NTC spectra at $M_J = 1.2$ and $M_T = 0.0$
θ_T: (a) 20°, (b) 30°, (c) 60°
⊡ Daisy lobe nozzle, ⊙ conical nozzle

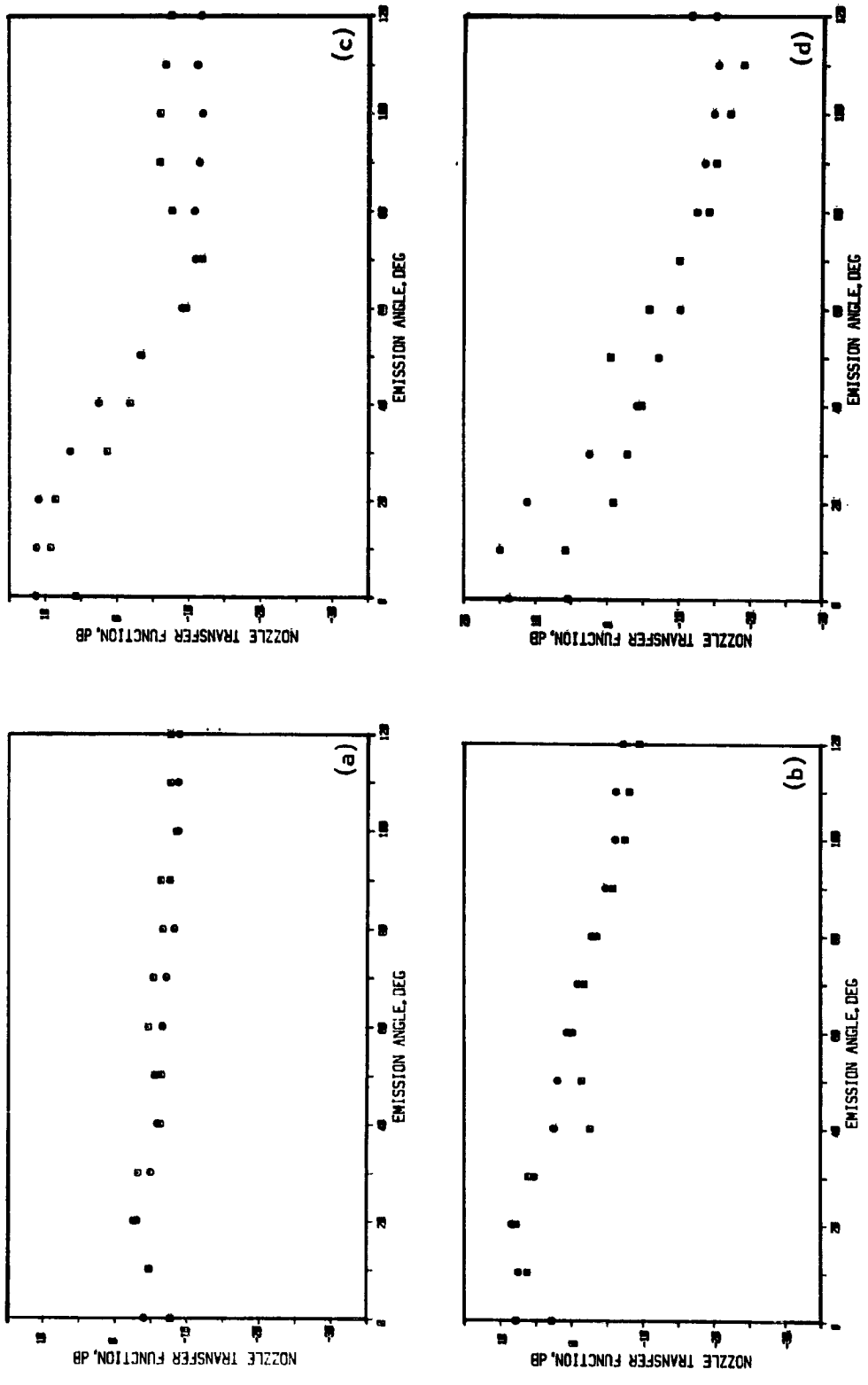

Figure 3.16 Effect of nozzle geometry on 1/3 octave NTC directivities at $M_j = 0.0$
f (KHz): (a) 1.0, (b) 4.0, (c) 8.0 and (d) 16.0
⊡ daisy lobe nozzle; ⊙ conical nozzle

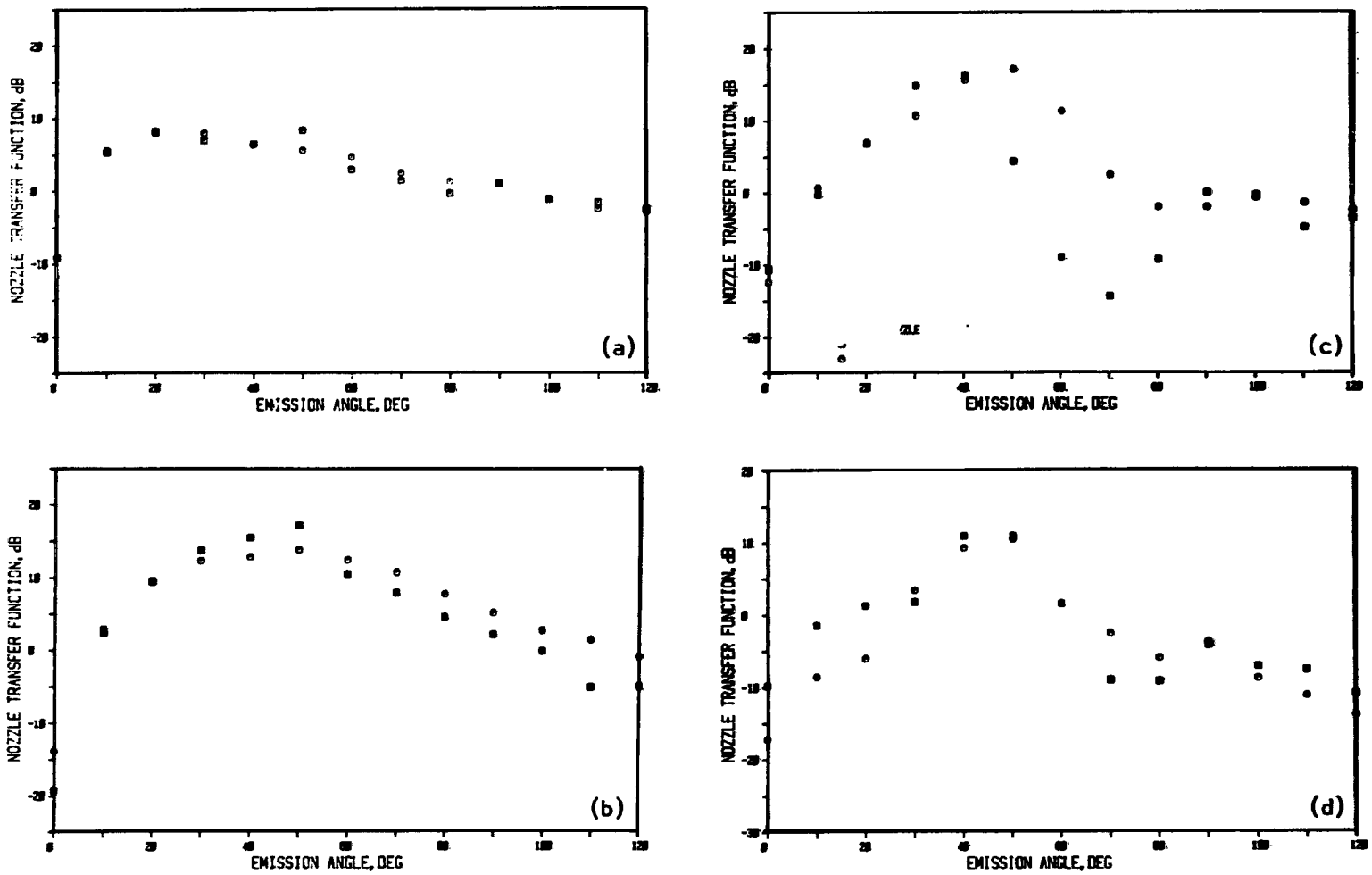

Figure 3.17 Effect of nozzle geometry on 1/3 octave NTC directivities at $M_J = 0.4$ (unheated)
f (KHz): (a) 1.0, (b) 4.0, (c) 8.0 and (d) 16.0
⊡ daisy lobe nozzle; ⊙ conical nozzle

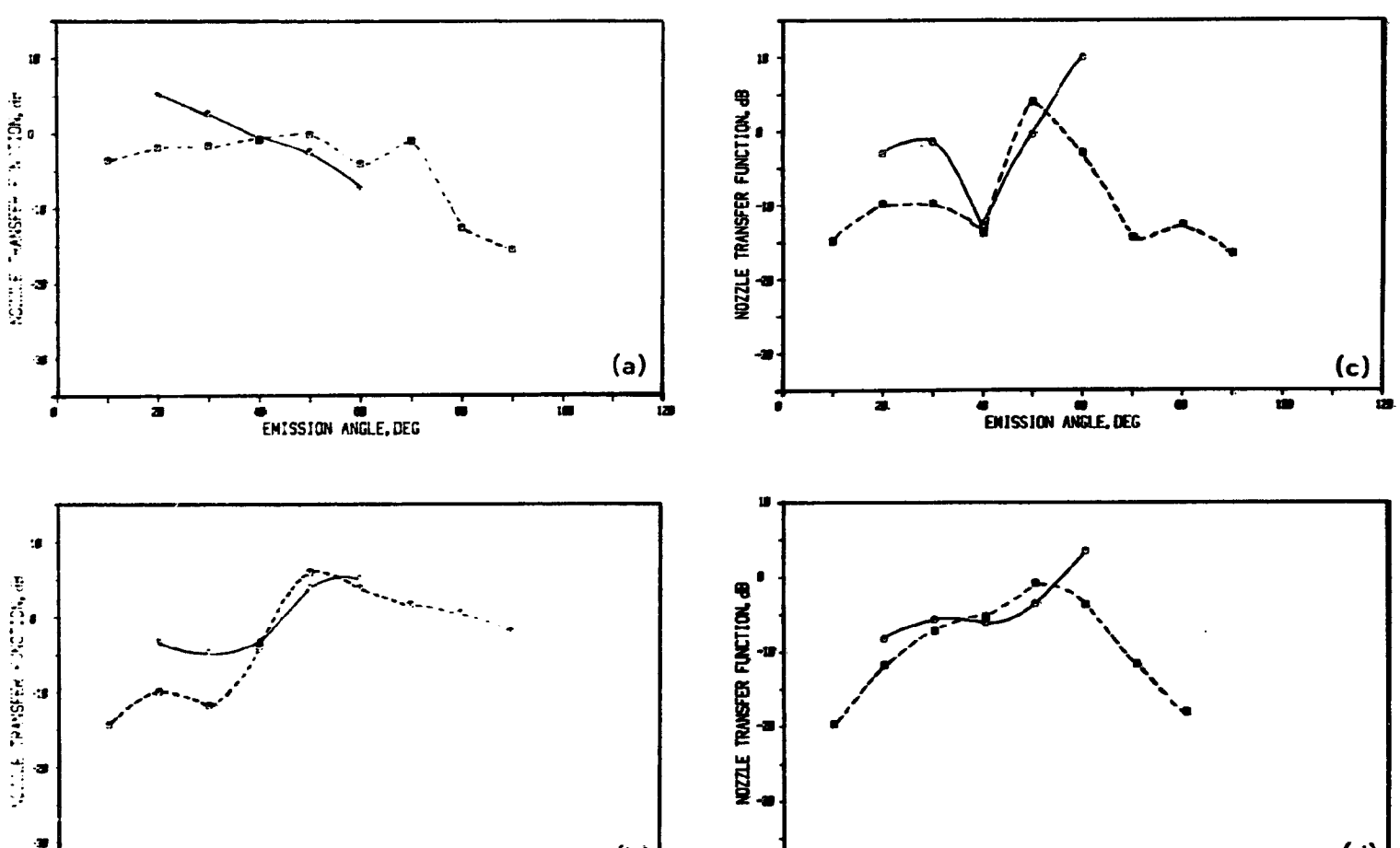

Figure 3.18 Effect of nozzle geometry on 1/3 octave NTC directivities at $M_J = 1.2$ (unheated).
f (KHz): (a) 1.0, (b) 4.0, (c) 8.0 and (d) 16.0
⊡ daisy lobe nozzle; ⊙ conical nozzle

3.1.5 Acoustic Power

Figures 3.19 (a), (b) and (c) show a comparison of the far-field acoustic power spectra normalized with respect to the incident power spectra for the daisy lobe and the reference conical nozzle for M_J = 0, 0.4, 0.6 and 0.8 respectively. For almost all flow conditions the results show little difference in the radiated acoustic power levels for the two nozzles. Just like the NTC spectra and the directivities, the shapes of these power spectra are also almost identical for the two nozzles thus further confirming that equivalent diameter (or equivalent radius) is a good parameter to incorporate in frequency (e.g. as in kR) to compare the nozzles of different shapes.

Other observations that can be made from these far-field acoustic power plots are summarized below:

(1) For low frequencies (i.e., f<4KHz; kR_n<3.8; kR_j<2.3) the far-field acoustic power is always less than the incident power. This behavior is consistent with what one would expect from theory. It is known from duct acoustics that at low frequencies, the open end of a tube has quite small resistance, so that very little energy is radiated outside. "Open tubes having cross sectional perimeters much smaller than the sound wave length are nearly as good hoarders of energy as closed tubes, for only a small percentage of the stored energy can be radiated away" [ref. 3.4, p. 246]. For short wave lengths or high frequencies, the impedance is almost entirely resistive, approaching in value the characteristic acoustic resistance ρc. As the frequency increases, more and more of the energy reaching the open end is radiated out. This is indeed what we see at each Mach number (Figure 3.19).

(2) At each Mach number the low frequency radiated power follows a 6 dB/octave, i.e. $W_f \sim \omega^2$, relationship. As shown in Figure 3.19, a mean straight line with a slope of 6 dB per octave can be drawn through the low frequency data. This proportionality of far-field power (W_f) with ω^2 can be explained following the arguments given by Lighthill [3.5]. According to Lighthill, for the plane waves propagating in the x direction along a tube of uniform cross section area A, we can assume simple proportionality between excess pressure and the component of fluid velocity in the direction of propagation given by

$$p - p_o = \rho_o c u \tag{3.1}$$

Thus if the plane waves are generated at x=o by a fluctuating noise outflow

$$q(t) = A\rho_o(u)_{x=o} = A\, c^{-1}\, (p-p_o)_{x=o} \tag{3.2}$$

The excess pressure for x>o takes the form

$$p - p_o = cA^{-1}\ \ q\ (t - x/c) \tag{3.3}$$

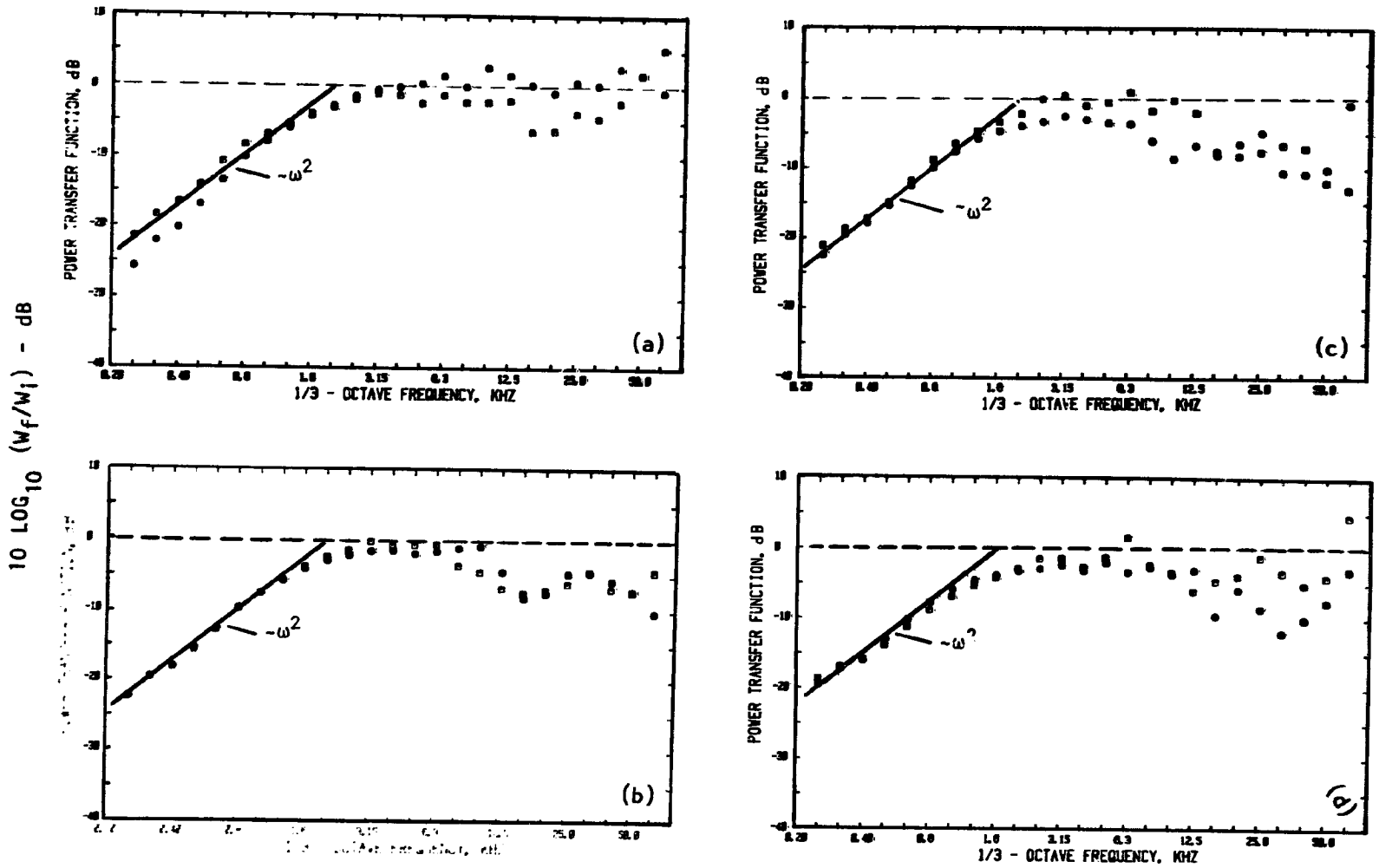

Figure 3.19 Effect of nozzle geometry on far-field acoustic power normalized with respect o incident power.
M_j = (a) 0.0, (b) 0.4, (c) 0.6 and (d) 0.8
Legend: ⊡ daisy lobe nozzle; ⊙ conical nozzle

The above expression is true for one dimensional propagation. If we were to consider three-dimensional propagation the excess pressure can be shown [3.5] to be

$$p - p_o = \frac{dq}{dt}(t - R/c)\ /4\pi R \qquad (3.4)$$

Here it is assumed that variations of mass outflow q(t) are spread over a region whose dimension is small compared with c/ω.

Figure 3.20 shows how a positive pulse of mass outflow generates a proportional positive pulse of pressure excess in one-dimensional propagation, but generates a pulse of quite different shape obtained by differentiation in three-dimensional propagation. (This is consistent with the time history shapes as measured in-duct and in the far-field, see Figures 3.9 and 3.10).

From equation (3.4) it is obvious that the far-field acoustic power ($W_f \sim (p - p_o)^2$) should follow an ω^2 relationship, as indeed it does in the measured results shown here (Figure 3.17). The incident pulse propagates as a one-dimensional wave while the propagation outside the duct is three-dimensional.

(3) Effect of jet Mach number on far-field acoustic power is stronger for the conical nozzle than for the daisy lobe nozzle. This is shown in Figures 3.21 (a) and 3.21 (b) where data for M_J = 0, 0.4, 0.6, 0.8 and also for 1.2 are plotted.* Data for the conical nozzle (Figure 3.21 (a)) clearly indicate that more and more of the low frequency incident energy is radiated to the far-field as the jet Mach number is increased with opposite effect at high frequencies. Acoustic powers for the daisy lobe nozzle (Figure 3.21 (b)), however, first decrease and then start increasing with increasing jet Mach number. This behavior certainly does not correlate with the reflection coefficient data where with increasing jet Mach number higher reflection coefficients were obtained for the daisy lobe nozzle thus implying a reduction in far-field acoustic power with increasing Mach number.

No explanations are currently available for this behavior. It is worth pointing out, however, that such a behavior has been noticed by others also, for example by Abrishaman [3.6].

POWER BALANCE. Far-field acoustic power (W_f) will now be compared with the transmitted acoustic power (W_t). The transmitted power was calculated by subtracting the reflected acoustic power from that associated with the incident signal measured inside the duct. A comparison of PTF_t on this basis for the two nozzles for M_J = 0, 0.4, 0.6 and 0.8 is made in Figures 3.22 (a), (b), (c) and (d) respectively. In fact PTF_t was found to be almost independent of M_J at low frequencies (see Figure 3.23).

* *Due to high jet noise levels the plots for M_J = 1.2 exclude data at a few angles and actual values may be 3 to 4 dB higher than shown here.*

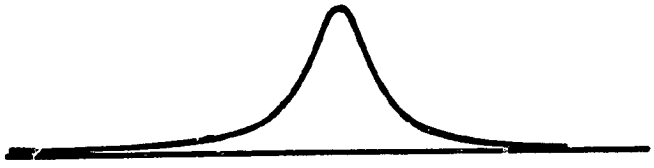

One-dimensional

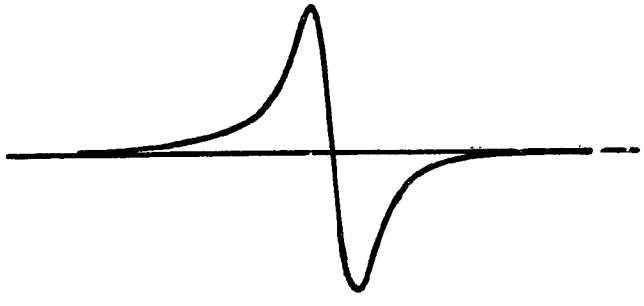

Three-dimensional

Figure 3.20 Sound pulses generated by a positive pulse of mass outflow (varying with time t like $(t^2+\tau^2)^{-1}$, where τ is constant) in one-dimensional and three-dimensional propagation. The pulses (illustrated with arbitrary vertical scales) are proportional to the mass outflow and to its first derivative respectively. [Taken from reference 3.5].

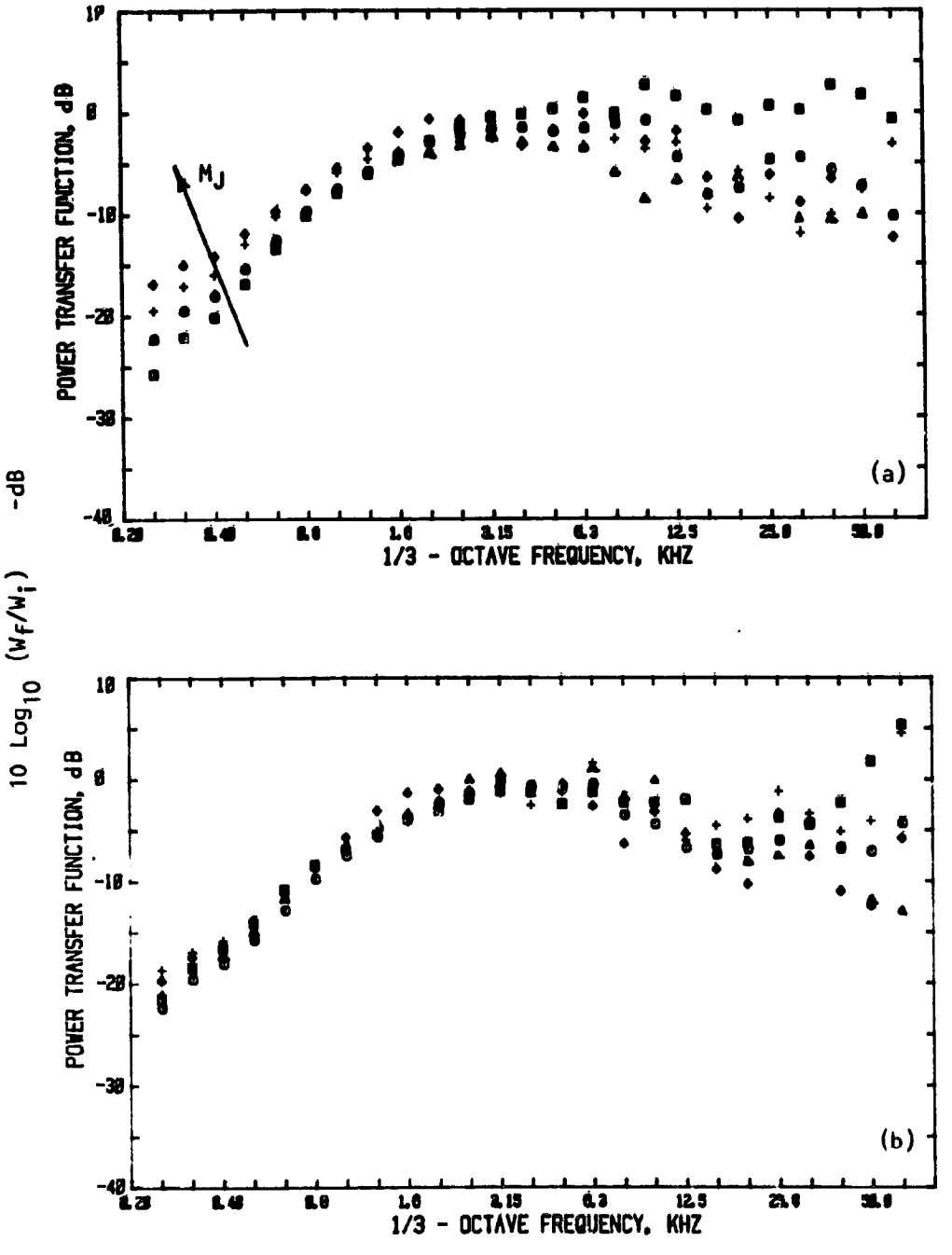

Figure 3.21 Effect of jet Mach number on far-field acoustic power spectra for (a) conical nozzle and (b) the daisy lobe nozzle.
Legend for M_j ⊡, 0.0; ⊙, 0.4; △, 0.6; +, 0.8; ◇, 1.2

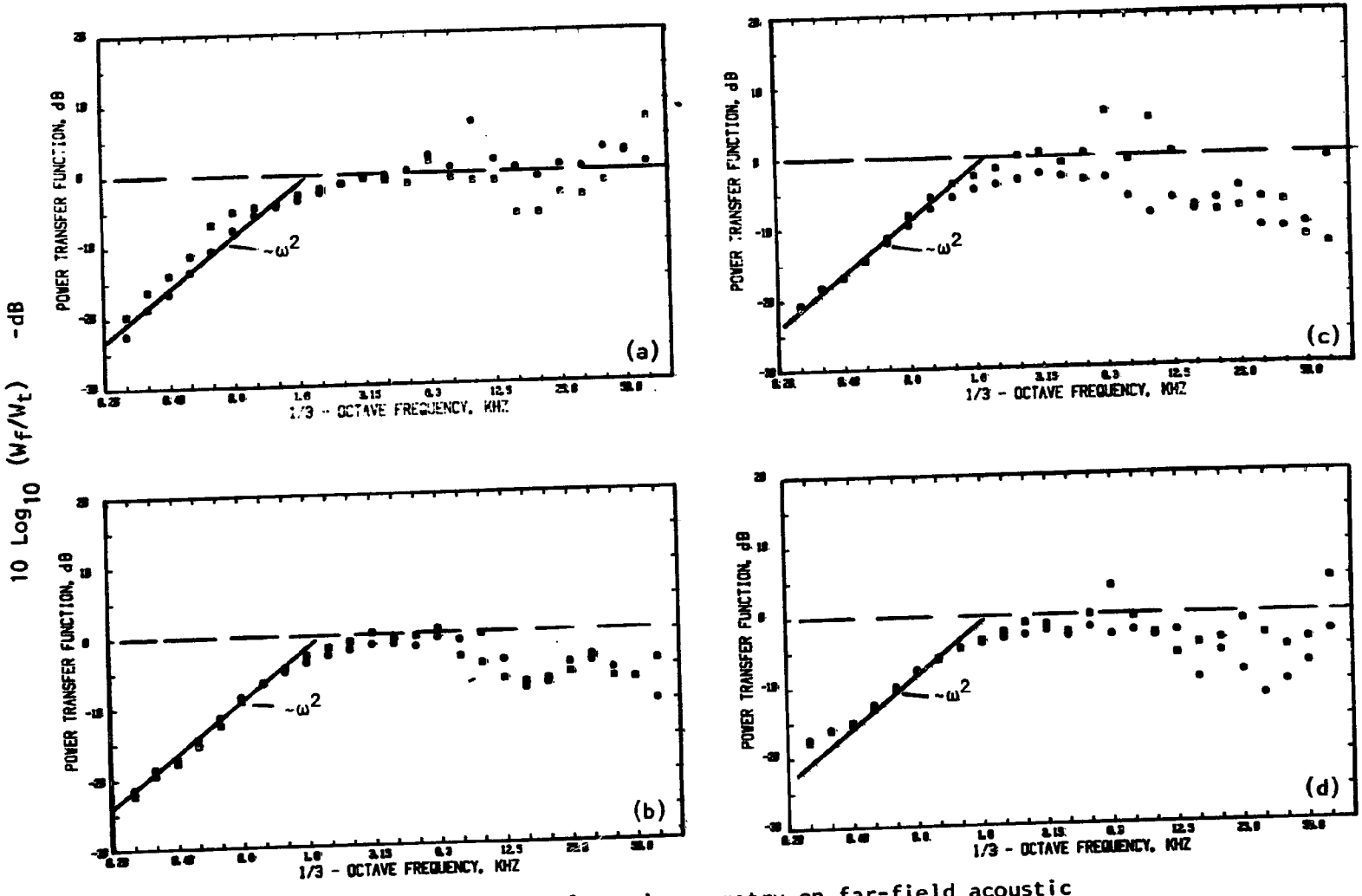

Figure 3.22 Effect of nozzle geometry on far-field acoustic power normalized w.r.t. transmitted power
M_J: (a) 0.0, (b) 0.4, (c) 0.6 and (d) 0.8
⊡ daisy lobe nozzle, ⊙ conical nozzle

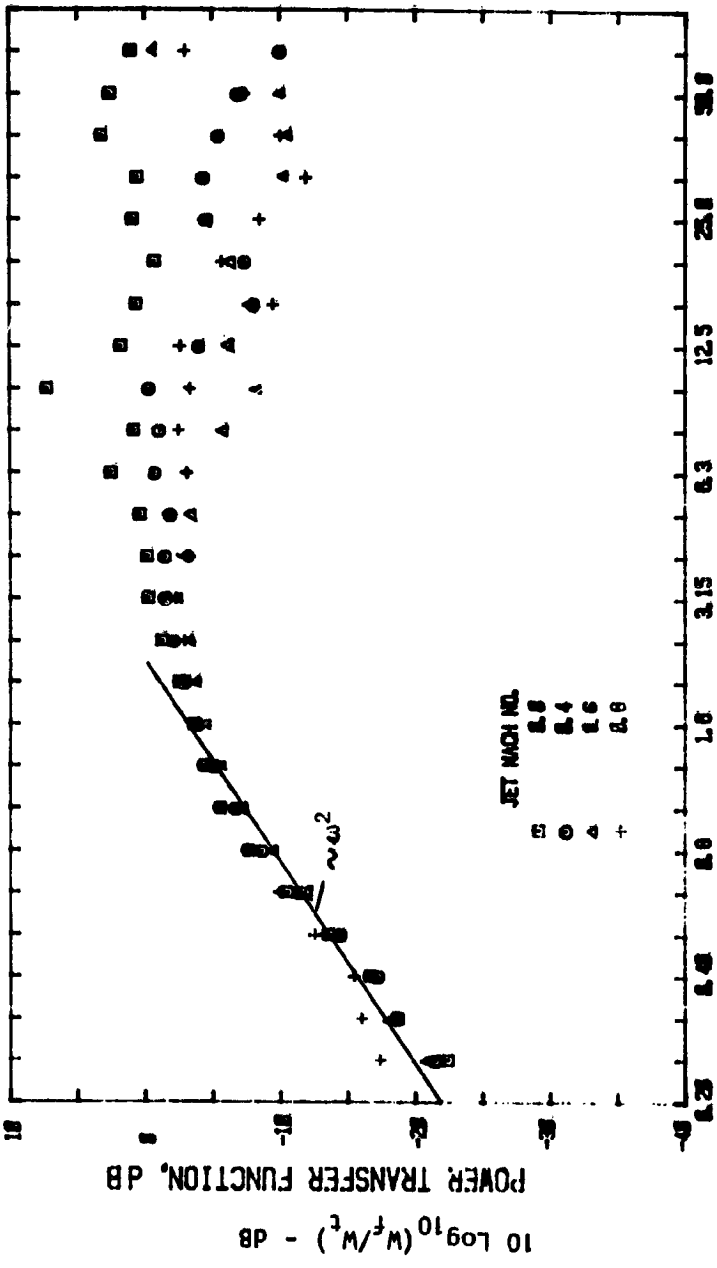

Figure 3.23 Effect Of Jet Mach Number On Far-field Acoustic Power For Conical Nozzle, Normalized W.R.T. Transmitted Power

These results are quite interesting in that the low frequency data once again shows a second power of frequency dependence. Instead of obtaining power balance a *decrease* in acoustic power is noticed at *low frequencies* for all jet Mach numbers including $M_J = 0$. Of course, levels at low frequencies can be expected to be higher (by about 2.5 dB), since the far-field power has been calculated for the angular range of 5° to 125° with the jet axis. This does not, however, account for the 20 to 25 dB missing near 200 Hz.

Various possible sources of error were first looked into. They are summarized below but were unable to account for this loss.

(1) Possible Error in Reflection Coefficient. The following expression was utilized for the calculation of the transmitted power:

$$W_t = \frac{A_D}{\rho_c} p_i^2 (1 - \psi)(1 + M_D)^2 \qquad (3.5)$$

where

$$\psi = \left(\frac{1-M_D}{1+M_D}\right)^2 \frac{p_r^2}{p_i^2} \qquad (3.6)$$

In terms of decibels, if the value of ψ is very close to unity, then a small error in ψ can cause a considerable error in the calculations of the acoustic power in decibels. To illustrate this point, the variation of $10 \text{ Log}_{10} (1-\psi)$ and $10 \text{ Log}_{10} (\psi)$ as a function of $(1-\psi)$ is shown in Figure 3.24. These plots make it quite clear that for large values of ψ (i.e. intensity reflection coefficient), approaching unity an error of 1dB in $10 \text{ Log } \psi$ can cause an error of 7 dB or even higher depending upon how close the value of ψ is to unity.

With the exception of $M_J = 1.2$ data and the first two low frequency points for the conical nozzle at $M_J = 0.8$ and 1.2, the value of ψ in the present study is mostly less than 0.5. Since ψ is the product of the reflection coefficient and a Mach number term which is always less than unity and decreases with M_D, ψ is reduced further and further with increasing M_D. Thus most data-points lie in the right half of Figure 3.24 (right of the dotted line shown in the figure). In this region an error of 1 db in ψ produces less than 1 dB error in $10 \text{ Log}_{10} (1-\psi)$ and thus in the power calculation. We believe that our reflection coefficients are correct within 1 dB as demonstrated in Phase 1 studies [3.7] by comparing the reflection coefficients for straight unflanged ducts with Levine and Schwinger's theory [3.8] and also comparison of data from the impulse technique with similar data from the impedance tube method.

Error in the measurement of reflection coefficients was thus ruled out as a possible reason for the missing low frequency in the power balance plots.

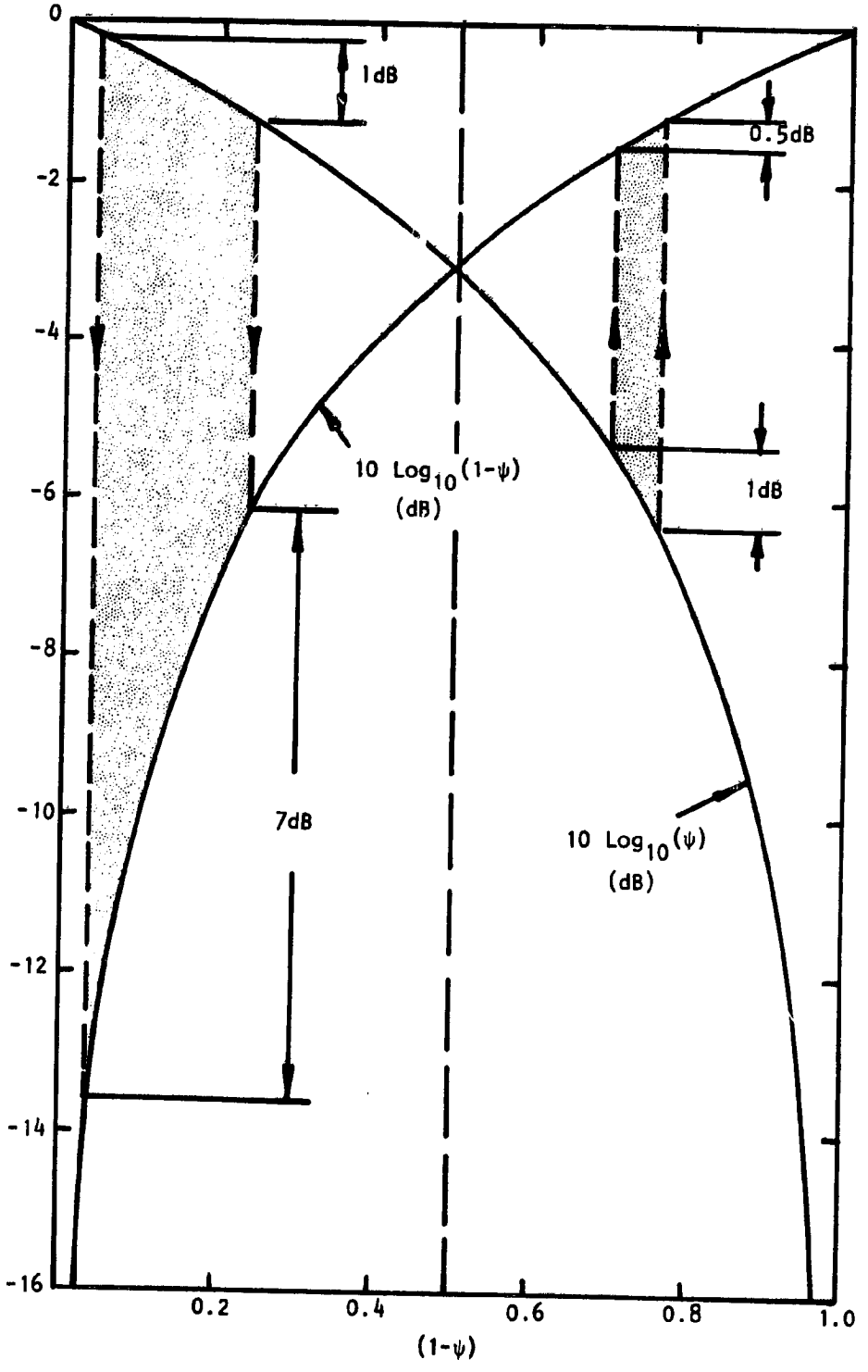

Figure 3.24 Variation of 10 $\text{Log}_{10}(\psi)$ and 10 $\text{Log}_{10}(1-\psi)$ with $(1-\psi)$

(2) Possible non-linear propagation in the far-field. Since high intensity pulses were used in the program it was first suspected that far-field pulses might not be following an inverse square law, as assumed, in the far-field power calculations. Time histories were, therefore, measured at various distances from the exit of the straight duct. Measurements made at $\theta = 0$, $20°$, $60°$ and $90°$ as a function of distance showed that the inverse square law was followed at all distances beyond about 3 diameters and the pulses had identical shapes at each measurement point. Typical time histories for $\theta = 60°$ are shown in Figure 3.25. These time histories have been adjusted for inverse square law by adjusting the amplified gain setting and are found to be identical in shapes and amplitudes in the far-field. Possible non-linear propagation was thus also ruled out as a possible candidate to explain the low frequency power imbalance.

Bechert [3.3, 3.9] recently reported the effect of nozzles on sound transmission to the far-field by injecting pure tones. With the exception of zero Mach number, his data with flow also shows considerable attenuation at low frequencies. The underlying physical mechanism behind this low frequency absorption, according to Bechert, is the shedding of fluctuating vorticity at the nozzle exit. The sound absorption is of the same kind as the fluid energy losses in a separated flow.

If this explanation fits the present data with flow, it is difficult to explain the low frequency power imbalance at the no flow condition. It is conceivable that the sound level at the exit at zero flow was strong enough to generate vortices (i.e. *acoustic streaming*) at the nozzle exit.

It was found in this study that the loss at low frequency was identical at all Mach numbers including $M_J = 0$.

Further work is needed to properly understand the above behavior.

3.1.6. Mach Number Effects - Summary

The results for the daisy lobe nozzle and the conical nozzle tested statically and unheated can be summarized as follows:

(1) The daisy lobe nozzle displays higher reflection coefficients than the conical nozzle.

(2) For both nozzles, the effect of flow is to gradually reduce the reflection from the jet opening and increase the reflection from the solid parts (i.e. nozzle shoulder and parts on to which the lobes and the tubes are attached). At the under-expanded flow condition, all reflection appears to be from the solid parts.

(3) The trends in variation of reflection coefficient with frequency are exactly opposite for the two nozzles. The daisy lobe reflection coefficient increases with frequency while that for the conical nozzle decreases with frequency almost at all Mach numbers.

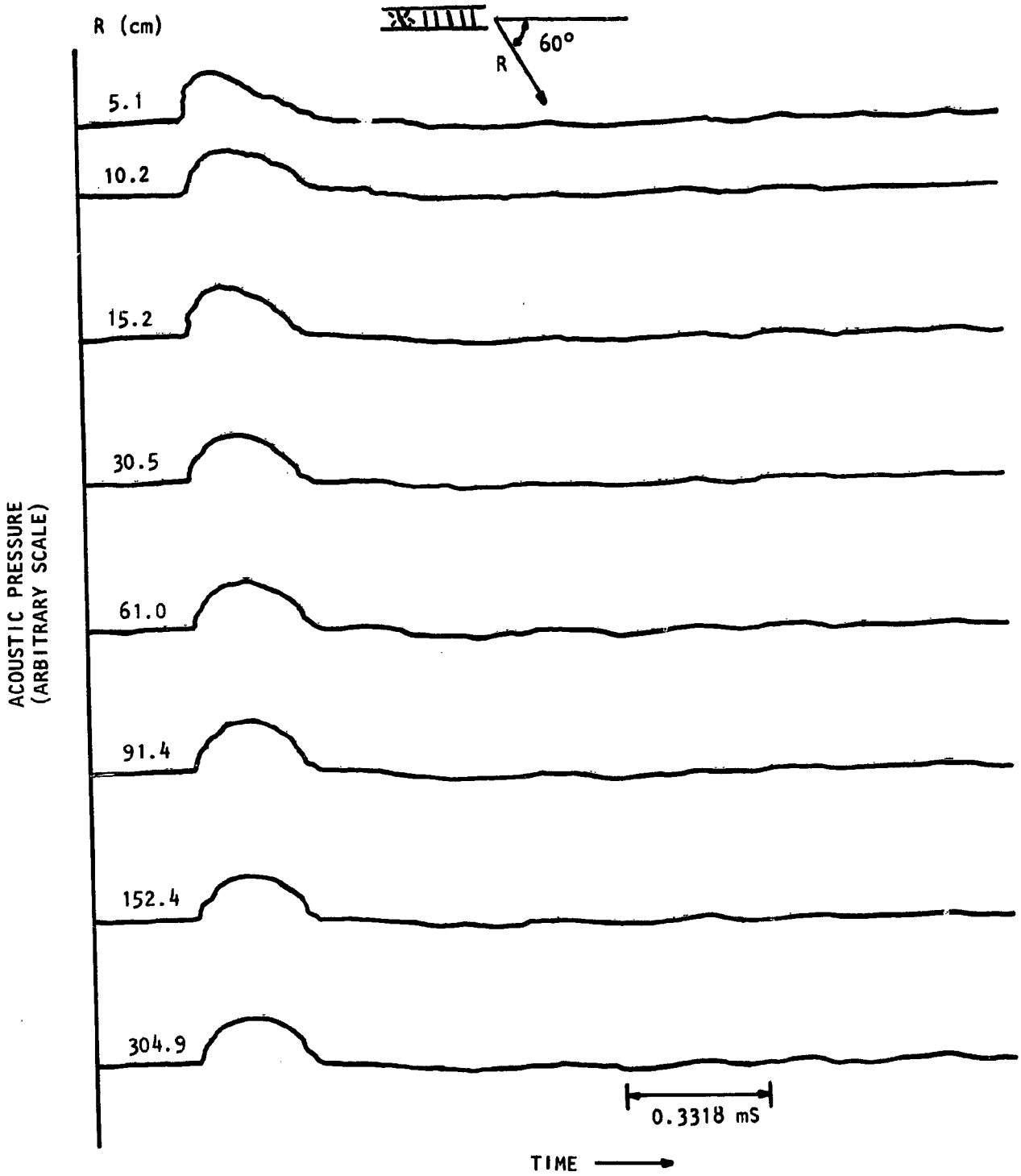

Figure 3.25 Far-field time histories for 10.16 cm diameter straight duct at $\theta = 60°$ as a function of measurement distance at $M_J = 0$. (amplitudes adjusted for $1/R^2$ law).

(4) Reflection coefficients at very low frequencies for the conical nozzle are higher than unity for high Mach numbers.

(5) At zero flow conditions, the radiation is predominantly towards the jet axis. With flow the refraction effect becomes important and the peaks in the directivities shift towards higher angles.

(6) Deductions made about far-field radiation based upon reflection coefficients do not necessarily hold. In fact both nozzles, despite completely different geometry, and different reflection characteristics show remarkably similar far-field NTC directivity and PTF except at the highest jet Mach number (M_J = 1.2). At M_J = 1.2 far-field levels are higher for the conical nozzle.

(7) Exit area appears to determine the shape and levels of the far-field spectra instead of geometric details of the nozzle.

(8) The far-field acoustic power at low frequencies follows a 6 dB/octave law.

(9) At low frequencies, the far-field acoustic power is always less than the incident power.

(10) Jet Mach number has little effect on power transmission.

(11) Power balance especially at low frequencies is not obtained. No firm explanations are available to account for this missing low frequency.

3.2 TEMPERATURE EFFECTS

Results similar to those presented in section 3.1 for unheated jets will now be presented for the jets heated to 600K. For this condition the nozzles were operated at only two jet Mach numbers (fully-expanded) namely, M_J = 0.8 and 1.2. Due to very high jet exit velocities (and therefore high amplitude of jet-mixing noise), the data at M_J = 1.2, particularly for the conical nozzle, was valid only for a few angles. For comparison with the unheated jets, therefore, only the M_J = 0.8 data will be discussed here.

3.2.1 Time Histories

The far-field time histories for the daisy lobe nozzle at M_J = 0.8 are shown in Figure 3.26 for both the unheated and the heated jet measured at θ = 30°, 60°, 90° and 120°. Corresponding data for the reference conical nozzle is shown in Figure 3.27. Both of these figures indicate that the time histories at θ = 30° have become wider as a result of heating the jet. This is a result of increased refraction as can be seen by inspecting the following equation relating the emerging angle θ_0 to the (incident) angle θ_i across a jet moving at a Mach number M_J (Ref. 3.10).

$$\cos \theta_i = 1/\left(\frac{c_0/c_J}{\cos \theta_0} - M_J\right) \qquad (3.7)$$

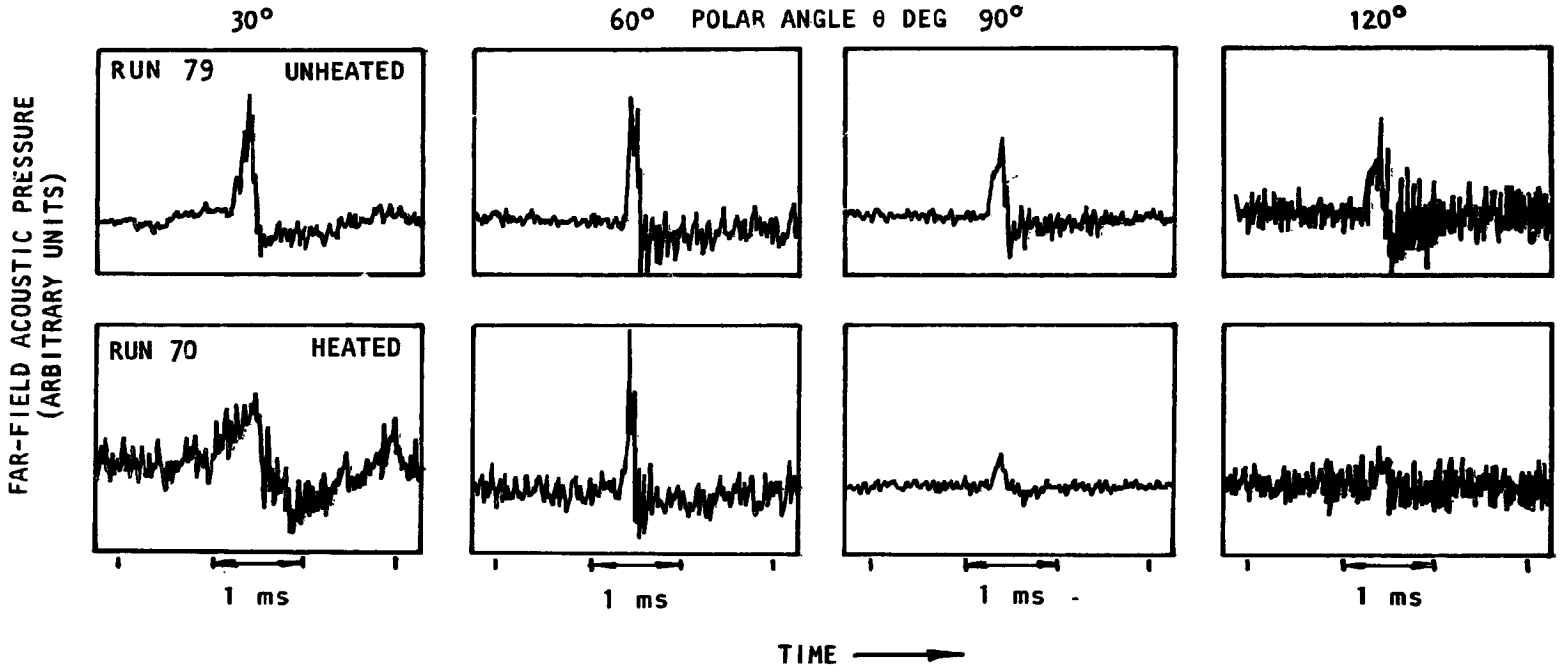

Figure 3.26 Far-field time histories for the daisy lobe nozzle (unheated versus heated) at various measurement angles and $M_j = 0.8$.

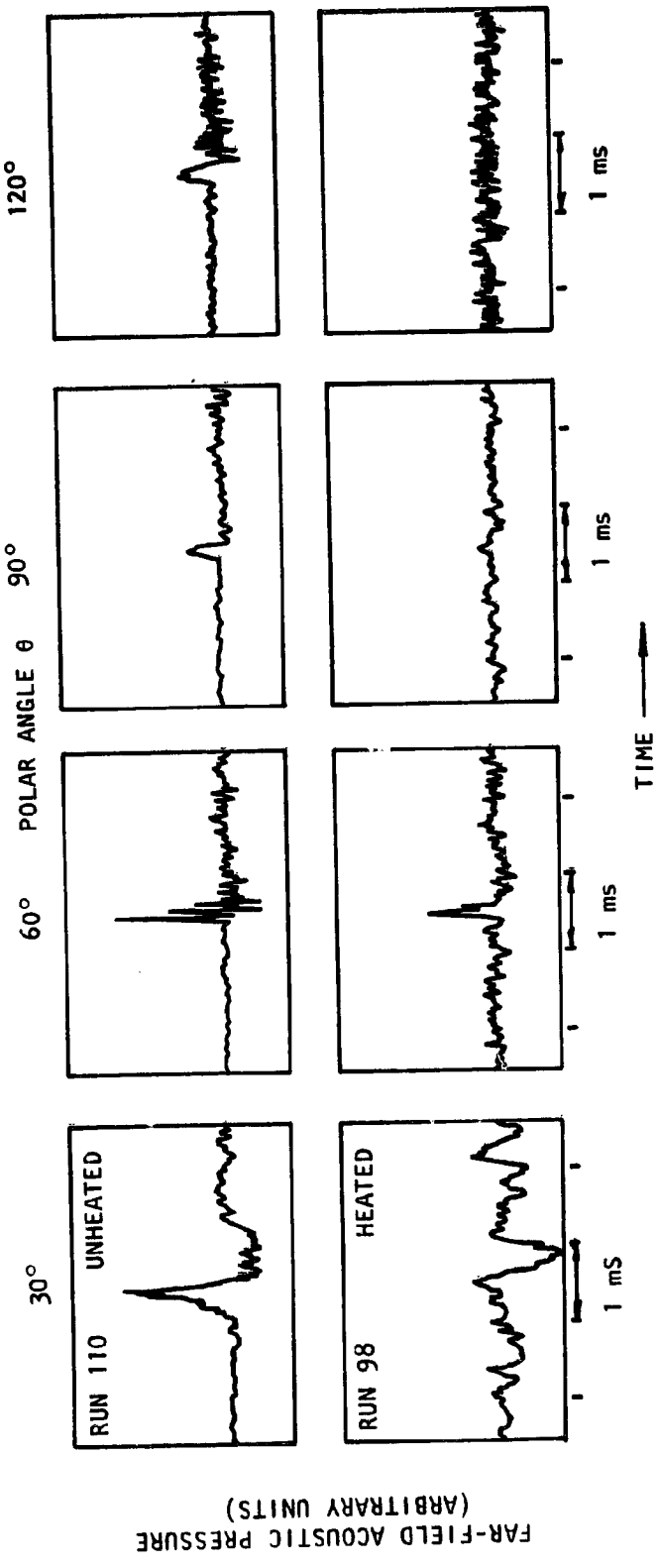

Figure 3.27 Far-field time histories for the conical nozzle (unheated versus heated) at various measurement angles and $M_J = 0.8$

It is clear from this equation that increasing M_j and/or c_j (i.e. jet temperature) increases the angle of refraction. These trends were found at $M_j = 1.2$ also, but inadequate signal to noise ratios at this Mach number made it difficult to isolate the pulse at many angles (see Figure 3.28).

NTC spectra were obtained from the Fourier transforms of these far-field time histories and also of those measured in-duct. Since the in-duct time histories followed a trend similar to that discussed for the unheated jets they are not discussed separately. Instead the reflection coefficients obtained from these time histories are presented.

3.2.2 Reflection Coefficients

Effect of heating on reflection coefficients for the daisy lobe nozzle at $M_j = 0.8$ and 1.2 is shown in Figure 3.29. It is seen that for the subsonic jet Mach number, heating reduces the reflection coefficients in most of the plane wave region, while at $M_j = 1.2$, heating increases the reflection coefficient considerably above unity at low frequencies and decreases it at higher frequencies (still within the plane wave region, f<2KHz).

Since, as pointed out earlier, even the unheated results on reflection coefficients can not be explained without further work (primarily theoretical), no attempts will be made to expalin the reflection coefficients for the heated data. Besides, only one heated condition was available, hardly enough to generalize the conclusions. It is certain, however, that heating the jet to 600K affects the low frequency reflection coefficients considerably. As for the daisy lobe nozzle, the conical nozzle reflection coefficients also decrease at low frequencies as a result of heating. This is shown in Figure 3.30 for $M_j = 0.8$. The effect of heating on reflection coefficients of the conical nozzle is not as drastic as it was for the daisy lobe nozzle.

Nozzle transfer coefficients and power transfer functions for the heated jets and their relationsh ps with these reflection coefficients will now be discussed.

3.2.3 One Third-Octave NTC

SPECTRA AND DIRECTIVITIES. Effect of heating on 1/3-octave NTC spectra at $\theta = 30°$, 60° and 90° is shown in Figure 3.31. It is found that the effect of heating is to reduce the NTC value at very low frequencies (f≤400Kz). At higher frequencies, effect of heating is to increase the NTC values especially at angles close to $\theta = 60°$. It is believed that this is because of refraction effects. This effect is best illustrated by comparing the directivities of NTC for the unheated and the heated condition, as shown in Figure 3.32 for frequencies of 1, 4, 8 and 16 KHz. Here the unheated-jet data for angles smaller than 20° were found to have some instrumentation problem (as discovered at a later stage), and is, therefore, not plotted. There is an indication, however, that the refraction effects at small angles tend to reduce the far-field radiation and increase it at larger angles. That this is a result of refraction is further confirmed by the acoustic power results shown later where it is shown that, except for the very low frequencies, there is little difference between the acoustic power transfer functions for the heated and the unheated jets.

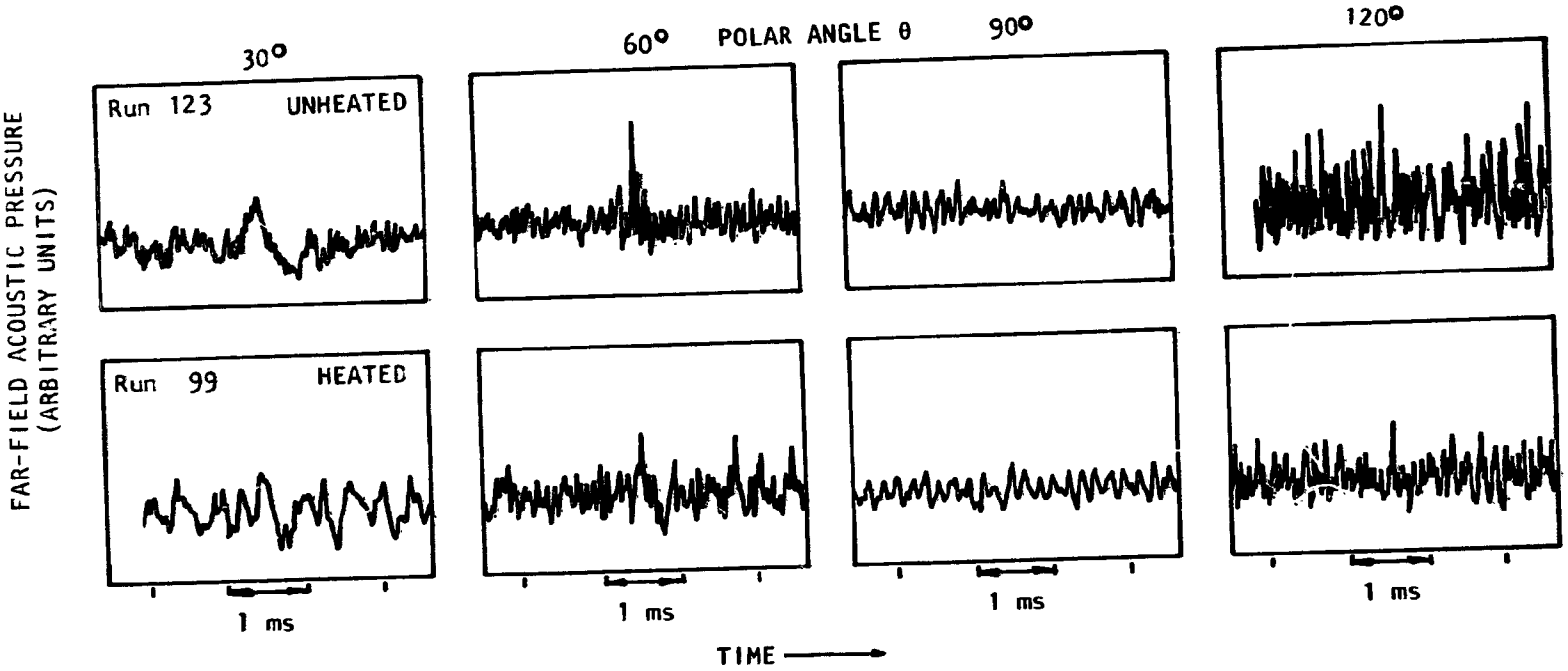

Figure 3.28 Far-field time histories for the daisy lobe nozzle (unheated versus heated) at various measurement angles and $M_J = 1.2$

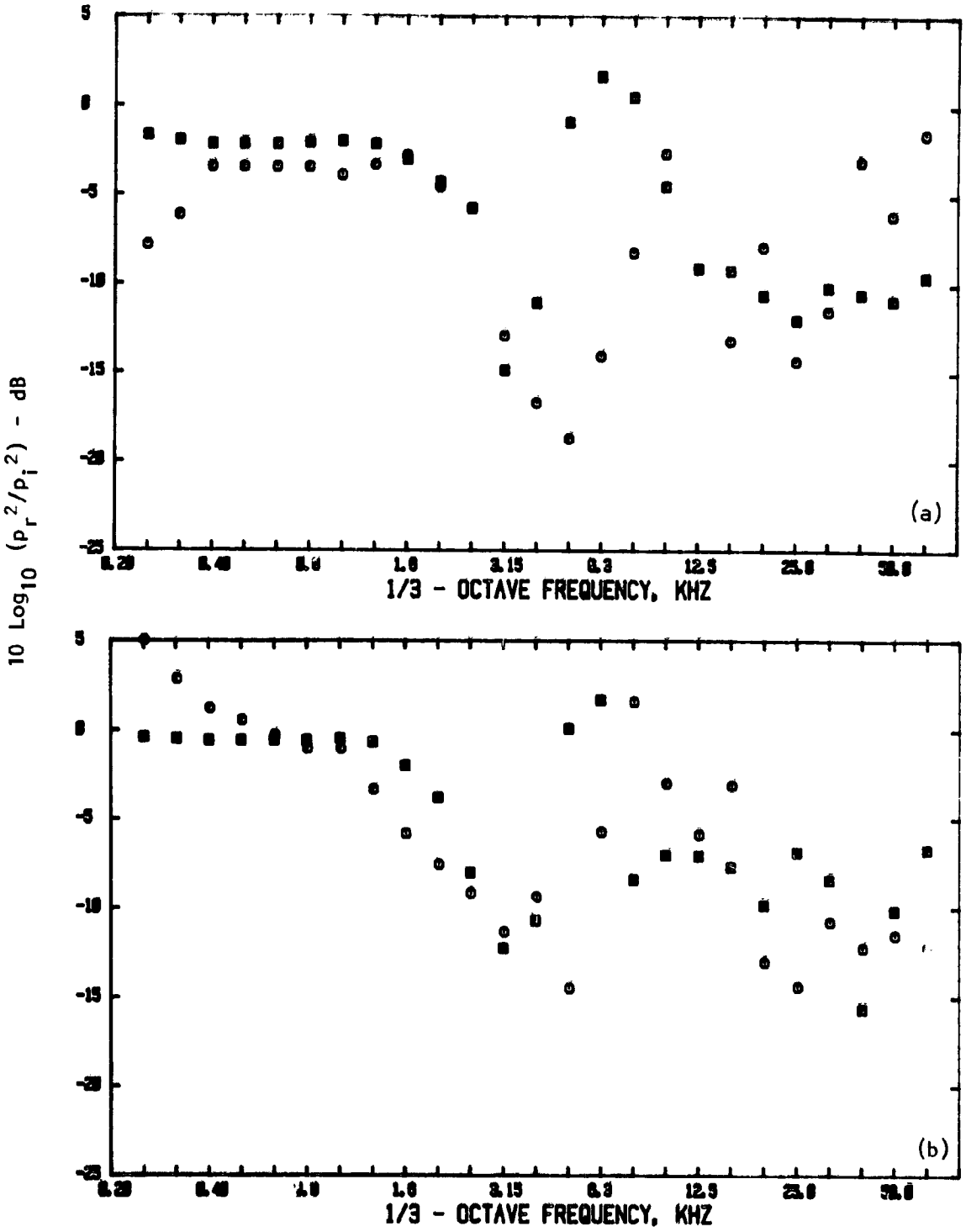

Figure 3.29 Effect on heating the jet on reflection coefficient spectra for the daisy lobe nozzle at (a) $M_J = 0.8$ and (b) $M_J = 1.2$
T_R: ⊡ , Ambient; ⊙ , 600K

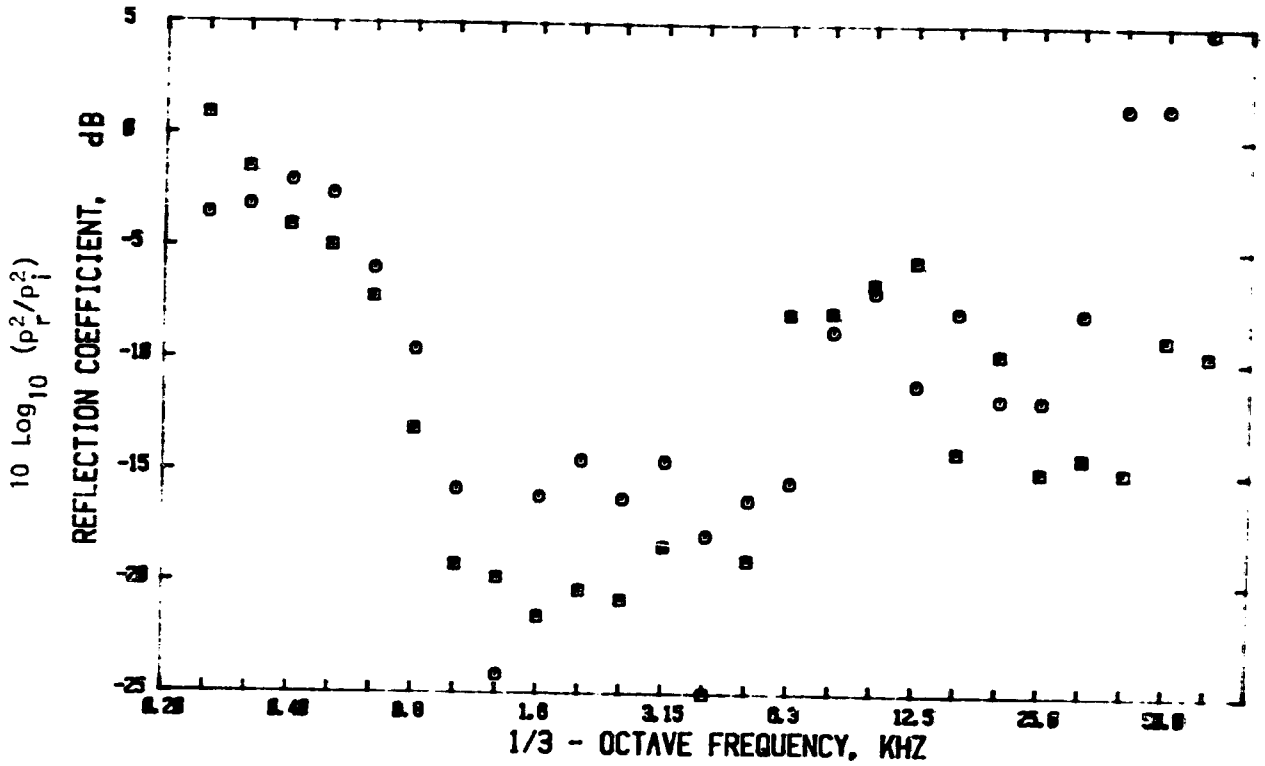

Figure 3.30 Effect of heating the jet on reflection coefficient spectra for the conical nozzle at $M_j = 0.8$
TR: ⊡ , Ambient; ⊙ , 600K

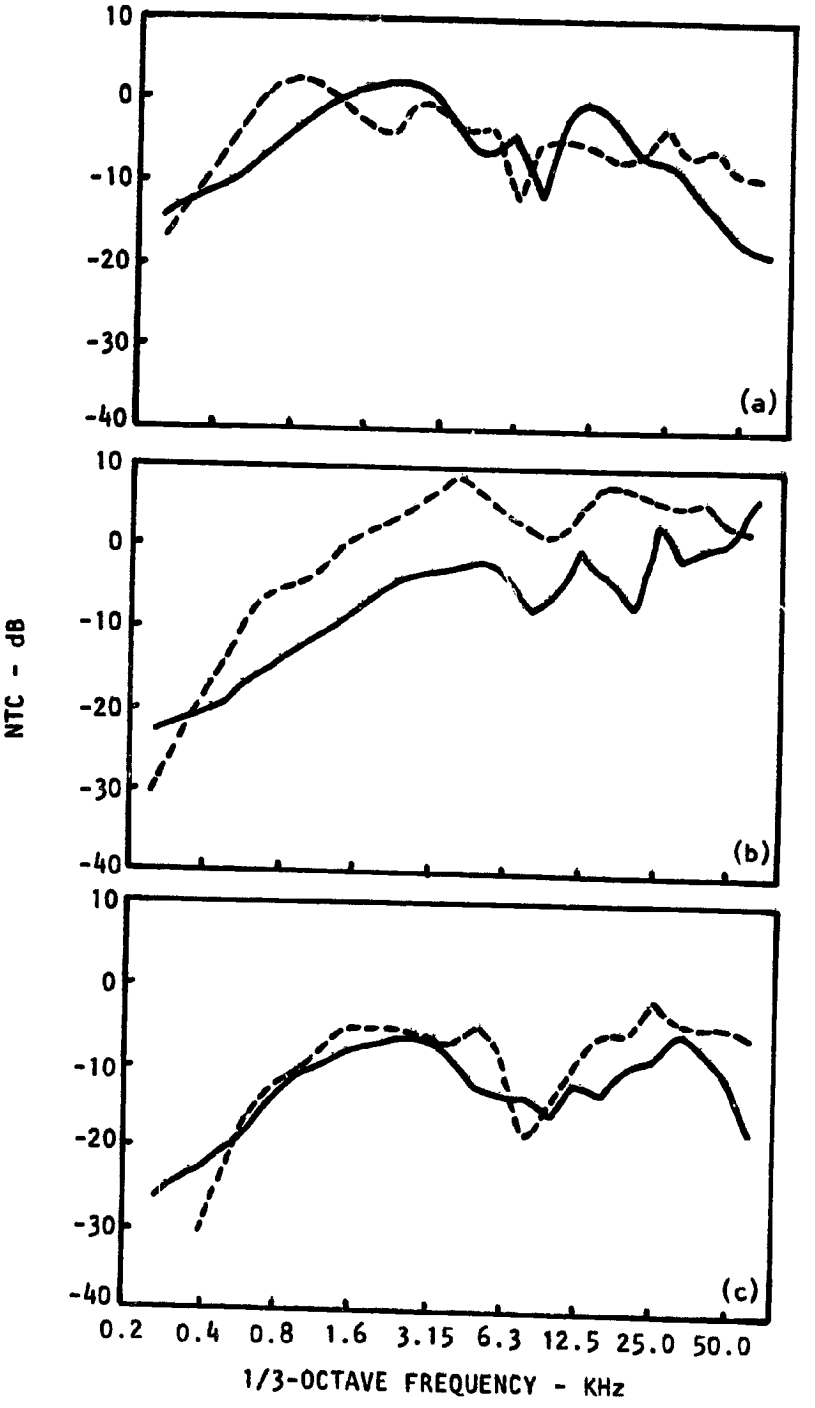

Figure 3.31 Heating effects on 1/3 octave NTC spectra of the daisy lobe nozzle, operated at $M_J = 0.8$
θ: (a) 30°, (b) 60° and (c) 90°
T_R: ———— , Ambient; – – – – – – 600K

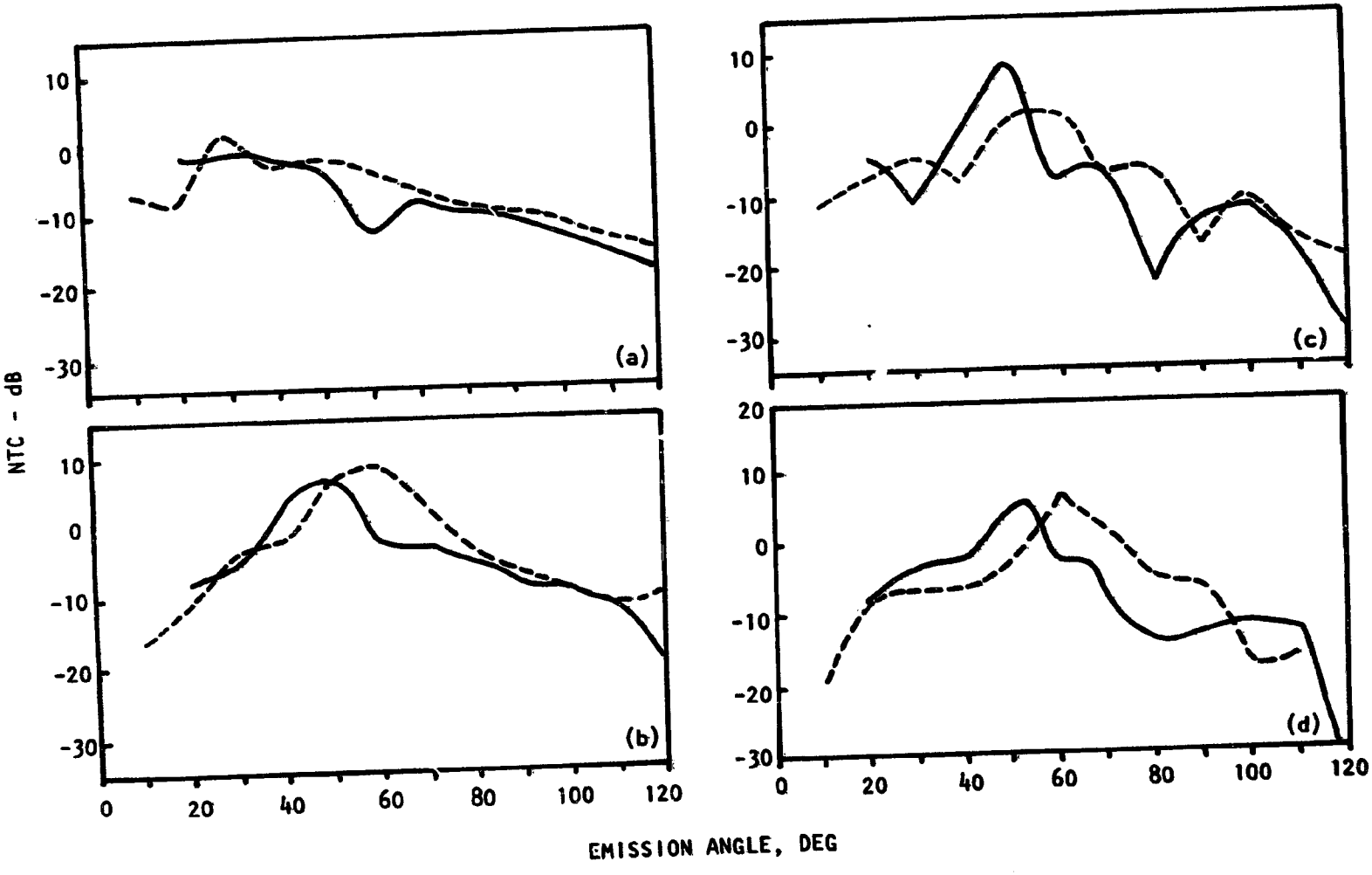

Figure 3.32 Effect of heating on daisy lobe nozzle NTC directivities at $M_J = 0.8$
T_R: ———, Ambient, - - - - - - - 600K
f (KHz): (a) 1, (b) 4, (c) 8 and (d) 16

COMPARISON WITH REFERENCE CONICAL NOZZLE. Typical NTC spectra at $M_J = 0.8$ and $T_R = 600K$ for both the daisy lobe nozzle and the conical nozzle are compared in Figure 3.33 at $\theta = 30°$, 60° and 90°. Clearly with the exception of some low frequency data, there is a general tendency for the daisy lobe nozzle to have lower NTC amplitudes. Similar results were obtained at other angles as seen in Figure 3.34 where the NTC directivities at $M_J = 0.8$ and $T_R = 600K$ for both the daisy lobe nozzle and the conical nozzle are compared for four frequencies, i.e., 1, 4, 8 and 16 KHz. These results show that the conical nozzle radiates more efficiently than the daisy lobe nozzle at almost all angles and particularly so at small angles. This effect was not so obvious for the unheated conditions. No clear cut explanation is available for this behavior.

3.2.4 Acoustic Power

A comparison of the radiation performance of the two nozzles is best assessed by comparing the radiated far-field acoustic powers for a given incident power. This is shown in Figure 3.35. Far-field acoustic power from the two nozzles normalized with respect to the incident power at $M_J = 0.8$ and $T_R = 600K$ is compared. The shapes of these PTF_1 spectra are very similar, with no change at low frequencies (up to a frequency of about 800 Hz). Thereafter the conical nozzle is 5 to 8 dB noisier than the daisy lobe nozzle.

The 1/3-octave spectra of the power transmission function with respect to the incident power for the daisy lobe nozzle operated at $M_J = 0.8$ is compared for the unheated and the heated condition in Figure 3.36. The general shapes of the spectra at both conditions are the same with 2 to 3 dB reduction at low frequencies ($f<12.5KHz$) and 4 to 5 dB increase at high frequencies ($f>12.5KHz$). The same far-field acoustic power when plotted with respect to the transmitted power does not show as much difference except for very low frequencies ($f<500Hz$) where the heated jet transmits much less power than the unheated jet. This is shown in Figure 3.37.

As observed for the heated jets, a low frequency absorption is noticed for the heated jets also but instead of following an ω^2 relationship the PTF follows a ω^4 relationship. Further comments on this will be reserved until similar data with flight simulation has been examined (see section 3.3.4).

3.2.5 Temperature Effects - Summary

Effect of heating on the time histories, reflection coefficients, NTC spectra and PTF spectra have been described for both the daisy lobe suppressor nozzle and the reference conical nozzle. Data for $M_J = 0.8$ and 1.2 at ambient conditions and $T_R = 600K$ were acquired but due to the dominance of jet mixing noise and shock noise, particularly for the conical nozzle, only $M_J = 0.8$ data has been discussed. Effects of heating can be summarized as follows:

(1) Effect of heating on time histories is to widen them at small angles (to the jet axis) and contract them around $\theta = 60°$. This effect is due to refraction and shows up in NTC directivities as reduced levels at

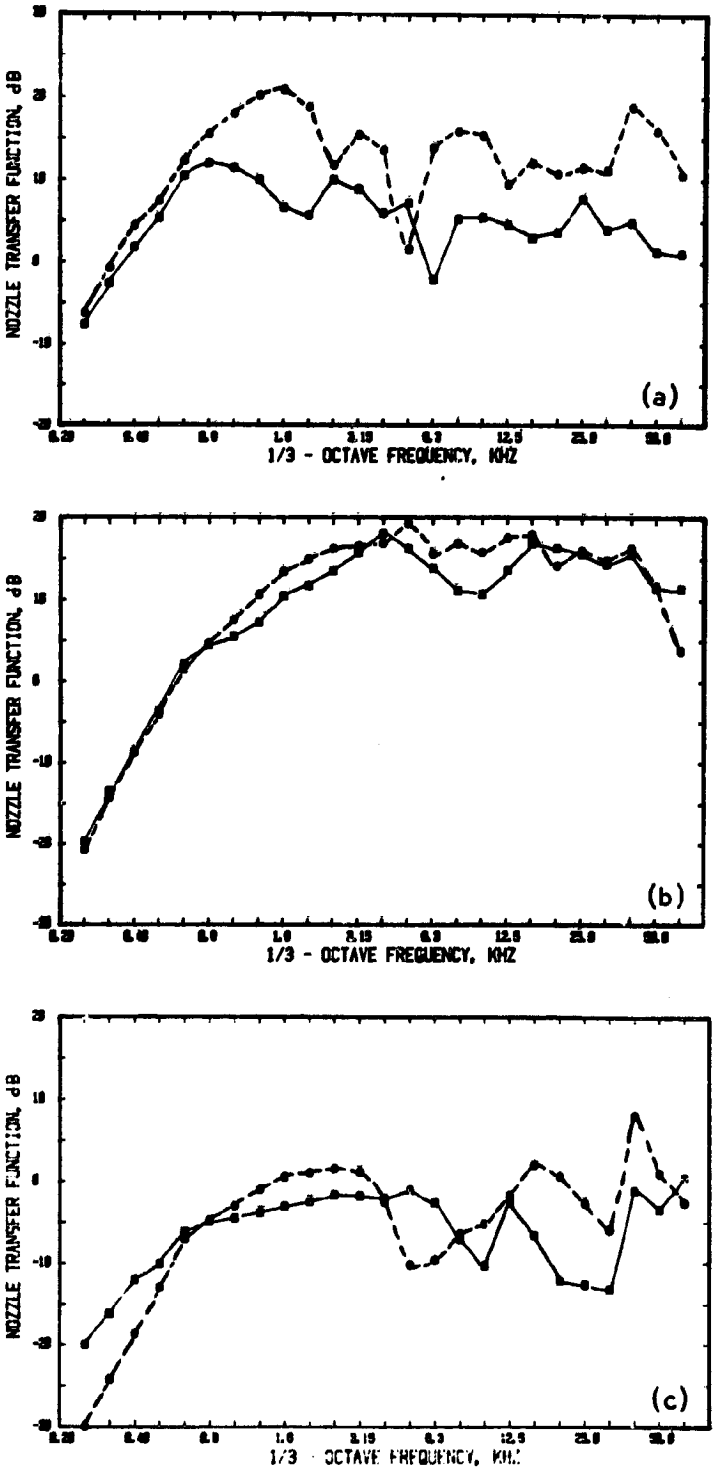

Figure 3.33 Effect of nozzle geometry on NTC spectra at $M_J = 0.8$ and $T_R = 600K$
θ: (a) 30°, (b) 60°, and (c) 110°
-□-, daisy lobe nozzle, -⊙-, reference conical nozzle

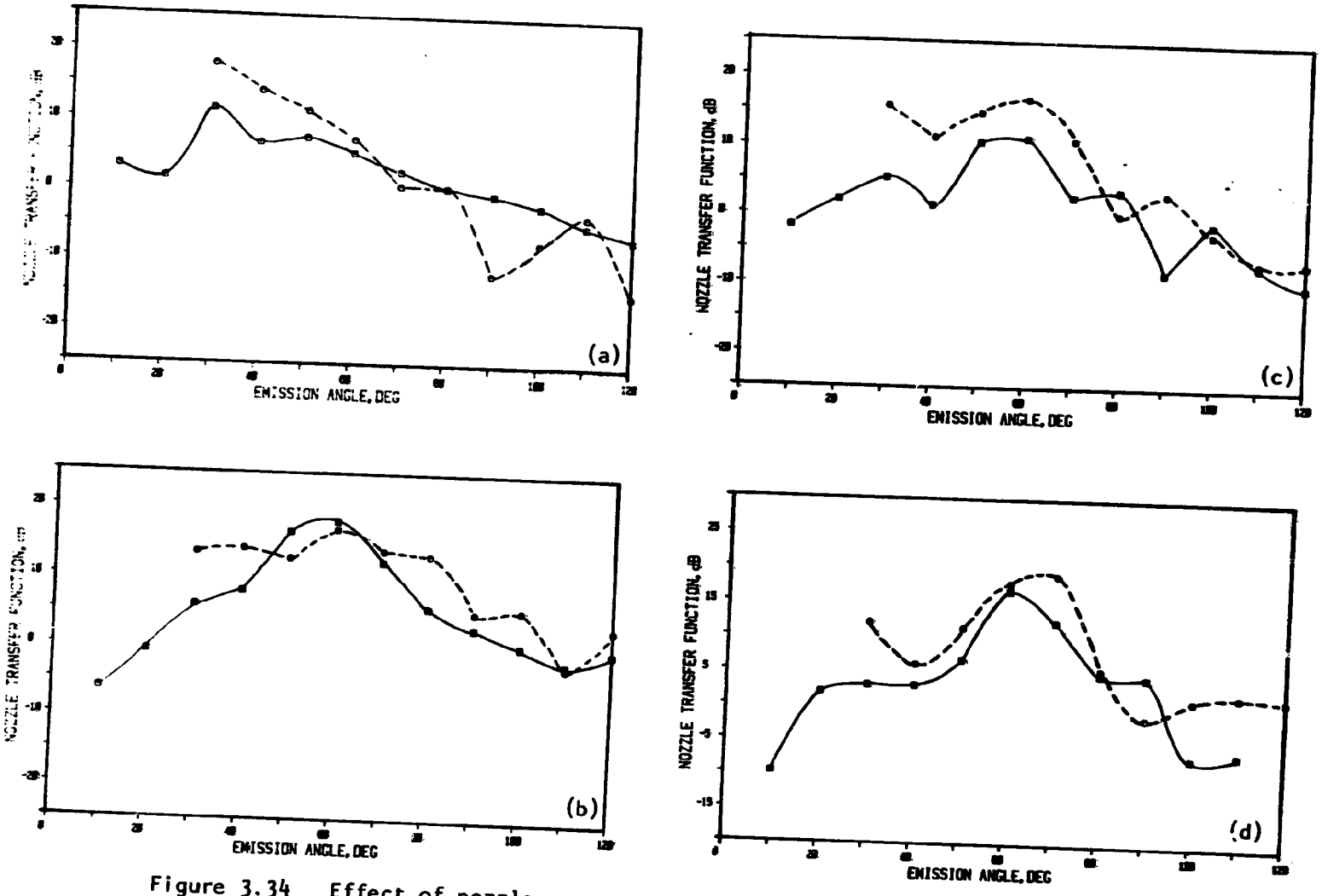

Figure 3.34 Effect of nozzle geometry on NTC directivities at $M_J = 0.8$ and $T_R = 600K$
f (KHz): (a) 1, (b) 4, (c) 8 and (d) 16
—⊡—, daisy lobe nozzle —⊙—, reference conical nozzle

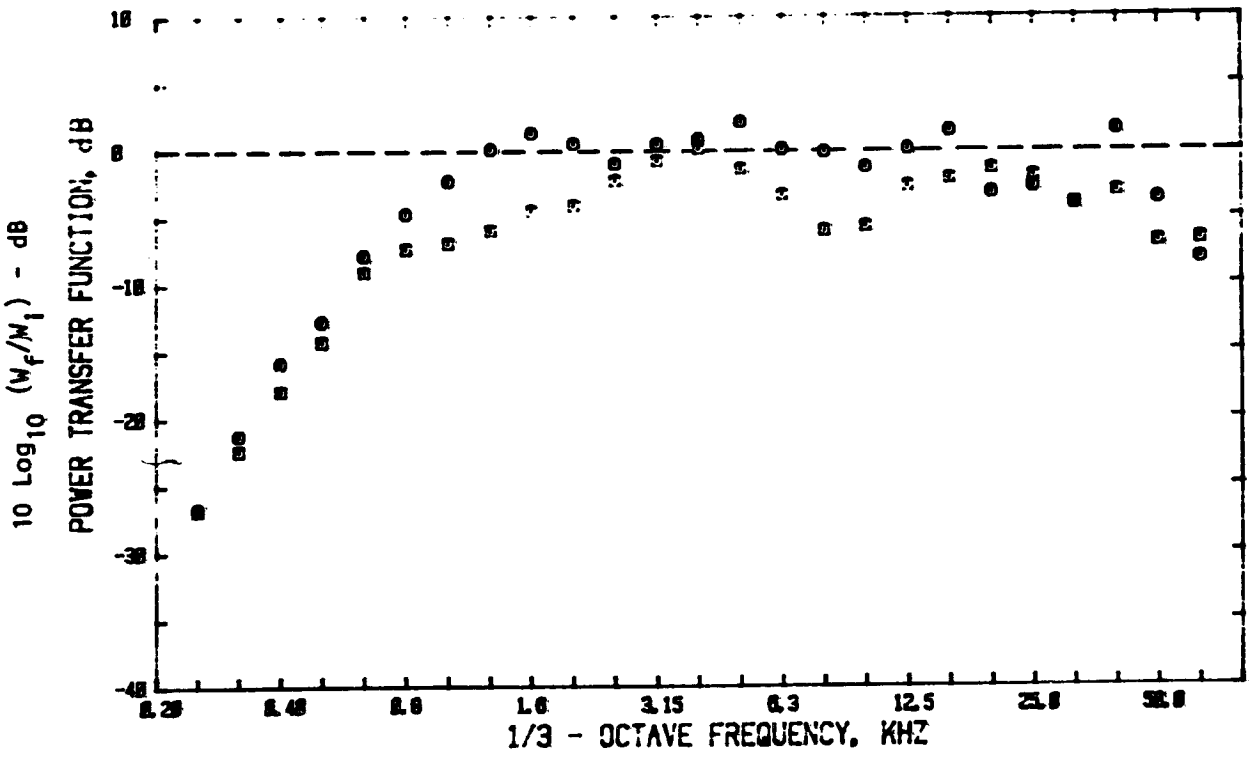

Figure 3.35 Effect Of Nozzle Geometry On Far-field Acoustic Power Normalized W.R.T. Incident Power, For M_J = 0.8, M_T = 0.00, T_R = 600 K

⊡ , daisy lobe nozzle; ⊙ , reference conical nozzle

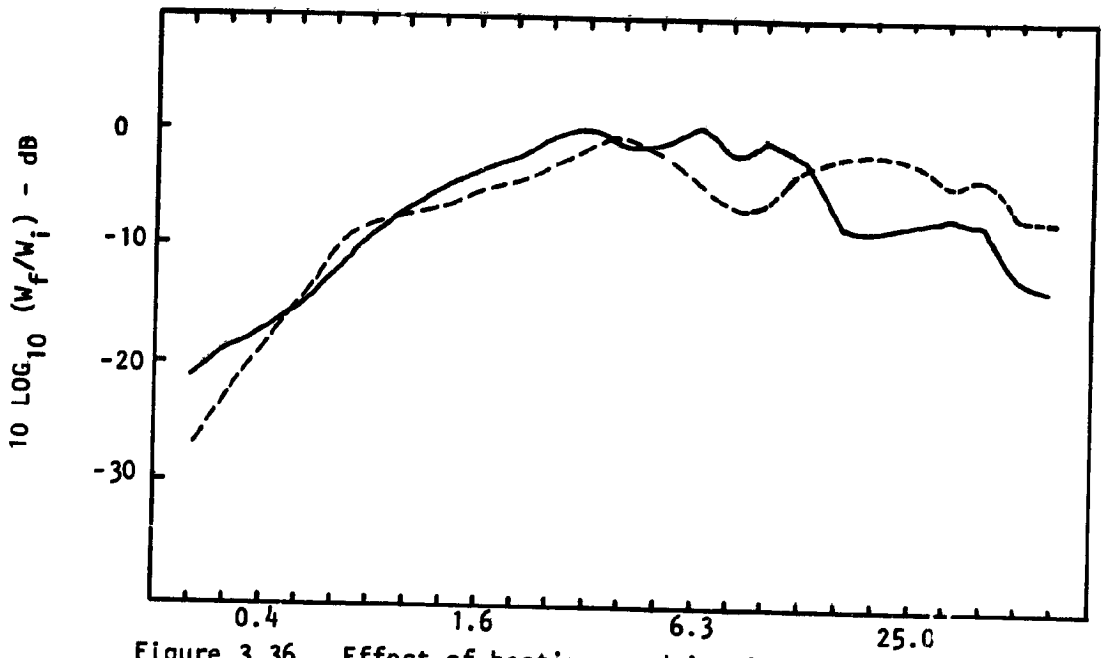

Figure 3.36 Effect of heating on daisy lobe nozzle far-field acoustic power normalized w.r.t. incident power at $M_J = 0.8$
T_R: ———, Ambient; – – – –, 600 K

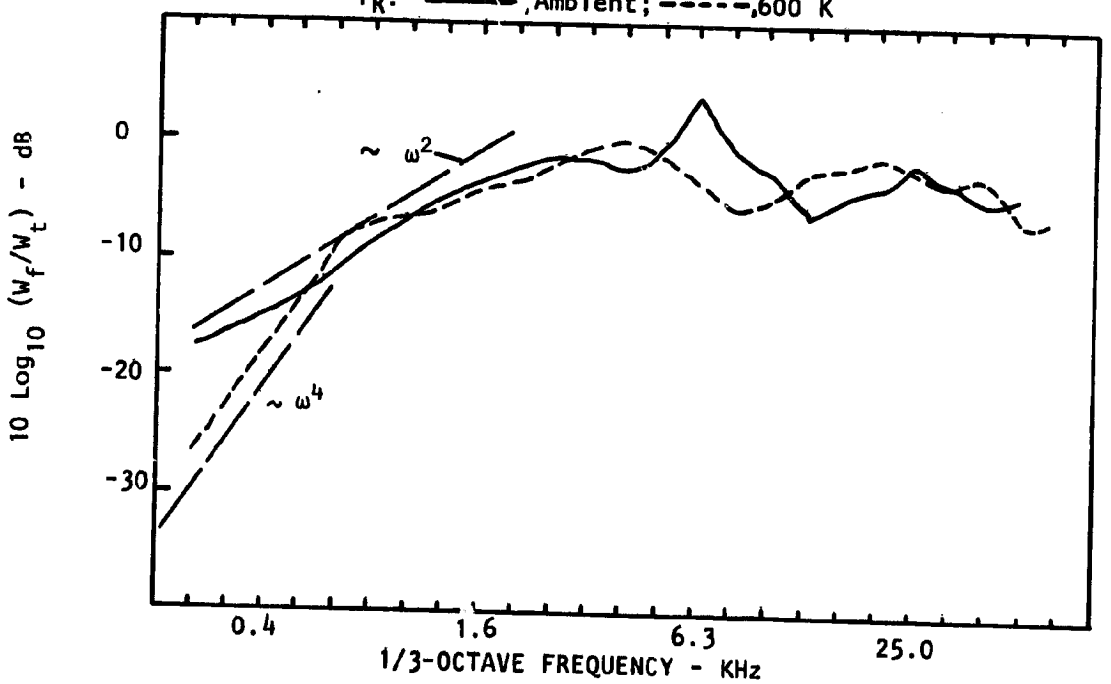

Figure 3.37 Effect of heating on daisy lobe nozzle far-field acoustic power normalized w.r.t. transmitted power at $M_J = 0.8$.
T_R: ———, Ambient; – – – –, 600 K

small angles and increased levels at larger angles.

(2) Conical nozzles radiate more efficiently than the daisy lobe nozzle when the jets are heated. This effect is more important at small angles to the jet axis.

(3) For a given incident power, the daisy lobe nozzle, when heated, transmits 2 to 3 dB less than the conical nozzle at frequencies lower than 12.5KHz. At higher frequencies the daisy lobe nozzle radiates 4 to 5 dB higher than the conical nozzle.

(4) Power conservation results for the heated data are similar to those for the unheated jets. Considerable power loss at low frequencies is noticed and it is even higher than the unheated jets for f<500Hz. Here the PTF follows a fourth power of the frequency dependence .

(5) As for the unheated jets no clear cut answers are available to explain many of these results.

3.3 FLIGHT EFFECTS

Results similar to those presented in sections 3.1 and 3.2 for the static conditions will now be presented for both nozzles operated under flight simulation. All data presented here are corrected to ideal wind tunnel conditions (IWT) using a free-jet shear layer correction program developed at Lockheed (ref. 3.10). It should be noted that whenever reference is made to an *angle* it is the emission angle and not the measured angle. It was assumed, in these calculations, that the source was located at the center of the nozzle exit.

3.3.1 Time Histories

Time histories, both in-duct and far-field, measured under flight simulation had shapes very similar to those measured statically, but had certain quantitative differences. For example, the in-duct time histories for the daisy lobe nozzle operated at $M_j = 0.6$ (unheated) at various tunnel velocities are shown in Figure 3.38. An important observation to be made here is that as the flight velocity is increased the relative peak levels between the incident and the reflected signals change. Similar results were obtained for the conical nozzle.

Far-Field time histories were very similar to those observed for the static case. Since to study flight effects one is really interested in the ideal wind tunnel data, which in this case is obtained by applying angle, amplitude and distance corrections to the measured free-jet data, there is not much one can gain from the far-field time histories unless free-jet corrections are applied in the time domain also. We shall, therefore, proceed to discuss the NTC spectra obtained from the IWT data. Some reflection coefficient data will, however, be presented first.

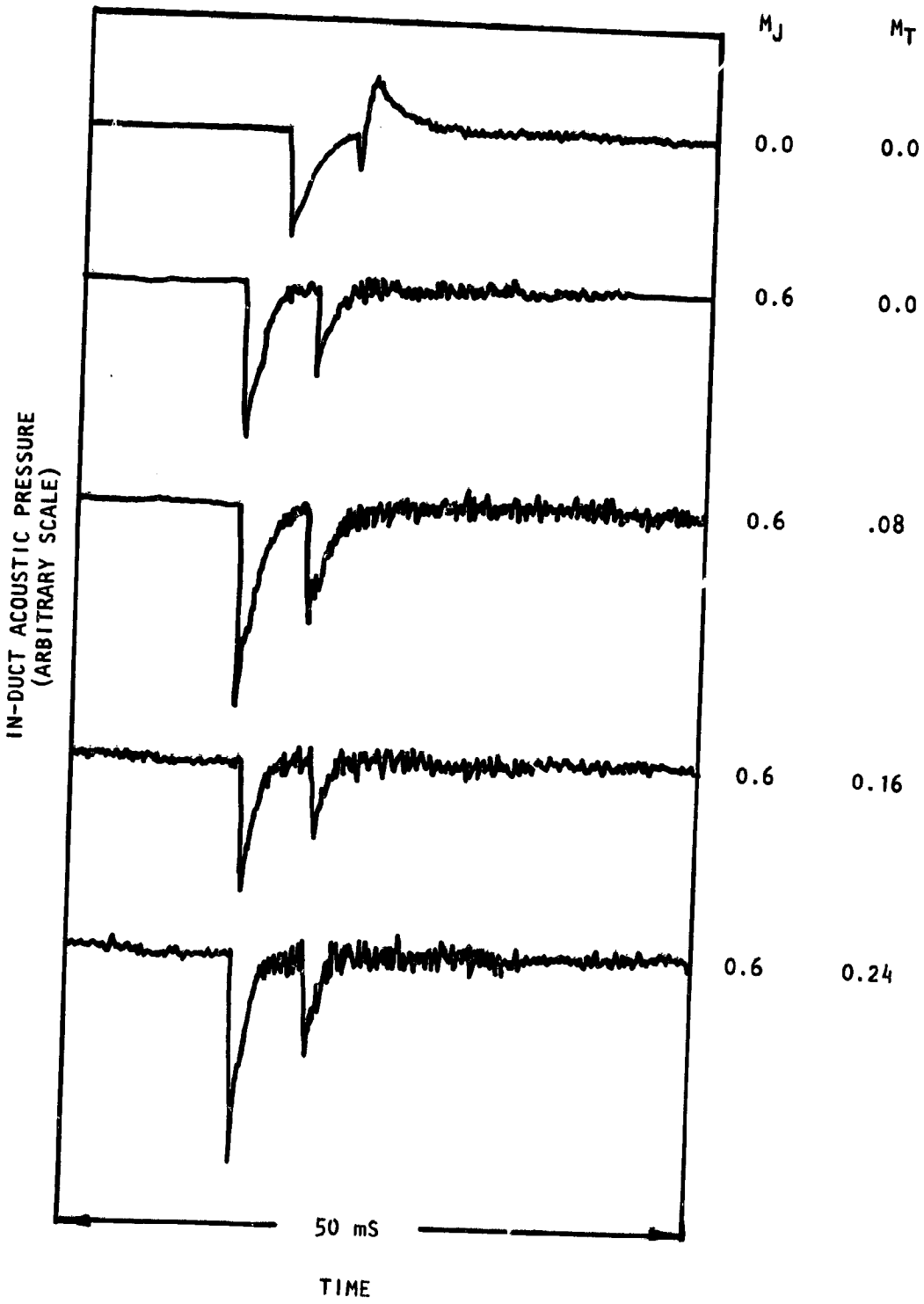

Figure 3.38 Effect of free-jet Mach number on daisy lobe nozzle in-duct time histories (unheated).

3.3.2 Reflection Coefficients

The reflection coefficients as a function of frequency for the time histories presented in Figure 3.38 are shown in Figure 3.39. Reflection coefficient spectra for $M_J = 1.2$ (unheated) are also shown. It is clear from these figures that flight velocity has a consistent trend of either increasing or decreasing the reflection coefficients, depending upon the frequencies (i.e. low or high, etc), as shown by arrows in the figures. But after examining reflection coefficients at other Mach numbers also, it appears that the effect of flight is to reduce the reflection coefficients (in the plane wave region) for the daisy lobe nozzle for all Mach numbers. This is best shown by plotting the reflection coefficients as a function of duct Mach number as shown in Figure 3.40 for frequencies of 400, 630, 800, 1000, 1250 and 1600 KHz. It is found that for the daisy lobe nozzle, the higher the duct Mach number the higher the difference between the static and the flight reflection coefficients. This effect is not as dominant for the conical nozzle as shown in the same figure. As pointed out earlier, since even the static reflection coefficients are not well understood, it is difficult to offer a suitable explanation for the observed effects. Theoretical work in progress at Lockheed under an IRAD program to understand these effects. All that one can say at present is that inducing a secondary stream over nozzles modifies the base pressures which in turn is bound to change the nozzle termination impedance and hence the reflection coefficients.

3.3.3 One-third Octave NTC

We shall start out here by presenting 1/3-octave NTC data at $M_J = 0$ as a function of free-jet Mach number. 1/3-octave NTC corrected for IWT conditions at emission angles of 30°, 60° (rear arc), 90° and 110° (forward arc) are compared in Figure 3.41 for four free-jet Mach numbers, namely, 0.0, 0.08, 0.16 and 0.24. These results are very similar to those observed in our earlier studies (ref. 3.10) for NASA Lewis (Contract NAS3-20050) on effects of flight on jet noise contaminated with internal noise. There it was found that flight simulation reduces noise in the rear arc, has little change at 90° and increases noise in the forward arc. These effects were attributed to the so-called "convective amplification" of internal noise by the free jet. A closer examination of the data presented here discloses the same trend *(as indicated by arrows in Figures 3.41 (a) thru 3.41 (d))*. Similar results were obtained at other jet Mach numbers also as shown in Figure 3.42 for $M_J = 0.8$ for the unheated jet. For the heated jets, however, this effect was not so strong as shown by the 1/3-octave NTC spectra for $M_J = 0.8$ and $T_R = 600K$ in Figure 3.43. This may have been due to the dominance of jet mixing noise at certain frequencies. Directivities for the data of Figure 3.43 are plotted in Figure 3.44 for three typical frequencies, namely 1, 4 and 8 KHz for both the static ($M_T = 0$) and the flight case ($M_T = 0.24$). Here the difference between the static and the flight NTC directivities appears to be a function of frequency. Even though some "convective amplification" type of phenomenon appears to be taking place, the results are contrary to the popular belief that "convective amplification" is independent of frequency. In most published work, however, these effects have been investigated based upon OASPL only [3.10, 3.11, 3.12].

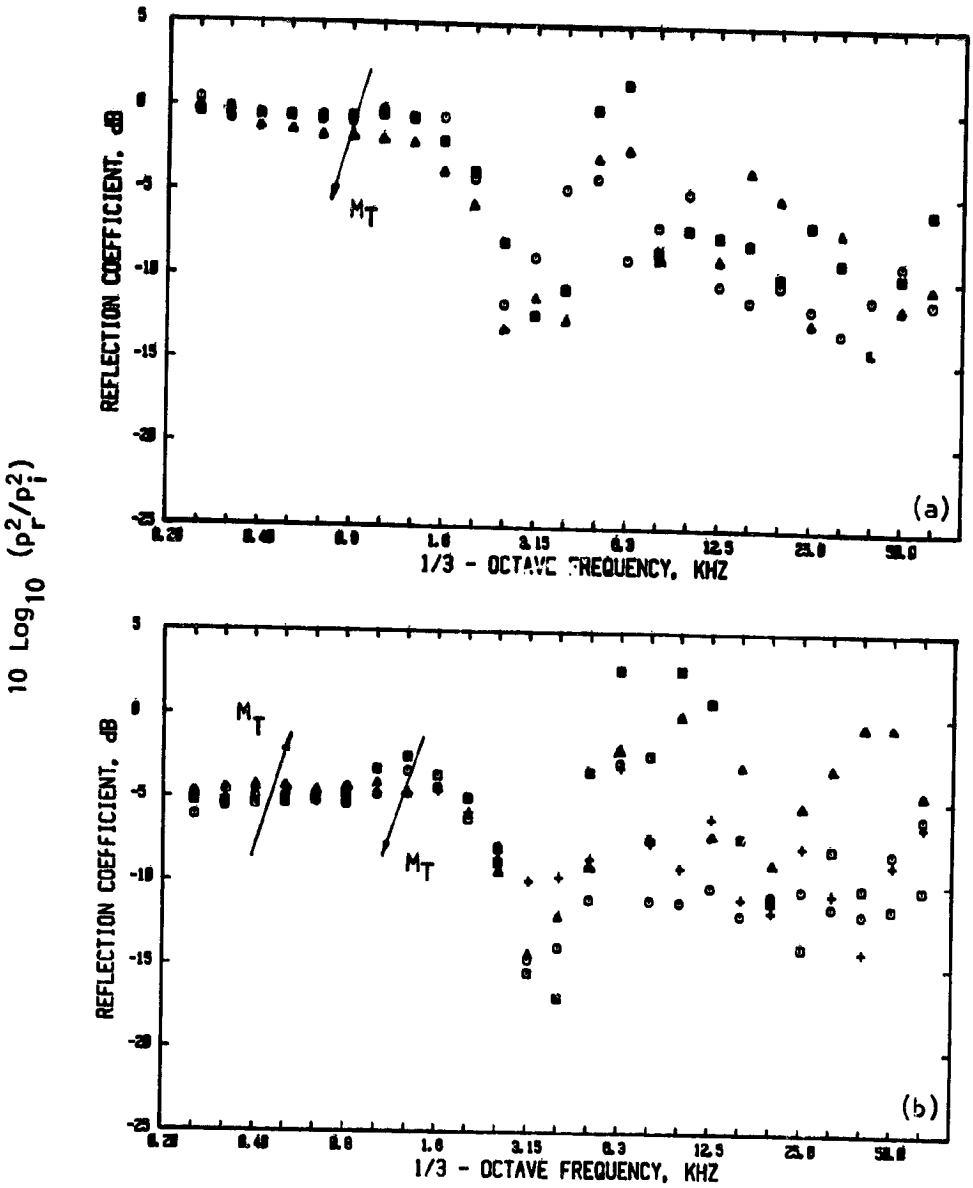

Figure 3.39 Effect of free jet Mach number on reflection coefficients for daisy lobe nozzle at (a) $M_J = 0.6$ and (b) $M_J = 1.2$
M_T: ⊐, 0.0; ⊙ 0.08; △ , 0.16 and + 0.24 (unheated)

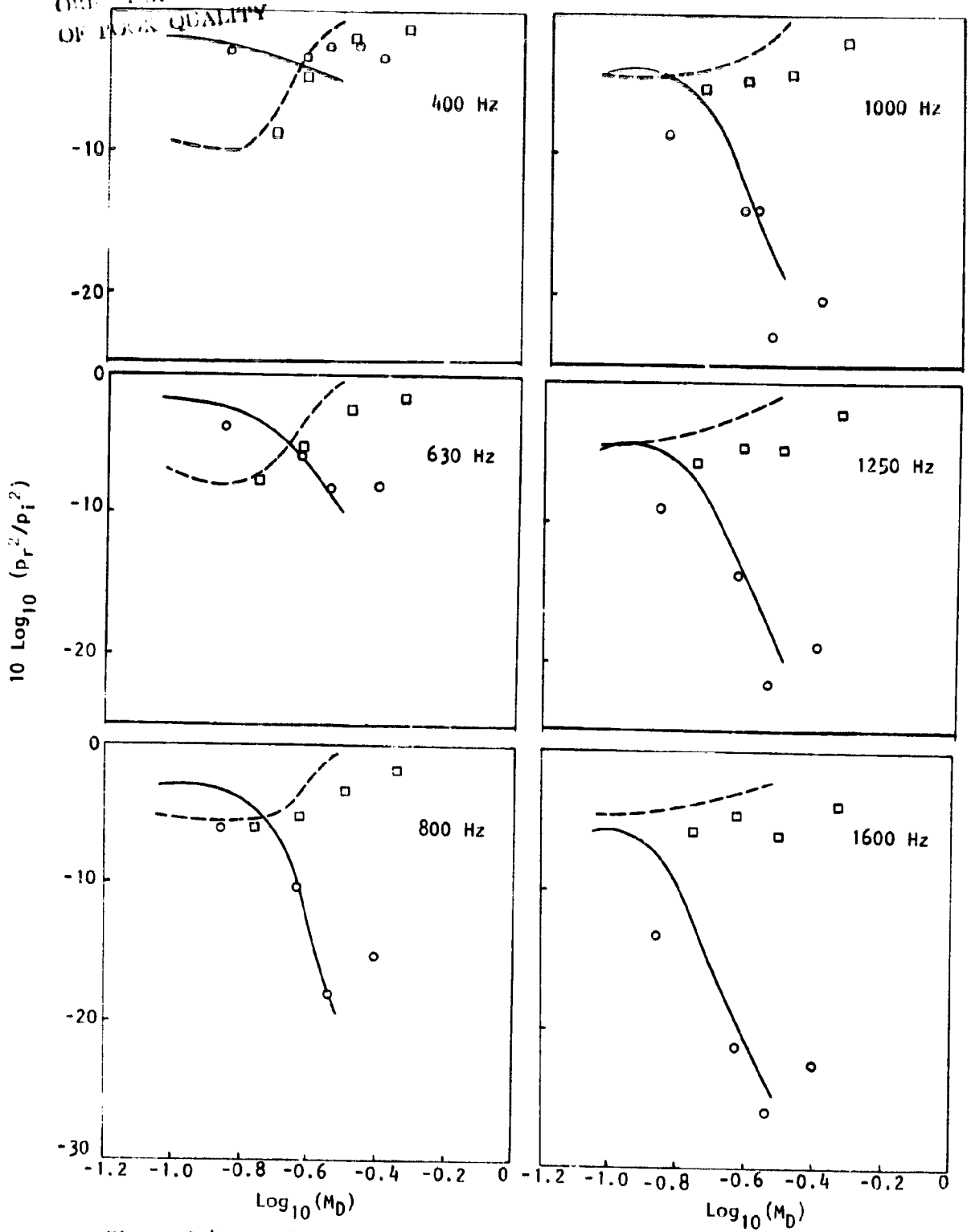

Figure 3.40 Effect of duct Mach number on the reflection coefficients of the daisy lobe nozzle and the reference conical nozzle at various 1/3-octave frequencies.

LEGEND: M_T = 0. - - - - - -, daisy lobe nozzle; ——————, reference conical nozzle
M_T = 0.24. ⊡ , daisy lobe nozzle; ⊙ , reference conical nozzle

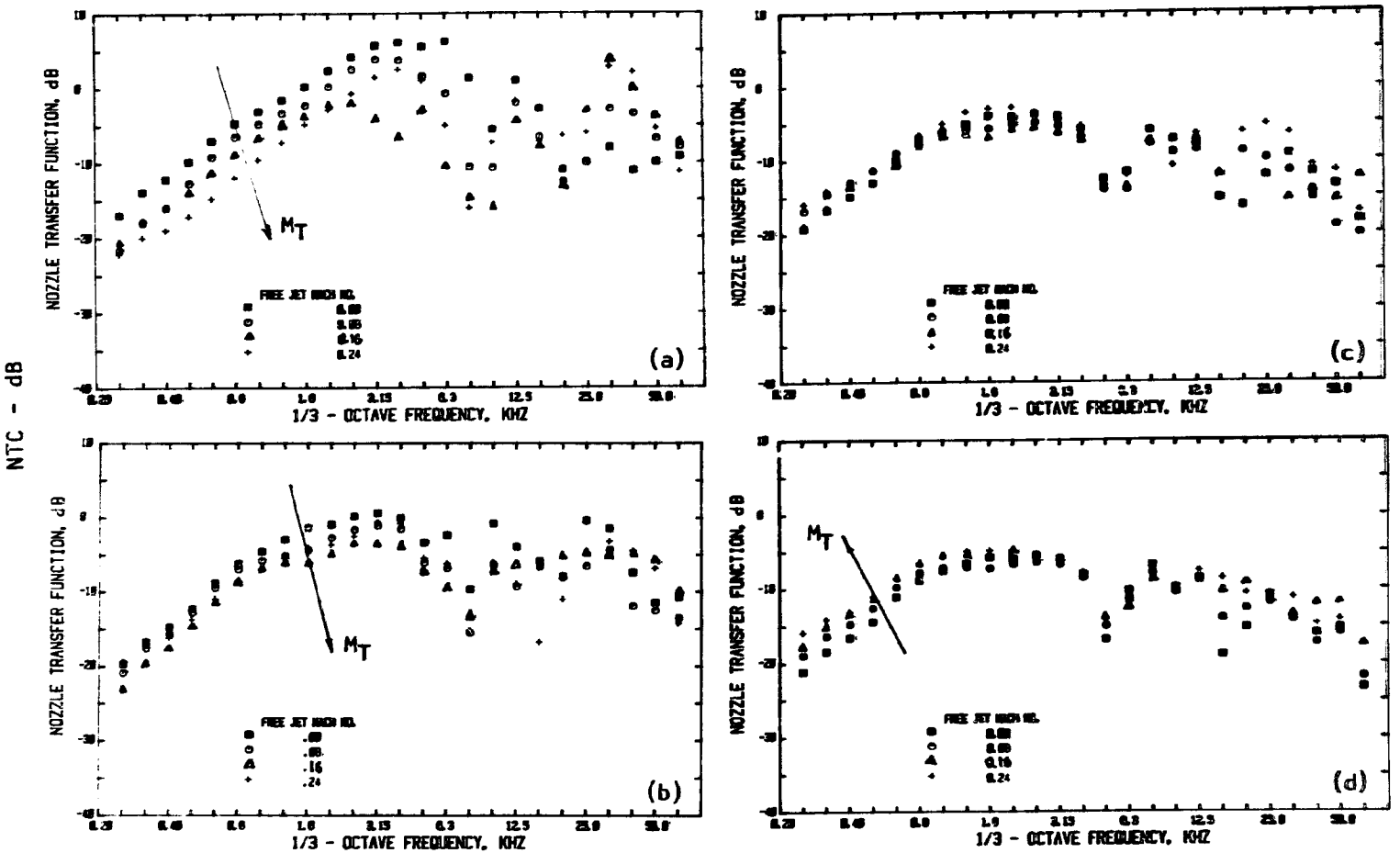

Figure 3.41 Effect of free-jet Mach number on 1/3-octave NTC spectra for the daisy lobe nozzle
θ: (a) 30°, (b) 60°, (c) 90° and (d) 110°
M_T: □ 0.0; o, 0.03; Δ, 0.16 and + 0.24.
($M_J = 0$)

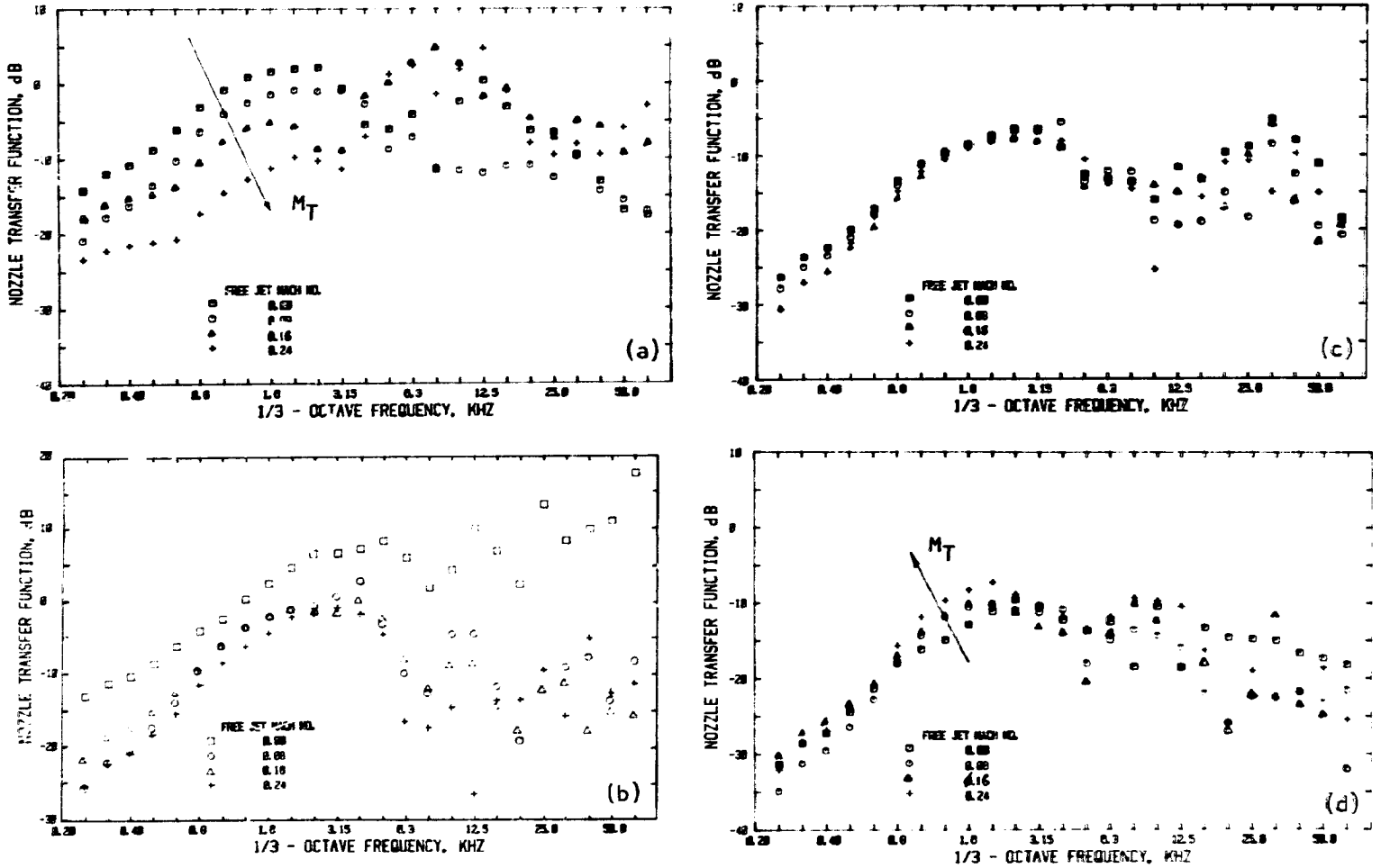

NTC - dB

Figure 3.42 Effect of free-jet Mach number on 1/3-octave NTC spectra for the daisy lobe nozzle
θ: (a) 30°, (b) 60°, (c) 90° and (d) 110°
M_T: □ , 0.0; O , 0.08; Δ , 0.16 and +, 0.24.
($M_J = 0.8$, unheated)

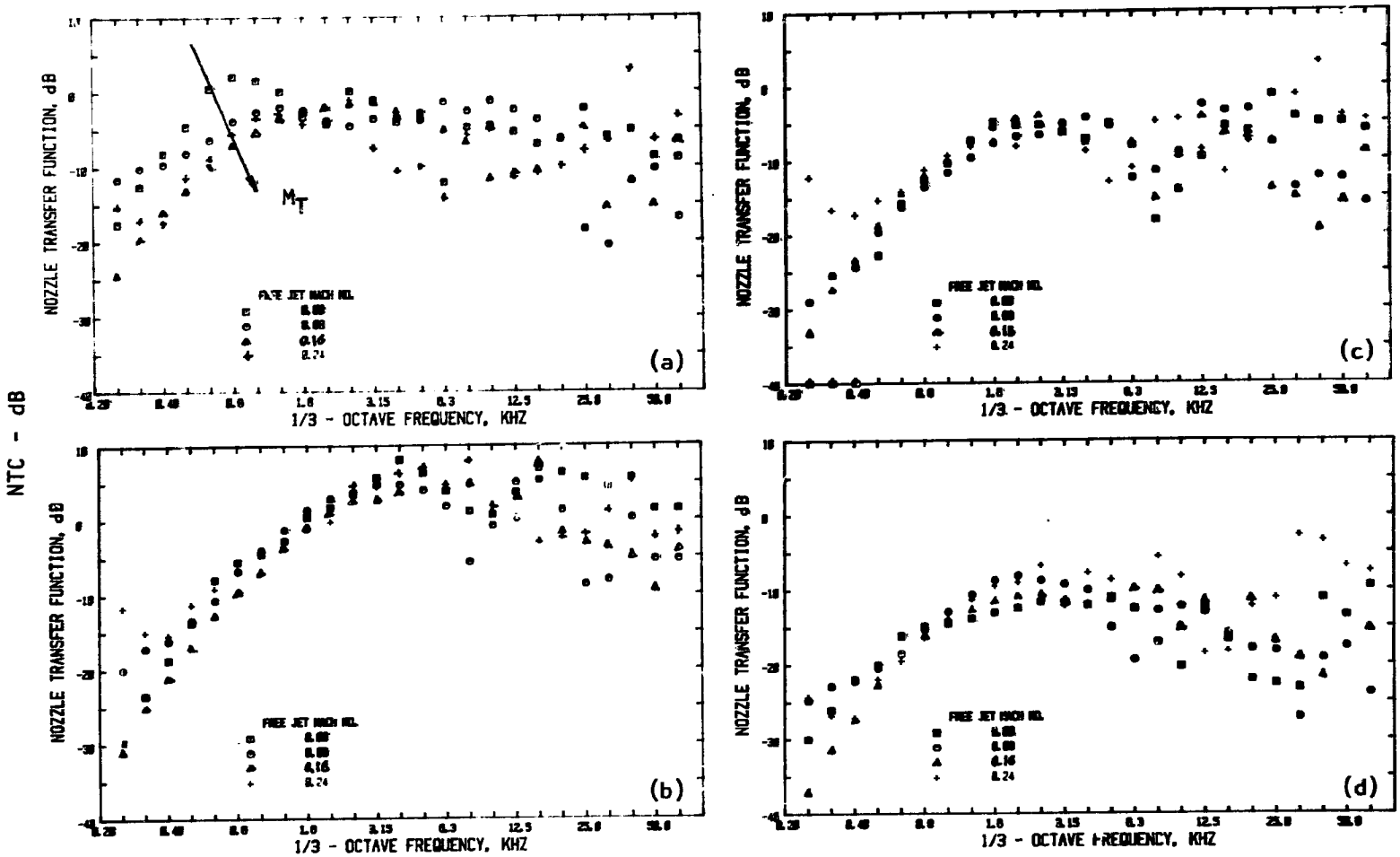

Figure 3.43 Effect of free-jet Mach number on 1/3-octave NTC spectra for the daisy lobenozzle
θ(a) 30°, (b) 60°, (c) 90° and (d) 110°
M_T: □ , 0.0; ○ , 0.08; △ , 0.16 and +, 0.24.
($M_J = 0.8$, $T_R = 600K$)

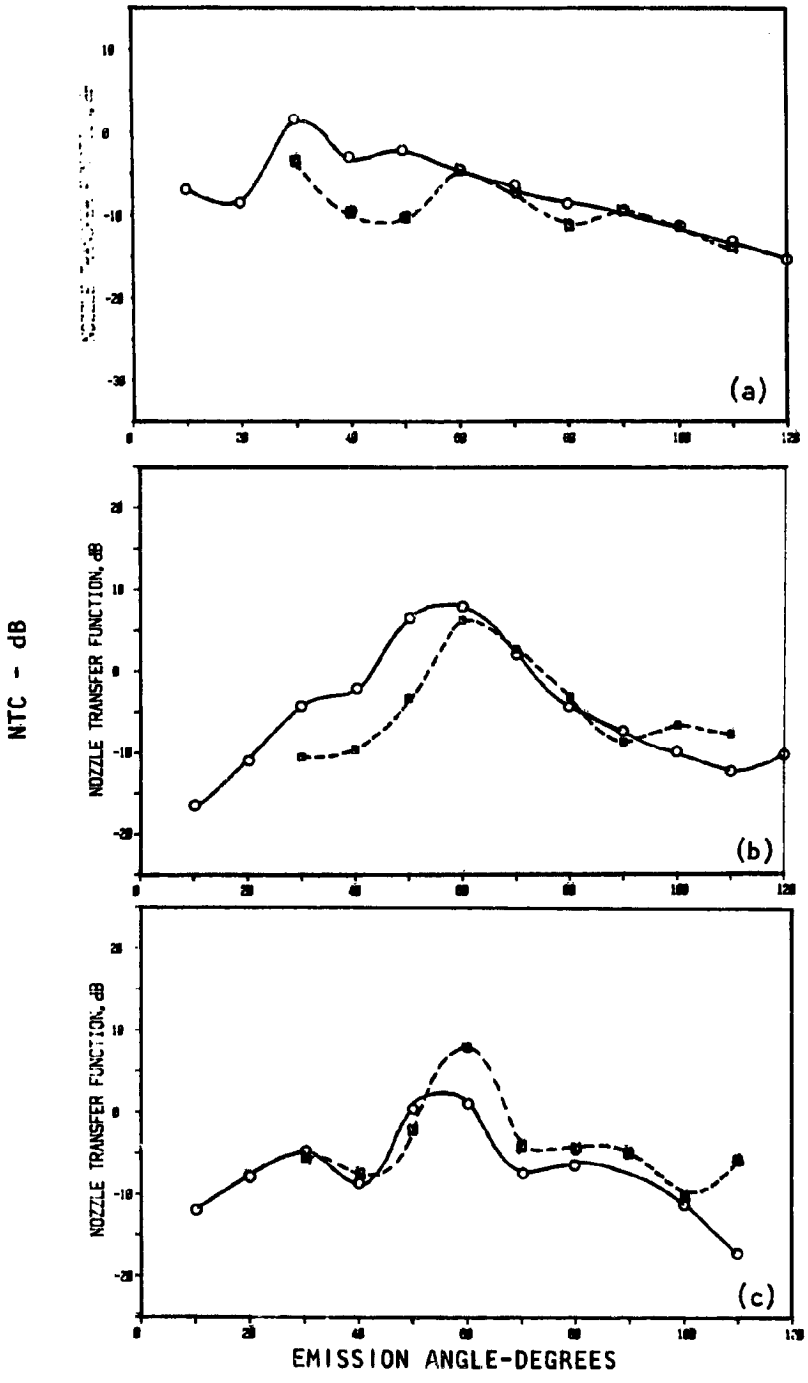

Figure 3.44 Effect free-jet Mach number on NTC directivities of the daisy lobe nozzle.
f: (a) 1 KHz, (b) 4 KHz and (c) 8 KHz
M_T: -○-, 0.0 and ··□··0.24
($M_J = 0.8$, $T_R = 600K$)

Further work is, therefore, needed to understand these results.

3.3.4 Acoustic Power

Far-field acoustic powers were found to decrease with forward velocity for all jet Mach numbers. This is shown in Figure 3.45. Far-field acoustic powers (W_f) normalized with respect to the incident power (W_i) for $M_J = 0$, 0.6 and 0.8 are shown as a function of free-jet Mach number. It is seen that there is up to 10 dB difference between the static and flight case (e.g., see Figure 3.45 (b) and compare $M_T = 0.0$ and 0.24 data). These results are further shown as a function of frequency and V_J/c_o in Figure 3.46. Here it is found that the slope of PTF_i versus Log (V_J/c_o) for the static case remains the same for each frequency but that for the flight case increases with frequency. The flight data is always lower than the static data.

The reason for the above behavior is not known. It is possible, however, that the low frequency absorption noticed in the static case has been augmented by the additional vortex shedding from the outer lip of the nozzles. Due to completely different exit geometries, the shear layer quite close to the exit in the flight simulation mode is expected to be quite different in terms of the local velocity and temperature gradients. If this is an important parameter in determining the far-field powers a comparison of these acoustic powers for the two nozzles should vary with respect to each other in some systematic manner as the relative velocities between the model jet and the free-jet are changed. It indeed was found to be so as shown in Figure 3.47. The far-field acoustic powers, for the two nozzles, normalized with respect to the incident power are compared in this figure at $M_J = 0.0$, 0.6 and 0.8 for a constant free-jet Mach number of 0.24. It is seen that as the jet Mach number is increased the daisy lobe acoustic power starts decreasing with respect to that from the reference conical nozzle.

To determine the effect of flight on low frequency absorption noticed earlier for the static case, the data of Figure 3.47 is replotted by normalizing the far-field power (W_f) with respect to the transmitted power (W_t). This is shown in Figure 3.48 for $M_J = 0.0$, 0.6 and 0.8 and tunnel Mach number, $M_T = 0.24$. Data for both the daisy lobe and the reference conical nozzle are compared. Similar to the results for the static case, low frequency absorption is noticed. At $M_J = 0$, the conical nozzle displays more low frequency absorption than the daisy lobe nozzle. At $M_J = 0.6$, this absorption is almost the same for both nozzles while the trend is reversed at $M_J = 0.8$ where the daisy lobe nozzle now displays more low frequency absorption than the conical nozzle. The reason for this is not quite clear. It is reasonable, however, to assume that due to different geometries of the two nozzles, the flow structure in the wake formed by each nozzle, operated in the flight-simulation mode, will be different. If the low-frequency absorption is indeed caused by the vortex shedding at the nozzle exit, as proposed by Bechert [3.3], it will undoubtedly be influenced by the fluid-dynamics of this nozzle-wake. Understanding this phenomenon in detail will require proper flow surveys and flow visualization at and downstream of the nozzle exit which was beyond the scope of the present program.

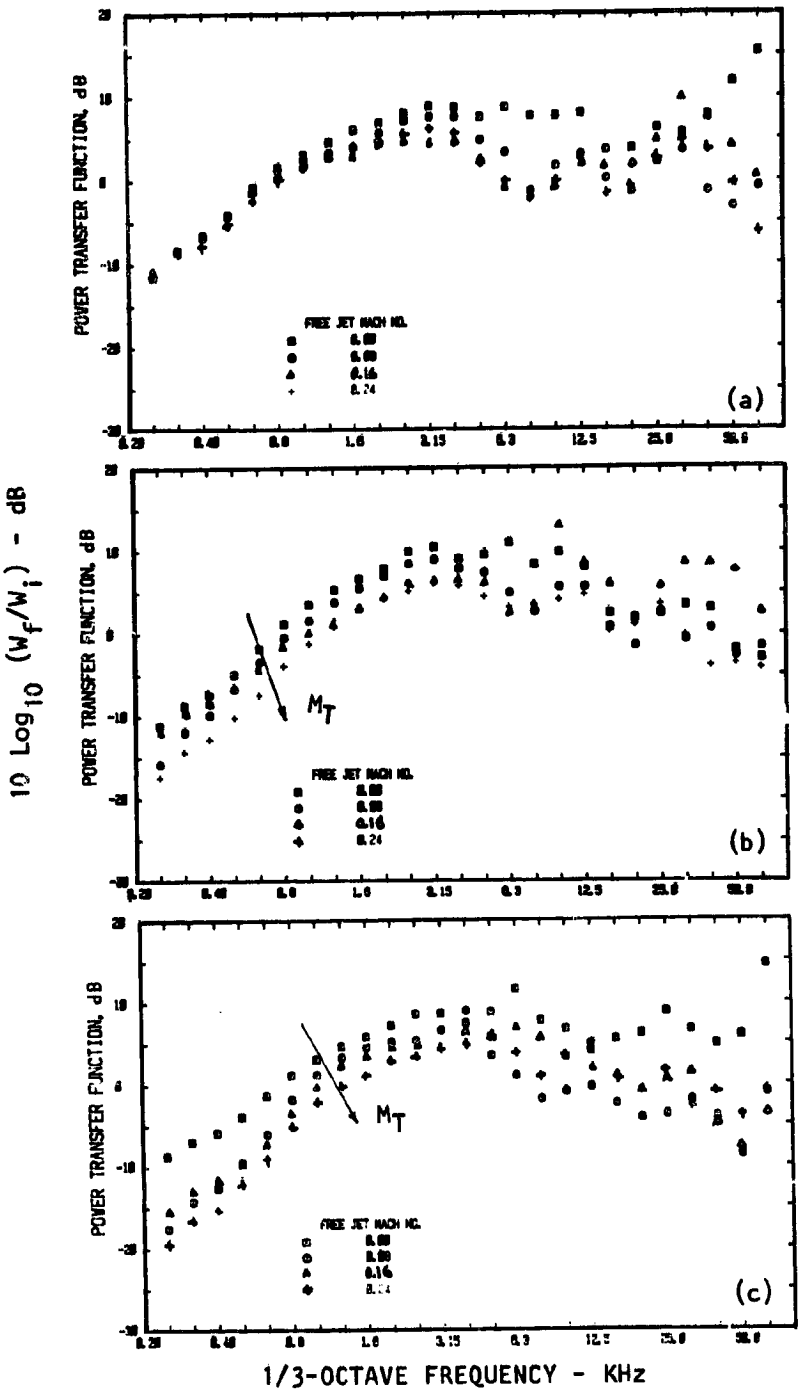

Figure 3.45 Effect of free-jet Mach number on far-field acoustic power levels of the daisy lobe nozzle at various jet Mach numbers (unheated)
M_J: (a) 0.0, (b) 0.6 and (c) 0.8
M_T: ⊡ , 0.0; ⊙ , 0.08; ▲ 0.16; + 0.24

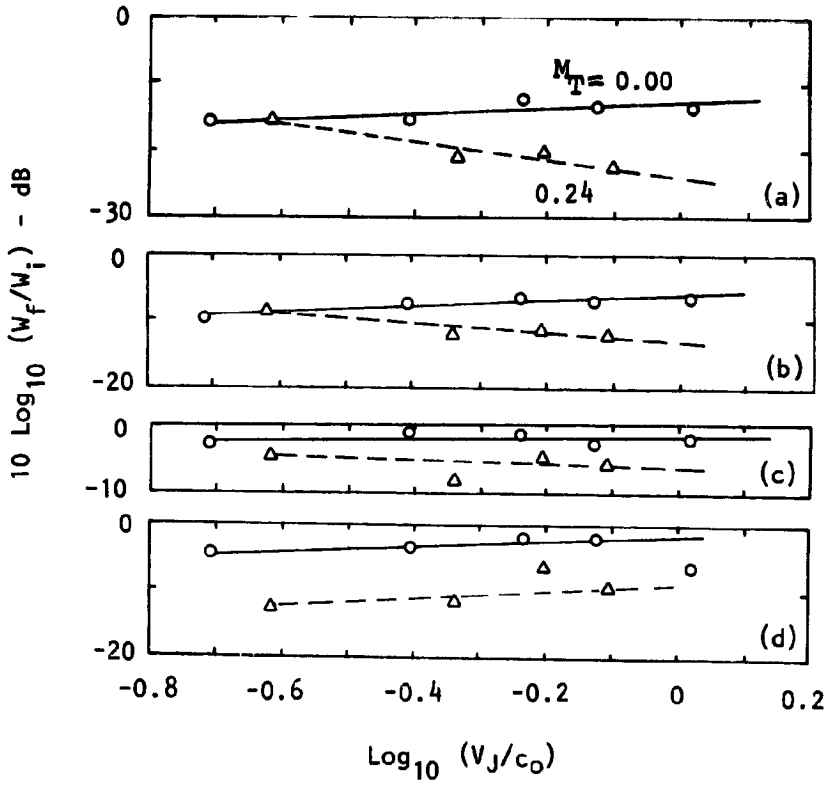

Figure 3.46 Effect of free-jet Mach number on the far-field acoustic power levels of the daisy lobe nozzle at various jet Mach numbers and frequencies, (a) f - 500 Hz, (b) f - 1 KHz, (c) f - 4 KHz, and (d) f - 8 KHz.

Legend: M_T = -0-, 0.0;--Δ--, 0.24

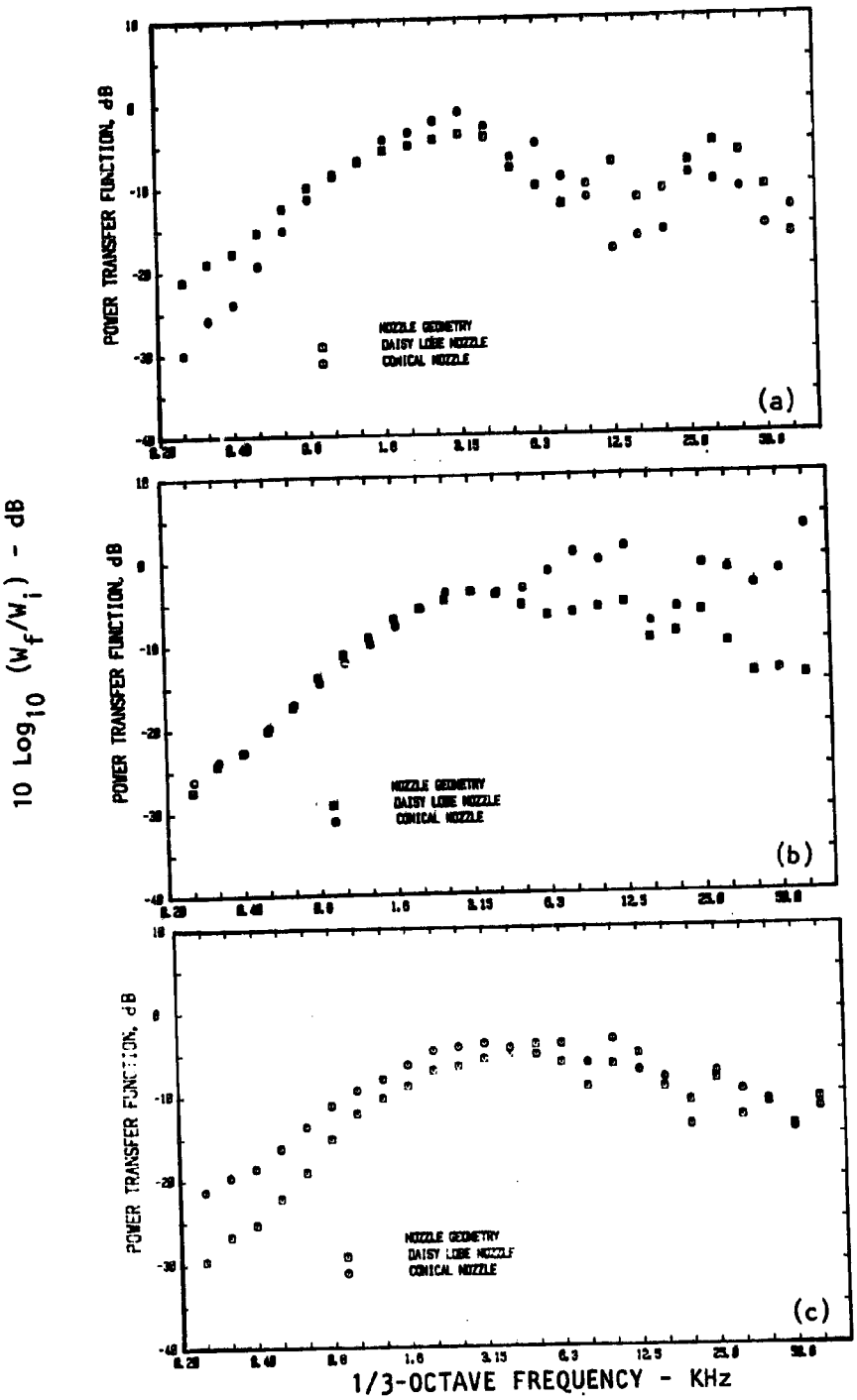

Figure 3.47 Effect of nozzle geometry on far-field acoustic power normalized w.r.t. incident power at $M_T = 0.24$. M_J: (a) 0.0, (b) 0.6 and (c) 0.8
⊡ , daisy lobe nozzle; ⊙ conical nozzle.

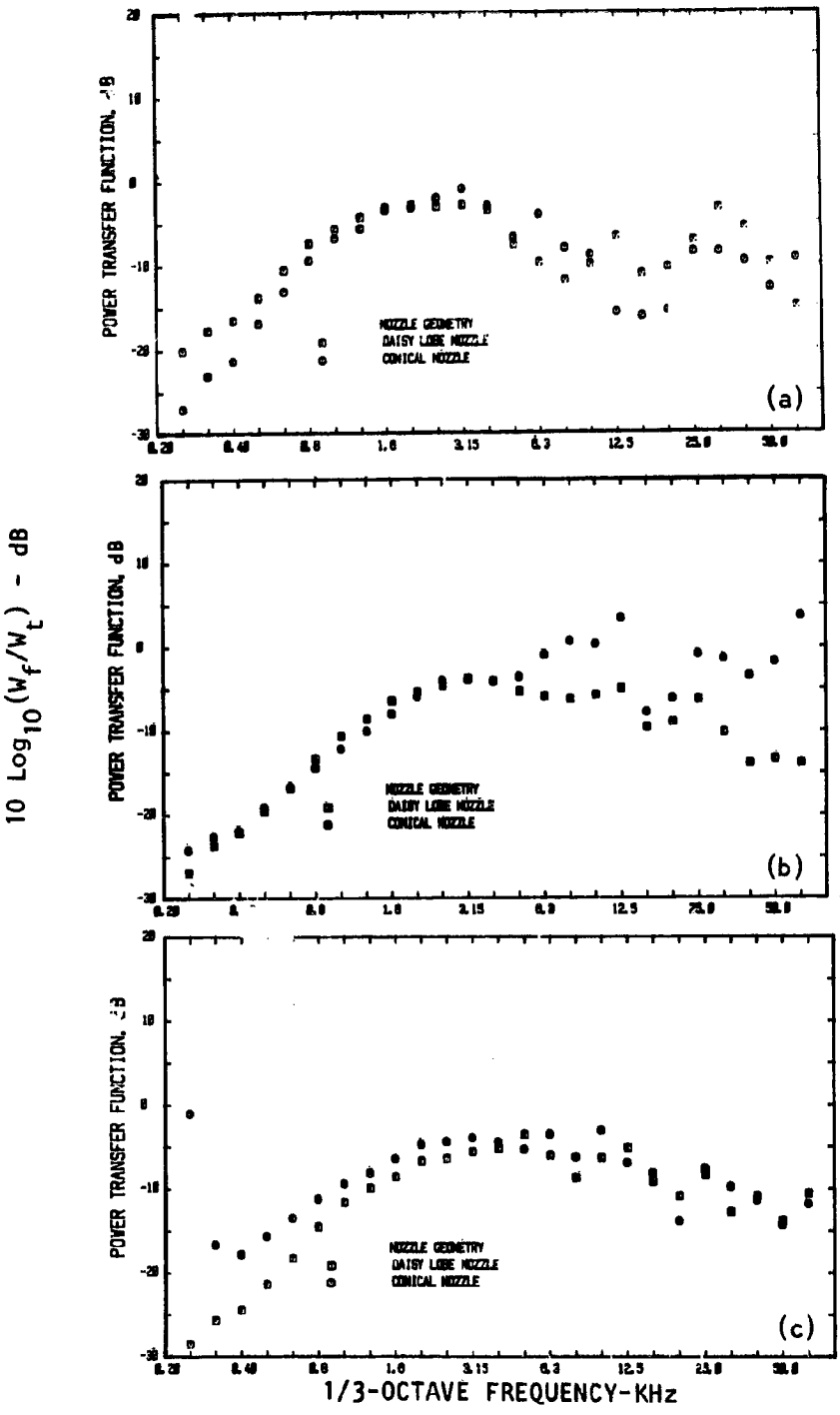

Figure 3.48 Effect of nozzle geometry on far-field acoustic power normalized w.r.t. transmitted power at $M_T = 0.24$. M_J: (a) 0.0, (b) 0.6 and (c) 0.8 (unheated) □ , daisy lobe nozzle; O , conical nozzle .

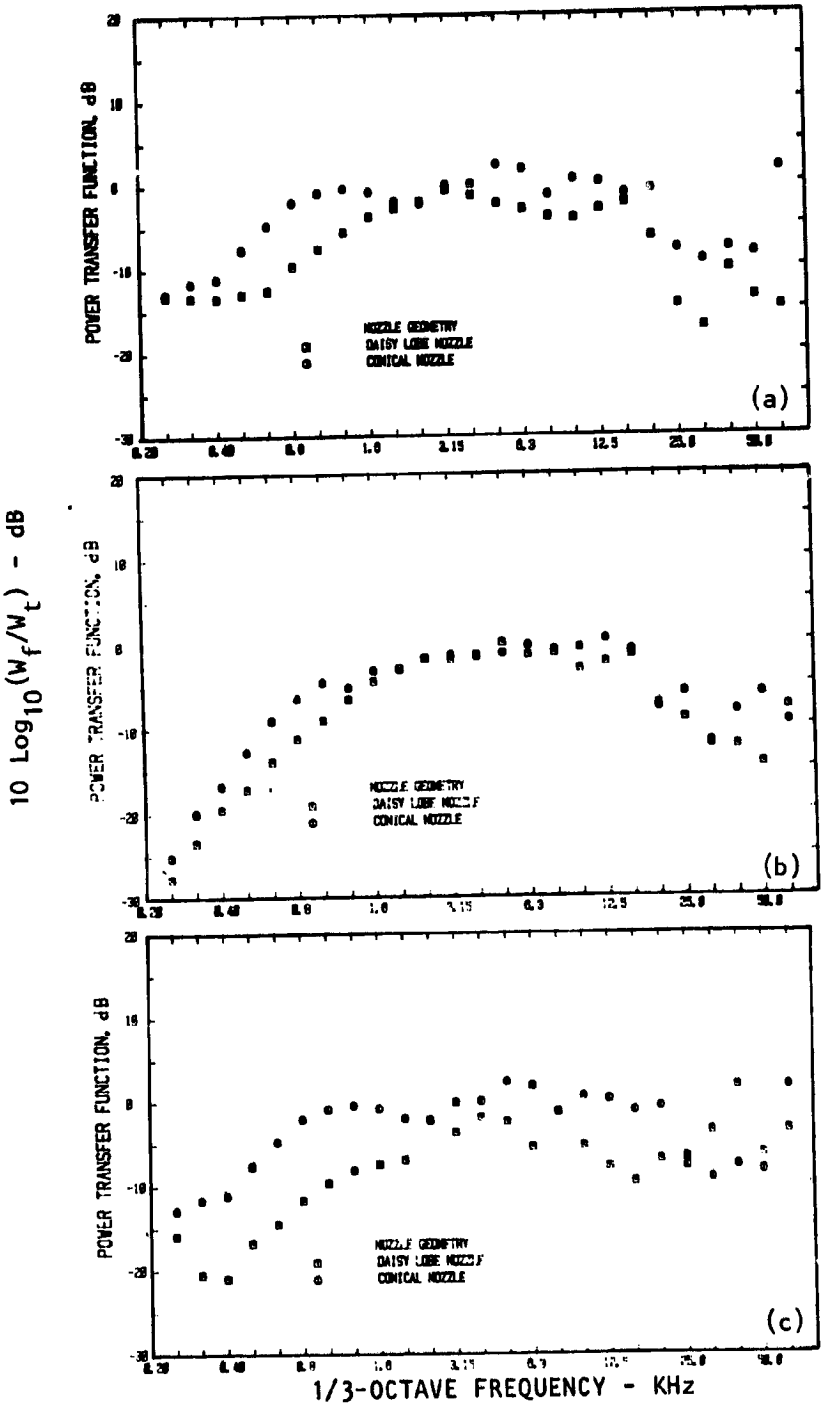

Figure 3.49 Effect of nozzle geometry on far-field acoustic power normalized w.r.t. transmitted power at $M_J = 0.8$ ($T_R = 600K$)
M_T: (a) 0.08, (b) 0.16 and (c) 0.24

Low frequency absorption was noticed for heated jets also, operated under flight simulation, as shown in Figure 3.49. Here the PTF_t spectra at $M_J = 0.8$ and $T_R = 600K$ for $M_T = 0.08$, 0.16 and 0.24 are plotted for both nozzles. The difference between the PTF_t values for the two nozzles changes as the relative velocity between the main jet and tunnel is varied. Due to a lack of data at other temperatures it is difficult to generalize these results at this stage.

Further work, both experimental and theoretical, is certainly warranted to understand these results. A theoretical study to understand the low frequency absorption has already been initiated at Lockheed.

3.3.5 Flight Effects - Summary

Results for free jet Mach numbers of 0.0, 0.08, 0.16 and 0.24 for the daisy lobe nozzle and the reference conical nozzle have been presented for a range of flow conditions. All data have been corrected for ideal wind tunnel conditions. The following four conclusions have been reached.

(1) The reflection coefficients decrease with free-jet Mach number.

(2) There is a tendency for the NTC values to decrease in the rear arc and increase in the forward arc with forward velocity.

(3) Far-field acoustic powers decrease with increasing free-jet Mach number.

(4) For $M_J>0$, there is more low frequency absorption for the daisy lobe nozzle (compared to the conical nozzle), and vice versa at $M_J = 0$.

Similar to the results for the static conditions, most results in this section can not be explained even though they were found to be consistent as a function of free-jet Mach number. A better plan should have been to complement the experimental program with a parallel theoretical study. Unfortunately the original program was only to obtain the nozzle transmission coefficients. A theoretical study to explain some of the observed effects has now been initiated at Lockheed and the results will be published in due course.

3.4 CONCLUSIONS

Important conclusions are summarized below:

Static Data

(1) The daisy lobe nozzle displays higher reflection coefficients than the reference conical nozzle at almost all flow conditions.

(2) For both nozzles, the effect of flow is to gradually reduce the reflection from the jet opening and increase the reflection from the solid parts (e.g. nozzle shoulder). At under-expanded conditions all reflection appears to be from the solid parts.

(3) The trends in variation of reflection coefficients with frequency are exactly opposite for the two nozzles. The daisy lobe reflection coefficient increases with frequency while that for the conical nozzle decreases with frequency for almost all frequencies.

(4) Reflection coefficients at very low frequencies for conical nozzles are higher than unity for high jet Mach numbers.

(5) At zero flow conditions, the radiation is predominantly towards the jet axis. With flow, refraction becomes important and the peaks in the directivities shift towards higher angles.

(6) Deductions made about the far-field radiation based upon reflection coefficients do not necessarily hold. For static conditions, both nozzles have remarkably similar far-field NTC directivities and spectra at subsonic Mach numbers even though the nozzle geometries and the reflection coefficient characteristics are quite different.

(7) Exit area of the nozzles appear to determine the shape and levels of the far-field spectra.

(8) The far-field acoustic power at low frequencies follows an ω^2 relationship for unheated jets and an ω^4 relationship for heated jets.

(9) At low frequencies, the far-field acoustic power is always less than the incident power.

(10) Jet Mach number has little effect on far-field power, especially at low frequencies.

(11) Power balance at low frequencies is not obtained both with and without flow. No immediate explanations are available for this result at the zero flow condition.

(12) When the jet is heated, the conical nozzle radiates more efficiently than the daisy lobe nozzle, especially at small angles to the jet .

Flight Simulation Data

(13) Forward velocity reduces reflection coefficients, decreases NTC in the rear arc, has little effect at 90° and increases radiation in the forward arc.

(14) Far-field acoustic powers are also reduced under flight simulation.

(15) Under flight conditions, exit area alone may not be a good parameter to determine the shape and levels of the far-field spectra. Further work needs to be done to determine the effect of true flow conditions at the nozzle exit on sound transmission.

(16) Under flight-simulation, the daisy lobe nozzle displayed more low frequency noise absorption than the conical nozzle, exept for $M_J = 0$.

4. TRANSMISSION RESULTS FOR MULTI-CHUTE SUPPRESSOR

Characteristics of internal noise radiation from the 36-chute coaxial suppressor nozzle tested only statically for both the unheated and the heated conditions are presented here. Effects of primary and secondary *jet Mach numbers* on the nozzle transmission coefficients and the power transfer functions are described first in section 4.1. Results showing the effects of *heating* either one or both of the coaxial streams on these transmission parameters are then presented in section 4.2. Wherever possible the results for the suppressor nozzle are compared with those for the reference coaxial nozzle for identical flow conditions. Finally, the conclusions are given in section 4.3.

4.1 MACH NUMBER EFFECTS

Experimental results showing the effects of changing the jet Mach number ratio for unheated jet conditions on the transmission characteristics of the multi-chute suppressor as well as the reference coaxial nozzle are presented in this section. The selection of the primary and the secondary jet Mach numbers for the present study, as stipulated by NASA-Lewis and described in section 2.2, was based upon the representative Mach numbers of the full-scale engines. The Mach numbers from one test point to another did not necessarily vary in a systematic manner. The limited test conditions, at which the data was acquired, were thus not altogether adequate for a fundamental study. The results presented here, therefore, are more representative of trends rather than conclusive evidence of the observed behavior.

4.1.1 Time Histories

As described in section 2.1.4, the source section for the multi-chute nozzle was different from that used for the daisy lobe nozzle. *First*, instead of a single spark plug, six spark plugs with their gaps located at the foci of paraboloidal reflectors were used as the impulsive sound source and were equi-spaced circumferentially within the annular plenum chamber upstream of the nozzle exit. *Second*, the source section was located only 74 cm upstream of the exit instead of 6 m as for the daisy lobe nozzle. For these reasons, both the in-duct and the far-field time histories for the multi-chute as well as the reference coaxial nozzle had different shapes compared with those for the daisy lobe suppressor nozzle tested in a different facility. For example, the incident wave, instead of being a single pulse, now consisted of four sharp pulses followed by minor fluctuations of much lower amplitude. This incident signal was found to be repeatable for fixed flow conditions. The reflected signal, however, was not defined well enough *for suitable editing* and has not been considered in this section.

Similar to the in-duct signal, the far-field signal also had multiple pulses. Identical signals were measured in the far-field as a function of azimuthal angle. Thus it did not matter whether the far-field arc was along one of the flow chutes or along one of the vented chutes. The measurements were made, however, with the polar arc lying in a plane passing through the center line of the jet system and also one of the flow chutes.

Typical in-duct and far-field time histories at $\theta = 10°$, 30", 50°, 90° and 120° (with the jet axis) are shown in Figure 4.1 for $M_{J1} = M_{J2} = 0$. In addition to the features discussed above, it is found that the pulses close to the jet axis are much peakier than those at larger angles. This indicates that the data at large angles is dominated by low frequency noise while that close to the jet axis contains all frequencies.

As the flow is superimposed, the high-frequency sound from small angles refracts to the higher angles. This effect is shown in Figure 4.2 for $M_{J1} = 0.4$ and $M_{J2} = 0.6$. The sharp peak at $\theta = 10°$ has virtually vanished and the pulse at 50° of Figure 4.1 has now become much peakier. As also seen for the daisy lobe suppressor, this is indicative of high frequency from the small angles being refracted to the larger angles. These results will now be considered in the frequency domain.

4.1.2 One Third Octave NTC

VARIATION WITH ANGLE. The variation of 1/3-octave NTC spectra with measurement angle and jet conditions are presented in Figures 4.3 [illegible] 4.6 for both the multi-chute suppressor as well as the reference coaxial nozzle. Details of the relevant conditions for the NTC data presented in these figures is given below in Table 4.1. All data is for both streams unheated ($T_{R_1}/T_{R_2} = 1$)

Table 4.1 Operating jet conditions for the data of figures 4.3 thru 4.6.

Figure No.	Nozzle Type	M_{J_1}	M_{J_2}	V_{J_2}/V_{J_1}
4.3(a)	Multi-chute	0.0	0.0	-
4.3(b)	Ref. Coaxial	0.0	0.0	-
4.4(a)	Multi-chute	0.4	0.6	1.50
4.4(b)	Ref. Coaxial	0.4	0.6	1.50
4.5(a)	Multi-chute	0.0	1.2	∞
4.5(b)	Ref. Coaxial	0.0	1.2	∞
4.6(a)	Multi-chute	0.8	1.2	1.40
4.6(b)	Ref. Coaxial	0.8	1.2	1.40

It should be noted that, for Figures 4.5 and 4.6, only 30° and 60° data is compared. The spectra in these figures are for the fan-jet operated at under-expanded conditions ($M_{J_2} = 1.2$). For these conditions, the reference coaxial nozzle produced much higher jet mixing and shock associated noise than the multi-chute nozzle. For the coaxial nozzle, the pulse in the far-field was, therefore, considerably contaminated at larger angles. Comparison at larger

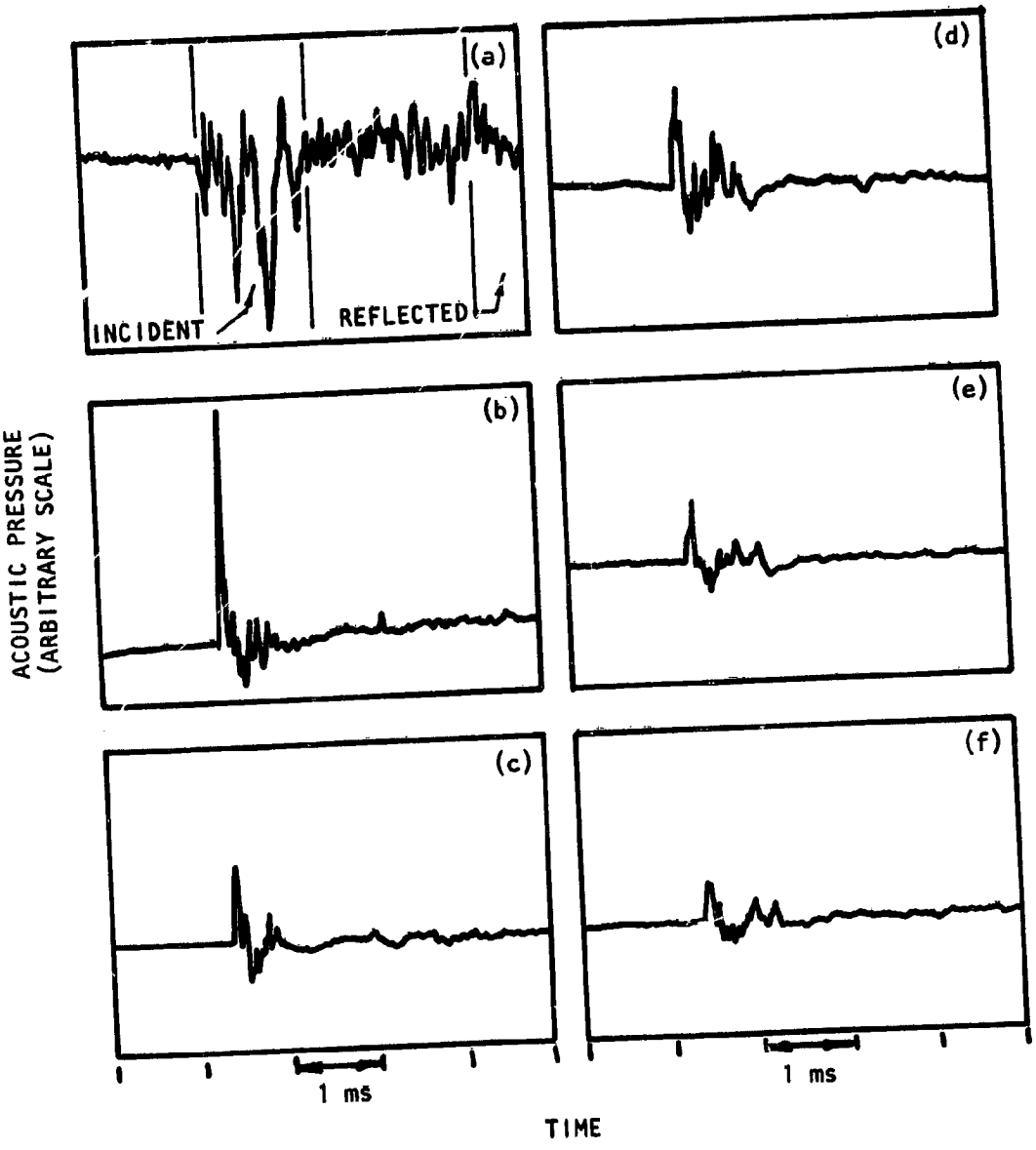

Figure 4.1 In-duct and far-field pressure time histories for the multi-chute suppressor nozzle at $M_{J_1} = M_{J_2} = 0$ (a) In-duct, (b) $\theta = 10°$, (c) $\theta = 30°$, (d) $\theta = 50°$ (e) $\theta = 90°$ and (f) 120°.

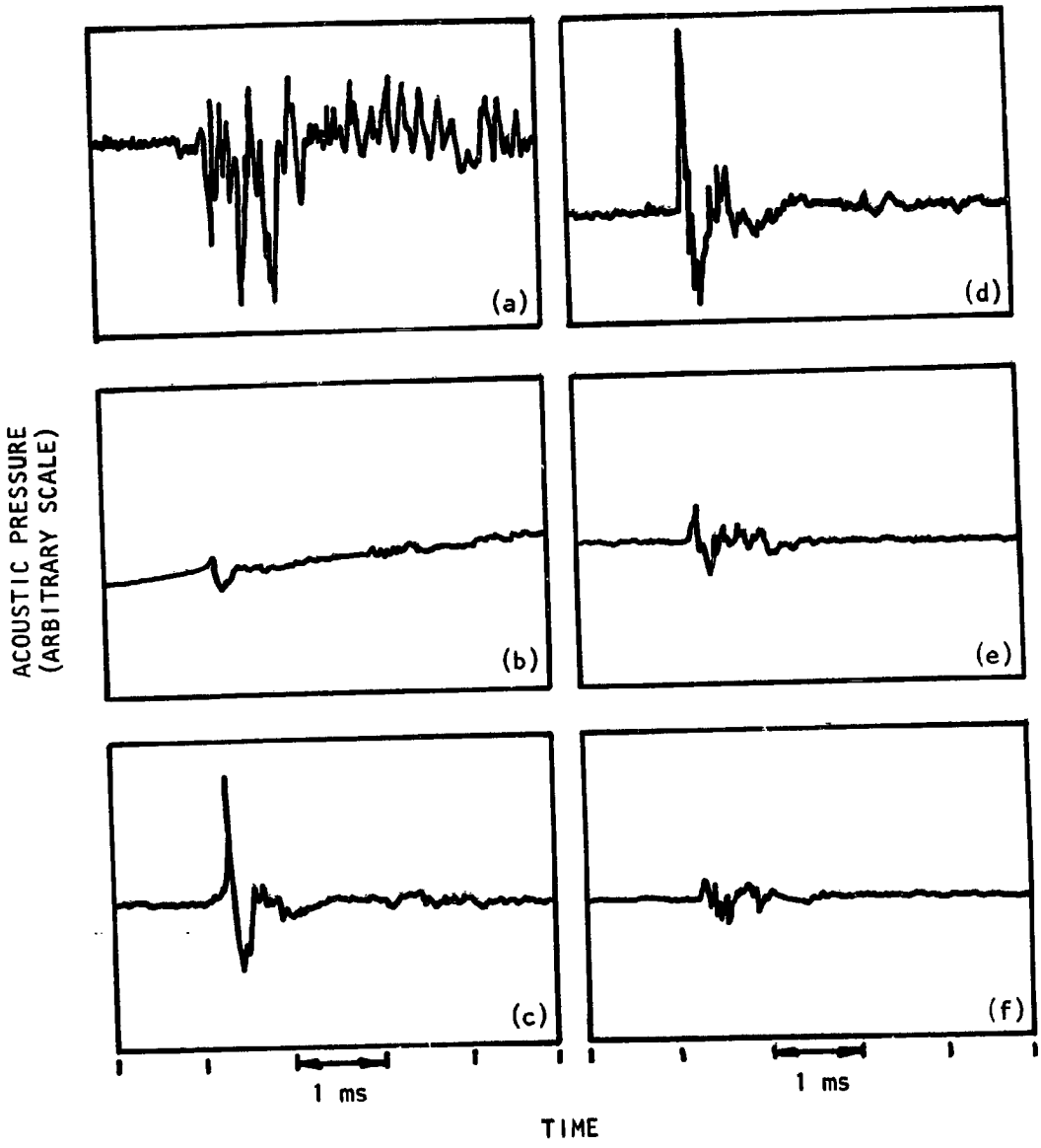

Figure 4.2 Pressure time histories for the multi-chute suppressor nozzle at $M_{J1} = 0.4$ and $M_{J2} = 0.6$ (unheated)
(a) In-duct, (b) $\theta = 10°$, (c) $\theta = 30°$, (d) $\theta = 50°$
(e) $\theta = 90°$ and (f) $\theta = 120°$

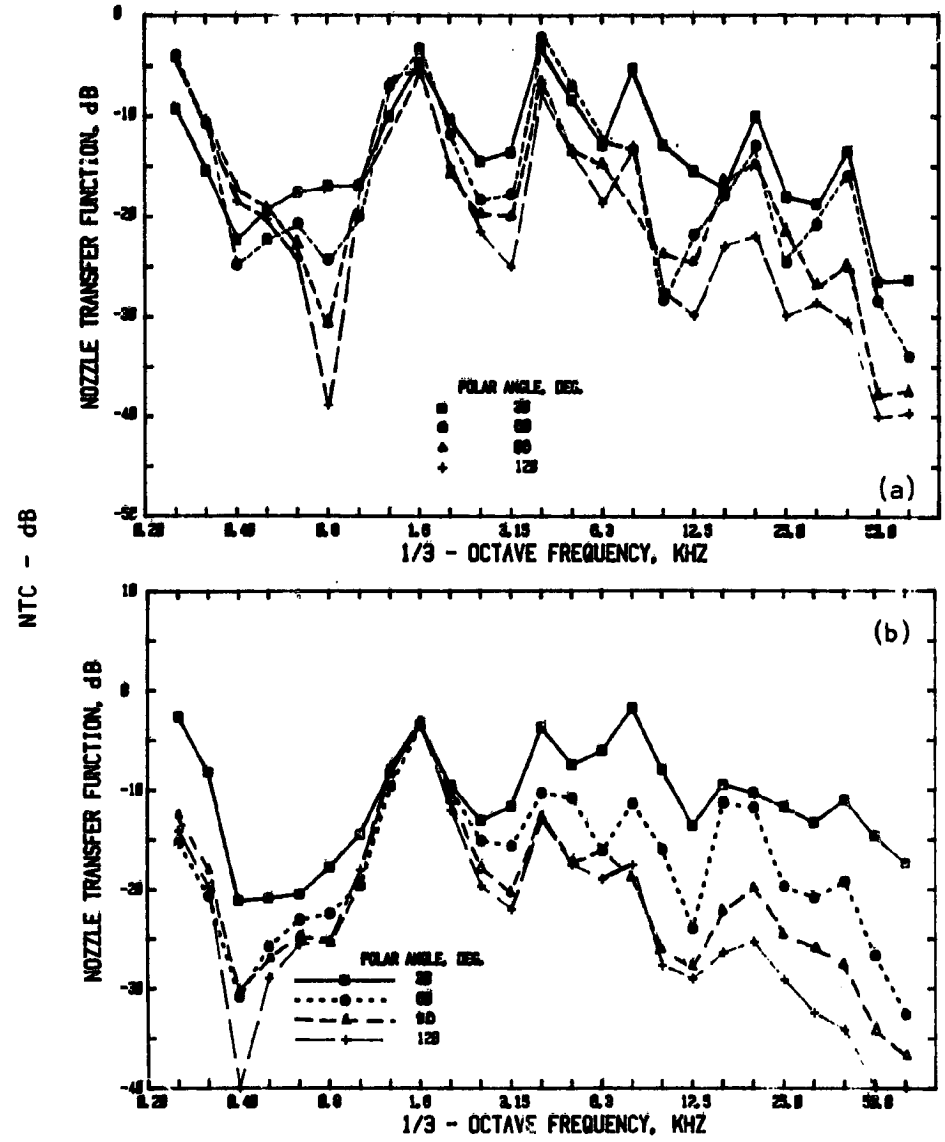

Figure 4.3 Variation of NTC spectra with polar angle for (a) the multi-chute suppressor and (b) the reference coaxial nozzle at $M_{J1} = 0$ $M_{J2} = 0$
(both jets unheated)
θ: —□—, 30°; ---○---, 60°; —△—, 90° and — + — , 120°

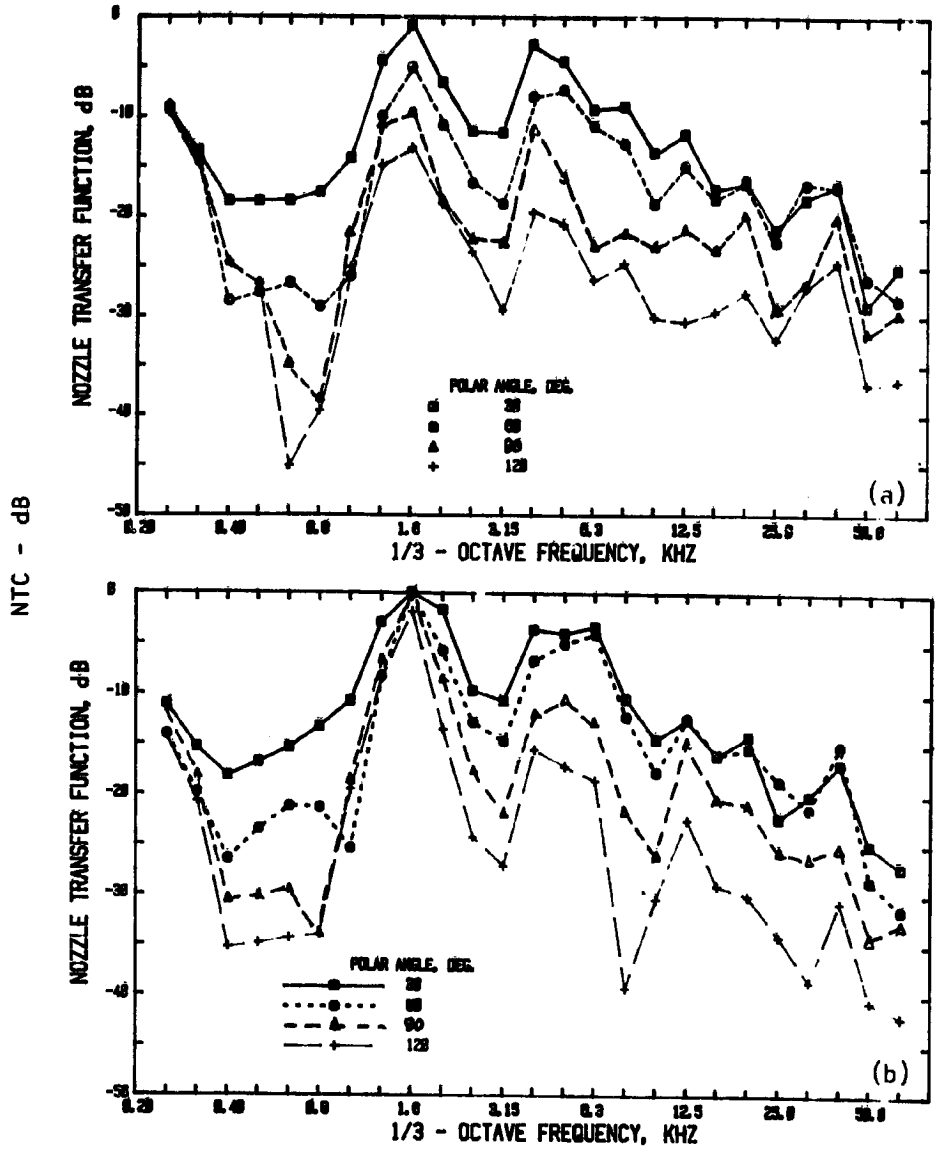

Figure 4.4 Variation of NTC spectra with polar angle for (a) the multi-chute suppressor and (b) the reference coaxial nozzle at $M_{J1} = 0.4$, $M_{J2} = 0.6$, $V_{J2}/V_{J1} = 1.50$
(both jets unheated)
θ: —□—, 30°; ---o---, 60°; -△-, 90° and — + — , 120°.

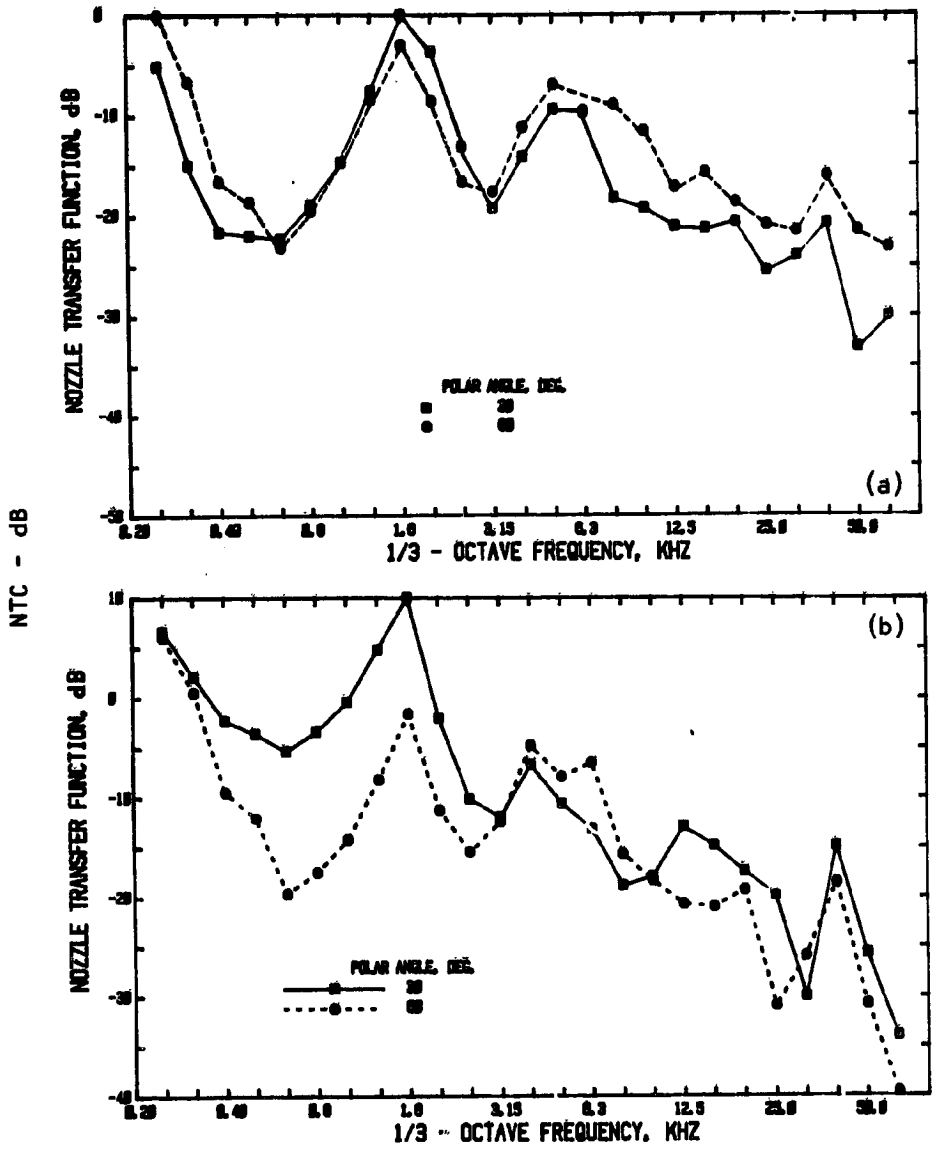

Figure 4.5 Variation of NTC spectra with polar angle for (a) the multi-chute suppressor and (b) the reference coaxial nozzle at $M_{J_1} = 0.0$ $M_{J_2} = 1.2$. (both jets unheated)
θ:—□—; 30° and ---○---, 60°

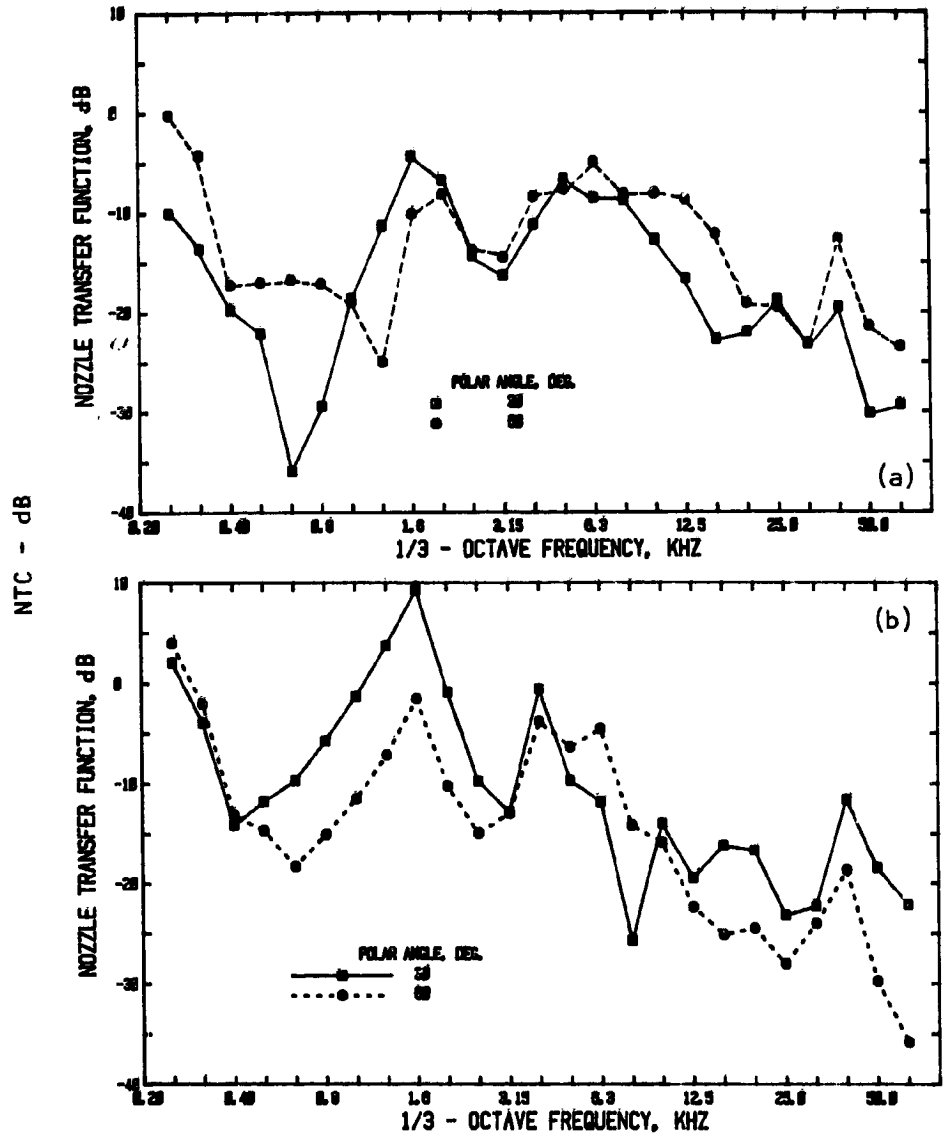

Figure 4.6 Variation of NTC spectra with polar angle for (a) the multi-chute suppressor and (b) the reference coaxial nozzle at $M_{J_1} = 0.8$ $M_{J_2} = 1.2$ $V_{J_2}/V_{J_1} = 1.40$ (both jets unheated)
θ:—□—, 30° and --o--, 60°

angles was, therefore, not possible for these conditions.

A closer inspection of the variation of NTC spectra with measurement angle for the multi-chute and the coaxial nozzle, as presented in Figures 4.3 thru 4.6, show that the spectral shapes for both nozzles are quite similar. For both of these d[illegible] stream nozzles, the NTC values start decreasing with frequency first and then start rising and then undergo three or four humps in the frequency domain. With the exception of the 30° data for the reference coaxial nozzle (see Figure 4.3(b)), the low frequency values at various angles are not too different from one another in amplitude indicating that the low frequency radiation is quite omnidirectional. At high frequencies the NTC values at a given frequency decrease with increasing angle for subsonic conditions (Figures 4.3 and 4.4), a trend found earlier for the single stream nozzles also. For shock containing jets, however, the NTC values do not decrease with angle as rapidly for the multi-chute suppressor nozzle as they do for the reference coaxial nozzle.

COMPARISON WITH DAISY LOBE SUPPRESSOR. The most important aspect of these NTC spectra is that their shapes have little resemblance with those for the single stream daisy lobe suppressor and the reference conical nozzle presented earlier in section 3.0. To show this, a typical NTC spectrum of the daisy lobe nozzle for the no flow condition and that for the multi-chute suppressor are compared in Figure 4.7 for $\theta = 90°$. Here the NTC spectra as a function of absolute frequency are compared. Except at very low frequencies (below 400 Hz) the multi-chute nozzle NTC values are lower than those for the daisy lobe nozzle at all frequencies. Similar results were obtained with flow as shown in Figure 4.8 where $\theta = 90°$ data for the two suppressor nozzles is compared for $M_J = 0.6$ for the daisy lobe nozzle and $M_{J_1} = 0.4$ and $M_{J_2} = 0.6$ for the muliti-chute nozzle. It should be noticed that for both nozzles, the stream containing the internal noise source is operated at the same jet Mach number. By comparing the results at $\theta = 90°$, the effects of refraction and convection have also been eliminated. Thus the difference between the two spectra is primarily a nozzle geometry effect. Note that any area effects are also not present here. This follows from the "area equivalence" effects discussed earlier in section 3. If the frequencies were to be non-dimensionalized by a factor of $\sqrt{A}$ then the multi-chute NTC spectra shown in Figures 4.7 and 4.8 will, for all intents and purposes, *not* shift with respect to each other since the two suppressors have almost identical equivalent exit areas.* Why the two spectra are so different is not amenable to explanations at this stage.

COMPARISON WITH REFERENCE COAXIAL NOZZLE. Variation of 1/3-octave NTC with angle has already been presented for both the multi-chute and the reference coaxial nozzles. Data for the two nozzles at identical conditions and the same angles will now be compared.

No flow case

The first obvious condition for this comparison is the no flow case. NTC spectra for the two nozzles at $M_{J_1} = 0$ and $M_{J_2} = 0$ for $\theta = 30°$, 60°, 90° and 120° are presented in Figure 4.9. The spectra at each angle for the two

* Daisy lobe exit area = 30.2 cm^2
Multi-chute exit area = 30.4 cm^2

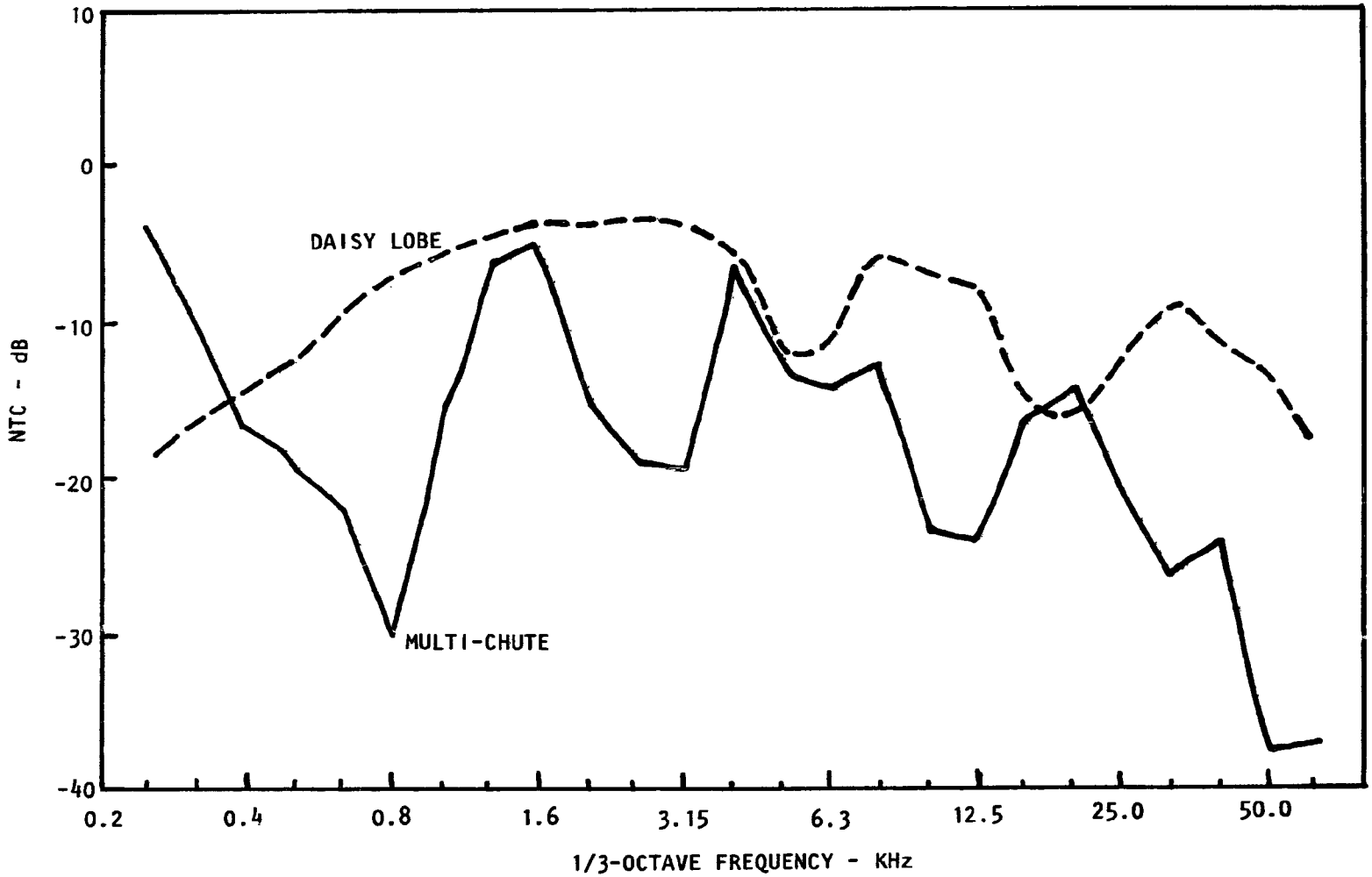

Figure 4.7 Comparison of typical NTC spectra at $\theta = 90°$ of the single stream daisy lobe supressor or (----) with those of the dual-stream multi-chute supressor (——) for no flow condition

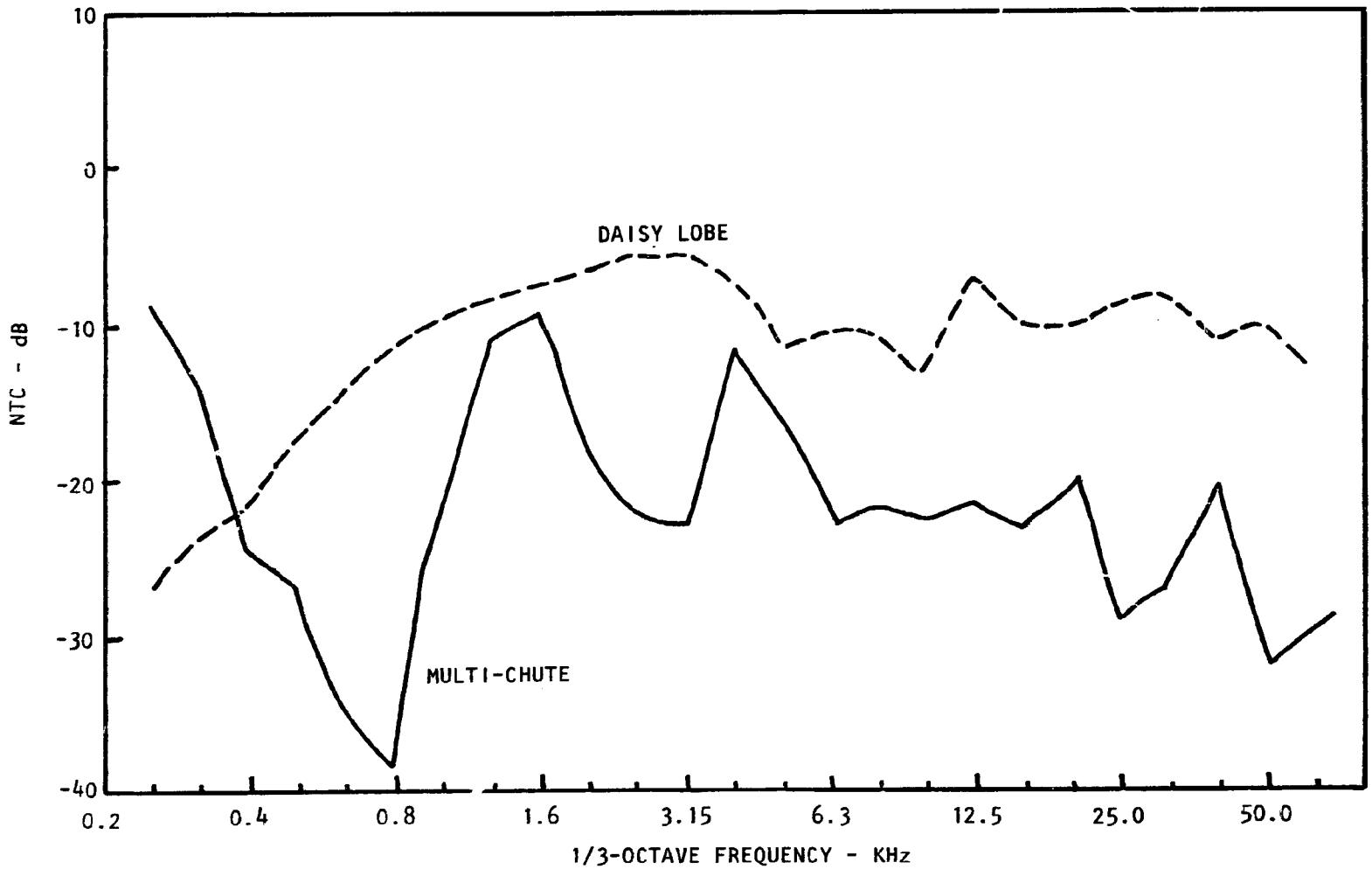

Figure 4.8 Comparison of typical NTC spectra at $\theta = 90°$ of the single stream daisy lobe suppressor (----) at $M_J = 0.6$ and the dual stream multi-chute suppressor (—) at $M_{J_1} = 0.4$ and $M_{J_2} = 0.6$

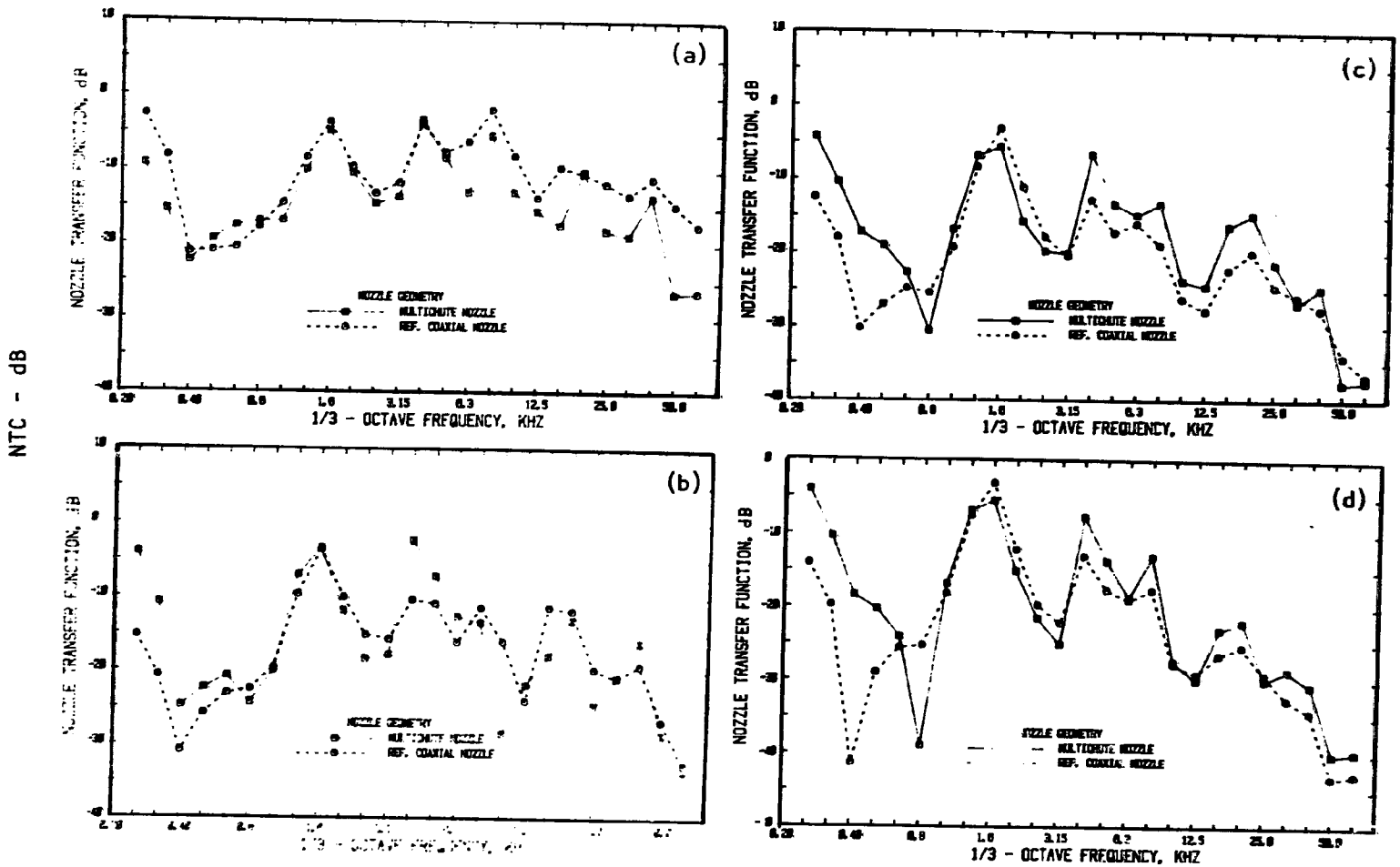

Figure 4.9 Effect of nozzle geometry on NTC spectra at $M_{J_1} = 0.0$, and $M_{J_2} = 0.0$ ($T_{R_1} = T_{R_2}$= Ambient).
θ: (a) 30°, (b) 60°, (c) 90° and (d) 120°
—□—, multi-chute nozzle;--○--, reference coaxial nozzle

nozzles have remarkably similar shapes and have almost identical amplitudes for frequencies higher than 800 Hz ($kh = 0.26$). Below 800 Hz, the suppressor appears to be a more efficient radiator of internal noise at all angles larger than 30°. At 30°, the trend is reversed in the low frequency range, i.e. the coaxial nozzle is more efficient now.

A good collapse up to almost 63 KHz is not too surprising. This is because some of the inhouse research at Lockheed has shown that the far-field NTC for nozzles can be collapsed up to $kD = 8$, where D is the diameter of the nozzle. Assuming that D can be replaced by h, then for the present configuration, where h = 1.78 cm for both nozzles, the NTC data for the two nozzles should collapse up to a frequency of 24.5 KHz. They appear to collapse even at higher frequencies.

It should be recalled that the reference coaxial nozzle used here was one of the existing nozzles used for Phase 1 studies [4.1]. During the design of the multi-chute nozzle it was possible to match only the values of the annulus height h and the ratio L/h (= 3) with those of the coaxial nozzle, but the exit areas of the annular jet could not be maintained the same. The flow area of the annulus in the multi-chute nozzle was 30.40 cm^2 while that in the reference coaxial nozzle was 64.14 cm^2. The primary jet exit area for both nozzles was, however, the same and was equal to 45.6 cm^2. Thus, following the "area equivalence" arguments given earlier, if we were to compare the data based upon normalized frequency given by $k\sqrt{A}$ instead of the absolute frequency, where A is the exit area, then the spectra for the coaxial jet will move to the right by just over a 1/3-octave with respect to the NTC spectra of the multi-chute nozzle. An inspection of the NTC spectra for the two nozzles shows that this does not modify the observed results considerably. Actually a systematic study, where h could be maintained constant and the exit area of the annulus could be varied, and vice versa, is needed to quantify the effects of the exit area and the annulus height.

Since here the annulus height is the same for the two nozzles and the area effects make a difference of only about one-third octave in the frequency normalization, the rest of the data is compared based upon absolute frequency itself. Also, since the shapes of the NTC spectra for both nozzles were the same at zero flow conditions, then under flow conditions, if there are any differences in their relative shapes they will be attributable to different flow conditions existent downstream of the respective nozzle exits.

Subsonic Mach numbers

Typical results in the presence of flow, comparing the NTC spectra for the two nozzles at $\theta = 30°$, 60°, 90° and 120°, are shown for $M_{J_1} = 0.4$, $M_{J_2} = 0.6$ in Figure 4.10 and for $M_{J_1} = 0.8$ and $M_{J_2} = 0.9$ in Figure 4.11. As for the zero flow case, the spectra for the flow case are similar in shape for the two nozzles but the reference coaxial data near the humps in the spectra are higher than those for the multi-chute nozzle.

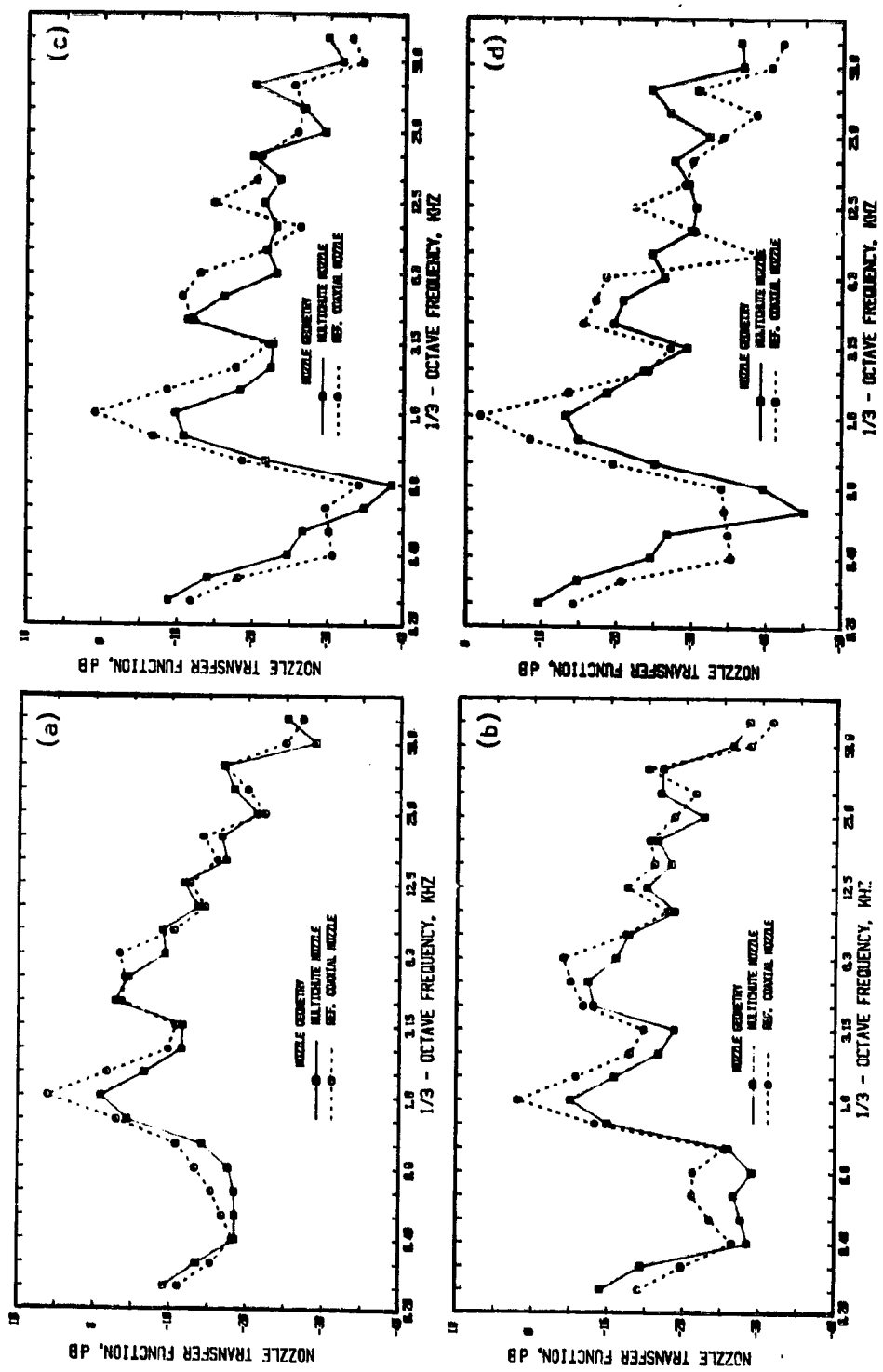

Figure 4.10 Effect of nozzle geometry on NTC spectra at $M_{J1} = 0.4$, and $M_{J2} = 0.6$, $V_{J2}/V_{J1} = 1.50$, ($T_{R1} = T_{R2}$ = Ambient).
θ: (a) 30°, (b) 60°, (c) 90° and (d) 120°
—□—, multi-chute nozzle; --o--, reference coaxial nozzle

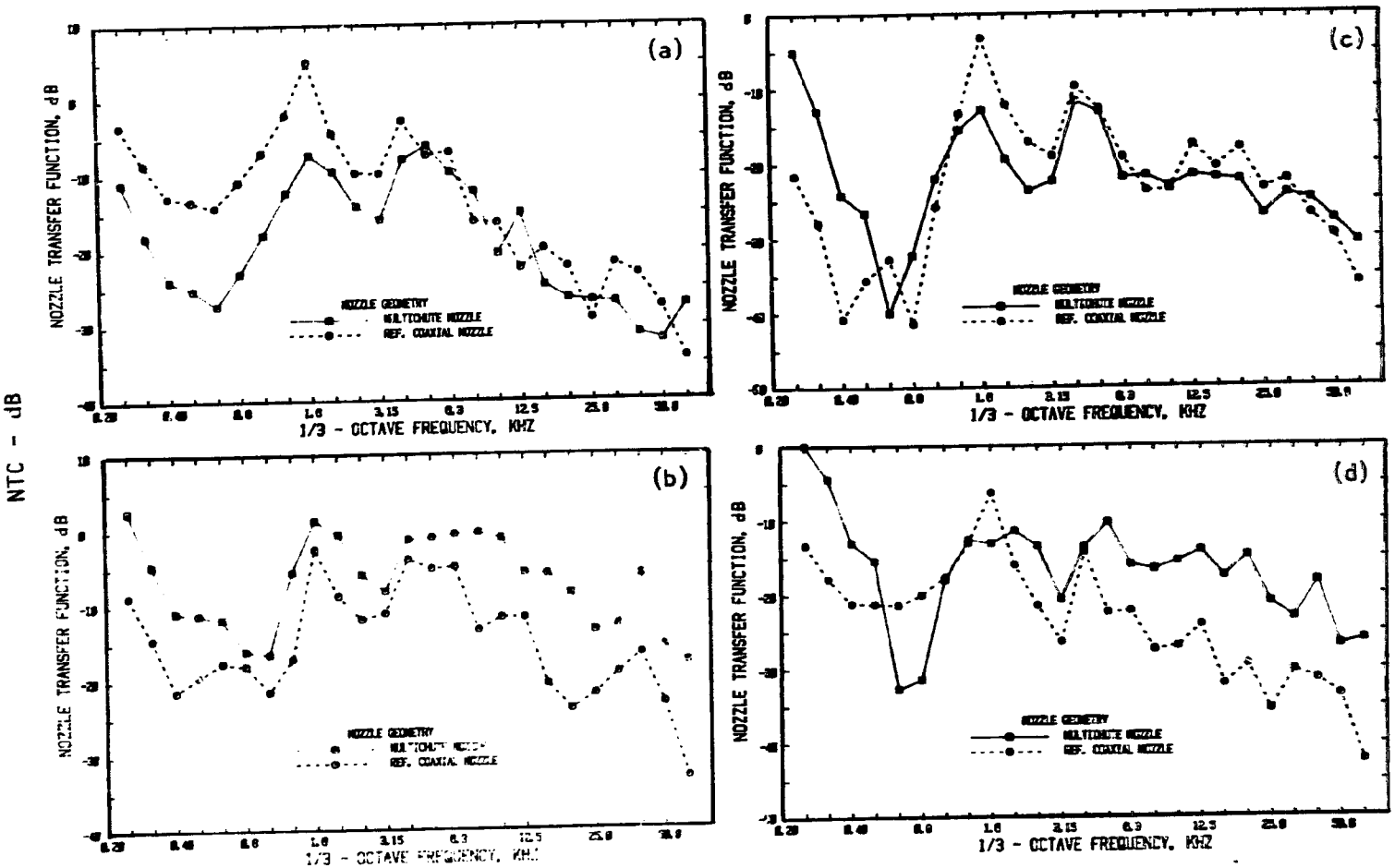

Figure 4.11 Effect of nozzle geometry on NTC spectra at $M_{J1} = 0.8$ and $M_{J2} = 0.9$, $V_{J2}/V_{J1} = 1.11$, ($T_{R1} = T_{R2}$ = ambient)
θ: (a) 30°, (b) 60°, (c) 90° and (d) 120°
—□—, multi-chute nozzle; —○--, reference coaxial nozzle

It is thus found that for zero flow and the subsonic flow conditions, except for a few frequencies, the multi-chute nozzle radiates either more efficiently than or at least as efficiently as the reference coaxial nozzle at almost all frequencies and angles. The only exception is the low frequency data at $\theta = 30°$ at $M_{J_1} = M_{J_2} = 0$ where the multi-chute nozzle is found to be less efficient than the reference coaxial nozzle.

Similar results can also be seen in the directivity plots for the two nozzles shown in Figure 4.12 for typical 1/3-octave frequencies of 1, 4, 8 and 16 KHz for a typical flow condition of $M_{J_1} = 0.4$ and $M_{J_2} = 0.6$. It is interesting to note that despite the odd looking NTC shapes, the directivity shapes are quite smooth and similar for both nozzles. Observations made above about the spectral shapes apply here also.

Supersonic Mach numbers

For the fan stream operated at *supercritical* pressure ratios, the coaxial jet at small angles is found to be *more* efficient than the multi-chute nozzle at *all* frequencies except at two or three frequencies where sharp dips in the coaxial data were noticed (see Figure 4.13(a) and 4.14(a)). At $\theta = 60°$, the multi-chute nozzle radiates *less* efficiently (by 2 to 3 dB) compared to the reference coaxial jet at *lower* frequencies (f<7KHz) and *more* efficiently at *higher* frequencies (see Figures 4.13(b) and 4.14(b)).

Notice that the fan-stream Mach number for the data presented in both of the Figures 4.13 and 4.14 is 1.2 but the primary Mach number (M_{J_1}), for the data presented in Figure 4.13, is zero while it is equal to 0.8 for the data of Figure 4.14. Thus any differences in the NTC spectra shown in these figures should also reflect the effects of the primary jet for internal noise radiating through the fan stream. A closer examination of the two figures shows only minor effects of the primary stream. However, since such tests were not conducted for other conditions, general conclusions about the effects of the primary stream can not be drawn from the limited data studied here.

EFFECT OF FAN STREAM MACH NUMBER. Effect of the fan stream Mach number was found to be more important for the reference coaxial nozzle than for the multi-chute nozzle. This is shown in Figure 4.15 for $\theta = 30°$ and Figure 4.16 for $\theta = 60°$. In both figures the NTC spectra for the multi-chute nozzle and also the conical nozzle are presented for two fan-jet Mach numbers, namely 0.0 and 1.2 with no flow through the primary stream. At $\theta = 30°$, both nozzles show the effect of refraction at high frequencies which is to be expected. At low frequencies, however, both nozzles appear to radiate more efficiently for the higher M_{J_2}. This effect of the fan jet Mach number is stronger for the coaxial nozzle than for the multi-chute nozzle.

4.1.3 Acoustic Power

Since the reflected signals were not processed for the dual stream nozzles, the far-field acoustic power normalized with respect to only the incident acoustic power, i.e. PTF_i, is considered here. PTF_i spectra for three flow conditions of M_{J_1}, M_{J_2} of 0.0, 0.0; 0.4, 0.6 and 0.8, 0.9 are presented in Figure 4.17 for both nozzles.

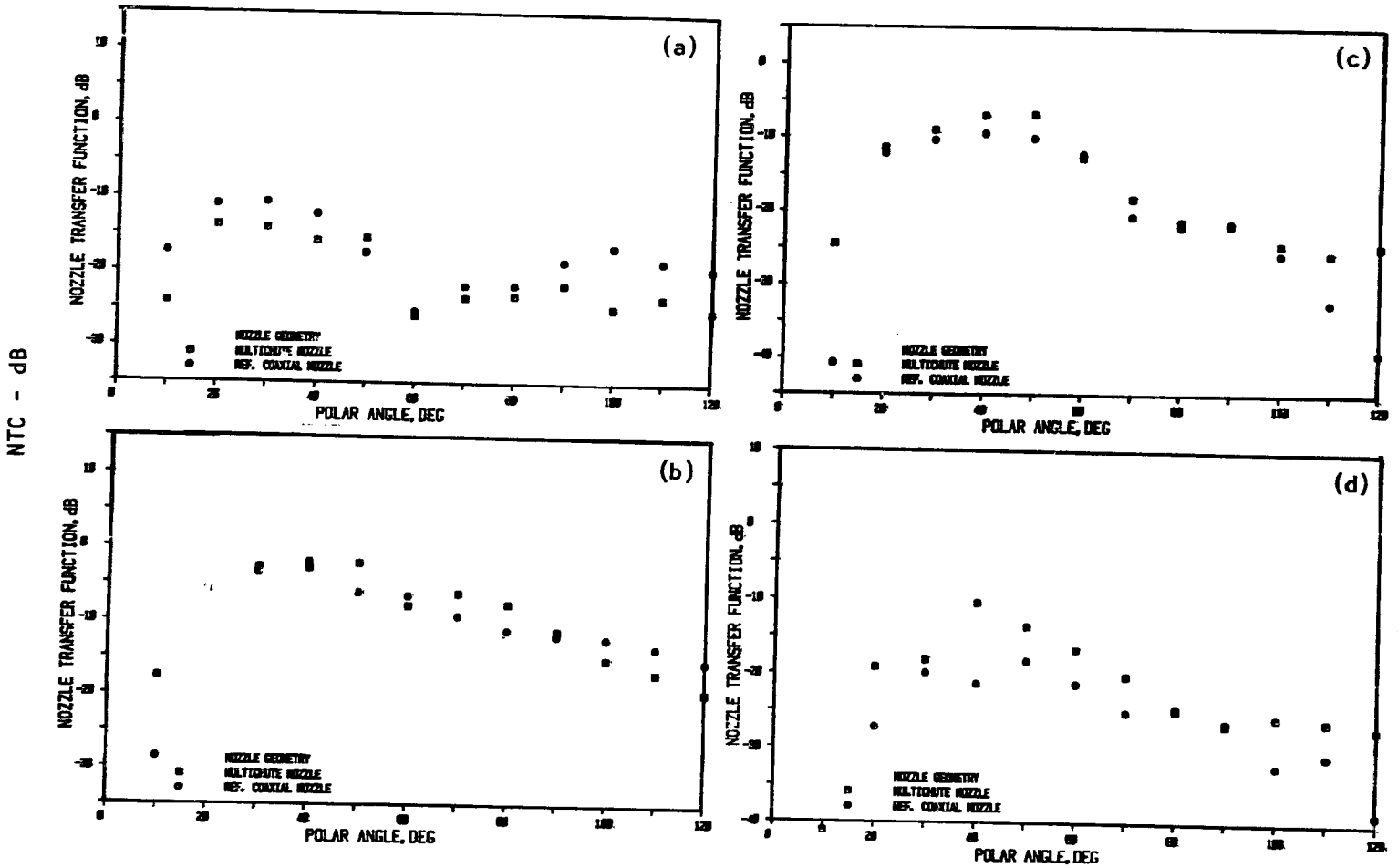

Figure 4.12 NTC directivities of the multi-chute (□) and the reference coaxial nozzle (○)
$M_{J1} = 0.4$, $M_{J2} = 0.6$, $V_{J2}/V_{J1} = 1.5$, ($T_{R_1} = T_{R2}$ = ambient)
f: (a) 1 KHz, (b) 4 KHz, (c) 8 KHz and (d) 16 KHz

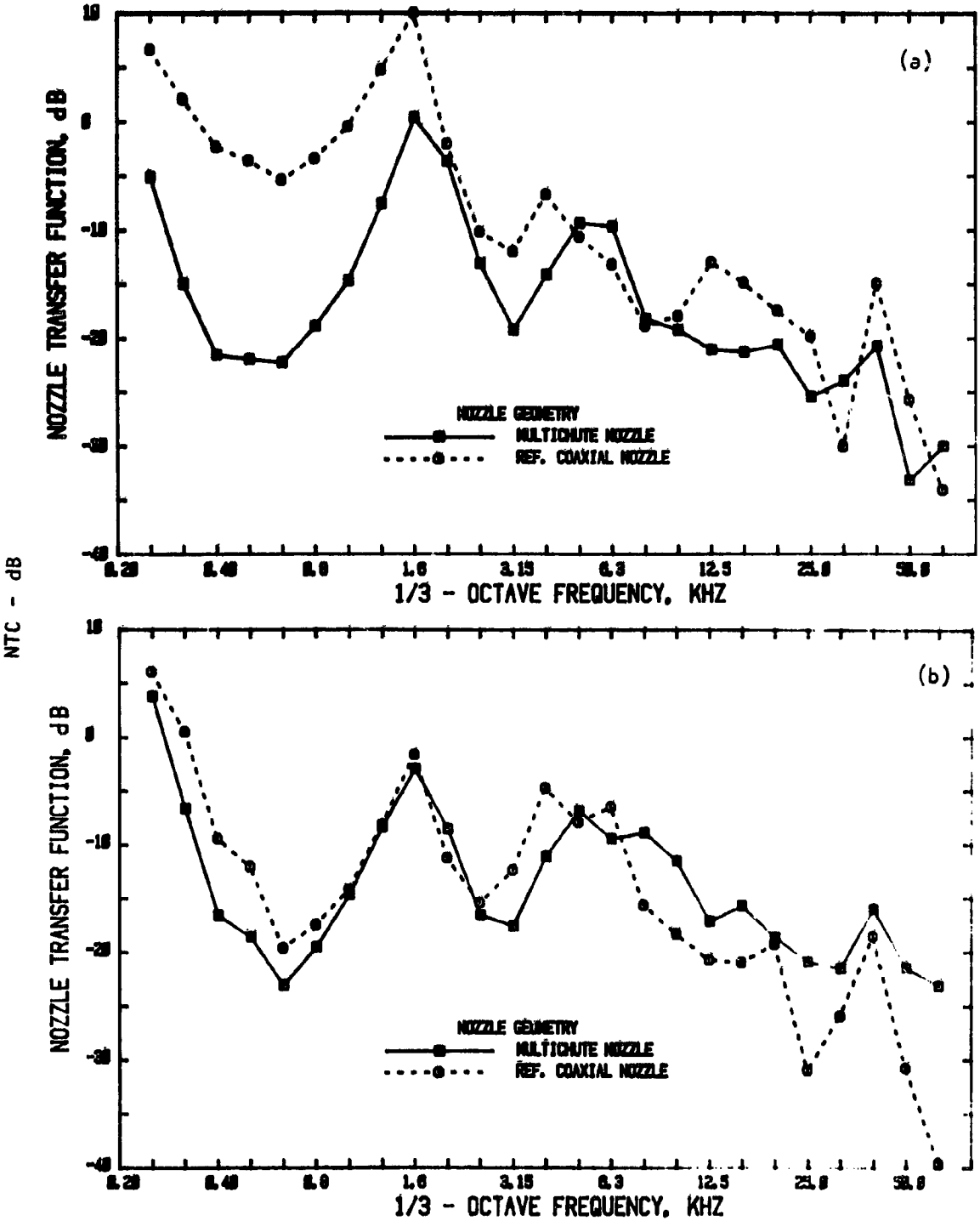

Figure 4.13 Effect of nozzle geometry on NTC spectra at $M_{J_1} = 0$ and $M_{J_2} = 1.2$ ($T_{R1} = T_{R2}$ = Ambient) θ: (a) 30° and (b) = 60°
—□—, multi-chute nozzle; --o--, reference coaxial nozzle

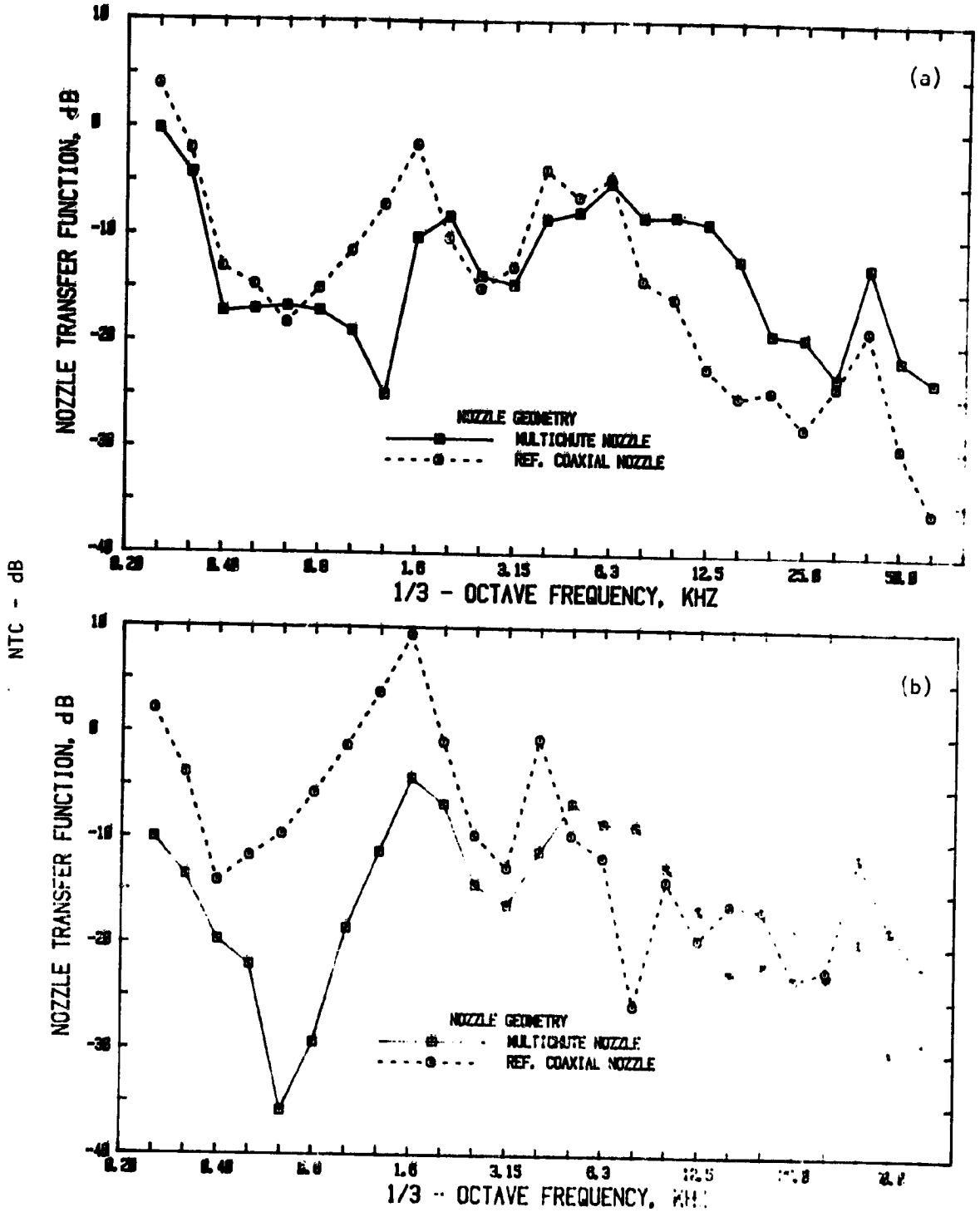

Figure 4.14 Effect of nozzle geometry on NTC spectra at $M_{J_1} = 0.8$ and $M_{J_2} = 1.2$, $V_{J_2}/V_{J_1} = 1.4$, ($T_{R_1} = T_{R_2}$ = ambient) θ: (a) 30° and (b) 60°

—□—, multi-chute nozzle; -○--, refe.ence coaxial nozzle.

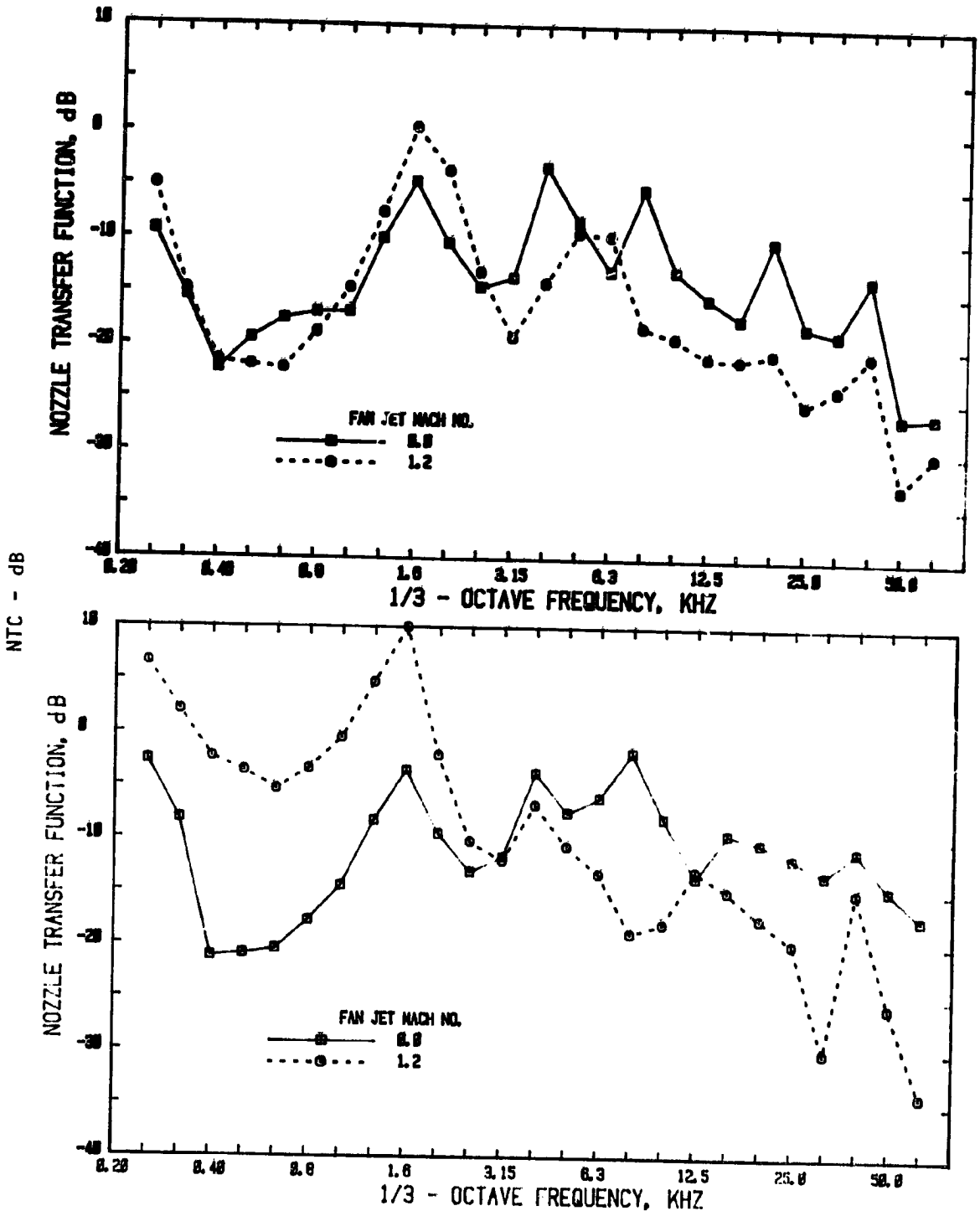

Figure 4.15 Effect of fan jet Mach number on NTC spectra of (a) multi-chute nozzle and (b) reference coaxial nozzle at $\theta = 30°$
$M_{J1} = 0.0$, $T_{R1} = T_{R2}$ = ambient
M_{J2}: —□—, 0.0; --o--, 1.2

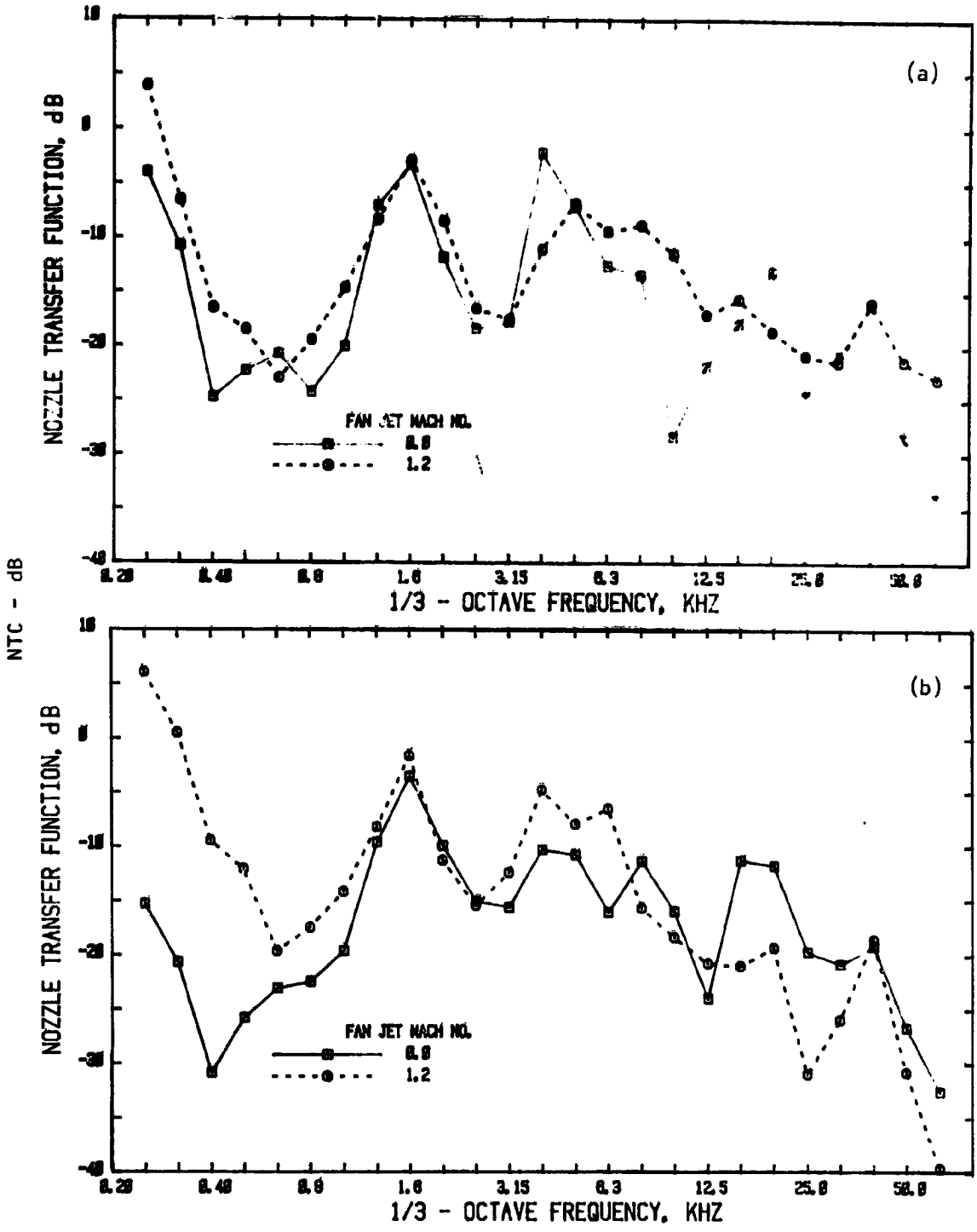

Figure 4.16 Effect of fan jet Mach number on NTC spectra of (a) multi-chute nozzle and (b) reference coaxial nozzle at $\theta = 60°$.
$M_{J1} = 0.0$, $T_{R1} = T_{R2}$ = ambient
M_{J2}: —□—, 0.0; ···o···, 1.2

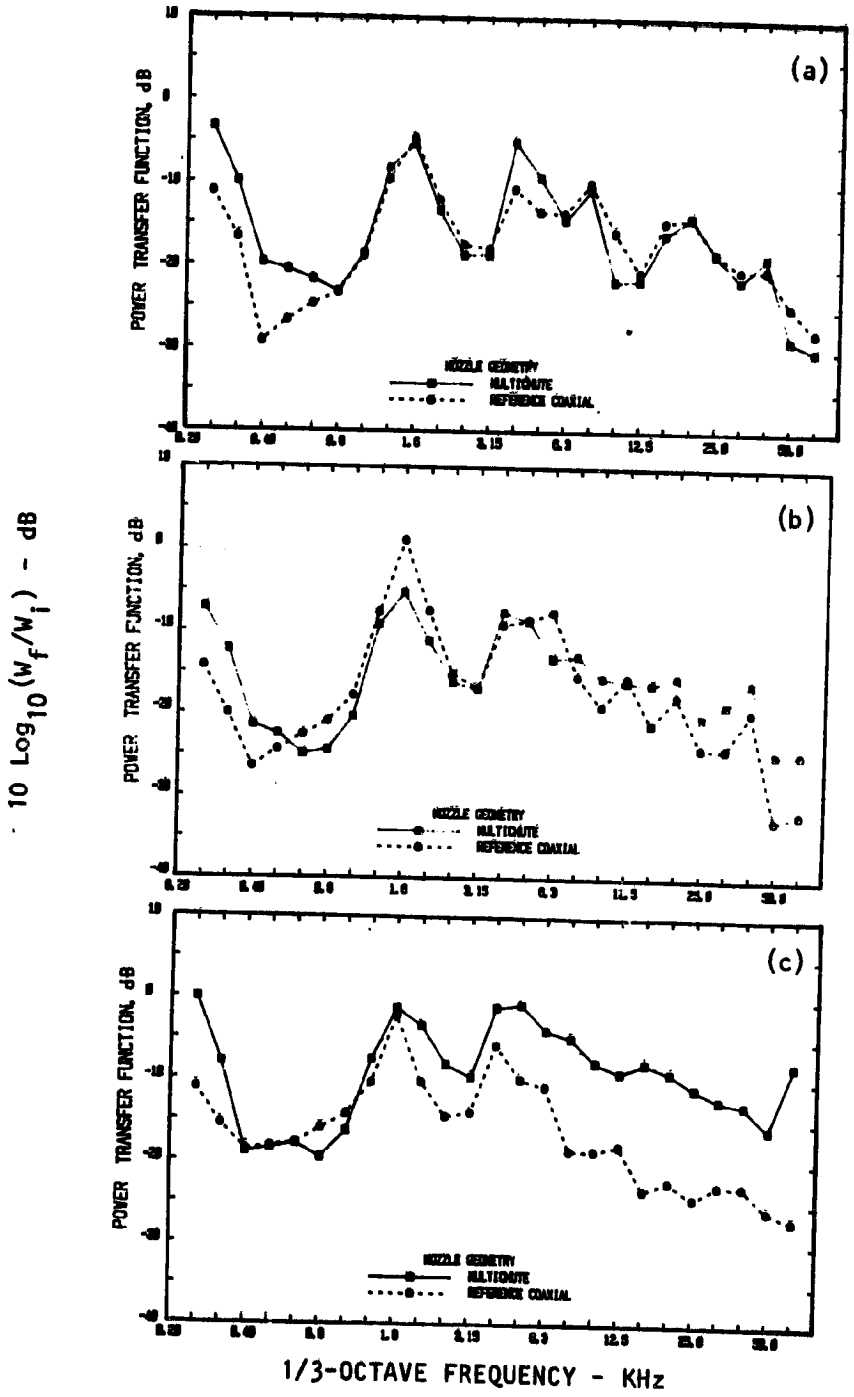

Figure 4.17 Effect of nozzle geometry on power transfer function (a) $M_{J_1} = 0.0$, $M_{J_2} = 0$, (b) $M_{J_1} = 0.4$, $M_{J_2} = 0.6$ and (c) $M_{J_1} = 0.8$, $M_{J_2} = 0.9$
($T_{R_1} = T_{R_2}$ = ambient)
—□— multi-chute nozzle, --o--reference coaxial nozzle

The zero Mach number data (Figure 4.17(a)) are particularly revealing in that beyond f = 800 Hz, the spectra for both nozzles are almost identical; indicating that, in the absence of the flow, the geometry of the nozzles does not affect the amplitudes of the far-field radiation except at low frequencies. At low frequencies the suppressor nozzle radiates more efficiently than the reference coaxial nozzle.

With flow the multi-chute nozzle appears to radiate more efficiently than the reference coaxial nozzle at almost all frequencies (e.g. see Figures 4.17(b) and 4.17(c)).

The spectral shapes of the acoustic powers presented are quite different from those obtained earlier for the single stream nozzles. For example, here the low frequency power decreases with frequency while that for the single stream nozzle was found to increase with frequency. Reasons for these differences are not known and further work needs to be done to understand these results.

4.1.4 Mach Number Effects - Summary

The results for the multi-chute suppressor nozzle and the reference coaxial nozzle tested statically and unheated can be summaried as below:

(1) Due to different source-section configuration for these nozzles, the in-duct and the far-field time histories consist of a multi-pulsed incident signal and are thus different from those obtained for the daisy lobe nozzle. It was not possible to properly isolate the reflected waves in this case. Reflection coefficient data are, therefore, not presented.

(2) Far-field radiation was found to be azimuthally symmetric.

(3) Low frequency radiation for both nozzles is omnidirectional.

(4) Dominant radiation for both nozzles is close to the jet axis.

(5) The multi-chute nozzle is a less efficient radiator of internal noise than the single stream daisy lobe nozzle (and therefore the conical nozzle).

(6) The NTC spectra and the directivities for the multi-chute and the reference coaxial nozzle are remarkably similar in shape and in most instances in amplitude also. It is below 800 Hz, that the suppressor radiates more efficiently at all angles except at angles smaller than 30° where the trend is opposite.

(7) For a fixed fan-jet Mach number, the primary jet has negligible effect on the transmission characteristics of these nozzles.

(8) Low frequency radiation increases with increasing fan-jet Mach number.

(9) At $M_J = 0$, the far-field acoustic powers, normalized with respect to the incident acoustic powers, are identical for the suppressor and the

reference nozzle for frequencies higher than 800 Hz. Below 800 Hz the multi-chute suppressor radiates more efficiently.

(10) With flow, the suppressor radiates more acoustic power than the reference conical nozzle at all frequencies.

4.2 TEMPERATURE EFFECTS

Results similar to those described in section 4.1 for unheated jets will now be presented for the heated jets. As already described in section 3 measurements were made only at a few test conditions as shown in Table 4.2.

Table 4.2 Multi-chute suppressor operating conditions for the heated jets.

Test No.	M_{J_1}	M_{J_2}	T_{R_1} (K)	T_{R_2} (K)	V_{J_2}/V_{J_1}
1	0.8	0.9	AMB	600	1.56
2	0.8	0.9	AMB	900	1.93
3	0.8	0.9	450	600	1.27
4	0.8	0.9	675	900	1.31
5	0.8	1.2	AMB	600	2.05

Data was obtained for both the multi-chute suppressor as well as the reference coaxial nozzle for the above conditions. Due to very high jet velocities (and therefore high amplitude of jet mixing noise), the data for $M_{J_2} = 1.2$ (test no. 5), particularly for the reference coaxial nozzle, was valid only for a few angles. Similarly, the data for test no. 4 was contaminated with jet mixing noise at many angles, both close to the jet axis where jet mixing noise is normally dominant and at 90° and in the forward arc where the pulse amplitude is normally low. For this reason data for the first three tests of table 4.2 only are discussed here. At other conditions, the data for those angles where the far-field pulse was detectable is shown in the print-outs given in Appendix C along with the rest of the data.

In view of the restrictions described above only two aspects of nozzle transmission are addressed here. These are:

(1) Effects of T_{R_2} for fixed M_{J_1}, M_{J_2} and T_{R_1} ($M_{J_1} = 0.8$, $M_{J_2} = 0.9$, T_{R_1} = ambient)

(2) Effects of T_{R_1} for fixed M_{J_1}, M_{J_2} and T_{R_2} ($M_{J_1} = 0.8$, $M_{J_2} = 0.9$ and $T_{R_2} = 600K$).

4.2.1 Effect of Heating the Fan Jet

Effects of heating the fan jet for $M_{J_1} = 0.8$ and $M_{J_2} = 0.9$ are shown in Figure 4.18. One-third octave NTC spectra at 30°, 60°, 90° and 120° are compared for T_{R_2} = ambient, 600K and 900K. For each of these conditions the primary jet was operated unheated. With the exception of the 90° data, the effect of heating the fan jet from ambient to 600K is to reduce the far-field radiation. Heating it further to 900K, however increases the far-field radiation at almost all frequencies. Inspection of similar data for the coaxial nozzle revealed that on heating the fan jet from ambient to 600K reduced the NTC values only for 60° and that also only at low frequencies. At other angles, effect of heating was mostly to increase the internal noise radiation. This coaxial nozzle data is shown in Figure 4.19 for the same condition at which the multi-chute data of the previous figure (Figure 4.18) were obtained.

It should be noted that for some of the angles, the 900K data have not been plotted since the jet mixing noise at these angles was more dominant than the far-field pulse itself. In view of the limited data, therefore, general conclusions can *not* be drawn from these results.

The data for the ambient and the 600K condition, however, indicates that for prediction purposes the effect of heating must be taken into account in working out a normalizing parameter for the frequency. For example, if the multi-chute data of Figure 4.18 for these two conditions are plotted as a function of kh instead of the absolute frequency, most of the humps in the spectra for the two conditions are found to lie under each other. Due to different speeds of sound (c) for the ambient and the 600K conditions the wave number k (= $2\pi f/c$) for the heated condition in this case is 1.4 times larger than the ambient condition. This means that, to compare the heated data on a kh basis, one should shift the heated jet spectrum to the left with respect to the ambient jet spectrum. When this is done, as shown in Figure 4.20, the two spectra show remarkable similarity. Only the 90° data shows some dissimilarity at low frequencies (f<1KHz). For other angles, the main conclusion to be derived from these results is that heating the jet to 600K reduces the radiation efficiency at almost all values of kh. On this basis, the differences in NTC between the ambient and the heated conditions are largest close to the jet axis.

The above observations about the NTC are true for the far-field acoustic powers as well. For example, the far-field acoustic powers normalized with respect to incident acoustic powers for the two conditions of the previous figure were found to have very similar shapes when compared on the non-dimensional frequency (kh) basis as shown in Figure 4.21. It is found that the effect of heating the fan-jet is to reduce the far-field radiation between 1 to 10 dB. Similar results were found for the reference coaxial nozzle. This is indicative of some form of shielding effect but a systematic study is needed to properly quantify these effects.

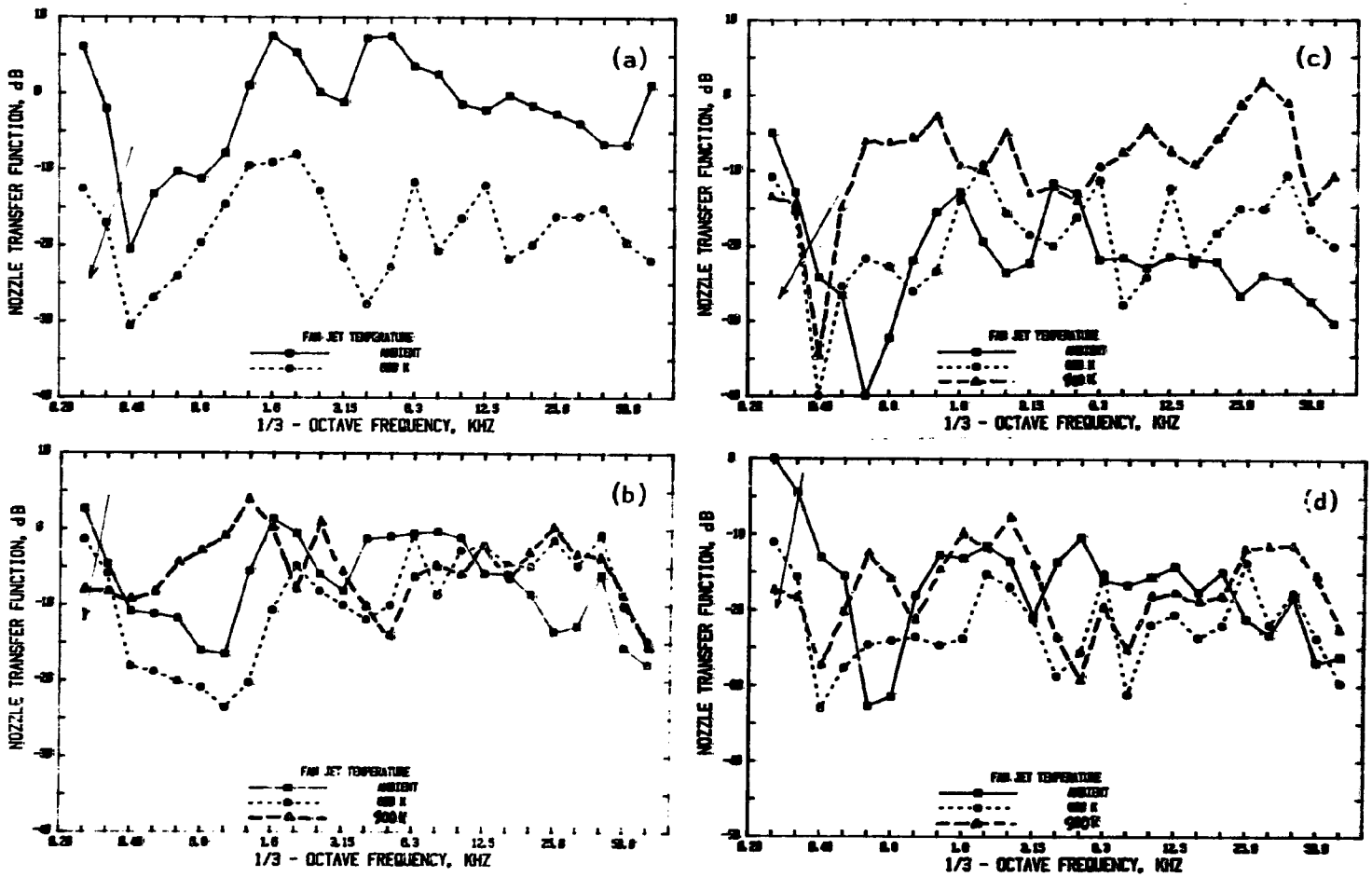

Figure 4.18 Effect of heating the fan jet on NTC spectra of the multi-chute nozzle at $M_{J_1} = 0.8$, and $M_{J_2} = 0.9$ (T_{R_1} = ambient).
θ: (a) 30°, (b) 60°, (c) 90° and (d) 120°
T_{R_2}: —□—, ambient; ---o---, 600K; —△—, 900K

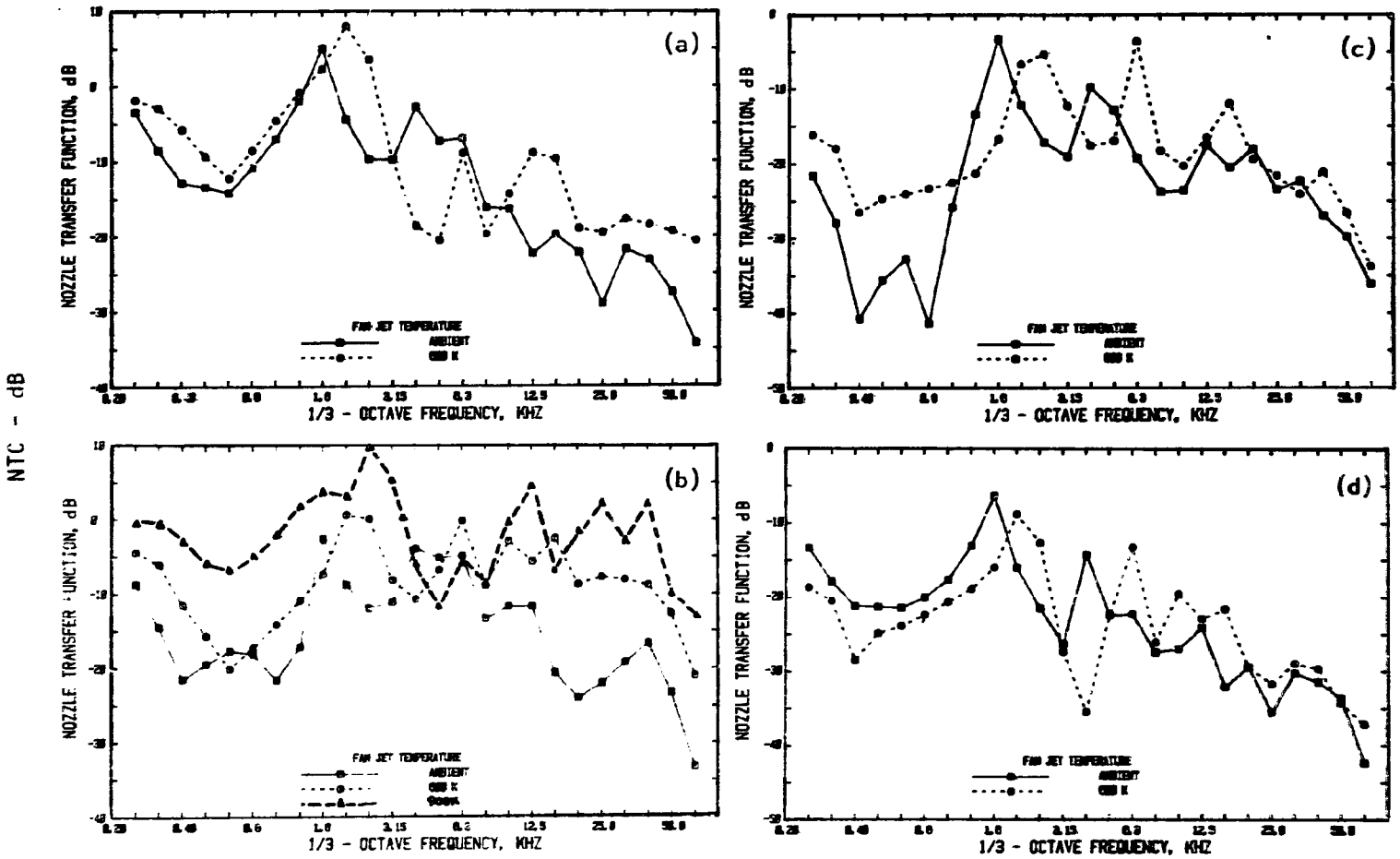

Figure 4.19 Effect of heating the fan jet NTC spectra of the reference coaxial nozzle at $M_{J_1} = 0.8$ and $M_{J_2} = 0.9$ (T_{R_1} = ambient).
θ: (a) 30°, (b) 60°, (c) 90° and (d) 120°
—□—, ambient; --o--, 600K; —△—, 900K.

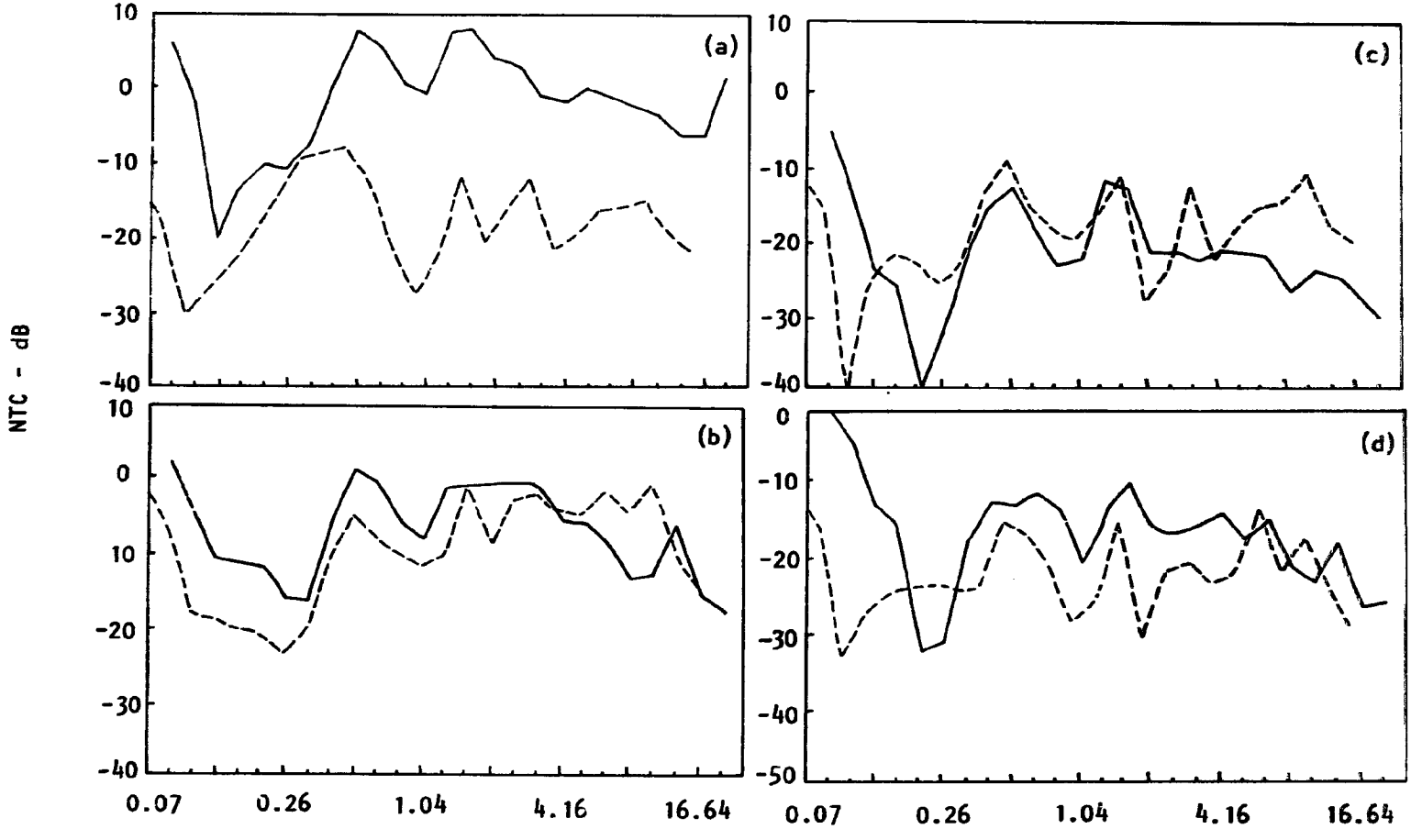

Figure 4.20 The ambient and the 600K data of figure 4.18 replotted as a function kh.
θ: (a) 30°, (b) 60°, (c) 90° and (d) 120°
T_{R2}: ——, ambient; — — —, 600K

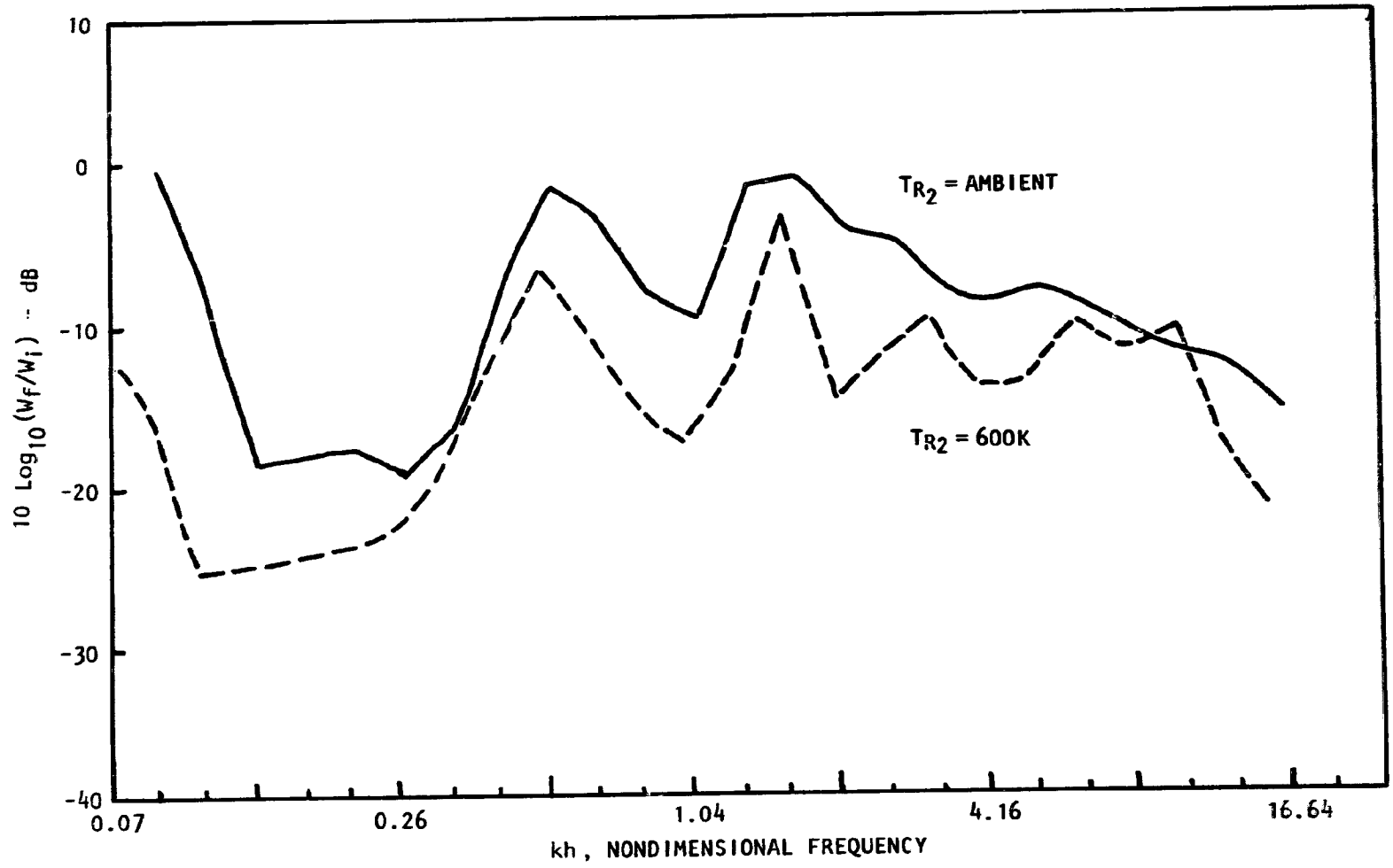

Figure 4.21 Effect of fan-jet temperature on far-field acoustic power for multi-chute nozzle normalized w.r.t. the incidnet power at $M_{J_1} = 0.8$, $M_{J_2} = 0.9$, T_{R_1} = ambient
——T_{R_2} = ambient, $T_{R_2}/T_{R_1} = 1$, $V_{J_2}/V_{J_1} = 1.11$
----T_{R_2} = 600K, $T_{R_2}/T_{R_1} = 2$, $V_{J_2}/V_{J_1} = 1.31$

4.2.2 Effect of Heating the Primary Jet

Strictly speaking only two test conditions, namely test numbers 1 and 3 of table 4.2 were available to determine the effects of heating the primary jet with other parameters remaining constant. Out of these two test points the latter was contaminated by jet mixing noise at many angles due to higher primary jet velocities. Reasonable data was available only at $\theta = 60°$ and 90°. A comparison of the 1/3-octave NTC spectra at these angles for the above two conditions (T_{R_1} = ambient and 450K with $M_{J_1} = 0.8$, $M_{J_2} = 0.9$ and $T_{R_2} = 600K$) is made in Figure 4.22(a) and (b) for $\theta = 60°$ and 90°, respectively. These results show that the far-field radiation of internal noise from noise sources imbedded within the fan stream, upstream of the fan jet exit, are not strongly influenced by the temperature of the primary stream. Compared to the unheated primary jet condition the NTC are found to be somewhat higher for the heated primary jet condition.

4.2.3 Temperature Effects - Summary

Effects of heating either one or both of the streams of the multi-chute and the reference coaxial nozzle on transmission characteristics of internal noise within the fan stream were investigated. Only limited conditions were tested and valid data was obtained for even less number of test conditions due to the dominance of jet mixing and sometimes shock-noise at many angles for the higher temperatures and Mach numbers. This was particularly true for the reference coaxial nozzle. Results presented here are thus more representative of trends rather than conclusive evidence of any phenomenon. The *observations* made about the temperature effects can be summarized as follows:

(1) For fixed M_{J_1}, M_{J_2} and T_{R_1}, the multi-chute suppressor radiates less efficiently at $T_{R_2} = 600K$ and more efficiently at $T_{R_2} = 900K$ with respect to the unheated fan jet.

(2) kh is a good normalizing frequency parameter for the configurations studied here.

(3) For fixed M_{J_1}, M_{J_2} and T_{R_2}, changing the primary jet total temperature tends to increase the far-field radiation.

4.3 CONCLUSIONS

Conclusions for this section basically consist of the summaries for the Mach number effects and the temperature effects which have already been given in subsections 4.1.4 and 4.2.3 respectively and are therefore not repeated.

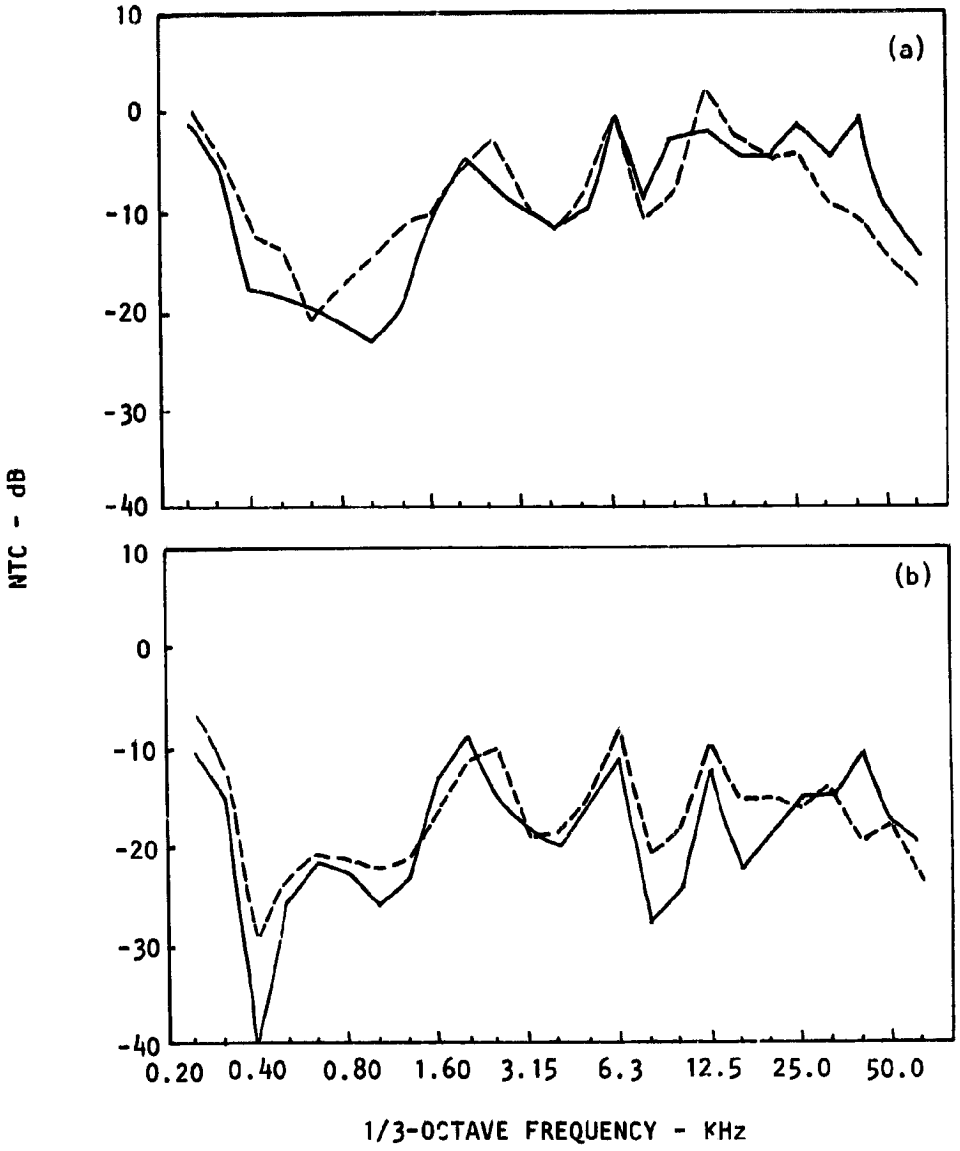

Figure 4.22 Effect of the primary temperature on the NTC of the multi-chute nozzle operated at $M_{J_1} = 0.8$, $M_{J_2} = 0.9$, $T_{R_2} = 600K$
T_{R_1}: ——, ambient; ---, 450K.

5. DEVELOPMENT OF SIGNAL AVERAGING TECHNIQUE FOR TRANSMISSION STUDIES

All acoustic data presented in the last two sections and also that obtained in Phase 1 [5.1] was based upon a single pulse analysis scheme where the pulse was produced by a high voltage spark discharge. It has by now become quite obvious that, in this method, whenever high levels of jet mixing or shock associated noise are superimposed as a background on the impulse received in the far-field, the pulse is either not detectable at all or there is considerable spectral contamination by the jet noise. This problem is found to be particularly severe close to the jet axis where the refraction effects reduce the pulse amplitude while the convective amplification increases the jet mixing noise and also at angles close to 90° and higher than 90°, where the pulse noise level is naturally low, while the shock associated noise from the supersonic jets is dominant.

In addition to this low signal to noise (S/N) ratio problem, a number of results obtained for the four nozzles investigated in this study, for those conditions whose S/N ratio was adequate, contradicted many of the conventional notions about transmission of sound through ducts and nozzles. For example, a comparison between the transmitted acoustic power (calculated from the in-duct measurements) and that measured in the far-field indicated a low frequency loss of up to 20 dB even when there was no flow through the nozzle system. Also at times, the predicted acoustic behavior in the far-field based upon the reflection coefficient data contradicted the measurements. For example, if the reflection coefficients decreased, one would expect to measure increased far-field sound levels but decreased far-field levels were measured instead.

Since high intensity pulses (spectrum level at the nozzle exit ≈ 130 dB) were generated by the spark discharge, it was suspected that possible non-linear problems associated with high intensity sound could be instrumental in explaining the above anomalies.*

The spark source had some other inherent operational problems as well. In particular, a high voltage electromagnetic pulse was generated whenever the spark was discharged. This led to numerous instrumentation and equipment problems. Furthermore, several minutes were required between discharges to recharge the capacitor bank.

In view of the above problems, a different technique was sought which could eliminate or minimize the above problems but at the same time retain the advantages of the impulse technique. Attempts were therefore made to develop a signal averaging technique. By this technique, a sufficient number of individual records are averaged, the stochastic contribution from the jet mixing noise should average to zero with a clean recovery of the pulse in the time domain. The other two main problems of very high noise levels (thus the associated possible non-linear effects) and the

* Based upon the results described in this section, similar results were found for low intensity sound as well.

electromagnetic radiation associated with the spark source can also be eliminated by this method.

The signal averaging technique was, therefore, first developed. An experimental investigation was then carried out with two objectives: (1) to substantiate the accuracy of the results obtained using the spark discharge method for low Mach numbers (M_j<0.8), and (2) to illustrate that for higher Mach numbers acoustic drivers in conjunction with signal averaging technique can be used instead of the spark discharge method.

The principle behind signal averaging for this investigation is first described in the next section. The actual method and the instrumentation together with the test plan are then described in section 5.2. This is followed by the test results in section 5.3. Finally, the general discussion and conclusions are presented in section 5.4.

5.1 PRINCIPLE OF SIGNAL AVERAGING

Signal averaging, sometimes also referred to as signal recovery, is averaging of time domain data containing a repetitive wave form (*signal*) contaminated with *noise*. It can recover repetitive wave forms from noise even when the raw data seems to contain little or no useful information.

In signal averaging the input signals are sampled at fixed time intervals, converted to digital form and then the sampled values are stored at separate locations in a memory. The sampling process is continued for a preset number of repetitions of the desired signal. The process is started out by storing the sample values in a memory, with each memory location corresponding to a definite sample time. Then, during subsequent repetitions, the new sample values are added algebraically to the values accumulated at the corresponding memory locations. After any given number of repetitions, the sum stored in each memory location is equal to the number of repetitions times the *average* of the samples taken at that point on the desired waveform.

To find the start of each repetition, a synchronizing signal must be available. Of course, the waveform of interest need not be periodic, but it must repeat exactly following each synchronizing pulse.

This simple summation process tends to enhance the signal with respect to noise. The signal portion of the input is a constant for any sample point, so its contribution to the stored sum is multiplied by the number of repetitions. On the other hand, the *noise* - which is random and not time-locked to the signal - makes both positive and negative contributions at any sample point during successive repetitions. Therefore, the noise portion of the stored sum grows more slowly than the signal portion.

This is a qualitative description of the signal averaging technique. A simple formulation can also be derived to determine the number of averages required to provide desired improvement in the S/N ratio. Following Trimble

[5.2] let the input be f(t), composed of a repetitive signal portion s(t) and a noise portion n(t). Let the kth repetition of s(t) begin at time t_k (and let $t_1 = o$). Then

$$f(t) = s(t) + n(t) \tag{5.1}$$

Let samples be taken ever T seconds, then

$$f(t + iT) = s(t_k + iT) + n(t_k + iT) \tag{5.2}$$

$$= s(iT) + n(t_k + iT)$$

For a given i and k, $n(t_k + iT)$ is a random variable and can in most practical cases be assumed to have a mean value of zero and an r.m.s. value of say β. And for different k's the noise samples are usually statistically independent.

Now the signal to noise ratio, (S/N) for the ith point on any particular repetition can be given by

$$S/N = \frac{s(iT)}{\beta} \tag{5.3}$$

After m repetitions, the value stored in the ith memory location is

$$\sum_{k=1}^{m} f(t_k + iT) = \sum_{k=1}^{m} s(iT) + \sum_{k=1}^{m} n(t_k + iT)$$

$$= m\, s(iT) + \sum_{k=1}^{m} n(t_k + iT) \tag{5.4}$$

Since the noise is random and the m samples are independent, the mean square value of the sum of the m noise samples is $m\beta^2$, and the r.m.s. value is $\beta\sqrt{m}$. Therefore, the signal - to - noise ratio after summation is

$$(S/N)_m = \frac{m s(iT)}{\beta\sqrt{m}} = \sqrt{m}\,(S/N) \tag{5.5}$$

Thus summing m repetitions improves the signal-to-noise ratio by a factor of $\sqrt{m}$. Thus an enhancement of signal-to-noise ratio by 20 dB (a factor of 10) will require 100 separate repetitions.

A total of 1024 repetitions were used in the present investigation which improved the signal-to-noise ratio by 30 dB over the single-shot spark source technique.

5.2 METHOD AND TEST SET-UP

5.2.1 The Source Section and the Instrumentation

A schematic showing the signal averaging procedure as adapted for the present investigation is given in Figure 5.1. A sharp pulse was fed through four electro-acoustic drivers into a source section. The electronic pulse that excites the drivers was also used as the triggering (or the synchronizing) signal which was fed to the real time analyzer SD-360 along with the actual pulse contaminated with jet-mixing noise. Typical time histories of the electronic signal, fed to the drivers and used as the trigger signal, together with the output of the drivers, jet mixing noise and the pulse before and after signal averaging are shown in Figure 5.1.

The source section, shown in Figure 5.2, consisted of four 100 watt electro-acoustic drivers arranged around the circumference of a 10 cm diameter duct connecting the test nozzles. This source section was physically located at the same position in the supply duct where the spark source was originally located for the daisy lobe and the reference conical nozzle.

The induct measurements were made by a 0.64 cm (1/4 in.) diameter B and K microphone (type 4136) mounted flush with the duct wall and was located 120 cm upstream of the nozzle exit. The far-field measurements were made by 1.28 cm (1/2 in.) diameter B and K microphones (type 4133) mounted, on a 1.2 meter radius polar arc, between the jet axis and 120° with the jet axis at 10° interval.

Other measurement and analysis details are identical to those described earlier for the spark discharge source except that the incident, reflected and the far-field pulses were now signal-averaged.

5.2.2 Test Plan

Since the present investigation was only a mini-study, designed primarily to substantiate the accuracy of the results obtained by using the spark discharge method and also to provide adequate data at high jet Mach number, data for only a limited number of test conditions was obtained. These are given in Table 5.1.

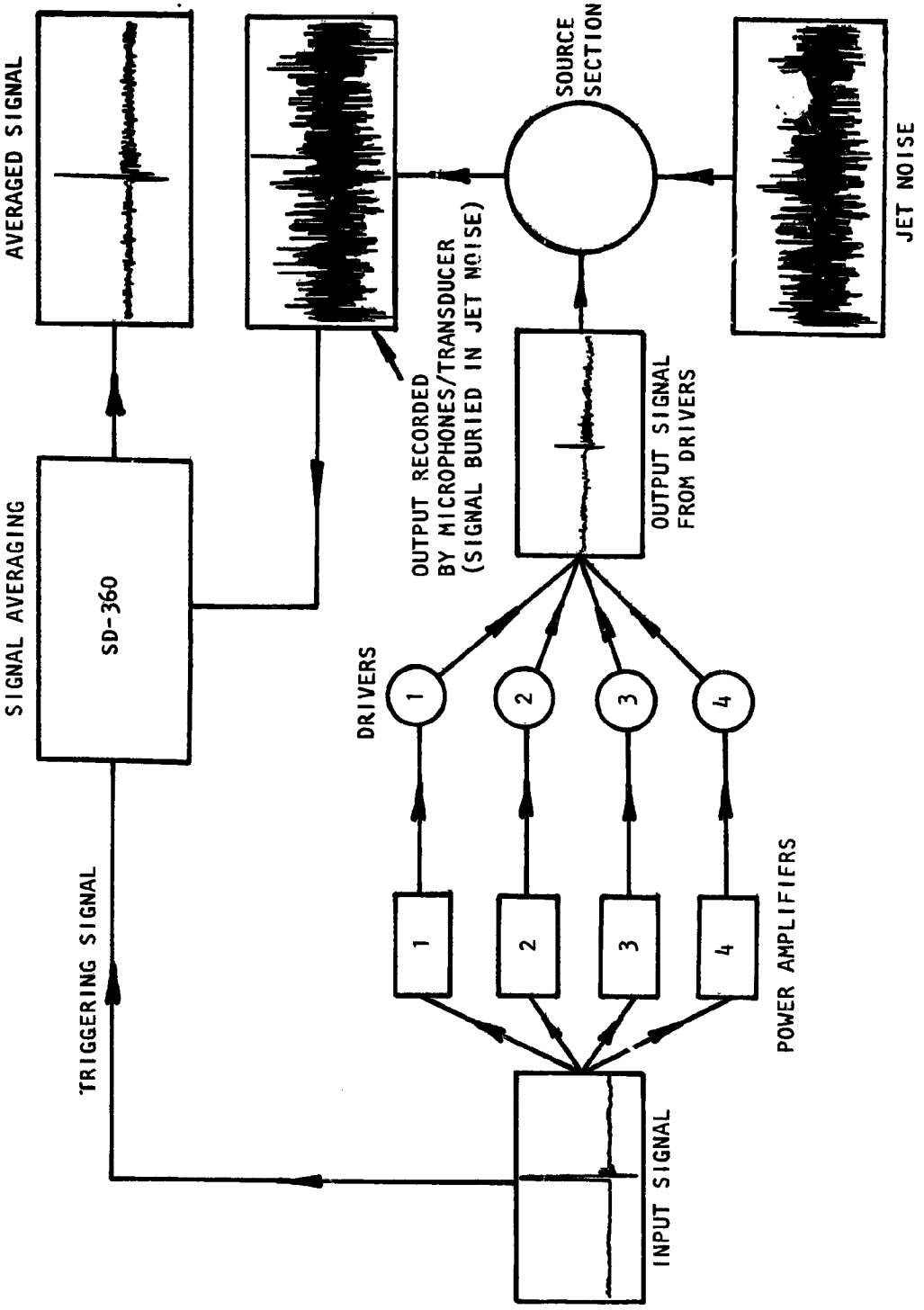

Figure 5.1 Schematic to show the signal averaging procedure.

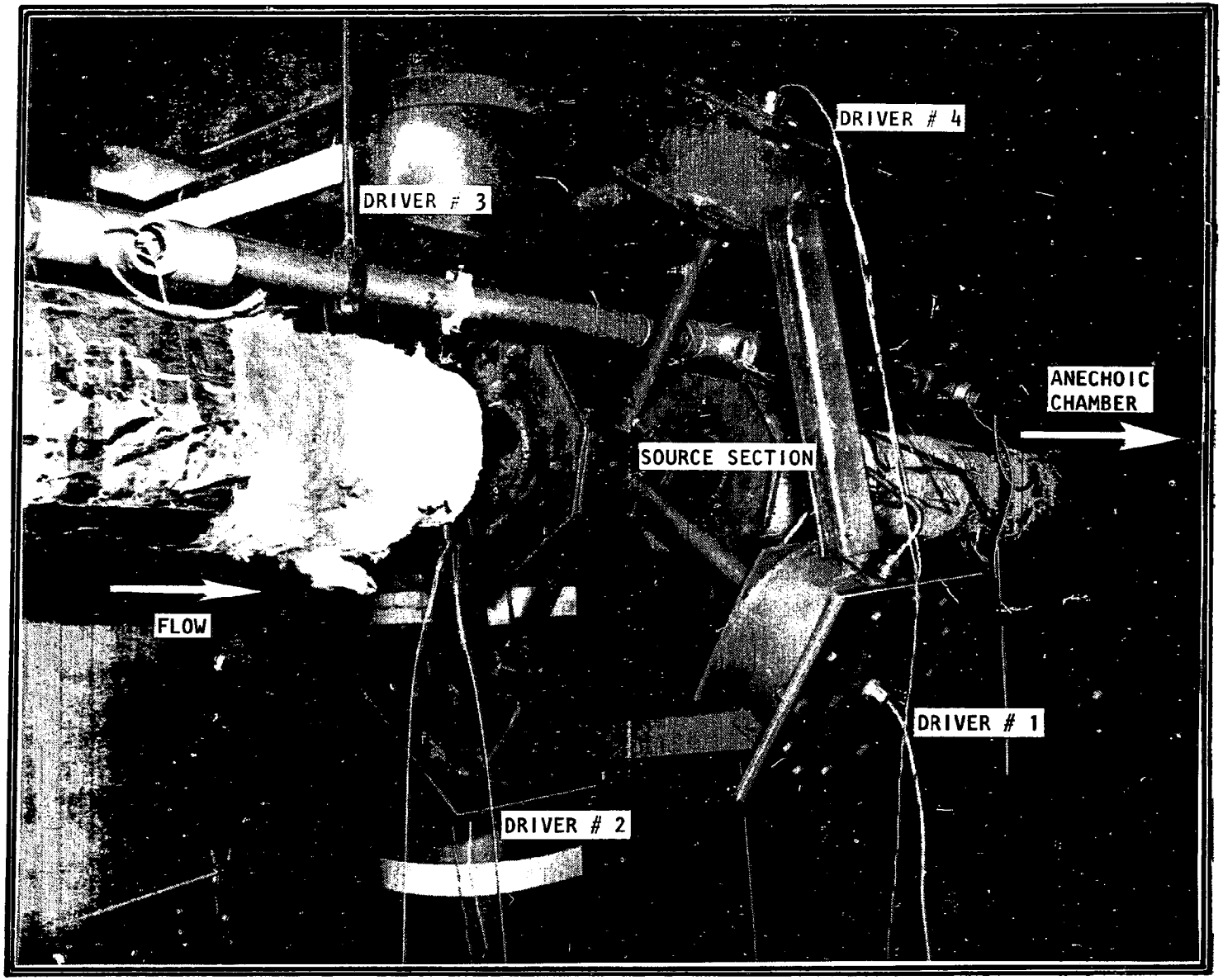

Figure 5.2 Photographic view of the drivers at the source section.

Table 5.1 Test plan for the data obtained with signal averaging.

Test Condition	Type of Nozzle	Jet Mach Number (M_J)	Temperature
1	Daisy Lobe	0.0	Ambient
2	Daisy lobe	0.6	Ambient
3	Daisy lobe	1.2	Ambient
4	Conical	0.0	Ambient
5	Conical	0.6	Ambient
6	Conical	1.2	Ambient

5.3 TEST RESULTS

5.3.1 Input and Output Signals

To investigate the internal noise transmission up to high enough frequencies the acoustic drivers must be capable of producing adequate levels of sound at all frequencies of interest. The spectral content of the output of the acoustic drivers, on the other hand, depends on the spectral content of the input signal and the frequency response of the drivers.

For this investigation an impulsive electronic signal, shown in Figure 5.3(a), was fed to each driver, periodically, at an interval of 33.33 ms. The spectrum (i.e. spectral content of the input signal) of this signal is shown in Figure 5.3(b) which is plotted up to 15 KHz (with 30 Hz bandwidth).

A typical time history of the output signal recorded by the in-duct microphone (after averaging) with the conical nozzle termination is shown in Figure 5.4(a) for zero flow conditions. The narrow band spectra (with 30 Hz bandwidth) of this incident pulse is shown in Figure 5.4(b). Due to the poor frequency response of the acoustic drivers, their acoustic output is very low at high frequencies. Therefore, the output of the acoustic drivers at higher frequencies needs to be improved. In view of the preliminary nature of this investigation, all the data analysis was, therefore, restricted to 10 KHz only. This frequency limitation was not considered to be a major restriction since one major objective was to resolve the *low* frequency absorption noticed at zero flow.

5.3.2 Recovery of the Pulse from the Dominant Jet Noise.

The random signals, plotted in Figure 5.5, show the time histories of the transmitted signal contaminated with jet noise for Mach numbers of 0.6 and 1.2

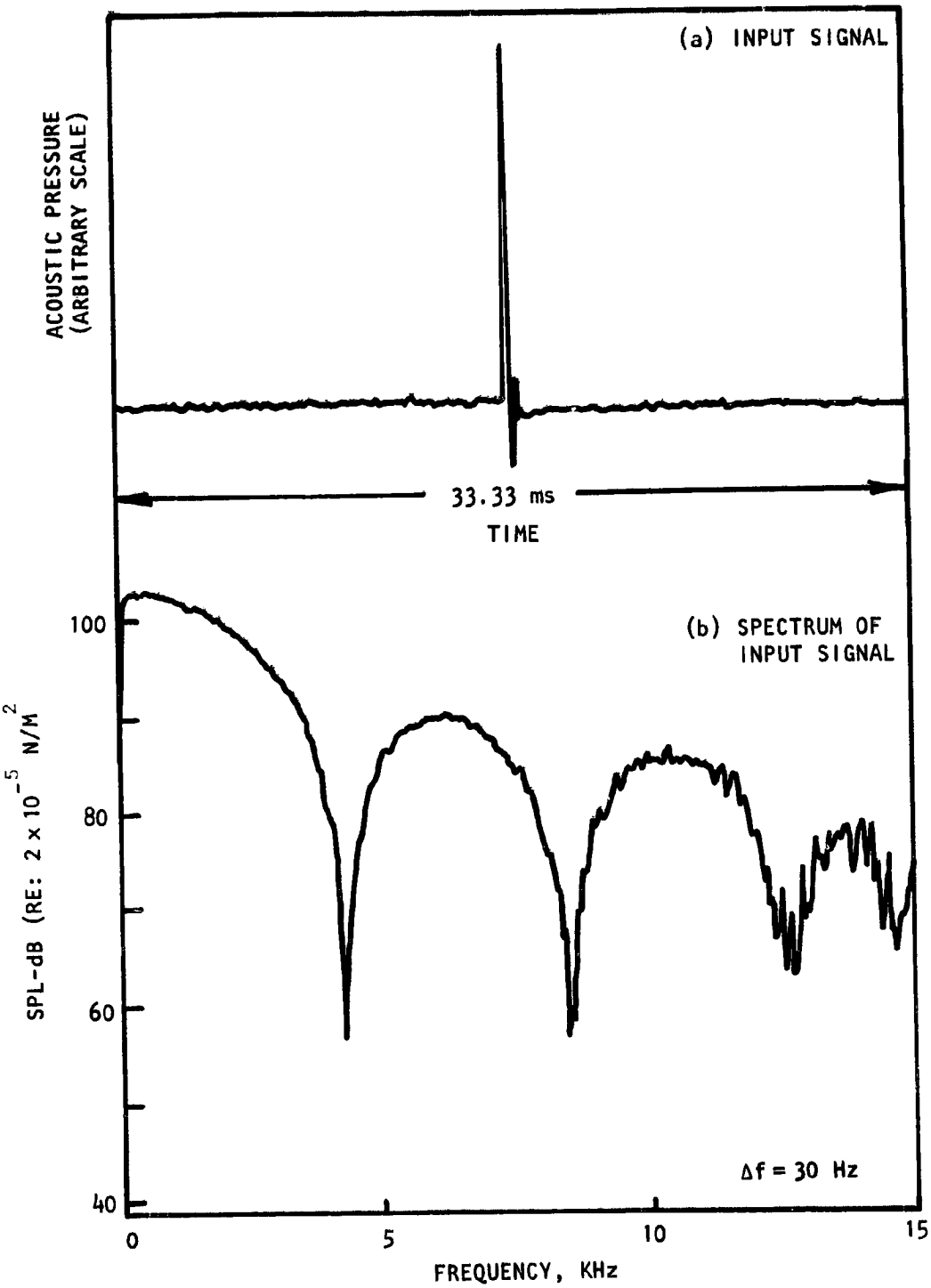

Figure 5.3. Time history and the spectrum of the input signal to drive each of the four drives located at the source section.

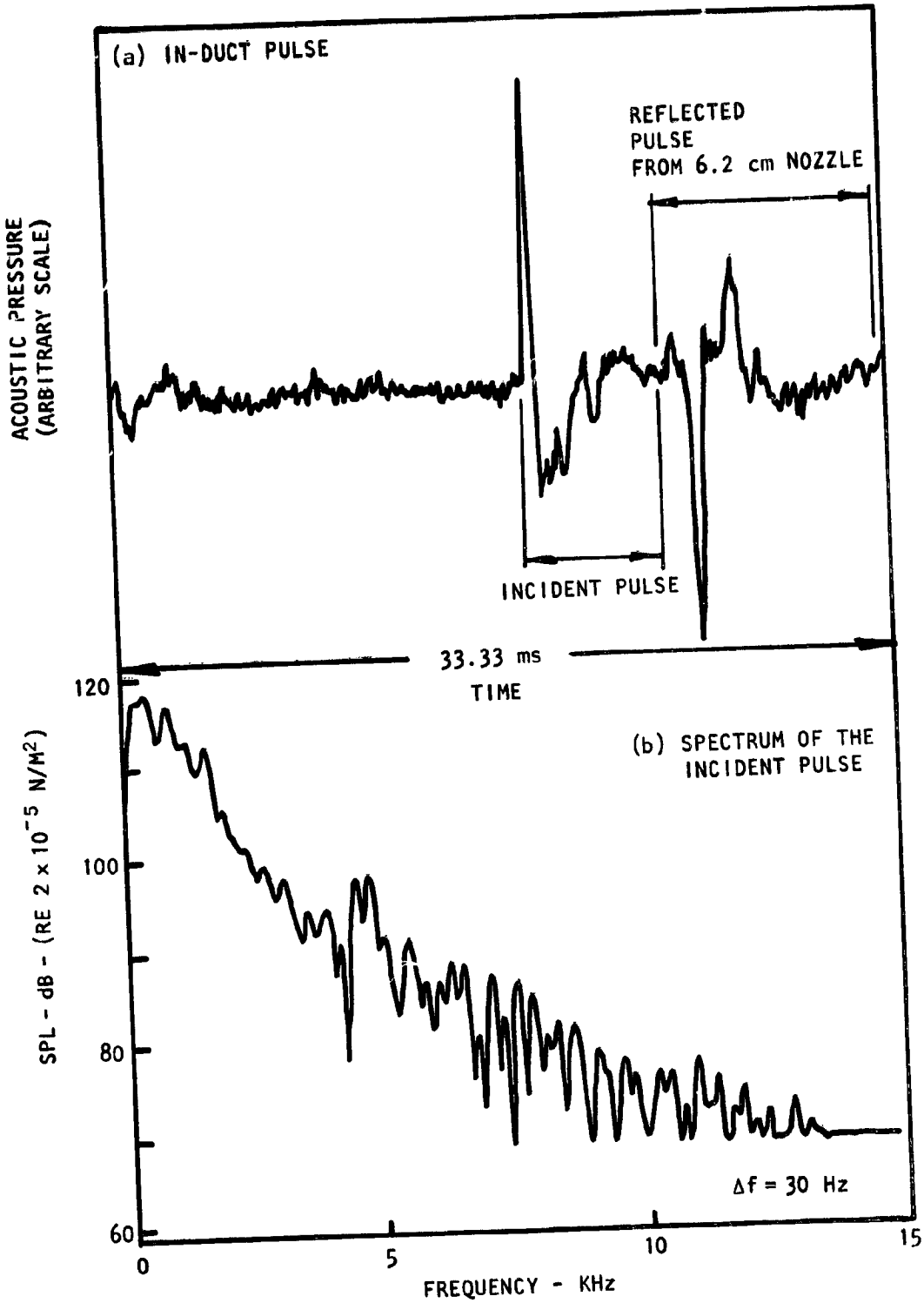

Figure 5.4. Time history of the in-duct (output) signal with 6.2 cm conical nozzle termination and the spectrum of the incident signal, $M_J = 0$

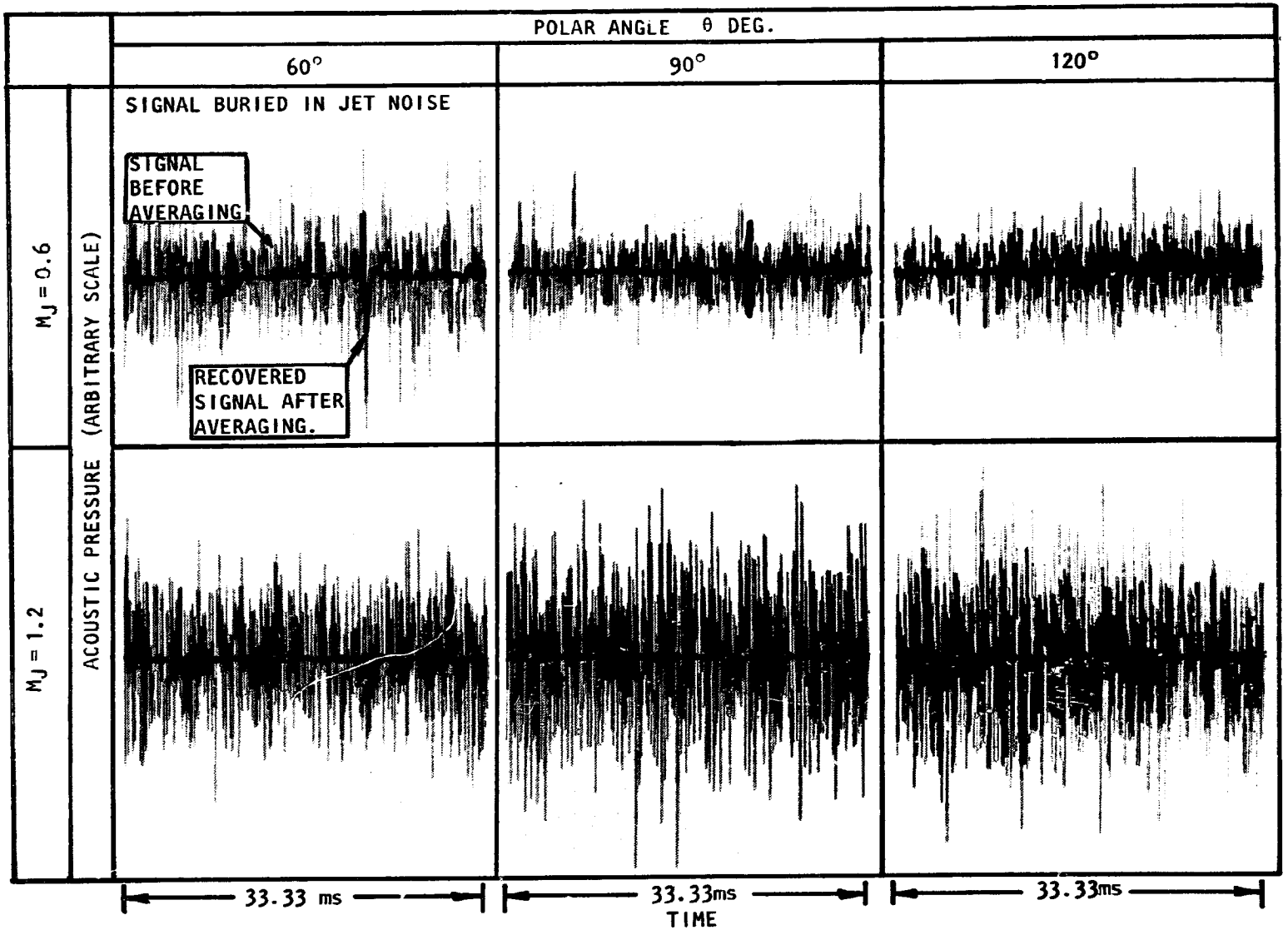

Figure 5.5. Recovery of the pulse from the jet noise by signal averaging process for the daisy lobe nozzle.

at various polar angles for the daisy lobe nozzle. It is impossible to identify the presence of the transmitted impulsive signal from this data. However, after signal averaging, these pulses stand-out clearly, as shown superimposed in a darker shade over the contaminated signal of Figure 5.5. Results similar to these were obtained for the conical nozzle and proved that the signal averaging technique is indeed a highly effective way of recovering the pulses buried in the jet mixing noise.

5.3.3 Comparison between the Spark Discharge and the Averaged Signal

Figures 5.6 and 5.7 show the comparison of far-field time histories for the daisy lobe and the conical nozzles, obtained using single spark discharge and averaged signal using acoustic drivers for jet Mach numbers of 0.6 and 1.2, respectively, at various polar angles. It is noticed that for the same condition of $M_J = 0.6$ the transmitted pulses, obtained using an acoustic driver source (without averaging), shown in Figure 5.5, are highly contaminated but those shown in Figure 5.6 obtained using a single spark discharge displays well defined shapes at each angle. This is due to much higher intensity of the spark discharge source compared to the output of the drivers.

At a jet Mach number of 0.6(see Figure 5.6), the signals obtained by single spark discharge and by signal averaging are quite clean. Therefore, it is expected that the spectral data for this condition, obtained by both the methods should compare well; which is shown, in the latter part of this section, to be true.

In Figure 5.7, where the far-field signals are compared at $M_J = 1.2$ as obtained by both the methods, one does not see the same trend as found in Figure 5.6 for $M_J = 0.6$. In this case, even for a spark discharge source, which was very intense, the transmitted pulse is not identified in the forward arc for both the nozzles. At those angles also, where the pulse appears to be present, it is highly contaminated. In contrast, the far-field signals obtained by signal averaging are clean at all polar angles for both the nozzles. In this situation, one should, therefore, expect to get more accurate results using the data obtained from the signal averaging technique. Data from the two schemes will now be compared in the frequency domain.

5.3.4 A Comparison of Spectral Data

NTC AT LOW MACH NUMBERS: Figure 5.8 shows the comparison of NTC for the daisy lobe nozzle for $M_J = 0$ and $M_J = 0.6$ at polar angles of 60° and 90°, obtained using the single spark discharge method and using the signal averaging method. For zero flow conditions, as shown in Figure 5.8(a), the agreement between the NTC values obtained by both the methods is excellent, except for very low frequencies (i.e. around 200 Hz). However, at $M_J = 0.6$ (see Figure 5.8(b)), though the overall agreement is good, the lower frequency NTC values obtained by signal averaging appear to be slightly higher compared to the NTC values obtained by spark discharge. As discussed later in section 5.4 one of the possible reasons for such a discrepancy could be the higher intensity of the signal generated by spark discharge. Another possible source of error could be the jitter of the impulses during averaging, a problem yet not resolved in this investigation (see section 5.4). However, the degree of

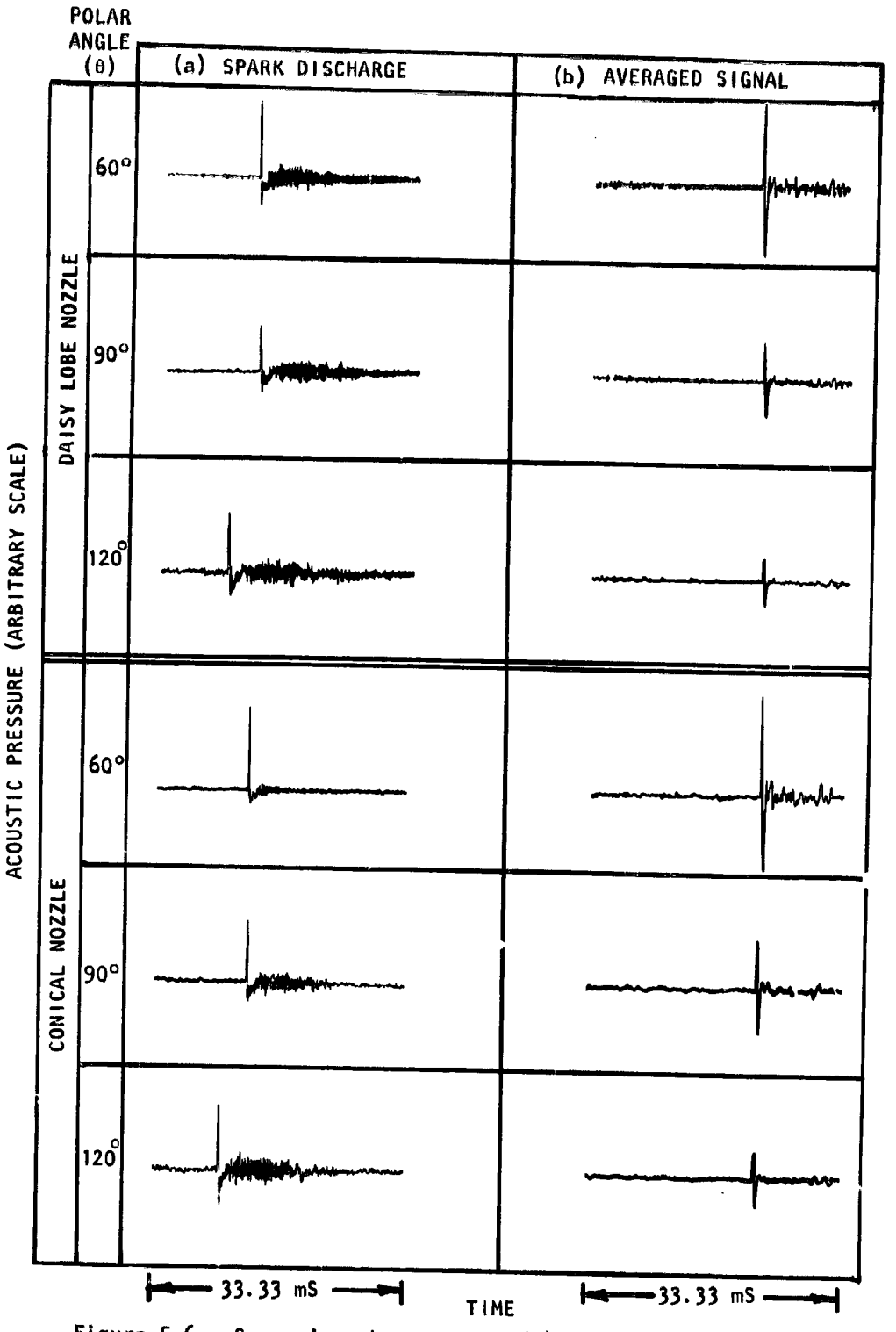

Figure 5.6 Comparison between the (a) signal obtained using single spark discharge and (b) averaged signal using acoustic drivers for daisy lobe nozzle and conical nozzle at $M_J = 0.6$

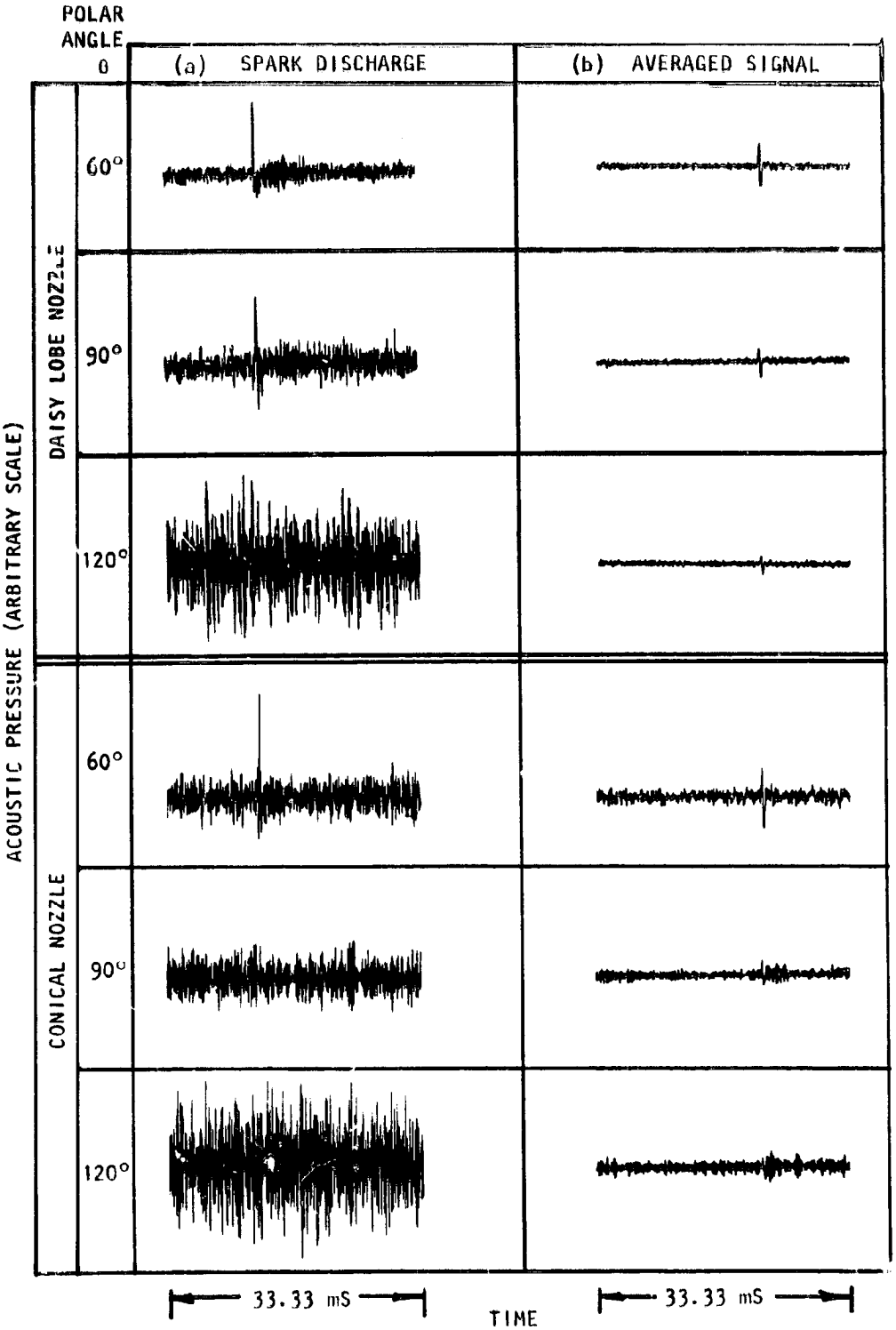

Figure 5.7 Comparison between the (a) signal obtained using single spark discharge and (b) averaged signal using acoustic drivers for daisy lobe nozzle and conical nozzle at $M_j = 1.2$

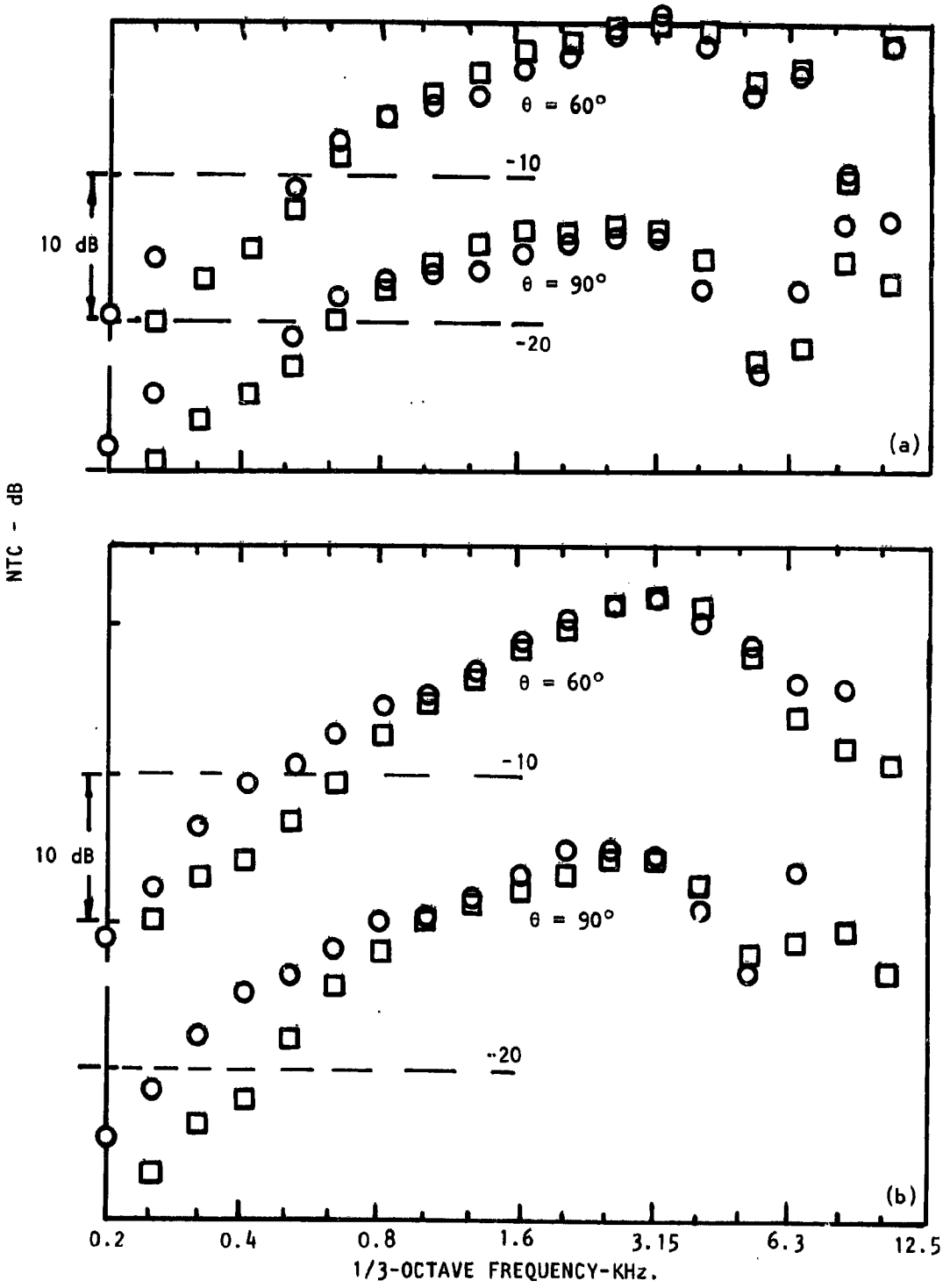

Figure 5.8 Comparison of NTC spectra obtained by using single shot spark source (□) and acoustic source with signal averaging (○) for daisy lobe nozzle. M_J: (a) 0.0, (b) 0.6

agreement, based upon a preliminary investigation, is rather good, and as observed in this figure, substantiates the quality of the data presented earlier in this report, using the spark discharge method, at least for lower jet Mach numbers.

NTC AT HIGH MACH NUMBER. Figure 5.9 shows the comparison of NTC spectra for the daisy lobe nozzle for $M_J = 1.2$ at polar angles of 60° and 90°, obtained by the two methods. Though the far-field time history at $\theta = 60°$ for the spark discharge case, as seen in Figure 5.7, is slightly contaminated with jet noise, the NTC spectrum compares well with that obtained by signal averaging. Whereas at $\theta = 90°$, where the jet noise was dominant over the transmitted pulse (see Figure 5.7) for the spark discharge case, the NTC spectra agreement between the two methods is very poor, which was expected. Therefore, for higher flow conditions, the signal averaging seems to be a more accurate method to evaluate internal noise transmission characteristics of nozzles.

ACOUSTIC POWERS. Figure 5.10 shows the comparison of power transfer functions for the daisy lobe nozzle obtained by the spark discharge and by signal averaging methods at $M_J = 0$ and $M_J = 1.2$. As expected, the agreement between the power transfer functions at $M_J = 0$, obtained by both the methods, is very good. However, at $M_J = 1.2$, the power transfer functions, obtained by both the methods, also agree well even though the individual NTC spectra do not compare well in the forward arc (see Figure 5.9). It could be due to higher values of NTC around $\theta = 60°$ where the comparison between NTC spectra obtained by both methods, as shown in Figure 5.9, is good and the power transfer function calculations are primarily affected by these high levels.

The main purpose of presenting these acoustic power comparisons, however, is to show that the low frequency absorption noticed with the spark discharge method is still noticeable indicating that it must be a genuine phenomenon.

REFLECTION COEFFICIENTS. Figure 5.11 shows the comparison of reflection coefficient spectra for the daisy lobe nozzle obtained by the spark discharge and by signal averaging methods at $M_J = 0$ and $M_J = 1.2$. The agreement between the reflection coefficient spectra is very good up to first radial cut-on frequency ($\simeq$ 4 KHz) for $M_J = 0$ and up to 1.25 KHz for $M_J = 1.2$. The discrepancy at higher frequencies is mainly due to the difference in higher mode contents in the signals, by the two methods, since the higher mode contents are influenced by the source orientation and strength.

Since the objectives of this investigation are fulfilled by discussing the daisy lobe nozzle data, presented in Figures 5.8 through 5.11, the conical nozzle data are not presented here. However, similar observations were made from the results obtained for the conical nozzle also.

5.4 DISCUSSION AND CONCLUSIONS

5.4.1 Effect of Source Intensity on Nozzle Transmission Characteristics

It has been observed in the Figures 5.8 through 5.11 that, at lower frequencies, the NTC, power transfer functions and reflection coefficients, obtained by the signal averaging method are relatively higher compared to the corresponding

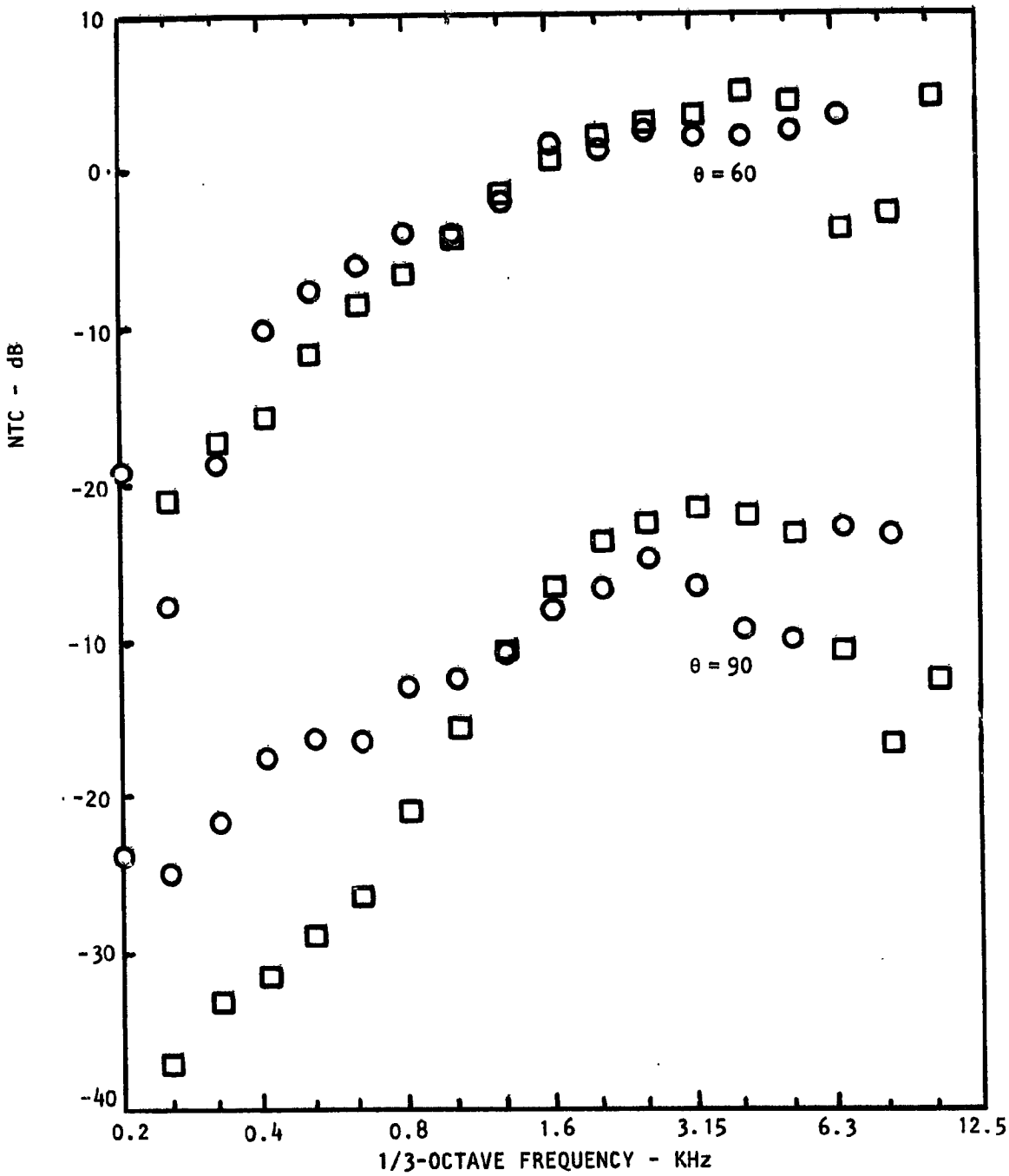

Figure 5.9 Comparison of NTC spectra obtained by using single shot spark source (□) and acoustic source with signal averaging (O) for daisy lobe nozzle, $M_J = 1.2$

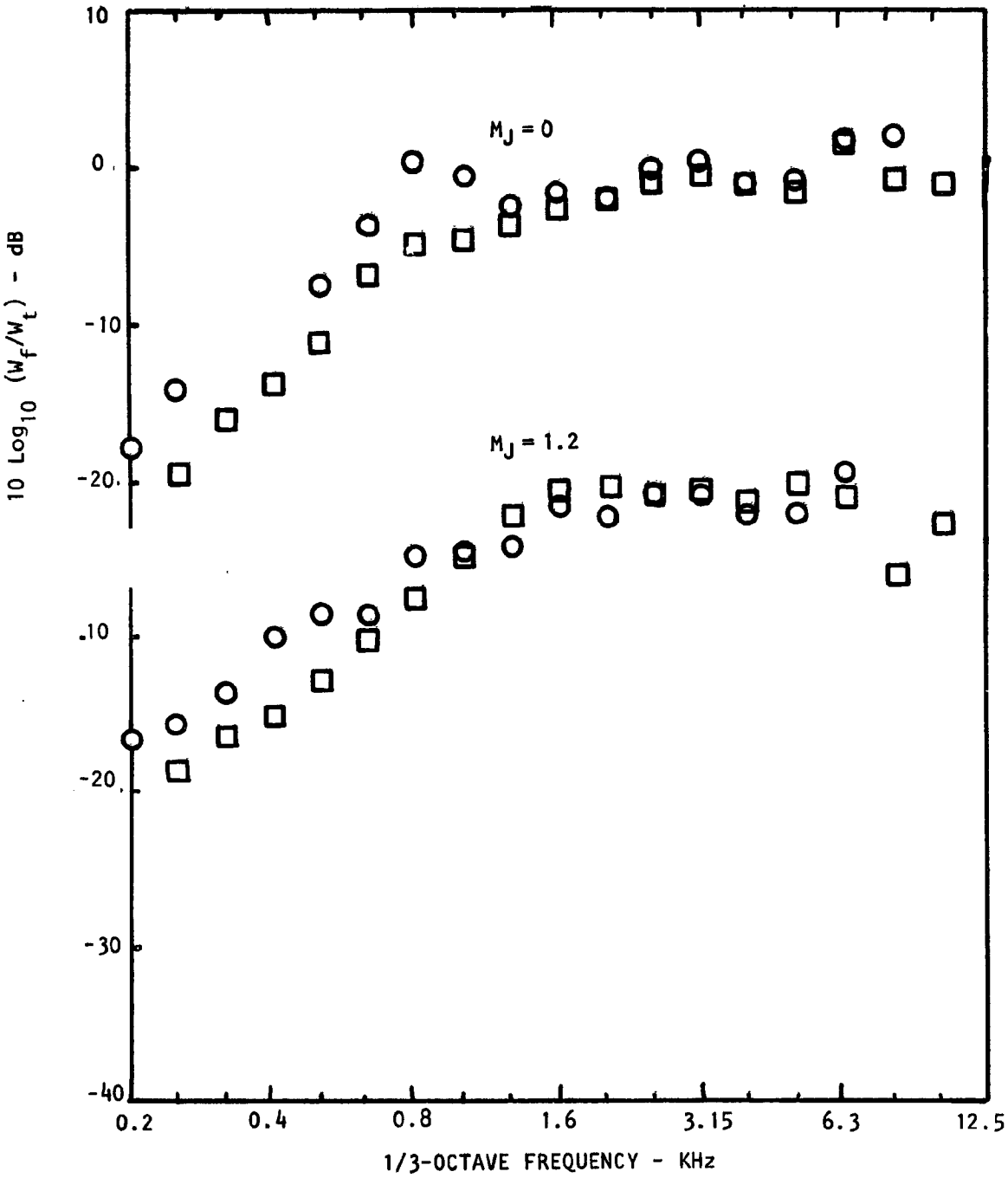

Figure 5.10 Comparison of far-field power normalized with respect to transmitted power obtained by using single shot spark source (□) and acoustic source with signal averaging (○) for daisy lobe nozzle.

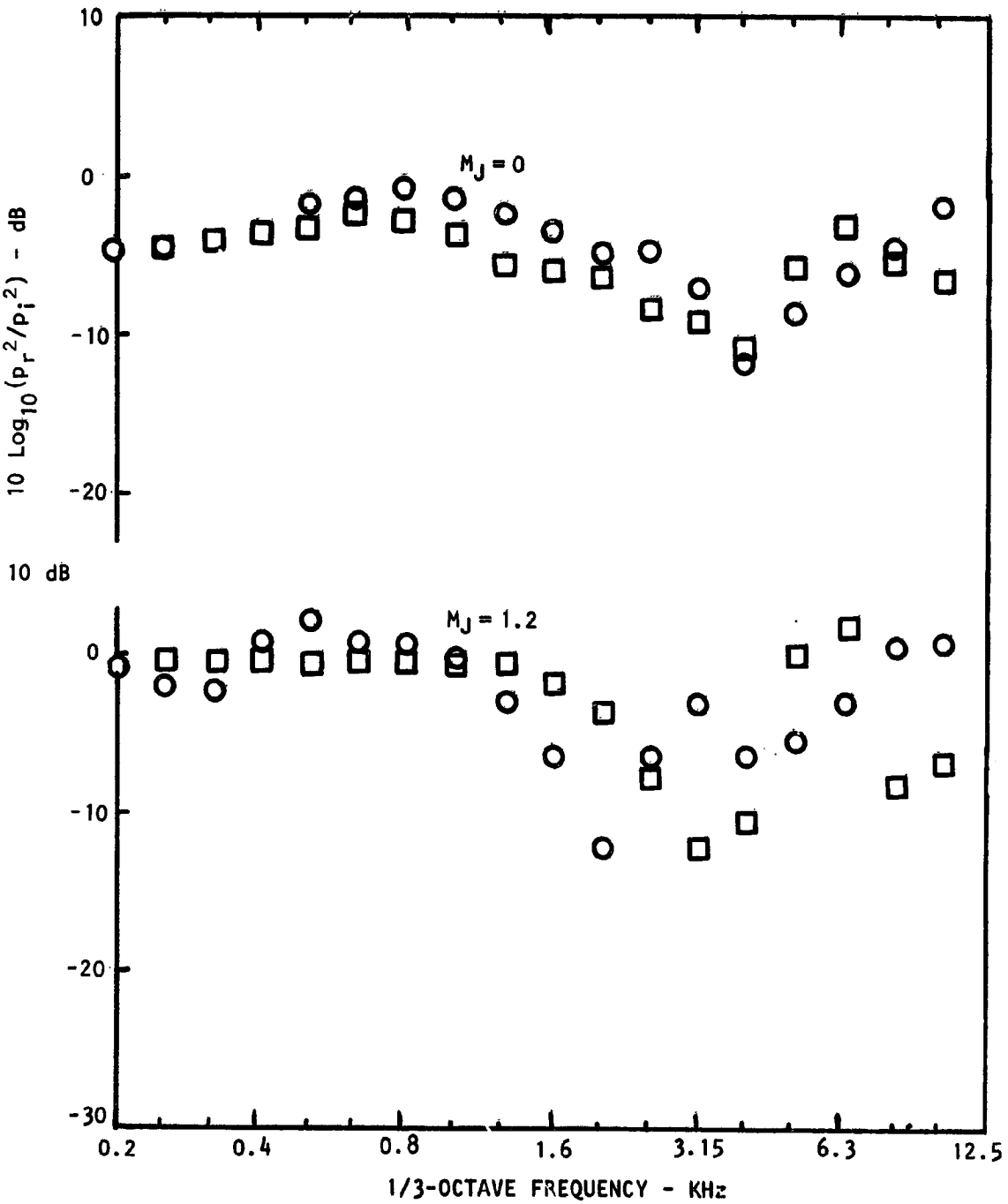

Figure 5.11 Comparison of reflection coefficient spectra obtained by using single shot spark source (□) and acoustic source with signal averaging (O) for daisy lobe nozzle.

values obtained by the spark discharge method. Since the spark discharge intensity was much higher compared to the output of the drivers in the signal averaging technique, it was felt that the discrepancy mentioned above could be due to the intensity of the source type. To substantiate this hypothesis some tests were conducted for a 10 cm diameter duct using a spark discharge source with varying spark discharge voltage. Three different spark discharge intensities are considered here, for which the discharge voltages were 4 KV, 7 KV and 10 KV. The corresponding narrow band (bandwidth = 40 Hz) spectra of the incident pulses are plotted in Figure 5.12. It is observed that the SPL values for 10 KV discharge voltage are about 20 dB higher than those for 4 KV discharge voltage test. Similarly the far-field transfer functions obtained for the tests with 4 KV and 7 KV discharge voltages with respect to those for the 10 KV case are plotted in Figure 5.13 for polar angles of 60°, 90° and 120°. If the above hypothesis is true, then the relative transfer functions plotted for 4 KV and 7 KV in Figure 5.13 will show positive values. In fact, for lower frequencies, (up to 3 KHz) where the spectral levels of the incident pulses are high (see Figure 5.12), the relative transfer functions appear to be identical for each discharge voltage.

It should be noticed that the data shown in Figures 5.12 and 5.13 are for a 10 cm diameter straight duct. With the nozzle attached to this duct, the acoustic intensities at their exits will, however, be somewhat higher . What effect the nozzles have on the NTC as a function of sound intensity is not quite clear and needs further investigation.

Results presented here for the straight duct, however, do not explain why there are differences, even though not large, between the two methods as noted earlier. Other reasons must, therefore, be found to explain these differences.

5.4.2 Effect of Jitter on Signal Averaging

During the analysis of the present data using signal averaging, it was observed that even for zero flow, minor jitters were present in the signal as it was being averaged. These could be due to slight changes in the physical conditions while acquiring the data. Such effects could be even more pronounced in the presence of the flow where physical conditions are difficult to maintain constant. It is conceivable that this effect was responsible for the differences noticed in the data obtained by the two methods.

5.5 CONCLUSIONS

Minor differences were noticed between the data obtained from the two methods. It was, not possible to establish precise reason(s) for these differences. Original objectives, however, were basically accomplished. In view of the preliminary nature of this investigation, the agreement, on the average, between the two schemes was quite good. The signal averaging technique also proved to be superior over the spark discharge method for the higher flow conditions.

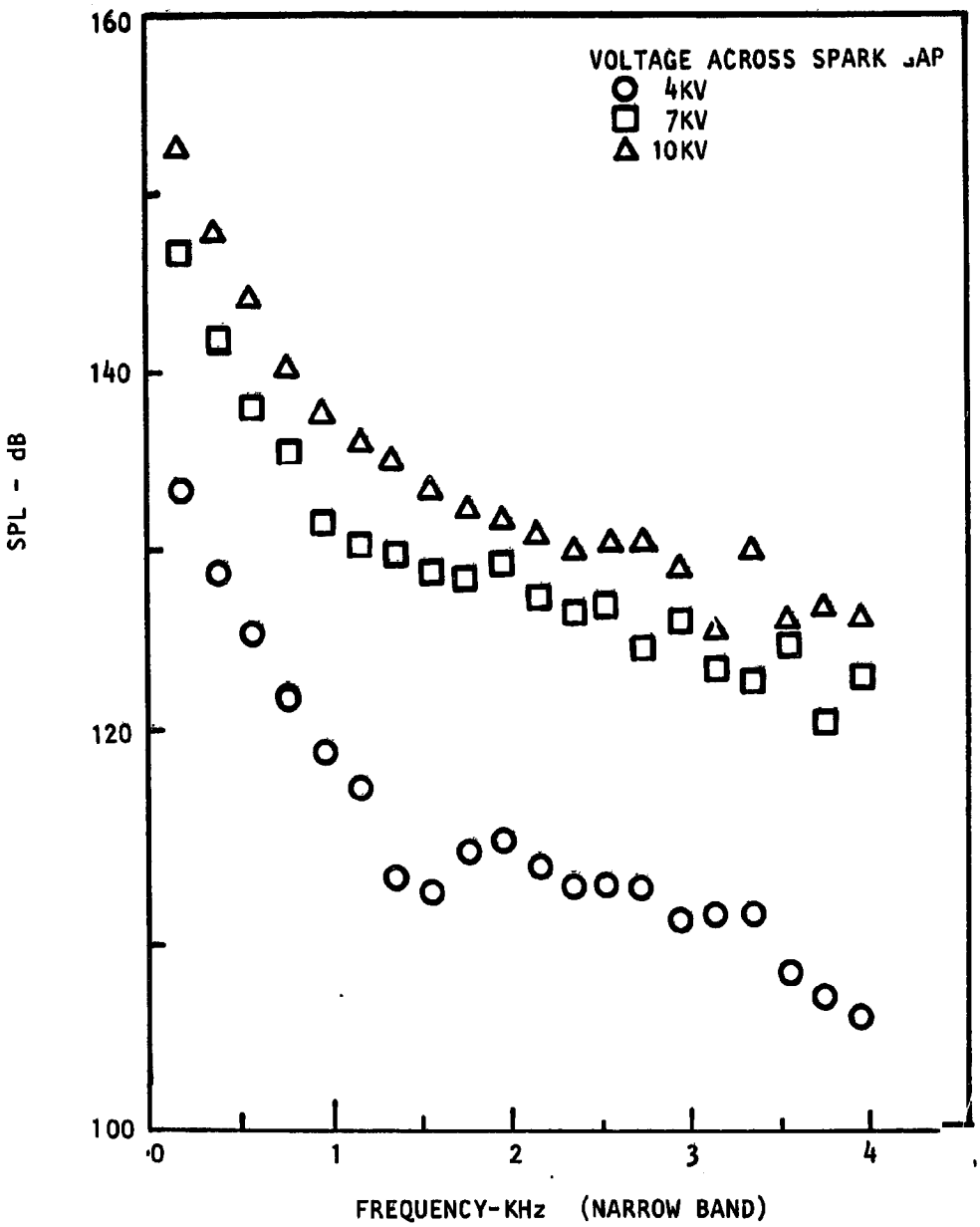

Figure 5.12 Spectra of the incident pulses at various source intensities generated by varying spark discharge voltage for a 10cm straight duct

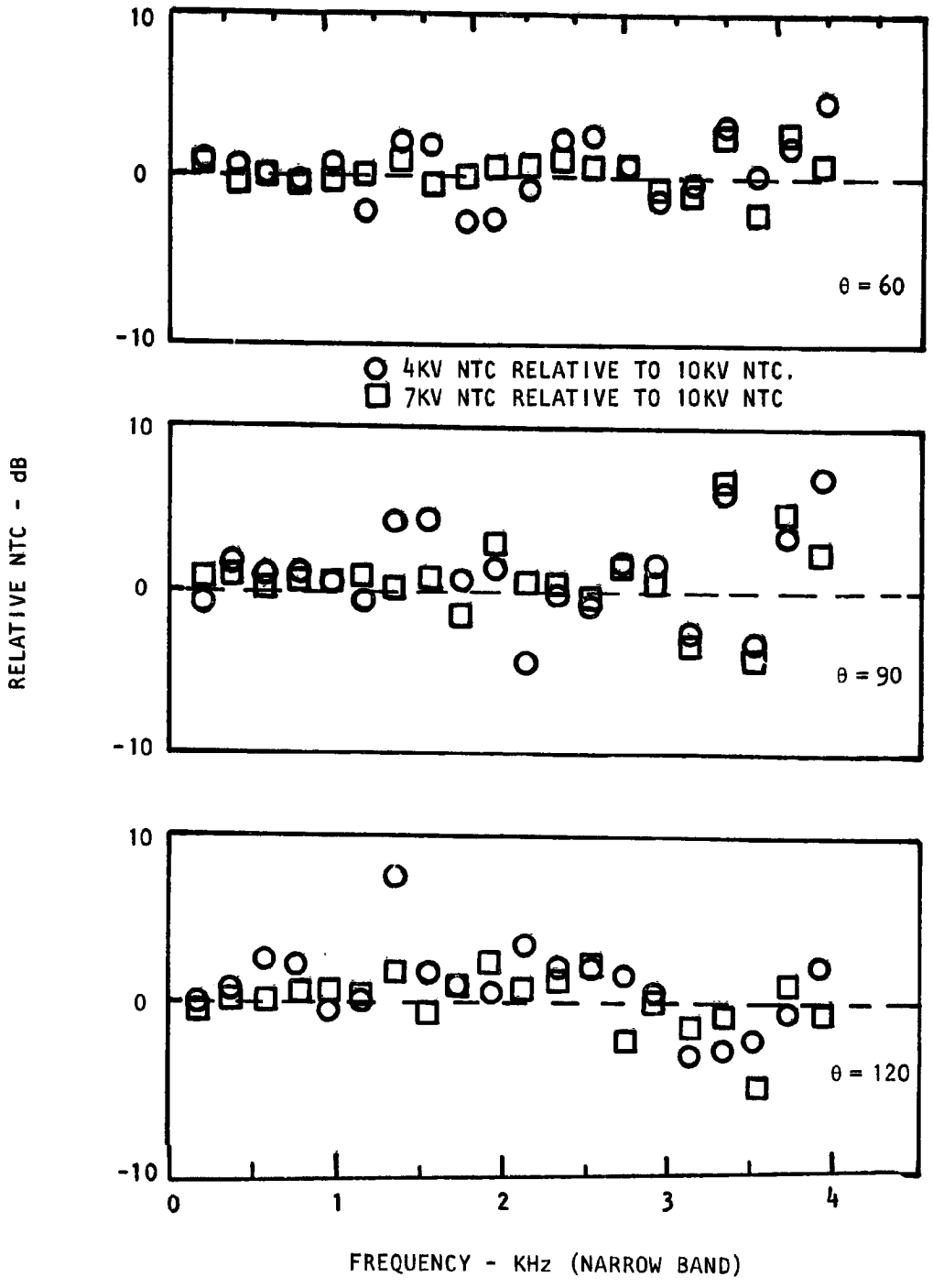

Figure 5.13 Relative far-field transfer function spectra at various source intensities generated by varying spark discharge voltage for a 10cm straight duct.

5.6 FUTURE WORK

The signal averaging technique described here is undoubtedly a superior technique to determine the transmission characteristics of the nozzles. Two particular areas, however, require considerable further work. These are concerned with (1) increasing of the range of frequencies over which the acoustic drivers produce strong acoustic signals and (2) the jitter effect while averaging.

These problems are now under investigation at Lockheed-Georgia Company.

6. MISCELLANEOUS RESULTS AND FINAL CONCLUSIONS

The work presented in this report describes an experimental program for understanding the characteristics of internal noise radiation through multi-element, single as well as dual stream, mechanical suppressors. Over and above the transmission results, some other interesting results were also acquired as a by-product of this study. These primarily concerned the jet-noise amplification and the suppression of jet mixing and shock-associated noise. Due to their interesting nature, some typical results are presented in the next section under "Miscellaneous Results". This section also includes base pressure profiles with and without the tunnel flow for the single stream daisy lobe suppressor. General discussion followed by the final conclusions are then presented.

6.1 MISCELLANEOUS RESULTS

6.1.1 Jet Noise Amplification

It has recently been shown by many researchers [6.1, 6.2] that above a certain excitation level, broad band jet noise can be amplified considerably by pure tone or broad band sources. Such effects were noticed in the present results also.

Typical far-field time histories measured at 70° for $M_J = 0$ and $M_J = 0.6$ for the daisy lobe nozzle are shown in Figure 6.1(a). The corresponding in-duct time histories are shown in Figure 6.1(b). The amplification of jet noise following the pulse is quite obvious in this figure which first gets amplified and then decays to a level that existed prior to the pulse.

Results with signal averaging presented in section 5 indeed confirm the presence of this jet noise amplification. Due to the stochastic nature of both the unamplified and the amplified jet mixing noise, it is virtually averaged out to zero after many averages. It was found that the averaged far-field pulses did not display amplification following the main pulse (for example see Figure 5.6). This indicated that the amplified part of the time history obtained using a single shot spark source was not related to the pulse but to the jet mixing noise.

Similar results were obtained at other angles and Mach numbers with maximum amplification noticed at 50° to the jet axis. Limited data inspected from the jet-noise amplification point of view for both the daisy lobe suppressor and the conical nozzle disclosed that jet noise amplification by upstream pulses was significant only for the daisy lobe suppressor nozzle for which the jet mixing noise was considerably lower than that for the reference conical nozzle.

Similarly, the dual stream nozzles did not appear to indicate strong jet noise amplification following the pulse.

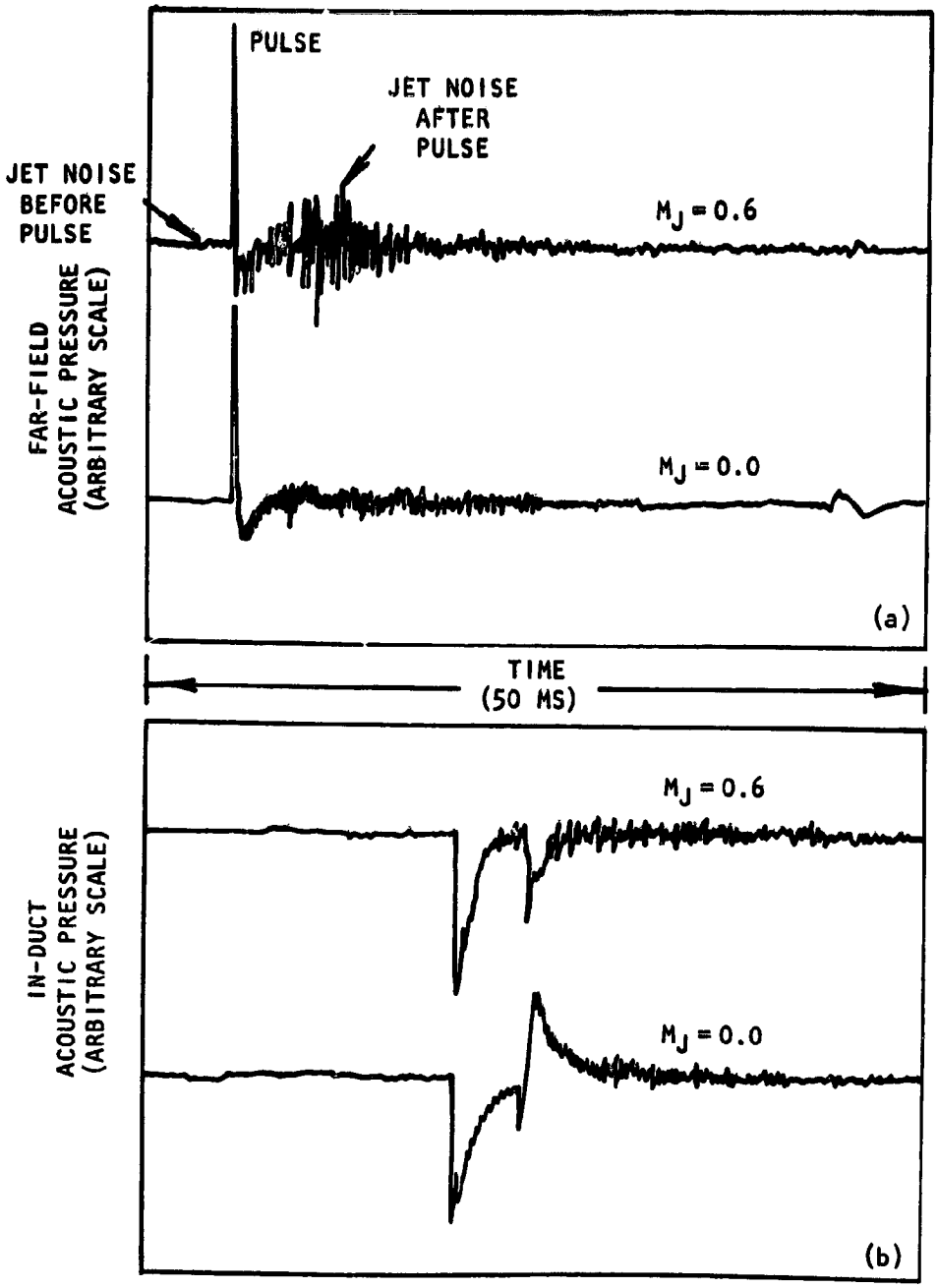

Figure 6.1 (a) Typical far-field signals ($\theta = 70°$) demonstrating jet noise amplification following the pulse and (b) the corresponding in-duct time histories

6.1.2 Jet Mixing Noise

STATIC DATA. Typical 1/3-octave SPL for the two nozzles operated at $T_R = 600K$ for $M_J = 1.2$ are shown in Figure 6.2. Spectra at polar angles of 30°, 60°, 90° and 110° are presented. Clearly, maximum reduction is obtained at $\theta = 30°$. The peak SPL has reduced by about 25 dB. Even though the jet is operated at supercritical conditions, conical nozzle data at small angles is dominated by jet mixing noise at all frequencies. At $\theta = 90°$ and in the forward arc shock associated noise is dominant at high frequencies and the jet mixing noise at low frequencies. Comparison of the spectra for the conical and the suppressor nozzle in Figure 6.2 thus indicates that the daisy lobe nozzle reduces both the jet mixing noise and peak levels of the shock associated noise. In addition to reduction in peak levels a frequency shift in the spectrum of the suppressor with respect to the conical nozzle is also noticed. This is attributable to shock-cell noise from the smaller elements of the suppressor.

The reduction in shock-cell noise produced by the suppressor can be explained by the fact that breaking up a large, round jet into very small, individual jets cause the shock-cell formation to be dissipated rapidly. The shock-cell spacings and cross-sectional dimensions are much smaller and the cells are likely to be fewer in number. The resulting shock associated noise is therefore likely to be much lower in level and higher in frequency than that for the reference conical nozzle.

Reduction of jet mixing noise from the daisy lobe nozzle in the rear arc is primarily due to a reduction in convective amplification as a result of lower convective eddy velocities [6.3] and due to lower turbulence levels. Due to mixing by the additional entrainment air for the multi-lobe multi-tube nozzle the mean velocities decay quite rapidly and therefore the majority of the noise-producing turbulent eddies in the plume convect downstream at a substantially lower velocity than in a conical nozzle.

Flow and sound measurements made by Regan and Meecham [6.4] for multi-tube nozzles suggest that the turbulence intensity in multi-tube suppressor flows can reduce in excess of 20% compared with the unsuppressed jet exhaust of equal area. Their work also demonstrated that the high-frequency sound radiated directly to the far-field by a multi-tube suppressor nozzle is primarily from the exterior tubes and that the overall suppression of jet-mixing noise can be attributed to a reduction in turbulence intensity.

Noise comparisons between the daisy lobe nozzle and a reference conical nozzle have also been given by Douglas Aircraft Company [6.5], but their data shows much less reduction at small angles compared to that shown here.

FLIGHT DATA. Effect of free-jet velocity on jet noise spectra of the daisy lobe nozzle operated at $M_J = 1.2$ and $T_R = 600K$ is shown in Figure 6.3. It is seen that at all angles the low frequency noise is reduced while the high frequency noise is increased.

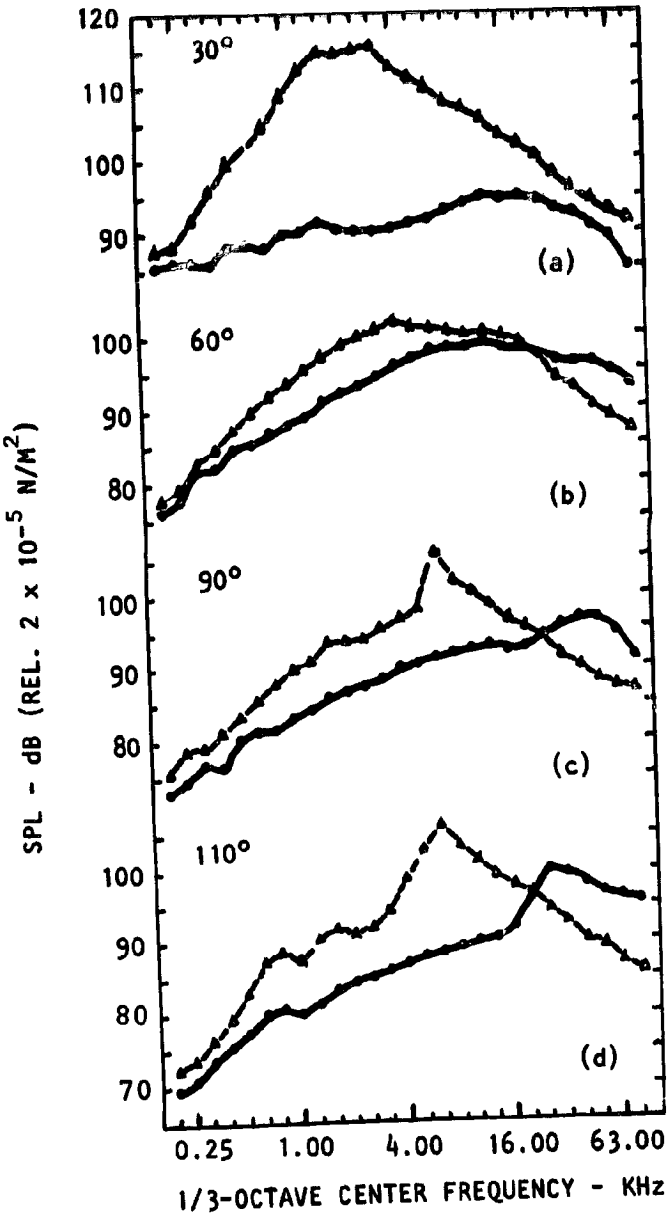

Figure 6.2 1/3-octave jet noise spectra for the daisy lobe nozzle (-●-) and the reference conical nozzle (-Δ-) at $M_J = 1.2$ and TR = 600 K.

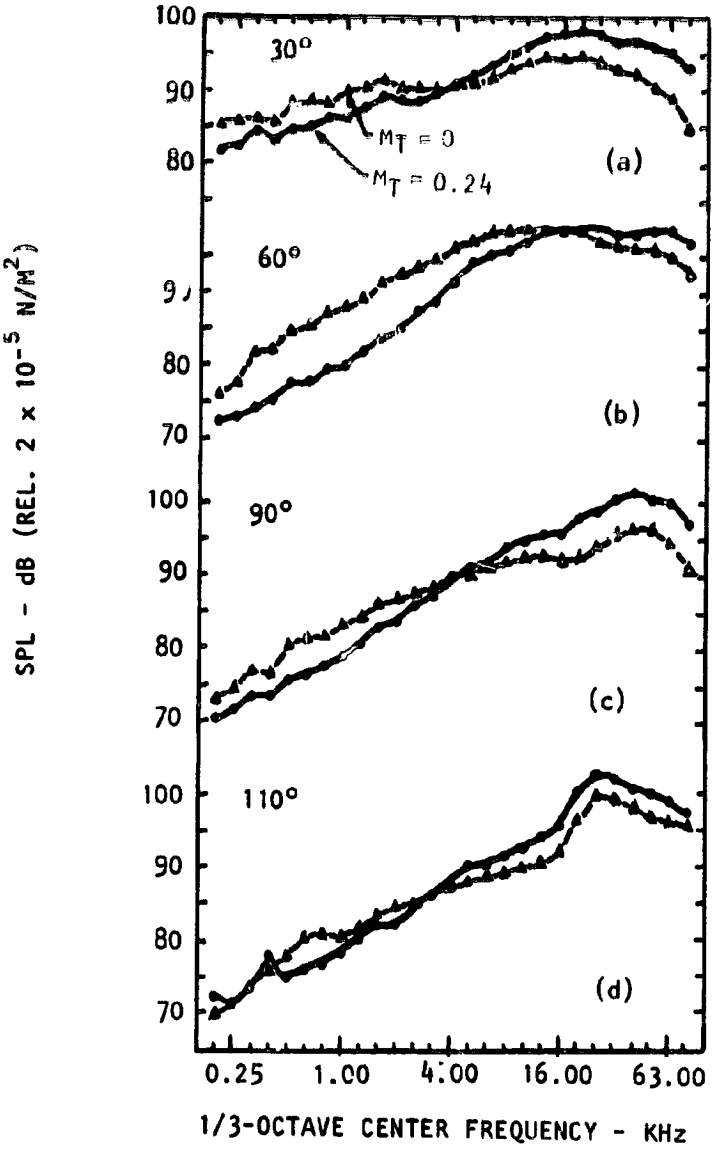

Figure 6.3 Effect of free-jet velocity on jet noise of the daisy lobe nozzle at $M_J = 1.2$ and TR = 600 K for $M_T = 0.0$ (-Δ-) and $M_T = 0.24$ (—●—)

The reduction at low frequencies is understandable. Low frequency noise for the daisy lobe nozzle emanates from the so called "merged flow region" of the nozzle system [6.6]. In this region the jet system can be treated as a single jet moving at the finally merged velocity. Effect of forward velocity is then to reduce the jet mixing noise normally associated with relative velocity reduction [6.6, 6.7]. It is not quite clear, however, why the high frequency noise has increased at all angles. One would expect to see such an increase in noise only in the forward arc as noticed in our earlier studies on shock containing single jets [6.7]. This observed effect at high frequencies emanating from "pre-merged" flow regions needs further investigation since in other studies [6.6] it is found that source alteration due to flight appears to be primarily confined to the "merged flow region" only.

The increase at high frequencies noted at all angles could be a result of the under-expanded jet becoming highly unstable when confined by a subsonic co-flowing stream. It was noticed by Ahuja [6.8] and Bhutiani [6.9] that under certain conditions if an under-expanded jet was superimposed by a coflowing subsonic stream the jet became highly unstable resulting in increased levels of noise.

In summary, the daisy lobe nozzle is indeed a good jet noise suppressor but the effects of flight largely remain to be understood.

Jet mixing noise from the dual stream nozzles were not analyzed in detail at the time of writing this report. Limited inspection of the data, however, indicated that the noise benefits of the 36-chute suppressor were only marginal compared to the reference coaxial nozzle.

6.1.3 Base Drag Data

We were required to provide some data on static pressures measured in the base of the daisy lobe nozzle. Base pressures were measured through three pressure ports on the center plug and four pressure ports located between the lobes as shown in Figure 2.6. Base pressure data for $M_J = 0.4$, 0.6, 0.8, 1.2, and 1.4 with the nozzle operated statically and also at $M_T = 0.08$, 0.16 and 0.24, is given in Table 6.1. Ratios of the measured base pressure and the ambient pressure ($=P_{Base}/P_{Ambient}$) as a function of the radial distance of the pressure ports are given in the table and also plotted in Figures 6.4(a) thru 6.4(d) for free-jet Mach numbers of 0.0, 0.08, 0.16 and 0.24 respectively. By assuming that each measurement point is representative of the base pressure over a circular strip of finite width, the data given in Figures 6.4(a) thru 6.4(d) should suffice to provide a measure of the base drag.

6.2 FINAL CONCLUSIONS

The work described in this report represents a first step in understanding and evaluating how internal noise radiates through multi-element, single as well as dual stream, mechanical suppressors.

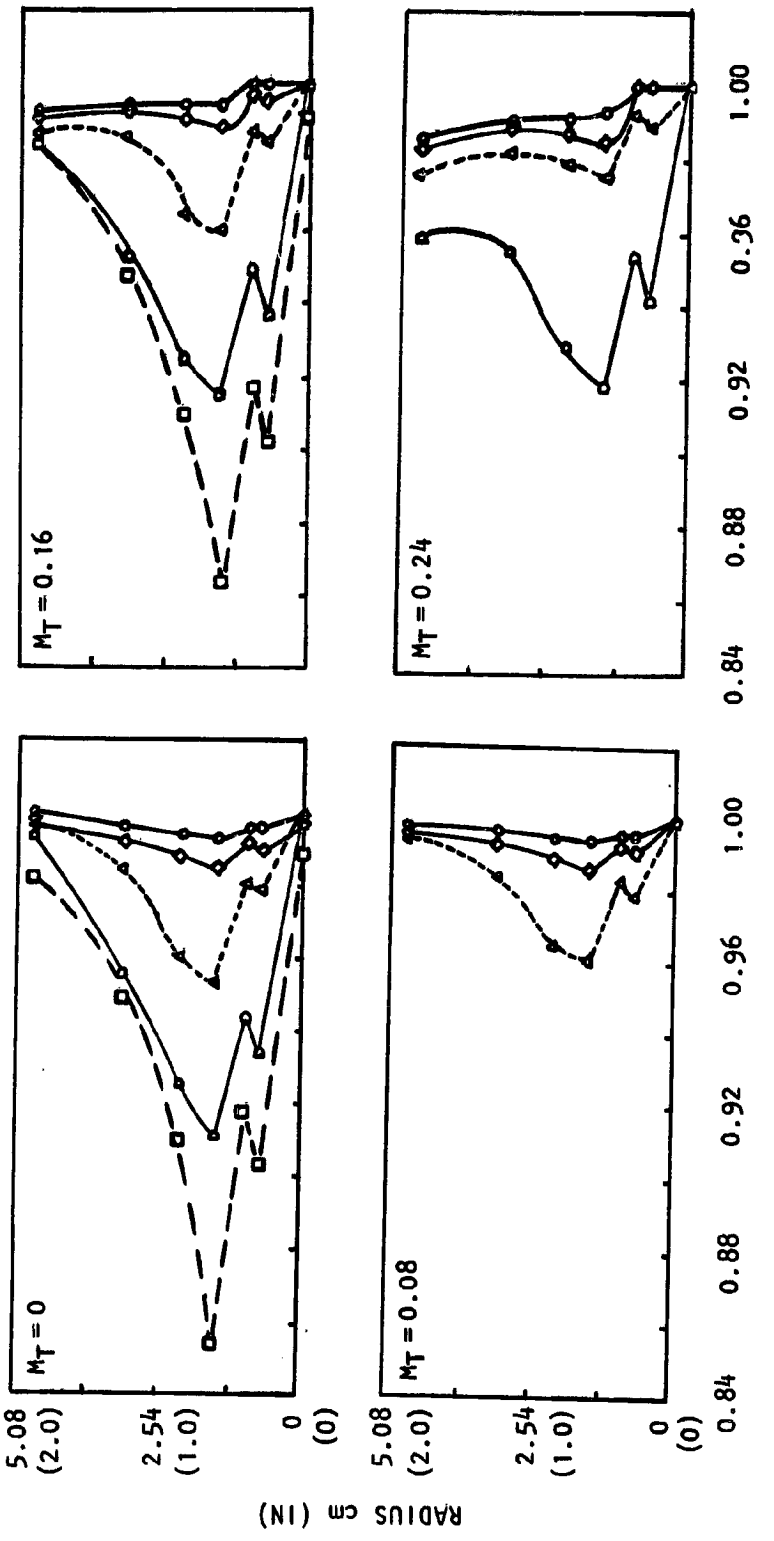

Figure 6.4 Measured base pressures for the daisy lobe nozzle.

Legend for M_J: —○—, 0.4; —◇—, 0.6; --△--, 0.8; —○—, 1.2 and —□—1.4

Table 6.1 Normalized base pressures for the daisy lobe nozzle.

Nominal M_J	Nominal M_T	Nozzle Reservoir Pressure $(N/m^2) \times 10^5$	Ambient Pressure $(N/m^2) \times 10^5$	RADIAL DISTANCE						
				0.000 cm (0")	0.732 cm (0.228")	0.986 cm (0.388")	1.524 cm (0.600")	2.159 cm (0.850")	3.112 cm (1.225")	4.798 cm (1.889")
				$P_{Base}/P_{Amb.}$						
0.40	0.0	1.1439	0.9781	1.000	0.996	0.996	0.993	0.994	0.996	0.999
0.60	0.0	2.6944	0.9779	1.001	0.990	0.992	0.985	0.988	0.992	0.998
0.80	0.0	5.1339	0.9772	1.001	0.979	0.981	0.953	0.960	0.984	0.996
1.20	0.0	13.9408	0.9750	0.997	0.932	0.944	0.911	0.925	0.955	0.993
1.40	0.0	21.3556	0.9740	0.989	0.904	0.918	0.854	0.910	0.949	0.982
0.40	0.08	1.1439	0.9739	1.001	0.996	0.996	0.994	0.995	0.997	0.997
0.60	0.08	2.6944	0.9739	1.002	0.991	0.993	0.986	0.989	0.993	0.996
0.80	0.08	5.1339	0.9739	1.001	0.979	0.983	0.961	0.965	0.984	0.994
0.40	0.16	1.1439	0.9598	1.005	1.000	1.001	0.994	0.994	0.994	0.992
0.60	0.16	2.6944	0.9598	1.006	0.995	0.997	0.988	0.990	0.993	0.990
0.80	0.16	5.1339	0.9598	1.006	0.984	0.987	0.960	0.964	0.985	0.986
1.20	0.16	13.9408	0.9598	1.000	0.936	0.949	0.915	0.925	0.953	0.983
1.40	0.16	21.3556	0.9598	0.991	0.902	0.917	0.864	0.910	0.948	0.983
0.40	0.24	1.1439	0.9386	1.008	1.003	1.006	0.993	0.991	0.990	0.985
0.60	0.24	2.6944	0.9386	1.011	1.000	1.003	0.985	0.987	0.989	0.982
0.80	0.24	5.1339	0.9386	1.013	0.989	0.993	0.975	0.979	0.982	0.975
1.20	0.24	13.9408	0.9386	1.005	0.942	0.954	0.918	0.929	0.955	0.958

The objective of this program was to conduct a series of tests to determine the efficiency of internal noise radiation for two mechanical suppressor nozzles, namely, a single stream 12-lobe 24-tube suppressor nozzle and a dual stream 36-chute suppressor nozzle. An equivalent single round conical nozzle and an equivalent coannular nozzle system were also tested to provide a reference for the two suppressors.

An impulse test technique developed in Phase 1 of this program was used to study the radiation characteristics of these nozzles. This technique utilizes a high voltage spark discharge as a noise source within the test duct and enables one to separate the incident, reflected and transmitted signals in the time domain. These signals are then Fourier transformed to obtain various transmission parameters, in particular, the nozzle transmission coefficients (NTC) and the power transfer functions (PTF).

These transmission parameters for the 12-lobe, 24-tube suppressor nozzle and the reference conical nozzle are presented as a function of jet Mach number, duct Mach number, polar angle and temperature. Effects of simulated forward flight are also considered for this nozzle.

For the dual stream, 36-chute suppressor, the NTC and PTF are presented as a function of velocity ratios and temperature ratios. Where possible data for the equivalent coaxial nozzle is also presented.

Many of the results described here are new and are not amenable to immediate explanations. Due to the interesting nature of these results and their usefulness, the transmission data has been included in this report as an appendix.

6.2.1 Daisy Lobe Suppressor - Transmission Results

Static Data

(1) The daisy lobe nozzle displays higher reflection coefficients than the reference conical nozzle at almost all flow conditions.

(2) For both nozzles, the effect of flow is to gradually reduce the reflection from the jet opening and increase the reflection from the solid parts (e.g. nozzle shoulder). At under-expanded conditions all the reflection appears to be from the solid parts.

(3) The trends in variation of reflection coefficients with frequency are exactly opposite for the two nozzles. The daisy lobe reflection coefficient increases with frequency while that for the conical nozzle decreases with frequency for almost all frequencies.

(4) Reflection coefficients at very low frequencies for conical nozzles are higher than unity for high jet Mach numbers.

(5) At zero flow conditions, the radiation is predominently towards the jet axis. With flow, refraction becomes important and the peaks in the directivities shift towards higher angles.

(6) Deductions made about the far-field radiation based upon reflection coefficients do not necessarily hold. For static conditions, both nozzles have remarkably similar far-field NTC directivities and spectra at subsonic Mach numbers even though the nozzle geometries and the reflection coefficient characteristics are quite different.

(7) Exit area of the nozzles appears to determine the shape and levels of the far-field spectra.

(8) The far-field acoustic power at low frequencies follows an ω^2 relationship for unheated jets and an ω^4 relationship for heated jets.

(9) At low frequencies, the far-field acoustic power is always less than the incident power.

(10) Jet Mach number has little effect on far-field power, especially at low frequencies.

(11) Power balance at low frequencies is not obtained both with and without flow. No immediate explanations are available for this result at zero flow conditions.

(12) When the jet is heated, the conical nozzle radiates more efficiently than the daisy lobe nozzle, especially at small angles to the jet .

Flight Simulation Data

(13) Forward velocity reduces reflection coefficients, decreases NTC in the rear arc, has little effect at 90° and increases radiation in the forward arc.

(14) Far-field acoustic powers are also reduced under flight simulation.

(15) Under flight conditions exit area alone may not be a good parameter to determine the shape and levels of the far-field spectra. Further work needs to be done to determine the effect of true flow conditions at the nozzle exit on sound transmission.

(16) Under flight-simulation, the daisy lobe nozzle displayed more low frequency noise absorption than the conical nozzle except for $M_J = 0$.

6.2.2 Multi-chute Suppressor - Transmission Results

Unheated Jets

(1) Due to different source-section configurations for these nozzles, the in-duct and the far-field time histories consist of multi-pulsed incident signals and are thus different from those obtained for the daisy lobe nozzle. It was not possible to properly isolate the reflected waves in this case. Reflection coefficient data are, therefore, not presented

(2) Far-field radiation was found to be azimuthally symmetric.

(3) Low frequency radiation for both nozzles is omnidirectional.

(4) Dominant radiation for both nozzles is close to the jet axis.

(5) The multi-chute nozzle is a less efficient radiator of internal noise than the single stream daisy lobe nozzle (and therefore the conical nozzle).

(6) The NTC spectra and the directivities for the multi-chute and the reference coaxial nozzle are remarkably similar in shape and in most instances in amplitude also. It is below 800 Hz, that the suppressor radiates more efficiently at all angles except at angles smaller than 30° where the trend is opposite.

(7) For a fixed fan-jet Mach number, the primary jet has negligible effect on the transmission characteristics of these nozzles.

(8) Low frequency radiation increases with increasing fan-jet Mach number.

(9) At $M_J = 0$, the far-field acoustic powers, normalized with respect to the incident acoustic power, are identical for the suppressor and the reference nozzle for frequencies higher than 800 Hz. Below 800 Hz the multi-chute suppressor radiates more efficiently.

(10) With flow, the suppressor radiates more acoustic power at all frequencies.

Heated Jets

(11) For fixed M_{J1}, M_{J2} and T_{R1}, the multi-chute suppressor radiates less efficiently at $T_{R2} = 600K$ and more efficiently at $T_{R2} = 900K$ with respect to the unheated fan jet.

(12) kh is a good normalizing frequency parameter for the configurations studied here.

(13) For fixed M_{J1}, M_{J2} and T_{R2}, changing the primary jet total temperature tends to increase the far-field radiation.

6.2.3 Jet Noise Results

(1) For the daisy lobe suppressor, jet mixing noise in the absence of internal noise is considerably reduced compared with the reference conical nozzle. Reductions of the order of 25 dB were obtained at 30° to the jet axis.

(2) For the daisy lobe suppressor, jet mixing noise following the pulse, is amplified. Such amplification was not so clear for the other three nozzles tested in this investigation.

(3) Forward velocity reduces the jet mixing noise at all angles for the daisy lobe suppressor but if shocks are present in the jet, the noise levels increase at all angles.

6.2.4 Signal Averaging Technique

To clarify some of the doubts about the validity of the data acquired using a single-shot spark discharge method and to improve the quality of the transmission data at high jet Mach numbers a signal averaging technique was developed. An electro-acoustic driver was excited with pulses located 33.33 mS apart in the time domain. Three main conclusions were reached:

(1) In view of the preliminary nature of the signal averaging technique development study, the agreement between the two schemes, on the average, was quite good.

(2) The signal technique was superior to the spark discharge method for the higher Mach numbers.

(3) The existence of the low frequency absorption phenomenon noticed with the spark source method was confirmed by the signal averaging technique.

APPENDIX A

IN-DUCT WAVE STRUCTURE FROM POINT IMPULSIVE SOURCE

An impulsive point source in a free-field environment will radiate spherically. At some point in the far-field, the wave front will have such a large radius of curvature that it will appear essentially as a plane wave, which is the desired in-duct condition. Shock tube studies have shown that a point source will propagate down the tube as a spherical wave followed by a reflected wave structure from the wall. This reflected wave field is a function of axial distance from the source. Figure A-1 shows the evolution of this wave structure as a function of time and distance from the source. As a result of propagation non-linearities, the wave fronts of the reflections gradually catch up to and coalesce with the initial spherical shock and produce a relatively clean wave front. However, multiple reflections of those parts of the initial spherical wave which are at high angles of incidence to the duct wall are unable to coalesce with the initial spherical wave due to their long travel times. This is illustrated in Figure A-2(a). It can be shown that after n reflections, a ray between an on-axis source and an on-axis receiver x distance apart in a duct of diameter D, will arrive at Δt seconds after the direct ray such that

$$\Delta t \simeq \frac{n^2 D^2}{2x\, c_o} \qquad \text{(A-1)}$$

It can be seen from Figure A-2(a) that as the angle of incidence, θ, is increased, the number of reflections, n, for the corresponding ray also increases, which in turn increases the value of Δt. This phenomenon introduces a "train" of oscillations following the incident pulse in the pressure time history of the point impulsive source. This phenomenon is quite pronounced when the source section of the duct is unlined. These oscillations can, however, be minimized by the addition of an absorbent lining to attenuate the high angle reflections as illustrated in Figure A-2(b) . This process, which effectively limits the pulse length, also reduces the total available energy by reducing the conical "capture window" θ_c of the test duct. This reduction can however be optimized by proper selection of the absorption material and the length "ℓ" of absorbent lining downstream of the impulsive source. In the present work, for daisy lobe and reference conical nozzles, 2.5 cm thick ceramic wool lining in the 10 cm diameter duct with 15 cm length was used and produced an acceptable in-duct time history at x = 60D as shown in Figure A-3.

First, the incident (*outgoing*) pulse is seen in Figure A-3 to be a steep-fronted positive pressure wave followed by a rarefaction wave. It is similar to a one-dimensional travelling shock wave. The width of the pulse is a function of the distance from the source and the initial pulse amplitude. The second feature is the reflected (*ingoing*) pulse, which is shown to be a steep-fronted *negative* ressure wave. Close examination reveals that the leading edge slope is not as sharp as that of the incident wave. Physically, this signifies an escape of high-frequency energy at the termination. Since

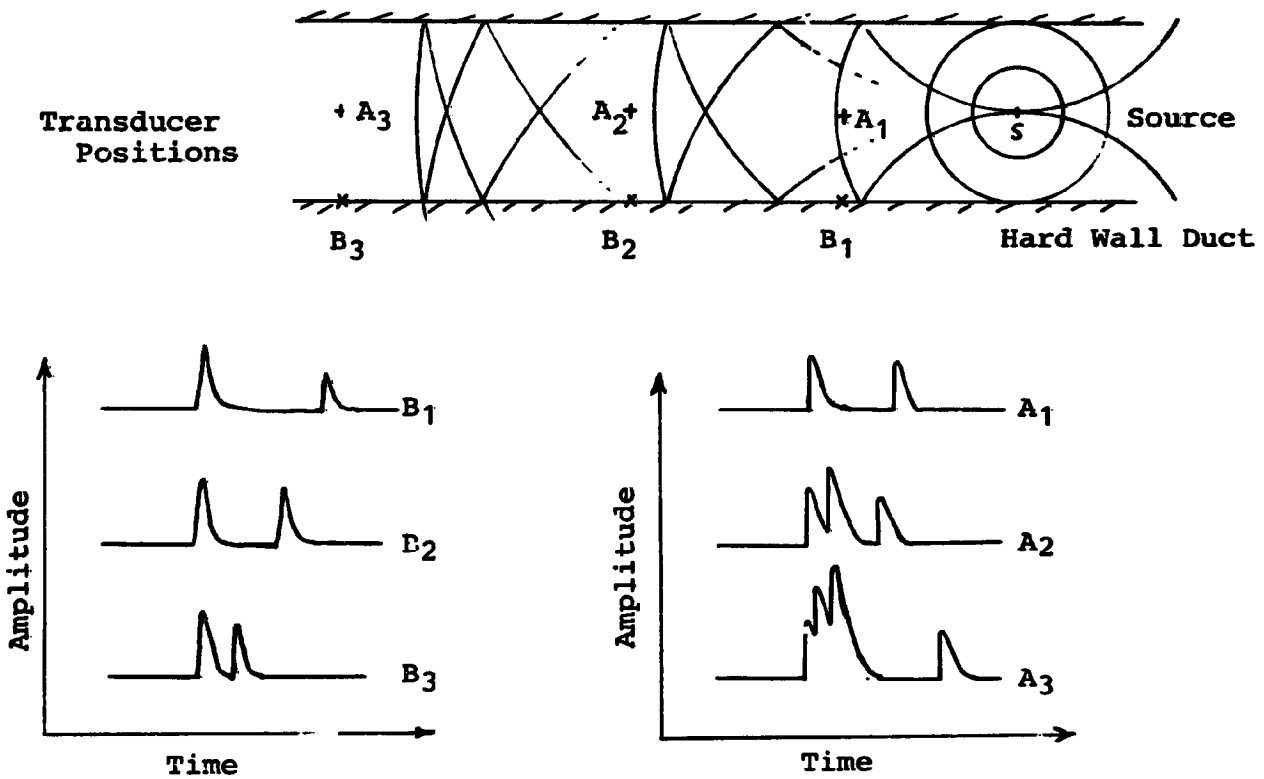

Figure A-1 Characteristic effects of source/microphone position on measured time histories.

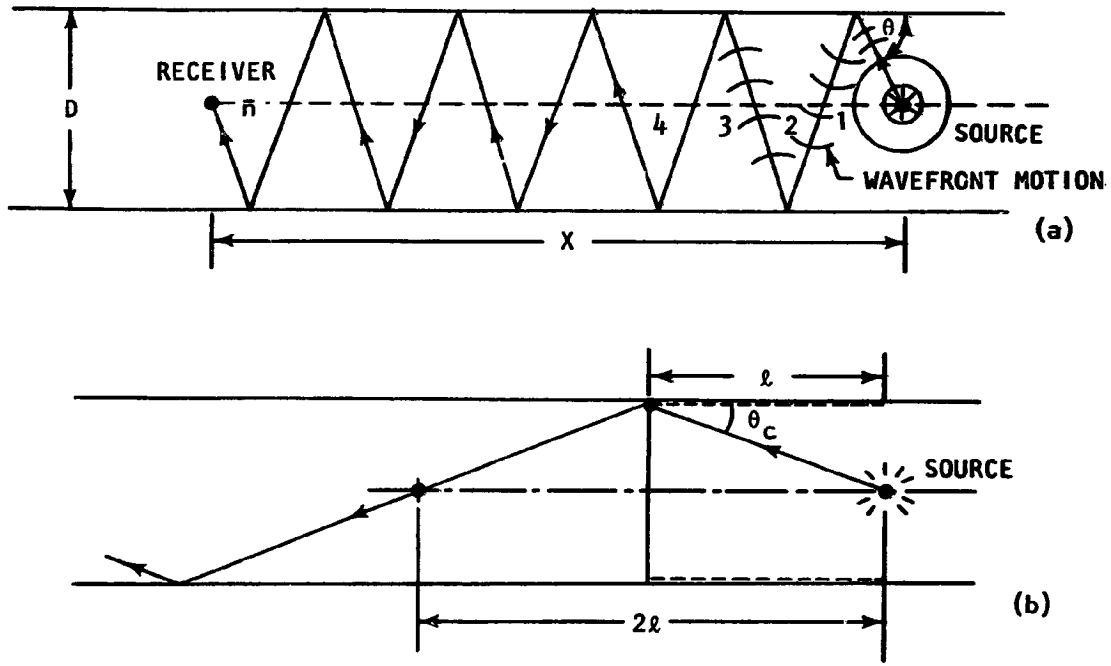

Figure A-2 (a) Structure of pressure time-history from point impulsive source. (b) Effect of absorbent duct lining around the source.

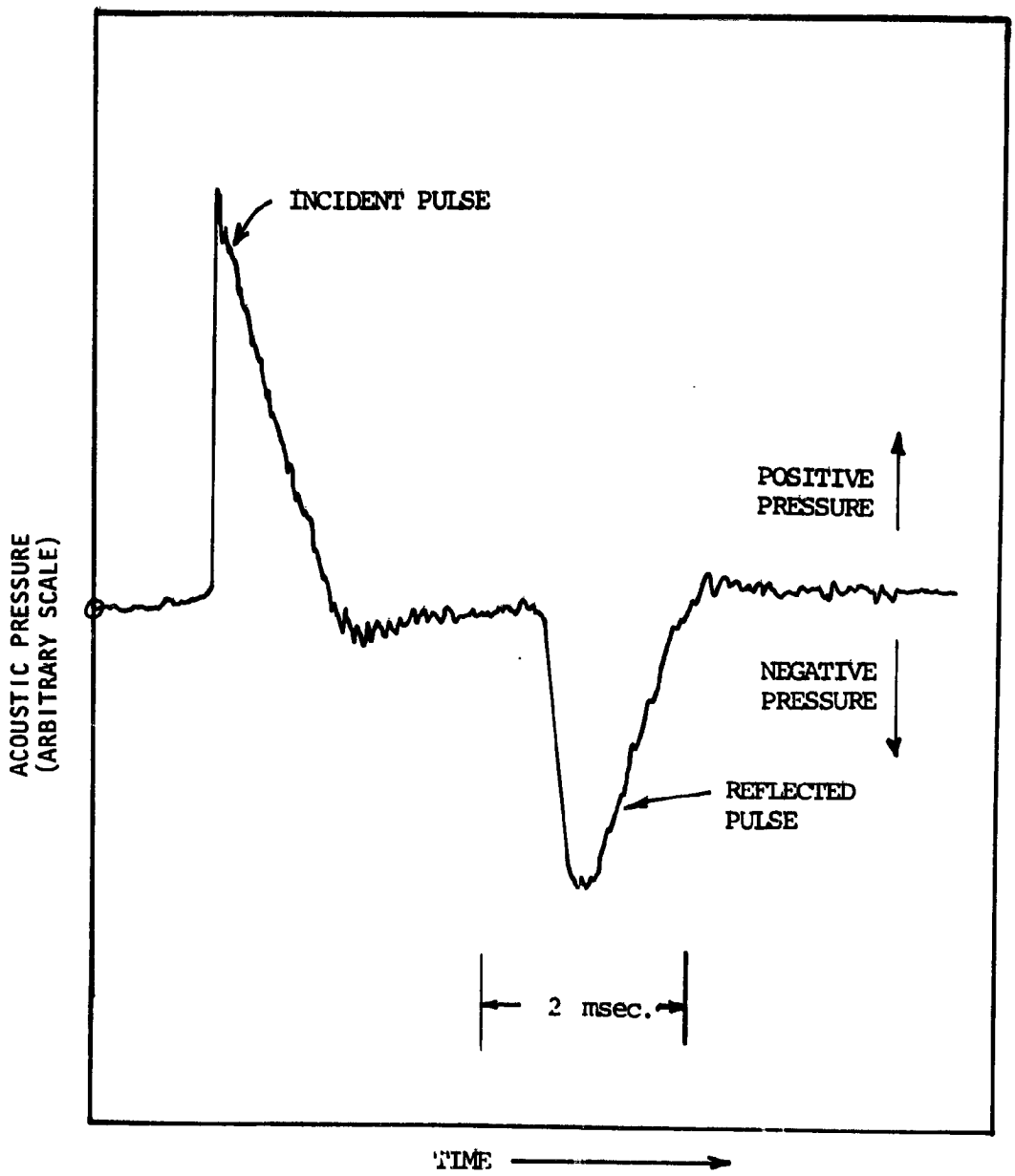

Figure A-3 In-duct time history for 10 cm diameter duct at zero flow.

each pulse is propagating at approximately the ambient speed of sound, pulse separation in time can only be achieved by proper transducer placement upstream of the termination. Another point worthy of mention is that the measured time interval between the incident and reflected pulse leading edges fairly accurately defines the geometric location at which reflection takes place.

APPENDIX B

DATA ANALYSIS

In this Appendix the data analysis procedure to compute one-third octave NTC and PTF values from the measured narrow band SPL data is described. The narrow band SPL data for incident, reflected and far-field pulses is obtained by the Fourier transform of each pulse using a digital FFT Signal analyzer (see Section 2).

The various parameters involved in this analysis can be broadly divided into three categories, namely, input data, intermediate outputs and the final outputs. Various parameters in these categories are defined below.

Input Data:

a) Physical and Geometric parameters.

D_{eq}	Equivalent nozzle exit diameter.
D_D	Duct diameter (for co-annular, outer diameter of the inner duct).
D_p*	Primary nozzle diameter.
DS	Distance of the in-duct transducer from the exit plane.
h*	Height of the annulus at the nozzle exit.
h_D*	Height of the annulus at the straight part of the co-annular nozzle.
P_D†	Static pressure in the duct.
P_o	Ambient pressure.
P_T	Total pressure in the duct
T_D	Static temperature in the duct
T_o	Ambient temperature
$R_m(\theta)$	Position of far-field microphone at a polar angle θ from the nozzle exit.
R_H	Relative humidity (%)

$$A_D = \pi D_D^2/4 \quad \text{Cross sectional area of the duct} \qquad (B\text{-}1)$$

$$= \pi/4 \left| (D_D + h_D)^2 - D_D^2 \right| \quad \text{Cross sectional area of annular duct} \qquad (B\text{-}2)$$

---

* only for co-annular nozzles.
† only for single nozzles in free-jet facility.

b) Calibration Data (all in decibels)

To obtain calibration or transfer function between two pressure measuring probes it is necessary to expose them to the same pressure field. In the present investigation the calibration of quarter inch B&K microphones were needed with respect to a Sundstrand piezoelectric pressure transducer. A pressure field of very high intensity (of the order of 140 dB) was required to obtain a good signal from the transducer. At this level of pressure field, the quarter inch B&K microphones with conventional cathode followers, were getting saturated. Therefore, to avoid this problem, a quarter-inch B&K microphone with a special cathode follower, (Type 2618) which had a built-in amplifier to amplify or attenuate the signal by 20 dB, was used. This probe, referred as a special microphone (SM), could measure a high intensity pressure field, with 20 dB attenuation to the built-in amplifier, when placed against the transducer and also could measure moderate pressure fields without any amplification or attenuation when placed against a conventional microphone-cathode follower probe. Therefore, the special microphone was used as an intermediate probe to obtain the calibration between conventional microphones with respect to the transducer.

To read absolute SPL values of the experimental data, recorded in the tape, a reference sine wave signal at 1000 Hz with 114 dB amplitude, read by each microphone, was also recorded in the corresponding tape recorder channels using a standard pistonphone calibrator. The recorded test data was analyzed using a dual channel FFT signal analyzer (SD-360) which has got a built-in attenuator to attenuate the input signal up to a maximum of 60 dB. To initialize this equipment (SD-360), the recorded sine wave signal, from one of the channels, (for this investigation the channel corresponding to $\theta = 120^{\circ}$ was chosen) was Fourier transformed with a suitable attenuation setting (reference attenuation, RATN) and the transformed value at 1000 Hz was set to zero. Therefore, the zero reading with this attenuation setting (RATN) would correspond to a value of 114 dB for that microphone channel. The sine wave signal recorded in the remaining tape-recorder channels for other microphone angles (θ) were then Fourier transformed and the corresponding readings at 1000 Hz (FC(θ)) were noted down. These readings were used in the data analysis to evaluate the SPL values.

During the data acquisition process, using SD-360, the attenuation settings (ATN(θ)) were different for different channels and were also different from the reference attenuation value (RATN). Therefore, the difference between the individual attenuation settings with respect to the reference attenuation (DATN(θ)) were used in the data analysis to get proper SPL values.

SM/T(f)	Calibration between a special microphone and in-duct transducer at a frequency f (narrow band)
M/SM(f,θ)	Calibration between the microphone positioned at θ and the special microphone at a frequency f (narrow band)
WC(f)	Effect of wind screen on far-field SPL at frequency f (narrow band).

$FC(\theta)$	Values read for 114dB at 1000 Hz with reference amplification, RAMP (θ) and reference attenuation, RATN on SD-360, for the microphone positioned at θ, with respect to that at $\theta = 120°$.
$FR(\theta, f_{1/3})$	Frequency response of microphone positioned at θ, at a 1/3-octave frequency of $f_{1/3}$.
$FFC(f_{1/3})$	Free-field correction of microphone for a 1/3-octave frequency of $f_{1/3}$.
$AMP(\theta)$	Amplifier setting for the microphone at θ during the test.
$ATN(\theta)$	Attenuation setting on SD-360 for the microphone at θ during data acquisition.
f	Narrow band center frequency with a fixed bandwidth
$f_{1/3}$	One-third octave center frequency.

c) Acoustic Data

$SPL'_i(f)$	Incident SPL at frequency f, (narrow band)
$SPL'_r(f)$†	Reflected SPL at frequency f, (narrow band)
$SPL'_f(f,\theta)$	Far-field SPL for microphone at θ, at frequency f, (narrow band)

Note: $SPL'_i(f)$, $SPL'_r(f)$ and $SPL'_f(f,\theta)$ are measured with respect to 114 dB at 1000 Hz for microphone at $\theta = 120°$ with RAMP(θ) and RATN.

Intermediate Outputs (all in decibels)

$C_h(f)$	Humidity correction at frequency f, per unit distance, = function of R_H, P_o, T_o.
$C_d(\theta)$	Distance correction to obtain the SPL level at 100 x D_{eq} for microphone at θ $= 20 \text{ Log}_{10}(R_m(\theta)/(100 \times Deq))$ (B-3)
$DAMP(\theta)$	$RAMP(\theta) - AMP(\theta)$ (B-4)
$DATN(\theta)$	$ATN(\theta) - RATN$ (B-5)
$M/T(f,\theta)$	Calibration between microphone at θ with respect to in-duct transducer at frequency f $= SM/T(f) + M/SM(f,\theta)$ (B-6)
$[M/T(f)]_{AVR}$	Average calibration value at frequency f. $= 10 \text{ Log}_{10}\left\{ \left[\sum_{j=1}^{n} (10)^{\frac{1}{10}(M/T(f,\theta_j))} \right]/n \right\}$, (B-7) n being the total number of far-field microphones.

† Only for single nozzles in free-jet facility.

$SPL_i(f)$ Absolute value of incident SPL at frequency f, (narrow band)

$$= SPL'_i(f) + [M/T(f)]_{AVR} + 114 \quad \text{(B-8)}$$

$SPL_r(f)$‡ Absolute value of reflected SPL at frequency f (narrow band)

$$= SPL'_r(f) + [M/T(f)]_{AVR} + 114 \quad \text{(B-9)}$$

$SPL_f(f,\theta)$ Absolute value of far-field SPL for the microphone positioned at θ, at frequency f (narrow band)

$$= SPL'_f(f,\theta) + C_h(f) \times (R_m(\theta) + DS) - FC(\theta) + C_d(\theta) + DAMP(\theta) + DATN(\theta) + WC(F)^{**} \quad \text{(B-10)}$$

Note: $SPL_i(f)$, $SPL_r(f)$ and $SPL_f(f,\theta)$ are calculated assuming flat frequency response for far-field microphones and without any free-field corrections, since these corrections were not available at narrow band frequency. However, frequency response ($FR(f_{1/3},\theta)$) and free-field corrections ($FFC(f_{1/3})$) were available for 1/3-octave frequencies, and therefore, were applied to the final 1/3-octave SPL data.

$[FR(f_{1/3})]_{AVR}$ Average frequency response at $f_{1/3}$

$$= 10\ Log_{10}\left\{ \left[\sum_{j=1}^{n} (10)^{\frac{1}{10}(FR(f_{1/3},\theta_j))} \right] /n \right\} \quad \text{(B-11)}$$

$SPL_f(f_{1/3},\theta)$ Absolute 1/3-octave far-field SPL at θ and at frequency $f_{1/3}$

$$= 10\ Log_{10}\left[\sum_{f_l}^{f_u} (10)^{SPL_f(f,\theta)/10} \right] + FR(f_{1/3},\theta) + FFC(f_{1/3}) + \text{Free jet correction} \quad \text{(B-12)}$$

$SPL_i(f_{1/3})$ Absolute 1/3-octave incident SPL at frequency $f_{1/3}$

$$= 10\ Log_{10}\left[\sum_{f_l}^{f_u} (10)^{SPL_i(f)/10} \right] + [FR(f_{1/3})]_{AVR} + FFC(f_{1/3}) \quad \text{(B-13)}$$

---

‡ Only for single nozzles in free-jet facility.

** Windscreens were used to minimize the flow noise at small angles to the jet axis for microphones placed at polar angles of 0°, 10°, 20° and 30°. Therefore, windscreen correction is applied to these microphone data.

$SPL_r(f_{1/3})$† Absolute 1/3-octave reflected SPL at frequency $f_{1/3}$

$$= 10 \text{ Log}_{10} \left[\sum_{f_l}^{f_u} (10)^{SPL_r(f)/10} \right] + [FR(f_{1/3})]_{AVR} + FFC(f_{1/3}) \quad \text{(B-14)}$$

where

f_l lower frequency for 1/3-octave center frequency of $f_{1/3}$

$$= f_{1/3} / (2)^{\frac{1}{6}} \quad \text{(B-15)}$$

f_u Upper frequency for 1/3-octave center frequency of $f_{1/3}$

$$= f_{1/3} \times (2)^{\frac{1}{6}} \quad \text{(B-16)}$$

$OASPL_f(\theta)$ Far-field OASPL at θ

$$= 10 \text{ Log}_{10} \left[\sum_{j=1}^{m} 10^{(SPL_f(f_{1/3},\theta)/10)} \right], \quad \text{(B-17)}$$

m being the member of one third-octave frequencies

$OASPL_i$ Incident OASPL

$$= 10 \text{ Log}_{10} \left[\sum_{j=1}^{m} 10^{SPL_f(f_{1/3})_j/10} \right] \quad \text{(B-18)}$$

$OASPL_r$‡ Reflected OASPL

$$= 10 \text{ Log}_{10} \left[\sum_{j=1}^{m} 10^{SPL_r(f_{1/3})_j/10} \right] \quad \text{(B-19)}$$

$OASPL_t$† Transmitted OASPL

$$= 10 \text{ Log}_{10} \left[\sum_{j=1}^{m} \left| (10^{SPL_i(f_{1/3})_j/10})(1+M_D)^2 - (10^{SPL_r(f_{1/3})_j/10})(1-M_D)^2 \right| \right] \quad \text{(B-20)}$$

$PWL_f(f_{1/3})$ Far-field PWL at frequency $f_{1/3}$

$$= 10 \text{ Log}_{10} \left[\frac{1}{\rho_o c_o} \sum_{j=1}^{n} 10^{SPL_f(f_{1/3},\theta_j)/10} \cdot \Delta S_j \right] \quad \text{(B-21)}$$

where, ΔS_j = elemental area associated with microphone at θ_j

$PWL_i(f_{1/3})$ Incident PWL at frequency $f_{1/3}$

$$= SPL_i(f_{1/3}) + 10 \text{ Log}_{10} \left(\frac{(1+M_D)^2 \cdot A_D}{\rho_D c_D} \right) \quad \text{(B-22)}$$

† Only for single nozzles in free-jet facility.

$PWL_r(f_{1/3})^{\ddagger}$ Reflected PWL at frequency $f_{1/3}$

$$= SPL_r(f_{1/3}) + 10\ Log_{10}\left(\frac{(1-M_D)^2 \cdot A_D}{\rho_D c_D}\right) \quad \text{(B-23)}$$

$PWL_t(f_{1/3})^{\ddagger}$ Transmitted PWL at frequency $f_{1/3}$

$$= 10\ Log_{10}\left[\left|10^{SPL_i(f_{1/3})/10}\right|(1+M_D)^2 - \left|10^{SPL_r(f_{1/3})/10}\right| (1-M_D)^2\right] + 10\ Log_{10}\left(\frac{A_D}{\rho_D c_D}\right) \quad \text{(B-24)}$$

$OPWL_f$ Overall far-field PWL

$$= 10\ Log_{10}\left[\sum_{j=1}^{m} 10^{(PWL_f(f_{1/3})_j/10)}\right] \quad \text{(B-25)}$$

$OPWL_i$ Overall incident PWL

$$= 10\ Log_{10}\left[\sum_{j=1}^{m} 10^{(PWL_i(f_{1/3})_j/10)}\right] \quad \text{(B-26)}$$

$OPWL_r^{\ddagger}$ Overall reflected PWL

$$= 10\ Log_{10}\left[\sum_{j=1}^{m} 10^{(PWL_r(f_{1/3})_j/10)}\right] \quad \text{(B-27)}$$

$OPWL_t^{\ddagger}$ Overall transmitted PWL

$$= 10\ Log_{10}\left[\sum_{j=1}^{m} 10^{(PWL_t(f_{1/3})_j/10)}\right] \quad \text{(B-28)}$$

Final Outputs (all in decibels)

$NTC_i(f_{1/3},\theta)$ Normalized transfer function (or coefficient) with respect to incident SPL at a frequency $f_{1/3}$ for emission angle θ.

$$= SPL_f(f_{1/3},\theta) - SPL_i(f_{1/3}) + 10\ Log_{10}\ (FACT\ 1)$$

where $$FACT\ 1 = \frac{4\pi(100 x D_{eq})^2 P_D}{A_D(1+M_D)^2 P_o}\sqrt{\frac{T_o}{T_D}} \quad \text{(B-29)}$$

‡ Only for single nozzles in free-jet facility.

$NTC_t(f_{1/3},\theta)^{\ddagger}$ Normalized transfer function (or coefficient) with respect to transmitted SPL at a frequency $f_{1/3}$ for emission angle θ.

$$= SPL_f(f_{1/3},\theta) - 10\ Log_{10}\left[\left|10^{SPL_i(f_{1/3})/10}\right|(1+M_D)^2 - \left|10^{SPL_r(f_{1/3})/10}\right|(1-M_D)^2\right] + 10\ Log_{10}\ (FACT\ 2)$$

where

$$FACT\ 2 = \frac{4\pi(100 \times D_{eq})^2 P_D}{A_D \cdot P_o}\sqrt{\frac{T_o}{T_D}} \qquad (B\text{-}30)$$

$PTF_i(f_{1/3})$ Power transfer function with respect to incident power at frequency $f_{1/3}$

$$= PWL_f(f_{1/3}) - PWL_i(f_{1/3}) \qquad (B\text{-}31)$$

$PTF_t(f_{1/3})^{\ddagger}$ Power transfer function with respect to transmitted power at frequency $f_{1/3}$

$$= PWL_f(f_{1/3}) - PWL_t(f_{1/3}) \qquad (B\text{-}32)$$

$\sigma(f_{1/3})^{\ddagger}$ Reflection coefficient* at a frequency $f_{1/3}$

$$= SPL_r(f_{1/3}) - SPL_i(f_{1/3}) \qquad (B\text{-}33)$$

$\sigma_M(f_{1/3})^{\ddagger}$ Reflection coefficient, corrected for Mach number*, at frequency $f_{1/3}$

$$= \sigma(f_{1/3}) + 20\ Log_{10}\left[\frac{1-M_D}{1+M_D}\right] \qquad (B\text{-}34)$$

$NOSPL_i(\theta)$ Normalized far-field OASPL with respect to incident OASPL at θ

$$= OASPL_f(\theta) - OASPL_i + 10\ Log_{10}\left[\frac{4\pi(100 D_{eq})^2 P_D}{A_D(1+M_D)^2 \cdot P_o}\sqrt{\frac{T_o}{T_D}}\right] \qquad (B\text{-}35)$$

---

‡ Only for single nozzles in free-jet facility.

* $\sigma(f_{1/3})$ and $\sigma_M(f_{1/3})$ do not appear in the data tables. These are plotted in the main text.

$NOSPL_t(\theta)^{\ddagger}$ Normalized far-field OASPL with respect to transmitted OASPL at θ

$$= OASPL_f(\theta) - OASPL_t + 10\ Log_{10}\left\{\frac{4\pi(100 \times D_{eq})^2 P_D}{A_D \cdot P_o}\sqrt{\frac{T_o}{T_D}}\right\} \quad (B\text{-}36)$$

$OPTF_i$ Overall power transfer function with respect to overall incident power

$$= OPWL_f - OPWL_i \quad (B\text{-}37)$$

$OPTF^{\dagger}$ Overall power transfer function with respect to overall transmitted power

$$= OPWL_f - OPWL_t \quad (B\text{-}38)$$

---

‡ Only for single nozzles in free-jet facility.

APPENDIX C

TEST CONDITIONS AND CORRESPONDING TRANSMISSION DATA

The purpose of this section is to tabulate all the nozzle transmission data obtained from the measurements after applying the needed corrections and transformations described in Appendix B. The test conditions, both nominal and exact, are tabulated in Tables C.1 through C.6. The 1/3-octave normalized transfer function and power transfer function data for daisy lobe nozzle and the corresponding reference conical nozzle are tabulated simultaneously. These transfer functions are obtained both with respect to incident (NTC_i and PTF_i) and transmitted (NTC_t and PTF_i) SPL. The 1/3-octave normalized transfer function and power transfer function data for multi-chute suppressor nozzle and the corresponding reference coaxial nozzle are only presented with respect to incident SPL (NTC_i and PTF_i). The corresponding overall SPL values of normalized transfer function and power transfer function data with respect to incident ($NOSPL_i$ and $OPTF_i$) and transmitted ($NOSPL_t$ and $OPTF_t$) data are also presented.

Various parameters presented in the data tables are described in Appendix B. But, for the convenience of the reader, important parameters that appear in the data tables are listed below:

$NTC_i\ (f_{1/3},\theta)$	Normalized transfer function (or coefficient) with respect to incident SPL at 1/3-octave center frequency of $f_{1/3}$ and at emission angle θ.
$NTC_t(f_{1/3},\theta)$ ‡	Normalized transfer function (or coefficient) with respect to transmitted SPL at 1/3-octave center frequency of $f_{1/3}$ and at emission angle θ. *
$PTF_i\ (f_{1/3})$	Power transfer function with respect to incident power at 1/3-octave frequency of $f_{1/3}$
$PTF_t\ (f_{1/3})$ ‡	Power transfer function with respect to transmitted power at 1/3-octave frequency of $f_{1/3}$
$NOSPL_i(\theta)$	Normalized far-field overall SPL with respect to incident overall SPL at emission angle θ.
$NOSPL_t(\theta)$ ‡	Normalized far-field overall SPL with respect to transmitted overall SPL at emission angle θ.

---

‡ Only for single nozzles in free-jet facility.

* The NTC_t values, even though not presented in the main text, were calculated after the text had already been written up. Due to the useful nature of this parameter and for the sake of completness this is also tabulated in this appendix.

$OPTF_I$	Overall power transfer function with respect to overall incident power
$OPTF_t$ ‡	Overall power transfer function with respect to overall transmitted power.
M_J ‡	Fully expanded model jet Mach number
M_T ‡	Free jet Mach number
T_R ‡	Reservoir temperature for model jet, K
T_o	Ambient temperature, K
P_o	Ambient pressure, N/m^2
M_{J_1} ‡‡	Fully expanded primary jet Mach number
M_{J_2} ‡‡	Fully expanded secondary (co-annular) jet Mach number
T_{R_1} ‡‡	Reservoir temperature for primary jet, K
T_{R_2} ‡‡	Reservoir temperature for secondary jet, K

Note: The linear value of the reflection coefficient, corrected for duct Mach number (i.e. $[p_r^2(1-M_D)^2] / [p_i^2(1+M_D)^2]$) becomes greater than unity for certain frequencies for a few flow conditions *(actually only for 8 out of a total of 1350 spectral points)*. This was found to be so only at high frequencies and is attributable to possible errors in single point in-duct measurements at high frequencies. For these cases, asterisk (*) marks are put against the corresponding frequencies in the data table.

For some test conditions, the data was analyzed only for a limited number of polar angles. Since the signal was highly contaminated with jet noise for the remaining angles, the data was not analyzed for those angles. Therefore, the power transfer functions, calculated for these cases were based on the limited number of polar angle data covering a fraction of the spherical area at the polar radius.

---

‡ Only for single nozzles in free-jet facility.
‡‡ Only for co-annular nozzles.

Table C.1 Nominal operating conditions for the daisy lobe and the reference conical nozzle

Run No.		Model Jet		Free Jet	Page No.	
Daisy Lobe Nozzle	Conical Nozzle	Mach No. M_J	Reservoir Temp., T_R	Mach No. M_T	NTC_i	NTC_t
19	89	0.0	Ambient	0.0	192	193
20	116	0.2	Ambient	0.0	194	195
13	91	0.4	Ambient	0.0	196	197
14	106	0.6	Ambient	0.0	198	199
15	110	0.8	Ambient	0.0	200	201
17	123	1.2	Ambient	0.0	202	203
41	121	0.0	Ambient	0.08	204	205
46	93	0.4	Ambient	0.08	206	207
81	109	0.6	Ambient	0.08	208	209
53	113	0.8	Ambient	0.08	210	211
39	120	0.0	Ambient	0.16	212	213
48	96	0.4	Ambient	0.16	214	215
36	108	0.6	Ambient	0.16	216	217
54	112	0.8	Ambient	0.16	218	219
56	115	1.2	Ambient	0.16	220	221
38	119	0.0	Ambient	0.24	222	223
49	97	0.4	Ambient	0.24	224	225
37	107	0.6	Ambient	0.24	226	227
55	111	0.8	Ambient	0.24	228	229
70	98	0.8	600K	0.00	230	231
86	100	0.8	600K	0.08	232	233
85	101	0.8	600K	0.16	234	235
128	103	0.8	600K	0.24	236	237
83	99	1.2	600K	0.00	238	239
84	105	1.2	600K	0.08	240	241
129	102	1.2	600K	0.16	242	243
130	104	1.2	600K	0.24	244	245

Table C.2 Nominal operating conditions for the multi-chute and the reference coaxial nozzles.

Run No.		Model Jet Mach Numbers		Model Jet Reservoir Temp.		Page No.
Multi-chute Nozzle	Reference Coaxial Nozzle	M_{J_1}	M_{J_2}	T_{R_1}	T_{R_2}	NTC_i
144	168	0.0	0.0	Ambient	Ambient	246
145	169	0.4	0.6	Ambient	Ambient	247
152	174	0.0	1.2	Ambient	Ambient	248
153	172	0.8	1.2	Ambient	Ambient	249
154	171	0.8	0.9	Ambient	Ambient	250
157	176	0.8	1.2	Ambient	600K	251
159	177	0.8	0.9	Ambient	900K	252
160	179	0.8	0.9	450K	600K	253
162	178	0.8	0.9	675K	900K	254
162	175	0.8	0.9	Ambient	600K	255

Table C. 3 Exact operating conditions for the daisy lobe nozzle.

Run No.	Model Jet		Free Jet	Ambient		Page No.	
	Mach No. M_J	Reservoir Temp. T_R (K)	Mach No. M_T	Temp. T_o (K)	Pressure $P_o(N/m^2)\times10^{-4}$	NTC_j	NTC_t
19	0.0	294	0.0	297	9.75	192	193
20	0.2007	294	0.0134	299	9.75	194	195
13	0.4100	294	0.0215	297	9.75	196	197
14	0.6025	293	0.0323	297	9.75	198	199
15	0.8036	292	0.0437	297	9.75	200	201
17	1.205	294	0.0671	297	9.75	202	203
41	0.0	295	0.0795	297	9.75	204	205
46	0.4115	292	0.0805	298	9.75	206	207
81	0.604	289	0.080	296	9.80	208	209
53	0.8059	292	0.0804	296	9.79	210	211
39	0.0	295	0.1654	297	9.75	212	213
48	0.436	292	0.1598	297	9.75	214	215
36	0.6258	293	0.1598	296	9.75	216	217
54	0.8197	292	0.1596	296	9.79	218	219
56	1.2152	293	0.1596	295	9.79	220	221
38	0.0	293	0.238	297	9.75	222	223
49	0.4732	292	0.237	297	9.75	224	225
37	0.6539	292	0.2371	296	9.75	226	227
55	0.8424	293	0.2366	295	9.79	228	229
70	0.8087	606	0.0436	302	9.80	230	231
86	0.8107	591	0.0827	297	9.80	232	233
85	0.8261	600	0.1613	297	9.80	234	235
128	0.8470	594	0.2391	295	9.72	236	237
83	1.2087	600	0.0662	308	9.80	238	239
84	1.2093	597	0.0758	308	9.80	240	241
129	1.2123	597	0.1610	298	9.72	242	243
130	1.2242	596	0.2348	296	9.72	244	245

Table C.4 Exact operating conditions for the reference conical nozzle.

Run No.	Model Jet		Free Jet	Ambient		Page No.	
	Mach No. M_J	Reservoir Temp. T_R (K)	Mach No. M_T	Temp. T_o (K)	Pressure P_o (N/m^2)x10^{-4}	NTC_i	NTC_t
89	0.0	303.3	0.0	295	9.72	192	193
116	0.2014	290.6	0.0170	296	9.72	194	195
91	0.4007	294	0.0217	296	9.72	196	197
106	0.6009	294.4	0.0345	296	9.72	198	199
110	0.8022	292	0.0457	296	9.72	200	201
123	1.2026	290	0.0711	296	9.72	202	203
121	0.0	293.3	0.0829	296	9.72	204	205
93	0.4092	291	0.0811	295	9.72	206	207
109	0.6057	294.4	0.0794	296	9.72	208	209
113	0.8068	289.4	0.0784	297	9.72	210	211
120	0.0	291.7	0.1594	296	9.72	212	213
96	0.4325	289	0.1601	294	9.72	214	215
108	0.6251	290.6	0.1638	298	9.72	216	217
112	0.8187	289.4	0.1594	298	9.72	218	219
115	1.2161	389.4	0.1571	298	9.72	220	221
119	0.0	290	0.2375	296	9.72	222	223
97	0.4547	289	0.2343	294	9.72	224	225
107	0.6517	291.7	0.2388	298	9.72	226	227
111	0.8418	290	0.2375	298	9.72	228	229
98	0.8162	605.6	0.043	305	9.72	230	231
100	0.8117	600	0.0817	300	9.72	232	233
101	0.8260	600	0.1598	296	9.72	234	235
103	0.8386	595.6	0.2388	297	9.72	236	237
99	1.2103	595.6	0.0684	308	9.72	238	239
105	1.2003	599	0.0828	307	9.72	240	241
102	1.2156	600	0.1615	29_	9.72	242	243
104	1.2342	600	0.2388	297	9.72	244	245

Table C.5 Exact operating conditions for the multi-chute nozzle

Run No.	Jet Model Mach No.		Reservoir Temperatures (K)		Ambient		Page No. NTC$_1$
	M_{J_1}	M_{J_2}	T_{R_1}	T_{R_2}	Temp. T_o(K)	Pressure P_o (N/m^2)X10^{-4}	
144	0.0	0.0	287.2	285.6	297.2	9.79	246
145	0.4	0.604	283.9	284.4	285.2	9.79	247
152	0.0	1.196	286.1	286.1	286.4	9.79	248
152	0.8	1.196	286.1	285.6	286.6	9.79	249
154	0.8	0.903	286.7	286.1	286.6	9.79	250
157	0.802	1.237	289.4	594.4	290.4	9.86	251
159	0.8	0.961	296.1	877.8	292.3	9.86	252
160	0.821	0.917	441.1	597.8	295.9	9.86	253
161	0.837	0.970	654.4	902.8	309.1	9.86	254
162	0.799	0.925	302.8	594.4	295.8	9.86	255

Table C.6 Exact operating conditions for the reference coaxial nozzle.

Run No.	Jet Model Mach No.		Reservoir Temperatures (K)		Ambient		Page No. NTC$_1$
	M_{J_1}	M_{J_2}	T_{R_1}	T_{R_2}	Temp. T_o(K)	Pressure P_o (N/m^2)X10^{-4}	
168	0.0	0.0	292.2	286.1	294.3	9.76	246
169	0.399	.599	281.0	282.2	284.4	9.76	247
174	0.141	1.196	281.0	281.0	296.0	9.76	248
172	0.799	1.196	280.6	281.0	296.0	9.76	249
171	0.807	0.895	280.0	281.0	284.9	9.76	250
176	0.8	1.228	298.3	593.3	295.1	9.73	251
177	0.797	0.975	295.6	898.9	301.7	9.73	252
179	0.818	0.929	446.1	597 8	302.2	9.73	253
178	0.840	0.964	658.3	873.3	311.2	9.73	254
175	0.795	0.931	292.2	601.1	293.0	9.73	255

1/3 OCTAVE NTC (dB) WITH RESPECT TO INCIDENT SPL (NTC_i)

$M_J = 0$ $M_T = 0$

DAISY LOBE NOZZLE (RUN NO = 19)

EMISSION ANGLE (RELATIVE TO JET EXHAUST) REFERENCED TO NOZZLE EXIT (DEGREES)

FREQ KHZ	PTF_i	0.	10.	20.	30.	40.	50.	60.	70.	80.	90.	100.	110.	120.
.250	-21.6	-22.8	-20.6	-17.6	-17.0	-23.8	-20.4	-19.8	-20.3	-21.7	-19.3	-22.0	-21.2	-21.6
.315	-18.6	-19.4	-17.0	-14.2	-13.9	-20.4	-17.4	-16.8	-17.3	-18.6	-16.7	-18.9	-18.5	-18.8
.400	-16.6	-17.6	-15.2	-12.4	-12.2	-18.3	-15.8	-14.8	-15.3	-16.6	-14.9	-17.1	-16.6	-16.9
.500	-14.2	-14.3	-12.0	-9.9	-9.8	-15.5	-13.0	-12.3	-12.9	-14.1	-13.1	-14.8	-14.5	-14.6
.630	-10.9	-11.0	-8.9	-6.7	-7.0	-11.7	-9.4	-8.8	-9.4	-10.6	-10.1	-11.6	-11.2	-11.1
.800	-8.4	-9.0	-6.4	-4.2	-4.7	-8.6	-7.0	-6.2	-6.8	-7.9	-7.7	-9.8	-8.9	-8.8
1.00	-8.0	-7.7	-4.8	-2.6	-3.1	-6.2	-5.6	-4.6	-5.3	-6.8	-6.3	-8.4	-7.8	-7.9
1.25	-5.4	-6.2	-3.2	-0.9	-1.6	-3.9	-3.7	-3.0	-3.7	-4.9	-5.1	-7.8	-6.7	-6.6
1.60	-4.0	-4.2	-1.2	1.0	0.2	-1.8	-2.2	-1.4	-2.3	-3.8	-4.1	-6.7	-5.8	-6.1
2.00	-3.1	-1.8	1.2	3.2	2.3	-1.2	-1.6	-0.9	-1.8	-3.8	-4.2	-8.1	-6.0	-6.3
2.50	-2.0	0.9	3.4	5.2	4.1	-0.6	-0.6	0.2	-1.1	-2.8	-3.8	-8.9	-5.6	-6.2
3.15	-1.2	2.4	4.9	7.0	5.7	-1.0	-0.1	0.6	-0.7	-2.6	-4.1	-6.3	-6.0	-6.9
4.00	-1.3	2.8	6.3	7.9	6.1	-2.8	-1.3	-0.9	-1.7	-3.8	-5.0	-7.4	-6.7	-6.8
5.00	-2.8	3.4	7.6	8.4	6.8	-5.8	-6.7	-3.4	-5.7	-8.7	-12.7	-15.6	-16.9	-17.8
6.30	-1.3	5.7	9.0	9.7	8.2	-3.7	-6.8	-2.4	-5.5	-9.2	-11.8	-11.4	-10.4	-11.1
8.00	-2.3	5.7	9.3	8.6	7.3	-1.8	-3.3	-0.7	-2.0	-5.3	-7.3	-10.9	-9.9	-9.8
10.0	-2.3	5.1	8.6	5.3	-5.0	2.9	-1.0	-0.8	-1.8	-3.3	-7.3	-10.9	-9.9	-9.8
12.5	-2.0	8.1	10.2	0.8	1.0	3.6	1.5	-4.0	-4.3	-6.8	-7.8	-7.4	-8.7	-13.8
16.0	-0.4	8.4	9.7	-0.9	-2.8	-4.8	-0.8	-5.8	-10.2	-14.3	-15.3	-17.2	-19.0	-11.6
20.0	-0.3	4.5	1.7	0.7	-11.0	-4.8	2.6	-7.9	-13.9	-15.5	-16.3	-20.2	-15.3	-10.5
25.0	-3.8	9.1	-3.0	3.9	-10.0	3.7	2.4	-0.4	-7.9	-13.2	-12.3	-14.0	-11.0	-10.9
31.5	-4.5	8.5	-1.9	-1.9	-8.0	4.9	-1.1	-1.5	-10.7	-12.3	-9.3	-16.8	-14.2	-13.4
40.0	-2.3	13.2	2.8	-8.7	-11.2	7.7	-0.7	-7.4	-10.2	-10.1	-11.9	-16.5	-16.1	-10.8
50.0	1.8	20.3	13.8	-10.2	-10.0	10.6	6.2	-11.5	-9.6	-9.6	-13.6	-16.4	-19.4	-16.0
63.0	8.4	25.1	19.4	-7.8	-9.2	5.6	11.6	-10.8	-16.0	-17.8	-18.3	-12.6	-23.4	-21.1

$OPTF_i$	$NOSPL_i$
21.8	-0.8 -3.9 -5.3 -6.5 -10.0 -6.6 -9.9 -10.9 -12.4 -11.8 -14.0 -13.7 -13.8

CONICAL NOZZLE (RUN NO = 89)

EMISSION ANGLE (RELATIVE TO JET EXHAUST) REFERENCED TO NOZZLE EXIT (DEGREES)

FREQ KHZ	PTF_i	0.	10.	20.	30.	40.	50.	60.	70.	80.	90.	100.	110.	120.
.250	-25.8	-24.6	-30.7	-31.6	-21.9	-28.1	-23.7	-24.2	-25.0	-29.9	-22.0	-27.7	-24.5	-23.8
.315	-22.2	-20.2	-24.8	-24.8	-18.4	-23.4	-20.1	-20.4	-21.2	-22.1	-19.0	-23.6	-21.2	-20.7
.400	-20.3	-18.5	-22.8	-22.7	-16.5	-21.2	-18.2	-18.6	-19.2	-20.1	-17.3	-21.5	-19.4	-18.9
.500	-17.0	-13.7	-15.0	-13.0	-14.1	-17.1	-15.2	-15.3	-16.0	-16.9	-15.3	-18.0	-16.8	-16.4
.630	-13.8	-10.8	-10.8	-8.6	-11.0	-13.1	-11.8	-11.9	-12.4	-13.3	-12.5	-14.3	-13.7	-13.4
.800	-10.2	-6.7	-7.5	-5.5	-7.3	-9.9	-8.7	-8.6	-9.1	-10.1	-9.6	-10.7	-10.7	-10.5
1.00	-7.9	-4.0	-4.6	-2.9	-4.8	-6.8	-6.3	-6.4	-7.0	-8.1	-7.4	-8.6	-8.6	-8.6
1.25	-6.8	-1.5	-2.1	-0.6	-2.8	-3.1	-4.2	-4.6	-5.3	-6.6	-6.0	-6.9	-6.9	-6.9
1.60	-4.3	0.7	-0.0	1.6	-0.8	-1.0	-2.6	-2.9	-3.7	-5.0	-4.7	-6.9	-6.0	-6.8
2.00	-2.8	3.0	2.2	3.7	1.2	0.6	-1.0	-1.5	-2.3	-3.5	-3.8	-6.2	-5.1	-5.9
2.50	-1.0	5.1	4.6	6.1	3.1	1.9	0.8	-0.2	-1.2	-2.6	-3.3	-4.9	-4.8	-5.1
3.15	-0.6	6.8	6.2	7.6	4.5	2.8	1.8	0.6	-0.5	-2.4	-3.6	-4.9	-4.9	-5.8
4.00	-0.2	7.9	7.6	8.6	5.3	2.5	2.1	0.8	-0.8	-2.7	-4.8	-6.1	-6.3	-7.2
5.00	0.3	9.5	9.5	10.3	6.0	3.3	1.6	0.0	-2.0	-4.3	-7.2	-8.3	-8.9	-9.8
6.30	1.4	11.0	11.3	12.9	8.1	4.6	2.0	-1.0	-4.5	-7.7	-11.1	-12.1	-12.3	
8.00	0.1	11.4	11.2	11.0	6.8	2.5	-3.4	-9.8	-11.0	-10.8	-11.7	-12.1	-11.4	-11.9
10.0	2.6	15.3	15.4	14.7	8.9	-1.0	-6.1	-6.0	-5.0	-6.8	-8.9	-9.9	-10.3	-10.6
12.4	1.8	13.3	14.1	12.8	6.9	0.8	-2.8	-3.4	-6.0	-9.3	-11.1	-12.0	-12.3	-13.7
16.0	0.2	13.8	15.0	11.2	2.4	-4.2	-7.2	-1.3	-10.2	-12.8	-13.6	-14.9	-15.8	-15.0
20.0	-0.9	14.3	15.8	8.7	1.0	-2.3	-6.6	-8.7	-12.2	-15.9	-16.8	-3.8	-16.1	-18.8
25.0	0.6	17.1	17.7	7.4	2.0	-2.7	-8.8	-9.3	-10.7	-13.8	-14.8	-18.7	-17.2	-17.6
31.5	0.2	17.4	17.0	1.9	0.9	-6.0	-8.5	-11.7	-15.1	-14.4	-17.1	-21.3	-19.8	-20.2
40.0	2.6	20.8	18.8	4.7	0.0	-7.9	-10.5	-12.8	-13.8	-15.6	-19.1	-19.1	-16.7	-20.9
50.0	1.7	18.8	18.1	6.3	-4.6	-11.1	-12.1	-13.9	-16.0	-16.8	-18.1	-21.8	-19.6	-22.8
63.0	-0.7	16.1	15.8	6.6	-10.4	-8.8	-18.6	-14.3	-19.4	-18.3	-14.2	-19.2	-23.4	-25.1

$OPTF_i$	$NOSPL_i$
23.7	1.4 4.8 -1.3 -5.3 -7.6 -8.8 -9.8 -10.7 -12.2 -11.4 -13.3 -13.3 -13.2

1/3 OCTAVE NTC (dB) WITH RESPECT TO TRANSMITTED SPL (NTC_t)

$M_J = 0$ $M_T = 0$

DAISY LOBE NOZZLE (RUN NO= 19)

EMISSION ANGLE (RELATIVE TO JET EXHAUST) REFERENCED TO NOZZLE EXIT (DEGREES)

FREQ KHZ	PTF_t	0.	10.	20.	30.	40.	50.	60.	70.	80.	90.	100.	110.	120.
.250	-19.7	-21.0	-18.7	-15.6	-18.2	-22.0	-16.6	-17.9	-18.5	-19.8	-17.4	-20.1	-19.3	-19.8
.315	-16.3	-17.2	-14.9	-12.0	-11.8	-18.2	-18.3	-14.6	-15.1	-16.5	-14.6	-16.7	-16.3	-16.6
.400	-14.0	-14.9	-12.6	-9.8	-9.6	-15.7	-12.6	-12.2	-12.8	-14.1	-12.4	-14.5	-14.1	-14.3
.500	-11.3	-11.4	-9.1	-6.7	-6.9	-12.6	-11.1	-9.4	-10.0	-11.2	-10.2	-11.6	-11.6	-11.6
.630	-8.9	-7.0	-4.9	-2.7	-3.0	-7.7	-8.4	-4.8	-5.4	-6.6	-6.1	-7.6	-7.2	-7.1
.800	-5.1	-5.6	-3.1	-0.9	-1.4	-5.3	-3.6	-2.6	-3.4	-4.6	-4.3	-6.2	-5.6	-5.5
1.00	-4.6	-5.2	-2.4	-0.1	-0.7	-3.8	-3.1	-2.1	-2.9	-4.1	-3.8	-5.9	-5.2	-5.2
1.25	-3.9	-4.7	-1.7	0.6	-0.1	-2.4	-2.2	-1.8	-2.2	-3.4	-3.6	-6.0	-5.2	-5.2
1.60	-2.7	-3.0	0.0	2.2	1.4	-0.6	-1.0	-0.1	-1.1	-2.6	-2.9	-5.5	-4.6	-4.8
2.00	-2.0	-0.4	2.4	4.4	3.5	-0.1	-0.8	0.2	-0.7	-2.4	-3.1	-4.9	-4.6	-5.2
2.50	-1.3	1.6	4.1	5.9	4.8	0.1	0.1	0.9	-0.4	-2.1	-3.1	-5.3	-4.9	-5.5
3.15	-0.6	2.6	5.8	7.6	6.3	-0.4	0.5	1.2	-0.1	-2.0	-3.5	-5.7	-5.4	-6.3
4.00	-0.9	3.2	6.6	8.2	6.5	-2.1	-0.5	0.4	-1.3	-3.2	-5.5	-7.2	-7.8	-9.1
5.00	-1.4	4.5	6.7	9.4	6.6	-4.8	-5.7	-2.3	-4.6	-7.7	-11.6	-14.5	-15.9	-16.9
6.30	1.7	8.6	12.0	12.7	9.2	-0.7	-3.6	0.6	-2.5	-6.2	-8.8	-8.4	-7.4	-8.1
8.00	-4.7	7.3	10.9	10.2	2.6	-0.2	-1.7	-8.1	-10.4	-6.2	-4.4	-4.5	-5.2	-6.0
10.0	-1.2	6.2	9.7	6.4	-4.8	3.9	0.0	0.3	-0.4	-2.3	-6.2	-9.8	-8.8	-8.6
12.5	-1.2	8.8	11.0	1.6	1.7	4.3	2.6	-3.2	-3.6	-5.0	-7.0	-6.6	-7.9	-12.7
16.0	-5.9	5.9	6.2	-0.4	-2.3	-4.3	0.0	-5.3	-9.7	-13.8	-14.8	-16.7	-18.5	-11.1
20.0	-6.0	4.9	2.1	1.1	-10.7	-4.4	2.6	-7.6	-13.6	-15.1	-16.0	-19.9	-15.0	-10.2
25.0	-3.1	9.8	-2.4	4.6	-9.4	4.4	3.0	0.3	-7.2	-12.5	-11.6	-13.3	-10.3	-10.2
31.5	-3.5	9.5	-0.9	-1.0	-7.0	6.0	-0.0	-0.5	-9.7	-11.2	-8.3	-15.7	-13.2	-12.4
40.0	-1.8	13.9	3.6	-7.9	-10.4	8.5	4.5	-6.6	-9.4	-9.4	-11.1	-15.7	-15.3	-10.0
50.0	2.0	21.4	14.6	-9.1	-8.9	11.8	7.3	-10.4	-8.4	-8.5	-12.4	-15.5	-14.3	-14.9
63.0	7.4	27.2	21.4	-5.4	-7.3	7.6	13.0	-8.7	-14.0	-18.7	-16.1	-10.0	-21.5	-18.9

$OPTF_t$	← $NOSPL_t$ →												
24.2	1.4	-1.7	-3.0	-4.3	-7.7	-6.7	-7.6	-8.7	-10.2	-9.5	-11.7	-11.5	-11.6

CONICAL NOZZLE (RUN NO = 80)

EMISSION ANGLE (RELATIVE TO JET EXHAUST) REFERENCED TO NOZZLE EXIT (DEGREES)

FREQ KHZ	PTF_t	0.	10.	20.	30.	40.	50.	60.	70.	80.	90.	100.	110.	120.
.250	-22.8	-21.3	-27.4	-28.3	-18.6	-24.8	-20.4	-20.9	-21.7	-22.6	-18.7	-24.4	-21.2	-20.8
.315	-18.7	-16.8	-21.4	-21.4	-15.0	-19.9	-16.7	-17.0	-17.8	-18.7	-15.6	-20.1	-17.9	-17.2
.400	-16.7	-14.9	-19.2	-19.1	-12.9	-17.6	-14.6	-14.9	-15.6	-16.8	-13.7	-17.9	-15.6	-15.3
.500	-13.6	-10.3	-11.6	-9.6	-10.7	-13.7	-11.8	-12.0	-12.6	-13.5	-11.9	-14.6	-13.4	-13.1
.630	-10.6	-7.1	-7.5	-5.7	-8.1	-10.2	-8.6	-8.9	-9.5	-10.4	-9.6	-11.4	-10.7	-10.5
.800	-7.7	-4.2	-4.9	-2.9	-4.8	-6.3	-4.1	-6.0	-6.6	-7.6	-7.0	-8.2	-8.1	-7.9
1.00	-5.6	-1.7	-2.3	-0.6	-2.5	-3.4	-4.0	-4.1	-4.7	-5.7	-5.1	-6.2	-6.3	-6.3
1.25	-4.4	0.6	-0.6	1.0	-1.3	-1.6	-2.7	-3.1	-3.8	-5.1	-4.4	-5.3	-5.4	-5.4
1.60	-3.6	1.4	0.7	2.3	-0.1	-0.3	-1.6	-2.2	-2.9	-4.3	-3.9	-6.2	-5.3	-5.0
2.00	-2.8	3.3	2.5	4.0	1.8	0.9	-0.7	-1.1	-2.0	-3.2	-3.6	-4.9	-4.8	-4.7
2.50	-1.3	5.3	4.7	6.2	3.2	2.0	1.0	-0.1	-1.0	-2.4	-3.1	-4.8	-4.6	-4.9
3.15	-0.3	7.0	6.4	7.7	4.7	3.0	2.0	0.8	-0.3	-2.1	-3.3	-4.7	-4.7	-5.8
4.00	-0.2	8.0	7.6	8.6	5.3	2.8	2.1	0.8	-0.7	-2.7	-4.7	-6.1	-6.2	-7.2
5.00	0.4	9.6	9.5	10.4	6.1	3.3	1.9	0.1	-2.0	-4.3	-7.1	-8.3	-8.8	-9.7
6.30	2.8	12.1	12.4	13.1	9.2	5.7	3.1	0.1	-3.4	-6.6	-10.0	-11.0	-11.0	-11.2
8.00	6.6	12.2	12.1	11.8	7.4	3.4	-2.6	-8.2	-10.2	-10.1	-10.8	-11.2	-10.5	-11.0
*10.0	7.2	20.1	20.0	19.3	10.6	3.7	-1.5	-0.3	-0.6	-2.1	-4.1	-5.3	-5.7	-6.1
12.5	1.8	13.5	14.4	13.1	7.2	0.7	-2.3	-3.1	-5.8	-9.1	-10.9	-11.7	-12.1	-13.5
16.0	0.6	14.2	15.4	11.6	2.9	-3.7	-6.7	-9.8	-9.7	-12.1	-13.2	-14.4	-15.0	-14.6
20.0	-0.7	14.5	15.7	8.9	1.2	-2.2	-6.5	-8.5	-12.0	-15.8	-16.6	-18.6	-18.0	-18.5
25.0	0.9	17.4	18.0	7.7	2.3	-2.4	-8.5	-9.0	-10.4	-13.2	-14.5	-18.4	-16.9	-17.3
31.5	0.5	17.7	17.3	2.3	1.2	-5.6	-8.6	-11.4	-14.8	-14.1	-16.8	-20.9	-19.5	-19.8
40.0	3.2	21.3	19.3	5.2	0.5	-7.4	-10.4	-12.3	-13.2	-15.1	-18.6	-18.6	-18.2	-20.4
50.0	2.6	19.7	19.0	7.2	-3.7	-10.2	-11.2	-13.1	-15.1	-15.7	-17.2	-20.9	-18.7	-22.0
63.0	1.0	16.9	17.2	8.4	-8.7	-7.1	-13.2	-12.5	-17.7	-13.8	-12.4	-17.2	-21.9	-27.4

$OPTF_t$	← $NOSPL_t$ →												
20.8	3.8	3.3	1.5	-2.4	-4.7	-6.5	-6.7	-7.8	-9.3	-8.7	-10.5	-10.5	-10.4

1/3 OCTAVE NTC (dB) WITH RESPECT TO INCIDENT SPL (NTC_i)

$M_J = 0.2 \quad M_T = 0$

DAISY LOBE NOZZLE (RUN NO = 20)

EMISSION ANGLE (RELATIVE TO JET EXHAUST) REFERENCED TO NOZZLE EXIT (DEGREES)

FREQ KHZ	PTF_i	0.	10.	20.	30.	40.	50.	60.	70.	80.	90.	100.	110.	120.
.250	-21.0	-18.3	-37.1	-18.9	-19.3	-21.4	-18.3	-20.2	-20.3	-22.1	-13.8	-27.0	-23.0	-23.5
.315	-19.0	-15.6	-34.5	-19.5	-16.5	-20.7	-15.4	-17.6	-17.6	-19.4	-13.0	-23.4	-20.6	-21.0
.400	-17.8	-14.2	-33.1	-20.1	-15.0	-20.2	-13.6	-16.2	-16.2	-17.9	-12.4	-21.9	-19.3	-19.6
.500	-15.9	-11.6	-30.9	-21.4	-12.4	-19.7	-11.1	-13.8	-13.9	-15.5	-12.5	-18.1	-17.3	-17.6
.630	-13.4	-8.8	-28.2	-26.9	-9.5	-18.8	-8.1	-11.0	-11.1	-12.7	-12.6	-14.8	-14.7	-15.0
.800	-11.1	-6.7	-25.9	-23.2	-7.1	-18.8	-5.6	-8.8	-8.8	-10.2	-10.3	-12.2	-12.6	-12.7
1.00	-9.6	-6.2	-24.2	-15.7	-5.2	-19.0	-4.0	-7.4	-7.4	-8.6	-9.1	-10.6	-11.3	-11.3
1.25	-7.8	-6.2	-22.6	-10.0	-3.3	-17.4	-1.8	-5.7	-5.7	-7.1	-8.0	-9.4	-10.3	-10.4
1.60	-6.3	-7.0	-21.4	-6.3	-1.4	-14.8	-0.0	-4.3	-4.3	-5.9	-6.4	-8.7	-9.2	-9.6
2.00	-5.2	-9.9	-20.7	-3.5	0.2	-15.1	1.8	-3.3	-3.0	-4.6	-6.1	-8.9	-8.5	-9.0
2.50	-4.2	-13.0	-20.7	-1.4	1.4	-14.8	2.6	-2.8	-2.4	-4.3	-5.9	-8.3	-8.5	-9.3
3.15	-3.4	-19.2	-21.4	0.8	2.9	-14.8	3.6	-2.0	-1.7	-4.0	-5.7	-8.3	-8.9	-10.0
4.00	-3.3	-22.8	-22.7	3.1	3.9	-11.9	3.7	-2.9	-2.8	-5.2	-8.1	-9.8	-11.5	-13.2
5.00	-4.9	-32.7	-24.3	3.5	3.9	-10.1	1.6	-7.7	-6.6	-9.9	-14.2	-18.5	-22.0	-25.1
6.30	-4.1	-26.9	-26.5	3.6	6.1	-6.9	1.6	-11.0	-9.8	-13.4	-14.6	-13.2	-15.0	-16.6
8.00	-4.6	-30.3	-29.8	0.2	5.7	-2.6	1.3	-10.4	-17.9	-14.0	-10.8	-8.8	-13.7	-14.5
10.0	-2.8	-23.5	-24.8	-7.2	5.2	2.0	5.8	-5.9	-7.8	-11.3	-14.0	-14.1	-12.3	-12.5
12.5	-1.8	-23.5	-28.0	1.9	3.5	1.8	7.4	-3.0	-11.0	-10.5	-12.8	-12.5	-15.3	-18.6
16.0	-3.1	-29.4	-24.5	6.9	1.3	2.1	4.2	-9.6	-14.7	-15.7	-17.8	-18.8	-18.4	-13.9
20.0	-3.9	-25.8	-31.4	4.9	-2.9	3.4	2.5	-6.4	-19.3	-21.1	-17.8	-18.2	-15.1	-15.4
25.0	-6.1	-19.1	-18.8	-1.1	-1.4	-1.1	2.2	-7.4	-10.8	-10.1	-10.7	-13.4	-13.4	-20.5
31.5	-4.1	-26.8	-19.5	0.3	-1.0	5.1	1.4	-7.8	-7.9	-12.5	-10.0	-17.1	-15.8	-12.3
40.0	-2.6	-27.8	-29.0	1.6	5.6	1.4	5.0	-2.1	-12.4	-9.8	-10.8	-15.8	-19.3	-13.6
50.0	-1.6	-26.1	-31.4	-4.0	9.8	2.2	6.8	-6.1	-11.1	-12.5	-12.2	-16.3	-18.4	-19.9
63.0	3.9	-19.9	-28.2	6.9	13.4	5.7	9.2	6.9	-16.8	-17.0	-8.7	-16.3	-25.8	-23.2

$OPTF_i$	$NOSPL_i$
22.3	-11.6 -28.3 -7.4 -4.0 -10.9 -4.6 -9.6 -10.9 -12.7 -11.3 -15.3 -15.6 -15.9

CONICAL NOZZLE (RUN NO = 116)

EMISSION ANGLE (RELATIVE TO JET EXHAUST) REFERENCED TO NOZZLE EXIT (DEGREES)

FREQ KHZ	PTF_i	20.	30.	40.	50.	60.	70.	80.	90.	100.	110.	120.
.250	-25.6	-17.7	-32.0	-29.3	-23.5	-24.6	-24.7	-24.1	-23.5	-27.8	-25.2	-24.7
.315	-22.0	-14.4	-26.6	-23.8	-19.5	-20.8	-20.9	-20.7	-20.1	-23.9	-22.0	-21.5
.400	-20.3	-12.8	-24.6	-21.6	-17.8	-18.5	-19.2	-19.1	-18.5	-22.3	-20.5	-20.0
.500	-17.0	-10.1	-18.9	-18.0	-14.1	-15.6	-15.7	-16.0	-15.4	-18.9	-17.8	-17.4
.630	-14.0	-7.4	-15.1	-12.2	-11.0	-12.5	-12.6	-13.1	-12.5	-15.8	-15.1	-14.8
.800	-10.8	-4.4	-11.1	-8.2	-7.7	-8.8	-9.4	-10.4	-9.9	-12.6	-12.3	-12.0
1.00	-8.4	-2.2	-7.9	-4.9	-5.4	-5.7	-7.2	-8.5	-8.0	-10.1	-10.4	-10.2
1.25	-6.2	-0.4	-5.2	-1.8	-3.7	-3.0	-5.8	-6.6	-6.2	-8.2	-8.4	-8.4
1.60	-4.5	1.7	-3.6	0.3	-1.8	-1.4	-4.0	-4.6	-4.9	-6.8	-6.6	-6.7
2.00	-3.2	3.6	-3.0	1.5	0.2	-0.8	-2.1	-3.3	-4.0	-6.4	-5.9	-5.9
2.50	-2.1	4.5	-2.2	3.1	1.5	0.8	-1.4	-2.4	-3.2	-5.8	-5.7	-5.7
3.15	-1.3	5.4	-1.1	4.2	2.9	2.2	-0.7	-2.3	-3.3	-6.2	-6.2	-6.5
4.00	-1.2	5.5	-0.2	4.6	3.8	1.7	-0.9	-2.4	-4.8	-6.6	-7.5	-8.5
5.00	-0.8	5.4	0.8	6.4	4.2	2.2	-1.6	-3.7	-7.2	-9.8	-10.5	-11.8
6.30	-0.2	5.6	1.8	8.8	4.1	1.7	-3.9	-8.2	-12.6	-15.2	-16.0	-16.8
8.00	0.9	5.5	5.7	10.9	3.9	-2.1	-9.5	-8.4	-8.9	-9.8	-9.8	-10.8
10.0	-4.9	0.3	-2.6	5.3	-3.2	-7.3	-8.6	-10.0	-11.9	-15.1	-16.2	-17.1
12.4	-3.6	-1.3	-5.6	6.1	-3.0	-10.5	-12.5	-12.0	-16.5	-17.6	-18.9	-20.2
16.0	-8.7	-5.6	-9.3	2.5	-10.1	-12.7	-20.1	-18.2	-19.2	-21.3	-20.8	-22.9
20.0	-9.2	2.7	-3.1	-4.8	-9.6	-10.3	-13.7	-14.1	-16.4	-18.8	-18.1	-19.2
25.0	-6.5	0.2	-5.7	-0.6	-2.2	-6.9	-9.2	-11.1	-13.0	-16.7	-19.0	-19.4
31.5	-11.1	-2.4	-3.6	-7.9	-7.0	-6.8	-15.1	-13.2	-17.6	-19.9	-21.7	-22.4
40.0	-14.5	-6.4	-3.3	-2.2	-7.2	-16.2	-15.9	-15.4	-19.2	-20.7	-23.0	-23.4
50.0	-1.6	-6.1	12.0	-2.6	-7.0	-13.2	-19.4	-17.3	-19.9	-23.6	-25.6	-25.6
63.0	4.4	-3.4	17.6	-7.2	-10.6	-11.8	-18.6	-13.4	-12.4	-16.4	-24.4	-26.7

$OPTF_i$	$NOSPL_i$
24.1	-3.7 -1.9 -3.6 -6.5 -7.6 -10.0 -11.1 -11.0 -13.7 -13.8 -13.7

1/3 OCTAVE NTC (dB) WITH RESPECT TO TRANSMITTED SPL (NIC_t)

$M_J = 0.2$ $M_T = 0$

DAISY LOBE NOZZLE (RUN NO= 20)

FREQ KHZ	PTF_t	0.	10.	20.	30.	40.	50.	60.	70.	80.	90.	100.	110.	120.
	EMISSION ANGLE (RELATIVE TO JET EXHAUST) REFERENCED TO NOZZLE EXIT (DEGREES)													
.250	-24.8	-18.1	-36.9	-18.7	-19.1	-21.2	-18.1	-20.0	-20.1	-21.9	-13.6	-26.8	-22.8	-23.3
.315	-18.7	-15.4	-34.3	-19.2	-16.2	-20.4	-15.1	-17.3	-17.4	-19.1	-12.8	-23.2	-20.4	-20.8
.400	-17.5	-13.9	-32.8	-19.8	-14.7	-19.8	-13.6	-15.8	-15.9	-17.6	-12.1	-21.5	-19.0	-19.3
.500	-15.5	-11.2	-30.5	-21.0	-12.1	-19.3	-10.7	-13.4	-13.5	-15.1	-12.1	-17.7	-16.9	-17.2
.630	-12.9	-8.2	-27.6	-26.4	-9.9	-18.3	-7.5	-10.4	-10.6	-12.2	-12.1	-14.2	-14.2	-14.4
.800	-10.3	-5.9	-25.0	-22.3	-6.3	-17.6	-4.6	-7.9	-8.0	-9.4	-9.5	-11.3	-11.8	-11.8
1.00	-8.6	-5.2	-23.3	-14.7	-4.2	-18.0	-3.0	-6.4	-6.5	-7.6	-8.1	-9.6	-10.4	-10.4
1.25	-6.9	-5.2	-21.7	-9.7	-2.4	-16.4	-1.5	-4.8	-4.8	-6.1	-7.0	-8.4	-9.4	-9.5
1.60	-5.4	-6.1	-20.6	-5.4	-0.5	-13.6	0.9	-3.4	-3.3	-5.0	-5.5	-7.8	-8.3	-8.7
2.00	-4.2	-8.9	-19.8	-2.5	1.2	-14.1	2.3	-2.3	-2.1	-3.9	-5.2	-7.9	-7.6	-8.1
2.50	-3.2	-12.0	-19.7	-0.4	2.4	-13.5	3.6	-1.8	-1.4	-3.3	-4.9	-7.3	-7.5	-8.2
3.15	-2.6	-18.4	-20.6	1.6	3.7	-13.7	4.3	-1.2	-0.9	-3.2	-4.9	-7.5	-8.2	-9.2
4.00	-3.1	-22.6	-22.5	3.3	4.1	-11.7	3.5	-2.6	-2.5	-5.0	-7.9	-9.6	-11.3	-12.9
5.00	-4.7	-32.5	-24.1	3.8	4.1	-9.8	1.6	-7.4	-6.3	-9.6	-14.0	-18.3	-21.8	-24.9
6.30	-3.3	-25.3	-25.8	4.2	6.8	-6.2	2.4	-10.2	-9.0	-12.7	-13.9	-12.4	-14.3	-15.9
8.00	-3.8	-29.6	-29.0	1.0	6.5	-1.8	1.1	-9.6	-17.1	-13.3	-10.0	-8.0	-12.9	-13.7
10.0	-1.4	-22.4	-23.7	-6.1	6.3	3.1	6.8	-4.9	-6.7	-10.3	-12.9	-13.0	-11.3	-11.4
12.5	-1.4	-23.1	-28.2	2.3	3.9	1.5	7.6	-2.5	-10.6	-10.0	-12.4	-12.1	-14.8	-18.2
16.0	-3.0	-29.3	-26.4	7.0	1.4	2.2	4.3	-9.5	-14.6	-15.6	-17.7	-18.7	-18.3	-13.7
20.0	-3.8	-25.7	-31.3	5.0	-2.9	3.4	3.0	-6.3	-19.3	-21.0	-17.7	-18.2	-15.1	-15.4
25.0	-6.0	-19.0	-18.6	-1.9	-1.2	-0.9	2.3	-7.2	-10.7	-9.9	-10.5	-13.2	-13.3	-20.4
31.5	-3.9	-26.6	-19.4	0.5	-0.8	5.3	1.0	-7.6	-7.7	-12.3	-9.8	-17.0	-15.6	-12.1
40.0	-2.6	-26.8	-28.8	1.8	5.7	1.5	5.2	-2.0	-12.2	-9.6	-10.7	-15.7	-19.2	-13.4
50.0	-1.8	-26.0	-31.3	-3.9	9.9	2.3	0.6	0.0	-10.9	-12.3	-12.1	-16.2	-18.2	-19.8
63.0	4.3	-19.4	-27.8	7.3	13.9	6.2	9.6	7.3	-16.3	-16.5	-8.2	-15.4	-25.3	-22.8
	$OPTF_t$ ←						$NOSPL_t$ →							
	22.7	-11.2	-27.9	-7.0	-3.6	-10.8	-4.2	-9.2	-10.5	-12.3	-10.9	-14.9	-15.2	-15.5

CONICAL NOZZLE (RUN NO = 116)

FREQ KHZ	PTF_t	20.	30.	40.	50.	60.	70.	80.	90.	100.	110.	120.
	EMISSION ANGLE (RELATIVE TO JET EXHAUST) REFERENCED TO NOZZLE EXIT (DEGREES)											
.250	-23.1	-15.1	-29.5	-26.6	-21.0	-22.1	-22.2	-21.6	-21.0	-25.3	-22.7	-22.1
.315	-19.4	-11.8	-24.0	-21.2	-17.0	-18.0	-18.3	-18.1	-17.8	-21.4	-19.4	-19.0
.400	-17.7	-10.2	-22.0	-19.2	-15.2	-16.3	-16.6	-16.5	-15.9	-19.7	-17.9	-17.4
.500	-14.4	-7.5	-16.3	-13.4	-11.5	-13.0	-13.1	-13.4	-12.8	-16.3	-15.2	-14.8
.630	-11.4	-4.8	-12.8	-9.7	-8.4	-9.5	-10.1	-10.5	-9.9	-13.3	-12.8	-12.2
.800	-8.9	-2.5	-9.3	-6.4	-5.8	-6.9	-7.8	-8.5	-8.0	-10.7	-10.4	-10.2
1.00	-7.1	-0.9	-6.6	-3.6	-4.2	-4.4	-6.0	-7.3	-6.7	-8.8	-9.1	-8.9
1.25	-5.2	0.6	-4.1	-0.8	-2.7	-2.6	-4.7	-6.6	-5.2	-7.1	-7.4	-7.4
1.60	-3.6	2.5	-2.7	1.1	-1.0	-0.6	-3.1	-3.8	-4.1	-6.0	-6.8	-6.9
2.00	-2.9	3.9	-2.7	1.9	0.5	-0.5	-1.8	-2.9	-3.7	-6.1	-5.6	-6.6
2.50	-2.6	4.7	-2.0	3.3	1.6	0.9	-1.3	-2.2	-3.0	-5.6	-5.5	-6.6
3.15	-1.2	5.5	-1.1	4.3	3.0	2.2	-0.7	-2.3	-3.3	-6.1	-6.2	-6.4
4.00	-1.2	5.5	-0.2	4.0	3.8	1.7	-0.9	-2.3	-4.7	-6.6	-7.5	-8.4
5.00	-8.7	5.5	0.9	6.5	4.3	2.3	-1.5	-3.7	-7.1	-9.5	-10.4	-11.7
6.30	-6.7	6.5	2.7	9.7	5.0	2.6	-3.0	-7.3	-11.8	-14.3	-15.1	-15.9
8.00	1.6	6.7	6.6	11.7	4.7	-1.2	-8.6	-7.5	-8.1	-8.9	-9.0	-9.9
10.0	12.3	17.4	13.9	21.5	13.6	8.9	12.2	6.3	3.0	3.1	1.6	7.1
12.5	-1.3	1.0	-3.4	10.3	-0.7	-8.2	-10.3	-9.8	-14.2	-15.4	-16.7	-18.1
16.0	-8.6	-5.5	-9.2	2.6	-10.0	-12.6	-20.0	-18.1	-19.1	-21.2	-20.7	-22.8
20.0	-9.1	2.8	-3.0	-4.7	-9.8	-10.2	-13.6	-14.0	-16.3	-18.7	-18.0	-19.1
25.0	-6.3	6.4	-5.6	-0.4	-2.0	-6.8	-9.1	-11.0	-12.9	-16.5	-18.9	-19.2
31.5	-14.9	-2.2	-3.4	-7.6	-6.8	-6.6	-14.9	-12.9	-17.4	-19.6	-21.5	-22.2
40.0	-14.1	-6.6	-3.0	-1.8	-6.8	-9.4	-15.6	-15.0	-18.8	-20.4	-22.7	-23.0
50.0	-1.0	-8.5	12.6	-2.0	-6.4	-12.7	-18.8	-16.7	-19.4	-22.9	-25.1	-25.0
63.0	9.1	6.7	22.6	-2.4	-6.0	-6.7	-14.0	-8.6	-7.8	-11.8	-19.5	-24.0
	$OPTF_t$ ←						$NOSPL_t$ →					
	26.2	-1.7	0.1	-1.5	-4.4	-5.8	-7.9	-9.1	-9.0	-11.7	-11.7	-11.6

1/3 OCTAVE NTC (dB) WITH RESPECT TO INCIDENT SPL (NTC_i)

$M_J = 0.4$ $M_i = 0$

DAISY LOBE NOZZLE (RUN NO = 13)

EMISSION ANGLE (RELATIVE TO JET EXHAUST) REFERENCED TO NOZZLE EXIT
(DEGREES)

FREQ KHZ	PTF_i	0.	10.	20.	30.	40.	50.	60.	70.	80.	90.	100.	110.	120.
.250	-22.5	-38.7	-13.8	-15.2	-16.8	-26.4	-17.5	-21.7	-22.8	-25.2	-27.4	-29.4	-26.6	-26.3
.315	-19.7	-34.6	-11.9	-12.1	-13.9	-21.8	-14.6	-19.0	-20.2	-22.5	-23.1	-25.3	-23.8	-23.7
.400	-16.2	-32.8	-10.9	-11.0	-12.8	-19.5	-13.0	-17.6	-18.9	-21.1	-21.3	-23.5	-22.4	-22.3
.500	-15.8	-28.8	-9.7	-8.6	-10.3	-15.6	-10.6	-16.6	-16.8	-18.9	-16.2	-19.1	-20.1	-20.1
.630	-12.9	-25.5	-8.1	-6.0	-7.8	-11.7	-7.6	-12.9	-14.2	-16.2	-12.6	-15.7	-17.3	-17.3
.800	-9.8	-22.1	-6.0	-3.8	-5.0	-7.0	-4.1	-9.6	-11.0	-12.9	-10.4	-12.9	-14.0	-14.3
1.00	-7.5	-19.3	-4.6	-1.7	-3.0	-3.5	-1.6	-7.1	-8.5	-10.5	-8.9	-11.2	-11.6	-12.5
1.25	-5.7	-17.5	-3.7	-0.4	-1.4	-0.7	0.9	-4.9	-6.4	-8.5	-7.8	-10.0	-10.1	-11.2
1.60	-3.6	-17.0	-3.4	0.9	0.4	1.7	2.6	-2.7	-4.3	-6.5	-6.7	-9.1	-8.7	-9.7
2.00	-2.4	-18.0	-3.6	1.6	2.0	2.9	4.3	-1.1	-2.8	-5.1	-6.0	-8.6	-7.7	-9.2
2.50	-1.4	-22.4	-4.6	1.3	3.0	3.5	5.7	0.2	-1.7	-4.0	-5.7	-8.4	-8.0	-9.5
3.15	-0.2	-34.5	-5.6	0.6	3.9	5.1	7.4	1.6	-0.5	-3.3	-5.0	-8.5	-9.4	-10.6
4.00	-0.7	-29.3	-7.7	-0.6	3.7	5.4	7.2	0.4	-2.2	-5.4	-7.8	-10.3	-15.1	-15.1
5.00	-1.7	-25.4	-9.4	-1.4	2.8	6.5	7.6	-1.0	-4.5	-8.4	-11.6	-15.1	-25.8	-22.3
6.30	-0.5	-29.2	-9.0	-0.5	3.4	9.0	5.9	-6.7	-12.5	-18.4	-10.6	-10.7	-17.6	-17.4
8.00	-3.6	-26.8	-10.4	-3.2	4.8	6.2	-5.6	-19.0	-24.5	-19.4	-9.9	-10.4	-15.0	-13.7
10.0	-4.5	-23.3	-10.0	-8.3	5.3	0.3	1.6	-9.9	-9.8	-22.5	-16.6	-12.9	-14.0	-13.8
12.5	-6.8	-20.0	-12.8	-8.9	1.5	-0.7	-0.2	-6.3	-11.4	-16.3	-17.5	-18.2	-20.1	-18.7
16.0	-7.5	-19.8	-11.6	-8.8	-8.2	0.9	0.6	-8.5	-19.1	-19.3	-14.4	-17.2	-17.7	-21.0
20.0	-7.0	-16.5	-11.5	-12.6	-7.8	1.8	0.6	-10.4	-18.0	-24.7	-13.7	-16.6	-18.9	-18.9
25.0	-6.8	-14.2	-13.3	-9.4	-2.4	3.7	-4.4	-3.9	-5.9	-10.5	-12.2	-12.8	-17.8	-21.8
31.5	-4.4	-14.1	-15.6	-8.6	-3.9	2.8	-1.2	3.7	-8.8	-7.1	-14.1	-20.1	-12.9	-17.1
40.0	-6.8	-20.3	-20.4	-13.5	0.9	1.8	0.0	-17.0	-10.4	-9.9	-14.6	-16.6	-17.7	-17.9
50.0	-7.1	-24.2	-21.6	-27.6	3.6	-0.4	-1.6	-12.7	-11.1	-14.4	-20.8	-21.9	-19.1	-22.8
63.0	-4.4	-20.5	-22.0	-24.6	8.2	-3.6	-6.7	-11.9	-15.6	-20.1	-16.8	-20.8	-28.6	-25.2

$OPTF_i$	$NOSPL_i$
23.8	-24.8 -8.9 -6.2 -4.0 -4.1 -3.2 -9.1 -11.3 -13.8 -13.0 -15.8 -16.4 -17.1

CONICAL NOZZLE (RUN NO = 91)

EMISSION ANGLE (RELATIVE TO JET EXHAUST) REFERENCED TO NOZZLE EXIT
(DEGREES)

FREQ KHZ	PTF_i	0.	10.	20.	30.	40.	50.	60.	70.	80.	90.	100.	110.	120.
.250	-22.3	-29.2	-16.1	-12.7	-17.4	-21.2	-20.6	-19.9	-25.2	-24.7	-22.8	-28.3	-15.9	-24.7
.315	-19.5	-28.0	-13.8	-10.6	-14.2	-17.7	-17.6	-17.0	-21.8	-21.4	-20.1	-24.8	-23.4	-26.2
.400	-16.2	-27.3	-12.7	-9.8	-12.9	-16.2	-16.0	-15.7	-20.4	-20.1	-18.9	-23.4	-22.2	-24.8
.500	-15.8	-27.5	-10.5	-8.3	-9.8	-12.7	-12.3	-12.9	-17.2	-16.7	-16.6	-19.8	-19.9	-21.2
.630	-12.6	-27.9	-8.0	-6.3	-6.9	-9.6	-9.1	-10.0	-14.2	-13.7	-14.1	-16.7	-17.4	-18.0
.800	-9.7	-23.4	-5.9	-3.9	-3.8	-6.1	-6.1	-7.3	-10.6	-10.8	-10.9	-13.4	-14.8	-15.0
1.00	-7.5	-19.1	-4.3	-1.9	-1.9	-3.4	-4.3	-5.3	-7.5	-8.6	-8.9	-11.1	-12.5	-12.9
1.25	-5.8	-16.0	-3.6	-0.6	-0.4	-1.3	-2.6	-3.3	-4.8	-7.0	-7.5	-9.4	-10.5	-11.3
1.60	-4.1	-13.7	-3.6	0.5	1.0	0.7	-0.6	-1.5	-2.8	-5.5	-6.3	-8.1	-8.9	-9.9
2.00	-2.9	-12.9	-3.7	1.1	2.2	2.3	0.7	-0.3	-1.3	-4.0	-5.1	-7.0	-7.8	-8.8
2.50	-2.2	-14.6	-4.5	0.8	2.8	2.7	2.2	1.0	-1.1	-3.1	-4.4	-6.7	-7.4	-8.3
3.15	-1.6	-21.5	-5.4	0.7	3.0	3.3	3.2	2.0	-0.6	-2.9	-4.2	-6.2	-7.4	-8.4
4.00	-1.5	-23.8	-7.1	-0.5	2.3	2.8	3.8	2.5	0.8	-2.3	-4.9	-7.2	-8.5	-10.9
5.00	-1.9	-31.9	-8.8	-2.2	1.1	3.0	4.8	2.5	-0.6	-3.4	-7.6	-10.2	-13.2	-15.0
6.30	-1.6	-29.4	-8.9	-2.5	0.9	4.3	6.5	2.4	-1.3	-7.0	-13.3	-16.4	-19.9	-21.0
8.00	-1.1	-22.4	-9.3	-3.0	0.7	5.6	7.2	1.3	-7.5	-12.1	-12.0	-10.8	-11.4	-12.5
10.0	-0.8	-23.3	-10.7	-4.1	0.3	6.2	7.6	-1.8	-2.8	-4.5	-6.5	-9.9	-14.0	-15.4
12.4	-4.4	-26.5	-17.2	-11.6	-4.5	0.3	6.1	-8.0	-8.4	-11.3	-14.4	-19.5	-19.5	-21.8
16.0	-8.1	-27.3	-18.7	-16.1	-6.5	-0.7	0.4	-8.5	-12.7	-16.1	-13.8	-18.9	-21.3	-23.9
20.0	-7.8	-19.7	-16.4	-16.4	-6.3	1.8	-2.1	-8.0	-9.8	-17.7	-17.8	-19.4	-22.8	-24.9
25.0	-4.6	-26.2	-13.4	-10.2	-6.6	6.4	1.9	-7.7	-8.2	-16.9	-16.8	-18.4	-17.1	-19.1
31.5	-4.5	-19.6	-18.2	-15.5	-7.4	5.5	1.4	-2.2	-8.2	-14.2	-15.6	-17.5	-17.8	-20.3
40.0	-5.7	-19.8	-22.1	-18.4	-9.9	5.7	-4.8	-7.1	-11.7	-13.0	-14.7	-17.3	-21.2	-25.3
50.0	-7.2	-18.2	-22.5	-21.6	-8.2	4.3	-5.7	-7.0	-13.6	-17.0	-17.8	-23.6	-23.6	-25.4
63.0	-10.2	-16.8	-18.6	-16.8	-11.5	0.7	-5.1	-12.2	-15.2	-17.3	-16.8	-20.9	-14.8	-30.2

$OPTF_i$	$NOSPL_i$
24.0	-21.8 -8.7 -5.4 -4.6 -3.9 -4.1 -6.3 -8.8 -11.1 -11.5 -14.2 -15.3 -16.2

1/3 OCTAVE NTC (dB) WITH RESPECT TO TRANSMITTED SPL (NTC_t)

$M_J = 0.4$ $M_T = 0$

DAISY LOBE NOZZLE (RUN NO= 13)

FREQ KHZ	PTF_t	EMISSION ANGLE (RELATIVE TO JET EXHAUST) REFERENCED TO NOZZLE EXIT (DEGREES) 0.	10.	20.	30.	40.	50.	60.	70.	80.	90.	100.	110.	120.
.250	-22.3	-38.6	-13.7	-15.1	-16.7	-26.2	-17.3	-21.5	-22.7	-25.0	-27.2	-24.2	-26.4	-26.2
.315	-19.5	-34.4	-11.7	-12.2	-13.7	-21.6	-14.3	-18.6	-20.0	-22.3	-22.9	-26.1	-23.6	-23.5
.400	-17.8	-32.6	-10.6	-10.7	-12.3	-19.7	-12.6	-17.4	-18.6	-20.8	-21.1	-23.3	-22.1	-22.1
.500	-15.5	-28.5	-9.4	-8.3	-10.0	-15.3	-10.3	-15.3	-16.6	-18.6	-16.0	-18.9	-19.9	-19.8
.630	-12.6	-25.1	-7.7	-5.6	-7.4	-11.3	-7.2	-12.8	-13.8	-15.8	-12.3	-15.3	-17.0	-17.0
.800	-9.1	-21.4	-5.3	-2.8	-4.3	-6.3	-3.4	-8.9	-10.3	-12.2	-9.7	-12.2	-13.3	-13.7
1.00	-6.6	-18.3	-3.6	-0.8	-2.1	-2.5	-0.6	-6.1	-7.5	-9.5	-7.9	-10.3	-10.6	-11.5
1.25	-4.6	-16.4	-2.6	0.7	-0.3	0.3	1.4	-3.9	-5.3	-7.4	-6.7	-8.9	-9.0	-10.1
1.60	-2.8	-16.0	-2.4	1.9	1.4	2.7	3.5	-1.7	-3.3	-5.5	-5.7	-8.1	-7.7	-8.7
2.00	-1.7	-17.3	-2.9	2.2	2.7	3.6	5.0	-0.4	-2.1	-4.4	-5.3	-7.9	-7.0	-8.5
2.50	-1.0	-21.9	-4.1	1.8	3.5	4.0	6.2	0.7	-1.2	-3.6	-5.2	-8.0	-7.5	-9.0
3.15	-0.2	-34.1	-5.2	1.1	4.2	5.4	7.6	1.9	-0.2	-3.0	-4.7	-8.1	-9.0	-10.2
4.00	-0.5	-29.2	-7.8	-0.4	3.9	5.5	7.3	1.6	-2.1	-5.3	-7.7	-10.2	-15.0	-15.0
5.00	-0.4	-25.1	-9.1	-1.1	3.1	6.8	7.5	-0.7	-4.2	-8.2	-11.3	-14.9	-25.5	-22.0
6.30	-0.6	-28.1	-7.8	0.7	4.5	10.1	7.1	-5.5	-11.3	-17.3	-9.4	-9.5	-16.4	-16.2
8.00	-3.4	-20.6	-10.2	-3.0	5.0	6.4	-5.4	-18.9	-24.3	-19.2	-9.8	-10.3	-14.8	-13.5
10.0	-4.4	-23.3	-9.9	-8.2	5.4	0.4	1.6	-9.8	-9.7	-22.5	-16.5	-12.8	-13.9	-13.7
12.5	-6.7	-19.9	-12.7	-8.6	1.6	-0.6	-1.1	-6.2	-11.3	-16.2	-17.4	-18.1	-20.0	-18.6
16.0	-7.3	-19.7	-11.4	-8.6	-8.0	1.1	1.0	-8.3	-19.0	-19.1	-14.2	-17.1	-17.5	-20.8
20.0	-6.8	-16.3	-11.3	-12.4	-7.6	2.0	0.7	-10.2	-17.8	-24.5	-13.6	-16.5	-18.7	-18.8
25.0	-5.9	-14.1	-13.1	-6.3	-2.3	3.9	-4.2	-3.8	-5.8	-10.3	-12.0	-12.6	-17.6	-21.6
31.5	-3.6	-13.3	-14.8	-7.8	-3.2	3.6	-0.4	4.5	-8.0	-6.3	-13.4	-19.3	-12.1	-16.4
40.0	-6.7	-20.2	-20.3	-13.4	1.0	1.5	0.1	-16.9	-10.3	-9.8	-14.5	-16.5	-17.6	-17.8
50.0	-6.9	-23.9	-21.4	-27.4	3.9	-0.2	-1.7	-12.4	-10.8	-14.1	-20.6	-21.6	-18.9	-22.5
63.0	-4.2	-20.4	-21.8	-23.9	8.3	-3.5	-6.6	-11.8	-15.4	-20.0	-16.7	-20.7	-28.5	-25.1

$OPTF_t$	$NOSPL_t$											
23.8	-24.5	-8.6	-5.8	-3.7	-3.6	-2.5	-8.8	-10.9	-13.8	-12.6	-15.4	-16.1	-16.8

CONICAL NOZZLE (RUN NO = 91)

FREQ KHZ	PTF_t	EMISSION ANGLE (RELATIVE TO JET EXHAUST) REFERENCED TO NOZZLE EXIT (DEGREES) 0.	10.	20.	30.	40.	50.	60.	70.	80.	90.	100.	110.	120.
.250	-21.8	-28.4	-15.3	-11.9	-10.6	-20.4	-20.1	-19.1	-24.4	-23.9	-22.0	-27.5	-25.1	-28.9
.315	-19.7	-27.1	-13.0	-10.9	-13.4	-18.8	-16.6	-16.2	-21.0	-20.6	-19.3	-24.0	-22.6	-25.4
.400	-17.3	-26.4	-11.9	-9.0	-12.0	-15.4	-15.2	-14.9	-19.5	-19.2	-18.0	-22.5	-21.4	-24.0
.500	-14.5	-26.6	-9.5	-7.3	-8.8	-11.8	-11.4	-11.9	-16.3	-15.8	-15.6	-18.9	-19.0	-20.2
.630	-11.8	-26.7	-6.9	-5.2	-5.7	-8.4	-8.0	-8.9	-13.1	-12.8	-12.9	-15.5	-16.3	-16.9
.800	-8.6	-22.3	-4.8	-2.8	-2.7	-5.1	-5.1	-6.2	-9.5	-9.7	-9.9	-12.3	-13.8	-13.9
1.00	-6.7	-18.3	-3.5	-1.1	-1.1	-2.6	-3.6	-4.5	-6.7	-7.8	-8.1	-10.3	-11.7	-12.1
1.25	-5.2	-19.4	-3.0	0.0	0.2	-0.7	-2.0	-2.7	-4.3	-6.4	-6.9	-8.8	-9.9	-10.8
1.60	-3.9	-13.4	-3.3	0.7	1.3	0.9	-0.4	-1.3	-2.5	-5.2	-6.0	-7.8	-8.6	-9.7
2.00	-2.9	-12.8	-3.6	1.1	2.3	2.3	0.7	-0.3	-1.3	-4.0	-5.1	-7.0	-7.7	-8.7
2.50	-2.1	-14.6	-4.5	0.9	2.8	2.7	2.2	1.0	-1.1	-3.0	-4.4	-6.7	-7.4	-8.3
3.15	-1.5	-21.4	-5.3	0.6	3.1	3.4	3.3	2.1	-0.6	-2.8	-4.1	-6.2	-7.3	-8.3
4.00	-1.5	-23.8	-7.0	-0.5	2.3	2.8	3.6	2.8	0.8	-2.3	-4.9	-7.2	-8.5	-10.9
5.00	-1.9	-31.9	-8.8	-2.2	1.1	3.0	4.5	2.8	-0.6	-3.4	-7.6	-10.2	-13.2	-14.9
6.30	-4.7	-28.6	-8.1	-1.6	1.8	5.1	6.7	3.3	-0.4	-6.1	-12.4	-15.6	-19.0	-20.1
8.00	-5.0	-22.4	-9.2	-2.9	0.8	5.7	7.2	1.4	-7.4	-12.0	-12.0	-10.7	-11.4	-12.4
10.0	-6.3	-22.7	-10.2	-3.5	0.8	5.7	8.3	-1.0	-2.3	-4.0	-6.0	-9.4	-13.5	-14.8
12.5	-4.0	-26.1	-16.8	-11.2	-4.1	0.7	6.5	-4.6	-5.1	-10.9	-14.0	-19.1	-19.1	-21.4
16.0	-8.1	-27.3	-18.6	-16.1	-6.5	-0.7	6.5	-8.4	-12.6	-16.0	-13.8	-18.8	-21.2	-23.9
20.0	-7.4	-19.7	-16.4	-16.4	-6.2	1.9	-2.0	-7.9	-9.8	-17.7	-17.8	-19.4	-22.8	-24.8
25.0	-4.5	-20.1	-13.3	-19.1	-6.5	0.5	1.6	-7.6	-8.1	-16.7	-16.7	-18.3	-17.0	-19.0
31.5	-4.4	-18.9	-18.1	-15.4	-7.3	5.6	0.5	-2.1	-8.1	-14.1	-15.5	-17.4	-17.5	-20.2
40.0	-5.5	-19.6	-21.9	-18.7	-9.7	5.6	-4.0	-6.9	-11.5	-12.8	-14.5	-17.1	-21.0	-25.1
50.0	-6.9	-17.9	-22.2	-21.3	-7.9	4.6	-6.3	-6.7	-13.3	-16.6	-17.4	-23.3	-23.3	-25.1
63.0	-10.9	-15.8	-18.4	-16.5	-11.3	0.9	-8.5	-12.0	-15.0	-17.1	-16.6	-20.7	-14.6	-29.9

$OPTF_t$	$NOSPL_t$											
24.8	-21.8	-7.9	-4.7	-3.8	-3.1	-2.4	-8.5	-8.1	-10.3	-10.8	-13.4	-14.5	-15.5

1/3 OCTAVE NTC (dB) WITH RESPECT TO INCIDENT SPL (NTC_i)

$M_J = 0.6 \quad M_T = 0$

DAISY LOBE NOZZLE (RUN NO = 14)

FREQ KHZ	EMISSION ANGLE (RELATIVE TO JET EXHAUST) REFERENCED TO NOZZLE EXIT (DEGREES)											
	PTF_i	10.	20.	30.	40.	50.	60.	70.	80.	90.	100.	110.	120.
.250	+21.2	+13.0	+13.2	+15.3	+20.8	+15.7	+19.8	+22.8	+26.2	+27.2	+31.1	+33.3	+29.9
.315	+18.8	+11.8	+11.4	+13.0	+17.8	+12.9	+17.0	+19.8	+22.3	+23.6	+27.3	+29.0	+26.8
.400	+17.4	+11.0	+10.4	+11.7	+15.9	+11.4	+16.7	+18.4	+20.8	+22.1	+25.7	+27.2	+25.2
.500	+15.0	+9.7	+8.9	+9.5	+12.8	+8.7	+13.2	+15.8	+18.1	+18.1	+21.7	+21.8	+22.3
.630	+11.9	+7.5	+6.8	+6.6	+9.2	+5.3	+10.4	+12.8	+14.8	+14.8	+18.2	+17.4	+18.8
.800	+8.8	+6.0	+3.7	+3.6	+5.3	+2.0	+7.4	+9.6	+11.1	+11.9	+14.8	+15.0	+14.9
1.00	+6.5	+5.5	+2.0	+1.6	+2.2	0.4	+6.0	+7.3	+8.6	+10.0	+12.5	+13.2	+13.2
1.25	+4.7	+6.0	+4.9	0.1	0.1	2.3	+3.0	+5.5	+7.4	+8.7	+11.1	+11.6	+12.8
1.60	+3.4	+7.5	+6.8	1.4	1.9	3.8	+1.4	+4.1	+7.0	+8.0	+10.1	+10.5	+12.0
2.00	+2.2	+8.6	+6.7	2.4	3.8	5.3	+0.1	+3.0	+6.0	+7.1	+9.1	+9.7	+11.9
2.50	+8.1	+8.6	+6.7	4.2	5.5	8.1	1.4	+2.0	+3.7	+5.7	+8.4	+8.7	+11.5
3.15	+9.5	+9.3	+2.0	4.1	6.1	9.0	2.0	+1.9	+4.2	+5.7	+8.9	+10.1	+12.1
4.00	+1.0	+14.5	+5.3	1.2	4.4	7.7	1.5	+2.4	+5.8	+7.5	+10.4	+13.7	+17.4
5.00	+8.5	+12.3	+5.6	0.6	5.9	9.0	+2.0	+6.4	+7.2	+12.2	+13.6	+15.7	+23.3
6.30	1.0	+9.4	+6.8	1.8	8.8	10.1	+6.1	+12.9	+13.7	+10.8	+9.9	+10.4	+15.4
8.00	+1.7	+19.6	+5.6	+0.5	9.2	3.1	+8.1	+16.7	+13.8	+10.8	+12.4	+17.8	+15.2
10.0	+8.2	+16.6	+6.4	+0.6	10.0	6.6	+9.1	+6.0	+14.0	+13.6	+13.7	+12.2	+16.1
12.5	+2.6	+15.9	2.3	0.2	4.2	6.5	+2.5	+7.8	+9.7	+7.1	+12.2	+13.1	+20.5
16.0	+7.6	+23.9	+4.8	+8.5	+0.9	0.1	+6.8	+9.2	+12.2	+10.2	+11.2	+15.4	+25.4
20.0	+8.2	+22.4	+8.1	+9.8	+4.5	0.6	+10.1	+8.7	+9.8	+10.6	+15.1	+16.3	+28.2
25.0	+7.6	+19.2	+6.2	+7.6	+3.1	0.1	+7.0	+5.6	+9.8	+9.0	+11.8	+12.2	+27.2
31.5	+6.6	+20.6	+6.8	+3.8	1.3	0.6	+8.6	+6.8	+7.2	+8.3	+13.6	+16.7	+21.7
40.0	+7.6	+26.7	+19.7	+9.9	+1.3	3.7	+6.8	+11.9	+7.8	+11.6	+13.9	+20.1	+21.5
50.0	+12.8	+31.4	+24.0	+14.0	+7.3	+3.4	+12.1	+11.6	+10.5	+10.5	+16.3	+16.8	+22.9
63.0	+13.8	+32.4	+24.2	+20.9	+9.5	+4.4	+10.1	+13.7	+19.6	+13.4	+16.7	+23.0	+28.0

$OPTF_i$	$NOSPL_i$									
24.0	+10.1	+7.1	+5.3	+3.2	+1.4	+8.0	+11.0	+13.4	+13.7	+16.9	+17.8	+19.3

CONICAL NOZZLE (RUN NO = 106)

FREQ KHZ	EMISSION ANGLE (RELATIVE TO JET EXHAUST) REFERENCED TO NOZZLE EXIT (DEGREES)											
	PTF_i	10.	20.	30.	40.	50.	60.	70.	80.	90.	100.	110.	120.
.250	+22.8	+18.8	+11.4	+15.9	+19.9	+26.7	+24.8	+23.3	+27.3	+27.2	+30.4	+29.6	+28.4
.315	+19.5	+13.8	+8.9	+12.6	+16.2	+22.3	+20.4	+20.4	+24.1	+24.2	+26.7	+26.7	+25.7
.400	+17.9	+12.6	+7.6	+11.1	+14.5	+20.5	+18.6	+19.0	+22.6	+22.7	+25.1	+25.2	+24.3
.500	+15.4	+10.8	+5.4	+8.2	+11.4	+16.7	+14.8	+16.7	+19.8	+20.6	+21.3	+22.7	+22.1
.630	+12.6	+8.7	+3.0	+5.3	+8.4	+13.4	+11.5	+14.1	+17.0	+18.1	+18.0	+20.0	+19.7
.800	+9.9	+7.3	+1.2	+2.6	+5.0	+9.3	+7.6	+11.5	+14.4	+14.9	+15.6	+17.6	+17.3
1.00	+7.5	+6.4	0.1	+0.9	+1.9	+6.2	+4.2	+8.8	+11.7	+11.8	+13.2	+15.1	+14.9
1.25	+5.8	+5.4	0.9	+0.2	0.4	+4.3	+1.8	+6.7	+9.8	+9.2	+11.4	+13.1	+12.9
1.60	+4.6	+5.4	0.8	0.8	1.7	+3.7	+0.4	+4.7	+7.6	+7.1	+9.9	+11.4	+11.3
2.00	+3.9	+6.3	0.4	1.5	2.2	+3.6	0.2	+2.9	+5.7	+5.7	+8.7	+9.8	+9.9
2.50	+3.3	+7.9	+1.0	0.7	2.5	+1.7	1.0	+1.0	+3.7	+5.1	+7.7	+8.4	+8.9
3.15	+2.5	+9.4	+1.7	0.1	2.4	+0.5	2.7	0.6	+2.1	+5.9	+7.0	+7.8	+8.9
4.00	+2.9	+13.2	+2.8	+1.7	1.2	+0.7	2.6	1.2	+1.8	+7.4	+8.0	+9.4	+11.7
5.00	+3.4	+15.5	+3.6	+2.9	+0.6	+1.1	3.4	0.3	+3.2	+7.9	+11.3	+14.9	+19.4
6.30	+3.6	+16.6	+5.7	+3.4	+0.9	1.1	4.4	+1.7	+8.3	+13.7	+20.1	+19.2	+17.9
8.00	+6.0	+18.6	+9.0	+5.6	+2.0	+0.9	1.7	+6.6	+13.6	+11.4	+12.7	+14.5	+15.9
10.0	+8.5	+20.2	+13.6	+9.0	+6.5	+1.8	+0.9	+11.4	+10.9	+16.3	+19.2	+24.0	+24.6
12.4	+6.7	+19.0	+10.0	+7.4	+5.8	2.4	+2.2	+6.8	+12.3	+14.2	+18.6	+16.9	+19.0
16.0	+8.0	+23.7	+13.9	+8.9	+14.7	1.9	+4.1	+8.3	+12.2	+16.5	+22.9	+22.4	+22.3
20.0	+6.5	+27.1	+17.7	+10.2	+9.7	2.7	+0.0	+7.7	+16.3	+24.4	+28.5	+30.9	+28.3
25.0	+4.8	+22.9	+13.4	+9.6	+8.2	6.3	+3.7	+8.9	+15.6	+14.1	+16.9	+23.8	+20.8
31.5	+10.6	+27.4	+26.0	+7.8	+12.4	+2.0	+3.4	+10.8	+12.7	+15.9	+28.1	+27.3	+24.7
40.0	+10.7	+31.6	+24.4	+11.4	+7.6	1.2	+14.4	+11.6	+23.2	+20.8	+29.1	+32.5	+29.3
50.0	+14.1	+22.8	+29.4	+16.6	+10.2	1.8	+12.1	+14.0	+24.0	+32.2	+33.4	+31.9	+29.0
63.0	+4.8	+18.9	+24.7	+23.5	+16.1	10.3	+12.4	+17.0	+26.4	+23.6	+28.8	+35.8	+33.3

$OPTF_i$	$NOSPL_i$									
23.8	+10.5	+4.6	+5.3	+5.2	+3.4	+5.3	+9.1	+12.4	+13.4	+15.9	+17.4	+17.6

1/3 OCTAVE NTC (dB) WITH RESPECT TO TRANSMITTED SPL (NTC_t)

$M_J = 0.6$ $M_T = 0$

DAISY LOBE NOZZLE (RUN NO= 14)

EMISSION ANGLE (RELATIVE TO JET EXHAUST) REFERENCED TO NOZZLE EXIT (DEGREES)

FREQ KHZ	PTF_t	10.	20.	30.	40.	50.	60.	70.	80.	90.	100.	110.	120.
.250	-2.4	-10.5	-11.7	-4.4	-4.4	-13.4	-14.4	-22.5	-24.7	-26.7	-30.6	-32.8	-29.4
.315	-14.3	-11.7	-14.9	-12.5	-17.0	-12.4	-16.6	-19.3	-21.8	-23.1	-26.3	-28.5	-26.3
.400	-16.9	-14.5	-9.9	-11.2	-15.4	-16.5	-15.2	-17.9	-20.3	-21.6	-25.2	-26.7	-24.7
.500	-14.5	-9.2	-8.4	-9.0	-12.3	-8.2	-12.7	-16.0	-17.6	-17.6	-21.2	-21.0	-21.8
.630	-11.3	-7.0	-6.0	-6.1	-6.7	-4.8	-9.6	-12.0	-14.2	-14.0	-17.3	-16.9	-18.3
.800	-8.2	-5.5	-3.2	-3.0	-4.8	-1.4	-6.8	-9.0	-10.8	-11.4	-14.2	-14.5	-14.4
1.00	-5.6	-4.6	-1.2	-0.8	-1.3	1.2	-4.2	-6.5	-7.8	-9.2	-11.6	-12.3	-12.4
1.25	-3.7	-5.0	0.1	1.1	1.1	3.3	-1.9	-4.5	-6.4	-7.7	-10.1	-10.6	-11.8
1.60	-2.6	-6.7	0.3	2.1	2.7	4.6	-0.6	-3.3	-6.3	-7.2	-9.4	-9.8	-11.2
2.00	-1.6	-8.1	-0.2	2.9	4.0	5.5	0.4	-2.5	-5.4	-6.6	-8.6	-9.2	-11.4
2.50	-0.1	-8.3	-0.5	4.4	5.8	6.3	1.7	-1.8	-3.5	-5.5	-8.2	-8.5	-11.3
3.15	0.5	-9.3	-1.9	4.1	6.1	9.1	2.0	-1.8	-4.2	-5.7	-8.9	-10.0	-12.0
4.00	-0.9	-14.5	-5.3	1.3	4.4	7.7	1.5	-2.3	-5.8	-7.4	-10.3	-13.6	-17.3
5.00	0.3	-11.5	-4.8	1.4	6.8	9.8	-1.2	-5.6	-6.4	-11.4	-12.8	-14.9	-22.5
6.30	0.2	-4.2	4.4	7.0	14.1	15.3	-0.8	-7.7	-8.4	-5.5	-4.7	-5.1	-10.1
8.00	-0.7	-18.5	-4.5	0.5	10.2	4.1	-7.1	-15.6	-12.4	-9.8	-11.3	-16.5	-14.1
10.0	0.2	-11.2	-1.0	4.8	15.4	12.0	-3.7	-0.7	-8.6	-8.1	-8.4	-9.3	-10.8
12.5	-0.4	-13.6	4.7	2.0	6.6	8.9	-0.6	-5.5	-7.3	-4.0	-9.8	-10.7	-18.4
16.0	-7.3	-23.6	-4.5	-8.2	-0.6	0.4	-0.5	-8.8	-11.9	-9.8	-10.8	-15.1	-25.1
20.0	-8.1	-22.3	-7.9	-9.6	-4.4	0.7	-10.0	-8.6	-9.3	-10.5	-15.0	-15.2	-28.1
25.0	-7.8	-19.1	-6.1	-7.5	-3.0	0.1	-7.6	-5.5	-9.7	-9.0	-11.4	-12.2	-27.1
31.5	-6.3	-20.4	-6.5	-3.6	1.6	0.3	-5.4	-6.6	-6.2	-8.1	-13.3	-16.4	-21.4
40.0	-0.8	-2.4	-19.5	-9.7	-1.1	3.9	-6.6	-11.6	-7.6	-11.3	-13.7	-19.9	-21.2
50.0	-11.9	-31.3	-23.9	-13.8	-7.2	-3.2	-12.6	-11.4	-10.3	-10.3	-16.2	-16.7	-22.8
63.0	-12.9	-31.9	-24.0	-20.7	-9.4	-4.2	-10.6	-13.6	-19.5	-13.2	-16.5	-22.6	-27.9

$OPTF_t$	← $NOSPL_t$ →									
24.6	-9.5	-6.5	-4.1	-2.7	-0.8	-7.5	-10.5	-12.9	-13.2	-16.3	-17.3	-18.8

CONICAL NOZZLE (RUN NO = 106)

EMISSION ANGLE (RELATIVE TO JET EXHAUST) REFERENCED TO NOZZLE EXIT (DEGREES)

FREQ KHZ	PTF_t	10.	20.	30.	40.	50.	60.	70.	80.	90.	100.	110.	120.
.250	-24.3	-14.3	-9.9	-14.4	-18.4	-25.2	-23.2	-21.8	-25.7	-25.6	-28.9	-28.1	-26.9
.315	-18.3	-12.6	-7.7	-11.4	-15.0	-21.1	-19.2	-19.2	-22.9	-23.0	-25.5	-25.5	-24.5
.400	-17.4	-11.7	-6.7	-10.1	-13.6	-19.6	-17.7	-18.0	-21.6	-21.7	-24.1	-24.3	-23.4
.500	-14.6	-10.0	-4.6	-7.4	-10.6	-15.9	-14.0	-15.9	-19.0	-19.7	-20.5	-21.9	-21.3
.630	-12.0	-8.1	-2.4	-4.7	-7.8	-12.8	-10.9	-13.5	-16.4	-17.5	-17.4	-19.5	-19.1
.800	-9.6	-7.0	-0.9	-2.3	-4.7	-9.0	-7.3	-11.2	-14.1	-14.6	-15.3	-17.2	-17.0
1.00	-7.3	-6.2	0.2	-0.7	-1.7	-6.0	-4.0	-8.7	-11.5	-11.6	-13.1	-14.9	-14.7
1.25	-5.7	-5.3	1.1	-0.0	0.6	-4.1	-1.7	-6.6	-9.4	-9.0	-11.2	-12.9	-12.8
1.60	-4.6	-5.4	0.8	0.9	1.8	-3.6	-0.3	-4.7	-7.6	-7.0	-9.9	-11.4	-11.3
2.00	-3.9	-6.3	0.4	1.5	2.3	-3.4	0.2	-2.9	-5.7	-5.6	-8.7	-9.8	-9.9
2.50	-3.3	-7.8	-1.0	0.8	2.5	-1.7	1.0	-1.0	-3.7	-5.1	-7.7	-8.4	-8.8
3.15	-2.5	-9.4	-1.6	0.1	2.4	-0.5	2.7	0.6	-2.1	-5.8	-7.0	-7.8	-8.9
4.00	-2.9	-13.1	-2.8	-1.6	1.2	-0.7	2.8	1.2	-1.8	-7.3	-8.0	-9.4	-11.7
5.00	-3.4	-15.5	-3.6	-2.9	-0.0	-1.1	3.4	0.3	-3.2	-7.9	-11.3	-14.9	-19.4
6.30	-3.2	-16.2	-5.3	-3.0	-0.5	1.8	4.8	-1.3	-7.9	-13.3	-19.7	-18.8	-17.8
8.00	-5.9	-17.9	-8.9	-5.6	-1.9	-0.9	1.7	-6.5	-13.4	-11.4	-12.6	-14.4	-15.8
10.0	-8.3	-20.0	-13.5	-8.8	-6.3	-1.6	-0.7	-11.3	-10.7	-16.1	-19.0	-23.8	-24.4
12.5	-6.3	-18.5	-9.6	-7.0	-5.4	-2.8	-1.8	-6.4	-11.8	-13.7	-15.1	-16.4	-18.7
16.0	-7.9	-23.6	-13.8	-8.8	-14.6	-2.0	-4.0	-8.2	-12.1	-16.4	-22.8	-22.3	-22.3
20.0	-8.4	-27.0	-17.7	-10.1	-9.6	-2.8	-0.8	-7.7	-18.3	-24.3	-25.4	-30.8	-25.2
25.0	-4.7	-22.8	-13.3	-9.4	-8.1	-6.4	-3.7	-8.9	-15.5	-14.0	-18.8	-23.7	-20.7
31.5	-10.5	-27.3	-19.9	-7.7	-12.3	-2.0	-3.3	-10.7	-12.6	-15.9	-25.1	-27.2	-24.6
40.0	-10.7	-31.5	-24.4	-11.4	-7.6	-1.3	-14.4	-11.6	-23.2	-20.8	-29.0	-32.5	-29.3
50.0	-10.0	-22.7	-29.3	-16.6	-10.2	-1.8	-12.1	-13.9	-24.0	-22.1	-33.4	-31.9	-28.9
63.0	-8.7	-18.9	-24.7	-23.4	-16.1	-10.4	-12.3	-16.9	-26.4	-23.5	-28.8	-35.7	-33.3

$OPTF_t$	← $NOSPL_t$ →									
24.5	-9.7	-3.9	-4.5	-4.4	-2.7	-4.6	-8.3	-11.7	-12.7	-15.1	-16.7	-16.8

1/3 OCTAVE NTC (dB) WITH RESPECT TO INCIDENT SPL (NTC_i)

$M_J = 0.8 \quad M_T = 0$

DAISY LOBE NOZZLE (RUN NO = 15)

EMISSION ANGLE (RELATIVE TO JET EXHAUST) REFERENCED TO NOZZLE EXIT (DEGREES)

FREQ KHZ	PTF_i	20.	30.	40.	50.	60.	70.	80.	90.	100.	110.	120.
.250	-18.7	-10.2	-14.2	-19.0	-21.4	-23.0	-23.6	-26.4	-26.3	-27.1	-31.4	-34.2
.315	-17.0	-9.0	-12.0	-16.1	-18.2	-21.3	-20.9	-23.5	-23.7	-24.4	-28.6	-31.6
.400	-15.0	-8.3	-10.9	-14.7	-16.6	-20.4	-19.6	-22.2	-22.4	-23.0	-27.3	-30.3
.500	-13.9	-6.9	-8.8	-11.9	-12.7	-18.6	-16.9	-19.3	-20.0	-20.4	-24.8	-27.7
.630	-11.3	-4.9	-6.1	-8.8	-6.0	-16.2	-13.9	-16.1	-17.2	-17.6	-21.4	-24.7
.800	-8.8	-3.4	-3.1	-5.3	-8.6	-14.1	-10.5	-12.7	-13.5	-15.5	-18.0	-21.5
1.00	-6.9	-1.6	-0.8	-2.3	-2.8	-12.5	-8.5	-10.3	-11.2	-13.6	-16.2	-19.6
1.25	-6.4	-1.2	0.9	0.5	-0.2	-9.7	-6.5	-8.6	-9.8	-11.8	-14.9	-18.5
1.60	-4.2	-2.1	1.6	2.2	1.8	-7.5	-4.7	-7.6	-8.6	-10.2	-12.9	-17.4
2.00	-2.8	-2.2	2.0	4.2	3.5	-5.3	-3.8	-8.9	-7.4	-9.2	-11.2	-15.6
2.50	-1.4	-2.2	2.1	5.6	6.5	-3.5	-2.8	-4.3	-6.5	-8.2	-9.6	-14.9
3.15	-1.4	-3.4	-0.6	4.9	6.8	-3.4	-1.7	-3.5	-6.5	-8.2	-10.5	-16.4
4.00	-2.6	-7.9	-5.8	2.7	6.8	-2.8	-2.8	-5.5	-9.0	-9.6	-12.3	-19.6
5.00	-1.2	-6.7	-6.1	3.7	8.6	-1.7	-6.2	-9.5	-12.7	-14.0	-13.7	-22.0
6.30	1.6	-4.8	-4.1	3.6	12.6	-4.0	-8.5	-16.1	-13.3	-11.8	-12.5	-23.1
8.00	-2.3	-4.3	-11.5	-1.2	8.6	-8.1	-6.5	-23.2	-13.7	-12.0	-18.5	-29.5
10.0	-3.3	-8.0	-2.4	-4.6	7.0	-5.8	-7.3	-9.8	-16.0	-16.3	-10.5	-25.7
12.5	-6.8	-6.7	0.4	-0.8	-0.6	-0.0	-10.2	-17.2	-11.7	-21.7	-18.5	-32.6
16.0	-4.6	-7.0	-3.1	-2.3	5.3	-3.1	-8.4	-14.7	-13.3	-11.9	-13.3	-36.3
20.0	-4.6	-5.3	-6.3	-5.8	6.2	-7.8	-4.8	-8.7	-9.7	-20.5	-14.6	-38.3
25.0	-1.2	-4.7	-6.5	-7.4	6.0	3.3	-6.3	-6.3	-8.9	-16.7	-14.8	-40.1
31.5	-3.4	-10.6	-9.5	-8.8	7.4	-1.8	-2.6	-8.3	-5.2	-13.5	-15.0	-36.3
40.0	-5.2	-23.9	-13.1	-10.7	5.5	-0.0	-5.4	-7.7	-8.0	-15.5	-16.7	-41.3
50.0	-4.1	-25.6	-16.9	-13.6	6.5	1.0	-7.5	-13.9	-11.2	-18.3	-17.4	-44.8
63.0	4.8	-24.7	-17.7	-16.6	16.2	7.5	-4.2	-15.6	-18.5	-17.8	-18.2	-38.3

$OPTF_i$	← $NOSPL_i$ →									
24.7	-6.5	-5.7	-4.9	0.2	-8.8	-11.3	-14.1	-14.8	-16.9	-19.3	-24.4

CONICAL NOZZLE (RUN NO = 110)

EMISSION ANGLE (RELATIVE TO JET EXHAUST) REFERENCED TO NOZZLE EXIT (DEGREES)

FREQ KHZ	PTF_i	10.	20.	30.	40.	50.	60.	70.	80.	90.	100.	110.	120.
.250	-19.5	-8.2	-14.4	-10.2	-20.2	-16.0	-20.1	-22.2	-25.0	-26.7	-42.1	-39.5	-40.0
.315	-17.1	-6.9	-11.8	-7.9	-16.0	-15.0	-17.0	-19.4	-22.5	-23.6	-35.6	-34.6	-35.1
.400	-16.1	-6.3	-10.8	-6.9	-14.6	-13.9	-15.8	-18.3	-21.2	-22.3	-34.0	-33.2	-33.6
.500	-13.0	-4.2	-6.1	-4.5	-9.9	-10.7	-12.1	-15.8	-17.2	-18.3	-24.7	-27.3	-27.8
.630	-14.2	-2.1	-2.9	-2.1	-6.4	-7.8	-9.1	-13.2	-14.1	-15.2	-20.6	-23.7	-24.1
.800	-7.7	-1.5	-2.7	0.6	-2.5	-4.9	-6.2	-9.6	-10.7	-12.7	-16.9	-19.6	-20.1
1.00	-5.9	-3.0	-3.2	2.1	0.6	-3.0	-4.1	-6.4	-8.7	-10.9	-14.1	-15.8	-16.8
1.25	-4.6	-5.4	-3.3	2.2	2.7	-1.8	-2.0	-4.8	-7.3	-9.0	-12.1	-12.6	-13.4
1.60	-3.9	-5.8	-7.6	1.6	3.2	-0.0	-0.2	-3.7	-5.5	-7.1	-10.8	-10.2	-11.3
2.00	-3.2	-8.2	-12.6	2.3	2.6	1.0	0.3	-1.8	-4.2	-5.1	-8.5	-8.6	-9.7
2.50	-2.9	-10.9	-7.3	1.2	1.3	1.9	1.6	-1.1	-3.3	-4.1	-7.0	-8.7	-9.4
3.15	-2.3	-12.8	-9.8	-0.2	0.3	2.8	3.5	0.6	-2.3	-4.9	-8.4	-10.5	-10.0
4.00	-3.1	-14.8	-11.0	-0.0	-2.7	2.3	3.0	0.0	-3.8	-6.9	-9.0	-13.4	-15.1
5.00	-2.0	-17.9	-12.2	-2.4	-0.6	4.0	5.0	0.7	-2.9	-7.7	-11.7	-17.6	-26.8
6.30	-3.3	-13.6	-7.6	-3.7	-2.6	2.5	4.2	-0.9	-6.9	-9.6	-12.6	-14.2	-15.4	-16.1
8.00	-2.7	-15.9	-16.0	-7.8	-1.9	2.2	5.6	-2.3	-4.0	-8.5	-9.8	-12.4	-17.9
10.0	-3.6	-18.6	-13.0	-8.2	-9.1	-0.4	6.1	-2.6	-10.3	-16.7	-14.0	-19.6	-18.1
12.4	-3.0	-22.8	-13.8	-8.9	-13.6	-0.5	7.6	-7.6	-10.2	-16.9	-16.5	-19.3	-23.3
16.0	-9.5	-27.4	-11.8	-9.2	-13.0	-4.5	-3.4	-3.6	-14.3	-13.5	-16.6	-21.8	-22.9
20.0	-5.9	-28.7	-14.5	-11.8	-8.9	1.8	-3.0	-0.4	-9.9	-13.2	-15.4	-21.9	-19.2
25.0	-8.5	-25.0	-17.1	-10.1	-4.6	-2.2	-2.6	-4.8	-12.5	-13.1	-15.4	-23.1	-27.0
31.5	-12.0	-29.8	-21.8	-11.0	-12.2	-11.0	-1.6	-14.6	-13.8	-18.4	-22.7	-28.5	-24.7
40.0	-14.1	-33.1	-26.4	-10.1	-8.8	-3.2	-2.7	-9.2	-9.7	-17.3	-18.0	-24.6	-18.8
50.0	-7.6	-28.5	-23.1	-7.1	-3.2	-2.3	0.9	-5.1	-10.2	-18.0	-18.5	-22.9	-19.5
63.0	-3.1	-25.8	-20.9	-12.0	-12.0	7.2	-1.3	-11.5	-14.6	-18.0	-19.3	-25.4	-26.6

$OPTF_i$	← $NOSPL_i$ →									
28.1	-5.5	-7.1	-2.6	-3.9	-3.4	-2.8	-7.5	-10.6	-12.1	-15.9	-17.5	-18.2

1/3 OCTAVE NTC (dB) WITH RESPECT TO TRANSMITTED SPL (NTC_t)

$M_J = 0.8$ $M_T = 0$

DAISY LOBE NOZZLE (RUN NO = 15)

EMISSION ANGLE (RELATIVE TO JET EXHAUST) REFERENCED TO NOZZLE EXIT (DEGREES)

FREQ KHZ	PTF_t	20.	30.	40.	50.	60.	70.	80.	90.	100.	110.	120.
.250	+17.8	-9.2	-13.3	-18.0	-20.6	-22.0	-22.6	-25.4	-25.3	-26.1	-30.4	-33.3
.315	+16.1	-8.1	-11.1	-15.2	-17.3	-20.4	-20.0	-22.7	-22.8	-23.5	-27.7	-30.7
.400	+15.1	-7.5	-10.1	-13.5	-15.6	-19.5	-18.8	-21.4	-21.6	-22.2	-26.5	-29.5
.500	+13.1	-6.1	-7.9	-11.1	-11.6	-17.7	-16.1	-18.4	-19.2	-19.5	-23.6	-26.8
.630	+11.6	-4.1	-5.3	-8.0	-8.2	-15.4	-13.1	-16.2	-16.3	-16.8	-20.5	-23.8
.800	+8.0	-2.5	-2.2	-4.4	-4.8	-13.2	-9.7	-11.8	-12.7	-14.6	-17.1	-20.6
1.00	+6.1	-4.9	0.0	-1.4	-1.9	-11.6	-7.6	-9.4	-10.4	-12.7	-15.3	-18.7
1.25	+4.5	-0.3	1.7	1.3	1.7	-8.8	-5.7	-7.8	-9.0	-11.0	-14.1	-17.6
1.60	+3.5	-1.4	2.3	2.9	2.5	-6.9	-4.1	-6.9	-7.9	-9.5	-12.3	-16.7
2.00	+2.3	-1.7	2.5	4.7	4.4	-4.8	-3.3	-5.4	-6.9	-8.7	-10.7	-15.1
2.50	+1.1	-1.8	2.5	6.0	6.3	-3.7	-2.4	-3.9	-6.1	-7.8	-9.2	-14.6
3.15	+1.4	-3.3	-0.6	4.5	6.5	-3.4	-1.6	-3.5	-6.5	-8.2	-10.4	-16.4
4.00	+2.5	-7.8	-5.4	2.5	6.6	-2.7	-2.7	-5.4	-8.9	-9.5	-12.2	-19.5
5.00	+4.1	-5.9	-4.9	4.5	10.6	-0.5	-5.0	-8.3	-11.5	-12.8	-12.6	-20.8
6.30	4.8	-2.3	-1.7	6.0	10.0	-1.6	-6.0	-13.6	-10.9	-9.4	-10.1	-20.6
8.00	+3.5	-2.0	-9.8	0.6	10.4	-0.4	-4.8	-21.4	-11.9	-10.3	-10.7	-27.8
10.0	+2.9	-7.5	-1.9	-4.4	7.5	-5.3	-0.8	-9.4	-15.6	-15.8	-10.0	-25.2
12.5	+5.6	-6.0	0.6	-0.7	-1.7	0.1	-10.0	-17.0	-11.6	-21.6	-18.4	-32.4
16.0	+4.4	-6.9	-3.0	-2.1	5.5	-2.9	-8.2	-14.8	-13.2	-11.8	-13.2	-36.1
20.0	+3.9	-5.2	-6.2	-5.7	6.4	-7.7	-4.7	-8.6	-9.6	-20.4	-14.5	-38.2
25.0	+1.1	-4.6	-6.4	-7.3	9.1	3.4	-6.2	-6.2	-8.8	-16.6	-14.7	-40.0
31.5	+3.3	-10.5	-9.4	-8.6	7.9	-1.7	-2.5	-8.2	-5.1	-13.3	-14.9	-36.2
40.0	+5.1	-23.8	-13.0	-10.6	5.6	0.1	-0.3	-7.6	-7.9	-15.3	-10.6	-41.2
50.0	+4.9	-25.5	-16.8	-13.5	7.0	1.1	-7.4	-13.8	-11.1	-18.2	-17.3	-44.7
63.0	4.7	-24.5	-17.5	-16.4	10.3	7.6	-4.0	-15.5	-18.4	-17.6	-18.1	-38.2

$OPTF_t$	$NOSPL_t$
25.6	-5.7 -4.9 -4.1 1.6 -8.0 -10.5 -13.3 -14.0 -16.1 -18.4 -23.6

CONICAL NOZZLE (RUN NO = 110)

EMISSION ANGLE (RELATIVE TO JET EXHAUST) REFERENCED TO NOZZLE EXIT (DEGREES)

FREQ KHZ	PTF_t	10.	20.	30.	40.	50.	60.	70.	80.	90.	100.	110.	120.
.250	+17.4	-6.4	-12.3	-8.1	-18.1	-15.5	-15.0	-20.0	-23.9	-24.6	-39.9	-37.4	-37.8
.315	+16.0	-5.8	-10.8	-8.6	-14.9	-14.0	-15.9	-18.3	-21.4	-22.4	-34.5	-33.5	-34.0
.400	+15.0	-5.7	-10.2	-6.3	-14.1	-13.4	-15.2	-17.7	-20.7	-21.8	-33.4	-32.6	-33.0
.500	+12.6	-3.6	-5.7	-4.1	-9.4	-10.2	-11.6	-15.3	-16.8	-17.9	-24.2	-20.9	-27.3
.630	+10.6	-1.9	-2.6	-1.8	-6.2	-7.5	-8.8	-13.6	-13.8	-15.0	-20.3	-23.4	-23.9
.800	+7.6	-1.5	-2.6	0.6	-2.5	-5.8	-6.1	-9.5	-10.7	-12.6	-16.8	-19.5	-20.0
1.00	+6.9	-3.0	-3.2	2.1	0.6	-3.0	-4.1	-6.4	-8.6	-10.9	-14.1	-15.8	-16.5
1.25	+4.5	-5.0	-3.3	2.2	2.7	-1.5	-2.0	-4.5	-7.3	-9.0	-12.0	-12.6	-13.4
1.60	-3.9	-5.8	-7.6	1.0	3.2	-0.6	-0.2	-3.7	-5.5	-7.1	-10.8	-10.2	-11.3
2.00	-3.2	-8.2	-12.6	2.3	2.6	1.0	0.3	-1.8	-4.2	-5.1	-8.5	-8.6	-9.7
2.50	-2.6	-10.9	-7.3	1.2	1.3	1.9	1.6	-1.0	-3.3	-4.1	-7.0	-8.7	-9.4
3.15	-2.3	-12.7	-9.8	-0.2	0.3	2.8	3.5	0.6	-2.3	-4.9	-8.4	-10.5	-10.0
4.00	-3.1	-14.8	-11.0	-0.6	-2.7	2.3	3.0	0.0	-3.5	-6.8	-9.0	-13.4	-15.1
5.00	-1.6	-17.9	-12.2	-2.4	-0.6	4.0	5.1	0.8	-2.8	-7.7	-11.6	-17.6	-26.8
6.30	-3.1	-13.3	-7.4	-3.6	-2.4	2.7	4.4	-0.7	-5.6	-12.4	-14.0	-15.2	-16.9
8.00	-2.5	-15.7	-9.7	-7.0	-1.3	2.5	5.8	-2.1	-3.8	-8.3	-9.5	-12.2	-17.7
10.0	-3.3	-18.3	-12.7	-7.9	-8.7	-0.1	6.5	-2.2	-10.0	-16.4	-13.7	-19.3	-17.8
12.5	-2.7	-22.2	-13.4	-8.5	-13.1	-0.1	7.9	-7.3	-9.7	-16.5	-16.2	-18.9	-23.0
16.0	-8.8	-27.4	-11.8	-9.2	-13.0	-4.4	-3.4	-3.5	-14.2	-13.4	-16.5	-21.5	-22.9
20.0	-5.7	-25.5	-14.4	-11.7	-5.7	2.0	-2.8	-0.3	-9.7	-13.1	-15.3	-21.7	-19.0
25.0	-8.4	-25.0	-17.1	-10.1	-4.6	-2.1	-2.6	-4.7	-12.9	-13.1	-15.4	-23.0	-27.0
31.5	-12.0	-29.7	-21.7	-10.9	-12.2	-10.9	-1.5	-14.6	-13.8	-18.3	-22.7	-28.5	-24.6
40.0	-16.1	-33.9	-26.4	-10.0	-5.7	-3.1	-2.6	-4.2	-9.6	-17.3	-18.0	-24.5	-18.4
50.0	-7.4	-28.3	-22.9	-6.9	-3.1	-2.1	1.1	-4.9	-10.0	-17.8	-18.3	-22.7	-19.4
63.0	-3.0	-25.7	-20.7	-11.8	-11.8	7.3	-1.1	-11.3	-14.5	-17.8	-15.2	-25.2	-26.4

$OPTF_t$	$NOSPL_t$
25.6	-4.9 -6.6 -2.0 -3.3 -2.8 -2.3 -7.0 -10.0 -11.6 -15.3 -17.0 -17.6

1/3 OCTAVE NTC (dB) WITH RESPECT TO INCIDENT SPL (NTC_i)

$M_J = 1.2 \quad M_T = 0$

DAISY LOBE NOZZLE (RUN NO = 17)

EMISSION ANGLE (RELATIVE TO JET EXHAUST) REFERENCED TO NOZZLE EXIT (DEGREES)

FREQ KHZ	PTF_i	10.	20.	30.	40.	50.	60.	70.	80.	90.
.250	-19.8	-16.6	-13.1	-10.5	-14.1	-24.7	-31.1	-14.9	-29.8	-36.9
.315	-17.5	-14.1	-10.9	-8.7	-15.0	-19.4	-17.5	-12.6	-23.9	-33.1
.400	-16.4	-12.8	-9.7	-7.7	-13.7	-18.1	-16.0	-11.5	-22.8	-31.6
.500	-13.6	-8.9	-6.9	-5.4	-11.1	-12.9	-11.9	-10.0	-21.4	-29.1
.630	-11.2	-5.7	-4.1	-3.7	-8.3	-9.1	-8.6	-8.0	-19.9	-26.2
.800	-8.8	-4.5	-2.8	-1.4	-4.6	-4.8	-6.4	-4.6	-16.8	-20.9
1.00	-5.7	-3.6	-1.9	-1.0	-0.7	-0.2	-4.0	-0.9	-12.6	-15.8
1.25	-3.1	-4.3	-1.9	-2.8	2.4	3.5	-1.6	1.9	-8.6	-10.6
1.60	-1.4	-7.6	-2.0	-1.2	4.1	5.8	0.6	3.0	-5.1	-6.4
2.00	-1.0	-13.1	-5.5	-2.2	3.8	6.4	2.2	2.3	-2.5	-3.6
2.50	-1.2	-11.3	-12.4	-5.1	2.4	6.2	2.7	1.5	-1.0	-2.3
3.15	-2.7	-15.0	-10.6	-8.1	1.3	6.6	3.5	2.4	0.3	-1.4
4.00	-1.3	-14.5	-9.9	-12.0	-3.9	5.9	3.9	1.7	0.5	-1.9
5.00	-1.2	-9.5	-12.0	-6.3	-9.6	7.4	3.4	0.8	0.3	-3.1
6.30	-2.7	-10.2	-11.3	-4.2	-11.7	8.2	-4.1	-6.3	-4.6	-10.6
8.00	-6.4	-14.8	-9.7	-9.8	-13.9	4.1	-2.9	-14.3	-12.7	-16.6
10.0	-3.2	-18.1	-9.9	-6.2	-9.6	5.1	4.6	-7.5	-12.0	-12.6
12.5	-5.4	-19.4	-14.8	-11.7	-11.8	-5.9	5.4	-10.3	-15.4	-15.3
16.0	-8.8	-19.8	-11.8	-7.2	-5.2	-0.7	-3.7	-11.8	-18.1	-10.4
20.0	-14.4	-15.4	-5.6	-8.2	-8.6	-3.1	-5.6	-13.7	-18.8	-13.6
25.0	-3.4	-9.1	1.1	-0.5	-5.7	2.6	3.0	-12.2	-9.7	-1.2
31.5	-7.6	-18.4	-7.6	-2.2	-2.7	-5.8	-1.1	-13.7	-7.7	-5.6
40.0	-11.1	-21.7	-16.5	-3.6	-8.7	-2.5	-6.2	-13.2	-6.8	-19.8
50.0	-12.5	-18.1	-21.1	-7.9	-7.2	-9.0	-11.5	-11.2	-5.3	-11.4
63.0	-6.8	-11.3	-13.0	-5.5	-4.7	0.7	-9.1	-6.6	-2.3	-0.6

$OPTF_i$	← $NOSPL_i$ →							
23.9	-9.4	-7.1	-5.8	-6.1	-2.8	-5.0	-6.2	-11.9	-12.5

CONICAL NOZZLE (RUN NO = 123)

EMISSION ANGLE (RELATIVE TO JET EXHAUST) REFERENCED TO NOZZLE EXIT (DEGREES)

FREQ KHZ	PTF_i	20.	30.	40.	50.	60.
.250	-10.9	-5.0	-6.8	-15.9	-17.4	-24.7
.315	-15.1	-4.0	-5.3	-13.4	-14.5	-21.2
.400	-14.3	-3.3	-4.7	-12.5	-13.6	-20.1
.500	-12.0	-0.8	-2.9	-10.1	-9.6	-14.9
.630	-9.7	1.4	-1.0	-7.8	-6.7	-11.7
.800	-7.6	3.4	0.9	-4.2	-4.8	-8.5
1.00	-5.8	5.2	2.7	-0.7	-2.3	-7.4
1.25	-3.5	6.7	4.3	2.4	-0.4	-8.3
1.60	-2.0	7.6	5.4	5.1	1.4	-3.1
2.00	-0.7	8.1	6.0	7.0	3.2	-0.7
2.50	-0.8	6.9	5.0	7.0	4.2	1.0
3.15	-1.8	3.9	2.0	4.5	5.0	3.3
4.00	-3.3	-3.2	-4.6	-3.4	4.1	8.2
5.00	-1.8	-8.1	0.3	3.0	1.5	7.4
6.30	-4.2	1.9	1.1	1.4	-1.0	9.5
8.00	-3.7	-2.9	-1.4	-12.8	-0.4	10.0
10.0	-2.9	-12.5	-10.0	-3.6	1.0	7.4
12.4	-1.9	-11.6	-8.4	-0.6	4.4	7.4
16.0	-5.8	-8.2	-5.7	-6.1	-3.6	3.6
20.0	-14.6	-11.9	-3.7	-6.3	-9.0	-2.6
25.0	-6.2	-8.6	-6.2	-2.6	0.9	1.5
31.5	-8.9	-11.4	-7.0	-11.0	-7.6	1.8
40.0	-6.6	-13.2	-3.0	-6.7	-0.3	4.0
50.0	-7.4	-12.5	-3.2	-3.3	-3.4	3.4
63.0	-12.4	-12.6	-8.1	-10.7	-6.4	-2.8

DATA FOR THE REMAINING ANGLES NOT ANALYZED DUE TO JET NOISE CONTAMINATION

$OPTF_i$	← $NOSPL_i$ →				
26.2	1.5	-0.3	-1.9	-3.1	-2.0

1/3 OCTAVE NIC (dB) WITH RESPECT TO TRANSMITTED SPL (NIC_t)

$M_j = 1.2$ $M_T = 0$

DAISY TUBE NOZZLE (RUN NO = 17)

EMISSION ANGLE (RELATIVE TO JET EXHAUST) REFERENCED TO NOZZLE EXIT (DEGREES)

FREQ KHZ	PIE,	10.	20.	30.	40.	50.	60.	70.	80.	90.
.250	-18.9	-15.9	-12.3	-9.0	-17.2	-23.8	-21.2	-14.0	-24.9	-36.0
.315	-10.7	-13.3	-10.0	-7.9	-14.2	-19.0	-16.7	-11.8	-23.0	-32.3
.400	-15.5	-12.0	-8.9	-6.4	-12.9	-17.3	-15.2	-10.7	-22.0	-30.8
.500	-13.1	-8.1	-6.1	-5.1	-10.3	-12.1	-11.1	-9.2	-20.6	-28.3
.630	-10.4	-4.9	-3.3	-2.9	-7.5	-8.3	-7.8	-7.2	-18.7	-25.4
.800	-7.7	-3.7	-1.7	-1.0	-3.8	-3.7	-5.5	-3.7	-15.7	-20.1
1.00	-4.9	-2.7	-1.0	-0.8	0.1	0.7	-3.2	-0.1	-11.8	-14.7
1.25	-2.3	-3.5	-1.1	-2.0	3.2	4.3	-0.7	2.7	-7.8	-9.8
1.60	-4.8	-7.1	-1.4	-0.7	4.6	6.4	1.1	3.5	-4.5	-5.9
2.00	-6.7	-12.7	-5.1	-1.8	4.1	6.6	2.6	2.7	-2.1	-3.3
2.50	-1.1	-11.2	-12.2	-4.9	2.5	6.4	2.8	1.7	-0.9	-2.1
3.15	-0.7	-14.9	-10.6	-8.0	1.3	6.7	3.6	2.5	0.4	-1.3
4.00	-1.3	-14.4	-9.8	-11.9	-3.9	6.0	3.9	1.8	0.6	-1.9
5.00	-8.2	-8.5	-11.1	-5.3	-8.7	6.3	4.4	1.8	1.2	-2.2
6.30	-1.2	-8.7	-9.8	-2.7	-10.2	6.7	-2.7	-4.8	-3.1	-9.2
8.00	-6.2	-14.7	-9.6	-9.0	-13.8	4.2	-2.7	-14.2	-12.5	-16.4
10.0	-3.0	-17.9	-9.8	-6.1	-9.4	5.3	4.8	-7.3	-11.8	-12.4
12.5	-5.2	-19.2	-14.7	-11.0	-11.6	-6.7	5.6	-16.1	-15.2	-15.2
16.0	-8.7	-19.6	-11.7	-7.9	-5.1	-0.6	-3.5	-11.6	-18.0	-10.3
20.0	-10.2	-14.9	-5.5	-8.2	-8.8	-3.0	-4.9	-13.6	-18.7	-13.5
25.0	-3.2	-8.9	1.3	-0.3	-5.6	2.8	3.1	-12.0	-9.5	-1.0
31.5	-7.5	-17.8	-7.5	-2.0	-2.6	-5.7	-0.9	-13.6	-7.6	-6.4
40.0	-11.0	-21.7	-16.5	-3.6	-8.7	-2.5	-8.2	-13.2	-6.5	-19.4
50.0	-12.4	-18.0	-21.0	-7.8	-7.2	-8.5	-11.4	-11.2	-5.2	-11.3
63.0	-5.6	-11.2	-12.8	-5.4	-4.5	0.9	-8.9	-6.4	-2.2	-0.4

$OPTE_t$ ← $NOSPL_t$ →

24.7 -8.7 -6.4 -5.0 -5.4 -2.0 -4.3 -5.4 -11.2 -11.8

CONICAL NOZZLE (RUN NO = 123)

EMISSION ANGLE (RELATIVE TO JET EXHAUST) REFERENCED TO NOZZLE EXIT (DEGREES)

FREQ KHZ	PIE_t	20.	30.	40.	50.	60.
.250	-12.5	-1.5	-2.4	-11.5	-13.0	-20.3
.315	-13.7	-2.6	-3.9	-12.8	-13.1	-19.8
.400	-13.9	-2.9	-4.3	-12.1	-13.2	-19.7
.500	-11.7	-0.5	-2.6	-9.6	-9.3	-14.7
.630	-9.6	1.5	-0.9	-7.7	-6.6	-11.6
.800	-7.6	3.4	0.9	-4.2	-4.4	-9.5
1.00	-5.8	5.2	2.7	-0.7	-2.3	-7.3
1.25	-3.8	6.7	4.3	2.4	-0.4	-5.2
1.60	-2.0	7.6	5.4	5.1	1.4	-3.1
2.00	-0.6	8.1	6.0	7.0	3.2	-0.7
2.50	-0.7	6.9	5.0	7.6	4.2	1.6
3.15	-1.7	3.9	2.0	4.5	5.0	3.3
4.00	-3.3	-3.2	-4.6	-3.4	4.1	5.2
5.00	-1.8	-5.1	0.3	3.0	1.8	7.4
6.30	0.1	2.2	1.4	1.7	-0.7	10.2
8.00	-0.6	-2.9	-1.3	-12.8	-0.3	11.1
10.0	-2.8	-12.4	-5.9	-3.5	1.1	7.8
12.5	-1.7	-11.3	-8.1	-0.3	4.6	7.6
16.0	-6.5	-8.2	-5.7	-6.0	-3.6	3.6
20.0	-10.3	-11.8	-3.6	-6.2	-9.0	-2.6
25.0	-0.1	-8.4	-6.0	-1.9	1.0	1.7
31.5	-8.8	-11.3	-7.6	-10.9	-7.6	1.9
40.0	-6.8	-15.1	-2.9	-6.6	-0.2	4.1
50.0	-7.2	-12.3	-3.0	-3.1	-3.3	3.6
63.0	-12.3	-12.5	-8.6	-10.6	-6.3	-2.7

$OPTE_t$ ← $NOSPL_t$ →

26.7 2.1 0.2 -1.3 -2.5 -1.4

DATA FOR THE REMAININGANGLES NOT ANALYZED DUE TO JET NOISE CONTAMINATION

1/3 OCTAVE NTC (dB) WITH RESPECT TO INCIDENT SPL (NTC_i)

$M_J = 0$ $M_T = 0.08$

DAISY LOBE NOZZLE (RUN NO = 41)

FREQ KHZ	PTF$_i$	10.	20.	30.	40.	50.	60.	70.	80.	90.	100.	110.
	EMISSION ANGLE (RELATIVE TO JET EXHAUST) REFERENCED TO NOZZLE EXIT (DEGREES)											
.250	+21.4	+17.2	+22.2	+21.0	+20.7	+19.4	+20.9	+21.0	+19.7	+16.8	+21.7	+19.0
.315	+18.8	+16.9	+18.9	+18.4	+17.4	+15.7	+17.7	+17.8	+17.0	+14.2	+18.7	+16.4
.400	+16.8	+17.1	+17.2	+16.9	+15.8	+13.7	+15.7	+15.9	+15.3	+13.0	+16.9	+14.8
.500	+14.2	+17.8	+14.0	+12.8	+12.8	+8.6	+12.8	+13.0	+13.1	+11.4	+14.6	+12.7
.630	+11.8	+17.4	+10.7	+9.2	+9.8	+6.1	+6.8	+9.6	+10.1	+9.0	+11.6	+9.8
.800	+8.6	+19.1	+7.8	+6.5	+8.8	+3.6	+7.0	+7.9	+7.6	+7.0	+9.1	+7.9
1.00	+7.4	+18.3	+6.1	+4.8	+4.7	+2.8	+5.8	+6.6	+6.9	+6.1	+8.0	+7.2
1.25	+6.7	+13.8	+4.4	+3.4	+3.3	+1.5	+5.1	+6.0	+6.3	+5.8	+7.9	+7.2
1.60	+6.0	+11.3	+3.1	+2.3	+2.3	+0.7	+4.4	+5.4	+6.2	+5.8	+7.7	+7.3
2.00	+4.3	+11.4	+0.4	0.2	0.0	1.2	+2.7	+3.8	+5.0	+5.2	+6.7	+6.7
2.50	+2.9	+9.9	1.6	2.5	1.8	2.5	+1.6	+3.0	+4.2	+4.9	+5.7	+6.5
3.15	+2.4	+7.5	3.4	3.8	2.2	2.6	+1.1	+2.8	+4.5	+5.4	+6.4	+6.8
4.00	+2.4	+6.4	4.0	3.7	2.0	3.8	+1.8	+3.8	+5.3	+6.9	+8.0	+8.6
5.00	+5.2	+5.7	2.8	1.6	+0.9	1.3	+6.1	+8.9	+10.8	+14.1	+15.6	+15.1
6.30	+6.7	+5.7	0.7	+0.7	+2.0	+0.3	+6.8	+11.1	+12.7	+14.1	+12.0	+11.4
8.00	+11.3	+12.2	+6.0	+10.6	+13.1	+12.3	+15.0	+15.3	+9.9	+7.8	+7.8	+7.9
10.0	+8.3	+8.1	+9.6	+10.7	+6.7	+1.2	+6.4	+6.2	+7.6	+9.0	+11.3	+10.5
12.5	+6.9	+8.5	+5.4	+2.0	+1.2	+0.6	+9.3	+6.5	+8.2	+8.7	+11.8	+8.7
16.0	+9.8	+6.8	+5.5	+6.6	+8.8	+4.2	+6.6	+10.0	+11.0	+12.2	+15.7	+14.1
20.0	+11.4	+6.9	+7.7	+12.6	+13.0	+8.8	+8.1	+9.8	+8.2	+8.9	+16.8	+12.8
25.0	+7.8	+1.1	+6.1	+10.9	+5.4	+0.0	+6.5	+5.6	+13.8	+9.9	+10.7	+11.9
31.5	+6.8	+2.8	+3.8	+2.9	0.0	1.2	+4.3	+11.4	+12.4	+11.7	+13.5	+14.0
40.0	+11.4	+5.7	+10.7	+3.5	+5.7	+4.2	+12.0	+15.5	+15.1	+15.3	+15.2	+17.4
50.0	+13.2	0.4	+8.1	+6.8	+13.4	+12.7	+12.6	+19.9	+19.0	+19.1	+18.8	+16.0
63.0	+10.8	4.3	+5.0	+7.9	+11.8	+11.5	+13.6	+18.8	+21.4	+20.2	+21.9	+21.9
	OPTF$_i$ ←						NOSPL$_i$ →					
	21.8	+13.4	+8.1	+7.4	+8.0	+6.4	+10.0	+11.1	+11.6	+10.5	+13.0	+12.1

CONICAL NOZZLE (RUN NO = 121)

FREQ KHZ	PTF$_i$	10.	20.	30.	40.	50.	60.	70.	80.	90.	100.	110.
	EMISSION ANGLE (RELATIVE TO JET EXHAUST) REFERENCED TO NOZZLE EXIT (DEGREES)											
.250	+28.3	+26.6	+27.7	+28.4	+28.8	+28.1	+24.6	+26.2	+26.8	+26.0	+29.1	+25.3
.315	+24.4	+22.0	+23.2	+23.4	+24.5	+24.0	+21.2	+22.7	+22.8	+22.1	+24.9	+21.7
.400	+22.7	+19.9	+21.5	+22.0	+22.6	+22.2	+19.6	+21.0	+21.0	+20.3	+22.0	+20.1
.500	+18.7	+14.9	+15.9	+17.4	+18.4	+18.7	+16.2	+17.4	+17.2	+16.0	+18.4	+16.6
.630	+14.8	+10.7	+11.6	+13.3	+14.4	+15.0	+12.6	+13.7	+13.4	+12.1	+14.3	+12.9
.800	+11.3	+7.2	+8.2	+9.4	+10.4	+10.6	+9.6	+10.6	+10.1	+9.0	+10.7	+9.7
1.00	+8.9	+4.0	+5.4	+6.6	+7.4	+7.6	+7.2	+8.2	+7.9	+6.9	+8.5	+7.7
1.25	+6.9	+1.4	+3.0	+4.1	+4.8	+5.5	+5.1	+6.2	+6.3	+5.2	+6.8	+6.4
1.60	+5.0	1.5	+0.6	+1.6	+2.1	+3.6	+3.8	+4.8	+4.6	+3.8	+5.3	+5.1
2.00	+3.2	4.4	1.7	0.9	0.4	+1.8	+2.3	+3.2	+2.9	+2.8	+4.6	+4.4
2.50	+1.8	6.8	3.8	2.9	2.3	+0.2	+1.0	+1.9	+2.1	+2.4	+4.5	+3.9
3.15	+6.5	9.1	6.0	4.8	3.7	1.0	+0.4	+0.9	+2.0	+2.2	+4.5	+4.2
4.00	+2.8	12.1	8.1	6.1	4.8	2.3	0.1	+0.7	+1.2	+2.8	+5.1	+5.2
5.00	1.6	14.1	9.3	6.9	5.2	3.3	1.0	+1.9	+2.5	+5.0	+7.2	+7.0
6.30	1.6	15.8	9.9	6.4	4.7	2.1	+1.6	+5.5	+6.8	+9.8	+12.2	+11.0
8.00	1.0	17.0	8.0	4.0	2.3	+4.8	+11.1	+10.5	+7.4	+8.4	+9.9	+9.0
10.0	+2.2	16.7	4.5	+3.3	+4.9	+3.2	+7.6	+4.6	+3.2	+8.2	+8.7	+8.0
12.4	+2.2	13.6	1.9	+2.7	+0.7	+0.5	+9.6	+7.5	+9.0	+12.2	+14.3	+12.8
16.0	+4.2	13.0	+3.4	+11.1	+6.8	+8.0	+12.0	+11.2	+10.7	+14.3	+17.5	+17.3
20.0	+6.8	10.5	+3.1	+7.5	+4.0	+3.9	+12.7	+15.9	+14.3	+19.4	+20.6	+19.2
25.0	+4.8	11.7	+3.1	+9.5	+1.3	+1.4	+7.6	+11.8	+10.2	+14.6	+17.8	+15.4
31.5	+4.7	11.7	+3.8	+8.4	+3.8	+2.9	+10.8	+13.8	+11.8	+13.2	+20.6	+23.0
40.0	+10.1	3.9	+11.0	+8.0	+6.2	+4.0	+13.6	+15.1	+15.6	+15.5	+18.1	+18.9
50.0	+11.6	3.1	+8.0	+8.0	+8.6	+9.2	+15.2	+19.2	+15.2	+16.3	+23.1	+23.5
63.0	+12.7	+0.2	+9.0	+9.2	+8.3	+11.8	+16.3	+19.7	+13.4	+12.3	+17.3	+23.4
	OPTF$_i$ ←						NOSPL$_i$ →					
	22.9	0.7	+4.6	+6.2	+7.3	+9.2	+10.0	+11.2	+11.4	+10.6	+12.9	+12.4

1/3 OCTAVE NIL (dB) WITH RESPECT TO TRANSMITTED SPL (NIL)

M_j = M_f = 0.28

DAISY LOBE NOZZLE (RUN NO = 41)

EMISSION ANGLE (RELATIVE TO JET EXHAUST) REFERENCED TO NOZZLE EXIT (DEGREES)

FREQ KHZ	PIF	10.	20.	30.	40.	50.	60.	70.	80.	90.	100.	110.
.250	-20.3	-10.1	-21.1	-20.5	-19.8	-18.3	-16.8	-15.9	-18.6	-19.7	-20.9	-17.9
.315	-17.1	-15.4	-17.4	-16.6	-16.0	-14.2	-16.2	-10.4	-15.6	-13.1	-17.3	-19.0
.400	-19.0	-15.3	-19.4	-14.2	-13.7	-11.5	-13.5	-14.2	-13.5	-11.2	-15.1	-19.9
.500	-12.2	-15.0	-12.0	-10.8	-10.8	-7.9	-11.6	-11.0	-11.1	-9.5	-12.7	-10.7
.630	-8.8	-14.9	-8.2	-6.8	-7.1	-3.6	-7.1	-7.2	-7.7	-6.6	-9.2	-7.4
.800	-5.5	-10.0	-4.7	-3.4	-3.5	-0.8	-3.5	-4.3	-4.8	-3.9	-5.6	-4.8
1.000	-4.7	-15.6	-3.4	-2.9	-1.9	0.2	-3.0	-3.9	-4.1	-3.4	-5.4	-4.5
1.250	-4.5	-11.7	-2.3	-1.2	-1.1	0.6	-2.4	-3.8	-4.1	-3.7	-5.7	-5.0
1.600	-4.4	-9.7	-1.5	-0.7	-0.7	1.0	-2.7	-3.8	-4.5	-4.1	-6.1	-5.7
2.000	-2.5	-9.2	1.5	2.0	1.8	3.0	-0.4	-2.0	-3.2	-3.3	-4.8	-4.9
2.500	-1.6	-8.6	2.9	3.7	3.1	3.8	-0.3	-1.7	-3.0	-3.6	-4.4	-5.2
3.150	-1.6	-6.9	4.0	4.5	2.6	3.2	-0.5	-2.2	-3.8	-4.8	-5.8	-6.2
4.000	-2.3	-5.9	4.1	3.8	2.1	3.6	-1.4	-3.6	-5.2	-6.8	-7.9	-8.4
5.000	-3.5	-4.9	4.5	3.3	0.8	3.0	-4.4	-7.2	-9.1	-12.5	-13.9	-13.4
6.300	0.4	1.4	7.8	6.4	5.1	6.7	0.2	-4.0	-5.7	-7.1	-4.9	-4.3
8.000	-10.8	-11.7	-5.5	-10.1	-12.6	-11.8	-15.1	-14.8	-9.4	-7.3	-7.3	-7.4
10.000	-7.7	-7.5	-8.9	-10.1	-6.1	-0.6	-5.8	-5.6	-7.0	-8.4	-10.7	-9.9
12.500	-6.0	-7.6	-4.5	-1.1	-0.3	-0.6	-6.4	-5.6	-7.3	-7.7	-10.9	-7.8
16.000	-9.6	-6.6	-5.2	-6.3	-5.5	-4.6	-6.4	-9.8	-10.8	-12.0	-15.4	-12.1
20.000	-11.0	-6.5	-7.2	-12.1	-12.8	-8.4	-7.6	-9.3	-7.8	-8.5	-8.8	-9.3
25.000	-7.1	-0.4	-5.3	-9.2	-4.7	0.7	-5.8	-4.9	-13.0	-9.1	-7.6	-11.2
31.500	-3.6	-0.2	-1.3	-0.1	2.8	3.7	-1.8	-8.9	-9.9	-9.2	-10.9	-11.4
40.000	-14.7	-5.1	-10.0	-2.8	-5.0	-3.5	-11.3	-14.8	-14.5	-14.6	-14.5	-16.7
50.000	-11.3	1.9	-6.2	-4.9	-11.8	-10.5	-10.0	-18.0	-17.1	-17.2	-16.8	-14.1
*63.000	-7.1	8.0	-1.5	-4.2	-8.0	-7.7	-9.6	-14.7	-17.8	-16.4	-17.6	-18.3

OPTF$_t$ ← NOSPL$_t$ →

23.4 -11.7 -6.4 -5.8 -6.4 -4.7 -8.4 -9.4 -10.0 -8.8 -11.3 -10.4

CONICAL NOZZLE (RUN NO = 121)

EMISSION ANGLE (RELATIVE TO JET EXHAUST) REFERENCED TO NOZZLE EXIT (DEGREES)

FREQ KHZ	PIF	10.	20.	30.	40.	50.	60.	70.	80.	90.	100.	110.
.250	-26.1	-25.8	-26.1	-26.8	-27.2	-26.4	-23.0	-24.6	-24.9	-24.4	-27.8	-23.7
.315	-22.9	-20.8	-21.7	-22.4	-23.0	-22.5	-19.7	-21.2	-21.3	-20.6	-23.3	-20.2
.400	-21.3	-18.5	-20.1	-20.6	-21.2	-20.8	-18.2	-19.6	-19.6	-18.9	-21.5	-18.7
.500	-17.4	-13.6	-14.7	-16.2	-17.2	-17.5	-15.0	-16.1	-16.0	-14.8	-17.1	-15.3
.630	-13.8	-9.7	-10.7	-12.4	-13.5	-14.1	-11.7	-12.7	-12.8	-11.1	-13.4	-12.0
.800	-10.3	-6.1	-7.2	-8.4	-9.3	-9.5	-8.5	-9.6	-9.1	-8.0	-9.7	-8.6
1.000	-7.8	-2.9	-4.3	-5.6	-6.4	-6.6	-6.1	-7.1	-6.8	-5.8	-7.4	-6.6
1.250	-6.1	-0.6	-2.2	-3.4	-4.1	-4.7	-4.3	-6.4	-6.5	-4.4	-6.0	-5.7
1.600	-4.5	2.0	-0.2	-1.0	-1.6	-3.1	-3.1	-4.1	-4.1	-3.4	-4.9	-4.6
2.000	-2.5	4.7	2.0	1.2	0.7	-1.5	-2.0	-2.9	-2.6	-2.5	-4.3	-4.1
2.500	-1.7	6.9	3.9	3.0	2.4	-0.1	-0.8	-1.8	-2.0	-2.3	-4.3	-3.8
3.150	-0.3	9.3	6.2	5.0	3.8	1.1	-0.3	-0.8	-1.8	-2.0	-4.3	-4.1
4.000	0.8	12.1	8.1	6.1	4.8	2.4	0.1	-0.6	-1.2	-2.8	-5.1	-5.2
5.000	1.7	14.1	9.4	7.0	5.2	3.4	1.1	-1.8	-2.5	-4.9	-7.1	-6.9
6.300	4.0	18.1	12.2	8.7	7.0	4.4	0.7	-3.1	-4.1	-7.4	-9.8	-8.7
8.000	1.8	17.4	8.4	4.4	2.7	-4.3	-10.6	-10.1	-6.9	-7.9	-9.4	-8.6
10.000	2.6	19.1	6.5	-0.6	-2.5	-0.7	-5.2	-2.2	-0.8	-3.8	-6.3	-5.6
12.500	3.2	18.8	7.3	2.8	4.7	5.0	-4.6	-2.6	-3.6	-6.1	-9.2	-7.7
16.000	-4.1	13.1	-3.2	-11.0	-6.3	-4.9	-11.8	-11.1	-10.5	-14.2	-17.3	-17.2
20.000	-6.4	10.6	-3.0	-7.4	-3.8	-3.6	-12.6	-15.8	-14.2	-19.3	-20.5	-19.1
25.000	-4.6	11.9	-2.9	-9.0	-1.0	-1.2	-7.3	-11.3	-9.9	-14.4	-17.6	-19.2
31.5	-4.4	12.1	-3.5	-8.1	-3.5	-2.8	-10.4	-13.5	-11.5	-12.8	-20.3	-22.7
40.0	-9.3	4.7	-10.2	-7.2	-5.4	-3.2	-12.8	-14.3	-14.8	-14.7	-17.3	-18.1
50.0	-14.3	4.3	-6.6	-6.7	-7.3	-7.6	-13.9	-17.9	-13.9	-15.0	-21.7	-22.2
*63.0	-8.2	4.7	-4.2	-5.2	-3.7	-6.1	-12.8	-15.3	-10.5	-7.6	-4.7	-20.2

OPTF$_t$ ← NOSPL$_t$ →

24.2 2.0 -3.3 -5.0 -6.1 -7.9 -8.7 -10.0 -10.2 -9.3 -11.6 -11.1

1/3 OCTAVE NTC (dB) WITH RESPECT TO INCIDENT SPL (NTC_i)

M_J= 0.4 M_T = 0.08

DAISY LOBE NOZZLE (RUN NO = 46)

FREQ KHZ	PTF$_i$	10.	20.	30.	40.	50.	60.	70.	80.	90.	100.	110.
	EMISSION ANGLE (RELATIVE TO JET EXHAUST) REFERENCED TO NOZZLE EXIT (DEGREES)											
.250	-27.1	-21.6	-24.3	-25.2	-26.8	-21.8	-27.4	-28.5	-27.4	-22.1	-35.1	-27.1
.315	-23.3	-17.7	-20.3	-20.8	-22.0	-17.8	-23.2	-24.2	-23.0	-19.3	-30.2	-23.6
.400	-21.2	-15.5	-18.4	-18.6	-19.7	-15.7	-21.0	-22.0	-20.8	-17.5	-27.8	-21.6
.500	-18.3	-13.2	-15.1	-15.2	-16.2	-13.2	-17.8	-18.7	-16.9	-15.7	-23.5	-18.7
.630	-15.1	-10.3	-11.8	-11.8	-12.7	-10.3	-14.4	-15.4	-13.3	-13.4	-19.7	-15.7
.800	-11.5	-6.3	-8.2	-8.0	-8.8	-6.6	-10.6	-11.5	-10.0	-10.7	-15.8	-13.1
1.00	-8.8	-3.0	-5.0	-4.7	-4.7	-3.2	-7.1	-8.1	-8.4	-8.8	-12.3	-11.6
1.25	-6.8	-0.5	-2.4	-2.1	-1.7	-0.4	-4.2	-5.4	-7.4	-7.3	-9.6	-10.3
1.60	-3.9	1.3	-0.4	0.0	0.6	1.8	-1.9	-3.3	-5.8	-6.0	-7.7	-9.5
2.00	-3.1	1.8	0.5	0.8	1.5	2.9	-0.9	-2.5	-4.7	-5.3	-7.2	-9.3
2.50	-1.7	2.6	1.8	2.0	2.8	4.6	0.4	-1.3	-3.2	-3.9	-6.4	-8.3
3.15	-1.2	2.2	2.2	2.4	3.0	5.6	0.8	-1.2	-2.3	-3.3	-6.4	-8.0
4.00	-1.9	0.5	0.9	2.5	2.8	5.3	-0.4	-2.8	-3.8	-5.9	-8.6	-11.3
5.00	-4.5	-2.6	-2.3	2.0	1.8	1.8	-3.7	-5.9	-7.4	-11.1	-17.7	-21.6
6.30	-4.8	-1.5	-0.6	3.3	2.9	1.6	-5.6	-8.2	-9.7	-10.2	-12.1	-12.4
8.00	-8.8	-4.6	-1.9	0.4	-1.9	-9.6	-19.9	-16.0	-16.7	-13.7	-13.9	-16.8
10.0	-9.3	-2.3	-3.8	-3.5	-4.6	-2.9	-10.6	-10.9	-17.1	-19.1	-18.2	-14.3
12.5	-7.8	-5.6	-8.3	-4.9	-0.8	1.8	-8.7	-15.4	-14.9	-17.7	-16.7	-15.8
16.0	-10.1	-11.6	-11.2	-9.0	-2.1	-3.4	-13.9	-13.2	-10.4	-14.4	-14.7	-16.5
20.0	-14.8	-7.5	-7.5	-5.5	-4.4	-3.6	-11.7	-17.3	-7.3	-14.2	-13.8	-16.5
25.0	-9.2	-6.8	-3.7	-5.2	-3.5	-5.6	-6.4	-10.0	-9.3	-11.9	-13.1	-12.5
31.5	-9.6	-6.6	-6.8	-10.3	-6.3	-1.8	-7.2	-11.1	-7.2	-9.4	-16.1	-15.9
40.0	-9.8	-8.8	-10.9	-9.9	-5.9	-3.1	-6.1	-7.6	-7.2	-12.4	-10.7	-16.1
50.0	-12.8	-9.7	-9.8	-12.9	-10.0	-8.2	-5.8	-6.6	-13.2	-13.3	-16.4	-13.3
63.0	-16.9	-3.7	-4.1	-12.5	-8.4	-4.4	-9.8	-13.8	-15.0	-14.7	-15.1	-17.1
	OPTF$_i$	←				NOSPL$_i$						→
	22.1	-6.6	-7.8	-7.0	-6.6	-5.8	-9.4	-11.1	-12.1	-12.0	-15.6	-16.0

CONICAL NOZZLE (RUN NO = 93)

FREQ KHZ	PTF$_i$	10.	20.	30.	4..	50.	60.	70.	80.	90.	100.	110.
	EMISSION ANGLE (RELATIVE TO JET EXHAUST) REFERENCED TO NOZZLE EXIT (DEGREES)											
.250	-24.8	-16.9	-18.6	-21.1	-25.4	-21.8	-24.0	-23.0	-28.5	-23.0	-28.3	-28.7
.315	-21.5	-13.9	-15.6	-17.7	-21.1	-18.4	-20.2	-19.9	-22.1	-20.4	-24.8	-23.1
.400	-24.1	-12.4	-14.5	-16.3	-19.5	-17.0	-18.6	-18.5	-20.7	-19.1	-23.3	-21.9
.500	-17.0	-9.7	-11.2	-13.3	-15.3	-13.7	-15.1	-15.5	-17.4	-17.0	-19.9	-19.8
.630	-14.2	-7.0	-8.4	-10.5	-11.9	-10.7	-12.0	-12.7	-14.4	-14.6	-16.8	-17.4
.800	-11.1	-4.4	-5.7	-7.3	-8.0	-7.9	-8.2	-9.8	-11.8	-11.8	-13.9	-14.7
1.00	-8.8	-2.3	-3.8	-4.8	-5.1	-5.7	-5.6	-7.7	-9.6	-9.8	-11.8	-12.2
1.25	-6.8	-0.3	-2.0	-2.7	-2.7	-3.5	-4.0	-5.8	-8.1	-8.3	-9.8	-10.1
1.60	-5.4	1.2	-0.6	-1.2	-1.4	-1.8	-2.8	-4.4	-6.5	-6.6	-8.3	-8.9
2.00	-4.3	1.7	0.2	-0.3	-0.3	-0.6	-0.9	-3.4	-4.8	-5.6	-7.5	-8.2
2.50	-3.1	2.0	0.8	0.6	1.0	1.3	0.4	-2.2	-3.7	-5.1	-7.0	-7.1
3.15	-2.4	2.1	0.9	1.0	1.6	2.6	1.1	-1.3	-3.0	-4.9	-6.7	-7.0
4.00	-2.3	0.6	0.2	0.0	1.1	3.4	2.1	-1.1	-2.0	-5.8	-8.0	-8.4
5.00	-2.4	-1.0	-0.8	0.4	1.4	3.7	2.6	-0.9	-3.8	-8.6	-10.9	-13.1
6.30	-0.2	-0.1	0.6	2.0	3.4	6.4	5.6	1.4	-3.8	-12.2	-12.6	-17.4
8.00	-2.2	-2.2	-0.6	0.9	2.6	5.9	1.5	-6.0	-10.5	-11.3	-11.3	-11.2
10.0	-4.3	-3.4	-4.4	-3.2	1.8	3.9	-6.1	-4.2	-7.4	-10.2	-12.4	-18.9
12.4	-5.0	-6.9	-7.1	-5.4	-1.7	3.3	-0.8	-3.9	-11.2	-14.7	-17.5	-17.5
16.0	-8.0	-14.4	-8.4	-4.3	-3.1	-0.4	-5.4	-6.4	-13.9	-13.8	-18.9	-21.1
20.0	-6.2	-8.4	-5.5	-4.5	-1.7	1.9	-3.1	-7.1	-16.3	-17.3	-19.1	-21.8
25.0	-5.6	-6.6	-3.3	-1.8	2.2	0.9	-5.6	-5.3	-10.2	-13.3	-16.4	-16.9
31.5	-5.2	-9.4	-2.2	1.1	2.7	0.4	-4.9	-6.7	-9.1	-15.3	-18.3	-17.1
40.0	-14.5	-16.4	-13.7	-5.5	-6.1	-2.3	-7.3	-8.1	-12.0	-15.5	-18.5	-19.4
50.0	-11.9	-14.6	-14.5	-5.7	-6.0	-4.4	-9.2	-11.6	-13.7	-19.3	-21.9	-22.9
63.0	-14.0	-17.5	-14.3	-9.8	-7.4	-8.6	-11.7	-13.4	-17.5	-19.2	-17.6	-28.3
	OPTF$_i$	←				NOSPL$_i$						→
	22.9	-5.3	-6.6	-6.7	-6.3	-5.2	-6.7	-9.3	-11.7	-12.2	-14.5	-15.1

1/3 OCTAVE NTC (dB) WITH RESPECT TO TRANSMITTED SPL (NTC_t)

$M_J = 0.4$ $M_T = 0.08$

DAISY LOBE NOZZLE (RUN NO= 46)

EMISSION ANGLE (RELATIVE TO JET EXHAUST) REFERENCED TO NOZZLE EXIT (DEGREES)

FREQ KHZ	PTF_t	10.	20.	30.	40.	50.	60.	70.	80.	90.	100.	110.
.250	+27.0	+21.5	+24.2	+25.1	+26.4	+21.4	+27.3	+28.4	+27.3	+22.0	+35.0	+27.0
.315	+23.1	+17.6	+20.1	+20.7	+21.8	+17.7	+23.0	+24.1	+22.9	+19.1	+30.0	+23.4
.400	+21.0	+15.2	+18.2	+18.4	+19.8	+16.8	+20.8	+21.8	+20.6	+17.2	+27.6	+21.3
.500	+18.0	+12.9	+14.8	+15.0	+16.0	+13.0	+17.6	+18.5	+16.7	+15.5	+23.2	+18.5
.630	+14.8	+10.0	+11.5	+11.5	+12.6	+10.0	+14.2	+15.1	+13.0	+13.1	+19.4	+15.4
.800	+11.0	+5.8	+7.7	+7.0	+8.0	+6.1	+10.1	+11.1	+9.6	+10.2	+15.3	+12.6
1.00	+7.7	+2.2	+4.1	+3.0	+3.9	+2.3	+6.3	+7.3	+7.5	+8.0	+11.5	+10.8
1.25	+4.8	0.7	+1.2	+0.9	+0.6	0.6	+3.0	+4.2	+6.2	+6.2	+8.4	+9.1
1.60	+2.6	2.6	0.9	1.3	1.9	3.1	+0.6	+2.0	+4.2	+4.7	+6.4	+8.2
2.00	+2.1	2.7	1.5	1.8	2.5	3.9	0.1	+1.5	+3.7	+4.3	+6.2	+8.4
2.50	+1.0	3.2	2.4	2.6	3.5	6.3	1.1	+0.6	+2.6	+3.2	+5.0	+7.6
3.15	+1.0	2.4	2.4	2.0	3.2	5.8	1.0	+1.0	+2.1	+3.1	+6.2	+7.8
4.00	+1.6	0.8	1.1	2.7	3.0	6.6	+0.1	+2.5	+3.6	+5.7	+8.3	+11.0
5.00	+2.9	+1.1	+0.8	3.6	3.3	3.3	+2.1	+4.4	+5.9	+9.5	+16.1	+20.1
6.30	+6.6	1.8	2.7	6.7	6.2	4.9	+2.3	+4.9	+6.4	+6.9	+8.8	+9.1
8.00	+8.0	+3.9	+1.1	1.2	+1.1	+8.9	+19.1	+17.3	+15.9	+12.9	+13.1	+16.0
10.0	+9.2	+2.2	+3.6	+3.3	+4.4	+2.8	+10.4	+10.8	+17.0	+18.9	+18.0	+14.2
12.5	+6.9	+5.6	+6.2	+4.8	+0.4	1.9	+6.6	+15.3	+14.8	+17.6	+16.7	+15.7
16.0	+10.0	+11.6	+11.2	+9.0	+2.0	+3.4	+13.9	+13.2	+10.4	+14.4	+14.6	+16.4
20.0	+10.8	+7.4	+7.4	+8.4	+4.3	+3.8	+11.7	+17.3	+7.2	+14.1	+13.7	+16.4
25.0	+9.1	+6.0	+3.6	+5.2	+3.5	+5.6	+6.3	+10.0	+9.3	+11.8	+13.1	+12.5
31.5	+9.6	+6.6	+6.8	+10.3	+6.3	+1.7	+7.2	+11.1	+7.1	+9.3	+16.1	+15.9
40.0	+9.7	+7.9	+10.8	+9.8	+5.8	+2.9	+6.0	+7.5	+7.1	+12.3	+10.6	+16.0
50.0	+11.8	+9.5	+9.6	+12.7	+9.8	+8.0	+5.6	+6.4	+13.0	+13.1	+16.2	+13.1
63.0	+10.6	+3.4	+3.9	+12.2	+8.1	+4.1	+9.3	+13.6	+14.8	+14.4	+14.8	+16.9

$OPTF_t$	← $NOSPL_t$ →									
22.4	+6.3	+7.5	+6.7	+6.3	+4.7	+9.1	+10.8	+11.9	+11.7	+15.3	+15.7

CONICAL NOZZLE (RUN NO = 93)

EMISSION ANGLE (RELATIVE TO JET EXHAUST) REFERENCED TO NOZZLE EXIT (DEGREES)

FREQ KHZ	PTF_t	10.	20.	30.	40.	50.	60.	70.	80.	90.	100.	110.
.250	+24.0	+16.1	+17.8	+20.3	+24.6	+21.0	+23.2	+22.2	+24.7	+22.2	+27.5	+24.9
.315	+20.7	+13.1	+14.8	+16.9	+20.3	+17.6	+19.3	+19.1	+21.3	+19.5	+24.0	+22.3
.400	+19.3	+11.6	+13.7	+15.5	+18.6	+16.2	+17.8	+17.6	+19.8	+18.3	+22.5	+21.0
.500	+16.1	+8.8	+10.3	+12.4	+14.4	+12.8	+14.2	+14.6	+16.8	+16.1	+19.0	+19.9
.630	+13.2	+6.0	+7.4	+9.0	+10.9	+9.8	+11.0	+11.7	+13.4	+13.6	+15.9	+16.4
.800	+10.2	+3.5	+4.9	+6.5	+7.2	+7.0	+7.4	+8.9	+10.6	+10.9	+13.0	+13.8
1.00	+8.2	+1.7	+3.2	+4.2	+4.5	+5.1	+5.0	+7.1	+9.0	+9.2	+11.1	+11.6
1.25	+6.4	0.1	+1.5	+2.3	+2.3	+3.0	+3.8	+5.4	+7.6	+7.9	+9.3	+9.6
1.60	+5.2	1.4	+0.3	+1.0	+1.1	+1.6	+2.5	+4.2	+6.2	+6.4	+8.1	+8.7
2.00	+4.2	1.8	0.3	+0.3	+0.3	+0.5	+0.8	+3.3	+4.8	+5.6	+7.4	+8.1
2.50	+3.1	2.0	0.6	0.0	1.0	1.4	0.4	+2.2	+3.7	+5.0	+7.0	+7.1
3.15	+2.4	2.2	0.9	1.0	1.7	2.6	1.2	+1.3	+2.9	+4.9	+6.6	+7.0
4.00	+2.3	0.6	0.2	0.0	1.1	3.4	2.1	+1.1	+2.0	+5.8	+7.9	+8.4
5.00	+2.4	+1.0	+0.8	0.4	1.8	3.7	2.6	+0.9	+3.8	+8.6	+10.9	+13.1
6.30	0.6	0.7	1.3	2.7	4.1	7.1	6.3	2.1	+3.0	+11.4	+11.9	+16.6
8.00	+2.1	+2.1	+0.5	1.0	2.7	6.0	1.6	+5.9	+10.4	+11.2	+11.2	+11.1
10.0	+3.4	+2.5	+3.5	+2.3	2.8	4.8	+5.1	+3.2	+6.4	+9.3	+11.5	+15.0
12.5	+4.2	+6.1	+6.3	+4.6	+0.9	4.1	+0.0	+3.1	+10.4	+13.9	+16.7	+16.7
16.0	+7.9	+14.3	+8.4	+4.2	+3.1	+0.4	+5.3	+6.4	+13.8	+13.7	+18.9	+21.1
20.0	+6.1	+8.3	+5.4	+4.4	+1.6	2.0	+3.0	+7.0	+15.2	+17.2	+19.0	+21.7
25.0	+5.5	+5.4	+3.1	+1.7	2.4	1.1	+5.5	+5.1	+10.0	+13.2	+16.3	+16.8
31.5	+5.1	+9.2	+2.1	1.3	2.8	0.6	+4.8	+6.5	+8.8	+15.2	+18.1	+17.0
40.0	+10.4	+16.4	+13.6	+5.4	+5.0	+2.2	+7.2	+8.0	+11.9	+15.4	+18.4	+19.3
50.0	+11.7	+14.5	+14.3	+5.5	+4.9	+4.3	+9.1	+11.4	+13.6	+19.2	+21.7	+22.8
63.0	+13.8	+17.2	+14.0	+9.5	+7.1	+8.3	+11.4	+13.1	+17.2	+18.9	+17.3	+25.0

$OPTF_t$	← $NOSPL_t$ →									
23.6	+4.6	+5.5	+6.0	+5.6	+4.4	+6.0	+8.6	+10.9	+11.5	+13.8	+14.4

1/3 OCTAVE NTC (dB) WITH RESPECT TO INCIDENT SPL (NTC_i)

$M_J = 0.6$ $M_T = 0.08$

DAISY LOBE NOZZLE (RUN NO = 81)

FREQ KHZ	PTF_i	10.	20.	30.	40.	50.	60.	70.	80.	90.	100.	110.
	EMISSION ANGLE (RELATIVE TO JET EXHAUST) REFERENCED TO NOZZLE EXIT (DEGREES)											
.250	-25.9	-21.4	-19.1	-21.2	-23.8	-21.6	-22.5	-24.8	-28.4	-27.5	-30.8	-29.7
.315	-22.6	-18.8	-15.4	-17.3	-19.6	-17.9	-18.8	-20.9	-23.9	-23.5	-26.7	-26.1
.400	-19.9	-14.4	-13.6	-15.2	-17.4	-15.9	-16.8	-18.8	-21.8	-21.4	-24.6	-24.2
.500	-16.7	-10.1	-10.0	-11.7	-14.1	-13.8	-14.1	-15.8	-17.8	-17.9	-21.0	-21.4
.630	-13.5	-6.4	-6.7	-8.3	-10.7	-11.0	-11.6	-12.6	-14.2	-14.4	-17.6	-18.3
.800	-10.8	-3.7	-4.4	-5.8	-7.2	-7.1	-8.1	-9.6	-11.1	-12.0	-14.8	-15.8
1.00	-8.4	-1.6	-2.7	-3.7	-4.8	-4.7	-6.0	-7.6	-9.2	-10.3	-13.2	-13.9
1.25	-6.2	0.2	-0.3	-0.9	-1.7	-2.4	-3.8	-5.8	-7.9	-8.7	-11.9	-12.2
1.60	-4.6	0.5	1.1	1.3	0.7	-0.6	-1.9	-4.5	-6.7	-8.2	-10.7	-10.6
2.00	-3.1	0.5	2.4	3.0	2.4	0.7	-0.4	-3.1	-5.3	-7.1	-9.0	-9.1
2.50	-1.6	0.1	3.3	4.8	4.2	2.6	1.3	-1.3	-4.5	-5.8	-8.3	-9.2
3.15	-1.1	-1.3	3.2	5.7	5.1	3.0	2.0	-1.7	-5.3	-6.1	-9.2	-9.5
4.00	-2.2	-2.7	1.4	4.0	4.4	2.5	1.1	-3.9	-6.1	-8.1	-10.5	-12.3
5.00	-2.7	-2.6	0.3	3.6	5.4	2.6	-1.3	-7.4	-11.0	-13.0	-14.7	-16.4
6.30	-6.1	-6.6	-4.2	-0.0	3.9	0.6	-9.7	-16.0	-16.7	-13.3	-13.3	-12.0
8.00	-7.4	-9.4	-7.0	-4.2	3.8	-4.7	-13.3	-17.7	-16.9	-18.3	-21.4	-17.1
10.0	-4.4	-9.4	-3.0	1.6	5.3	-3.5	-14.0	-4.8	-9.5	-11.2	-12.3	-9.5
12.5	-4.4	-8.8	-2.5	1.8	4.2	-0.6	-9.6	-6.9	-6.8	-6.6	-12.6	-14.6
16.0	-9.2	-9.1	-3.9	-2.6	-2.2	-4.4	-12.1	-12.8	-12.5	-12.7	-16.8	-16.2
20.0	-11.6	-11.1	-4.2	-6.4	-7.5	-10.0	-20.5	-10.3	-11.7	-11.6	-13.2	-12.0
25.0	-7.5	-8.9	-3.8	-6.2	-2.3	-5.5	-18.8	-2.7	-9.6	-4.2	-10.2	-8.3
31.5	-10.8	-10.3	-6.1	-7.5	-6.6	-9.3	-12.2	-10.9	-11.1	-6.5	-11.4	-11.2
40.0	-9.4	-10.6	-12.6	-5.6	-5.1	-5.9	-11.5	-7.0	-7.2	-5.6	-7.9	-12.7
50.0	-12.8	-13.2	-16.1	-9.8	-10.0	-7.3	-13.4	-10.6	-11.2	-9.0	-15.8	-9.5
63.0	-11.7	-4.2	-9.1	-8.6	-9.4	-10.2	-12.8	-11.4	-9.5	-9.9	-11.6	-11.8
	$OPTF_i$ ←					$NOSPL_i$ →						
	22.6	-6.8	-5.8	-4.9	-4.4	-6.8	-6.7	-10.6	-13.0	-12.9	-16.2	-16.4

CONICAL NOZZLE (RUN NO = 109)

FREQ KHZ	PTF_i	10.	20.	30.	40.	50.	60.	70.	80.	90.	100.	110.
	EMISSION ANGLE (RELATIVE TO JET EXHAUST) REFERENCED TO NOZZLE EXIT (DEGREES)											
.250	-21.9	-11.9	-10.2	-17.0	-21.6	-23.2	-24.5	-26.6	-29.3	-21.8	-34.6	-36.4
.315	-19.5	-9.4	-8.6	-14.7	-18.0	-19.3	-20.8	-23.0	-25.8	-19.6	-30.0	-31.5
.400	-16.3	-8.2	-8.1	-13.4	-16.6	-17.8	-19.3	-21.1	-24.3	-18.5	-28.3	-29.9
.500	-15.8	-5.7	-6.4	-10.9	-13.2	-13.4	-16.0	-17.9	-20.6	-16.7	-23.6	-26.1
.630	-13.2	-3.4	-4.7	-8.2	-10.1	-10.6	-12.9	-14.8	-17.8	-14.6	-20.0	-22.8
.800	-10.8	-1.6	-3.0	-5.2	-6.7	-7.1	-9.0	-11.6	-14.4	-12.0	-15.9	-19.0
1.00	-8.3	-0.3	-2.0	-3.1	-4.1	-5.2	-5.9	-8.8	-11.2	-9.7	-12.8	-15.7
1.25	-6.6	0.5	-1.2	-1.6	-2.0	-3.6	-3.6	-6.4	-8.5	-7.8	-10.6	-12.9
1.60	-6.0	0.8	-0.1	-0.3	-0.4	-1.8	-2.1	-4.1	-6.1	-6.3	-9.5	-10.3
2.00	-4.1	-0.2	0.6	0.4	0.2	-0.6	-1.6	-2.2	-4.1	-5.2	-9.0	-8.3
2.50	-3.9	-2.9	-1.2	-0.6	0.4	-0.2	-1.1	-1.2	-3.0	-4.7	-8.2	-7.3
3.15	-3.6	-4.4	-2.9	-0.6	1.6	1.0	1.1	-0.6	-2.9	-4.3	-6.4	-7.9
4.00	-3.6	-5.2	-4.3	-1.7	1.3	0.3	1.1	-0.7	-3.4	-5.7	-9.1	-12.3
5.00	-4.1	-9.0	-7.1	-4.0	-0.4	0.2	2.0	-1.0	-3.3	-7.9	-12.5	-16.8
6.30	-5.7	-11.2	-10.7	-6.7	-2.4	-0.1	1.4	-2.8	-6.5	-16.0	-22.8	-18.5
8.00	-6.8	-13.4	-11.8	-7.4	-3.2	-0.2	-0.4	-5.4	-14.8	-11.8	-13.0	-13.8
10.0	-8.1	-13.6	-12.8	-7.5	-2.9	-1.6	-2.1	-9.5	-9.3	-14.4	-19.9	-19.4
12.4	-9.3	-15.5	-15.8	-11.2	-3.7	-2.1	-4.3	-8.3	-18.8	-15.9	-18.4	-22.0
16.0	-13.8	-17.4	-21.2	-18.2	-11.2	-7.7	-10.1	-8.5	-14.8	-16.6	-20.6	-23.6
20.0	-8.6	-12.6	-16.4	-16.2	-7.6	0.9	-6.5	-9.4	-10.9	-15.7	-19.2	-24.3
25.0	-8.6	-14.0	-16.9	-7.9	-0.6	4.8	-7.3	-9.6	-10.8	-14.1	-15.9	-18.8
31.5	-11.7	-15.1	-13.0	-12.1	-7.4	-3.4	-7.4	-10.4	-13.7	-14.5	-21.1	-21.0
40.0	-12.7	-19.7	-22.5	-12.4	-10.2	-4.0	-12.1	-6.0	-17.7	-15.6	-20.3	-22.5
50.0	-16.8	-12.7	-22.6	-18.7	-13.0	-6.7	-15.0	-9.7	-19.8	-19.0	-24.9	-23.6
63.0	-16.4	-10.7	-17.0	-14.6	-11.7	-9.7	-14.2	-13.9	-22.3	-22.2	-25.4	-27.2
	$OPTF_i$ ←					$NOSPL_i$ →						
	22.5	-4.8	-5.5	-6.8	-6.6	-6.6	-7.2	-9.5	-12.2	-11.9	-15.9	-17.4

1/3 OCTAVE NTC (dB) WITH RESPECT TO TRANSMITTED SPL (NTC_t)

$M_J = 0.6$ $M_T = 0.08$

DAISY LOBE NOZZLE (RUN NO= 81)

EMISSION ANGLE (RELATIVE TO JET EXHAUST) REFERENCED TO NOZZLE EXIT (DEGREES)

FREQ KHZ	PTF_t	10.	20.	30.	40.	50.	60.	70.	80.	90.	100.	110.
.250	-25.4	-21.0	-18.7	-20.8	-23.3	-21.2	-22.1	-24.4	-28.0	-27.0	-30.4	-29.3
.315	-21.5	-18.3	-14.9	-16.8	-19.0	-17.4	-18.3	-20.4	-23.5	-23.0	-26.2	-25.6
.400	-19.4	-13.9	-13.1	-14.6	-16.8	-15.4	-16.3	-18.3	-21.2	-20.9	-24.0	-23.6
.500	-16.2	-9.6	-9.5	-11.2	-13.6	-13.2	-13.5	-15.2	-17.3	-17.3	-20.5	-20.8
.630	-12.9	-5.9	-6.1	-7.8	-10.2	-10.5	-10.6	-12.0	-13.6	-13.9	-17.0	-17.7
.800	-10.0	-3.2	-3.9	-5.3	-6.7	-6.6	-7.6	-9.1	-10.6	-11.5	-14.3	-15.3
1.00	-7.8	-0.9	-2.1	-3.1	-3.9	-4.1	-5.5	-7.0	-8.7	-9.8	-12.7	-13.3
1.25	-5.4	1.1	0.5	-0.1	-0.8	-1.6	-3.0	-5.0	-7.1	-7.8	-11.1	-11.3
1.60	-3.9	1.2	1.8	1.9	1.4	0.1	-1.3	-3.8	-6.1	-7.5	-10.0	-9.9
2.00	-2.7	0.9	2.8	3.5	2.8	1.1	0.0	-2.8	-4.9	-6.7	-8.6	-8.7
2.50	-1.3	0.4	3.5	5.0	4.5	2.8	1.6	-1.0	-4.3	-5.6	-8.1	-8.9
3.15	-1.0	-1.2	3.2	5.6	5.2	3.0	2.1	-1.6	-5.3	-6.0	-9.1	-9.5
4.00	-2.1	-2.7	1.5	4.1	4.5	2.6	1.1	-3.8	-6.0	-8.0	-10.4	-12.2
5.00	-2.5	-2.5	0.4	3.7	5.5	2.7	-1.2	-7.2	-10.9	-12.8	-14.6	-18.3
6.30	-4.2	-5.6	-3.2	0.9	4.9	1.8	-8.7	-15.1	-15.7	-12.3	-12.3	-11.0
8.00	-7.2	-9.3	-6.9	-4.0	3.6	-4.6	-13.1	-17.6	-16.7	-18.1	-21.3	-17.0
10.0	-4.3	-9.3	-2.9	1.7	5.4	-3.3	-13.9	-4.6	-9.3	-11.0	-12.1	-9.4
12.5	-4.3	-8.6	-2.3	2.0	4.3	-0.4	-9.3	-6.8	-6.7	-6.4	-12.5	-14.5
16.0	-9.1	-9.6	-3.8	-2.6	-2.1	-4.2	-12.0	-12.7	-12.4	-12.6	-16.7	-16.1
20.0	-11.4	-14.9	-4.0	-6.3	-7.3	-9.8	-20.4	-10.2	-11.5	-11.5	-13.1	-11.9
25.0	-7.3	-8.8	-3.6	-6.0	-2.2	-5.4	-18.7	-2.5	-9.4	-4.0	-10.1	-8.2
31.5	-14.7	-14.2	-6.0	-7.4	-6.8	-9.2	-12.1	-10.8	-11.0	-6.4	-11.3	-11.1
40.0	-9.3	-14.5	-12.5	-5.5	-5.0	-5.8	-11.4	-6.9	-7.1	-5.5	-7.8	-12.6
50.0	-12.5	-13.0	-15.8	-9.2	-9.7	-7.0	-13.1	-10.3	-10.9	-8.7	-16.5	-9.3
63.0	-11.3	-3.8	-8.7	-8.2	-9.0	-9.8	-12.3	-11.0	-9.1	-9.5	-11.2	-11.4

$OPTF_t$ ←	$NOSPL_t$ →									
23.0	-6.3	-5.4	-4.4	-4.0	-4.3	-6.2	-10.1	-12.6	-12.4	-15.7	-16.0

CONICAL NOZZLE (RUN NO = 109)

EMISSION ANGLE (RELATIVE TO JET EXHAUST) REFERENCED TO NOZZLE EXIT (DEGREES)

FREQ KHZ	PTF_t	10.	20.	30.	40.	50.	60.	70.	80.	90.	100.	110.
.250	-10.0	-9.6	-7.3	-14.7	-18.7	-20.3	-21.6	-23.6	-26.4	-18.9	-31.7	-32.6
.315	-17.7	-7.7	-6.9	-13.0	-16.3	-17.6	-19.0	-21.2	-24.0	-17.9	-28.3	-29.7
.400	-17.2	-7.1	-7.0	-12.3	-15.5	-16.7	-18.2	-20.4	-23.2	-17.4	-27.2	-28.9
.500	-14.9	-4.8	-5.5	-10.0	-12.3	-12.5	-15.1	-17.0	-20.0	-15.8	-22.7	-25.2
.630	-12.6	-2.8	-4.1	-7.6	-9.5	-9.4	-12.3	-14.2	-17.2	-13.9	-19.4	-22.2
.800	-10.3	-1.4	-2.8	-5.0	-6.5	-6.9	-8.8	-11.4	-14.2	-11.8	-15.7	-18.8
1.00	-8.3	-0.2	-1.9	-3.0	-4.0	-5.1	-6.8	-8.7	-11.2	-9.6	-12.7	-15.6
1.25	-6.5	0.6	-1.2	-1.5	-2.0	-3.4	-3.5	-6.3	-8.4	-7.7	-10.5	-12.8
1.60	-5.0	0.8	-0.1	-0.3	-0.4	-1.4	-2.1	-4.1	-6.1	-6.3	-9.5	-10.3
2.00	-4.1	-0.1	0.6	0.4	0.2	-0.6	-1.6	-2.2	-4.1	-5.2	-9.0	-8.3
2.50	-3.9	-2.8	-1.1	-0.6	0.4	-0.2	-1.1	-1.1	-3.0	-4.7	-8.2	-7.3
3.15	-3.6	-4.3	-2.8	-0.4	1.7	1.1	1.2	-0.5	-2.8	-4.2	-6.3	-7.8
4.00	-3.6	-5.2	-4.3	-1.7	1.3	0.4	1.1	-0.7	-3.4	-5.7	-9.1	-12.3
5.00	-4.1	-5.8	-7.1	-4.6	-0.4	0.2	2.0	-1.0	-3.3	-7.9	-12.5	-16.8
6.30	-5.4	-11.0	-10.5	-6.4	-2.1	0.1	1.6	-2.8	-8.2	-15.8	-22.6	-18.3
8.00	-6.7	-13.3	-11.7	-7.4	-3.1	-0.1	-0.3	-5.4	-14.8	-11.6	-12.9	-13.8
10.0	-7.9	-13.5	-12.3	-7.3	-2.7	-1.5	-1.9	-9.4	-9.2	-14.2	-19.8	-19.3
12.5	-9.2	-10.4	-10.7	-11.1	-3.6	-2.0	-4.2	-8.2	-18.7	-15.8	-18.3	-21.8
16.0	-13.8	-17.3	-21.1	-18.8	-11.2	-7.6	-10.0	-8.5	-14.7	-16.6	-20.6	-23.6
20.0	-8.8	-12.6	-16.3	-16.2	-7.5	1.0	-6.4	-9.3	-10.9	-15.6	-19.2	-24.2
25.0	-8.5	-13.9	-16.8	-7.6	-0.4	4.7	-7.1	-9.4	-10.7	-13.9	-15.8	-18.6
31.5	-11.6	-15.0	-12.9	-12.0	-7.3	-3.3	-7.3	-10.3	-13.6	-14.4	-21.0	-20.9
40.0	-12.7	-19.6	-22.5	-12.3	-10.2	-4.0	-12.0	-5.9	-17.7	-15.6	-20.3	-22.4
50.0	-15.9	-12.7	-22.6	-18.7	-13.0	-6.8	-15.0	-9.6	-19.8	-19.0	-24.9	-23.5
63.0	-16.3	-10.6	-16.9	-14.5	-11.6	-9.6	-14.1	-13.8	-22.2	-22.1	-25.3	-27.1

$OPTF_t$ ←	$NOSPL_t$ →									
23.5	-3.8	-4.6	-5.9	-5.6	-5.6	-6.3	-8.5	-11.2	-11.0	-15.0	-16.4

1/3 OCTAVE NTC (dB) WITH RESPECT TO INCIDENT SPL (NTC_i)

$M_J = 0.8$ $M_T = 0.08$

DAISY LOBE NOZZLE (RUN NO = 53)

EMISSION ANGLE (RELATIVE TO JET EXHAUST) REFERENCED TO NOZZLE EXIT (DEGREES)

FREQ KHZ	PTF_i	20.	30.	40.	50.	60.	70.	80.	90.	100.	110.
.250	-27.6	-20.1	-20.9	-27.0	-21.9	-25.7	-31.6	-29.0	-27.8	-35.0	-34.9
.315	-24.3	-16.5	-17.8	-23.4	-19.1	-22.3	-27.0	-25.6	-25.0	-30.4	-31.3
.400	-22.7	-15.1	-16.3	-21.7	-17.6	-20.6	-25.0	-23.9	-23.5	-28.5	-29.6
.500	-19.6	-10.9	-13.5	-18.1	-15.1	-17.5	-21.9	-20.9	-21.0	-24.2	-26.4
.630	-16.1	-7.3	-10.3	-14.3	-11.9	-14.0	-16.8	-17.3	-17.8	-20.1	-22.8
.800	-11.9	-3.4	-6.4	-10.4	-8.2	-9.6	-11.2	-13.0	-14.1	-14.7	-18.1
1.00	-8.5	-0.5	-4.0	-8.4	-5.4	-6.2	-7.2	-9.6	-11.3	-10.9	-14.4
1.25	-6.7	1.5	-2.5	-7.3	-3.3	-3.7	-4.3	-7.0	-9.5	-8.4	-11.9
1.60	-5.6	2.3	-1.4	-5.9	-2.0	-2.2	-2.9	-5.5	-8.6	-7.7	-10.6
2.00	-4.9	2.6	-0.8	-4.8	-0.8	-1.1	-2.0	-4.5	-8.1	-8.1	-10.2
2.50	-4.7	2.8	-1.0	-3.9	0.4	-0.6	-3.2	-4.1	-7.9	-9.5	-10.9
3.15	-3.6	1.8	-0.9	-2.2	3.1	0.6	-2.2	-3.0	-6.8	-9.0	-11.3
4.00	-1.1	-2.1	-2.7	-1.1	7.3	2.8	1.0	-1.4	-5.6	-8.8	-10.9
5.00	-0.6	-7.5	-8.7	-7.6	2.9	-3.0	-7.3	-8.8	-13.6	-15.8	-18.0
6.30	-9.0	-1.2	-7.1	-12.9	-0.5	-9.9	-14.0	-12.6	-12.2	-10.5	-14.9
8.00	-12.3	-4.2	-11.2	-18.2	-8.6	-12.5	-6.9	-9.8	-12.3	-10.8	-13.6
10.0	-11.1	-6.6	-11.6	-17.0	-7.0	-4.6	-7.0	-10.7	-16.8	-14.7	-14.4
12.5	-12.5	-8.9	-11.9	-16.6	-2.1	-4.5	-13.4	-18.2	-19.4	-15.5	-15.9
16.0	-12.5	-8.0	-11.0	-13.2	-2.4	-11.7	-20.5	-27.2	-19.0	-19.6	-22.0
20.0	-14.3	-8.3	-10.9	-9.8	-6.3	-15.0	-17.0	-17.6	-15.[illegible]	-21.4	-25.9
25.0	-13.8	-9.5	-12.6	-12.6	-10.7	-12.0	-9.5	-10.2	-18.4	-13.3	-22.4
31.5	-12.1	-8.8	-9.8	-11.7	-8.4	-8.9	-9.9	-12.5	-8.3	-11.3	-22.5
40.0	-14.2	-20.1	-14.3	-13.4	-10.2	-7.4	-10.1	-24.0	-12.[illegible]	-12.8	-21.7
50.0	-18.7	-19.5	-15.6	-21.2	-12.2	-13.6	-17.2	-17.2	-19.6	-17.2	-23.2
63.0	-11.2	-14.6	-17.0	-17.1	-2.6	-8.0	-5.4	-11.8	-20.8	-12.9	-21.6

$OPTF_i$	$NOSPL_i$									
24.1	-6.6	-9.4	-12.9	-7.3	-9.6	-11.7	-13.6	-15.5	-16.2	-19.3

CONICAL NOZZLE (RUN NO = 113)

EMISSION ANGLE (RELATIVE TO JET EXHAUST) REFERENCED TO NOZZLE EXIT (DEGREES)

FREQ KHZ	PTF_i	10.	20.	30.	40.	50.	60.	70.	80.	90.	100.	110.
.250	-19.3	-8.7	-8.8	-12.9	-16.0	-17.2	-23.5	-26.3	-31.6	-35.5	-38.7	-37.6
.315	-17.9	-6.6	-6.8	-10.5	-13.3	-14.6	-19.6	-23.1	-27.5	-30.1	-33.9	-33.3
.400	-16.5	-5.6	-6.2	-9.5	-12.3	-13.6	-18.4	-22.0	-26.1	-28.6	-32.4	-32.0
.500	-13.4	-3.2	-3.7	-6.9	-9.7	-10.7	-14.2	-18.7	-21.2	-21.4	-26.2	-27.0
.630	-10.9	-0.8	-1.5	-4.5	-7.0	-8.1	-11.1	-15.9	-17.9	-17.6	-22.6	-23.7
.800	-8.2	0.9	0.8	-1.7	-4.0	-5.4	-7.2	-12.6	-14.2	-13.8	-18.9	-19.9
1.00	-6.3	1.8	2.0	-0.0	-1.6	-3.2	-4.1	-9.1	-10.9	-10.3	-15.4	-16.4
1.25	-4.9	1.3	2.3	0.6	-0.1	-1.6	-2.6	-6.2	-8.0	-7.4	-12.3	-13.4
1.60	-3.9	0.2	2.2	1.3	0.9	0.1	-1.9	-3.7	-5.5	-5.1	-9.6	-10.8
2.00	-3.0	-0.7	0.9	1.2	2.2	1.5	-0.7	-1.7	-3.5	-3.6	-7.5	-8.8
2.50	-2.4	-2.8	-0.1	1.6	2.7	2.5	0.1	-0.9	-2.6	-3.4	-6.5	-8.3
3.15	-2.2	-5.2	-1.1	0.9	2.1	3.3	1.7	-0.7	-2.3	-3.4	-6.6	-9.5
4.00	-2.5	-4.1	-0.8	-1.7	0.0	3.6	1.3	-0.5	-2.0	-4.2	-8.9	-14.3
5.00	-3.2	-8.6	-4.2	-5.[illegible]	-2.6	3.3	2.5	0.2	-2.3	-6.7	-13.2	-20.9
6.30	-3.0	-8.7	-5.2	-3.7	-2.4	3.7	3.8	-0.3	-6.8	-12.4	-17.8	-16.7
8.00	-5.0	-10.2	-8.3	-9.6	-4.7	2.7	2.4	-6.3	-14.3	-10.6	-14.7	-18.8
10.0	-5.8	-13.5	-10.5	-11.4	-6.4	1.9	1.7	-6.5	-9.7	-14.4	-22.9	-19.6
12.4	-5.0	-11.7	-8.7	-11.6	-9.8	1.9	3.3	-5.4	-10.2	-13.9	-18.6	-22.5
16.0	-9.9	-20.5	-17.1	-15.1	-10.2	-1.3	-2.9	-13.2	-15.3	-23.1	-23.2	-25.3
20.0	-12.8	-17.0	-12.4	-17.3	-13.6	-3.7	-12.2	-10.5	-17.3	-14.6	-22.4	-23.6
25.0	-3.9	-9.5	-5.3	-6.3	-2.7	4.4	1.8	-3.3	-9.1	-7.7	-16.7	-18.0
31.5	-4.2	-18.0	-9.9	-6.3	-2.2	4.4	3.0	-5.2	-9.1	-9.0	-13.7	-22.7
40.0	-3.7	-12.6	-10.5	-3.9	-2.4	6.6	2.5	-4.0	-8.5	-8.4	-15.0	-17.0
50.0	-10.3	-11.2	-17.1	-13.6	-9.8	-0.3	-3.8	-12.2	-16.9	-14.0	-22.7	-25.4
63.0	-11.9	-7.7	-14.0	-15.3	-11.0	-3.4	-7.4	-13.2	-19.2	-18.1	-19.3	-29.1

$OPTF_i$	$NOSPL_i$									
24.7	-2.7	-2.5	-4.1	-4.6	-3.4	-4.7	-8.6	-11.1	-11.1	-15.7	-17.7

1/3 OCTAVE NTC (dB) WITH RESPECT TO TRANSMITTED SPL (NTC_t)

$M_J = 0.8$ $M_T = 0.08$

DAISY LOBE NOZZLE (RUN NO = 53)

FREQ KHZ	EMISSION ANGLE (RELATIVE TO JET EXHAUST) REFERENCED TO NOZZLE EXIT (DEGREES)										
	PTF_t	20.	30.	40.	50.	60.	70.	80.	90.	100.	110.
.250	-26.6	-19.1	-19.9	-26.0	-21.0	-24.7	-30.6	-28.0	-26.8	-34.0	-33.9
.315	-23.4	-15.6	-16.9	-22.0	-18.2	-21.4	-26.0	-24.7	-24.1	-29.5	-30.4
.400	-21.9	-14.3	-15.4	-20.9	-16.8	-19.6	-24.2	-23.1	-22.6	-27.6	-28.7
.500	-18.8	-10.1	-12.7	-17.3	-14.2	-16.7	-20.1	-20.1	-20.2	-23.4	-25.6
.630	-15.3	-6.6	-9.5	-13.0	-11.1	-13.2	-16.0	-16.6	-17.1	-19.3	-22.0
.800	-11.2	-2.6	-5.6	-9.0	-7.4	-8.8	-10.4	-12.3	-13.3	-14.0	-17.3
1.00	-8.0	0.4	-3.1	-7.6	-4.8	-5.4	-6.3	-8.7	-10.5	-10.0	-13.5
1.25	-5.5	2.6	-1.4	-6.1	-2.1	-2.8	-3.1	-5.8	-8.3	-7.2	-10.7
1.60	-4.7	3.1	-0.6	-5.2	-1.2	-1.4	-2.1	-4.7	-7.8	-6.9	-9.8
2.00	-4.2	3.3	-0.2	-4.1	-0.1	-0.4	-1.9	-3.8	-7.4	-7.4	-9.5
2.50	-4.4	2.3	-0.7	-3.7	0.6	-0.3	-2.9	-3.8	-7.6	-9.2	-10.6
3.15	-3.2	1.3	-0.6	-1.9	3.4	0.9	-1.9	-2.7	-6.5	-8.8	-11.0
4.00	-6.8	-1.8	-2.4	-0.8	7.6	3.1	1.0	-1.1	-6.3	-8.5	-10.6
5.00	-6.1	-7.0	-8.2	-7.4	3.4	-2.6	-6.9	-8.3	-13.1	-15.4	-17.6
6.30	-8.0	-4.2	-6.1	-11.0	0.5	-8.8	-13.6	-11.6	-11.2	-9.5	-13.9
8.00	-11.3	-3.5	-10.8	-17.6	-7.9	-11.8	-8.2	-9.1	-11.5	-10.1	-12.9
10.0	-14.8	-6.4	-11.3	-16.8	-6.8	-4.3	-7.3	-10.4	-18.6	-14.5	-14.1
12.5	-13.1	-8.5	-11.6	-16.2	-1.7	-4.1	-13.0	-17.8	-19.0	-15.1	-15.6
16.0	-12.5	-7.9	-11.0	-13.1	-2.3	-11.6	-20.4	-27.2	-18.9	-19.5	-22.0
20.0	-14.1	-8.1	-10.7	-9.6	-6.1	-16.8	-16.7	-17.4	-14.8	-21.2	-25.7
25.0	-13.7	-9.3	-12.4	-12.4	-10.5	-11.5	-9.7	-10.6	-18.2	-13.1	-22.2
31.5	-12.0	-8.7	-9.6	-11.5	-8.2	-8.6	-9.8	-12.4	-8.4	-11.2	-22.3
40.0	-14.1	-20.0	-14.2	-13.4	-10.2	-7.3	-10.1	-23.9	-12.5	-12.7	-21.7
50.0	-16.0	-19.4	-15.5	-21.1	-12.1	-13.5	-17.1	-17.1	-19.5	-17.1	-23.1
63.0	-11.0	-14.4	-16.8	-16.9	-2.4	-7.6	-5.2	-11.6	-20.6	-12.8	-21.4

$OPTF_t$ ← $NOSPL_t$ →

24.8 -5.8 -8.7 -12.1 -6.8 -6.6 -10.9 -12.8 -14.8 -15.5 -18.5

CONICAL NOZZLE (RUN NO = 113)

FREQ KHZ	EMISSION ANGLE (RELATIVE TO JET EXHAUST) REFERENCED TO NOZZLE EXIT (DEGREES)										
	PTF_t	10.	20.	30.	40.	50.	60.	70.	80.	90.	100.	110.
.250	-14.0	-3.4	-3.6	-7.7	-10.7	-11.9	-18.2	-21.0	-26.4	-30.2	-33.5	-32.3
.315	-15.0	-4.7	-4.9	-8.5	-11.4	-12.6	-17.7	-21.2	-25.5	-28.1	-31.9	-31.4
.400	-15.2	-4.9	-5.5	-8.7	-11.8	-12.8	-17.6	-21.2	-25.4	-27.8	-31.6	-31.2
.500	-12.8	-2.6	-3.2	-6.4	-9.1	-10.1	-13.6	-18.1	-20.6	-20.8	-25.6	-26.5
.630	-14.6	-4.6	-1.2	-4.2	-6.9	-7.9	-10.8	-15.6	-17.6	-17.4	-22.3	-23.4
.800	-8.2	0.9	0.9	-1.7	-3.9	-5.3	-7.1	-12.4	-14.2	-13.7	-18.8	-19.8
1.00	-6.2	1.8	2.0	-0.9	-1.6	-3.2	-4.1	-9.1	-10.9	-10.3	-15.4	-16.4
1.25	-4.9	1.3	2.3	0.9	0.1	-1.6	-2.0	-6.2	-8.0	-7.4	-12.3	-13.4
1.60	-3.9	0.2	2.2	1.3	0.9	0.1	-0.9	-3.7	-6.8	-5.1	-9.6	-10.8
2.00	-3.4	-0.7	0.9	1.2	2.2	1.8	-0.7	-1.7	-3.8	-3.6	-7.5	-8.8
2.50	-2.4	-2.7	-0.1	1.0	2.7	2.5	0.1	-0.9	-2.6	-3.4	-6.5	-8.3
3.15	-2.2	-5.2	-1.1	0.9	2.1	3.4	1.8	-0.7	-2.3	-3.3	-6.6	-9.4
4.00	-2.8	-4.1	-0.8	-1.7	0.0	3.0	1.3	-0.4	-2.0	-4.1	-8.9	-14.3
5.00	-3.2	-8.6	-4.2	-5.8	-2.6	3.3	2.6	0.2	-2.3	-6.7	-13.2	-20.9
6.30	-2.7	-8.3	-4.8	-3.3	-2.0	4.1	4.2	0.1	-6.4	-12.1	-17.4	-16.3
8.00	-4.9	-10.2	-8.2	-9.0	-4.6	2.8	2.4	-6.3	-14.3	-10.5	-14.6	-18.7
10.0	-5.5	-13.3	-10.2	-11.1	-6.1	2.1	1.9	-6.2	-9.4	-14.1	-22.6	-19.3
12.5	-4.8	-11.2	-8.2	-11.1	-9.3	2.5	3.8	-4.9	-9.7	-13.3	-18.1	-22.0
16.0	-9.9	-20.4	-17.0	-15.0	-10.1	-1.3	-2.9	-13.2	-15.3	-23.1	-23.2	-25.3
20.0	-12.8	-17.0	-12.4	-17.2	-13.6	-3.7	-12.1	-10.5	-17.3	-14.6	-22.4	-23.6
25.0	-3.8	-9.4	-5.2	-6.2	-2.6	4.8	1.9	-3.2	-9.0	-7.6	-16.6	-17.9
31.5	-4.0	-14.8	-9.7	-6.1	-2.0	4.8	3.2	-5.0	-9.0	-8.8	-13.5	-22.6
40.0	-3.6	-12.5	-10.4	-3.8	-2.3	6.6	2.6	-3.9	-8.4	-8.3	-14.9	-16.9
50.0	-10.1	-11.0	-16.9	-13.4	-9.6	-0.1	-3.6	-12.0	-16.7	-13.8	-22.5	-26.2
63.0	-11.8	-7.5	-13.9	-15.2	-10.8	-3.2	-7.3	-13.1	-19.1	-17.9	-19.2	-29.0

$OPTF_t$ ← $NOSPL_t$ →

25.6 -1.8 -1.6 -3.2 -3.8 -2.5 -3.8 -7.7 -10.2 -10.3 -14.9 -16.8

1/3 OCTAVE NTC (dB) WITH RESPECT TO INCIDENT SPL (NTC_i)

$M_J = 0$ $M_T = 0.16$

DAISY LOBE NOZZLE (RUN NO = 39)

FREQ KHZ	PTF_i	20.	30.	40.	50.	60.	70.	80.	90.	100.	110.
	EMISSION ANGLE (RELATIVE TO JET EXHAUST) REFERENCED TO NOZZLE EXIT (DEGREES)										
.250	-20.8	-10.3	-20.6	-23.9	-25.0	-26.5	-22.4	-20.1	-17.3	-22.0	-18.3
.315	-18.3	-8.8	-17.7	-20.4	-21.0	-22.1	-19.0	-17.3	-14.8	-18.7	-15.7
.400	-16.6	-8.0	-16.0	-18.4	-18.6	-19.6	-16.9	-15.5	-13.1	-16.6	-13.9
.500	-14.4	-6.2	-13.9	-15.7	-15.2	-15.0	-14.1	-13.4	-11.5	-14.2	-11.8
.630	-11.5	-4.2	-11.2	-12.4	-11.6	-11.0	-10.8	-10.6	-9.1	-11.1	-9.0
.800	-9.3	-3.9	-9.0	-9.3	-8.7	-8.4	-8.1	-8.2	-6.8	-8.1	-7.0
1.00	-7.8	-2.6	-6.8	-7.0	-6.9	-7.0	-6.5	-6.8	-5.5	-6.7	-5.9
1.25	-7.1	-1.6	-5.0	-5.7	-5.9	-6.1	-6.1	-6.2	-5.2	-6.7	-5.9
1.60	-7.0	-0.4	-3.9	-5.2	-5.6	-5.6	-6.3	-6.7	-5.6	-6.9	-6.0
2.00	-5.9	0.0	-2.3	-3.6	-4.1	-4.2	-5.0	-5.5	-4.8	-6.1	-5.1
2.50	-5.3	1.5	-2.1	-3.4	-3.0	-3.3	-3.8	-4.8	-4.9	-6.0	-5.6
3.15	-5.6	3.6	-4.2	-5.6	-2.9	-3.2	-3.9	-5.3	-6.2	-7.1	-6.6
4.00	-5.3	0.4	-6.7	-8.1	-3.0	-3.2	-4.5	-6.4	-7.6	-9.3	-8.4
5.00	-7.3	4.9	-3.0	-6.0	-5.9	-6.3	-8.4	-11.7	-13.6	-17.8	-13.7
6.30	-11.6	-0.4	-10.6	-11.2	-7.2	-8.1	-11.4	-14.9	-13.8	-13.0	-12.4
8.00	-11.9	-7.5	-14.8	-15.7	-14.0	-15.2	-13.2	-9.5	-7.5	-9.1	-8.4
10.0	-14.8	-7.1	-15.9	-14.7	-9.7	-9.0	-5.6	-8.5	-9.4	-11.8	-10.2
12.5	-8.2	-6.4	-4.5	-6.6	-7.9	-7.3	-5.0	-9.7	-6.8	-12.4	-7.8
16.0	-8.4	2.8	-7.8	-9.3	-5.2	-8.6	-8.0	-10.3	-11.7	-16.9	-10.3
20.0	-8.2	2.3	-13.2	-13.9	-8.3	-8.0	-2.8	-7.0	-8.4	-15.5	-9.2
25.0	-5.1	9.0	-3.1	-5.4	-5.2	-5.5	-4.2	-11.8	-11.5	-14.3	-11.0
31.5	-4.3	14.5	3.6	-3.6	-4.4	-4.1	-4.6	-14.5	-12.0	-12.1	-13.6
40.0	-2.7	8.2	-6.1	-7.4	-6.2	-5.9	-2.6	-14.2	-13.4	-13.2	-12.6
50.0	-5.9	4.7	-3.9	-10.1	-8.0	-6.1	-4.6	-14.3	-13.7	-13.1	-13.1
63.0	-9.4	2.7	-7.4	-11.5	-11.7	-9.8	-9.9	-18.5	-14.7	-13.5	-16.5
	$OPTF_i$ ←					$NOSPL_i$ →					
	21.0	-3.9	-16.7	-12.1	-11.5	-11.5	-11.5	-11.9	-10.4	-12.4	-11.1

CONICAL NOZZLE (RUN NO = 120)

FREQ KHZ	PTF_i	10.	20.	30.	40.	50.	60.	70.	80.	90.	100.	110.
	EMISSION ANGLE (RELATIVE TO JET EXHAUST) REFERENCED TO NOZZLE EXIT (DEGREES)											
.250	-14.8	0.6	-19.7	-30.3	-31.0	-29.2	-28.6	-40.0	-28.8	-25.8	-27.7	-23.2
.315	-12.6	4.7	-17.1	-25.8	-26.4	-24.9	-24.4	-32.4	-24.8	-21.8	-23.6	-19.9
.400	-15.7	1.1	-17.2	-23.8	-24.4	-22.9	-22.4	-30.0	-22.8	-20.0	-21.6	-18.2
.500	-15.6	-6.5	-14.4	-19.3	-19.8	-18.5	-17.9	-19.2	-17.8	-16.1	-17.6	-15.1
.630	-15.2	-14.9	-15.6	-15.3	-15.3	-14.5	-14.0	-14.2	-13.8	-12.2	-13.6	-11.7
.800	-11.9	-11.5	-11.4	-11.7	-11.8	-11.1	-10.7	-10.7	-10.6	-9.1	-10.3	-8.8
1.00	-9.4	-7.9	-7.8	-8.8	-8.8	-8.5	-8.2	-8.3	-8.2	-8.8	-8.1	-8.7
1.25	-7.1	-4.2	-4.3	-6.2	-6.9	-6.4	-6.0	-6.1	-6.2	-4.7	-5.9	-4.9
1.60	-5.5	-1.4	-2.1	-2.6	-3.9	-5.0	-4.4	-4.2	-4.8	-3.8	-4.9	-3.8
2.00	-4.1	1.2	-0.4	-0.9	-2.3	-3.6	-2.8	-2.5	-2.7	-2.7	-4.4	-3.2
2.50	-2.5	4.7	1.6	0.0	-0.4	-1.3	-0.6	-1.6	-2.1	-1.5	-3.6	-2.3
3.15	-1.5	7.9	3.1	2.0	1.5	0.7	0.1	-2.1	-2.0	-1.7	-3.4	-2.8
4.00	-0.4	11.4	4.9	2.8	2.4	1.6	1.1	-3.0	-1.2	-1.9	-3.2	-4.4
5.00	-0.5	13.5	4.3	2.8	2.4	1.2	0.0	-4.1	-4.1	-4.5	-6.7	-7.3
6.30	-0.6	14.6	3.9	2.8	2.4	-0.3	-4.0	-8.1	-9.9	-10.1	-12.0	-12.0
8.00	-0.4	11.2	-3.0	-3.5	-5.7	-9.5	-11.0	-15.5	-15.0	-11.8	-13.6	-12.4
10.0	-7.0	7.9	-9.4	-9.9	-6.9	-5.1	-6.4	-9.0	-11.8	-9.0	-10.8	-11.5
12.4	-11.6	1.9	-5.9	-10.2	-10.1	-8.4	-11.7	-16.7	-17.5	-13.9	-16.1	-16.4
16.0	-11.3	3.3	-9.9	-10.6	-8.6	-8.4	-12.3	-17.6	-14.1	-13.1	-15.3	-16.6
20.0	-9.1	7.2	-1.0	-6.8	-8.5	-10.0	-14.1	-22.3	-20.3	-17.1	-16.6	-13.5
25.0	-8.9	6.0	-4.1	-5.4	-3.8	-7.5	-17.3	-19.3	-12.7	-13.1	-13.4	-14.4
31.5	-10.3	4.1	-5.0	-9.6	-10.7	-9.1	-10.9	-11.4	-13.9	-13.7	-13.4	-14.4
40.0	-10.5	4.8	-10.0	-8.4	-11.1	-11.1	-11.5	-14.3	-20.9	-14.9	-13.9	-16.0
50.0	-12.5	3.5	-9.2	-11.4	-16.3	-17.1	-16.6	-20.6	-15.7	-13.6	-18.9	-22.9
63.0	-11.3	4.8	-12.3	-12.9	-14.2	-17.2	-14.4	-21.0	-15.0	-11.5	-14.3	-26.0
	$OPTF_i$ ←					$NOSPL_i$ →						
	23.1	4.1	-8.4	-9.5	-10.2	-10.9	-10.9	-12.3	-12.2	-10.7	-12.6	-11.5

1/3 OCTAVE NTC (dB) WITH RESPECT TO TRANSMITTED SPL (NTC_t)

$M_J = 0$ $M_T = 0.16$

DAISY LOBE NOZZLE (RUN NO = 39)

EMISSION ANGLE (RELATIVE TO JET EXHAUST) REFERENCED TO NOZZLE EXIT (DEGREES)

FREQ KHZ	PTF_t	20.	30.	40.	50.	60.	70.	80.	90.	100.	110.
.250	-18.8	-8.3	-18.6	-21.9	-23.0	-24.5	-20.4	-18.1	-18.3	-20.0	-16.4
.315	-15.8	-6.3	-15.3	-18.0	-18.6	-16.7	-16.5	-14.8	-12.4	-16.2	-13.2
.400	-13.6	-4.9	-13.0	-15.3	-15.9	-16.8	-13.9	-12.5	-10.1	-13.6	-10.9
.500	-11.1	-2.9	-10.6	-12.3	-11.9	-11.7	-10.8	-10.1	-8.2	-10.8	-8.5
.630	-7.4	-0.0	-7.1	-8.2	-7.5	-6.8	-6.6	-6.4	-5.0	-6.9	-4.9
.800	-5.8	0.0	-5.2	-5.4	-4.9	-4.6	-4.2	-4.4	-3.0	-4.2	-3.1
1.00	-5.0	0.2	-3.9	-4.2	-4.1	-4.1	-3.7	-3.9	-2.7	-3.9	-3.0
1.25	-5.1	1.1	-2.9	-3.7	-3.9	-4.0	-4.0	-4.1	-3.2	-4.7	-3.8
1.60	-5.3	1.3	-2.2	-3.4	-3.8	-3.5	-4.8	-5.0	-3.9	-5.2	-4.3
2.00	-4.6	1.3	-1.0	-2.3	-2.8	-2.5	-3.7	-4.3	-3.6	-4.8	-3.8
2.50	-4.5	2.3	-1.2	-2.0	-2.2	-2.5	-3.0	-4.0	-4.1	-5.2	-4.8
3.15	-5.1	4.0	-3.7	-5.2	-2.5	-2.8	-3.5	-4.9	-5.8	-6.7	-6.1
4.00	-5.2	6.5	-6.6	-8.0	-2.8	-3.1	-4.4	-6.3	-7.5	-9.2	-8.3
5.00	-5.2	6.9	-6.9	-3.9	-3.8	-4.2	-6.3	-9.7	-11.5	-15.7	-11.6
* 6.30	-3.5	7.1	-3.0	-3.7	0.3	-0.7	-3.9	-7.5	-6.4	-5.5	-4.9
8.00	-11.4	-7.0	-14.3	-15.2	-13.3	-14.7	-12.7	-9.0	-7.0	-8.6	-7.8
10.0	-10.3	-6.5	-15.4	-14.1	-9.1	-8.5	-8.0	-7.5	-8.8	-11.3	-9.6
12.5	-6.2	1.7	-2.4	-4.5	-5.8	-5.2	-3.1	-7.7	-4.7	-10.4	-5.8
16.0	-6.0	3.2	-7.4	-8.9	-4.8	-5.1	-7.6	-5.9	-11.3	-16.8	-9.9
20.0	-7.9	2.7	-12.8	-13.5	-8.0	-7.7	-2.5	-5.7	-8.0	-15.1	-8.9
25.0	-4.4	9.7	-2.4	-4.7	-4.5	-4.8	-3.4	-11.1	-10.8	-13.5	-10.3
31.5	2.0	16.9	5.9	-1.5	-2.1	-1.6	-2.2	-12.2	-9.7	-9.8	-11.2
40.0	-6.5	10.5	2.0	-5.3	-4.0	-3.5	-0.4	-12.1	-11.3	-10.9	-10.5
50.0	4.6	17.5	5.4	-0.5	1.2	6.2	4.0	-5.5	-5.1	4.7	-3.7
*63.0	8.1	12.8	4.0	-2.5	0.3	-3.2	-0.4	-8.2	-7.1	-5.1	-4.9

$OPTF_t$	← $NOSPL_t$ →								
23.5	-1.4	-8.2	-9.6	-9.0	-9.0	-9.0	-9.4	-7.9	-9.9	-8.6

CONICAL NOZZLE (RUN NO = 120)

EMISSION ANGLE (RELATIVE TO JET EXHAUST) REFERENCED TO NOZZLE EXIT (DEGREES)

FREQ KHZ	PTF_t	10.	20.	30.	40.	50.	60.	70.	80.	90.	100.	110.
.250	-8.2	11.2	-15.1	-25.7	-26.4	-24.6	-24.0	-35.4	-24.2	-21.2	-23.1	-18.6
.315	-8.0	9.3	-12.5	-21.1	-21.7	-20.2	-19.7	-27.8	-19.8	-17.2	-19.0	-15.2
.400	-11.6	5.8	-12.5	-19.1	-19.7	-18.2	-17.7	-25.3	-17.8	-15.3	-16.9	-13.5
.500	-11.0	4.0	-9.8	-14.8	-15.0	-13.9	-13.3	-14.6	-13.2	-11.5	-13.0	-10.5
.630	-10.8	-10.6	-11.3	-11.0	-11.0	-10.1	-9.7	-9.9	-9.4	-7.9	-9.3	-7.4
.800	-8.2	-7.8	-7.6	-8.0	-8.1	-7.4	-7.0	-7.0	-6.9	-5.4	-6.6	-5.1
1.00	-5.9	-4.4	-4.3	-5.0	-5.3	-5.0	-4.7	-4.7	-4.7	-3.2	-4.6	-3.2
1.25	-4.7	-1.9	-2.0	-2.8	-3.6	-4.0	-3.6	-3.7	-3.8	-2.3	-3.6	-2.6
1.60	-4.2	-0.1	-0.8	-1.3	-2.6	-3.7	-3.1	-2.9	-3.2	-2.3	-3.6	-2.5
2.00	-2.8	2.5	0.8	0.2	-1.1	-2.4	-1.2	-1.3	-1.4	-1.4	-3.1	-1.9
2.50	-2.1	5.2	2.0	1.0	0.1	-0.8	-0.2	-1.1	-1.6	-1.0	-3.1	-1.8
3.15	-1.2	8.2	3.5	2.3	1.9	1.1	0.5	-1.7	-1.7	-1.4	-3.1	-2.5
4.00	-0.4	11.4	4.9	2.6	2.4	1.6	1.1	-3.0	-1.2	-1.9	-3.2	-4.4
5.00	-0.4	13.6	4.4	2.9	2.5	1.3	0.1	-4.0	-4.0	-4.4	-6.6	-7.2
* 6.30	1.3	16.7	6.0	5.0	4.5	1.8	-2.6	-6.0	-7.8	-8.0	-9.9	-9.9
8.00	-5.0	11.6	-2.6	-3.4	-5.3	-9.5	-11.4	-15.1	-14.6	-11.4	-13.2	-12.0
10.0	-8.0	9.9	-7.4	-7.9	-4.9	-3.1	-4.4	-7.0	-9.5	-7.0	-8.8	-9.5
12.5	1.3	14.1	6.8	3.2	3.1	4.8	2.6	-5.7	-4.2	3.7	-4.2	-4.5
16.0	-14.9	3.7	-9.5	-10.2	-8.2	-8.0	-11.9	-17.2	-13.7	-12.7	-14.9	-16.2
20.0	-8.6	7.7	-0.5	-6.2	-7.9	-9.4	-13.6	-21.7	-19.8	-16.6	-16.0	-12.9
25.0	-8.4	6.5	-3.6	-4.9	-3.3	-7.4	-16.8	-18.8	-12.2	-12.6	-12.9	-13.9
31.5	-9.5	4.9	-4.2	-8.8	-9.9	-8.3	-10.1	-10.6	-13.1	-12.9	-12.6	-13.6
40.0	-9.6	5.5	-9.2	-7.7	-10.4	-10.4	-10.8	-13.7	-20.2	-14.2	-13.2	-16.3
50.0	-16.2	5.8	-7.0	-9.0	-13.9	-14.7	-14.3	-18.2	-13.3	-11.2	-16.6	-20.8
*63.0	-7.1	8.9	-8.4	-8.6	-9.9	-13.0	-10.1	-16.7	-11.0	-7.4	-9.6	-20.8

$OPTF_t$	← $NOSPL_t$ →								
27.1	8.1	-4.4	-5.5	-6.2	-7.0	-7.0	-8.3	-8.3	-6.8	-8.7	-7.6

1/3 OCTAVE NTC (dB) WITH RESPECT TO INCIDENT SPL (NTC_i)

$M_J = 0.4$ $M_T = 0.16$

DAISY LOBE NOZZLE (RUN NO = 48)

FREQ KHZ	PTF$_i$	10.	20.	30.	40.	50.	60.	70.	80.	90.	100.	110.
	EMISSION ANGLE (RELATIVE TO JET EXHAUST) REFERENCED TO NOZZLE EXIT (DEGREES)											
.250	-3.5	14.8	-22.1	-25.8	-26.2	-26.1	-26.4	-27.2	-30.8	-25.1	-29.3	-27.6
.315	-5.6	11.9	-18.5	-21.4	-22.0	-24.1	-23.0	-23.8	-26.7	-22.1	-25.9	-24.8
.400	-9.2	8.2	-17.6	-19.5	-20.1	-22.3	-21.2	-22.1	-24.8	-20.5	-24.1	-23.2
.500	-10.7	6.5	-14.1	-15.7	-16.5	-18.5	-18.6	-19.3	-21.3	-18.4	-21.2	-21.0
.630	-10.3	-6.4	-12.5	-12.1	-12.9	-15.4	-15.6	-16.2	-17.8	-15.7	-18.1	-18.3
.800	-13.1	-9.1	-8.4	-8.1	-9.1	-11.5	-12.0	-12.9	-13.8	-12.4	-15.0	-15.4
1.00	-10.2	-3.2	-5.1	-4.8	-5.8	-8.3	-9.2	-10.2	-10.6	-9.7	-12.4	-13.0
1.25	-8.0	-2.1	-3.0	-2.5	-3.4	-5.5	-7.0	-8.4	-8.2	-7.9	-10.6	-11.5
1.60	-6.3	-1.1	-1.9	-0.7	-1.2	-3.6	-5.2	-6.7	-6.3	-6.8	-9.1	-9.9
2.00	-5.3	-0.4	-1.8	0.2	0.3	-2.1	-4.0	-5.3	-5.1	-6.3	-8.3	-9.6
2.50	-4.6	0.6	-1.1	1.5	2.0	-0.6	-3.0	-3.7	-4.0	-5.8	-7.8	-9.0
3.15	-2.8	2.1	1.6	3.6	3.1	0.0	-2.4	-2.3	-3.3	-5.9	-8.0	-8.5
4.00	-2.8	4.0	2.9	4.4	3.2	-1.2	-3.8	-2.1	-4.3	-7.5	-11.0	-11.4
5.00	-4.4	3.9	3.4	3.8	1.2	-3.8	-7.4	-7.3	-9.4	-12.3	-18.2	-20.7
6.30	-4.5	4.7	5.3	4.3	-0.2	-7.1	-11.8	-14.1	-15.3	-14.1	-14.4	-15.3
8.00	-3.3	3.3	7.6	5.2	1.6	-8.2	-25.0	-16.2	-13.9	-11.8	-13.1	-12.6
10.0	-1.9	-0.3	7.4	5.8	4.9	1.3	-8.5	-6.7	-19.4	-15.6	-15.9	-9.5
12.5	-5.1	1.7	-0.2	1.6	2.7	-1.1	-10.5	-12.6	-11.3	-11.0	-17.4	-12.4
16.0	-7.7	1.7	-9.3	-3.0	0.4	-3.2	-12.2	-15.8	-15.2	-10.9	-15.8	-11.4
20.0	-6.5	1.7	-1.0	-0.6	0.5	-3.4	-14.9	-15.9	-10.4	-8.2	-14.0	-13.0
25.0	-5.7	4.4	4.2	-5.0	-0.7	-0.1	-10.0	-1.8	-8.8	-13.0	-15.9	-11.3
31.5	-5.3	3.5	2.1	2.1	0.1	-2.7	-7.9	-6.6	-12.6	-8.6	-16.2	-10.3
40.0	-7.1	-9.2	-7.1	-1.5	-0.8	-0.4	-8.9	-4.5	-5.1	-8.7	-17.0	-16.3
50.0	-6.2	-5.8	0.8	-0.9	-1.0	0.4	-14.9	-5.2	-12.0	-12.5	-19.6	-21.1
63.0	-8.4	-5.9	9.4	6.2	5.3	2.3	-11.7	-7.8	-16.2	-17.4	-19.8	-20.6
	OPTF$_i$ ← NOSPL$_i$ →											
	27.2	9.9	-4.1	-4.3	-5.2	-8.2	-11.4	-11.8	-12.8	-12.7	-15.6	-16.2

CONICAL NOZZLE (RUN NO = 96)

FREQ KHZ	PTF$_i$	10.	20.	30.	40.	50.	60.	70.	80.	90.	100.	110.
	EMISSION ANGLE (RELATIVE TO JET EXHAUST) REFERENCED TO NOZZLE EXIT (DEGREES)											
.250	-25.8	-20.5	-17.7	-23.5	-24.0	-22.8	-22.9	-27.8	-27.4	-23.9	-31.5	-26.5
.315	-22.8	-16.9	-15.7	-20.2	-20.7	-19.7	-19.9	-23.6	-23.7	-21.0	-27.1	-23.7
.400	-21.5	-15.5	-15.1	-18.9	-19.2	-18.4	-18.6	-22.1	-22.2	-19.6	-25.4	-22.5
.500	-18.3	-9.9	-13.1	-16.0	-16.9	-15.2	-15.8	-18.3	-18.5	-17.0	-21.1	-20.1
.630	-15.4	-7.3	-11.1	-13.2	-12.6	-12.3	-13.0	-15.1	-15.4	-14.4	-17.6	-17.6
.800	-12.7	-6.5	-6.7	-10.1	-10.0	-9.8	-10.2	-11.5	-12.2	-11.4	-13.7	-14.8
1.00	-10.3	-6.3	-6.5	-7.2	-7.5	-7.6	-7.7	-8.6	-10.0	-9.6	-10.5	-12.0
1.25	-8.1	-3.5	-3.7	-5.0	-5.2	-5.1	-5.2	-6.5	-8.9	-8.3	-8.6	-9.9
1.60	-6.4	-0.4	-2.2	-3.2	-3.0	-2.7	-3.2	-5.6	-7.8	-6.8	-7.5	-8.2
2.00	-5.0	2.9	-0.8	-1.8	-1.3	-1.1	-2.0	-5.3	-6.4	-5.9	-7.0	-7.1
2.50	-3.9	5.4	0.7	-1.0	-0.3	0.0	-1.8	-4.4	-5.4	-6.0	-6.4	-6.8
3.15	-3.3	6.2	1.6	-0.6	-0.0	0.8	-0.8	-2.9	-5.2	-6.2	-6.6	-6.7
4.00	-3.0	6.4	3.4	0.2	0.1	0.6	-0.1	-1.7	-5.2	-7.2	-7.2	-8.4
5.00	-2.8	4.0	3.9	0.1	0.2	1.8	0.5	0.5	-6.3	-9.2	-8.8	-12.3
6.30	-3.4	3.9	3.7	-1.2	-0.5	2.4	1.4	-2.7	-11.9	-17.4	-21.8	-19.5
8.00	-7.0	4.9	-1.6	-9.6	-6.3	1.0	-2.1	-16.4	-19.3	-17.8	-16.1	-11.6
10.0	-7.8	-0.9	-2.7	-7.9	-3.0	0.8	-8.6	-14.3	-16.2	-14.9	-17.4	-15.6
12.4	-5.8	-4.5	-3.7	-8.9	-4.6	0.2	-11.1	-13.1	-18.3	-20.2	-20.8	-16.6
16.0	-8.1	-1.8	-4.1	-3.8	-1.2	-1.3	-5.6	-11.3	-21.2	-16.8	-19.7	-14.0
20.0	-9.7	-2.5	-2.4	-4.8	-2.8	-4.6	-16.7	-17.8	-22.8	-17.8	-24.3	-16.0
25.0	-9.8	-6.5	-2.3	-2.8	-1.1	-4.4	-10.1	-15.2	-17.4	-14.8	-22.0	-14.8
31.5	-8.2	-6.3	-7.3	-0.9	-0.6	-4.1	-7.8	-7.8	-15.2	-16.9	-24.0	-18.2
40.0	-8.7	-4.3	-8.2	-1.2	-1.2	-2.2	-8.5	-10.8	-14.5	-19.4	-18.6	-18.7
50.0	-10.1	-6.2	-13.1	-3.9	-2.0	-3.5	-8.8	-13.3	-16.3	-22.2	-21.5	-20.0
63.0	-12.9	-5.2	-7.2	-10.8	-8.6	-6.6	-11.2	-17.2	-17.6	-18.8	-18.7	-26.3
	OPTF$_i$ ← NOSPL$_i$ →											
	21.9	-4.8	-6.4	-8.4	-7.9	-6.9	-6.4	-10.9	-13.3	-12.6	-14.1	-14.7

1/3 OCTAVE NTC (dB) WITH RESPECT TO TRANSMITTED SPL (NTC_t)

$M_J = 0.4$ $M_T = 0.16$

DAISY LOBE NOZZLE (RUN NO =)

EMISSION ANGLE (RELATIVE TO JET EXHAUST) REFERENCED TO NOZZLE EXIT (DEGREES)

FREQ KHZ	PTF_t	10.	20.	30.	40.	50.	60.	70.	80.	90.	100.	110.
.250	-3.3	14.1	-21.8	-25.7	-26.1	-28.0	-26.2	-27.1	-30.7	-25.0	-29.2	-27.5
.315	-6.4	12.1	-18.4	-21.3	-21.9	-24.1	-22.8	-23.6	-26.5	-21.9	-25.7	-24.6
.400	-9.0	8.5	-17.4	-19.3	-19.9	-22.1	-21.0	-21.8	-24.6	-20.3	-23.9	-23.0
.500	-14.5	6.7	-13.9	-15.5	-16.3	-16.8	-16.4	-19.1	-21.1	-18.2	-21.0	-20.8
.630	-16.1	-5.7	-12.3	-11.9	-12.7	-15.2	-15.3	-16.0	-17.6	-15.5	-17.8	-18.0
.800	-12.6	-4.6	-8.8	-7.7	-8.7	-11.1	-11.6	-12.4	-13.4	-12.0	-14.5	-14.9
1.00	-9.5	-2.5	-4.4	-4.1	-5.1	-7.6	-8.5	-9.5	-9.9	-9.0	-11.7	-12.3
1.25	-7.2	-1.2	-2.1	-1.7	-2.5	-4.9	-6.1	-7.5	-7.3	-7.0	-9.8	-10.6
1.60	-5.4	-0.2	-1.0	0.2	-0.3	-2.7	-4.3	-5.8	-5.4	-5.9	[illegible]	-7.0
2.00	-4.5	0.3	-1.1	0.9	1.0	-1.3	-3.3	-4.6	-4.4	-5.6	[illegible]	-6.9
2.50	-3.6	1.0	-0.7	1.9	2.4	-0.2	-2.6	-3.3	-3.6	-5.4	[illegible]	-6.6
3.15	-2.7	2.3	1.6	3.0	3.2	0.1	-2.3	-2.2	-3.2	-5.8	-7.[illegible]	-6.4
4.00	-2.5	4.3	3.1	4.7	3.[illegible]	-0.9	-3.8	-1.9	-4.0	-7.2	-10.7	-11.2
5.00	-3.5	4.9	4.3	4.8	2.2	-2.9	-6.5	-6.4	-8.5	-11.4	-17.2	-19.7
6.30	-3.6	5.5	6.2	5.2	0.6	-6.2	-11.9	-13.2	-14.5	-13.2	-13.6	-14.5
8.00	-3.9	3.7	7.9	5.5	1.8	-7.9	-24.6	-15.9	-13.5	-11.5	-12.7	-12.3
10.0	-1.7	-0.2	7.6	5.9	5.0	1.4	-8.3	-6.5	-19.2	-15.4	-15.7	-9.4
12.5	-4.5	1.9	-0.1	1.8	2.9	-1.0	-10.3	-12.4	-11.1	-10.9	-17.2	-12.2
16.0	-7.7	1.8	-9.2	-3.0	0.5	-3.1	-12.2	-15.9	-15.1	-10.9	-15.7	-11.4
20.0	-6.5	1.8	-0.9	-0.5	0.6	-3.3	-14.8	-15.5	-10.3	-8.1	-14.0	-13.0
25.0	-5.7	4.5	0.3	-5.9	-0.7	-0.0	-10.0	-1.8	-8.8	-12.9	-15.9	-11.3
31.5	-6.2	3.6	2.2	2.2	0.2	-2.6	-7.8	-6.5	-12.5	-8.5	-16.1	-10.2
40.0	-7.0	-9.2	-7.1	-1.4	-0.8	-0.3	-6.8	-4.4	-5.0	-8.6	-16.9	-10.3
50.0	-6.1	-5.7	0.8	-0.5	-1.0	0.4	-14.8	-5.2	-1.9	-12.4	-19.5	-21.0
63.0	0.3	-5.2	18.1	7.0	6.0	3.0	-11.1	-7.1	-15.4	-16.8	-19.3	-19.8

$OPTF_t$ ← $NOSPL_t$ →

27.4 10.2 -3.9 -4.0 -4.9 -7.9 -11.1 -11.6 -12.5 -12.4 -15.3 -18.9

CONICAL NOZZLE (RUN NO = 96)

EMISSION ANGLE (RELATIVE TO JET EXHAUST) REFERENCED TO NOZZLE EXIT (DEGREES)

FREQ KHZ	PTF_t	10.	20.	30.	40.	50.	60.	70.	80.	90.	100.	110.
.250	-24.7	-19.4	-16.6	-22.3	-22.9	-21.7	-21.8	-26.4	-26.3	-22.8	-31.4	-25.3
.315	-21.7	-15.8	-14.7	-19.2	-19.6	-18.6	-18.8	-22.6	-22.6	-19.9	-26.0	-22.7
.400	-20.5	-14.5	-14.1	-17.8	-18.2	-17.3	-17.5	-21.1	-21.2	-18.6	-24.4	-21.4
.500	-17.2	-8.8	-12.0	-14.9	-14.9	-14.1	-14.7	-17.2	-17.5	-16.0	-20.0	-19.1
.630	-14.4	-6.2	-10.1	-12.1	-11.8	-11.2	-11.9	-14.0	-14.3	-13.3	-16.5	-16.6
.800	-11.9	-5.7	-7.9	-9.3	-9.2	-9.0	-9.4	-10.7	-11.3	-10.6	-12.9	-13.9
1.00	-9.7	-5.7	-5.9	-6.7	-7.0	-7.0	-7.1	-8.0	-9.4	-9.0	-10.0	-11.4
1.25	-7.7	-3.0	-3.2	-4.5	-4.7	-4.7	-4.7	-6.0	-8.4	-7.9	-8.1	-9.4
1.60	-6.1	-0.2	-2.0	-3.0	-2.8	-2.8	-2.9	-5.4	-7.6	-6.6	-7.3	-8.0
2.00	-4.8	3.0	-0.7	-1.7	-1.2	-1.0	-2.0	-5.3	-6.4	-5.8	-7.0	-7.0
2.50	-3.9	5.4	0.7	-1.0	-0.3	0.1	-1.6	-4.4	-5.4	-6.0	-6.4	-6.9
3.15	-3.2	6.3	1.6	-0.0	0.0	0.8	-0.5	-2.9	-5.1	-6.1	-6.5	-6.7
4.00	-2.9	6.4	3.4	0.2	0.2	0.6	-0.1	-1.7	-5.2	-7.2	-7.2	-8.4
5.00	-2.8	4.0	3.9	0.2	0.2	1.5	1.5	0.6	-6.3	-9.2	-8.8	-12.3
6.30	-2.3	5.0	4.8	-0.1	0.6	3.5	2.6	-1.6	-10.8	-16.3	-20.7	-18.4
8.00	-0.9	1.0	-1.4	-9.0	-6.2	1.1	-2.0	-16.3	-19.2	-17.7	-16.0	-11.5
10.0	-7.4	-0.4	-2.3	-7.4	-3.2	1.2	-8.1	-13.9	-15.7	-14.5	-17.0	-15.1
12.5	-8.5	-4.2	-3.4	-8.0	-4.2	0.6	-10.8	-17.3	-17.9	-19.5	-20.5	-15.3
16.0	-8.0	-1.8	-4.0	-3.8	-1.1	-1.2	-9.6	-11.3	-21.1	-16.4	-19.6	-13.9
20.0	-9.6	-2.4	-2.3	-4.6	-2.3	-4.5	-16.6	-17.6	-22.7	-17.4	-24.1	-15.8
25.0	-8.9	-3.4	-2.2	-2.7	-1.0	-4.2	-10.6	-15.1	-17.3	-14.7	-21.8	-14.7
31.5	-7.9	-5.9	-7.0	-0.0	-0.3	-3.8	-7.5	-7.5	-14.9	-16.6	-23.6	-17.9
40.0	-8.5	-4.1	-8.0	-1.4	-1.0	-2.0	-6.3	-10.6	-14.3	-19.2	-18.4	-18.5
50.0	-9.5	-5.9	-12.8	-3.0	-1.7	-3.3	-8.5	-13.1	-1[illegible]1	-22.0	-21.2	-19.8
63.0	-12.7	-5.0	-7.0	-10.6	-8.4	-6.4	-10.9	-17.0	-1[illegible]	-18.6	-18.4	-20.1

$OPTF_t$ ← $NOSPL_t$ →

22.7 -3.1 -5.0 -7.0 -7.1 -6.0 -7.6 -10.0 -12.8 -11.8 -13.3 -13.9

1/3 OCTAVE NTC (dB) WITH RESPECT TO INCIDENT SPL (NTC_i)

$M_J = 0.6$ $M_T = 0.16$

DAISY LOBE NOZZLE (RUN NO = 36)

EMISSION ANGLE (RELATIVE TO JET EXHAUST) REFERENCED TO NOZZLE EXIT (DEGREES)

FREQ KHZ	PTF_i	20.	30.	40.	50.	60.	70.	80.	90.	100.	110.
.250	-22.2	-16.1	-20.8	-17.1	-14.4	-24.6	-24.4	-24.5	-24.6	-28.3	-25.6
.315	-19.9	-13.6	-18.9	-15.8	-12.3	-20.8	-20.9	-21.8	-21.7	-24.8	-23.1
.400	-18.6	-12.6	-17.8	-14.9	-11.2	-19.1	-19.3	-20.1	-20.2	-23.0	-21.8
.500	-16.8	-10.5	-17.0	-14.2	-9.6	-18.8	-18.3	-17.8	-18.5	-19.9	-19.9
.630	-14.8	-8.3	-15.8	-13.0	-7.0	-12.6	-13.3	-14.8	-16.3	-16.8	-17.5
.800	-11.9	-5.3	-13.0	-10.9	-5.6	-9.1	-11.2	-12.2	-12.7	-13.8	-15.3
1.00	-10.1	-2.8	-10.7	-9.5	-4.7	-7.0	-8.5	-10.7	-9.9	-11.7	-13.6
1.25	-8.7	-4.8	-9.2	-8.1	-3.4	-6.2	-7.4	-9.7	-8.2	-10.4	-11.9
1.60	-7.0	0.9	-7.7	-6.2	-1.0	-5.2	-5.8	-8.9	-6.8	-8.8	-10.7
2.00	-5.6	2.5	-5.7	-4.7	0.1	-2.9	-4.3	-7.6	-5.9	-7.4	-9.3
2.50	-4.9	3.4	-2.9	-2.1	1.8	-0.6	-3.1	-6.1	-5.6	-6.6	-7.2
3.15	-3.7	3.3	-0.8	-0.9	1.3	0.4	-3.0	-5.8	-6.4	-7.1	-7.4
4.00	-3.6	3.4	0.9	0.4	1.8	0.3	-4.3	-7.1	-7.3	-8.7	-11.1
5.00	-4.0	3.1	-0.8	0.4	3.0	-1.0	-5.5	-8.3	-11.5	-12.6	-14.6
6.30	-7.7	3.1	-6.0	-5.3	-1.2	-9.4	-12.3	-13.5	-15.4	-10.9	-10.6
8.00	-0.6	9.0	2.6	0.4	-6.4	-14.4	-11.6	-13.3	-17.5	-13.1	-15.1
10.0	2.9	11.1	12.7	10.1	1.8	-9.2	-6.6	-10.5	-14.6	-11.1	-9.3
12.5	-1.6	4.1	7.6	6.5	0.3	-8.1	-13.7	-19.7	-20.7	-17.0	-14.4
16.0	-4.2	2.1	4.3	3.3	-1.7	-7.9	-11.6	-13.5	-13.4	-9.2	-13.0
20.0	-8.8	-2.3	-2.3	-2.1	-6.3	-11.1	-9.5	-13.1	-18.0	-13.5	-10.6
25.0	-4.3	-5.7	6.5	4.6	-0.8	-3.8	-5.5	-10.9	-10.1	-7.7	-6.6
31.5	-1.6	-2.8	5.9	6.4	0.6	-3.7	-2.1	-10.0	-8.7	-5.3	-4.0
40.0	-1.5	-0.6	6.8	7.1	3.2	-2.7	-5.0	-5.5	-8.7	-4.7	-2.8
50.0	-2.6	-10.0	3.4	5.9	2.9	-0.9	-3.4	-8.6	-12.5	-5.9	-5.9
63.0	-7.6	-13.8	-1.6	2.2	-5.4	-12.5	-13.3	-15.7	-23.5	-12.9	-15.4

$OPTF_i$ ← $NOSPL_i$ →

22.6	-3.8	-5.7	-5.9	-5.5	-9.0	-11.4	-13.6	-12.8	-14.2	-15.2

CONICAL NOZZLE (RUN NO = 108)

EMISSION ANGLE (RELATIVE TO JET EXHAUST) REFERENCED TO NOZZLE EXIT (DEGREES)

FREQ KHZ	PTF_i	10.	20.	30.	40.	50.	60.	70.	80.	90.	100.	110.
.250	-26.9	-13.3	-21.8	-25.2	-25.4	-26.3	-26.5	-34.6	-31.7	-26.1	-28.5	-37.9
.315	-24.1	-11.5	-18.0	-21.2	-22.9	-24.4	-22.6	-26.6	-27.2	-22.8	-25.7	-33.4
.400	-22.8	-10.5	-16.9	-19.6	-21.7	-23.8	-21.0	-25.4	-25.8	-21.4	-24.3	-31.7
.500	-19.7	-9.2	-11.8	-15.3	-20.0	-22.9	-17.5	-20.8	-20.6	-18.6	-21.8	-27.2
.630	-16.9	-7.7	-8.6	-11.9	-18.5	-22.6	-14.2	-17.4	-17.0	-15.8	-19.1	-23.6
.800	-13.8	-5.7	-6.0	-8.8	-14.7	-18.2	-10.3	-14.1	-13.2	-12.3	-16.4	-19.6
1.00	-11.3	-3.9	-4.6	-6.7	-11.7	-14.6	-7.3	-11.3	-10.3	-9.6	-13.9	-16.1
1.25	-9.2	-2.5	-2.6	-4.7	-9.3	-11.7	-4.9	-8.6	-8.4	-7.6	-11.8	-13.1
1.60	-7.3	-0.9	-0.7	-2.[illegible]	-6.7	-9.1	-3.3	-6.1	-7.4	-6.7	-9.9	-10.4
2.00	-5.7	0.7	0.8	[illegible]	-4.4	-6.9	-2.1	-3.7	-6.3	-6.1	-8.0	-8.1
2.50	-4.7	1.3	1.7	[illegible]	-2.7	-6.2	-1.0	-2.2	-4.9	-5.3	-6.9	-7.3
3.15	-4.3	0.7	3.1	1.[illegible]	-2.0	-6.3	0.0	-1.7	-4.4	-5.3	-6.9	-8.4
4.00	-4.5	-0.5	2.9	0.[illegible]	-2.8	-4.4	0.5	-3.2	-4.8	-7.8	-9.5	-13.2
5.00	-4.4	-0.9	2.6	1.2	-0.8	-1.5	0.0	-4.4	-8.9	-11.2	-13.8	-16.2
6.30	-5.2	-3.5	1.3	-1.2	-1.8	-0.3	0.9	-6.2	-11.3	-12.9	-21.6	-20.4
8.00	-6.7	-7.1	-2.0	-4.8	-3.3	0.1	-0.9	-11.3	-12.6	-11.8	-14.3	-15.1
10.0	-6.9	-7.4	-3.8	-5.2	-1.8	1.4	-4.4	-12.3	-10.6	-14.5	-19.3	-24.6
12.5	-5.6	-5.9	-2.0	-8.2	-3.4	4.0	-3.5	-13.7	-13.6	-16.2	-21.1	-20.2
16.0	-9.3	-8.9	-5.7	-6.2	-4.3	-1.5	-4.2	-13.6	-14.5	-16.3	-23.7	-22.8
20.0	-7.8	-7.7	-3.2	-3.9	-1.1	-0.7	-7.8	-19.0	-16.3	-18.2	-31.6	-22.7
25.0	-2.2	-3.7	3.0	1.2	5.6	5.6	-3.9	-10.7	-8.6	-13.9	-20.1	-17.7
31.5	-5.4	-14.9	-1.1	-1.1	1.8	3.1	-9.1	-7.9	-10.8	-17.1	-29.4	-24.1
40.0	-8.8	-13.5	-10.3	-6.4	-3.8	1.5	-5.9	-11.8	-13.8	-19.8	-28.6	-29.0
50.0	-9.1	-13.9	-19.7	-8.3	-0.9	0.7	-12.5	-18.7	-18.7	-21.9	-30.7	-28.8
63.0	-3.2	-7.0	-7.8	-6.8	2.3	6.4	-10.4	-21.0	-17.8	-20.9	-26.7	-26.6

$OPTF_i$ ← $NOSPL_i$ →

21.7	-6.2	-5.8	-7.3	-8.4	-7.0	-7.9	-11.7	-13.2	-12.7	-16.0	-17.6

1/3 OCTAVE NTC (dB) WITH RESPECT TO TRANSMITTED SPL (NTC_t)

$M_J = 0.6$ $M_T = 0.16$

DAISY LOBE NOZZLE (RUN NO= 36)

EMISSION ANGLE (RELATIVE TO JET EXHAUST) REFERENCED TO NOZZLE EXIT (DEGREES)

FREQ KHZ	PTF_t	20.	30.	40.	50.	60.	70.	80.	90.	100.	110.
.250	-21.6	-15.5	-20.2	-16.8	-13.8	-20.0	-23.8	-23.9	-23.9	-27.7	-25.0
.315	-15.2	-13.0	-18.3	-15.2	-11.7	-20.2	-21.3	-20.9	-21.1	-24.1	-22.5
.400	-18.0	-12.8	-17.2	-14.2	-10.8	-18.4	-18.7	-19.4	-19.6	-22.4	-21.2
.500	-16.1	-9.8	-16.4	-13.0	-8.9	-15.2	-15.7	-16.9	-17.9	-19.3	-19.2
.630	-13.9	-7.7	-15.2	-12.4	-7.8	-12.0	-12.7	-14.2	-15.7	-16.2	-16.9
.800	-11.2	-4.6	-12.4	-10.3	-5.0	-8.5	-9.6	-11.6	-12.1	-13.1	-14.7
1.00	-9.4	-2.1	-10.1	-8.9	-4.1	-6.3	-7.8	-10.1	-9.2	-11.1	-12.9
1.25	-8.1	-0.2	-8.6	-7.8	-2.8	-5.6	-6.8	-8.1	-7.6	-9.9	-11.4
1.60	-6.4	1.5	-7.1	-5.8	-0.3	-4.5	-5.2	-6.3	-6.2	-8.2	-10.1
2.00	-5.2	2.9	-5.2	-4.3	0.6	-2.4	-3.5	-7.2	-5.5	-7.0	-8.9
2.50	-3.8	3.6	-2.8	-2.0	2.0	-0.4	-2.9	-5.9	-5.4	-6.4	-7.0
3.15	-3.7	3.4	-0.7	-0.9	1.3	0.4	-2.9	-5.7	-6.4	-7.0	-7.3
4.00	-3.4	3.5	1.0	1.0	1.9	0.4	-4.2	-7.0	-7.2	-8.6	-11.0
5.00	-3.6	3.3	-0.6	0.0	3.3	-0.6	-5.3	-8.1	-11.3	-12.4	-14.4
6.30	-6.5	4.3	-4.8	-4.2	-0.1	-8.2	-11.1	-12.4	-14.2	-9.7	-9.4
8.00	-1.3	0.4	2.9	1.2	-6.0	-14.1	-11.3	-13.0	-17.2	-12.7	-14.8
10.0	5.0	13.1	14.8	12.2	3.8	-7.1	-4.5	-8.4	-12.5	-9.0	-7.2
12.5	-1.3	4.4	8.0	6.8	0.6	-7.8	-13.4	-19.4	-20.3	-16.7	-14.1
16.0	-3.3	3.8	5.2	4.2	-0.8	-6.9	-10.7	-12.5	-12.6	-8.3	-12.0
20.0	-6.6	-2.1	-2.1	-1.8	-6.1	-10.9	-5.3	-17.9	-17.8	-13.3	-10.4
25.0	-3.6	-5.2	1.0	5.1	-0.3	-3.3	-5.0	-10.4	-9.6	-7.2	-6.1
31.5	-6.8	-1.2	6.7	7.2	1.4	-2.5	-1.3	-9.2	-7.9	-4.5	-3.2
40.0	-6.4	-5.6	7.7	8.3	4.3	-1.5	-4.4	-4.3	-7.6	-3.6	-1.6
50.0	-6.3	-7.7	5.6	8.1	5.2	1.4	-1.2	-6.4	-10.3	-3.6	-3.7
63.0	-7.1	-13.3	-1.1	2.7	-4.9	-11.6	-12.8	-15.2	-22.9	-12.4	-14.8

$OFTF_t$ ← $NOSPL_t$ →

23.2 -3.2 -5.1 -5.3 -4.9 -8.4 -10.4 -13.1 -12.2 -13.6 -14.6

CONICAL NOZZLE (RUN NO = 108)

EMISSION ANGLE (RELATIVE TO JET EXHAUST) REFERENCED TO NOZZLE EXIT (DEGREES)

FREQ KHZ	PTF_t	10.	20.	30.	40.	50.	60.	70.	80.	90.	100.	110.
.250	-24.8	-11.3	-19.7	-23.1	-23.4	-24.2	-24.4	-28.5	-29.7	-24.0	-26.4	-38.8
.315	-22.7	-10.1	-16.6	-19.8	-21.8	-23.0	-21.2	-25.2	-25.8	-21.4	-24.3	-32.0
.400	-21.8	-9.5	-16.0	-18.7	-20.8	-22.6	-20.1	-24.1	-24.5	-20.8	-23.3	-30.8
.500	-18.9	-8.4	-11.0	-14.5	-19.2	-22.1	-16.7	-20.0	-19.8	-17.8	-21.0	-26.4
.630	-16.4	-7.1	-8.1	-11.3	-18.0	-22.1	-13.7	-16.8	-16.4	-15.3	-18.5	-23.1
.800	-13.6	-5.5	-5.8	-8.6	-14.5	-18.0	-10.1	-13.9	-13.0	-12.1	-16.2	-19.4
1.00	-11.2	-3.8	-4.5	-6.5	-11.6	-14.5	-7.1	-11.1	-10.2	-9.4	-13.8	-16.0
1.25	-9.1	-2.3	-2.5	-4.6	-9.2	-11.6	-4.8	-8.5	-8.3	-7.5	-11.7	-13.0
1.60	-7.3	-0.9	-0.6	-2.4	-6.7	-9.0	-3.2	-6.0	-7.3	-6.7	-9.9	-10.4
2.00	-5.6	0.8	0.9	-0.4	-4.3	-6.8	-2.0	-3.7	-6.3	-6.1	-8.0	-8.1
2.50	-4.6	1.3	1.8	0.3	-3.7	-6.2	-1.0	-2.2	-4.8	-5.3	-6.9	-7.3
3.15	-4.8	0.8	3.2	1.1	-2.9	-6.3	0.6	-1.7	-4.4	-5.2	-6.9	-6.4
4.00	-4.5	-0.5	2.9	0.8	-2.8	-4.4	0.5	-3.2	-4.8	-7.8	-9.5	-13.2
5.00	-4.3	-0.8	2.6	1.3	-0.8	-1.5	0.6	-4.4	-5.8	-11.1	-13.7	-16.2
6.30	-4.9	-3.2	1.6	-0.9	-1.5	-0.0	1.2	-5.9	-11.0	-12.6	-21.3	-20.1
8.00	-6.6	-7.1	-2.0	-4.7	-3.2	0.2	-0.8	-11.3	-12.5	-11.8	-14.3	-15.0
10.0	-6.8	-7.3	-3.7	-5.0	-1.7	1.6	-4.3	-12.2	-10.4	-14.4	-19.2	-24.5
12.5	-8.3	-5.6	-1.6	-2.8	-3.0	4.3	-3.1	-13.4	-13.2	-15.8	-20.7	-19.8
16.0	-9.0	-8.8	-5.7	-6.2	-4.3	-1.5	-4.2	-13.6	-14.5	-16.2	-23.7	-22.8
20.0	-7.8	-7.6	-3.1	-3.9	-1.1	-0.7	-7.7	-19.0	-16.3	-18.1	-31.6	-22.7
25.0	-2.2	-3.7	3.1	1.3	5.6	5.7	-3.8	-10.7	-8.5	-13.9	-20.0	-17.7
31.5	-5.3	-14.8	-1.0	-1.0	1.9	3.2	-4.0	-7.8	-10.4	-17.0	-29.3	-24.0
40.0	-8.5	-13.5	-10.2	-6.4	-3.4	1.5	-5.8	-11.8	-13.5	-19.8	-28.6	-20.0
50.0	-6.0	-13.8	-15.7	-8.2	-0.8	0.7	-12.5	-18.6	-18.6	-21.8	-30.6	-28.7
63.0	-3.1	-6.9	-7.4	-6.0	2.4	6.5	-10.2	-20.8	-17.6	-20.7	-26.8	-26.5

$OFTF_t$ ← $NOSPL_t$ →

22.5 -5.4 -5.0 -5.5 -7.7 -6.3 -7.1 -10.9 -12.4 -12.0 -15.2 -16.8

1/3 OCTAVE NTC (dB) WITH RESPECT TO INCIDENT SPL (NTC_i)

$M_J = 0.8$ $M_T = 0.16$

DAISY LOBE NOZZLE (RUN NO = 54)

EMISSION ANGLE (RELATIVE TO JET EXHAUST) REFERENCED TO NOZZLE EXIT (DEGREES)

FREQ KHZ	PTF_i	20.	30.	40.	50.	60.	70.	80.	90.	100.	110.
.250	-25.6	-18.0	-17.7	-21.4	-25.8	-21.7	-30.6	-27.8	-30.6	-33.5	-30.2
.315	-23.1	-15.4	-16.0	-19.0	-22.1	-18.9	-26.3	-24.2	-27.1	-30.0	-27.2
.400	-21.5	-14.5	-15.2	-17.9	-20.7	-17.6	-24.7	-22.7	-25.7	-28.4	-25.8
.500	-19.7	-12.1	-14.7	-16.1	-17.2	-16.2	-20.2	-20.1	-22.8	-24.9	-23.3
.630	-17.3	-10.6	-13.8	-14.4	-14.2	-12.7	-16.8	-17.3	-19.5	-21.8	-20.7
.800	-13.8	-8.9	-10.4	-11.0	-10.3	-9.3	-12.9	-12.6	-16.9	-18.4	-17.0
1.00	-10.3	-2.6	-7.7	-8.3	-6.0	-6.2	-8.5	-8.8	-12.9	-15.3	-13.8
1.25	-8.0	-0.4	-6.0	-6.4	-4.2	-3.5	-6.9	-6.2	-10.6	-12.9	-11.6
1.60	-6.3	0.6	-5.1	-5.2	-2.0	-2.1	-4.5	-4.6	-8.7	-11.0	-10.2
2.00	-5.6	1.0	-5.0	-5.3	-0.6	-1.4	-2.8	-4.5	-7.8	-9.6	-10.1
2.50	-5.0	1.1	-4.7	-7.2	0.0	-1.3	-1.6	-5.4	-7.8	-9.0	-11.3
3.15	-5.0	-0.6	-4.9	-6.7	0.1	-1.5	-0.8	-5.5	-8.2	-9.0	-13.4
4.00	-3.7	-1.7	-1.7	0.0	1.1	0.2	0.6	-3.6	-8.9	-8.8	-13.9
5.00	-4.6	-7.4	0.2	2.7	0.4	-2.2	-3.0	-6.7	-14.4	-12.3	-20.5
6.30	-3.3	-5.3	2.9	0.6	1.2	-7.9	-8.0	-7.5	-13.1	-10.8	-14.2
8.00	-4.4	-0.7	4.8	3.6	-4.1	-11.9	-11.3	-7.3	-13.6	-14.1	-10.3
10.0	-6.9	-4.7	2.7	0.7	-6.8	-8.7	-17.0	-10.0	-14.1	-20.7	-12.4
12.5	-8.3	-7.9	-1.8	0.2	-3.4	-8.6	-12.0	-18.2	-15.1	-25.0	-18.8
16.0	-9.1	-9.3	-0.6	-0.4	-7.0	-14.3	-13.6	-13.6	-13.0	-21.1	-18.0
20.0	-10.9	-10.7	-4.6	-2.6	-9.7	-17.7	-5.0	-11.9	-17.0	-19.0	-27.0
25.0	-9.6	-8.6	-7.1	-3.4	-6.3	-12.1	-10.1	-4.4	-10.0	-14.2	-22.1
31.5	-8.5	-10.9	-4.8	-3.4	-7.5	-11.1	-4.9	-4.8	-6.0	-12.3	-11.8
40.0	-14.9	-15.3	-5.7	-8.3	-12.9	-17.7	-14.2	-13.6	-16.2	-21.6	-23.5
50.0	-17.8	-16.8	-9.3	-11.4	-14.3	-15.1	-17.0	-19.2	-21.7	-23.1	-24.8
63.0	-13.7	-15.9	-7.3	-5.6	-10.7	-15.6	-15.5	-12.8	-19.6	-21.6	-32.1

$OPTF_i$	$NOSPL_i$									
21.5	-6.5	-7.5	-7.2	-7.6	-8.6	-10.0	-11.7	-14.7	-16.9	-17.5

CONICAL NOZZLE (RUN NO = 112)

EMISSION ANGLE (RELATIVE TO JET EXHAUST) REFERENCED TO NOZZLE EXIT (DEGREES)

FREQ KHZ	PTF_i	20.	30.	40.	50.	60.	70.	80.	90.	100.	110.
.250	-25.6	-12.7	-19.6	-22.7	-22.7	-24.0	-30.7	-32.8	-35.5	-41.8	-40.7
.315	-22.0	-10.5	-15.8	-18.4	-19.3	-21.0	-26.4	-28.5	-30.4	-35.9	-35.5
.400	-20.7	-9.9	-14.4	-17.3	-17.9	-19.7	-24.9	-26.9	-28.7	-34.0	-33.8
.500	-17.8	-7.9	-10.5	-13.6	-14.6	-16.8	-20.6	-22.4	-22.7	-27.0	-27.9
.630	-15.3	-7.2	-7.5	-10.6	-11.8	-14.2	-17.4	-19.1	-19.1	-23.1	-24.3
.800	-12.0	-3.6	-4.4	-7.0	-8.7	-11.5	-13.6	-15.5	-15.5	-19.3	-20.5
1.00	-9.2	-1.3	-2.2	-3.8	-5.7	-8.6	-10.1	-11.9	-12.0	-15.6	-16.8
1.25	-6.8	0.2	-0.3	-1.4	-3.2	-5.9	-7.0	-8.7	-8.9	-12.4	-13.6
1.60	-5.1	0.7	1.0	0.1	-1.3	-3.6	-4.5	-6.0	-6.3	-9.8	-11.0
2.00	-3.6	1.7	1.8	0.8	-0.1	-1.6	-2.9	-4.0	-4.2	-8.0	-9.3
2.50	-2.8	2.9	2.9	1.9	0.8	-0.1	-2.6	-3.1	-3.9	-7.4	-8.7
3.15	-2.3	2.1	3.9	3.3	1.4	0.9	-3.4	-3.1	-4.1	-8.3	-9.9
4.00	-3.2	1.2	3.8	2.2	-0.5	0.4	-4.3	-3.8	-5.4	-12.1	-14.6
5.00	-4.9	-2.5	2.4	1.8	-1.5	-1.7	-2.8	-1.9	-5.7	-13.5	-22.3
6.30	-4.8	-5.4	-1.0	1.3	-0.3	-1.3	-1.8	-4.7	-10.3	-19.3	-17.6
8.00	-4.8	-5.7	-3.2	0.5	2.6	-0.3	-4.9	-12.9	-9.9	-14.9	-19.0
10.0	-5.3	-7.5	-4.3	-0.2	4.0	-4.2	-9.5	-14.5	-14.6	-26.2	-19.2
12.4	-5.3	-8.8	-5.6	2.6	2.9	-7.1	-8.5	-10.9	-12.4	-20.7	-18.9
16.0	-5.8	-11.4	-7.0	0.3	2.8	0.2	-10.0	-19.8	-20.0	-23.1	-24.2
20.0	-8.1	-9.6	-7.1	-2.2	0.9	-6.3	-16.1	-19.7	-20.8	-22.5	-24.7
25.0	-7.5	-4.6	-3.0	-0.0	-0.3	-5.4	-11.4	-14.0	-17.8	-23.7	-21.2
31.5	-7.8	-8.3	-3.0	0.4	-1.3	-7.4	-9.1	-11.8	-16.0	-25.8	-29.4
40.0	-14.6	-14.3	-5.0	-2.7	-3.4	-7.5	-11.1	-15.0	-17.0	-25.7	-24.1
50.0	-16.7	-19.4	-11.6	-8.4	-9.8	-15.4	-15.2	-21.2	-22.3	-37.4	-29.2
63.0	-14.6	-16.3	-7.0	-2.6	-4.4	-11.0	-13.5	-20.9	-19.7	-23.3	-31.9

$OPTF_i$	$NOSPL_i$									
23.3	-4.7	-4.2	-4.5	-5.1	-7.6	-10.4	-11.8	-12.1	-16.7	-18.2

$M_J = 0.8$ $M_T = 0.16$

DAISY LOBE NOZZLE (RUN NO= 54)

EMISSION ANGLE (RELATIVE TO JET EXHAUST) REFERENCED TO NOZZLE EXIT (DEGREES)

FREQ KHZ	PTF_t	20.	30.	40.	50.	60.	70.	80.	90.	100.	110.
.250	-24.4	-16.8	-16.4	-20.1	-24.6	-26.5	-26.3	-26.5	-29.3	-32.2	-29.0
.315	-21.0	-14.2	-14.9	-17.8	-21.0	-17.7	-25.2	-23.1	-26.0	-28.8	-26.0
.400	-20.6	-13.4	-14.1	-16.8	-19.6	-16.5	-23.0	-21.7	-24.6	-27.3	-24.8
.500	-18.6	-11.1	-13.6	-15.1	-16.2	-14.2	-16.2	-19.0	-21.8	-23.9	-22.3
.630	-16.4	-9.1	-12.9	-13.0	-13.3	-11.8	-15.9	-16.4	-18.6	-20.9	-19.8
.800	-12.8	-5.1	-9.6	-10.2	-9.5	-8.5	-12.1	-11.8	-15.1	-17.6	-16.2
1.00	-9.5	-1.8	-6.9	-7.0	-6.1	-5.4	-8.7	-8.0	-12.1	-14.8	-13.1
1.25	-7.2	0.4	-5.2	-5.6	-3.5	-3.1	-6.1	-6.5	-9.9	-12.2	-10.9
1.60	-5.7	1.2	-4.5	-4.0	-1.4	-1.6	-3.9	-4.1	-8.1	-10.4	-9.6
2.00	-5.3	1.2	-5.5	-5.1	-0.4	-1.1	-2.8	-4.3	-7.6	-9.4	-9.0
2.50	-5.4	1.1	-8.7	-7.1	0.1	-1.3	-1.6	-5.4	-7.7	-9.0	-11.2
3.15	-6.5	-0.5	-8.8	-6.7	0.2	-1.4	-0.7	-6.4	-8.2	-8.9	-13.3
4.00	-3.7	-1.6	-1.7	0.1	1.1	0.2	0.6	-3.6	-8.9	-8.8	-13.9
5.00	-4.3	-7.9	0.6	3.1	0.8	-1.8	-2.6	-6.3	-14.0	-11.9	-20.2
6.30	-1.1	-3.9	5.1	8.2	3.4	-6.7	-6.7	-6.3	-10.9	-8.6	-11.9
8.00	-3.6	0.1	5.6	4.4	-3.3	-11.1	-10.5	-6.4	-12.8	-13.3	-9.5
10.0	-6.8	-4.6	2.8	0.5	-6.7	-8.5	-10.8	-9.9	-14.0	-20.5	-12.3
12.5	-8.2	-7.8	-1.7	0.3	-3.3	-8.5	-11.8	-15.1	-15.0	-24.9	-18.7
16.0	-9.8	-9.2	-8.5	-0.3	-7.8	-14.2	-13.5	-13.5	-12.9	-20.9	-17.9
20.0	-16.5	-10.6	-4.6	-2.5	-9.6	-17.7	-9.6	-11.9	-16.9	-19.0	-26.9
25.0	-9.4	-8.5	-6.9	-3.3	-6.1	-11.5	-10.6	-4.2	-9.9	-14.0	-21.9
31.5	-8.1	-10.5	-4.5	-3.6	-7.1	-10.8	-4.5	-4.4	-5.6	-11.9	-11.4
40.0	-14.8	-15.2	-5.6	-8.2	-12.8	-17.6	-14.1	-13.5	-16.1	-21.5	-23.4
50.0	-17.7	-16.7	-9.2	-11.3	-14.1	-15.0	-10.8	-19.1	-21.6	-22.9	-24.6
63.0	-13.6	-14.8	-7.8	-8.4	-10.9	-18.4	-15.3	-12.7	-19.5	-21.5	-31.9

$OPTF_t$ ←	$NOSPL_t$ →								
22.3	-5.7	-6.6	-6.3	-6.8	-7.6	-9.1	-10.8	-13.9	-16.1	-16.6

CONICAL NOZZLE (RUN NO = 112)

EMISSION ANGLE (RELATIVE TO JET EXHAUST) REFERENCED TO NOZZLE EXIT (DEGREES)

FREQ KHZ	PTF_t	20.	30.	40.	50.	60.	70.	80.	90.	100.	110.
.250	-21.6	-9.5	-16.4	-19.5	-19.8	-20.8	-27.5	-29.6	-32.3	-38.6	-37.5
.315	-20.5	-9.0	-14.3	-17.2	-17.8	-19.4	-24.9	-26.9	-28.8	-34.4	-34.0
.400	-20.1	-9.2	-13.7	-16.6	-17.3	-15.0	-24.2	-20.2	-28.0	-33.4	-33.1
.500	-17.3	-2.4	-10.0	-13.1	-14.1	-16.3	-20.1	-21.9	-22.2	-26.5	-27.4
.630	-15.1	-7.0	-7.2	-10.4	-11.6	-14.0	-17.2	-18.9	-18.8	-22.9	-24.1
.800	-11.9	-3.6	-4.4	-6.9	-8.7	-11.4	-13.6	-15.4	-15.4	-19.2	-20.5
1.00	-9.1	-1.3	-2.1	-3.8	-5.6	-8.5	-10.1	-11.9	-11.9	-15.6	-16.8
1.25	-6.6	0.2	-0.3	-1.4	-3.2	-5.9	-7.0	-8.7	-8.9	-12.4	-13.6
1.60	-5.1	0.8	1.0	0.1	-1.3	-3.5	-4.5	-6.0	-6.3	-9.8	-11.0
2.00	-3.6	1.7	1.8	0.8	-0.1	-1.6	-2.9	-4.0	-4.8	-8.0	-9.2
2.50	-2.6	2.9	2.9	1.9	0.9	-0.1	-2.6	-3.1	-3.9	-7.4	-8.7
3.15	-2.3	2.1	4.0	3.3	1.4	1.0	-3.4	-3.1	-4.1	-8.3	-9.8
4.00	-3.2	1.2	3.8	2.2	-0.8	0.4	-4.3	-3.8	-5.4	-12.1	-14.6
5.00	-4.0	-2.5	2.4	1.8	-1.6	-1.7	-2.8	-1.9	-5.7	-13.8	-22.3
6.30	-4.5	-5.0	-0.6	1.6	0.1	-1.0	-1.5	-4.3	-10.0	-18.9	-17.3
8.00	-4.8	-5.6	-3.1	0.6	2.7	-0.3	-4.8	-12.8	-9.9	-14.9	-18.9
10.0	-4.9	-7.1	-3.9	0.2	4.3	-3.8	-9.1	-14.1	-14.2	-25.8	-18.8
12.5	-4.9	-8.5	-5.3	2.4	3.2	-6.8	-8.2	-10.5	-12.1	-20.4	-18.6
16.0	-5.6	-11.3	-7.0	0.3	2.8	0.3	-9.9	-19.5	-20.0	-23.0	-24.1
20.0	-8.1	-9.5	-7.0	-2.1	1.0	-6.3	-16.0	-19.6	-20.7	-22.4	-24.6
25.0	-7.8	-4.6	-3.0	0.0	-0.2	-5.3	-11.3	-14.0	-17.7	-23.6	-21.1
31.5	-7.8	-8.3	-3.0	0.4	-1.3	-7.3	-5.0	-11.8	-16.0	-25.7	-29.3
40.0	-14.6	-14.2	-6.0	-2.7	-3.3	-7.8	-11.1	-15.0	-16.9	-25.7	-24.0
50.0	-16.6	-19.4	-11.5	-8.4	-9.8	-15.3	-16.1	-21.2	-22.3	-37.3	-29.2
63.0	-10.8	-10.2	-6.9	-2.5	-4.3	-10.6	-13.4	-20.8	-19.6	-23.2	-31.8

$OPTF_t$ ←	$NOSPL_t$ →								
24.0	-4.0	-3.5	-3.8	-4.4	-6.5	-9.0	-11.0	-11.4	-16.0	-17.5

1/3 OCTAVE NTC (dB) WITH RESPECT TO INCIDENT SPL (NTC_i)

$M_J = 1.2$ $M_T = 0.16$

DAISY LOBE NOZZLE (RUN NO = 56)

EMISSION ANGLE (RELATIVE TO JET EXHAUST) REFERENCED TO NOZZLE EXIT (DEGREES)

FREQ KHZ	PTF_i	30.	40.	50.	60.	70.
.250	-24.1	-29.2	-29.3	-27.4	-18.6	-15.1
.315	-21.8	-23.9	-24.4	-23.6	-16.1	-11.9
.400	-19.8	-22.3	-22.8	-22.2	-15.0	-10.6
.500	-16.1	-14.9	-15.9	-17.3	-12.8	-7.1
.630	-12.9	-10.9	-12.0	-13.9	-10.3	-3.9
.800	-9.3	-7.2	-8.2	-10.[illegible]	-6.6	-0.3
1.00	-5.2	-3.3	-4.1	-6.0	-2.6	3.9
1.25	-1.3	0.1	-0.1	-2.1	1.0	7.8
1.60	2.0	2.9	2.8	1.2	4.1	11.2
2.00	1.7	1.6	1.7	1.0	3.4	11.1
2.50	2.4	0.8	1.7	1.8	3.8	12.0
3.15	3.0	-1.2	1.1	2.5	3.2	13.0
4.00	5.5	-4.5	0.9	4.7	4.8	15.8
5.00	8.4	-10.0	-0.9	7.3	5.6	16.9
6.30	4.8	-9.3	-2.8	2.7	-1.3	15.1
8.00	4.8	-8.1	-0.8	1.8	-0.4	16.7
10.0	-2.6	-13.1	-6.1	-2.3	-[illegible].7	7.5
12.5	-4.6	-12.0	-7.4	-4.1	-1.5	4.9
16.0	-[illegible].4	-14.8	-7.4	1.0	-1.4	9.8
20.0	-12.2	-23.4	-15.1	-9.5	-18.1	-1.9
25.0	-8.2	-16.6	-9.8	-5.3	-12.9	2.2
31.5	-12.5	-13.5	-12.2	-10.3	-12.0	-3.7
40.0	-13.8	-14.8	-13.0	-8.8	-[illegible].8	-5.8
50.0	-12.7	-12.5	-11.9	-10.1	-14.4	-1.6
63.0	-14.4	-15.5	-13.3	-10.9	-10.6	-5.1

DATA FOR REMAINING ANGLES NOT ANALYZED DUE TO JET NOISE CONTAMINATION

$OPTF_i$ ←	$NOSPL_i$ →
27.8	-9.1 -8.0 -6.1 -5.4 4.6

CONICAL NOZZLE (RUN NO = 115)

EMISSION ANGLE (RELATIVE TO JET EXHAUST) REFERENCED TO NOZZLE EXIT (DEGREES)

FREQ KHZ	PTF_i	30.	40.	50.	60.	70.
.250	-26.7	-15.4	-19.3	-26.4	-40.5	-44.0
.315	-23.9	-12.8	-16.6	-22.2	-33.0	-36.8
.400	-22.7	-11.7	-15.4	-20.8	-31.1	-34.9
.500	-20.0	-9.4	-13.2	-16.8	-21.9	-28.6
.630	-17.4	-7.9	-10.7	-13.9	-17.6	-21.3
.800	-14.1	-4.5	-7.6	-9.5	-12.4	-16.7
1.00	-11.1	-2.4	-4.7	-5.7	-8.3	-12.6
1.25	-8.5	-0.9	-2.2	-2.4	-4.8	-8.8
1.60	-6.2	-0.2	-0.1	0.6	-1.9	-5.2
2.00	-4.6	-1.5	1.2	2.4	0.1	-2.1
2.50	-4.0	-3.6	1.2	2.9	0.9	0.4
3.15	-4.3	-5.6	-0.6	1.5	1.0	1.9
4.00	-3.6	-3.7	-1.0	0.7	2.8	2.8
5.00	-3.1	-4.8	-0.9	2.6	4.1	1.7
6.30	-6.1	-6.9	-7.3	-3.0	3.1	-2.8
8.00	-8.7	-7.8	-8.4	-8.1	0.7	-9.1
10.0	-7.1	-2.5	-1.9	-1.6	-0.1	-7.6
12.4	-5.7	-1.3	1.0	1.4	-1.8	-6.3
16.0	-7.6	-3.0	-2.7	-0.9	-0.6	-11.1
20.0	-7.3	-5.6	-6.6	1.6	-3.8	-12.8
25.0	-3.2	-3.6	4.1	6.5	-1.8	-6.8
31.5	-6.3	-2.4	0.7	3.0	-6.6	-13.8
40.0	-7.2	-6.5	-6.8	-0.2	-4.6	-6.8
50.0	-6.0	-2.4	-1.7	2.5	-2.0	-6.1
63.0	-6.6	-4.6	-4.1	-2.5	3.1	-6.9

DATA FOR THEREMAINING ANGLES NOT ANALYZED DUE TO JET NOISE CONTAMINATION

$OPTF_i$ ←	$NOSPL_i$ →
22.1	-6.9 -5.7 -4.9 -5.0 -6.8

1/3 OCTAVE NTC (dB) WITH RESPECT TO TRANSMITTED SPL (NTC_t)

$M_J = 1.2$ $M_T = 0.16$

DAISY LOBE NOZZLE (RUN NO= 56)

FREQ KHZ	EMISSION ANGLE (RELATIVE TO JET EXHAUST) REFERENCED TO NOZZLE EXIT (DEGREES)					
	PTF_t	30.	40.	50.	60.	70.
.250	-23.4	-28.5	-28.6	-26.7	-17.8	-14.4
.315	-26.4	-23.3	-23.7	-23.0	-15.6	-11.3
.400	-19.3	-21.8	-22.2	-21.7	-14.5	-10.1
.500	-15.5	-14.4	-15.4	-16.8	-12.2	-6.8
.630	-12.4	-10.4	-11.4	-13.4	-9.8	-3.4
.800	-8.8	-6.7	-7.7	-9.7	-6.1	0.2
1.00	-4.6	-2.8	-3.5	-5.4	-2.0	4.5
1.25	-0.6	0.6	0.0	-1.6	1.8	8.4
1.60	2.5	3.5	3.1	1.8	4.6	11.7
2.00	1.9	1.9	2.0	1.3	3.6	11.3
2.50	2.4	0.8	1.8	1.8	3.5	12.0
3.15	3.0	-1.1	1.1	2.5	3.3	13.1
4.00	5.7	-4.3	1.1	4.9	4.7	16.0
5.00	8.6	-9.6	-0.7	7.5	5.9	19.1
6.30	4.5	-9.2	-2.7	2.8	-1.2	15.2
8.00	4.9	-8.4	-0.7	2.0	-6.3	15.8
10.0	-2.4	-12.9	-6.0	-2.1	-0.6	7.7
12.5	-4.5	-11.9	-7.3	-4.1	-1.4	4.6
16.0	-0.4	-14.8	-7.3	1.1	-1.3	9.9
20.0	-12.2	-23.4	-15.1	-9.5	-15.1	-1.6
25.0	-8.1	-16.5	-9.8	-6.3	-12.9	2.3
31.5	-12.4	-13.5	-12.2	-10.2	-12.0	-5.6
40.0	-13.6	-14.7	-13.0	-8.6	-8.5	-6.8
50.0	-12.6	-12.4	-11.8	-10.0	-14.3	-1.6
63.0	-14.4	-15.5	-13.2	-10.9	-10.6	-5.0

DATA FOR THEREMAINING ANGLES NOT ANALYZED DUE TO JET NOISE CONTAMINATION

$OPTF_t$ ←	→ $NOSPL_t$				
26.3	-8.7	-7.8	-5.6	-5.0	5.0

CONICAL NOZZLE (RUN NO = 115)

FREQ KHZ	EMISSION ANGLE (RELATIVE TO JET EXHAUST) REFERENCED TO NOZZLE EXIT (DEGREES)					
	PTF_t	30.	40.	50.	60.	70.
.250	-23.8	-12.5	-16.4	-23.4	-37.5	-41.0
.315	-22.7	-11.6	-15.3	-20.9	-31.8	-35.8
.400	-22.3	-11.3	-15.0	-20.4	-30.7	-34.8
.500	-19.7	-9.1	-12.9	-16.8	-21.6	-26.3
.630	-17.3	-6.9	-10.6	-13.8	-17.8	-21.2
.800	-14.0	-4.5	-7.8	-9.8	-12.4	-16.7
1.00	-11.1	-2.4	-4.7	-5.7	-8.3	-12.6
1.25	-8.5	-0.9	-2.2	-2.4	-4.8	-8.8
1.60	-6.2	-0.2	-0.1	0.5	-1.9	-5.2
2.00	-4.6	1.5	1.2	2.4	0.1	-2.1
2.50	-4.0	3.6	1.2	2.9	0.9	0.4
3.15	-4.3	0.6	-0.6	1.5	1.1	1.9
4.00	-3.6	3.7	-1.0	0.8	2.8	2.8
5.00	-3.1	-4.8	-0.9	2.0	4.1	1.7
6.30	-5.8	-6.6	-7.1	-2.7	3.3	-2.3
8.00	-8.7	-7.7	-8.4	-5.1	0.7	-9.1
10.0	-7.1	-2.5	-1.9	-1.6	-0.0	-7.6
12.5	-5.7	-1.2	1.1	1.8	-1.7	-6.2
16.0	-7.5	-3.9	-2.6	-0.8	-0.5	-11.0
20.0	-7.3	-5.5	-0.6	1.6	-3.7	-12.5
25.0	-3.1	-3.5	4.1	6.6	-1.8	-6.7
31.5	-6.2	-2.3	0.8	3.1	-8.5	-13.4
40.0	-7.1	-4.4	-6.7	-0.2	-4.6	-8.8
50.0	-5.9	-2.3	-1.5	2.6	-1.9	-8.0
63.0	-6.8	-4.5	-4.0	-2.4	3.2	-8.8

DATA FOR THEREMAINING ANGLES NOT ANALYZED DUE TO JET NOISE CONTAMINATION

$OPTF_t$ ←	→ $NOSPL_t$				
22.7	-5.4	-5.1	-4.3	-6.4	-8.2

1/3 OCTAVE NTC (dB) WITH RESPECT TO INCIDENT SPL (NTC_i)

$M_J = 0$ $M_T = 0.24$

DAISY LOBE NOZZLE (RUN NO = 38)

EMISSION ANGLE (RELATIVE TO JET EXHAUST) REFERENCED TO NOZZLE EXIT (DEGREES)

FREQ KHZ	PTF_i	30.	40.	50.	60.	70.	80.	90.	100.	110.
.250	-21.2	-22.1	-25.6	-24.1	-19.5	-21.7	-19.0	-15.9	-23.0	-15.9
.315	-19.6	-20.0	-22.2	-20.7	-17.3	-18.4	-16.8	-14.1	-20.3	-14.1
.400	-17.9	-19.8	-20.8	-19.3	-16.2	-17.5	-15.7	-13.2	-19.0	-13.2
.500	-16.4	-17.2	-16.8	-14.9	-13.8	-14.0	-13.3	-11.3	-16.8	-11.1
.630	-12.6	-14.8	-13.2	-11.3	-11.0	-10.7	-10.8	-8.9	-13.6	-8.5
.800	-10.1	-12.0	-10.3	-8.0	-8.6	-8.2	-7.9	-6.6	-10.3	-6.6
1.00	-8.5	-9.6	-8.6	-7.3	-6.9	-6.6	-6.2	-5.1	-7.9	-5.8
1.25	-7.0	-7.3	-7.3	-6.4	-5.5	-5.3	-4.4	-3.5	-6.5	-5.0
1.60	-5.7	-4.8	-4.9	-4.5	-4.1	-4.4	-3.6	-3.0	-3.0	-4.9
2.00	-5.1	-2.9	-4.1	-4.2	-3.7	-3.7	-3.1	-2.9	-1.7	-6.2
2.50	-4.5	-0.7	-2.7	-3.2	-2.5	-2.6	-3.3	-3.6	-1.2	-5.7
3.15	-3.9	1.5	-1.4	-1.9	-0.6	-3.1	-4.0	-4.7	-0.8	-5.9
4.00	-4.2	2.5	-0.6	-1.6	-0.8	-6.0	-5.5	-5.5	-1.9	-7.8
5.00	-8.0	1.6	-4.7	-7.3	-5.4	-9.7	-10.1	-12.9	-8.5	-15.0
6.30	-14.2	-5.0	-5.3	-6.1	-6.2	-9.5	-12.1	-12.2	-11.2	-11.9
8.00	-12.4	-16.1	-13.8	-13.6	-15.2	-11.7	-12.5	-7.6	-9.8	-7.9
10.0	-14.1	-7.3	-6.0	-6.1	-6.0	-7.6	-12.1	-10.9	-11.7	-10.1
12.5	-7.4	-1.7	-1.2	-4.5	-8.9	-7.0	-6.3	-6.5	-7.3	-7.6
16.0	-11.8	-7.2	-7.6	-10.7	-16.8	-11.5	-14.0	-11.8	-7.6	-8.6
20.0	-14.7	-6.4	-11.5	-14.0	-11.0	-8.1	-6.4	-6.3	-13.9	-10.7
25.0	-7.4	-6.0	-6.0	-4.8	-6.6	-6.3	-7.3	-5.3	-14.0	-11.1
31.5	-8.1	2.0	0.6	-0.3	-3.2	-7.6	-6.6	-6.8	-7.9	-11.3
40.0	-6.3	2.1	-1.0	-1.8	-4.5	-6.8	-10.0	-10.9	-7.1	-14.8
50.0	-14.5	-5.4	-7.4	-7.0	-6.8	-7.5	-11.1	-11.7	-10.0	-14.3
63.0	-16.2	-11.3	-11.7	-13.2	-14.3	-14.9	-15.6	-17.2	-12.7	-22.0

$OPTF_i$ ← $NOSPL_i$ →

21.3 -9.6 -11.1 -10.9 -10.0 -10.8 -10.4 -9.0 -10.4 -10.0

CONICAL NOZZLE (RUN NO = 119)

EMISSION ANGLE (RELATIVE TO JET EXHAUST) REFERENCED TO NOZZLE EXIT (DEGREES)

FREQ KHZ	PTF_i	30.	40.	50.	60.	70.	80.	90.	100.	110.
.250	-30.0	-32.7	-31.4	-28.2	-27.1	-31.6	-33.2	-31.2	-26.7	-24.1
.315	-25.9	-27.0	-26.8	-24.6	-23.2	-26.4	-27.6	-25.9	-22.8	-20.5
.400	-24.0	-24.9	-24.8	-22.8	-21.3	-24.3	-25.4	-23.7	-20.8	-18.8
.500	-19.4	-19.7	-20.8	-19.8	-17.6	-18.4	-18.8	-16.5	-16.8	-15.5
.630	-15.3	-15.5	-16.7	-16.3	-13.8	-13.8	-13.7	-11.8	-12.9	-11.8
.800	-11.5	-9.7	-11.8	-12.2	-10.0	-9.9	-9.7	-8.8	-9.4	-8.3
1.00	-8.8	-5.6	-7.9	-8.7	-7.1	-7.7	-7.7	-7.0	-6.6	-6.5
1.25	-7.0	-2.7	-4.8	-6.1	-5.4	-7.3	-7.3	-5.5	-4.8	-3.7
1.60	-4.5	0.8	-1.4	-3.3	-3.7	-5.1	-5.1	-2.7	-2.8	-1.6
2.00	-3.6	2.8	0.1	-2.6	-3.6	-5.3	-4.0	-2.1	-2.6	-1.0
2.50	-2.3	4.7	1.8	-1.1	-2.8	-5.2	-2.4	-0.3	-2.2	-0.1
3.15	-1.2	6.1	2.8	0.4	-0.6	-2.6	-1.1	0.1	-2.1	-0.3
4.00	-3.0	3.6	-0.4	-1.5	0.6	-2.8	-3.6	-2.9	-2.6	-3.6
5.00	-6.7	-2.7	-7.3	-6.0	-0.3	-3.7	-7.4	-7.2	-6.3	-8.0
6.30	-5.1	4.7	-1.3	-3.3	-1.3	-9.5	-6.5	-9.8	-11.8	-10.0
8.00	-9.1	1.0	-6.4	-10.9	-9.9	-11.7	-11.8	-14.1	-10.4	-7.3
10.0	-11.7	-8.8	-10.7	-9.8	-5.4	-10.6	-11.8	-13.1	-12.8	-10.6
12.4	-17.9	-10.2	-12.8	-14.0	-14.8	-18.4	-20.6	-20.8	-26.0	-23.8
16.0	-16.4	-6.8	-11.9	-15.3	-16.3	-17.6	-19.1	-17.6	-22.1	-18.2
20.0	-15.7	-5.4	-13.2	-18.1	-16.2	-19.6	-18.4	-18.0	-24.6	-17.6
25.0	-8.9	2.3	-5.2	-13.2	-15.4	-18.3	-12.9	-11.4	-20.3	-14.2
31.5	-9.8	0.5	-4.8	-8.1	-9.3	-12.0	-11.9	-10.8	-15.8	-16.8
40.0	-14.7	0.6	-7.7	-11.3	-11.9	-13.9	-13.4	-13.0	-12.3	-19.6
50.0	-15.2	-5.7	-12.3	-15.9	-14.8	-18.4	-12.7	-13.3	-21.7	-25.0
63.0	-13.0	-5.7	-10.9	-14.1	-11.7	-16.7	-11.6	-8.6	-12.8	-24.2

$OPTF_i$ ← $NOSPL_i$ →

26.7 -6.8 -9.9 -11.8 -11.1 -13.2 -12.8 -10.6 -11.5 -10.4

1/3 OCTAVE NTC (dB) WITH RESPECT TO TRANSMITTED SPL (NTC_t)

$M_J = 0$ $M_T = 0.24$

DAISY LOBE NOZZLE (RUN NO= 38)

EMISSION ANGLE (RELATIVE TO JET EXHAUST) REFERENCED TO NOZZLE EXIT (DEGREES)

FREQ KHZ	PTF_t	30.	40.	50.	60.	70.	80.	90.	100.	110.
.250	-24.1	-21.0	-24.5	-23.3	-18.4	-20.6	-17.9	-14.8	-21.9	-14.8
.315	-17.8	-18.8	-21.0	-19.4	-16.1	-17.6	-15.0	-12.9	-19.1	-12.9
.400	-16.1	-17.7	-19.5	-18.0	-14.2	-16.2	-14.4	-11.9	-17.7	-11.9
.500	-13.9	-15.6	-15.2	-13.1	-12.3	-12.5	-11.7	-9.8	-15.0	-9.8
.630	-14.6	-12.9	-11.3	-9.4	-9.0	-8.7	-8.5	-7.0	-11.6	-6.6
.800	-7.4	-9.4	-7.7	-5.9	-5.9	-5.5	-5.2	-4.0	-7.6	-3.9
1.00	-5.7	-6.8	-5.8	-4.5	-4.1	-3.8	-3.4	-2.2	-8.1	-3.0
1.25	-4.4	-4.6	-4.6	-3.8	-2.8	-2.6	-1.7	-0.9	-2.8	-2.4
1.60	-3.2	-2.3	-2.4	-2.3	-1.6	-1.9	-1.1	-0.5	-0.5	-2.4
2.00	-2.9	-0.7	-1.9	-2.2	-1.5	-1.5	-0.8	-0.7	0.5	-4.0
2.50	-3.1	0.7	-1.3	-1.6	-1.1	-1.4	-1.9	-2.2	0.2	-4.3
3.15	-2.9	2.4	-0.4	-0.9	0.4	-2.2	-3.1	-3.8	0.1	-5.0
4.00	-3.6	3.1	0.1	-1.0	-0.1	-5.3	-4.9	-4.8	-1.3	-7.2
5.00	-7.6	1.4	-4.3	-6.9	-5.1	-9.3	-9.8	-12.5	5.1	-14.6
6.30	-4.7	-4.5	-4.8	-5.7	-5.8	-9.5	-11.7	-11.8	-10.7	-11.5
8.00	-11.5	-15.6	-13.3	-13.1	-14.7	-11.2	-12.6	-7.6	-8.9	-7.3
10.0	-14.9	-7.2	-5.9	-6.0	-5.9	-7.5	-12.0	-10.8	-11.6	-9.9
12.5	-6.7	-1.8	-6.5	-3.8	-8.2	-6.3	-8.6	-5.9	-6.6	-6.9
16.0	-11.2	-6.6	-7.0	-10.1	-16.2	-10.9	-13.4	-11.2	-7.0	-8.0
20.0	-14.4	-6.9	-11.1	-13.6	-10.6	-7.7	-6.6	-5.9	-13.6	-10.3
25.0	-7.1	-5.7	-5.7	-4.6	-0.3	-6.0	-7.1	-5.6	-13.7	-10.8
31.5	-3.3	4.5	2.4	1.1	-1.4	-5.6	-4.9	-4.7	-6.2	-9.4
40.0	-5.6	2.8	-0.3	-1.1	-3.8	-6.1	-9.3	-10.2	-6.4	-14.1
50.0	-9.8	-4.7	-6.7	-6.3	-6.1	-6.8	-10.4	-11.0	-9.3	-13.6
63.0	-15.0	-10.1	-10.5	-12.1	-13.0	-13.7	-14.5	-15.9	-11.4	-20.9

$OPTF_t$	← $NOSPL_t$ →							
22.8	-8.1	-9.6	-9.4	-8.5	-9.3	-8.9	-7.5	-8.9	-8.5

CONICAL NOZZLE (RUN NO = 119)

EMISSION ANGLE (RELATIVE TO JET EXHAUST) REFERENCED TO NOZZLE EXIT (DEGREES)

FREQ KHZ	PTF_t	30.	40.	50.	60.	70.	80.	90.	100.	110.
.250	-26.9	-29.6	-28.2	-25.1	-23.9	-26.5	-30.1	-28.1	-23.6	-21.0
.315	-23.8	-24.1	-23.9	-21.7	-20.3	-23.5	-24.7	-22.9	-19.9	-17.6
.400	-21.2	-22.2	-22.1	-20.1	-18.6	-21.6	-22.6	-21.0	-18.1	-16.0
.500	-18.9	-17.1	-18.2	-17.2	-15.1	-18.8	-15.9	-14.0	-14.3	-13.0
.630	-13.1	-13.3	-14.6	-14.1	-11.7	-11.6	-11.5	-9.6	-10.7	-9.7
.800	-9.4	-7.7	-9.7	-10.1	-7.9	-7.8	-7.7	-6.8	-7.3	-6.2
1.00	-6.8	-3.7	-5.9	-6.6	-5.1	-5.7	-5.7	-5.0	-4.7	-3.6
1.25	-5.6	-1.4	-3.4	-4.7	-4.1	-5.9	-6.0	-4.1	-3.4	-2.3
1.60	-3.8	1.7	-0.8	-2.4	-2.8	-4.1	-4.1	-1.8	-1.8	-0.7
2.00	-3.2	3.2	0.5	-2.1	-3.2	-4.9	-3.6	-1.7	-2.1	-0.6
2.50	-2.0	5.0	2.1	-0.8	-2.5	-4.9	-2.1	-0.1	-2.0	0.2
3.15	-4.9	6.4	3.1	0.7	-0.3	-2.3	-0.8	0.4	-1.8	0.0
4.00	-3.0	3.7	-0.4	-1.4	0.7	-2.7	-3.4	-2.8	-2.6	-3.7
5.00	-6.7	-2.6	-7.2	-5.9	-0.2	-3.6	-7.3	-7.1	-8.2	-7.9
6.30	-4.0	8.9	-0.2	-2.2	-0.2	-8.3	-7.4	-8.7	-10.7	-8.9
8.00	-8.0	2.2	-5.3	-9.7	-8.7	-10.5	-10.7	-12.9	-9.2	-6.1
10.0	-8.8	-8.9	-7.9	-6.9	-2.5	-7.6	-8.9	-10.2	-9.6	-7.6
12.5	-15.6	-7.9	-10.2	-11.7	-12.2	-16.2	-18.3	-18.5	-23.7	-21.2
16.0	-16.1	-6.5	-11.6	-15.0	-16.0	-17.3	-18.8	-17.4	-21.8	-17.9
20.0	-18.4	-8.1	-13.0	-17.8	-15.9	-19.3	-18.2	-17.7	-24.3	-17.4
25.0	-8.4	2.7	-4.7	-12.8	-14.9	-14.8	-11.5	-11.0	-19.9	-13.7
31.5	-8.4	1.8	-3.5	-6.8	-8.0	-10.8	-10.6	-9.4	-14.2	-15.8
40.0	-9.6	1.7	-6.6	-10.2	-10.7	-12.8	-12.3	-11.9	-11.2	-18.5
50.0	-12.8	-3.3	-9.9	-12.6	-12.1	-13.0	-10.3	-10.8	-19.3	-22.6
63.0	-9.2	-2.2	-7.1	-10.2	-7.7	-12.0	-8.0	-4.8	-8.1	-20.6

$OPTF_t$	← $NOSPL_t$ →							
23.1	-4.4	-7.5	-9.4	-8.7	-10.7	-10.4	-8.2	-9.0	-7.9

1/3 OCTAVE NTC (dB) WITH RESPECT TO INCIDENT SPL (NTC_i)

$M_J = 0.4$ $M_T = 0.24$

DAISY LOBE NOZZLE (RUN NO = 49)

EMISSION ANGLE (RELATIVE TO JET EXHAUST) REFERENCED TO NOZZLE EXIT (DEGREES)

FREQ KHZ	PTF_i	30.	40.	50.	60.	70.	80.	90.	100.	110.
.250	-28.6	-34.2	-28.0	-26.5	-26.7	-25.2	-26.9	-23.6	-30.0	-28.2
.315	-25.4	-25.9	-24.0	-22.9	-23.5	-22.4	-23.8	-21.1	-26.6	-25.1
.400	-23.9	-24.1	-22.3	-21.3	-22.0	-20.9	-22.2	-19.8	-24.9	-23.5
.500	-21.3	-20.1	-18.9	-18.2	-19.4	-18.5	-19.9	-17.1	-16.2	-18.9	-18.1
.630	-18.4	-16.6	-15.5	-15.0	-16.5	-15.8	-17.1	-13.2	-12.5	-15.2	-14.3
.800	-14.6	-12.3	-11.3	-11.1	-12.7	-12.6	-13.2	-10.4	-9.8	-12.4	-11.6
1.00	-12.0	-9.1	-8.7	-8.7	-10.0	-10.4	-10.4	-8.7	-8.0	-10.8	-9.9
1.25	-10.5	-6.8	-7.9	-8.2	-8.3	-9.3	-8.7	-7.4	-6.6	-9.0	-8.4
1.60	-9.4	-4.7	-8.9	-9.6	-6.6	-8.3	-7.4	-6.6	-5.8	-8.0	-7.4
2.00	-8.2	-3.1	-6.4	-7.1	-5.4	-7.6	-6.8	-5.8	-5.5	-7.2	-6.7
2.50	-6.3	-1.6	-1.2	-1.8	-4.2	-6.8	-6.7	-5.5	-5.9	-7.3	-7.1
3.15	-5.2	-0.5	0.9	0.3	-3.6	-5.8	-7.3	-6.9	-8.1	-10.2	-11.2
4.00	-7.8	-1.1	-3.1	-4.7	-5.7	-6.7	-8.0	-8.1	-11.4	-15.3	-18.6
5.00	-8.7	-0.7	-1.1	-4.3	-11.1	-11.6	-10.1	-11.4	-15.3	-18.6	-13.1
6.30	-10.3	-1.2	-3.1	-7.1	-15.8	-21.9	-16.2	-12.8	-12.5	-13.1	-16.8
8.00	-11.5	-0.7	-7.0	-14.5	-22.5	-23.2	-15.8	-11.5	-12.4	-16.8	-11.0
10.0	-8.6	1.6	-2.6	-7.2	-11.9	-16.7	-15.8	-15.6	-13.2	-11.0	-16.0
12.5	-9.5	1.6	-4.7	-9.9	-12.4	-15.6	-11.9	-13.3	-14.8	-16.0	-17.3
16.0	-9.9	-2.6	-2.5	-5.6	-13.9	-17.7	-12.4	-9.7	-10.2	-17.3	-15.0
20.0	-14.5	-2.8	-4.4	-7.4	-13.5	-19.0	-13.9	-10.2	-9.4	-15.0	-16.2
25.0	-7.8	-2.6	-1.7	-3.1	-7.2	-8.3	-8.9	-6.0	-11.3	-16.2	-12.8
31.5	-12.2	-10.2	-8.2	-5.6	-9.5	-16.5	-11.6	-8.6	-13.9	-12.8	-16.2
40.0	-11.2	-7.3	-5.8	-5.3	-12.8	-17.6	-13.1	-9.2	-9.2	-16.2	-20.2
50.0	-14.2	-9.8	-10.0	-8.6	-11.8	-16.6	-11.8	-13.4	-16.1	-20.2	-20.1
63.0	-16.2	-12.8	-10.6	-12.0	-15.9	-15.2	-14.5	-16.5	-18.2	-20.1	

$OPTF_i$	$NOSPL_i$
-10.4	-8.1 -9.4 -10.6 -12.4 -13.6 -13.8 -12.2 -14.7 -14.8

CONICAL NOZZLE (RUN NO = 97)

EMISSION ANGLE (RELATIVE TO JET EXHAUST) REFERENCED TO NOZZLE EXIT (DEGREES)

FREQ KHZ	PTF_i	10.	20.	30.	40.	50.	60.	70.	80.	90.	100.	110.
.250	-29.0	-24.9	-27.0	-31.0	-28.6	-25.6	-24.8	-28.0	-28.9	-23.9	-32.5	-31.8
.315	-25.3	-20.4	-22.1	-26.2	-24.2	-22.2	-21.9	-24.4	-24.8	-21.3	-27.6	-27.2
.400	-23.7	-18.6	-20.6	-24.2	-22.4	-20.6	-20.5	-22.7	-23.0	-19.9	-25.6	-25.3
.500	-20.9	-13.6	-14.9	-18.6	-18.4	-17.8	-18.2	-19.3	-19.5	-18.0	-20.5	-20.6
.630	-16.8	-9.9	-11.1	-14.7	-15.0	-15.1	-16.7	-16.2	-16.3	-15.8	-16.6	-16.9
.800	-13.5	-7.6	-7.2	-10.9	-11.3	-11.8	-13.1	-13.4	-12.8	-13.1	-13.2	-13.4
1.00	-11.6	-6.3	-5.1	-7.8	-8.3	-9.2	-10.8	-10.9	-9.7	-10.7	-10.6	-10.9
1.25	-8.9	-6.4	-4.0	-4.9	-5.7	-7.0	-8.6	-8.4	-7.8	-8.6	-8.8	-9.4
1.60	-7.3	-4.2	-2.9	-2.3	-3.9	-5.5	-6.6	-6.9	-6.9	-8.1	-8.1	-8.7
2.00	-5.6	-1.6	-0.7	-0.1	-3.1	-4.9	-4.8	-3.3	-4.3	-5.3	-7.7	-7.3
2.50	-3.9	0.4	2.1	1.6	-2.9	-4.7	-2.4	-0.6	-2.8	-3.9	-6.3	-6.3
3.15	-2.8	0.4	5.2	2.1	-2.6	-3.9	-0.8	1.4	-3.1	-3.6	-5.9	-7.0
4.00	-2.6	1.4	6.8	1.1	-2.8	-3.2	0.6	3.0	-2.3	-4.3	-7.1	-7.8
5.00	-2.1	2.3	7.6	-3.7	-3.4	-0.9	1.3	2.8	-3.4	-7.8	-9.5	-11.7
6.30	-2.0	5.2	7.6	-0.6	-1.7	-0.1	2.8	1.6	-6.0	-15.1	-16.8	-18.6
8.00	-2.4	4.8	8.0	2.5	-0.1	-0.3	0.8	-7.5	-12.6	-8.6	-9.1	-8.8
10.0	-5.3	1.0	5.7	-0.7	-3.7	-4.4	-2.6	-6.6	-11.1	-10.3	-13.9	-16.6
12.4	-4.8	-1.0	6.4	3.6	-4.2	-6.5	-2.7	-6.5	-11.2	-17.1	-16.1	-16.4
16.0	-8.1	-3.8	2.3	-0.5	-6.6	-6.2	-7.6	-8.1	-11.7	-18.6	-16.9	-18.7
20.0	-4.9	-1.3	1.0	5.0	-2.0	-6.2	-4.6	-9.7	-11.9	-19.1	-20.4	-21.9
25.0	-6.8	3.4	2.8	-2.5	-2.0	-3.9	-6.6	-7.7	-8.5	-17.2	-16.7	-21.3
31.5	-8.2	-0.7	1.4	-2.9	-8.5	-8.9	-6.1	-4.3	-9.0	-14.4	-17.7	-22.8
40.0	-6.4	-5.0	3.9	-2.6	-7.0	-7.8	-9.0	-7.2	-10.1	-18.8	-18.1	-24.0
50.0	-14.7	-9.5	-1.4	-3.0	-9.2	-10.9	-11.6	-14.1	-19.8	-22.1	-21.8	-26.8
63.0	-12.5	-2.4	-2.1	-7.1	-12.6	-15.5	-12.4	-15.5	-19.7	-24.2	-23.2	-31.3

$OPTF_i$	$NOSPL_i$
-21.7	-7.0 -3.7 -6.4 -10.0 -10.8 -9.6 -9.1 -12.0 -12.4 -14.4 -15.0

1/3 OCTAVE NTC (dB) WITH RESPECT TO TRANSMITTED SPL (NTC_t)

$M_J = 0.4$ $M_T = 0.24$

DAISY LOBE NOZZLE (RUN NO = 49)

EMISSION ANGLE (RELATIVE TO JET EXHAUST) REFERENCED TO NOZZLE EXIT (DEGREES)

FREQ KHZ	PTF_t	30.	40.	50.	60.	70.	80.	90.	100.	110.
.250	-26.4	-30.0	-27.8	-26.3	-26.5	-25.0	-26.7	-23.4	-29.8	-28.1
.315	-25.2	-25.6	-23.8	-22.7	-23.3	-22.1	-23.5	-20.9	-26.3	-24.8
.400	-23.6	-23.8	-22.0	-21.0	-21.7	-20.6	-22.0	-19.5	-24.6	-23.2
.500	-21.0	-19.8	-18.6	-17.9	-19.1	-18.2	-19.6	-18.0	-21.7	-20.6
.630	-18.0	-16.2	-15.1	-14.7	-16.1	-15.4	-16.7	-15.8	-18.6	-17.7
.800	-14.9	-11.7	-10.7	-10.8	-12.2	-12.0	-12.7	-12.0	-14.6	-13.7
1.00	-11.3	-8.5	-8.1	-8.1	-9.4	-9.8	-9.8	-9.1	-11.7	-11.0
1.25	-9.9	-6.2	-7.3	-7.6	-7.7	-8.7	-8.1	-7.4	-9.9	-9.3
1.60	-8.8	-4.1	-8.3	-9.0	-6.0	-7.7	-6.8	-6.0	-8.4	-7.8
2.00	-7.6	-2.5	-5.8	-6.6	-4.9	-7.0	-6.2	-5.2	-7.4	-6.8
2.50	-5.9	-1.2	-8.9	-1.4	-3.9	-6.4	-6.4	-5.1	-6.8	-6.4
3.15	-5.1	-0.4	1.0	0.1	-3.6	-6.7	-7.2	-5.8	-7.2	-7.0
4.00	-7.7	-0.9	-2.9	-4.5	-5.5	-6.5	-7.8	-7.9	-10.0	-11.0
5.00	-8.1	-0.2	-0.5	-3.8	-10.5	-11.0	-5.6	-10.9	-14.8	-18.1
6.30	-9.6	-0.8	-2.6	-6.7	-15.3	-21.4	-15.8	-12.3	-12.1	-12.6
8.00	-11.4	-4.6	-6.9	-14.4	-22.4	-23.1	-15.7	-11.4	-12.3	-16.8
10.0	-8.6	1.8	-2.4	-7.0	-11.8	-16.5	-15.0	-15.5	-13.0	-10.9
12.5	-9.2	1.9	-4.3	-9.5	-12.0	-15.3	-11.5	-12.9	-14.8	-15.7
16.0	-9.8	-2.6	-2.4	-6.7	-13.9	-17.7	-12.4	-9.6	-10.1	-17.2
20.0	-10.4	-2.7	-4.4	-7.3	-13.5	-19.0	-13.9	-10.1	-9.3	-14.9
25.0	-7.7	-2.6	-1.6	-3.4	-7.1	-5.2	-6.9	-5.9	-11.3	-16.2
31.5	-12.0	-10.1	-8.0	-5.4	-9.3	-16.7	-11.4	-8.4	-13.8	-12.6
40.0	-11.1	-7.2	-5.7	-5.1	-12.7	-11.5	-13.0	-9.1	-9.1	-16.1
50.0	-14.1	-9.7	-9.9	-8.7	-11.7	-16.5	-11.7	-13.3	-16.0	-20.1
63.0	-16.0	-12.6	-10.4	-11.6	-15.7	-15.0	-14.4	-16.4	-18.0	-19.9

$OPTF_t$ ← $NOSPL_t$ →

19.6 -7.8 -9.1 -10.3 -12.0 -13.5 -13.5 -11.2 -14.4 -14.4

CONICAL NOZZLE (RUN NO = 97)

EMISSION ANGLE (RELATIVE TO JET EXHAUST) REFERENCED TO NOZZLE EXIT (DEGREES)

FREQ KHZ	PTF_t	10.	20.	30.	40.	50.	60.	70.	80.	90.	100.	110.
.250	-27.1	-23.0	-25.1	-29.6	-26.7	-23.6	-22.8	-26.1	-27.0	-22.0	-30.6	-29.9
.315	-23.7	-18.8	-20.4	-24.5	-22.6	-20.5	-20.2	-22.7	-23.1	-19.6	-25.9	-25.5
.400	-22.3	-17.2	-19.2	-22.7	-20.9	-19.2	-19.0	-21.3	-21.6	-18.4	-24.1	-23.8
.500	-18.6	-11.6	-13.5	-17.2	-17.0	-16.5	-16.8	-17.9	-18.1	-16.6	-19.1	-19.2
.630	-15.6	-8.7	-9.9	-13.5	-13.8	-13.9	-14.6	-15.0	-15.1	-14.6	-15.6	-15.7
.800	-12.9	-7.2	-6.8	-10.3	-10.6	-11.2	-12.4	-12.7	-11.8	-12.4	-12.6	-12.7
1.00	-10.6	-5.9	-4.8	-7.5	-8.0	-8.5	-10.4	-10.6	-9.3	-10.4	-10.2	-10.6
1.25	-8.6	-5.0	-3.7	-4.6	-5.4	-6.7	-8.3	-8.1	-7.1	-8.3	-8.5	-9.1
1.60	-7.2	-4.1	-2.8	-2.2	-3.8	-5.4	-6.6	-6.8	-5.8	-6.8	-6.0	-6.5
2.00	-5.5	-1.5	-0.6	-0.0	-3.0	-4.8	-4.6	-3.2	-4.3	-5.3	-7.7	-7.2
2.50	-3.9	0.4	2.1	1.6	-2.9	-4.7	-2.4	-0.8	-2.8	-3.9	-6.3	-6.3
3.15	-2.8	0.4	5.2	2.2	-2.6	-3.8	-0.8	1.5	-3.1	-3.6	-5.9	-7.0
4.00	-2.0	1.4	6.8	1.1	-2.8	-3.2	0.7	3.0	-2.3	-4.3	-7.0	-7.8
5.00	-2.1	2.3	7.7	-3.7	-3.3	-0.9	1.3	2.9	-3.4	-7.7	-9.4	-11.7
6.30	-1.3	5.9	8.1	0.1	-1.1	0.5	3.1	2.2	-4.3	-14.5	-16.1	-15.0
8.00	-2.2	5.0	8.1	2.7	0.1	-0.2	1.0	-7.3	-12.4	-8.5	-8.9	-8.6
10.0	-4.6	1.7	6.4	-0.0	-3.0	-3.7	-1.8	-4.9	-10.4	-9.7	-13.1	-15.9
12.5	-3.0	0.5	7.9	5.1	-2.6	-5.3	-1.1	-4.1	-9.6	-15.4	-14.6	-14.8
16.0	-8.1	-3.8	2.4	-0.4	-6.6	-9.2	-7.6	-8.0	-11.6	-18.6	-16.8	-18.6
20.0	-4.8	-1.2	1.1	5.1	-1.9	-6.1	-4.6	-9.6	-11.8	-19.0	-20.3	-21.8
25.0	-6.7	3.5	2.9	-2.4	-2.0	-3.8	-0.5	-7.6	-8.4	-17.1	-16.6	-21.3
31.5	-8.1	-0.5	1.6	-2.7	-8.3	-8.7	-5.9	-4.2	-8.8	-14.2	-17.5	-22.6
40.0	-6.2	-4.8	4.1	-1.9	-6.9	-7.3	-8.8	-7.6	-10.0	-18.7	-17.9	-23.8
50.0	-10.6	-9.4	-1.3	-3.5	-9.1	-10.8	-11.5	-14.0	-19.7	-22.1	-21.7	-26.7
63.0	-12.2	-2.1	-1.8	-6.9	-12.3	-15.3	-12.2	-15.2	-19.4	-23.9	-23.0	-31.1

$OPTF_t$ ← $NOSPL_t$ →

22.9 -5.8 -2.5 -5.7 -8.9 -6.7 -6.4 -8.0 -10.9 -11.3 -13.3 -13.8

1/3 OCTAVE NTC (dB) WITH RESPECT TO INCIDENT SPL (NTC_i)

$M_J = 0.6$ $M_T = 0.24$

DAISY LOBE NOZZLE (RUN NO = 37)

EMISSION ANGLE (RELATIVE TO JET EXHAUST) REFERENCED TO NOZZLE EXIT (DEGREES)

FREQ KHZ	PTF_i	20.	30.	40.	50.	60.	70.	80.	90.	100.	110.
.250	-27.5	-30.3	-31.9	-26.9	-24.9	-25.5	-24.2	-27.1	-23.6	-26.4	-26.0
.315	-24.4	-31.6	-27.5	-23.5	-21.6	-21.9	-21.0	-23.4	-21.2	-23.8	-23.3
.400	-22.8	-29.8	-26.6	-21.9	-20.0	-20.1	-19.3	-21.7	-19.9	-22.3	-21.9
.500	-28.2	-19.1	-21.9	-19.6	-17.5	-17.4	-16.8	-18.8	-18.4	-20.4	-19.7
.630	-17.5	-14.6	-18.8	-16.8	-14.9	-14.4	-14.1	-15.8	-16.4	-18.0	-17.3
.800	-14.0	-18.4	-14.4	-13.0	-11.2	-10.6	-10.8	-12.0	-13.5	-15.4	-14.7
1.00	-11.3	-6.1	-10.7	-9.7	-8.1	-7.4	-8.5	-9.4	-11.7	-14.9	-12.9
1.25	-9.2	-3.6	-7.8	-7.1	-5.7	-5.2	-6.8	-7.9	-10.4	-14.3	-11.2
1.60	-7.1	-0.2	-5.2	-4.5	-3.3	-3.1	-4.2	-6.8	-9.2	-13.1	-10.2
2.00	-5.8	1.7	-3.5	-2.7	-1.5	-1.9	-3.6	-6.5	-9.3	-12.6	-8.8
2.50	-4.9	2.5	-1.9	-1.2	-0.1	-0.6	-3.7	-7.2	-8.8	-12.2	-8.3
3.15	-3.9	2.5	-1.3	-0.4	1.3	1.4	-3.0	-7.3	-9.0	-11.3	-10.7
4.00	-4.3	3.1	-3.1	-1.4	1.1	1.5	-4.7	-5.9	-10.2	-11.4	-12.4
5.00	-5.6	4.7	-2.1	-3.3	-2.2	-1.1	-8.5	-6.5	-12.2	-13.9	-15.8
6.30	-6.8	4.7	-2.4	-4.8	-4.8	-4.8	-13.4	-10.6	-11.2	-12.5	-10.1
8.00	-6.5	6.6	-1.9	-4.0	-6.1	-7.9	-16.8	-15.7	-15.7	-16.8	-15.6
10.0	-6.0	7.8	-1.7	-7.5	-12.2	-12.8	-8.0	-10.0	-20.7	-20.6	-11.0
12.5	-5.4	5.8	4.0	-3.3	-8.7	-9.8	-14.1	-11.1	-17.7	-19.8	-12.6
16.0	-9.7	-4.7	-8.1	-4.9	-9.1	-11.2	-16.9	-13.7	-12.3	-21.1	-10.3
20.0	-9.0	-3.9	1.4	-9.5	-16.1	-12.9	-13.1	-8.8	-14.9	-16.5	-13.7
25.0	-8.5	-7.8	2.4	-2.9	-8.8	-7.8	-4.4	-4.8	-11.3	-13.0	-14.7
31.5	-14.3	-7.2	-3.7	-12.2	-13.2	-6.4	-7.7	-6.2	-9.6	-14.6	-13.8
40.0	-14.0	-9.2	-10.1	-14.8	-12.2	-8.5	-13.8	-9.2	-17.4	-18.3	-23.4
50.0	-13.7	-14.6	-9.0	-11.2	-9.8	-7.2	-11.7	-10.3	-15.8	-19.7	-18.2
63.0	-14.3	-14.5	-5.0	-11.3	-16.1	-12.2	-14.4	-12.3	-16.7	-19.3	-18.3

$OPTF_i$	← $NOSPL_i$ →								
21.0	-4.3	-8.5	-9.9	-8.8	-8.5	-11.3	-13.1	-14.8	-17.7	-15.9

CONICAL NOZZLE (RUN NO = 107)

EMISSION ANGLE (RELATIVE TO JET EXHAUST) REFERENCED TO NOZZLE EXIT (DEGREES)

FREQ KHZ	PTF_i	10.	20.	30.	40.	50.	60.	70.	80.	90.	100.	110.
.250	-26.3	-27.8	-12.9	-32.0	-33.2	-30.0	-26.2	-27.7	-26.9	-26.8	-33.2	-34.9
.315	-24.0	-23.5	-11.8	-26.6	-27.8	-26.7	-23.2	-24.8	-24.0	-23.9	-29.5	-30.1
.400	-22.9	-21.7	-11.1	-24.9	-26.0	-24.1	-21.9	-23.0	-22.7	-22.6	-27.9	-28.4
.500	-24.0	-17.6	-9.8	-17.6	-18.6	-18.4	-19.0	-20.0	-20.0	-20.3	-24.1	-23.4
.630	-17.2	-14.2	-8.0	-13.8	-14.5	-14.9	-16.1	-17.1	-17.3	-17.7	-20.9	-19.7
.800	-14.7	-14.4	-6.3	-11.2	-12.0	-12.5	-13.8	-14.1	-14.6	-14.8	-17.9	-15.8
1.00	-12.3	-6.9	-5.1	-8.9	-9.8	-10.3	-11.0	-11.4	-12.3	-11.6	-15.3	-12.8
1.25	-10.1	-4.0	-3.9	-6.9	-7.6	-8.1	-8.7	-8.7	-10.1	-9.2	-12.8	-10.8
1.60	-8.0	-1.3	-1.7	-4.5	-6.4	-5.9	-6.5	-6.2	-8.1	-7.5	-10.5	-10.0
2.00	-6.9	0.8	0.9	-1.9	-3.2	-4.0	-4.5	-3.8	-6.2	-6.6	-8.5	-9.8
2.50	-4.0	2.3	2.6	0.5	-0.7	-1.6	-2.2	-1.8	-4.5	-7.1	-7.1	-7.1
3.15	-4.0	1.2	0.8	1.4	-0.1	-1.0	-1.1	-1.8	-4.9	-9.0	-7.8	-8.2
4.00	-4.1	-2.9	-2.5	1.7	0.9	0.1	0.0	-3.3	-6.6	-7.8	-9.7	-10.6
5.00	-3.0	-4.3	-5.2	1.9	2.8	2.2	1.1	-7.5	-10.5	-9.7	-15.4	-16.1
6.30	-1.6	1.0	-4.4	2.2	4.7	5.3	3.2	-5.6	-12.7	-14.5	-14.7	-16.1
8.00	0.6	1.5	-7.0	0.9	7.3	8.6	3.9	-7.6	-8.3	-6.5	-6.6	-8.7
10.0	-0.3	-1.9	-8.0	-0.7	7.5	8.2	-0.1	-11.1	-10.8	-13.3	-15.6	-16.3
12.4	1.3	-6.8	-9.2	0.1	10.3	9.6	-3.0	-11.0	-2 .6	-21.6	-17.0	-14.9
16.0	-7.7	-7.9	-14.6	-17.5	-0.3	2.0	-16.5	-17.8	-18.6	-17.1	-24.6	-20.7
20.0	-6.1	-6.3	-7.4	-13.1	1.9	2.6	-14.8	-12.5	-19.0	-18.7	-21.7	-23.4
25.0	-2.9	-1.4	-0.7	-4.0	9.2	7.1	-12.0	-10.3	-13.4	-13.6	-17.4	-23.5
31.5	-1.6	-6.7	-5.2	-4.5	6.2	8.2	-5.3	-14.0	-10.0	-10.6	-24.4	-22.0
40.0	-3.5	-13.5	-6.3	-4.0	4.8	7.0	-8.0	-16.5	-12.7	-16.2	-19.9	-23.2
50.0	-1.8	-14.1	-8.8	-4.0	6.6	8.1	-7.1	-13.4	-14.9	-19.2	-23.8	-24.1
63.0	3.5	-6.9	-7.2	-7.3	12.3	11.6	-11.9	-17.0	-16.4	-17.3	-21.6	-26.5

$OPTF_i$	← $NOSPL_i$ →								
22.8	-7.5	-6.6	-7.6	-4.1	-4.0	-9.1	-11.7	-13.9	-13.9	-16.5	-16.1

1/3 OCTAVE NTC (dB) WITH RESPECT TO TRANSMITTED SPL (NTC_t)

$M_J = 0.6$ $M_T = 0.24$

DAISY LOBE NOZZLE (RUN NO= 37)

EMISSION ANGLE (RELATIVE TO JET EXHAUST) REFERENCED TO NOZZLE EXIT (DEGREES)

FREQ KHZ	PTF_t	20.	30.	40.	50.	60.	70.	80.	90.	100.	110.
.250	-26.9	-38.7	-31.4	-26.3	-24.3	-24.9	-23.6	-26.5	-23.0	-25.9	-25.4
.315	-23.8	-31.0	-26.9	-22.9	-21.0	-21.3	-20.4	-22.8	-20.6	-23.2	-22.7
.400	-22.2	-29.2	-25.0	-21.3	-19.4	-19.5	-18.7	-21.1	-19.3	-21.7	-21.2
.500	-19.7	-18.5	-21.3	-19.0	-17.0	-16.8	-16.3	-18.2	-17.8	-19.8	-19.2
.630	-17.0	-14.1	-18.3	-16.3	-14.4	-13.9	-13.6	-15.3	-15.9	-17.5	-16.8
.800	-13.4	-9.5	-13.8	-12.4	-10.7	-10.0	-10.3	-11.4	-13.0	-14.9	-14.2
1.00	-10.7	-5.5	-10.1	-9.1	-7.8	-6.8	-8.0	-8.8	-11.1	-13.9	-12.3
1.25	-8.6	-2.4	-7.3	-6.5	-5.1	-4.6	-6.2	-7.3	-9.8	-13.7	-10.7
1.60	-6.5	0.4	-4.6	-3.9	-2.7	-2.5	-3.6	-6.2	-8.6	-12.5	-9.6
2.00	-5.4	2.1	-3.0	-2.2	-1.1	-1.5	-3.2	-6.1	-8.8	-12.2	-8.4
2.50	-4.6	2.7	-1.6	-0.9	0.1	-0.3	-3.5	-7.0	-8.6	-11.9	-8.1
3.15	-3.8	2.7	-1.1	-0.2	1.5	1.6	-2.8	-7.1	-8.8	-11.2	-10.6
4.00	-4.1	3.3	-3.0	-1.2	1.2	1.7	-4.6	-5.8	-10.0	-11.2	-12.2
5.00	-5.3	4.9	-1.9	-3.1	-2.0	-0.9	-8.2	-6.3	-12.0	-13.6	-15.5
6.30	-5.9	5.6	-1.5	-3.9	-3.9	-3.9	-12.5	-9.8	-10.3	-11.6	-9.2
8.00	-6.2	6.9	-1.6	-4.3	-5.8	-7.6	-16.5	-15.4	-15.5	-16.5	-15.3
10.0	-5.8	8.0	-1.8	-7.0	-12.0	-12.6	-8.4	-9.7	-20.5	-20.4	-10.8
12.5	-5.0	6.2	4.5	-2.9	-8.3	-9.4	-13.7	-10.7	-17.3	-19.3	-12.2
16.0	-9.6	-4.6	0.0	-4.7	-9.0	-11.1	-16.8	-13.5	-12.2	-21.0	-10.2
20.0	-8.9	-3.8	1.5	-9.4	-16.0	-12.8	-13.0	-8.7	-14.8	-16.4	-13.6
25.0	-6.2	-7.5	2.7	-7.6	-8.5	-7.5	-4.1	-4.5	-11.0	-12.7	-14.4
31.5	-14.2	-7.8	-3.6	-12.1	-13.1	-6.2	-7.5	-6.0	-9.4	-14.5	-13.6
40.0	-13.9	-9.1	-10.1	-14.7	-12.1	-8.5	-13.4	-9.2	-17.3	-18.2	-23.4
50.0	-13.4	-14.2	-8.7	-10.9	-9.5	-6.9	-11.4	-10.0	-15.5	-19.4	-17.9
63.0	-13.8	-14.1	-4.6	-10.9	-15.7	-11.8	-14.0	-11.9	-18.3	-18.9	-17.9

$OPTF_t$ ← $NOSPL_t$ →

21.5 -3.8 -8.0 -9.4 -8.3 -8.0 -10.8 -12.6 -14.3 -17.2 -15.4

CONICAL NOZZLE (RUN NO = 107)

EMISSION ANGLE (RELATIVE TO JET EXHAUST) REFERENCED TO NOZZLE EXIT (DEGREES)

FREQ KHZ	PTF_t	10.	20.	30.	40.	50.	60.	70.	80.	90.	100.	110.
.250	-24.2	-25.8	-10.8	-30.0	-31.2	-28.0	-24.2	-25.7	-24.8	-24.8	-31.2	-32.8
.315	-22.7	-22.2	-10.2	-25.3	-26.8	-24.4	-21.9	-23.2	-22.7	-22.6	-28.2	-28.8
.400	-22.1	-20.9	-10.3	-24.0	-25.2	-23.2	-21.0	-22.2	-21.8	-21.7	-27.0	-27.5
.500	-19.3	-17.0	-8.8	-16.9	-17.9	-17.8	-18.3	-19.3	-19.3	-19.6	-23.4	-22.7
.630	-16.8	-13.8	-7.5	-13.4	-14.0	-14.5	-15.7	-16.7	-16.9	-17.3	-20.4	-19.3
.800	-14.5	-10.2	-6.1	-11.1	-11.9	-12.4	-13.3	-13.9	-14.5	-14.4	-17.8	-16.6
1.00	-12.2	-6.8	-5.0	-8.8	-9.7	-10.2	-11.0	-11.3	-12.2	-11.6	-15.2	-12.7
1.25	-10.1	-3.9	-3.8	-6.8	-7.6	-8.1	-8.7	-8.7	-10.0	-9.2	-12.7	-10.7
1.60	-8.0	-1.3	-1.7	-4.4	-5.4	-5.9	-6.8	-6.2	-8.1	-7.5	-10.5	-9.9
2.00	-5.9	0.8	1.0	-1.8	-3.2	-4.0	-4.8	-3.8	-6.1	-6.6	-8.5	-9.5
2.50	-4.0	2.4	2.6	0.6	-0.6	-1.8	-2.2	-1.8	-4.8	-7.1	-7.1	-7.1
3.15	-3.9	1.2	0.6	1.1	-0.1	-1.0	-1.0	-1.7	-4.9	-9.0	-7.8	-8.2
4.00	-4.1	-2.9	-2.5	1.7	0.9	0.1	0.0	-3.3	-6.6	-7.8	-9.7	-10.6
5.00	-3.6	-4.2	-5.2	1.9	2.5	2.3	1.2	-7.5	-10.5	-9.7	-15.4	-19.1
6.30	-4.9	1.6	-3.8	2.9	5.4	6.0	3.9	-4.9	-12.1	-13.8	-14.0	-15.5
8.00	-4.7	1.6	-6.9	1.1	7.4	8.9	4.0	-7.5	-8.2	-6.4	-6.5	-8.6
10.0	-4.4	-1.2	-7.3	-0.9	8.3	8.9	0.6	-10.4	-10.1	-12.6	-14.9	-15.6
12.5	3.8	-4.7	-7.1	2.3	12.5	11.8	-0.7	-8.9	-20.4	-19.2	-14.8	-12.8
16.0	-7.7	-7.8	-14.6	-17.5	-0.3	2.0	-16.5	-17.7	-18.6	-17.1	-24.6	-20.7
20.0	-6.1	-5.3	-7.4	-13.6	2.0	2.7	-14.7	-12.4	-19.0	-18.6	-21.6	-23.4
25.0	-4.8	-1.2	-0.6	-4.4	9.4	7.2	-11.9	-10.2	-13.2	-13.5	-17.2	-23.4
31.5	-1.3	-6.5	-4.9	-4.3	6.5	8.4	-6.1	-13.7	-9.8	-10.4	-24.2	-21.8
40.0	-3.5	-13.5	-6.2	-4.6	4.8	7.0	-7.9	-15.5	-12.6	-16.1	-19.8	-23.1
50.0	-1.7	-14.9	-8.4	-4.5	6.8	8.2	-7.0	-13.3	-14.8	-19.1	-23.4	-24.0
63.0	3.7	-6.7	-7.0	-7.1	12.6	11.8	-11.7	-16.8	-16.2	-17.1	-21.4	-26.2

$OPTF_t$ ← $NOSPL_t$ →

23.6 -6.7 -5.8 -7.1 -3.3 -3.2 -8.3 -10.9 -13.1 -13.1 -18.8 -15.3

1/3 OCTAVE NTC (dB) WITH RESPECT TO INCIDENT SPL (NTC_i)

$M_J = 0.8 \quad M_T = 0.24$

DAISY LOBE NOZZLE (RUN NO = 55)

FREQ KHZ	PTF$_i$	20.	30.	40.	50.	60.	70.	80.	90.	100.	110.
	EMISSION ANGLE (RELATIVE TO JET EXHAUST) REFERENCED TO NOZZLE EXIT (DEGREES)										
.250	-24.6	-21.4	-23.4	-28.3	-29.3	-28.6	-29.7	-30.3	-30.6	-37.8	-32.1
.315	-20.7	-18.3	-22.2	-26.1	-26.2	-22.5	-26.2	-27.2	-27.1	-33.3	-28.4
.400	-25.4	-17.3	-21.6	-25.1	-24.9	-21.2	-23.0	-25.8	-25.6	-31.5	-26.9
.500	-22.3	-13.5	-21.2	-23.2	-21.9	-18.8	-19.0	-22.9	-21.8	-26.4	-24.0
.630	-19.2	-16.2	-20.8	-21.3	-18.8	-15.6	-16.2	-19.8	-18.3	-22.4	-20.8
.800	-15.2	-8.6	-17.3	-17.4	-15.3	-11.6	-10.7	-16.2	-14.9	-18.7	-15.7
1.00	-12.2	-3.9	-14.6	-15.2	-12.5	-8.5	-7.5	-13.2	-12.2	-15.7	-11.9
1.25	-14.4	-2.2	-12.8	-13.5	-10.6	-6.3	-6.1	-11.5	-10.6	-13.6	-9.6
1.60	-8.9	-0.6	-11.3	-11.9	-8.7	-4.6	-5.3	-9.8	-9.1	-11.7	-8.2
2.00	-7.1	1.8	-9.8	-10.0	-6.4	-2.3	-4.4	-7.8	-7.3	-9.4	-7.2
2.50	-6.6	3.4	-10.3	-9.6	-5.3	-1.6	-5.0	-7.1	-7.0	-8.7	-8.8
3.15	-5.8	4.9	-11.4	-9.2	-3.8	-1.0	-5.3	-6.4	-6.8	-8.3	-10.4
4.00	-5.3	6.8	-7.0	-6.0	-3.0	-1.8	-7.2	-7.3	-8.1	-10.3	-11.8
5.00	-4.1	8.3	1.3	-0.9	-2.3	-4.6	-11.1	-11.0	-10.7	-15.5	-13.4
6.30	-6.3	4.4	2.4	-0.8	-7.1	-16.7	-24.6	-20.6	-13.9	-15.7	-11.8
8.00	-9.2	-2.6	-1.4	-1.4	-7.2	-17.5	-20.7	-19.0	-14.6	-16.0	-9.3
10.0	-6.5	2.9	0.9	0.1	-6.2	-14.7	-13.8	-12.1	-25.4	-17.9	-9.7
12.5	-5.3	4.2	4.7	0.4	-11.8	-26.5	-14.3	-12.7	-19.5	-24.0	-10.5
16.0	-9.3	-0.7	-1.0	-2.8	-6.7	-13.7	-22.8	-16.3	-15.7	-19.8	-16.3
20.0	-11.8	-4.4	-7.9	-4.2	-5.3	-13.5	-23.0	-11.7	-11.0	-14.8	-25.9
25.0	-8.4	-1.1	-9.5	-1.9	-1.5	-9.5	-10.2	-7.0	-10.9	-16.2	-19.0
31.5	-12.5	-1.3	-8.1	-9.6	-10.8	-18.7	-14.6	-12.0	-15.0	-14.6	-22.7
40.0	-11.1	-8.4	-9.8	-12.7	-8.9	-5.0	-11.5	-7.1	-9.8	-10.7	-21.9
50.0	-14.6	-18.9	-5.9	-7.1	-8.7	-12.5	-10.6	-15.6	-15.1	-16.4	-8.6
63.0	-14.9	-10.7	-2.9	-3.5	-7.8	-11.3	-17.3	-13.2	-19.1	-15.5	-25.5
	OPTF$_i$ ←					NOSPL$_i$ →					
	24.4	-3.4	-8.5	-10.4	-11.8	-10.1	-12.3	-15.1	-14.4	-17.2	-15.5

CONICAL NOZZLE (RUN NO = 111)

FREQ KHZ	PTF$_i$	10.	20.	30.	40.	50.	60.	70.	80.	90.	100.	110.
	EMISSION ANGLE (RELATIVE TO JET EXHAUST) REFERENCED TO NOZZLE EXIT (DEGREES)											
.250	-21.4	-4.8	-16.6	-25.0	-25.2	-25.1	-26.7	-31.2	-40.9	-41.4	-52.9	-40.7
.315	-19.7	-3.8	-13.3	-20.6	-20.8	-20.9	-22.8	-26.9	-34.4	-34.9	-44.3	-35.3
.400	-18.6	-3.8	-12.6	-19.0	-19.3	-19.4	-21.3	-25.4	-32.6	-33.1	-42.2	-33.7
.500	-16.3	-2.1	-8.4	-14.1	-14.2	-14.8	-17.7	-20.9	-23.9	-23.8	-29.1	-29.3
.630	-13.8	-0.7	-5.4	-10.6	-10.6	-11.5	-14.6	-17.5	-19.9	-19.7	-24.8	-25.7
.800	-11.3	-0.6	-2.6	-7.6	-7.4	-8.1	-10.7	-14.1	-16.2	-16.5	-21.2	-19.8
1.00	-9.4	-0.1	-1.0	-5.7	-5.7	-5.8	-7.3	-10.7	-12.8	-13.5	-18.0	-15.2
1.25	-8.1	-0.9	-0.3	-4.9	-5.8	-4.9	-4.6	-7.6	-9.7	-10.8	-15.0	-11.4
1.60	-6.4	-1.1	0.9	-3.4	-4.4	-3.8	-2.7	-4.7	-7.0	-8.4	-12.3	-8.2
2.00	-4.8	0.3	2.4	-2.3	-2.4	-1.8	-1.9	-2.2	-4.9	-6.6	-10.2	-6.1
2.50	-4.4	-0.5	1.6	-1.6	-1.6	-1.7	-2.3	-0.8	-4.1	-5.9	-9.3	-5.6
3.15	-4.0	-2.7	0.9	0.4	-1.8	-1.8	-0.2	0.1	-4.8	-6.4	-9.6	-7.2
4.00	-4.8	-6.7	0.6	0.9	-2.7	-3.0	1.2	-0.7	-6.1	-9.6	-13.0	-14.4
5.00	-5.3	-4.6	-0.4	-2.4	-4.4	-3.0	1.4	-1.3	-6.9	-13.7	-19.9	-22.6
6.30	-4.1	-6.8	-2.1	-4.5	-1.6	1.9	3.4	-2.6	-14.1	-18.7	-18.7	-19.0
8.00	-6.4	-2.3	0.2	-6.3	-5.0	-1.4	0.9	-11.7	-14.0	-9.8	-13.9	-17.5
10.0	-3.6	-4.3	2.1	-4.9	-0.6	3.0	2.9	-5.2	-9.8	-10.4	-20.6	-15.4
12.4	-7.3	-3.3	-1.0	-11.1	-4.7	0.1	-1.7	-12.1	-18.1	-14.5	-19.8	-22.0
16.0	-8.2	-8.7	-9.3	-7.8	-1.9	-0.6	-6.9	-8.1	-15.7	-14.2	-21.2	-24.7
20.0	-13.9	-8.0	-9.6	-15.1	-11.0	-8.2	-9.1	-14.1	-15.3	-16.5	-20.8	-25.3
25.0	-7.6	-6.4	-3.8	-5.3	-0.6	-0.6	-4.8	-9.0	-18.0	-12.6	-15.1	-22.2
31.5	-9.8	-9.4	-8.3	-6.1	-3.8	-2.6	-6.7	-9.3	-12.7	-16.5	-26.2	-28.1
40.0	-11.4	-6.7	-18.8	-10.7	-6.9	-2.3	-6.9	-15.1	-17.8	-20.1	-24.8	-26.1
50.0	-14.4	-9.3	-14.7	-8.9	-8.2	-7.0	-9.7	-17.8	-25.8	-24.4	-27.9	-30.5
63.0	-12.8	-2.8	-8.7	-9.7	-7.6	-7.3	-7.4	-12.5	-17.8	-20.1	-25.4	-28.6
	OPTF$_i$ ←					NOSPL$_i$ →						
	22.4	-2.3	-4.6	-8.0	-8.1	-7.3	-7.1	-9.7	-13.5	-14.3	-18.7	-15.9

1/3 OCTAVE NTC (dB) WITH RESPECT TO TRANSMITTED SPL (NTC_t)

$M_J = 0.8$ $M_T = 0.24$

DAISY LOBE NOZZLE (RUN NO = 55)

EMISSION ANGLE (RELATIVE TO JET EXHAUST) REFERENCED TO NOZZLE EXIT (DEGREES)

FREQ KHZ	PTF_t	20.	30.	40.	50.	60.	70.	80.	90.	100.	110.
.250	-28.8	-20.3	-22.3	-27.2	-28.1	-24.4	-26.5	-29.2	-29.5	-36.8	-30.9
.315	-25.7	-17.3	-21.2	-25.2	-25.3	-21.8	-24.3	-26.2	-26.1	-32.4	-27.4
.400	-24.8	-16.5	-20.7	-24.2	-24.0	-20.3	-22.7	-25.0	-24.7	-30.7	-26.0
.500	-21.5	-12.6	-20.3	-22.4	-21.0	-17.7	-18.2	-22.0	-20.6	-25.5	-23.2
.630	-18.4	-9.4	-20.0	-20.5	-18.0	-14.8	-14.8	-19.0	-17.8	-21.7	-20.1
.800	-14.6	-6.0	-16.7	-17.3	-14.7	-11.0	-10.1	-15.6	-14.3	-18.1	-15.1
1.00	-11.7	-3.4	-14.1	-14.7	-12.0	-8.0	-7.0	-12.7	-11.7	-15.2	-11.4
1.25	-10.0	-1.8	-12.4	-13.1	-10.2	-6.5	-5.7	-11.0	-10.2	-13.2	-9.2
1.60	-8.6	-0.2	-11.0	-11.6	-8.4	-4.1	-5.0	-9.5	-8.8	-11.4	-7.9
2.00	-8.7	2.1	-9.5	-9.7	-6.0	-1.9	-4.1	-7.4	-7.0	-9.1	-6.9
2.50	-8.4	3.2	-10.1	-9.4	-5.1	-1.4	-4.8	-6.9	-6.8	-8.5	-8.6
3.15	-8.6	5.1	-11.3	-9.0	-3.7	-0.8	-5.2	-6.2	-6.6	-8.2	-10.2
4.00	-8.3	6.8	-7.0	-6.0	-3.0	-1.8	-7.1	-7.2	-8.1	-10.2	-11.8
5.00	-3.6	8.7	1.7	-0.5	-1.9	-4.2	-10.7	-10.6	-10.3	-15.1	-13.0
6.30	-6.1	4.6	2.7	-0.0	-6.9	-16.5	-24.4	-20.4	-13.7	-15.5	-11.6
8.00	-6.7	-2.2	-0.9	-1.0	-6.8	-17.1	-28.3	-18.6	-14.2	-15.6	-8.9
10.0	-6.3	3.1	2.1	0.3	-6.8	-14.5	-13.6	-11.9	-25.1	-17.7	-9.5
12.5	-5.1	4.4	4.9	0.0	-11.6	-26.4	-14.2	-12.6	-19.4	-23.9	-10.3
16.0	-9.2	-6.6	-0.9	-2.0	-6.5	-13.6	-22.6	-16.2	-15.5	-19.7	-16.1
20.0	-10.9	-4.4	-7.9	-4.1	-5.2	-13.5	-22.9	-11.6	-10.9	-14.7	-25.8
25.0	-8.3	-0.9	-9.4	-1.8	-1.3	-9.4	-10.6	-6.8	-10.7	-16.1	-18.8
31.5	-12.8	-1.3	-8.0	-9.5	-10.7	-15.7	-18.5	-12.0	-15.0	-14.6	-22.6
40.0	-14.9	-8.3	-9.3	-12.6	-8.8	-4.9	-11.4	-7.0	-9.7	-10.6	-21.8
50.0	-13.8	-18.7	-5.7	-7.0	-8.5	-12.3	-16.4	-15.4	-14.9	-18.2	-18.4
63.0	-14.6	-14.4	-2.7	-3.2	-7.8	-11.0	-17.0	-12.9	-18.9	-15.3	-25.2
$OPTF_t$	21.1	-2.7	-7.8	-9.7	-11.0	-9.4	-11.8	-14.4	-13.7	-16.5	-14.7

$NOSPL_t$

CONICAL NOZZLE (RUN NO = 111)

EMISSION ANGLE (RELATIVE TO JET EXHAUST) REFERENCED TO NOZZLE EXIT (DEGREES)

FREQ KHZ	PTF_t	10.	20.	30.	40.	50.	60.	70.	80.	90.	100.	110.
.250	-1.0	15.5	3.8	-4.6	-4.8	-4.7	-6.3	-10.8	-20.8	-21.1	-32.5	-20.3
.315	-10.7	-0.8	-10.3	-17.6	-17.8	-17.9	-19.8	-23.9	-31.4	-31.9	-41.3	-32.3
.400	-18.0	-2.2	-11.7	-18.2	-18.8	-18.6	-20.5	-24.6	-31.8	-32.3	-41.4	-32.9
.500	-15.7	-1.5	-7.9	-13.5	-13.6	-14.2	-17.1	-20.3	-23.3	-23.2	-28.6	-28.7
.630	-13.6	-0.5	-5.2	-10.4	-10.4	-11.3	-14.4	-17.3	-19.6	-19.5	-24.6	-28.5
.800	-11.3	-0.0	-2.6	-7.4	-7.4	-8.1	-10.7	-14.0	-16.2	-16.5	-21.2	-19.8
1.00	-9.4	-0.1	-1.0	-5.7	-5.7	-5.8	-7.3	-10.7	-12.8	-13.5	-18.0	-18.2
1.25	-8.1	-0.9	-0.3	-4.9	-5.5	-4.9	-4.6	-7.6	-9.7	-10.8	-15.0	-11.4
1.60	-6.4	-1.1	0.9	-3.4	-4.4	-3.8	-2.0	-4.7	-7.0	-8.4	-12.3	-8.2
2.00	-4.7	0.3	2.4	-2.3	-2.4	-1.8	-1.9	-2.2	-4.9	-6.8	-10.2	-6.1
2.50	-4.4	-0.5	1.6	-1.6	-1.6	-1.7	-2.2	-0.8	-4.1	-5.9	-9.3	-6.6
3.15	-3.5	-2.6	1.0	0.4	-1.5	-1.7	-0.2	0.2	-4.4	-6.3	-9.6	-7.1
4.00	-4.4	-6.7	0.7	0.9	-2.7	-3.0	1.2	-0.7	-6.1	-9.6	-13.0	-14.4
5.00	-8.3	-4.6	-0.4	-2.3	-4.4	-3.0	1.4	-1.3	-6.8	-13.7	-19.9	-22.6
6.30	-3.5	-6.0	-1.5	-3.9	-1.1	2.4	4.0	-2.1	-13.6	-18.1	-18.1	-16.4
8.00	-6.2	-2.2	0.3	-6.2	-4.9	-1.3	1.0	-11.6	-13.9	-9.7	-13.8	-17.4
10.0	-3.0	-3.8	2.6	-4.3	-0.1	3.5	3.4	-4.6	-9.0	-9.8	-20.1	-14.8
12.5	-6.5	-2.9	-0.5	-10.7	-4.3	0.6	-1.3	-11.7	-17.6	-14.1	-19.4	-21.6
16.0	-8.1	-5.6	-5.2	-7.6	-1.8	-0.5	-6.8	-8.0	-15.6	-14.1	-21.1	-24.6
20.0	-13.9	-7.9	-9.4	-15.0	-10.9	-8.2	-9.6	-14.1	-19.2	-16.4	-20.7	-25.2
25.0	-7.8	-5.9	-3.8	-5.3	-0.5	-0.5	-4.7	-6.9	-14.9	-12.6	-15.0	-22.2
31.5	-9.7	-9.3	-5.3	-6.1	-3.7	-2.5	-6.6	-9.2	-12.7	-16.4	-26.1	-26.0
40.0	-11.4	-6.7	-10.8	-10.6	-6.8	-2.2	-5.8	-15.0	-17.7	-20.0	-24.8	-26.0
50.0	-14.3	-9.3	-14.7	-8.6	-8.1	-6.9	-9.6	-17.8	-28.5	-24.4	-27.9	-30.5
63.0	-11.8	-2.6	-8.5	-9.4	-7.4	-7.1	-7.1	-12.3	-17.5	-19.8	-25.2	-28.4
$OPTF_t$	23.7	-1.0	-3.3	-6.7	-6.8	-6.0	-5.8	-8.4	-12.1	-13.2	-17.5	-14.6

$NOSPL_t$

1/3 OCTAVE NTC (dB) WITH RESPECT TO INCIDENT SPL (NTC_i)

$M_J = 0.8$ $M_T = 0$ $T_R = 600K$

DAISY LOBE NOZZLE (RUN NO = 70)

EMISSION ANGLE (RELATIVE TO JET EXHAUST) REFERENCED TO NOZZLE EXIT (DEGREES)

FREQ KHZ	PTF	10.	20.	30.	40.	50.	60.	70.	80.	90.	100.	110.	120.
.250	-26.9	-14.0	-24.9	-17.6	-26.6	-29.2	-29.7	-33.6	-36.6	-39.2	-41.0	-30.0	-41.3
.315	-22.5	-11.4	-20.6	-12.6	-20.9	-22.6	-23.8	-27.2	-30.1	-46.2	-33.8	-26.2	-35.3
.400	-18.1	-7.4	-16.4	-8.1	-16.1	-17.7	-18.7	-22.3	-28.2	-40.7	-28.8	-22.1	-30.6
.500	-14.4	-5.5	-13.8	-4.6	-11.9	-12.0	-13.7	-16.8	-20.3	-22.8	-21.8	-20.1	-25.8
.630	-9.1	-1.8	-9.3	0.5	-6.4	-6.0	-7.9	-10.8	-14.4	-15.8	-15.4	-16.2	-20.1
.800	-7.4	-2.9	-8.1	2.1	-3.9	-3.6	-5.6	-8.6	-11.2	-12.7	-13.3	-15.0	-18.0
1.00	-7.0	-6.8	-8.3	1.8	-3.2	-2.8	-4.8	-7.1	-9.3	-10.4	-12.0	-14.6	-16.3
1.25	-8.0	-11.4	-8.7	0.1	-2.6	-0.9	-2.8	-4.2	-7.1	-7.3	-9.7	-13.9	-13.6
1.60	-4.6	-14.9	-11.3	-3.3	-2.2	0.9	0.4	-1.2	-5.8	-4.9	-7.9	-13.1	-11.1
2.00	-4.2	-18.1	-16.2	-4.3	-2.9	1.8	1.7	-0.8	-6.6	-5.3	-8.7	-12.6	-10.8
2.50	-2.3	-26.8	-13.5	0.1	-2.3	4.3	3.8	0.4	-4.0	-5.3	-8.8	-11.7	-9.3
3.15	-6.8	-17.6	-13.4	-1.1	-3.0	5.8	5.7	2.8	-2.5	-6.3	-9.7	-11.8	-8.9
4.00	-0.1	-16.3	-10.9	-4.1	-2.0	6.6	8.1	2.2	-4.3	-7.2	-9.6	-12.2	-10.4
5.00	-1.5	-13.4	-10.1	-2.9	-2.0	4.7	6.3	-0.4	-4.6	-5.1	-13.6	-11.1	-13.2
6.30	-3.4	-14.1	-7.0	-12.2	-1.9	1.0	3.9	-1.3	-1.4	-8.0	-11.9	-12.7	-21.7
8.00	-6.1	-11.8	-8.0	-4.8	-6.6	0.6	1.1	-7.2	-6.3	-18.2	-11.1	-17.2	-20.0
10.0	-5.8	-8.1	-5.9	-4.6	-1.6	-2.5	0.7	-2.9	-4.4	-14.1	-14.5	-20.4	-19.7
12.5	-2.8	-13.7	-6.2	-5.4	0.3	-2.8	3.6	2.8	-0.7	-9.6	-6.2	-12.7	-27.7
16.0	-2.3	-19.8	-8.2	-7.1	-7.1	-3.2	0.9	2.3	-5.2	-5.5	-17.2	-16.7	-40.9
20.0	-1.5	-12.2	-1.6	-6.4	3.9	1.7	6.3	-2.6	-5.0	-6.2	-11.3	-22.2	-31.0
25.0	-2.0	-13.6	0.1	-2.3	-0.7	-2.4	5.6	-3.2	0.3	-1.3	-8.7	-22.7	-30.8
31.5	-4.1	-17.1	-4.8	-6.0	-2.5	-2.6	4.4	-2.4	-1.8	-4.3	-12.3	-23.3	-34.4
40.0	-3.2	-18.6	-13.4	-5.2	-2.0	-4.8	5.6	-0.4	0.1	-5.0	-11.4	-11.2	-35.4
50.0	-6.9	-18.4	-19.4	-8.7	-7.1	-11.2	1.4	-0.9	-3.7	-5.0	-12.9	-13.6	-32.4
63.0	-6.7	-11.7	-12.7	-8.9	-7.8	-4.1	1.4	-3.4	-5.7	-6.0	-11.0	-9.6	-29.2

$OPTF_i$	← $NOSPL_i$ →									
20.6	-9.5	-15.4	-6.8	-10.7	-7.8	-6.9	-11.0	-14.9	-15.6	-18.8	-20.9	-22.1

CONICAL NOZZLE (RUN NO = 98)

EMISSION ANGLE (RELATIVE TO JET EXHAUST) REFERENCED TO NOZZLE EXIT (DEGREES)

FREQ KHZ	PTF_i	30.	40.	50.	60.	70.	80.	90.	100.	110.	120.
.250	-26.7	-16.3	-19.1	-26.3	-30.8	-30.2	-37.4	-31.3	-51.1	-40.9	-77.3
.315	-21.3	-10.8	-13.9	-19.9	-24.4	-25.4	-30.8	-28.8	-42.8	-34.3	-63.2
.400	-16.0	-5.5	-8.7	-14.4	-18.9	-20.3	-25.2	-25.0	-37.0	-28.8	-57.0
.500	-12.8	-2.5	-6.0	-9.6	-14.2	-17.7	-19.6	-24.6	-28.3	-23.1	-36.2
.630	-7.9	2.3	-1.3	-3.9	-8.8	-13.1	-13.6	-23.3	-21.8	-17.2	-29.3
.800	-4.8	5.6	1.8	-0.9	-5.4	-11.0	-11.3	-23.0	-19.3	-14.9	-26.7
1.00	-2.3	8.0	4.3	1.6	-2.8	-9.1	-9.4	-21.8	-17.2	-13.1	-24.4
1.25	-1.1	10.2	6.7	3.9	0.6	-6.8	-7.1	-19.7	-14.7	-11.1	-21.5
1.60	1.3	10.9	8.1	5.2	3.4	-4.6	-4.9	-17.1	-12.2	-9.5	-18.6
2.00	0.5	8.8	7.4	4.2	4.9	-3.0	-3.4	-14.9	-10.5	-9.0	-16.4
2.50	1.0	1.8	5.3	0.3	6.2	-0.7	-1.1	-11.8	-8.0	-8.8	-13.2
3.15	6.4	5.4	6.1	0.0	6.8	2.1	1.8	-7.7	-5.2	-8.9	-9.3
4.00	2.8	3.6	4.2	2.7	6.9	4.0	3.3	-4.8	-4.8	-12.6	-6.9
5.00	2.1	-8.5	9.4	-0.5	9.3	4.2	2.8	-3.2	-7.0	-20.3	-6.7
6.30	4.0	3.8	6.8	-2.0	5.6	3.2	-0.5	-2.8	-12.3	-19.7	-9.6
8.00	-4.2	5.8	1.2	4.9	6.9	1.0	-9.8	-6.7	-12.6	-16.5	-16.5
10.0	-1.3	5.3	-1.1	1.9	5.8	2.1	-4.7	-18.7	-18.4	-15.2	-17.2
12.5	0.0	-0.6	-4.2	1.3	7.5	7.1	-5.1	-9.9	-13.3	-11.8	-17.3
16.0	1.3	2.0	-4.0	1.4	7.9	9.2	-4.5	-11.4	-8.8	-8.0	-8.4
20.0	-3.3	0.7	-1.8	-1.2	4.1	-0.8	-6.6	-14.0	-10.5	-9.5	-9.2
25.0	-2.8	1.5	-6.2	0.5	6.0	-6.8	-7.2	-12.3	-8.8	-12.8	-14.0
31.5	-4.1	1.2	-6.8	1.0	4.8	-3.3	-11.2	-6.7	-10.2	-16.0	-19.0
40.0	1.5	8.8	2.2	0.3	6.3	1.5	-8.4	-2.9	-3.0	-2.0	-10.4
50.0	-3.7	5.9	-2.3	-3.2	1.6	-2.6	-7.0	-6.8	-14.0	-9.1	-11.3
63.0	-8.1	0.6	-2.8	-5.7	-6.2	-12.5	-10.1	-11.8	-10.2	-12.7	-25.3

$OPTF_i$	← $NOSPL_i$ →									
22.4	-1.6	-4.4	-7.6	-7.4	-12.6	-16.1	-21.5	-22.2	-21.5	-26.2

1/3 OCTAVE NTC (dB) WITH RESPECT TO TRANSMITTED SPL (NTC_t)

$M_J = 0.8$ $M_T = 0$ $T_R = 600K$

DAISY LOBE NOZZLE (RUN NO = 70)

EMISSION ANGLE (RELATIVE TO JET EXHAUST) REFERENCED TO NOZZLE EXIT (DEGREES)

FREQ KHZ	PTF	10.	20.	30.	40.	50.	60.	70.	80.	90.	100.	110.	120.
.250	-20.8	-13.8	-24.7	-17.4	-26.4	-20.0	-29.5	-33.4	-38.4	-59.0	-40.8	-29.8	-41.1
.315	-22.2	-10.7	-20.3	-12.3	-20.8	-22.3	-23.3	-26.9	-29.8	-45.9	-33.5	-25.9	-35.0
.400	-17.5	-6.8	-16.8	-7.0	-15.6	-17.2	-18.2	-21.8	-24.6	-40.2	-28.3	-21.5	-30.0
.500	-13.8	-5.8	-13.2	-4.9	-11.4	-11.5	-13.2	-15.9	-19.7	-22.3	-21.2	-19.6	-25.2
.630	-8.6	-1.2	-8.8	1.1	-5.9	-6.5	-7.4	-9.9	-13.9	-15.2	-14.9	-15.7	-19.5
.800	-6.8	-2.4	-7.6	2.0	-3.4	-3.1	-5.0	-8.1	-10.6	-12.1	-12.8	-14.4	-17.5
1.00	-6.5	-6.3	-7.8	2.0	-2.8	-2.0	-4.1	-6.7	-8.8	-9.9	-11.5	-14.1	-15.8
1.25	-5.5	-10.5	-8.1	0.0	-2.0	-0.3	-2.2	-3.6	-6.5	-6.8	-9.1	-13.3	-13.9
1.60	-3.5	-14.2	-10.7	-2.7	-1.5	1.5	1.1	-0.5	-4.9	-4.3	-7.3	-12.5	-10.4
2.00	-3.8	-17.7	-15.8	-4.9	-2.4	2.2	2.1	-0.4	-5.2	-4.9	-8.2	-12.1	-10.4
2.50	-2.0	-20.4	-13.2	0.4	-2.0	4.6	3.8	0.7	-3.6	-5.0	-8.5	-11.4	-9.0
3.15	-4.8	-17.5	-13.3	-1.1	-2.9	5.9	6.8	2.9	-2.5	-6.2	-9.6	-11.8	-8.8
4.00	-0.1	-16.3	-10.8	-4.1	-2.0	6.6	8.1	2.2	-4.3	-7.1	-9.6	-12.2	-10.3
5.00	-1.5	-13.3	-10.1	-2.9	-2.0	4.7	6.3	-0.4	-4.6	-5.1	-13.6	-11.1	-13.1
6.30	-3.4	-10.6	-7.0	-12.1	-1.8	1.0	3.9	-1.2	-1.4	-8.0	-11.9	-12.6	-21.6
8.00	-5.9	-11.7	-7.8	-4.6	-8.5	0.7	1.3	-7.1	-6.2	-18.1	-11.0	-17.0	-19.8
10.0	-5.1	-7.4	-5.2	-3.9	-0.9	-1.9	1.3	-2.3	-3.7	-13.4	-13.8	-19.7	-19.0
12.5	-2.0	-13.5	-6.1	-5.3	0.5	-2.7	3.8	2.9	-0.6	-9.5	-6.0	-12.5	-27.6
16.0	-2.2	-19.8	-8.1	-7.3	-7.0	-3.2	6.9	2.4	-5.1	-5.5	-17.2	-16.6	-40.9
20.0	-1.3	-12.0	-1.4	-6.2	3.5	1.9	6.5	-2.4	-4.8	-6.0	-11.1	-22.0	-30.8
25.0	-2.0	-13.6	0.2	-2.3	-0.7	-2.4	5.6	-3.2	0.3	-1.3	-8.7	-22.7	-30.7
31.5	-4.0	-17.0	-3.9	-5.9	-2.4	-2.5	4.6	-2.4	-1.4	-4.2	-12.3	-23.2	-34.4
40.0	-2.6	-18.6	-12.7	-4.6	-1.4	-4.2	6.2	0.2	0.7	-4.4	-10.8	-10.6	-34.8
50.0	-6.0	-18.1	-19.1	-8.4	-6.6	-10.9	1.7	-0.6	-3.4	-4.7	-12.7	-13.3	-32.1
63.0	-5.6	-10.9	-11.7	-8.1	-6.9	-3.3	2.3	-2.5	-4.9	-5.1	-10.1	-8.8	-28.1

$OPTF_t$	$NOSPL_t$
20.9	-9.2 -15.1 -6.5 -10.4 -7.6 -6.6 -10.7 -14.6 -15.3 -18.5 -20.6 -21.8

CONICAL NOZZLE (RUN NO = 98)

EMISSION ANGLE (RELATIVE TO JET EXHAUST) REFERENCED TO NOZZLE EXIT (DEGREES)

FREQ KHZ	PTF	30.	40.	50.	60.	70.	80.	90.	100.	110.	120.
.250	-20.0	-15.6	-18.4	-25.6	-30.1	-29.5	-36.7	-30.6	-50.4	-40.2	-76.6
.315	-20.5	-10.0	-13.1	-19.1	-23.6	-24.6	-30.0	-28.1	-42.0	-33.5	-62.4
.400	-15.0	-4.5	-7.7	-13.4	-17.9	-19.3	-24.2	-24.0	-36.0	-27.7	-55.9
.500	-12.0	-1.6	-5.1	-8.7	-13.3	-16.8	-18.7	-23.7	-27.4	-22.2	-35.3
.630	-7.5	2.7	-0.9	-3.8	-8.1	-12.8	-13.2	-22.9	-21.4	-16.8	-28.9
.800	-4.6	5.7	2.0	-0.7	-5.2	-10.9	-11.2	-22.8	-19.2	-14.7	-26.5
1.00	-2.3	8.0	4.3	1.5	-2.5	-9.1	-9.3	-21.7	-17.2	-13.1	-24.3
1.25	-0.1	10.2	6.8	3.9	0.6	-6.8	-7.1	-19.7	-14.7	-11.1	-21.5
1.60	1.2	11.0	8.1	5.2	3.4	-4.6	-4.9	-17.1	-12.2	-9.5	-18.0
2.00	0.5	8.8	7.4	4.3	5.0	-3.0	-3.3	-14.8	-10.4	-9.0	-16.3
2.50	-1.0	1.8	5.4	0.4	6.3	-0.7	-1.0	-11.7	-8.0	-8.5	-13.2
3.15	0.5	5.5	6.1	0.7	6.6	2.2	1.9	-7.6	-6.1	-8.9	-9.3
4.00	0.6	3.6	4.2	2.7	7.0	4.0	3.4	-4.8	-4.4	-12.6	-6.8
5.00	2.1	-8.4	9.3	-0.4	9.3	4.2	2.8	-3.2	-6.9	-20.2	-6.7
6.30	0.1	3.9	6.9	-1.9	5.7	3.3	-0.5	-2.7	-12.2	-19.7	-9.5
8.00	0.0	6.6	1.4	5.1	7.1	1.2	-5.6	-6.5	-12.4	-16.3	-16.3
10.0	-1.0	5.6	-6.8	2.2	6.1	2.4	-4.4	-18.4	-18.1	-14.9	-16.9
12.5	0.1	-6.5	-4.0	1.4	7.6	7.2	-5.0	-9.7	-13.2	-11.7	-17.2
16.0	1.6	2.3	-3.7	1.6	8.2	9.4	-4.2	-11.2	-8.5	-7.8	-8.2
20.0	-3.2	0.8	-1.7	-1.1	4.2	-0.7	-6.4	-13.9	-10.4	-9.4	-9.1
25.0	-2.7	1.6	-6.1	0.6	6.1	-6.7	-7.1	-12.2	-8.4	-12.7	-13.9
31.5	-3.8	1.4	-6.6	1.2	5.0	-3.0	-11.1	-6.4	-10.0	-15.8	-18.7
40.0	4.2	11.5	4.9	11.1	9.0	4.1	-5.8	-0.2	-0.2	0.6	-7.8
50.0	-6.9	8.6	6.5	-0.5	4.4	0.1	-4.2	-4.6	-11.4	-6.4	-8.5
63.0	7.5	11.0	33.1	5.3	8.5	4.6	-1.8	4.6	-5.2	-3.2	-17.1

$OPTF_t$	$NOSPL_t$
23.1	-1.1 -3.7 -6.9 -6.8 -11.9 -14.4 -20.9 -21.6 -20.8 -25.5

1/3 OCTAVE NTC (dB) WITH RESPECT TO INCIDENT SPL (NTC_i)

$M_J = 0.8$ $M_T = 0.08$ $T_R = 600K$

DAISY LOBE NOZZLE (RUN NO = 86)

FREQ KHZ	EMISSION ANGLE (RELATIVE TO JET EXHAUST) REFERENCED TO NOZZLE EXIT (DEGREES)										
	PTF_i	10.	20.	30.	40.	50.	60.	70.	80.	90.	100.	110.
.250												
.315												
.400												
.500												
.630												
.800												
1.00												
1.25												
1.60												
2.00												
2.50												
3.15												
4.00												
5.00												
6.30												
8.00												
10.0												
12.5												
16.0												
20.0												
25.0												
31.5												
40.0												
50.0												
63.0												
	$OPTF_i$	$NOSPL_i$										
	24.4	-10.5	-6.8	-6.1	-6.7	-3.3	-3.0	-7.2	-10.1	-11.0	-15.5	-16.0

CONICAL NOZZLE (RUN NO = 100)

FREQ KHZ	EMISSION ANGLE (RELATIVE TO JET EXHAUST) REFERENCED TO NOZZLE EXIT (DEGREES)										
	PTF_i	10.	20.	30.	40.	50.	60.	70.	80.	90.	100.
.250											
.315											
.400											
.500											
.630											
.800											
1.00											
1.25											
1.60											
2.00											
2.50											
3.15											
4.00											
5.00											
6.30											
8.00											
10.0											
12.5											
16.0											
20.0											
25.0											
31.5											
40.0											
50.0											
63.0											
	$OPTF_i$	$NOSPL_i$									
	28.7	4.0	2.2	1.0	-0.7	-1.2	-1.2	-4.1	-8.3	-10.2	-13.0

1/3 OCTAVE NIC (dB) WITH RESPECT TO TRANSMITTED SPL (NIC_t)

$M_J = 0.8$ $M_T = 0.08$ $T_R = 600K$

DAISY LOBE NOZZLE (RUN NO = 86)

EMISSION ANGLE (RELATIVE TO JET EXHAUST) REFERENCED TO NOZZLE EXIT (DEGREES)

FREQ KHZ	PTF_t	10.	20.	30.	40.	50.	60.	70.	80.	90.	100.	110.
.250	+13.2	+7.4	-6.4	-10.7	-10.3	-3.8	-15.1	-21.4	-38.2	-28.1	-21.9	-23.9
.315	+13.4	+8.6	-6.2	-9.4	-9.6	-4.8	-16.3	-18.8	-29.0	-24.7	-21.6	-22.1
.400	+13.6	+9.2	-6.4	-8.8	-9.4	-5.6	-15.4	-17.9	-27.8	-23.8	-21.7	-21.4
.500	+13.0	+10.6	-5.3	-7.3	-8.8	-6.6	-12.6	-14.9	-18.4	-18.8	-21.7	-19.8
.630	+12.6	+11.9	-4.3	-5.6	-8.8	-12.1	-9.9	-12.1	-14.3	-15.4	-21.8	-17.7
.800	+9.7	+11.3	-3.4	-3.0	-6.7	-6.9	-6.9	-8.9	-10.2	-12.7	-20.4	-14.5
1.00	+7.7	+11.8	-4.0	-1.8	-3.6	-3.9	+3.2	+6.5	-7.6	-10.8	-18.2	-12.1
1.25	+6.7	+10.9	-4.3	-1.2	-1.7	-1.4	+0.8	-3.9	-5.4	-8.8	-15.2	-9.9
1.60	+3.8	+10.7	-5.9	-1.6	-0.1	0.9	2.1	+1.3	-3.9	-6.9	-11.8	-7.9
2.00	+2.9	+11.2	-7.7	-3.2	0.3	2.2	3.6	0.4	-4.0	-6.2	-9.1	-7.6
2.50	+2.1	+11.4	-7.0	-4.1	0.4	3.7	4.1	1.4	-4.8	-6.1	-6.7	-8.3
3.15	+0.8	+10.2	-5.9	-3.4	1.4	5.9	5.0	2.3	-2.9	-4.9	-4.0	-9.1
4.00	+1.4	-6.3	-5.0	-3.4	0.7	5.3	4.8	0.0	-4.1	-4.2	-5.1	-10.1
5.00	+2.4	-5.7	-6.6	-3.7	+0.6	4.5	4.1	-2.0	-3.3	-5.3	-9.2	-15.1
6.30	+3.0	-7.2	-2.1	-1.1	1.1	4.0	2.1	-5.6	-2.3	-12.2	-17.7	-19.2
8.00	+4.6	-2.6	-0.9	+0.8	2.0	2.0	-3.8	-2.0	-3.7	-9.7	-14.7	-11.1
10.0	+4.2	+5.3	1.0	2.0	0.1	-5.1	2.8	+7.3	-10.1	-5.6	-9.2	-9.2
12.5	-3.1	+17.1	-7.3	-2.0	-2.6	-11.0	5.4	-2.0	-1.9	-2.2	-11.7	-12.7
16.0	-2.3	+16.8	-5.7	-3.6	-4.1	-8.8	6.0	+0.1	0.1	-2.6	-10.8	-18.2
20.0	-6.4	+14.2	-2.8	-5.0	-6.8	-18.5	1.9	-10.2	-10.8	-2.6	-13.9	-17.3
25.0	-14.6	+13.3	-11.7	-14.3	-17.8	-16.7	-8.6	-18.5	-20.2	-7.6	-19.2	-18.2
31.5	-17.2	-23.2	-21.7	-20.5	-19.7	-14.7	-8.0	-17.5	-17.9	-13.7	-26.0	-27.1
40.0	+12.3	+14.1	-14.6	-11.9	-16.5	-14.0	0.3	-13.6	-13.6	-12.2	-17.9	-19.1
50.0	-13.6	-16.9	-15.5	-9.9	-13.3	-13.0	-4.8	-14.9	-12.7	-12.0	-21.9	-17.2
63.0	-14.8	-9.9	-14.4	-16.6	-15.8	-14.2	-5.2	-14.2	-18.5	-15.7	-18.3	-23.8

$OPTF_t$ ←	$NOSPL_t$ →									
25.1	+9.8	+8.8	+5.4	+5.0	+2.6	+2.2	+6.5	+9.4	+10.3	+14.8	+14.3

CONICAL NOZZLE (RUN NO = 100)

EMISSION ANGLE (RELATIVE TO JET EXHAUST) REFERENCED TO NOZZLE EXIT (DEGREES)

FREQ KHZ	PTF_t	10.	20.	30.	40.	50.	60.	70.	80.	90.	100.
.250	+13.6	0.1	-4.6	-6.1	-10.1	-15.0	-16.7	-18.9	-21.9	-24.9	-27.2
.315	+11.7	0.8	-3.1	-4.7	-8.4	-12.6	-14.6	-17.1	-19.9	-23.0	-25.1
.400	+11.3	1.2	-3.0	-4.4	-8.0	-12.1	-14.2	-16.7	-19.4	-22.6	-24.6
.500	+7.7	4.3	1.3	-0.6	-4.3	-7.1	-9.9	-13.0	-14.6	-18.0	-20.5
.630	+4.8	6.9	4.3	2.0	-1.4	-3.8	-6.9	-10.1	-11.4	-14.8	-17.4
.800	+2.1	8.7	6.8	4.9	2.0	-0.3	-3.3	-6.4	-8.7	-12.1	-13.8
1.00	+1.0	8.2	7.5	6.1	4.0	1.9	-1.0	-3.9	-7.7	-10.7	-11.4
1.25	+0.8	4.8	6.8	6.2	5.2	3.9	1.1	-1.5	-7.1	-9.1	-9.4
1.60	-0.2	0.4	1.6	3.6	4.7	5.2	2.8	0.4	-5.8	-6.6	-8.0
2.00	-2.1	3.3	-2.8	-5.1	-0.0	4.7	3.0	0.6	-3.7	-4.4	-8.3
2.50	-2.4	-0.2	-3.5	-9.8	-7.0	3.6	4.3	0.9	-3.1	-3.6	-7.7
3.15	-0.2	1.7	0.0	-4.6	-2.7	2.4	7.2	4.8	-2.9	-3.2	-3.8
4.00	-0.1	1.2	1.3	-1.7	-4.8	-3.3	6.3	5.8	1.7	-1.6	-2.7
5.00	2.2	1.4	3.2	4.4	5.2	1.9	8.9	5.3	4.7	-1.4	-4.9
6.30	1.7	-2.6	1.4	3.6	2.9	1.0	7.7	6.7	5.3	-1.8	-12.7
8.00	-1.4	-6.3	-3.8	-2.4	-2.8	1.0	6.3	3.2	-0.7	-6.0	-12.4
10.0	4.8	-14.4	-2.1	-0.5	-0.1	3.6	9.0	2.7	-0.6	-4.3	-7.5
12.5	4.1	-13.8	-6.2	-2.0	0.8	1.5	9.0	2.9	-3.8	-3.3	-8.8
16.0	-1.3	-14.7	-8.7	-6.3	-3.3	-0.1	6.4	3.9	-1.5	-4.2	-7.2
20.0	-4.8	-14.2	-6.7	-6.0	-4.4	-3.6	7.0	4.7	-0.4	-5.9	-6.8
25.0	-7.9	-15.1	-12.6	-11.5	-6.6	-3.4	-1.6	-2.4	-12.1	-10.5	-14.8
31.5	-9.3	-17.2	-11.2	-11.8	-12.9	-8.0	-0.7	-9.2	-11.8	-8.6	-16.1
40.0	-7.8	-14.2	-14.4	-9.9	-12.4	-7.6	1.9	-4.7	-12.9	-7.8	-12.1
50.0	-8.4	-9.1	-12.7	-7.0	-11.2	-8.5	2.0	-3.2	-11.6	-13.8	-17.2
63.0	1.6	8.1	1.7	11.1	-0.5	0.6	6.8	3.9	14.6	-3.6	-7.4

$OPTF_t$ ←	$NOSPL_t$ →									
29.4	4.7	3.0	1.7	0.0	-0.5	+0.8	-3.4	-7.6	-9.8	-12.3

1/3 OCTAVE NTC (dB) WITH RESPECT TO INCIDENT SPL (NTC_i)

$M_J = 0.8$ $M_T = 0.16$ $T_R = 600K$

DAISY LOBE NOZZLE (RUN NO = 85)

EMISSION ANGLE (RELATIVE TO JET EXHAUST) REFERENCED TO NOZZLE EXIT (DEGREES)

FREQ KHZ	PTF_i	20.	30.	40.	50.	60.	70.	80.	90.	100.	110.
.250	-28.1	-16.0	-24.8	-26.4	-26.3	-31.1	-26.8	-32.1	-33.2	-41.2	-37.3
.315	-24.1	-13.6	-19.7	-21.6	-21.8	-25.3	-22.4	-27.2	-27.8	-34.3	-31.6
.400	-20.6	-10.4	-16.0	-17.8	-17.8	-21.3	-18.9	-23.4	-23.5	-30.0	-27.6
.500	-18.1	-8.8	-13.3	-15.2	-15.3	-17.1	-16.8	-20.3	-18.9	-24.4	-22.9
.630	-14.9	-6.9	-9.9	-11.7	-12.0	-12.9	-13.2	-16.5	-14.8	-19.7	-18.5
.800	-12.2	-8.5	-7.2	-8.4	-8.8	-9.7	-10.9	-14.0	-12.1	-15.8	-16.2
1.00	-9.9	-4.8	-6.3	-5.7	-5.7	-6.9	-8.8	-11.8	-10.0	-12.6	-14.5
1.25	-7.4	-4.6	-3.7	-2.8	-2.6	-3.8	-6.7	-8.9	-7.6	-9.6	-12.8
1.60	-5.3	-4.6	-2.8	-0.6	0.2	-1.0	-4.7	-6.6	-5.8	-7.8	-11.6
2.00	-3.8	-4.6	-2.0	0.7	2.3	0.9	-3.3	-6.0	-4.8	-6.9	-11.0
2.50	-2.3	-4.9	-1.7	1.9	4.3	2.6	-1.4	-3.8	-4.0	-7.8	-10.6
3.15	-2.2	-3.9	-1.6	2.0	4.8	2.6	-0.8	-4.5	-6.0	-9.7	-11.5
4.00	-1.7	-5.9	-2.6	2.5	5.6	3.5	0.6	-5.5	-7.8	-11.4	-12.1
5.00	-5.1	-8.9	-3.0	2.8	6.9	6.2	1.7	-2.4	-6.1	-14.5	-11.6
6.30	-1.6	-16.4	-5.3	1.3	5.5	4.8	-0.6	-3.5	-7.7	-9.5	-9.9
8.00	-1.9	-6.2	-6.8	-0.4	6.8	4.8	-9.0	-14.6	-16.2	-13.3	-10.2
10.0	-3.6	-8.1	-11.9	-3.9	5.9	0.9	-6.0	-9.2	-9.5	-10.8	-15.1
12.5	-2.7	-8.7	-10.9	-3.6	5.5	2.9	-4.3	-4.0	-4.2	-11.8	-11.6
16.0	-1.8	-11.9	-10.6	-6.0	1.3	7.6	-1.0	-4.4	-6.4	-7.6	-17.1
20.0	-7.5	-9.4	-6.4	-3.5	-3.4	-1.6	-11.9	-7.5	-7.1	-10.3	-11.5
25.0	-9.2	-4.7	-4.8	-4.1	-5.6	-3.2	-17.2	-9.7	-13.9	-14.1	-17.1
31.5	-12.1	-17.1	-15.4	-11.5	-5.3	-3.7	-15.2	-13.2	-15.2	-16.0	-19.2
40.0	-12.5	-20.0	-12.0	-9.9	-5.3	-4.8	-14.7	-12.4	-19.3	-14.5	-21.6
50.0	-14.7	-15.9	-15.2	-13.1	-7.2	-9.4	-13.1	-12.9	-16.6	-16.4	-17.7
63.0	-8.4	-7.0	-6.6	-4.0	-3.6	-4.1	-9.8	-9.2	-8.9	-7.1	-15.3

$OPTF_i$ ←	$NOSPL_i$ →								
20.7	-10.0	-10.8	-8.9	-6.3	-7.3	-11.8	-14.7	-13.9	-17.3	-19.8

CONICAL NOZZLE (RUN NO = 101)

EMISSION ANGLE (RELATIVE TO JET EXHAUST) REFERENCED TO NOZZLE EXIT (DEGREES)

FREQ KHZ	PTF_i	20.	30.	40.	50.	60.	70.	80.	90.	100.	110.
.250	-25.9	-17.1	-17.9	-20.4	-22.5	-25.4	-32.6	-37.8	-29.6	-37.1	-38.1
.315	-20.7	-11.6	-13.0	-15.4	-17.3	-19.6	-26.0	-31.0	-25.1	-31.1	-33.0
.400	-17.6	-8.9	-9.9	-12.3	-14.2	-16.8	-22.7	-27.6	-22.2	-27.8	-29.9
.500	-13.4	-2.9	-6.6	-8.9	-10.4	-12.6	-17.3	-21.4	-19.4	-23.1	-25.8
.630	-9.6	1.1	-2.9	-5.2	-6.6	-8.5	-12.8	-16.8	-16.2	-18.9	-21.9
.800	-6.7	3.3	-4.1	-2.0	-3.4	-6.3	-9.0	-13.1	-13.2	-15.3	-19.4
1.00	-4.7	4.8	1.9	0.3	-1.3	-3.0	-6.7	-9.8	-10.4	-12.8	-16.9
1.25	-5.3	6.1	-40.8	-34.8	-0.1	-1.5	-2.8	-6.8	-7.7	-10.2	-14.2
1.60	-3.3	2.8	2.2	1.2	-0.1	-0.8	-0.8	-4.8	-5.8	-9.0	-11.7
2.00	-3.2	-4.7	-1.2	0.7	1.1	1.7	0.8	-3.1	-4.7	-8.4	-9.2
2.50	-1.9	-2.6	-0.1	1.7	2.4	3.6	1.6	-2.9	-4.9	-7.0	-7.1
3.15	-1.6	-1.1	-0.6	0.0	1.2	4.3	3.6	-3.3	-4.7	-5.1	-5.6
4.00	-1.8	-4.9	-6.8	-4.2	2.6	3.2	3.8	-1.9	-2.0	-4.8	-5.8
5.00	-1.4	-6.1	-7.7	-5.8	-1.3	6.1	6.1	0.0	-2.8	-7.9	-9.6
6.30	-6.6	-16.6	-7.1	-2.4	1.1	6.8	6.4	0.4	-6.8	-5.4	-19.5
8.00	-1.2	-8.8	-8.8	-5.7	-0.7	7.3	3.4	0.4	-11.1	-9.3	-17.3
10.0	-6.9	-7.8	-8.8	-5.4	-3.6	7.3	6.9	-6.7	-8.4	-7.4	-17.0
12.5	-4.2	-6.6	-9.1	-8.5	-3.8	7.2	7.0	0.4	-0.8	-6.6	-11.6
16.0	-1.3	-11.2	-10.1	-7.9	-3.8	3.3	7.8	-1.4	-9.6	-7.2	-10.5
20.0	-7.9	-14.1	-15.1	-10.1	-5.1	-2.4	-1.3	-6.5	-11.1	-16.4	-22.5
25.0	-6.2	-12.6	-16.8	-11.8	-6.1	-2.4	2.6	-7.1	-13.8	-14.0	-25.4
31.5	-12.8	-16.9	-18.2	-15.7	-8.9	-3.8	-4.8	-11.2	-16.0	-21.4	-31.0
40.0	-8.5	-15.6	-13.9	-13.7	-6.6	0.4	-2.0	-11.0	-13.8	-17.6	-21.2
50.0	-7.5	-9.9	-9.2	-9.3	-4.7	0.5	0.7	-10.4	-9.6	-15.0	-19.2
63.0	-11.7	-6.2	-10.3	-11.8	-10.5	-4.0	-7.6	-14.4	-16.3	-17.0	-22.8

$OPTF_i$ ←	$NOSPL_i$ →								
23.3	-2.7	-5.8	-6.9	-6.7	-5.7	-7.1	-12.3	-13.0	-16.1	-18.6

1/3 OCTAVE NTC (dB) WITH RESPECT TO TRANSMITTED SPL (NTC_t)

$M_J = 0.8$ $M_T = 0.16$ $T_R = 600K$

DAISY LOBE NOZZLE (RUN NO = 85)

EMISSION ANGLE (RELATIVE TO JET EXHAUST) REFERENCED TO NOZZLE EXIT
(DEGREES)

FREQ KHZ	PTF_t	20.	30.	40.	50.	60.	70.	80.	90.	100.	110.
.250	-27.8	-15.7	-24.1	-26.0	-26.0	-30.7	-26.4	-31.7	-32.9	-40.8	-36.9
.315	-23.6	-12.4	-19.2	-21.0	-21.0	-24.8	-21.9	-26.7	-27.0	-33.7	-31.0
.400	-19.7	-9.8	-15.1	-16.9	-16.9	-20.4	-18.0	-22.5	-22.6	-29.1	-26.7
.500	-17.3	-7.9	-12.4	-14.3	-14.4	-16.2	-15.6	-19.4	-18.0	-23.6	-22.0
.630	-14.0	-6.1	-9.1	-10.9	-11.2	-12.1	-12.4	-15.7	-13.7	-18.9	-17.7
.800	-11.3	-4.6	-6.3	-7.6	-7.7	-8.5	-10.1	-13.1	-11.2	-15.0	-15.4
1.00	-9.1	-4.0	-4.5	-4.9	-4.9	-6.1	-8.1	-10.8	-9.2	-11.8	-13.7
1.25	-6.7	-3.9	-2.9	-2.1	-1.8	-3.0	-5.9	-8.1	-6.8	-8.8	-12.0
1.60	-4.6	-3.9	-1.8	0.1	0.9	-0.3	-4.0	-6.8	-4.9	-6.7	-10.9
2.00	-3.1	-4.0	-1.4	1.3	3.0	1.6	-2.6	-4.3	-3.9	-6.2	-10.4
2.50	-2.0	-4.5	-1.3	2.3	4.7	3.0	-1.0	-3.2	-3.6	-7.1	-10.2
3.15	-2.1	-3.8	-1.5	2.2	5.0	2.7	-0.4	-4.4	-5.9	-9.5	-11.4
4.00	-1.6	-5.8	-2.5	2.6	5.7	3.6	0.7	-5.4	-7.7	-11.4	-12.0
5.00	-2.1	-6.9	-3.0	2.8	6.9	6.2	1.7	-2.4	-5.1	-14.5	-11.6
6.30	-1.6	-10.4	-5.2	1.3	5.6	4.8	-0.6	-3.5	-7.7	-9.5	-9.9
8.00	-1.4	-5.6	-6.3	0.1	7.3	5.4	-6.4	-14.1	-14.6	-12.7	-9.6
10.0	-3.2	-7.8	-11.6	-3.6	6.2	1.2	-5.7	-8.9	-9.2	-10.5	-14.8
12.5	-2.5	-8.5	-10.7	-3.4	5.7	3.1	-4.1	-3.8	-4.0	-11.6	-11.4
16.0	-1.7	-11.8	-10.5	-5.9	1.4	7.8	-0.9	-4.3	-6.3	-7.5	-16.9
20.0	-7.8	-9.3	-6.3	-3.4	-3.3	-1.6	-11.8	-7.4	-7.0	-10.2	-11.4
25.0	-9.2	-4.7	-4.8	-4.1	-5.6	-3.1	-17.2	-9.7	-13.9	-14.1	-17.1
31.5	-12.1	-17.1	-15.4	-11.6	-5.3	-3.7	-15.2	-13.2	-15.1	-16.0	-19.2
40.0	-12.8	-19.9	-12.0	-9.8	-5.3	-4.7	-14.7	-12.4	-19.3	-14.4	-21.6
50.0	-14.6	-15.8	-15.1	-13.1	-7.2	-9.3	-13.0	-12.9	-15.6	-16.3	-17.6
63.0	-7.8	-6.4	-6.0	-3.4	-2.9	-3.5	-6.9	-8.6	-8.3	-6.5	-14.8

$OPTF_t$ ← $NOSPL_t$ →

21.3 -9.5 -10.3 -8.1 -5.8 -6.8 -11.3 -14.2 -13.4 -16.7 -19.3

CONICAL NOZZLE (RUN NO = 101)

EMISSION ANGLE (RELATIVE TO JET EXHAUST) REFERENCED TO NOZZLE EXIT
(DEGREES)

FREQ KHZ	PTF_t	20.	30.	40.	50.	60.	70.	80.	90.	100.	110.
.250	-25.3	-16.5	-17.3	-19.8	-21.9	-24.8	-31.9	-37.2	-29.0	-36.5	-37.5
.315	-20.1	-10.9	-12.3	-14.7	-16.7	-19.3	-25.4	-30.4	-24.5	-30.5	-32.4
.400	-17.0	-8.2	-9.3	-11.6	-13.6	-16.1	-22.0	-26.9	-21.6	-27.1	-29.2
.500	-12.9	-2.3	-6.0	-8.4	-9.8	-12.0	-16.7	-20.8	-18.8	-22.5	-25.2
.630	-9.1	1.5	-2.5	-4.8	-6.2	-8.1	-12.4	-16.4	-15.8	-18.8	-21.5
.800	-6.5	3.5	0.1	-1.8	-3.2	-5.1	-8.8	-12.9	-13.0	-15.1	-19.2
1.00	-4.7	4.6	2.0	0.3	-1.2	-2.9	-5.7	-9.8	-10.3	-12.4	-16.8
1.75	-5.3	5.1	-44.5	-34.5	-0.0	-1.5	-2.8	-6.8	-7.7	-10.1	-14.2
1.60	-3.3	2.8	2.2	1.2	-0.0	-0.6	-0.8	-4.5	-5.8	-9.0	-11.6
2.00	-3.2	-4.7	-1.2	0.7	1.1	1.7	0.6	-3.1	-4.7	-8.4	-9.2
2.50	-1.9	-2.6	-0.1	1.8	2.4	3.6	1.6	-2.9	-4.9	-7.0	-7.1
3.15	-1.6	-1.1	-0.6	0.0	1.2	4.3	3.8	-3.3	-4.6	-5.1	-5.6
4.00	-1.8	-4.9	-0.8	-4.2	2.0	3.3	3.8	-1.9	-2.0	-4.8	-5.8
5.00	-1.4	-6.1	-7.7	-5.8	-1.3	5.1	5.1	0.0	-2.8	-7.9	-9.6
6.30	-6.6	-10.6	-7.1	-2.4	1.2	5.8	6.4	0.4	-6.8	-5.4	-19.5
8.00	-1.0	-8.4	-8.4	-5.6	-0.6	7.5	3.5	0.5	-11.0	-9.2	-17.2
10.0	-6.8	-7.7	-5.4	-5.3	-3.5	7.4	6.1	-6.6	-8.3	-7.3	-16.9
12.5	-4.2	-6.5	-9.0	-8.4	-3.5	7.3	7.0	0.4	-0.6	-6.6	-11.5
16.0	-1.1	-11.1	-9.9	-7.7	-3.3	3.5	7.7	-1.2	-9.5	-7.0	-10.4
20.0	-7.9	-14.6	-15.1	-10.0	-5.1	-2.3	-1.3	-6.4	-11.1	-16.4	-22.5
25.0	-6.1	-12.5	-16.5	-11.5	-6.0	-2.4	2.7	-7.0	-13.8	-14.5	-25.4
31.5	-12.4	-15.9	-18.1	-15.7	-8.8	-3.5	-5.5	-11.2	-14.9	-21.4	-31.0
40.0	-8.3	-15.5	-13.7	-13.5	-6.5	0.6	-1.9	-10.9	-13.4	-17.6	-21.1
50.0	-6.3	-8.7	-8.0	-8.1	-3.4	1.6	1.9	-8.3	-8.4	-13.7	-18.0
63.0	-9.6	-4.0	-8.1	-9.6	-8.7	-1.5	-5.6	-12.6	-14.2	-15.3	-20.7

$OPTF_t$ ← $NOSPL_t$ →

23.7 -2.2 -5.3 -6.4 -6.2 -5.3 -6.6 -11.8 -12.8 -15.7 -18.2

1/3 OCTAVE NTC (dB) WITH RESPECT TO INCIDENT SPL (NTC_i)

$M_J = 0.8$ $M_T = 0.24$ $T_R = 600K$

DAISY LOBE NOZZLE (RUN NO = 128)

EMISSION ANGLE (RELATIVE TO JET EXHAUST) REFERENCED TO NOZZLE EXIT (DEGREES)

FREQ KHZ	PTF_i	30.	40.	50.	60.	70.	80.	90.	100.	110.
.250	-17.6	-16.3	-18.8	-16.8	-11.7	-18.3	-26.1	-12.2	-16.2	-24.4
.315	-24.9	-17.1	-21.6	-20.2	-15.0	-18.3	-26.4	-16.6	-20.3	-26.9
.400	-21.3	-17.4	-21.8	-20.7	-15.4	-18.6	-26.6	-17.3	-20.7	-27.2
.500	-17.2	-11.4	-17.3	-17.1	-11.3	-14.1	-18.8	-15.4	-19.0	-22.0
.630	-16.1	-8.8	-14.9	-15.0	-9.1	-11.8	-16.1	-14.2	-17.6	-19.6
.800	-12.2	-5.6	-11.7	-12.1	-6.6	-9.2	-13.4	-11.3	-14.0	-16.8
1.00	-10.1	-3.4	-9.8	-10.3	-4.6	-7.3	-11.3	-9.3	-11.8	-13.9
1.25	-8.7	-2.9	-9.2	-9.3	-2.6	-5.6	-10.0	-8.1	-10.0	-11.4
1.60	-7.9	-4.2	-9.6	-8.7	-1.1	-3.9	-9.2	-7.5	-9.8	-9.8
2.00	-7.1	-4.2	-8.7	-7.3	-0.2	-2.6	-8.0	-8.1	-10.5	-9.0
2.50	-2.8	-1.6	-4.8	-2.6	4.6	1.7	-3.4	-6.2	-8.7	-6.8
3.15	-4.8	-7.5	-8.6	-4.0	4.4	0.6	-4.4	-6.0	-8.8	-12.2
4.00	-2.4	-10.7	-9.6	-3.3	6.3	2.6	-3.2	-8.6	-6.7	-7.8
5.00	-2.7	-10.6	-9.7	-3.5	7.1	-1.8	-3.0	-13.0	-7.4	-8.7
6.30	-8.7	-14.2	-15.0	-7.6	4.8	-7.0	-9.3	-11.1	-18.4	-19.6
8.00	-1.8	-8.8	-7.4	-2.0	8.0	-4.1	-4.3	-4.8	-10.0	-5.6
10.0	-8.7	-8.1	-7.4	-5.4	1.8	-8.2	-6.9	-4.5	-4.8	-8.2
12.5	-8.0	-11.5	-12.2	-8.0	0.0	-8.4	-5.5	-8.6	-10.0	-18.6
16.0	-9.9	-11.6	-18.5	-15.8	-2.9	-8.3	-4.7	-11.7	-10.1	-18.3
20.0	-7.2	-9.9	-14.6	-12.4	-2.4	-4.8	-2.3	-7.6	-3.1	-12.3
25.0	-7.8	-7.8	-10.7	-9.5	-2.0	-6.4	-0.8	-7.5	-9.0	-11.2
31.5	-4.8	-6.6	-10.9	-7.1	1.2	-3.7	2.0	-1.3	-4.4	-2.8
40.0	-0.9	2.8	-3.8	-1.6	6.1	2.8	5.9	3.1	1.8	-3.5
50.0	-7.8	-6.4	-12.9	-11.3	-2.8	-3.2	-2.6	-4.1	-6.0	-6.9
63.0	-6.9	-3.3	-8.9	-10.1	-1.6	-1.8	-1.6	-4.6	-3.4	-7.6

$NOSPL_i$ →

$OPTF_i$									
22.9	-6.9	-12.2	-10.9	-3.1	-7.1	-10.6	-10.5	-12.6	-14.2

CONICAL NOZZLE (RUN NO = 103)

EMISSION ANGLE (RELATIVE TO JET EXHAUST) REFERENCED TO NOZZLE EXIT (DEGREES)

FREQ KHZ	PTF_i	30.	40.	50.	60.	70.	80.	90.	100.	110.
.250	-25.7	-16.6	-20.3	-22.9	-24.1	-26.4	-20.3	-27.1	-36.2	-36.7
.315	-21.2	-12.7	-18.4	-17.4	-19.0	-22.6	-22.6	-23.3	-30.8	-31.8
.400	-19.0	-10.7	-13.1	-15.0	-16.7	-19.8	-20.8	-20.3	-29.3	-29.4
.500	-15.2	-8.8	-8.9	-9.9	-12.4	-16.0	-17.6	-18.3	-23.0	-24.9
.630	-11.7	-5.6	-5.2	-6.0	-8.7	-12.6	-14.6	-15.1	-19.0	-21.0
.800	-8.8	-2.4	-2.2	-2.7	-5.5	-9.9	-12.7	-13.0	-16.7	-18.6
1.00	-7.3	-1.4	-0.8	-1.0	-3.6	-8.3	-11.6	-11.7	-15.1	-16.8
1.25	-6.6	-1.2	0.1	0.5	-1.9	-6.6	-10.0	-10.0	-12.9	-14.8
1.60	-5.4	-2.7	-0.2	1.1	-0.5	-4.8	-7.6	-7.9	-10.1	-11.6
2.00	-4.3	-6.1	-1.4	1.5	1.4	-2.3	-5.0	-4.9	-8.5	-8.1
2.50	-3.8	-5.5	-1.4	1.6	1.9	-1.4	-4.1	-4.7	-5.4	-6.9
3.15	-2.2	0.0	1.5	2.9	2.7	0.2	-2.3	-4.8	-3.9	-5.5
4.00	-3.3	-1.1	-2.3	-1.2	2.6	0.7	-1.7	-6.0	-5.0	-7.5
5.00	-4.0	-4.5	-1.4	1.2	1.4	-0.2	-3.4	-4.0	-10.1	-16.8
6.30	-0.3	-2.2	-4.1	-3.1	1.4	-2.2	-6.8	-6.2	-8.6	-15.9
8.00	-0.6	-4.4	-0.3	-2.6	3.1	-4.9	-14.2	-9.2	-9.1	-17.0
10.0	-3.7	1.2	1.0	0.9	2.3	-4.6	-12.3	-4.6	-6.3	-19.7
12.5	-0.9	2.5	2.7	4.7	9.1	-2.4	-4.7	-6.6	-9.2	-10.2
16.0	-2.6	-3.0	-1.9	1.2	6.0	-0.3	-4.4	-12.6	-12.2	-18.6
20.0	-6.6	-10.7	-10.3	-0.6	2.6	-3.6	-10.6	-14.1	-18.6	-15.6
25.0	-9.6	-11.4	-9.2	-6.1	-1.7	-6.5	-10.3	-14.3	-12.3	-16.6
31.5	-14.2	-12.4	-11.6	-6.6	-0.7	-6.7	-12.2	-20.6	-21.1	-21.1
40.0	-6.4	-6.0	-4.6	0.6	1.6	-6.6	-16.3	-16.2	-15.7	-20.5
50.0	-7.4	-8.1	-9.6	-4.7	2.1	-4.3	-12.3	-16.3	-17.6	-24.6
63.0	-14.1	-8.7	-16.6	-8.3	-0.8	-9.0	-16.7	-9.1	-22.0	-21.7

$NOSPL_i$ →

$OPTF_i$									
23.2	-6.6	-5.3	-4.7	-4.6	-9.2	-12.3	-12.3	-14.9	-17.0

1/3 OCTAVE NTC (dB) WITH RESPECT TO TRANSMITTED SPL (NTC_t)

$M_J = 0.8$ $M_T = 0.24$ $T_R = 600K$

DAISY LOBE NOZZLE (RUN NO = 128)

FREQ KHZ	PTF_t	30.	40.	50.	60.	70.	80.	90.	100.	110.
	EMISSION ANGLE (RELATIVE TO JET EXHAUST) REFERENCED TO NOZZLE EXIT (DEGREES)									
.250	+16.6	+13.7	+17.1	+15.2	+10.1	+13.7	+23.4	+10.6	+14.-	+22.8
.315	+20.6	+16.8	+21.1	+19.9	+14.7	+17.9	+26.1	+16.3	+19.9	+26.5
.400	+21.1	+17.1	+21.5	+20.4	+15.2	+18.4	+26.3	+17.1	+20.5	+26.9
.500	+16.9	+11.6	+16.9	+16.7	+11.0	+13.7	+18.5	+15.0	+18.7	+21.7
.630	+14.6	+8.4	+14.8	+14.6	+8.7	+11.3	+15.7	+13.8	+17.2	+19.2
.800	+11.8	+8.2	+11.3	+11.8	+6.3	+8.8	+13.0	+10.9	+13.7	+16.2
1.00	+9.8	+3.1	+9.4	+10.0	+4.1	+7.0	+11.0	+9.0	+11.2	+13.6
1.25	+8.3	+2.5	+8.8	+8.9	+2.2	+5.2	+9.6	+7.7	+9.6	+11.0
1.60	+7.8	+3.9	+9.3	+8.4	+0.7	+3.6	+8.8	+7.1	+9.4	+9.1
2.00	+7.0	+4.1	+8.5	+7.2	+0.1	+2.4	+7.9	+8.0	+10.3	+8.9
2.50	+2.3	+8.4	+4.3	+2.3	5.2	2.3	+2.8	+4.7	+5.1	+6.2
3.15	+3.8	+7.3	+8.3	+3.8	4.6	0.8	+4.2	+5.8	+8.6	+12.0
4.00	+2.0	+10.4	+9.3	+3.0	6.6	3.0	+2.9	+8.5	+6.3	+7.5
5.00	+2.5	+9.9	+9.6	+3.4	7.2	+1.4	+2.9	+12.9	+7.2	+8.5
6.30	+5.5	+14.1	+14.9	+7.4	4.9	+6.9	+9.2	+11.0	+18.2	+19.5
8.00	+1.4	+5.4	+7.0	+1.6	8.4	+3.7	+3.9	+4.4	+9.6	+5.2
10.0	+5.4	+4.8	+7.1	+5.1	2.2	+4.9	+6.6	+4.2	+4.6	+7.9
12.5	+7.9	+11.4	+12.1	+8.0	0.1	+5.4	+5.4	+8.6	+9.9	+18.5
16.0	+9.7	+10.9	+18.3	+15.6	+2.8	+8.2	+4.6	+11.5	+10.0	+18.2
20.0	+7.1	+9.8	+14.4	+12.3	+2.3	+4.7	+2.2	+7.5	+3.0	+12.2
25.0	+6.9	+7.8	+10.6	+9.4	+1.9	+6.3	+0.4	+7.5	+8.9	+11.1
31.5	+3.7	+6.3	+10.6	+6.9	1.5	+3.4	2.2	+1.1	+4.1	+2.6
40.0	1.6	3.6	+3.0	+0.8	5.8	3.3	6.6	3.8	2.6	+2.8
50.0	+6.4	+5.8	+12.4	+10.7	+2.0	+2.6	+2.0	+3.5	+5.5	+6.3
63.0	+3.6	+1.1	+6.6	+8.0	0.9	0.4	0.4	+2.3	+1.0	+5.4
	$OPTF_t$ ←					$NOSPL_t$ →				
	23.3	+6.5	+11.9	+10.6	+2.7	+6.7	+10.2	+10.2	+12.2	+13.9

CONICAL NOZZLE (RUN NO = 103)

FREQ KHZ	PTF_t	30.	40.	50.	60.	70.	80.	90.	100.	110.
	EMISSION ANGLE (RELATIVE TO JET EXHAUST) REFERENCED TO NOZZLE EXIT (DEGREES)									
.250	+22.4	+13.4	+17.1	+19.6	+20.8	+23.2	+23.0	+23.9	+33.0	+33.4
.315	+18.6	+10.1	+12.8	+14.8	+16.4	+19.4	+20.0	+20.8	+28.3	+29.2
.400	+17.0	+8.7	+11.1	+13.0	+14.7	+17.8	+18.7	+18.3	+27.3	+27.4
.500	+13.6	+6.4	+7.2	+8.3	+10.8	+14.4	+16.0	+16.6	+21.4	+23.2
.630	+14.7	+4.1	+4.3	+5.1	+7.8	+11.6	+13.8	+14.2	+18.0	+20.1
.800	+8.4	+2.8	+1.8	+2.3	+6.1	+9.5	+12.3	+12.6	+16.3	+18.1
1.00	+7.2	+1.3	+0.7	+0.9	+3.5	+8.2	+11.4	+11.6	+15.0	+16.7
1.25	+6.0	+1.2	0.1	0.5	+1.9	+6.6	+9.9	+10.0	+12.9	+14.5
1.60	+5.4	+2.7	+0.2	1.1	+0.5	+4.8	+7.7	+7.9	+10.1	+11.6
2.00	+4.3	+6.1	+1.4	1.5	1.4	+2.3	+4.9	+4.9	+6.5	+8.1
2.50	+3.8	+5.5	+1.4	1.0	1.9	+1.4	+4.1	+4.7	+6.4	+6.9
3.15	+2.1	0.1	1.6	2.9	2.7	0.2	+2.3	+4.8	+3.9	+5.5
4.00	+3.3	+1.1	+2.3	+1.2	2.6	0.7	+1.7	+6.0	+5.0	+7.5
5.00	+3.9	+4.4	+1.3	1.2	1.4	+0.5	+3.3	+3.9	+10.1	+16.8
6.30	+4.5	+1.7	+3.7	+2.6	1.9	+1.7	+6.4	+4.8	+8.2	+15.4
8.00	+5.3	+4.2	+5.1	+2.3	3.3	+4.6	+13.9	+8.9	+8.9	+16.8
10.0	+3.1	1.8	1.6	1.5	2.9	+4.0	+11.7	+4.0	+5.7	+10.1
12.5	1.8	2.7	2.9	4.9	9.3	2.6	+4.5	+5.4	+9.0	+10.1
16.0	+2.4	+2.8	+1.6	1.4	6.2	+0.1	+4.2	+12.4	+12.0	+18.4
20.0	+6.5	+10.7	+16.3	+5.8	2.8	+3.9	+10.5	+14.1	+15.6	+15.9
25.0	+9.5	+11.4	+9.2	+6.0	+1.7	+6.5	+10.3	+14.2	+12.3	+16.0
31.5	+10.2	+12.4	+11.8	+6.6	+0.7	+6.7	+12.2	+20.6	+21.1	+21.1
40.0	+6.3	+5.9	+4.4	0.6	1.8	+6.7	+16.2	+16.0	+15.5	+20.4
50.0	+6.9	+7.6	+9.0	+4.1	2.6	+3.8	+11.9	+15.8	+17.3	+24.3
63.0	+8.3	+6.9	+8.7	+6.6	1.1	+7.1	+13.9	+7.2	+20.4	+19.9
	$OPTF_t$ ←					$NOSPL_t$ →				
	24.7	+4.6	+3.8	+3.2	+3.4	+7.7	+10.8	+10.9	+13.5	+15.5

1/3 OCTAVE NTC (dB) WITH RESPECT TO INCIDENT SPL (NTC_i)

$M_J = 1.2$ $M_T = 0$ $T_R = 600K$

DAISY LOBE NOZZLE (RUN NO = 83)

EMISSION ANGLE (RELATIVE TO JET EXHAUST) REFERENCED TO NOZZLE EXIT (DEGREES)

FREQ KHZ	PTF_i	40.	50.	60.	70.
.250	+14.9	+11.9	+11.0	-7.5	+0.0
.315	+17.6	+18.0	+13.0	-10.4	-11.2
.400	+18.3	+20.7	+13.4	-11.1	-11.6
.500	+16.9	+23.2	+11.4	-10.3	+0.8
.630	+15.7	+31.0	+9.8	-9.6	+8.4
.800	+13.4	+27.6	+7.5	-7.6	+6.0
1.00	+11.1	+23.9	+5.2	-5.2	+3.8
1.25	+9.2	+19.8	+3.2	-3.2	+2.0
1.60	+7.0	+15.5	+0.9	-0.6	-0.2
2.00	+4.4	+11.0	1.7	2.6	1.7
2.50	+4.5	+8.9	1.8	3.4	0.2
3.15	+2.2	+4.6	4.0	6.6	+0.4
4.00	1.3	+0.5	5.3	9.8	+0.4
5.00	2.4	2.8	5.7	12.3	2.3
6.30	1.5	3.0	1.5	11.7	1.8
8.00	-2.2	0.2	-11.3	7.9	+0.6
10.0	-5.8	-2.7	-3.1	3.0	+1.7
12.5	-4.6	-2.3	4.2	+1.3	+0.5
16.0	-6.7	-2.4	-6.0	0.3	-3.8
20.0	-12.9	-4.8	-10.0	-0.4	-10.1
25.0	-14.4	-1.0	-4.7	-6.0	-9.4
31.5	-7.0	0.2	-0.7	-1.4	+4.0
40.0	-14.5	+0.7	-5.9	-3.5	+4.8
50.0	+4.7	2.1	+0.8	1.6	+0.0
63.0	-6.0	-3.5	4.5	2.2	+4.0

DATA FOR THE REMAINING ANGLES NOT ANALYZED DUE TO JET NOISE CONTAMINATION

$OPTF_i$ ← $NOSPL_i$ →

24.8 -6.2 -3.3 -0.2 +4.5

CONICAL NOZZLE (RUN NO = 99)

FREQ KHZ	PTF_i
.250	
.315	
.400	
.500	
.630	
.800	
1.00	
1.25	
1.60	
2.00	
2.50	
3.15	
4.00	
5.00	
6.30	
8.00	
10.0	
12.5	
16.0	
20.0	
25.0	
31.5	
40.0	
50.0	
63.0	

DATA NOT ANALYZED DUE TO JET NOISE CONTAMINATION

$OPTF_i$ ← $NOSPL_i$ →

1/3 OCTAVE NTC (dB) WITH RESPECT TO TRANSMITTED SPL (NTC_t)

$M_J = 1.2$ $M_T = 0$ $T_R = 600K$

DAISY LOBE NOZZLE (RUN NO = 83)

EMISSION ANGLE (RELATIVE TO JET EXHAUST) REFERENCED TO NOZZLE EXIT
(DEGREES)

FREQ KHZ	PTF_t 40.	50.	60.	70.
.250	-8.3	-8.3	-4.4	-0.9	-2.4
.315	-16.4	-16.7	-11.7	-9.2	-9.9
.400	-17.5	-19.9	-12.6	-10.3	-10.8
.500	-18.2	-22.5	-14.7	-9.6	-9.1
.630	-15.1	-30.4	-9.2	-9.0	-7.9
.800	-12.9	-27.2	-7.0	-7.2	-6.6
1.00	-14.7	-23.4	-4.7	-4.8	-3.4
1.25	-8.9	-19.5	-3.0	-2.9	-1.7
1.60	-6.6	-15.3	-0.8	-0.4	-0.0
2.00	-4.3	-16.9	1.8	2.7	1.8
2.50	-4.4	-8.9	1.9	3.6	0.3
3.15	-2.2	-4.6	4.0	6.7	-0.3
4.00	0.4	-6.4	5.6	9.8	-0.3
5.00	2.4	2.8	5.7	12.3	2.3
6.30	1.7	3.1	1.6	11.8	1.9
8.00	-1.3	1.1	-18.4	8.8	0.3
10.0	-5.6	-2.4	-2.8	3.3	-1.4
12.5	-4.8	-2.2	4.3	-1.1	-0.3
16.0	-6.4	-2.1	0.3	0.6	-3.8
20.0	-12.9	-4.8	-10.0	-6.3	-10.1
25.0	-10.3	-1.0	-4.7	-6.0	-9.4
31.5	-7.6	0.2	-0.6	-1.4	-3.9
40.0	-14.4	-6.7	-5.9	-3.4	-4.7
50.0	-4.7	2.1	-0.7	1.7	0.0
63.0	-6.0	-3.5	0.8	2.3	-4.0

DATA FOR
THE REMAINING ANGLES NOT ANALYZED
DUE TO JET NOISE CONTAMINATION

$OPTF_t$ ← $NOSPL_t$ →

25.3	-5.7	-2.8	0.3	-4.0

CONICAL NOZZLE (RUN NO = 99)

FREQ KHZ	PTF_t
.250	
.315	
.400	
.500	
.630	
.800	
1.00	
1.25	
1.60	
2.00	
2.50	
3.15	
4.00	
5.00	
6.30	
8.00	
10.0	
12.5	
16.0	
20.0	
25.0	
31.5	
40.0	
50.0	
63.0	

DATA NOT ANALYZED DUE
TO JET NOISE CONTAMINATION

$OPTF_t$ ← $NOSPL_t$ →

1/3 OCTAVE NTC (dB) WITH RESPECT TO INCIDENT SPL (NTC_i)

$M_J = 1.2$ $M_T = 0.08$ $T_R = 600K$

DAISY LOBE NOZZLE (RUN NO = 84)

	EMISSION ANGLE (RELATIVE TO JET EXHAUST) REFERENCED TO NOZZLE EXIT (DEGREES)								
FREQ KHZ	PTF_i	10.	20.	30.	40.	50.	60.	70.	80.	90.
.250	+23.2	+19.2	-29.3	+35.5	+39.5	+36.5	+18.0	+46.2	+20.2	+14.8
.315	+23.9	+18.2	-26.4	+31.1	+33.4	+29.4	+16.0	+37.0	+23.1	+19.0
.400	+22.8	+17.6	-23.8	+27.6	+29.0	+26.1	+12.9	+32.4	+22.6	+19.5
.500	+20.5	+17.7	-22.5	+24.7	+24.1	+18.0	+13.1	+20.2	+18.2	+17.1
.630	+19.6	+20.8	-20.2	+23.4	+19.6	+13.9	+16.3	+14.9	+15.7	+15.3
.800	+16.6	+21.3	-21.8	+20.6	+17.1	+11.4	+14.2	+12.6	+13.4	+13.0
1.00	+13.7	+18.4	-19.1	+18.3	+15.2	+8.9	+8.3	+10.6	+11.1	+10.9
1.25	+10.7	+15.8	-16.9	+16.3	+13.3	+6.3	+3.4	+8.5	+8.8	+8.9
1.60	+7.3	+12.5	-13.8	+13.4	+10.6	+3.3	1.1	+6.2	+6.3	+6.9
2.00	+4.6	+9.7	-11.3	+11.1	+8.6	+0.8	4.4	+4.5	+4.3	+5.5
2.50	+1.8	+6.1	+8.2	+8.4	+6.9	2.1	7.6	+2.4	1.6	+0.4
3.15	1.3	+2.2	+5.0	+5.4	+3.8	5.4	10.2	+0.5	2.4	+0.7
4.00	2.4	0.1	+3.1	+3.8	+1.6	6.6	11.1	0.4	4.8	0.4
5.00	3.6	2.3	+1.1	+1.9	0.3	8.3	12.4	1.4	4.6	+0.9
6.30	4.4	4.0	+2.8	+3.1	+1.1	8.4	9.3	+1.7	0.6	+5.3
8.00	+3.7	+4.5	+5.8	+5.3	+3.5	0.1	4.0	+7.4	+0.3	+4.3
10.0	+3.2	+11.6	+9.4	+6.6	+5.2	+8.4	+0.1	+8.0	5.9	+3.4
12.5	1.3	+11.8	+6.0	+0.6	1.4	+8.5	9.7	6.9	0.9	+4.0
16.0	+2.4	+13.8	+10.4	+5.7	+5.6	+13.1	6.3	3.4	+5.7	+8.4
20.0	+3.4	+12.4	+10.6	+6.3	+5.6	+10.0	4.4	+1.1	+2.8	0.9
25.0	+6.7	+6.6	1.0	3.6	4.6	2.6	4.9	+1.3	+4.3	+0.7
31.5	+3.4	+13.1	+11.1	+6.8	+4.3	+4.4	1.8	+5.4	2.5	3.3
40.0	4.3	+12.7	+11.1	+7.2	+6.1	+6.2	+1.6	+10.0	12.8	12.5
50.0	+1.4	+8.3	+5.6	+1.1	+1.4	+7.7	+1.8	+6.2	1.6	8.2
63.0	2.6	+1.5	0.3	3.1	6.3	4.8	0.1	1.2	9.5	6.2

$OPTF_i$	← $NOSPL_i$ →							
24.8	+13.7	+14.6	+13.0	+11.1	+7.9	+2.8	+10.4	+4.1	+2.9

CONICAL NOZZLE (RUN NO = 105)

	EMISSION ANGLE (RELATIVE TO JET EXHAUST) REFERENCED TO NOZZLE EXIT (DEGREES)							
FREQ KHZ	PTF_i	20.	30.	40.	50.	60.	70.	80.
.250	+26.0	+15.3	+16.6	+20.1	+21.1	+22.0	+26.4	+33.0
.315	+19.7	+16.3	+13.2	+14.4	+16.4	+17.0	+21.9	+26.9
.400	+16.9	+7.8	+10.3	+11.8	+12.6	+14.4	+19.7	+24.6
.500	+12.9	+4.4	+6.6	+7.4	+8.3	+10.1	+15.1	+16.7
.630	+9.2	+1.0	+3.0	+3.8	+4.4	+6.4	+11.4	+12.4
.800	+5.7	2.9	0.9	0.6	+0.9	+4.0	+9.3	+10.6
1.00	+2.7	6.2	4.2	3.7	1.9	+1.8	+6.9	+9.4
1.25	0.6	9.7	7.6	6.9	5.0	1.0	+6.1	+7.8
1.60	3.3	13.0	10.8	9.4	7.8	3.8	+3.7	+5.6
2.00	4.5	14.7	11.8	9.9	8.2	5.6	+0.3	+2.4
2.50	3.9	14.6	10.3	7.8	6.7	6.3	1.2	+1.2
3.15	1.8	12.8	8.4	2.9	2.8	4.9	3.8	1.1
4.00	0.8	8.4	3.3	0.2	0.9	6.2	6.3	2.7
5.00	0.8	6.8	0.0	+4.5	+1.9	7.4	7.0	2.6
6.30	2.3	11.2	4.5	+0.0	0.4	6.2	8.8	2.9
8.00	3.6	10.1	8.5	2.8	3.0	8.7	10.2	3.3
10.0	7.1	13.4	12.1	12.8	10.6	6.0	11.8	5.7
12.5	4.2	8.7	5.9	5.2	5.3	8.9	11.7	6.0
16.0	1.6	10.8	7.3	6.6	4.8	3.8	5.8	+6.2
20.0	+1.5	9.1	4.8	2.4	1.9	1.8	+3.4	+8.0
25.0	+2.8	8.8	4.0	1.7	0.4	+2.5	+8.0	+6.2
31.5	+1.4	8.5	5.0	5.8	3.9	1.3	+13.6	+8.4
40.0	+3.5	0.9	3.6	2.0	2.0	1.5	+1.6	+7.2
50.0	+3.3	1.6	3.4	2.2	2.9	+0.9	+2.0	+7.2
63.0	+5.4	1.1	+0.9	0.4	0.4	+1.4	+8.0	+9.4

DATA FOR THE REMAINING ANGLES NOT ANALYZED DUE TO JET NOISE CONTAMINATION

$OPTF_i$	← $NOSPL_i$ →						
28.9	4.5	1.7	0.6	+1.0	+2.5	+3.6	+8.3

1/3 OCTAVE NTC (dB) WITH RESPECT TO TRANSMITTED SPL (NTC_t)

$M_J = 1.2$ $M_T = 0.08$ $T_R = 600K$

DAISY LOBE NOZZLE (RUN NO = 84)

EMISSION ANGLE (RELATIVE TO JET EXHAUST) REFERENCED TO NOZZLE EXIT (DEGREES)

FREQ KHZ	PTF_t	10.	20.	30.	40.	50.	60.	70.	80.	90.
.250	-22.9	-18.9	-29.8	-35.2	-39.2	-36.2	-16.4	-45.9	-20.0	-14.6
.315	-23.6	-17.8	-26.0	-30.7	-33.0	-29.0	-14.6	-36.6	-22.7	-18.6
.400	-21.8	-16.3	-23.2	-27.0	-28.3	-24.4	-12.3	-31.7	-21.9	-18.9
.500	-19.9	-17.1	-21.9	-24.1	-23.5	-17.4	-12.4	-19.6	-17.5	-16.4
.630	-18.5	-25.3	-24.7	-22.9	-19.1	-13.4	-15.7	-14.4	-15.2	-14.8
.800	-16.1	-20.8	-21.1	-20.0	-16.6	-10.5	-13.7	-12.1	-12.9	-12.5
1.00	-13.3	-18.4	-18.6	-17.8	-14.7	-8.4	-7.8	-10.1	-10.6	-10.4
1.25	-14.3	-15.4	-16.5	-16.0	-12.9	-5.9	-3.0	-8.1	-8.4	-8.5
1.60	-6.9	-12.1	-13.8	-13.1	-10.2	-3.0	1.5	-5.8	-5.9	-6.6
2.00	-4.2	-9.3	-11.0	-10.8	-8.1	-0.5	4.7	-4.2	-4.0	-5.2
2.50	-6.7	-5.7	-7.9	-8.0	-5.5	2.5	7.8	-2.0	2.0	-0.1
3.15	1.8	-2.0	-4.8	-5.2	-2.9	5.6	10.4	-0.3	2.5	-0.5
4.00	2.5	0.1	-3.0	-3.8	-1.6	6.6	11.1	0.5	4.8	0.4
5.00	3.6	2.3	-1.1	-1.8	0.4	8.3	12.4	1.5	4.6	-0.9
6.30	4.5	0.6	-2.8	-3.1	-1.1	5.4	9.3	-1.7	0.1	-5.3
8.00	-2.0	-2.8	-4.1	-3.6	-1.8	1.8	5.7	-5.7	1.4	-2.6
10.0	-2.4	-10.8	-8.6	-5.8	-4.4	-7.6	0.7	-7.2	6.7	-2.6
12.5	2.1	-11.1	-5.3	0.2	2.1	-4.8	10.5	7.6	1.7	-3.3
16.0	-2.2	-13.6	-10.2	-5.4	-5.3	-12.9	6.6	3.7	-5.4	-8.1
20.0	-3.2	-12.3	-10.5	-6.2	-5.5	-9.9	4.8	-1.0	-2.6	1.1
25.0	-0.2	0.3	1.9	4.5	5.3	3.5	5.8	0.4	-3.4	0.3
31.5	-3.3	-13.8	-11.0	-6.8	-4.2	-4.4	1.6	-5.3	2.8	3.3
40.0	4.3	-12.7	-11.1	-7.2	-6.1	-6.1	-1.6	-9.9	12.8	12.6
50.0	-1.3	-8.2	-5.5	-1.0	-1.3	-7.6	-1.4	-6.1	1.7	8.3
63.0	2.9	-1.2	0.6	3.4	6.6	6.1	0.4	1.6	9.8	6.5

$OPTF_t$	← $NOSPL_t$ →							
24.9	-13.3	-14.2	-12.6	-10.7	-7.6	-2.4	-10.0	-3.7	-2.6

CONICAL NOZZLE (RUN NO = 105)

EMISSION ANGLE (RELATIVE TO JET EXHAUST) REFERENCED TO NOZZLE EXIT (DEGREES)

FREQ KHZ	PTF_t	20.	30.	40.	50.	60.	70.	80.
.250	-23.4	-13.7	-17.0	-18.5	-19.8	-20.4	-24.8	-31.4
.315	-18.4	-9.4	-11.9	-13.1	-14.1	-15.7	-20.6	-28.6
.400	-15.9	-6.9	-9.3	-10.5	-11.7	-13.4	-18.7	-23.6
.500	-12.2	-3.7	-5.9	-8.7	-7.8	-9.3	-14.3	-16.0
.630	-8.9	-0.7	-2.7	-3.2	-4.1	-6.1	-11.1	-12.1
.800	-5.8	3.1	1.0	0.6	-0.8	-3.8	-9.1	-10.5
1.00	-2.7	6.2	4.2	3.7	2.0	-1.7	-7.9	-9.4
1.25	-0.5	9.8	7.6	6.9	5.0	1.0	-6.1	-7.7
1.60	3.3	13.0	10.8	9.6	7.5	3.8	-3.7	-5.4
2.00	4.5	14.7	11.5	9.9	8.2	5.6	-0.3	-2.4
2.50	3.9	14.6	10.3	7.8	6.7	6.3	1.2	-1.2
3.15	1.5	12.0	6.4	2.9	2.8	4.9	3.6	1.1
4.00	-0.8	8.4	3.3	0.2	0.9	5.2	6.3	2.7
5.00	-0.6	6.8	0.1	-4.5	-1.9	7.4	7.0	2.6
6.30	2.3	11.2	4.5	-0.0	0.4	6.2	8.5	2.9
8.00	3.0	10.1	5.5	2.8	3.1	5.8	10.3	3.3
10.0	7.2	13.6	12.3	13.0	10.7	6.2	12.0	5.8
12.5	4.2	8.8	6.0	5.3	5.4	6.0	11.8	6.1
16.0	1.8	11.4	7.8	5.8	4.8	4.0	8.7	-6.0
20.0	-1.4	9.1	4.8	2.0	1.9	1.8	-3.3	-8.0
25.0	-2.8	8.6	4.0	1.7	0.4	-2.4	-7.9	-6.2
31.5	-1.4	5.5	5.0	5.5	3.9	1.3	-13.8	-8.4
40.0	-3.3	0.9	3.6	2.1	2.0	1.8	-1.6	-7.1
50.0	-3.1	1.8	3.8	2.3	3.1	-0.7	-1.8	-7.0
63.0	-4.9	1.5	-0.8	0.8	0.8	-0.9	-7.6	-9.0

DATA FOR THE REMAINING ANGLES NOT ANALYZED DUE TO JET NOISE CONTAMINATION

$OPTF_t$	← $NOSPL_t$ →							
29.7	5.4	2.6	1.4	-0.1	-1.7	-2.8	-7.4

1/3 OCTAVE NTC (dB) WITH RESPECT TO INCIDENT SPL. (NTC_i)

$M_J = 1.2$ $M_T = 0.16$ $T_R = 600K$

DAISY LOBE NOZZLE (RUN NO = 129)

EMISSION ANGLE (RELATIVE TO JET EXHAUST) REFERENCED TO NOZZLE EXIT
(DEGREES)

FREQ KHZ	PTF_i	50.
.250	-33.5	-21.8
.315	-28.6	-16.8
.400	-27.8	-15.8
.500	-18.1	-6.4
.630	-15.2	-3.5
.800	-13.2	-1.4
1.00	-11.8	0.3
1.25	-9.6	1.9
1.60	-7.3	4.5
2.00	-5.1	6.6
2.50	-6.7	5.1
3.15	-7.4	4.3
4.00	-9.5	2.4
5.00	-7.6	4.1
6.30	-8.4	3.4
8.00	-15.2	-3.5
10.0	-13.4	1.4
12.5	-15.6	-4.2
16.0	-17.1	-5.3
20.0	-13.9	-2.1
25.0	-14.1	1.7
31.5	-0.6	5.1
40.0	-.9	12.7
50.0	-.4	11.4
63.0	-2.9	8.8

DATA FOR
THEREMAINING ANGLES NOT ANALYZED
DUE TO JET NOISE CONTAMINATION

$OPTF_i$	$NOSPL_i$
21.1	-0.4

CONICAL NOZZLE (RUN NO = 102)

EMISSION ANGLE (RELATIVE TO JET EXHAUST) REFERENCED TO NOZZLE EXIT
(DEGREES)

FREQ KHZ	PTF_i	40.	50.	60.	70.	80.	90.
.250	-13.1	-16.0	-15.7	-3.1	-9.4	-38.6	-28.9
.315	-11.6	-11.4	-11.6	-1.9	-8.3	-32.3	-22.3
.400	-11.0	-10.1	-10.5	-1.4	-7.8	-30.9	-21.2
.500	-8.7	-3.2	-4.8	-0.3	-7.7	-20.0	-16.1
.630	-6.7	0.2	-1.9	0.9	-7.3	-16.6	-13.1
.800	-4.6	2.1	0.6	2.7	-4.1	-14.9	-11.2
1.00	-3.2	3.7	2.6	3.6	-2.0	-13.1	-9.6
1.25	-1.9	5.3	4.4	3.7	-0.8	-11.0	-7.8
1.60	-0.7	6.6	6.4	3.9	0.3	-8.6	-6.0
2.00	0.5	6.3	8.0	6.3	1.2	-6.6	-3.3
2.50	1.3	3.9	8.0	8.1	4.8	-4.2	-1.6
3.15	1.8	-0.6	6.7	8.6	6.4	-1.9	-0.6
4.00	3.0	3.9	8.1	9.9	8.1	0.2	1.0
5.00	2.3	2.1	5.1	8.9	8.8	0.9	0.3
6.30	2.2	-0.9	4.4	8.5	9.5	1.6	-1.0
8.00	5.1	1.7	9.6	11.3	12.1	3.1	-2.7
10.0	1.7	-1.8	7.3	8.3	7.9	-2.6	-8.2
12.5	3.1	2.5	7.9	11.2	7.8	-8.8	-6.8
16.0	4.4	6.5	4.9	9.6	2.8	-17.2	-6.8
20.0	-5.4	-3.4	1.6	2.0	-6.8	-20.6	-6.5
25.0	-7.5	-4.6	0.7	-0.6	-10.6	-19.0	-11.4
31.5	-3.2	-4.3	-0.1	7.9	-10.0	-9.4	-8.8
40.0	4.1	2.8	6.4	8.4	0.5	-7.0	-9.3
50.0	-4.0	-1.6	2.5	3.8	-6.5	-18.2	-9.6
63.0	-4.9	1.2	0.2	3.2	-12.5	-10.9	-7.6

DATA FOR THE REMAINING ANGLES NOT ANALYZED DUE TO JET NOISE CONTAMINATION

$OPTF_i$	$NOSPL_i$
29.3	0.8	1.6	3.1	-0.8	-10.4	-6.0

1/3 OCTAVE NTC (dB) WITH RESPECT TO TRANSMITTED SPL (NTC_t)

$M_J = 1.2$ $M_T = 0.16$ $T_R = 600K$

DAISY LOBE NOZZLE (RUN NO = 129)

EMISSION ANGLE (RELATIVE TO JET EXHAUST) REFERENCED TO NOZZLE EXIT (DEGREES)

FREQ KHZ	PTF_t	50.
.250	+33.4	+21.3
.315	+28.1	+16.4
.400	+27.2	+15.5
.500	+17.7	+6.4
.630	+14.8	+3.1
.800	+12.7	+1.0
1.00	+11.1	0.7
1.25	+5.6	2.2
1.60	+7.4	4.7
2.00	+4.8	6.9
2.50	+6.4	5.3
3.15	+7.4	4.4
4.00	+5.7	2.6
5.00	+7.0	4.2
6.30	+6.3	3.5
8.00	+19.1	+3.3
10.0	+1[illegible].3	1.4
12.5	+15.8	+4.6
16.0	+14.9	+5.1
20.0	+13.5	+2.1
25.0	+1[illegible].1	1.7
31.5	+4.6	5.2
40.0	1.1	12.8
50.0	+4.2	11.5
63.0	+2.3	9.7

DATA FOR
THE REMAINING ANGLES NOT ANALYZED
DUE TO JET NOISE CONTAMINATION

$OPTF_t$	$NOSPL_t$
21.5	+0.0

CONICAL NOZZLE (RUN NO = 102)

EMISSION ANGLE (RELATIVE TO JET EXHAUST) REFERENCED TO NOZZLE EXIT (DEGREES)

FREQ KHZ	PTF_t	40.	50.	60.	70.	80.	90.
.250	+11.8	+14.7	+14.4	+1.9	+8.1	+37.3	+24.[illegible]
.315	+14.8	+10.6	+10.8	+1.1	+7.5	+31.8	+21.8
.400	+14.9	+9.5	+9.9	+0.8	+7.2	+30.3	+20.6
.500	+8.2	+2.8	+4.3	0.2	+7.2	+19.5	+15.6
.630	+6.4	0.5	+1.6	1.2	+7.0	+16.2	+12.8
.800	+4.6	2.3	0.7	2.8	+4.0	+14.7	+11.1
1.00	+3.1	3.8	2.6	3.6	+2.0	+13.0	+9.5
1.25	+1.9	5.3	4.6	3.7	+0.4	+10.9	+7.6
1.60	+0.7	6.6	6.4	4.0	0.3	+8.6	+5.0
2.00	+0.8	6.3	8.0	6.3	1.2	+6.6	+3.3
2.50	1.3	4.0	8.0	8.1	4.6	+4.2	+1.6
3.15	1.5	+0.6	6.7	8.9	6.4	+1.9	+0.0
4.00	3.1	3.9	8.2	9.9	8.2	0.2	1.1
5.00	2.3	2.2	5.1	9.0	8.2	0.9	0.4
6.30	2.3	+0.9	4.4	8.6	9.5	1.6	+1.0
8.00	5.2	1.9	9.8	11.5	12.2	3.3	+2.5
10.0	1.8	+1.7	7.5	8.3	8.1	+2.4	+0.1
12.5	3.1	2.5	8.4	11.2	7.8	+5.8	+6.8
16.0	3.4	0.5	5.0	9.6	2.7	+17.2	+6.7
20.0	+5.4	+3.4	1.6	2.0	+6.8	+20.6	+6.5
25.0	+7.4	+4.6	0.7	+0.5	+10.6	+19.0	+11.4
31.5	+3.2	+4.3	+0.1	7.2	+10.0	+9.4	+5.8
40.0	4.2	3.0	6.6	8.6	0.6	+6.9	+9.1
50.0	+3.5	+1.4	2.7	4.0	+6.3	+15.1	+9.4
63.0	+3.8	2.7	1.7	4.6	+11.1	+5.3	+6.2

DATA FOR THE REMAINING ANGLES NOT ANALYZED DUE TO JET NOISE CONTAMINATION

$OPTF_t$	$NOSPL_t$					
29.7	1.2	2.0	3.5	+0.4	+10.0	+7.6

1/3 OCTAVE NTC (dB) WITH RESPECT TO INCIDENT SPL (NTC_i)

$M_J = 1.2$ $M_T = 0.24$ $T_R = 600K$

DAISY LOBE NOZZLE (RUN NO = [illegible])

EMISSION ANGLE (RELATIVE TO JET EXHAUST) REFERENCED TO NOZZLE EXIT (DEGREES)

FREQ KHZ	PTF_i	40.	50.
.250	-34.6	-23.0	-36.4
.315	-24.3	-18.2	-23.2
.400	-27.8	-16.8	-21.3
.500	-15.[illegible]	-10.0	-9.9
.630	-15.6	-7.4	-5.9
.800	-14.2	-6.0	-4.4
1.00	-12.[illegible]	-4.7	-3.1
1.25	-1[illegible].6	-2.6	-0.9
1.60	-7.6	0.5	2.2
2.00	-6.[illegible]	2.1	3.9
2.50	-6.1	2.0	3.7
3.15	-7.[illegible]	0.7	2.2
4.00	-6.7	1.9	2.8
5.00	-8.[illegible]	0.9	1.2
6.30	-8.7	0.0	0.6
8.00	-8.9	-0.7	0.6
10.0	-1[illegible].3	-7.3	-7.3
12.5	-1[illegible].3	-9.2	-5.3
16.0	-8.1	-0.1	1.3
20.0	-12.[illegible]	-3.6	-2.7
25.0	-5.[illegible]	-2.8	-0.1
31.5	-6.[illegible]	-0.2	4.0
40.0	4.[illegible]	10.9	14.7
50.0	1.4	8.7	11.8
63.0	-4.7	2.9	5.3

DATA FOR THE REMAINING ANGLES NOT ANALYZED DUE TO JET NOISE CONTAMINATION

$OPTF_i$ ← $NOSPL_i$ →

24.2 -5.1 -3.4

CONICAL NOZZLE (RUN NO = 104)

EMISSION ANGLE (RELATIVE TO JET EXHAUST) REFERENCED TO NOZZLE EXIT (DEGREES)

FREQ KHZ	PTF_i	30.	40.	50.	60.	70.
.250	-5.2	2.4	1.7	0.2	-2.3	-4.1
.315	-7.3	-0.1	-1.0	-2.4	-4.8	-4.0
.400	-7.8	-0.7	-1.6	-3.0	-5.4	-3.9
.500	-7.4	-0.2	-1.2	-2.6	-4.8	-3.6
.630	-6.8	0.5	-0.6	-1.9	-4.0	-3.4
.800	-4.6	3.1	2.0	0.6	-1.9	-2.6
1.00	-2.8	5.5	4.4	2.8	-0.1	-2.0
1.25	-0.2	8.2	6.9	5.1	1.9	-1.1
1.60	1.4	10.2	8.3	6.3	3.3	0.4
2.00	1.4	10.3	7.6	5.7	4.1	2.0
2.50	1.3	9.7	5.8	4.9	6.4	3.4
3.15	1.9	8.8	6.3	6.3	8.1	3.9
4.00	0.9	2.5	4.0	6.6	8.8	3.2
5.00	-1.8	0.9	-3.1	0.1	8.4	-2.2
6.30	0.8	0.1	-0.1	3.6	10.4	2.0
8.00	2.6	-1.4	1.6	4.7	8.2	11.2
10.0	0.9	0.8	-0.8	0.1	2.8	0.8
12.5	-0.3	3.1	-2.1	-3.6	0.8	9.4
16.0	0.3	-4.3	-8.1	-6.4	1.5	10.6
20.0	-5.2	-6.8	-7.0	-5.0	0.9	3.7
25.0	-10.4	-5.2	-6.2	-6.2	-3.2	-0.5
31.5	-2.0	2.5	0.6	2.2	5.9	1.6
40.0	-2.6	-0.3	-1.4	-0.5	3.9	4.3
50.0	-5.1	-1.8	-4.5	-3.4	3.6	-0.6
63.0	-7.3	0.3	-3.6	-2.6	-7.7	-3.8

DATA FOR THE REMAINING ANGLES NOT ANALYZED DUE TO JET NOISE CONTAMINATION

$OPTF_i$ ← $NOSPL_i$ →

34.3 4.5 2.9 1.5 0.8 -0.0

1/3 OCTAVE NTC (dB) WITH RESPECT TC TRANSMITTED SPL (NTC_t)

$M_J = 1.2$ $M_T = 0.24$ $T_R = 600K$

DAISY LOBE NOZZLE (RUN NO = 130)

EMISSION ANGLE (RELATIVE TO JET EXHAUST) REFERENCED TO NOZZLE EXIT (DEGREES)

FREQ KHZ	PTF_t	40.	80.
.250	-32.8	-21.2	-28.6
.315	-27.6	-18.5	-21.5
.400	-20.2	-15.2	-19.7
.500	-17.6	-8.5	-8.8
.630	-14.5	-6.2	-4.7
.800	-13.3	-5.1	-3.5
1.00	-12.1	-4.0	-2.3
1.25	-11.2	-2.8	-0.4
1.60	-7.1	1.0	2.7
2.00	-5.7	2.4	4.2
2.50	-5.9	2.2	3.9
3.15	-7.4	0.8	2.3
4.00	-6.6	2.0	2.9
5.00	-5.0	1.0	1.2
6.30	-5.5	0.2	0.8
8.00	-5.5	-0.3	0.5
10.0	-11.3	-7.3	-7.2
12.5	-15.2	-9.1	-5.2
16.0	-7.9	0.1	1.6
20.0	-12.6	-3.6	-2.7
25.0	-5.9	-2.8	-0.0
31.5	-0.5	-0.2	4.1
40.0	4.4	11.3	15.2
50.0	3.3	10.6	13.8
63.0	-4.0	3.6	6.0

DATA FOR THE REMAINING ANGLES NOT ANALYZED DUE TO JET NOISE CONTAMINATION

$OPTF_t$	$NOSPL_t$
21.2	-4.0 -2.3

CONICAL NOZZLE (RUN NO = 104)

EMISSION ANGLE (RELATIVE TO JET EXHAUST) REFERENCED TO NOZZLE EXIT (DEGREES)

FREQ KHZ	PTF_t	30.	40.	50.	60.	70.
.250	-3.6	4.0	3.3	1.8	-0.6	-2.8
.315	-6.0	0.3	-0.6	-2.0	-4.4	-3.6
.400	-7.6	-0.5	-1.4	-2.7	-5.2	-3.6
.500	-7.1	0.0	-0.9	-2.4	-4.8	-3.4
.630	-6.6	0.8	-0.4	-1.7	-3.8	-3.1
.800	-4.8	3.2	2.1	0.7	-1.9	-2.6
1.00	-2.5	5.5	4.4	2.8	-0.1	-2.0
1.25	-0.1	8.3	6.9	5.1	2.0	-1.0
1.60	1.4	10.2	8.3	6.3	3.3	0.4
2.00	1.4	10.3	7.6	5.7	4.1	2.0
2.50	1.3	9.7	5.8	4.9	6.4	3.4
3.15	1.9	8.4	6.3	6.3	8.1	3.6
4.00	0.9	2.5	4.0	6.5	8.8	3.2
5.00	-1.5	0.9	-3.1	0.1	8.4	-2.1
6.30	0.8	0.2	-0.1	3.8	10.5	2.1
8.00	2.8	-1.2	1.8	4.9	8.4	11.4
10.0	0.2	1.0	-0.4	0.3	3.0	9.6
12.5	-4.2	3.1	-2.1	-3.0	0.5	9.5
16.0	4.4	-4.3	-8.0	-6.4	1.8	10.6
20.0	-5.2	-6.8	-7.0	-5.0	0.9	3.7
25.0	-10.4	-5.2	-6.2	-6.2	-3.1	-8.4
31.5	-2.0	2.6	0.6	2.3	6.0	1.6
40.0	-2.8	-0.3	-1.4	-0.8	4.0	4.4
50.0	-5.0	-1.7	-4.8	-3.3	3.6	-0.4
63.0	-3.6	3.9	3.0	1.1	-4.0	-0.2

DATA FOR THE REMAINING ANGLES NOT ANALYZED DUE TO JET NOISE CONTAMINATION

$OPTF_t$	$NOSPL_t$
3.8	4.7 3.1 1.7 1.0 0.2

1/3 OCTAVE NTC (dB) WITH RESPECT TO INCIDENT SPL (NTC_i)

$M_{J1} = 0 \quad M_{J2} = 0$

MULTICHUTE NOZZLE (RUN NO = 144)

FREQ KHZ	PTF$_i$	0.	10.	20.	30.	40.	50.	60.	70.	80.	90.	100.	110.	120.
	EMISSION ANGLE (RELATIVE TO JET EXHAUST) REFERENCED TO NOZZLE EXIT (DEGREES)													
.250	-3.3	-8.6	11.2	-8.4	-9.3	-9.2	-4.1	-4.0	-4.9	-4.9	-4.3	-5.1	-4.9	-4.1
.315	-14.0	-16.8	4.6	-13.9	-15.5	-15.9	-10.5	-10.8	-11.7	-11.6	-10.5	-11.9	-11.5	-10.5
.400	-19.7	-23.8	-4.9	-18.6	-22.4	-27.1	-24.1	-24.9	-24.0	-23.4	-17.3	-26.0	-21.8	-18.5
.500	-20.6	-21.9	-7.4	-16.4	-19.4	-26.0	-16.2	-22.4	-24.2	-23.6	-19.1	-25.3	-22.7	-20.3
.630	-21.7	-20.1	-15.9	-14.9	-17.6	-23.6	-17.0	-20.8	-24.4	-23.8	-22.7	-24.8	-24.0	-24.1
.800	-23.2	-15.7	-13.9	-14.0	-17.0	-24.7	-19.0	-24.4	-28.6	-30.3	-30.6	-29.6	-31.3	-38.9
1.00	-18.6	-16.2	-11.6	-12.9	-16.9	-25.5	-18.4	-20.1	-18.9	-17.4	-16.9	-16.3	-17.7	-16.9
1.25	-8.2	-1.7	-6.9	-7.7	-10.0	-13.8	-5.2	-7.0	-7.9	-6.7	-6.8	-7.9	-7.0	-6.7
1.60	-5.3	-2.0	-4.6	-4.3	-4.7	-8.6	-0.7	-3.3	-4.5	-4.9	-5.0	-5.9	-5.3	-5.8
2.00	-13.4	-9.7	-11.3	-10.3	-10.4	-15.0	-8.0	-11.9	-13.3	-14.8	-15.7	-14.5	-14.9	-15.1
2.50	-18.7	-14.9	-16.4	-14.4	-14.6	-20.1	-14.1	-18.4	-19.8	-19.2	-19.8	-19.5	-19.8	-21.6
3.15	-18.7	-15.3	-14.8	-13.0	-13.6	-20.4	-14.4	-17.8	-18.1	-19.1	-20.1	-21.8	-22.8	-25.0
4.00	-5.0	-1.7	-2.1	-1.5	-3.2	-10.8	-1.0	-2.2	-2.8	-4.7	-6.6	-7.9	-6.7	-7.8
5.00	-9.3	-10.4	-8.9	-7.3	-8.3	-12.0	-3.0	-7.1	-9.3	-12.1	-13.4	-14.1	-13.1	-13.7
6.30	-14.5	-14.4	-13.2	-12.7	-13.0	-18.2	-5.5	-12.6	-15.2	-15.1	-14.9	-16.4	-17.3	-18.7
8.00	-10.7	-4.5	-3.2	-4.5	-5.2	-15.2	-6.5	-13.4	-13.7	-11.7	-13.4	-13.8	-13.7	-13.0
10.0	-21.8	-6.2	-15.7	-13.8	-12.9	-25.2	-23.2	-28.4	-22.9	-22.2	-23.8	-23.9	-24.6	-27.4
12.5	-21.6	-8.8	-14.2	-13.4	-15.5	-30.7	-20.5	-21.9	-19.6	-20.9	-24.6	-26.0	-31.0	-29.9
16.0	-16.1	-6.1	-7.7	-7.7	-17.4	-24.6	-14.1	-17.9	-12.9	-13.4	-16.4	-20.8	-26.8	-23.0
20.0	-14.4	-1.8	-4.5	-5.6	-10.1	-17.0	-11.2	-13.1	-19.8	-16.6	-14.8	-20.5	-19.2	-22.0
25.0	-18.4	-8.7	-9.8	-10.4	-18.1	-21.0	-13.0	-24.6	-21.4	-20.2	-21.5	-25.0	-27.0	-29.9
31.5	-21.6	-6.3	-13.2	-16.3	-18.8	-25.1	-17.0	-20.9	-19.5	-27.3	-26.9	-28.5	-29.2	-28.6
40.0	-18.8	-5.3	-11.2	-11.3	-13.6	-24.0	-18.3	-16.1	-16.6	-20.8	-24.8	-28.0	-27.7	-30.8
50.0	-28.7	-9.0	-18.5	-21.1	-26.6	-37.6	-25.0	-28.6	-27.7	-30.3	-37.8	-39.3	-37.8	-40.1
63.0	-34.0	-13.6	-21.7	-29.4	-26.4	-34.7	-23.6	-34.0	-31.2	-38.2	-37.8	-31.7	-37.7	-39.7
	OPTF$_i$ ← NOSPL$_i$ →													
	21.4	-9.8	-6.0	-12.2	-13.3	-19.2	-12.2	-14.9	-15.6	-16.6	-17.0	-17.3	-17.5	-17.7

REF. COAXIAL NOZZLE (RUN NO = 168)

FREQ KHZ	PTF$_i$	10.	20.	30.	40.	50.	60.	70.	80.	90.	100.	110.	120.
	EMISSION ANGLE (RELATIVE TO JET EXHAUST) REFERENCED TO NOZZLE EXIT (DEGREES)												
.250	-11.2	-2.8	-1.7	-2.6	-14.8	-16.6	-15.3	-14.2	-14.7	-12.5	-14.4	-13.8	-14.1
.315	-16.7	-8.3	-7.1	-8.2	-19.7	-22.3	-20.7	-19.8	-20.4	-18.0	-20.1	-19.5	-19.8
.400	-29.3	-20.9	-17.8	-21.2	-25.7	-38.6	-30.9	-35.9	-37.8	-30.3	-42.1	-44.5	-41.4
.500	-26.7	-20.3	-18.3	-21.0	-22.7	-28.4	-25.8	-28.1	-28.6	-27.1	-28.9	-29.2	-29.0
.630	-24.7	-19.6	-18.9	-20.5	-20.6	-25.0	-23.1	-25.0	-25.5	-24.9	-25.4	-25.7	-25.6
.800	-23.4	-16.3	-15.0	-17.8	-19.1	-23.9	-22.8	-25.4	-26.0	-25.8	-25.4	-25.4	-25.3
1.00	-18.9	-11.2	-10.8	-14.5	-17.4	-22.2	-19.7	-20.7	-20.7	-19.3	-18.7	-18.1	-18.1
1.25	-9.6	-4.4	-4.8	-8.3	-10.0	-13.5	-9.6	-9.3	-8.9	-8.3	-7.8	-7.4	-7.8
1.60	-4.6	-1.1	-2.5	-3.5	-3.9	-6.8	-3.5	-3.7	-3.4	-3.1	-2.9	-3.0	-3.1
2.00	-12.1	-9.1	-10.0	-9.5	-10.1	-13.0	-10.0	-10.9	-11.2	-11.1	-11.2	-11.9	-12.1
2.50	-17.5	-13.7	-13.3	-13.1	-14.0	-17.4	-16.1	-16.0	-17.3	-17.8	-17.8	-19.4	-19.7
3.15	-17.9	-12.8	-12.4	-11.7	-13.5	-17.4	-16.7	-17.4	-18.6	-20.4	-20.1	-21.7	-22.1
4.00	-14.7	-4.3	-4.3	-3.7	-6.7	-11.7	-10.4	-11.3	-12.1	-12.8	-12.5	-12.6	-13.0
5.00	-13.5	-7.8	-7.3	-7.5	-9.5	-12.3	-10.9	-12.9	-15.2	-17.3	-16.9	-16.9	-17.6
6.30	-13.7	-5.1	-5.7	-6.1	-9.0	-16.2	-16.1	-14.9	-15.0	-16.0	-16.1	-18.3	-19.0
8.00	-9.9	-0.4	-0.8	-1.8	-5.8	-10.8	-11.4	-12.5	-15.0	-16.9	-17.0	-16.4	-17.6
10.0	-16.9	-4.8	-5.7	-8.0	-14.8	-16.2	-16.0	-19.1	-24.5	-26.2	-25.9	-26.0	-27.7
12.5	-26.7	-9.9	-10.8	-13.6	-18.6	-21.7	-24.0	-23.3	-25.8	-27.9	-25.2	-27.1	-29.1
16.0	-14.6	-3.1	-4.5	-9.5	-16.0	-17.7	-11.3	-16.6	-20.6	-22.3	-22.3	-24.4	-26.5
20.0	-14.1	-2.1	-5.6	-10.4	-14.2	-14.0	-11.8	-15.0	-17.4	-20.0	-20.4	-22.4	-25.4
25.0	-18.3	-7.6	-7.8	-11.6	-18.1	-20.8	-19.7	-20.8	-23.0	-24.6	-24.5	-24.6	-29.2
31.5	-24.4	-9.4	-13.3	-13.3	-18.7	-19.9	-20.9	-22.1	-24.9	-26.0	-26.2	-27.5	-32.5
40.0	-24.3	-8.1	-16.1	-11.1	-18.0	-20.4	-19.2	-23.2	-28.7	-27.7	-27.5	-28.9	-34.2
50.0	-24.7	-11.1	-14.5	-14.7	-26.1	-30.8	-26.7	-29.9	-30.9	-34.1	-34.1	-36.1	-43.1
63.0	-27.6	-16.3	-18.1	-17.4	-20.1	-34.3	-32.6	-31.6	-38.0	-36.8	-30.9	-37.6	-42.7
	OPTF$_i$ ← NOSPL$_i$ →												
	22.4	-9.2	-9.3	-10.1	-13.7	-17.5	-15.6	-16.4	-17.5	-17.6	-17.4	-18.2	-18.5

1/3 OCTAVE NTC (dB) WITH RESPECT TO INCIDENT SPL (NTC_i)

$M_{J1} = 0.4$ $M_{J2} = 0.6$

MULTICHUTE NOZZLE (RUN NO = 145)

FREQ KHZ	PTF$_i$	10.	20.	30.	40.	50.	60.	70.	80.	90.	100.	110.	120.
	EMISSION ANGLE (RELATIVE TO JET EXHAUST) REFERENCED TO NOZZLE EXIT (DEGREES)												
.250	-7.1	7.9	-7.8	-8.1	-9.3	-6.0	-6.0	-9.7	-8.7	-8.8	-10.2	-9.8	-9.6
.315	-12.3	2.8	-11.7	-13.8	-14.6	-14.4	-14.4	-16.0	-18.1	-14.1	-15.5	-15.1	-14.8
.400	-21.4	-8.9	-16.3	-18.5	-20.7	-20.0	-20.5	-27.0	-27.2	-20.7	-20.6	-25.8	-24.6
.500	-22.5	-8.1	-15.8	-18.8	-24.7	-21.7	-27.7	-28.1	-20.6	-20.7	-28.5	-27.9	-26.8
.630	-24.9	-37.0	-16.8	-18.8	-22.7	-18.4	-26.7	-30.4	-32.2	-34.8	-35.7	-37.9	-45.1
.800	-24.8	-33.8	-16.7	-17.7	-20.9	-17.7	-24.1	-30.9	-45.6	-38.4	-66.6	-42.6	-39.6
1.00	-20.4	-24.2	-13.9	-14.2	-15.9	-15.6	-20.8	-23.8	-23.2	-21.7	-24.8	-21.4	-25.2
1.25	-9.1	-13.1	-8.1	-4.4	-5.8	-3.4	-6.0	-6.7	-10.6	-10.8	-13.4	-12.8	-15.0
1.60	-8.2	-14.6	-2.4	-0.8	-1.6	1.3	-5.0	-6.3	-8.1	-9.7	-12.2	-11.8	-13.2
2.00	-11.1	-18.3	-8.9	-6.6	-7.0	-4.3	-11.9	-13.8	-16.3	-18.3	-19.0	-17.6	-18.7
2.50	-16.1	-25.0	-14.6	-11.5	-11.9	-9.3	-16.7	-20.2	-22.1	-22.4	-21.9	-21.6	-23.6
3.15	-16.9	-25.4	-15.0	-11.6	-12.0	-10.3	-16.8	-22.2	-21.6	-22.7	-24.0	-25.8	-29.5
4.00	-7.5	-17.7	-5.9	-2.7	-3.0	-2.3	-6.0	-6.2	-7.6	-11.3	-15.3	-17.1	-19.7
5.00	-6.6	-19.8	-7.9	-4.4	-3.9	-2.7	-7.3	-7.7	-11.7	-16.1	-19.8	-20.1	-20.9
6.30	-13.2	-23.6	-11.2	-9.3	-7.8	-7.6	-11.0	-13.8	-20.8	-23.1	-23.0	-23.4	-26.4
8.00	-12.9	-24.5	-11.4	-8.9	-6.9	-6.8	-12.7	-18.3	-21.4	-21.8	-24.5	-25.8	-24.8
10.0	-18.5	-32.6	-18.2	-13.8	-10.1	-8.7	-16.8	-21.7	-19.8	-23.1	-24.3	-28.9	-30.2
12.5	-15.9	-28.5	-13.9	-11.6	-8.3	-11.9	-15.0	-16.9	-18.9	-21.4	-26.3	-30.6	-30.6
16.0	-16.2	-34.4	-19.8	-17.3	-8.3	-11.0	-16.2	-20.3	-18.8	-23.5	-28.2	-30.5	-29.6
20.0	-15.3	-30.4	-17.7	-16.7	-6.6	-10.7	-16.3	-21.7	-18.0	-19.9	-22.2	-23.5	-27.7
25.0	-26.2	-43.4	-23.5	-21.3	-11.3	-15.6	-22.5	-22.4	-24.9	-29.5	-24.5	-30.7	-32.4
31.5	-18.7	-41.2	-19.3	-18.3	-10.5	-13.7	-16.8	-20.2	-24.9	-26.7	-25.7	-26.2	-27.1
40.0	-16.4	-35.1	-20.0	-16.9	-9.3	-9.5	-17.0	-17.3	-17.7	-20.1	-23.8	-23.7	-24.6
50.0	-24.0	-40.4	-28.7	-29.0	-20.0	-17.4	-26.3	-23.1	-24.9	-31.7	-30.6	-32.7	-36.9
63.0	-24.0	-34.4	-31.0	-25.2	-20.6	-17.0	-26.4	-26.6	-29.2	-29.8	-24.5	-33.0	-36.6
	OPTF$_i$ ← NOSPL$_i$ →												
	22.4	-4.8	-13.2	-11.4	-10.5	-9.7	-15.3	-16.6	-18.0	-19.0	-20.2	-20.4	-20.9

REF. COAXIAL NOZZLE (RUN NO = 169)

FREQ KHZ	PTF$_i$	10.	20.	30.	40.	50.	60.	70.	80.	90.	100.	110.	120.
	EMISSION ANGLE (RELATIVE TO JET EXHAUST) REFERENCED TO NOZZLE EXIT (DEGREES)												
.250	-14.3	-13.7	-9.3	-11.1	-13.4	-16.2	-14.1	-13.8	-14.0	-11.8	-13.7	-12.8	-14.3
.315	-24.0	-17.2	-13.8	-15.4	-18.6	-21.7	-19.8	-20.1	-20.5	-18.1	-20.2	-18.9	-20.7
.400	-26.5	-19.1	-16.2	-18.2	-23.1	-27.1	-26.5	-31.3	-39.8	-30.6	-37.2	-33.5	-35.3
.500	-24.5	-19.2	-15.3	-16.9	-19.6	-22.7	-23.5	-28.0	-30.4	-30.2	-34.4	-33.1	-34.9
.630	-22.0	-19.3	-14.3	-15.4	-17.0	-19.9	-21.2	-25.6	-26.9	-29.7	-32.1	-32.6	-34.4
.800	-21.0	-18.6	-12.7	-13.3	-14.5	-17.7	-21.3	-27.2	-28.1	-34.1	-29.6	-32.3	-34.1
1.00	-17.8	-17.4	-11.1	-10.8	-12.4	-17.6	-25.4	-22.0	-21.9	-18.6	-16.7	-18.8	-19.5
1.25	-7.0	-13.6	-4.5	-2.9	-2.5	-8.6	-8.2	-7.4	-7.6	-6.7	-6.1	-7.7	-8.6
1.60	1.1	-8.3	3.7	6.1	6.9	2.1	2.0	1.3	1.0	1.0	0.7	-0.7	-1.9
2.00	-7.4	-18.0	-5.1	-1.7	-1.2	-5.6	-5.7	-7.0	-7.7	-8.6	-9.5	-11.6	-13.6
2.50	-15.1	-28.1	-14.1	-9.7	-8.5	-12.2	-12.9	-14.2	-15.7	-17.7	-18.9	-22.1	-24.3
3.15	-16.8	-32.3	-15.8	-10.7	-9.6	-13.3	-14.7	-17.0	-19.4	-22.0	-24.0	-26.3	-27.2
4.00	-9.1	-28.8	-8.0	-3.6	-2.2	-6.2	-6.7	-9.4	-11.3	-12.1	-12.5	-13.6	-15.6
5.00	-8.5	-35.9	-7.5	-4.0	-2.6	-5.4	-5.0	-7.7	-9.0	-10.6	-13.0	-14.3	-17.2
6.30	-7.5	-37.3	-6.9	-3.3	-1.7	-2.9	-4.0	-9.0	-13.1	-13.0	-14.0	-15.7	-18.6
8.00	-15.4	-40.9	-12.2	-10.5	-9.5	-10.2	-12.3	-20.7	-22.1	-21.7	-25.9	-32.6	-39.3
10.0	-9.0	-35.4	-15.6	-14.5	-14.0	-13.1	-17.8	-24.4	-25.9	-26.2	-27.8	-29.8	-30.5
12.5	-15.9	-38.0	-16.4	-12.6	-14.1	-11.8	-12.4	-12.6	-16.0	-14.8	-17.7	-23.5	-22.5
16.0	-21.2	-44.9	-21.4	-16.1	-17.4	-20.1	-16.0	-19.8	-20.6	-20.4	-23.7	-30.7	-29.1
20.0	-17.7	-38.3	-19.2	-14.2	-13.0	-12.6	-15.4	-17.8	-24.2	-21.0	-24.5	-28.0	-30.2
25.0	-24.0	-50.0	-25.8	-22.3	-22.6	-22.5	-18.6	-20.9	-20.7	-25.8	-26.2	-31.8	-34.2
31.5	-24.1	-51.4	-27.4	-20.1	-21.5	-18.3	-21.4	-25.1	-24.5	-26.5	-32.3	-30.9	-38.6
40.0	-19.6	-34.7	-21.7	-16.9	-17.1	-14.8	-15.1	-17.3	-18.0	-25.3	-23.8	-30.4	-30.8
50.0	-32.7	-39.2	-30.1	-25.0	-31.9	-29.8	-28.6	-31.2	-33.3	-34.3	-34.6	-37.9	-40.6
63.0	-31.6	-33.3	-30.5	-27.2	-24.7	-28.4	-31.5	-30.1	-33.6	-32.9	-33.8	-36.7	-42.1
	OPTF$_i$ ← NOSPL$_i$ →												
	22.6	-23.6	-13.8	-10.7	-10.0	-13.1	-13.9	-16.9	-17.4	-18.1	-19.1	-20.8	-22.6

1/3 OCTAVE NTC (dB) WITH RESPECT TO INCIDENT SPL (NTC_i)

$M_{J1} = 0$ $M_{J2} = 1.2$

MULTICHUTE NOZZLE (RUN NO = 152)

EMISSION ANGLE (RELATIVE TO JET EXHAUST) REFERENCED TO NOZZLE EXIT
(DEGREES)

FREQ KHZ	PTF$_i$	20.	30.	40.	50.	60.	70.	80.
.250	-3.9	-2.6	-5.1	-5.6	2.9	3.8	-10.5	-10.9
.315	-14.5	-13.2	-15.0	-15.4	-7.9	-0.6	-21.0	-21.4
.400	-26.3	-28.1	-21.6	-25.2	-25.6	-16.6	-39.5	-32.1
.500	-26.6	-27.5	-22.0	-23.4	-21.4	-18.6	-35.3	-34.9
.630	-26.9	-34.8	-22.3	-22.6	-19.2	-23.1	-47.8	-47.6
.800	-24.9	-30.5	-18.9	-19.0	-19.0	-16.6	-32.6	-34.9
1.00	-24.8	-18.8	-14.7	-14.4	-17.7	-14.7	-21.0	-24.8
1.25	-12.7	-8.9	-7.6	-7.3	-7.6	-8.4	-12.4	-15.6
1.60	-4.1	-1.6	0.4	0.7	2.9	-3.0	-5.0	-8.3
2.00	-7.6	-7.0	-3.7	-2.6	0.1	-8.6	-9.9	-13.2
2.50	-15.0	-16.9	-13.2	-10.1	-7.0	-16.6	-19.0	-22.3
3.15	-16.6	-21.4	-19.3	-12.0	-8.3	-17.6	-22.3	-23.4
4.00	-14.3	-18.8	-14.2	-7.0	-2.2	-11.2	-13.5	-13.2
5.00	-7.6	-17.1	-9.4	-4.6	-0.3	-6.9	-6.9	-8.4
6.30	-8.1	-13.2	-9.7	-6.1	-0.4	-9.5	-10.6	-15.3
8.00	-13.2	-16.1	-18.3	-16.1	-5.8	-8.9	-16.4	-19.0
10.0	-12.9	-19.5	-19.3	-16.6	-5.0	-11.6	-13.4	-17.6
12.5	-12.7	-21.6	-21.1	-15.6	-4.5	-17.2	-17.6	-16.5
16.0	-14.5	-18.3	-21.3	-13.5	-7.5	-15.7	-11.3	-17.5
20.0	-17.8	-22.2	-20.7	-16.4	-11.2	-18.7	-15.8	-15.6
25.0	-17.3	-25.0	-25.5	-24.3	-8.7	-20.9	-21.0	-20.4
31.5	-24.1	-25.7	-24.0	-24.2	-11.8	-21.5	-23.3	-23.4
40.0	-12.7	-18.6	-20.8	-17.8	-5.7	-16.0	-10.8	-8.5
50.0	-24.5	-31.4	-33.2	-29.1	-12.8	-21.5	-18.9	-18.7
63.0	-21.3	-32.7	-30.1	-28.9	-13.4	-23.2	-17.9	-21.6

DATA FOR THE REMAINING ANGLES NOT ANALYZED DUE TO JET NOISE CONTAMINATION

OPTF$_i$	NOSPL$_i$						
21.8	-17.9	-15.7	-12.9	-7.6	-13.8	-17.4	-18.8

REF. COAXIAL NOZZLE (RUN NO = 174)

EMISSION ANGLE (RELATIVE TO JET EXHAUST) REFERENCED TO NOZZLE EXIT
(DEGREES)

FREQ KHZ	PTF$_i$	30.	40.	50.	60.
.250	-1.1	6.7	-5.2	5.2	0.1
.315	-6.6	2.1	-8.1	-0.7	0.8
.400	-14.4	-2.3	-9.8	-23.4	-9.5
.500	-14.1	-3.6	-10.3	-8.7	-12.1
.630	-13.8	-5.3	-10.7	-5.8	-19.7
.800	-12.8	-3.4	-9.3	-5.2	-17.5
1.00	-10.7	-0.4	-6.9	-4.0	-14.2
1.25	-6.1	4.8	-1.8	-0.6	-8.2
1.60	-1.1	10.1	3.8	3.8	-1.6
2.00	-12.1	-2.6	-7.1	-6.6	-11.3
2.50	-16.6	-10.2	-12.7	-8.5	-15.6
3.15	-13.7	-12.6	-11.6	-4.8	-12.6
4.00	-7.3	-6.7	-6.5	1.6	-4.8
5.00	-13.6	-10.7	-11.0	-5.1	-7.9
6.30	-14.4	-13.2	-7.9	-2.3	-6.5
8.00	-22.9	-18.9	-18.3	-16.7	-15.7
10.0	-23.8	-18.6	-24.1	-16.6	-18.4
12.5	-22.8	-13.6	-23.6	-16.1	-20.8
16.0	-24.5	-14.9	-14.4	-13.1	-21.0
20.0	-22.4	-17.6	-18.5	-14.9	-19.3
25.0	-28.2	-19.8	-23.3	-20.9	-31.0
31.5	-34.1	-30.1	-25.0	-22.4	-26.0
40.0	-22.8	-14.9	-21.8	-15.7	-18.6
50.0	-32.7	-25.7	-31.8	-24.5	-30.8
63.0	-44.3	-34.0	-38.0	-32.2	-39.6

DATA FOR THE REMAINING ANGLES NOT ANALYZED DUE TO JET NOISE CONTAMINATION

OPTF$_i$	NOSPL$_i$				
23.1	-6.7	-13.2	-8.9	-11.2	

1/3 OCTAVE NTC (dB) WITH RESPECT TO INCIDENT SPL (NTC_i)

$M_{J1} = 0.8$ $M_{J2} = 1.2$

MULTICHUTE NOZZLE (RUN NO = 153)

FREQ KHZ	EMISSION ANGLE (RELATIVE TO JET EXHAUST) REFERENCED TO NOZZLE EXIT (DEGREES)							
	PTF$_i$	20.	30.	40.	50.	60.	70.	80.
.250	-7.6	-6.9	-10.1	-7.9	-1.3	-0.2	-4.1	-10.7
.315	-11.3	-10.1	-13.6	-10.2	-4.8	-4.3	-13.2	-13.8
.400	-18.3	-14.9	-19.8	-12.7	-10.8	-17.2	-27.9	-18.3
.500	-19.0	-14.1	-22.1	-13.1	-12.1	-17.0	-23.2	-18.8
.630	-23.1	-13.2	-35.9	-13.6	-14.7	-16.8	-20.6	-19.5
.800	-18.1	-11.8	-29.4	-12.7	-11.1	-17.2	-20.8	-17.1
1.00	-15.4	-11.4	-18.6	-11.6	-7.2	-19.0	-23.4	-14.9
1.25	-11.9	-11.7	-11.4	-9.2	-2.6	-25.0	-23.0	-12.4
1.60	-5.3	-7.9	-4.3	-2.9	3.4	-10.2	-6.3	-9.5
2.00	-7.4	-9.6	-6.8	-3.7	0.9	-8.2	-7.6	-15.7
2.50	-14.4	-10.9	-14.4	-10.6	-6.4	-13.8	-14.9	-22.7
3.15	-15.4	-20.9	-16.3	-14.1	-7.0	-14.6	-18.4	-20.9
4.00	-8.3	-19.1	-11.3	-8.2	0.2	-8.4	-12.7	-12.7
5.00	-5.2	-14.1	-6.6	-3.1	2.7	-7.7	-5.4	-6.8
6.30	-5.4	-12.1	-8.5	-6.0	2.2	-5.0	-5.4	-11.8
8.00	-14.6	-13.8	-8.8	-12.4	-3.1	-8.2	-12.9	-24.6
10.0	-15.4	-17.6	-12.7	-13.4	-2.4	-8.1	-16.9	-13.1
12.5	-9.6	-17.3	-16.6	-13.8	-1.8	-8.7	-18.0	-10.4
16.0	-15.8	-24.4	-22.7	-18.0	-8.2	-12.2	-23.5	-27.4
20.0	-16.7	-22.6	-22.0	-17.8	-11.0	-19.1	-23.6	-24.1
25.0	-14.0	-21.9	-18.7	-20.6	-8.4	-19.5	-18.4	-18.2
31.5	-18.1	-25.1	-23.2	-23.8	-9.6	-23.1	-19.2	-25.8
40.0	-11.1	-17.6	-19.5	-18.9	-2.8	-12.7	-12.1	-12.6
50.0	-16.4	-29.0	-30.2	-28.7	-7.8	-21.4	-20.4	-16.4
63.0	-24.5	-29.0	-29.4	-28.6	-11.6	-23.5	-22.0	-26.0

DATA FOR THE REMAINING ANGLES NOT ANALYZED DUE TO JET NOISE CONTAMINATION

OPTF$_i$	NOSPL$_i$						
23.9	-15.8	-14.8	-12.3	-5.3	-10.9	-15.3	-17.2

REF. COAXIAL NOZZLE (RUN NO = 172)

FREQ KHZ	EMISSION ANGLE (RELATIVE TO JET EXHAUST) REFERENCED TO NOZZLE EXIT (DEGREES)					
	PTF$_i$	30.	40.	50.	60.	70.
.250	-4.2	2.1	2.0	-5.5	4.0	-2.2
.315	-10.2	-3.9	-3.7	-11.8	-2.1	-8.4
.400	-20.6	-14.2	-11.2	-27.4	-13.2	-22.2
.500	-15.7	-11.8	-13.3	-20.6	-14.8	-14.2
.630	-18.7	-9.7	-20.6	-17.4	-18.4	-11.0
.800	-16.2	-5.8	-17.8	-14.0	-16.2	-10.1
1.00	-12.9	-1.3	-13.7	-11.0	-11.6	-9.9
1.25	-8.4	3.7	-8.4	-5.9	-7.2	-11.9
1.60	-2.6	9.2	-1.7	1.0	-1.6	-4.8
2.00	-11.2	-0.9	-9.4	-6.4	-10.3	-8.4
2.50	-16.3	-9.8	-13.0	-10.1	-18.0	-11.6
3.15	-15.0	-12.9	-10.4	-8.1	-13.0	-10.6
4.00	-6.8	-0.6	-1.7	-0.5	-3.8	-2.9
5.00	-12.3	-9.7	-7.2	-6.2	-6.4	-11.4
6.30	-12.7	-11.9	-14.5	-8.5	-4.6	-7.8
8.00	-21.6	-25.8	-17.5	-16.0	-14.2	-20.6
10.0	-20.3	-14.0	-18.5	-16.7	-15.9	-13.1
12.5	-20.1	-19.5	-16.8	-13.6	-22.4	-13.8
16.0	-21.2	-16.2	-19.0	-19.8	-25.2	-11.1
20.0	-19.0	-16.7	-18.4	-11.4	-24.6	-15.6
25.0	-20.3	-23.2	-27.2	-19.7	-28.1	-15.8
31.5	-24.8	-22.3	-30.5	-18.0	-24.1	-17.4
40.0	-16.8	-11.6	-17.3	-12.3	-18.7	-7.7
50.0	-24.6	-18.5	-24.2	-18.9	-29.8	-17.8
63.0	-31.4	-22.2	-36.6	-25.2	-35.9	-25.4

DATA FOR THE REMAINING ANGLES NOT ANALYZED DUE TO JET NOISE CONTAMINATION

OPTF$_i$	NOSPL$_i$					
23.4	-7.5	-10.6	-11.4	-5.8	-11.5	

1/3 OCTAVE NTC (dB) WITH RESPECT TO INCIDENT SPL (NTC_i)

$M_{J1} = 0.8$ $M_{J2} = 0.9$

MULTICHUTE NOZZLE (RUN NO = 154)

FREQ KHZ	PTF$_i$	20.	30.	40.	50.	60.	70.	80.	90.	100.	110.	120.
	EMISSION ANGLE (RELATIVE TO JET EXHAUST) REFERENCED TO NOZZLE EXIT (DEGREES)											
.250	-6.4	-5.5	-11.0	-9.0	6.1	2.6	-0.2	-6.5	-5.0	2.7	-0.5	3.2
.315	-7.9	-12.8	-18.1	-16.0	-2.0	-4.6	-14.2	-14.5	-12.9	-5.3	-8.6	-4.4
.400	-19.1	-19.5	-24.0	-21.4	-20.6	-10.9	-26.7	-28.5	-24.2	-19.0	-24.2	-13.1
.500	-18.5	-21.5	-25.2	-21.9	-13.3	-11.3	-26.4	-28.5	-26.7	-19.9	-23.3	-15.5
.630	-18.0	-27.6	-27.3	-22.0	-10.3	-11.8	-26.0	-28.3	-40.1	-21.3	-22.4	-32.7
.800	-19.7	-39.7	-23.0	-20.7	-11.3	-16.1	-25.7	-27.8	-32.4	-25.1	-25.9	-31.5
1.00	-16.4	-21.9	-17.9	-18.8	-7.9	-16.6	-27.7	-21.3	-22.1	-22.2	-22.3	-18.1
1.25	-7.5	-11.7	-12.3	-12.3	1.0	-5.5	-17.8	-13.7	-15.6	-11.9	-13.2	-12.7
1.60	-1.2	-5.9	-7.3	-4.6	7.6	1.3	-5.8	-10.0	-13.0	-8.6	-9.9	-13.2
2.00	-3.4	-9.8	-9.4	-6.3	5.3	-0.6	-12.3	-16.0	-19.5	-14.1	-10.6	-11.5
2.50	-8.1	-17.9	-14.2	-11.9	0.2	-5.9	-18.8	-23.6	-23.7	-12.8	-12.1	-13.5
3.15	-9.7	-20.6	-15.9	-14.4	-1.2	-8.1	-23.9	-25.3	-22.5	-13.6	-17.0	-20.7
4.00	-1.1	-12.1	-7.9	-5.1	7.3	-1.2	-10.1	-9.4	-11.8	-6.7	-10.4	-13.6
5.00	-4.7	-10.7	-6.1	-4.4	7.6	-0.9	-8.5	-10.3	-13.2	-6.4	-11.6	-10.4
6.30	-3.9	-12.2	-9.6	-8.3	3.6	-0.5	-14.0	-20.7	-22.0	-13.9	-16.6	-16.1
8.00	-4.6	-10.4	-12.2	-11.0	2.6	-0.3	-17.0	-19.9	-21.8	-10.9	-14.1	-16.7
10.0	-7.7	-19.6	-20.5	-12.4	-1.4	-1.1	-15.1	-16.6	-23.2	-11.9	-15.1	-15.6
12.5	-6.6	-16.1	-15.0	-12.2	-2.1	-5.8	-12.4	-17.7	-21.7	-10.5	-18.8	-14.2
16.0	-7.6	-23.5	-24.7	-22.2	-0.2	-5.9	-20.2	-20.0	-22.0	-16.9	-21.1	-17.6
20.0	-4.0	-29.8	-26.4	-21.2	-1.6	-8.5	-19.5	-19.9	-22.4	-17.3	-17.1	-14.9
25.0	-11.0	-31.9	-26.8	-24.4	-2.7	-13.6	-22.9	-22.9	-27.0	-15.9	-17.9	-21.2
31.5	-12.4	-27.8	-27.0	-25.1	-3.9	-12.8	-24.2	-24.2	-24.2	-20.7	-22.2	-23.2
40.0	-12.9	-26.4	-31.2	-21.4	-6.6	-6.0	-18.6	-21.5	-24.9	-17.8	-14.3	-18.3
50.0	-15.9	-32.9	-32.0	-32.4	-6.7	-15.7	-25.3	-27.9	-27.7	-22.8	-24.9	-26.9
63.0	-7.9	-32.2	-27.3	-33.3	1.2	-17.9	-26.3	-31.7	-30.7	-15.2	-22.9	-26.2
	OPTF$_i$ ← NOSPL$_i$ →											
	29.2	-16.3	-15.0	-12.8	0.3	-5.7	-17.0	-18.8	-19.2	-11.3	-13.8	-12.2

REF. COAXIAL NOZZLE (RUN NO = 171)

FREQ KHZ	PTF$_i$	10.	20.	30.	40.	50.	60.	70.	80.	90.	100.	110.	120.
	EMISSION ANGLE (RELATIVE TO JET EXHAUST) REFERENCED TO NOZZLE EXIT (DEGREES)												
.250	-11.2	-7.8	-0.9	-3.4	-8.2	-13.6	-8.7	-12.3	-22.4	-21.6	-22.6	-15.7	-13.3
.315	-15.6	-11.6	-5.8	-8.6	-9.3	-18.5	-14.6	-18.8	-26.6	-28.0	-28.3	-17.7	-17.9
.400	-18.7	-13.8	-9.8	-12.9	-9.6	-22.5	-21.6	-41.7	-29.4	-40.8	-34.6	-18.5	-21.2
.500	-18.3	-14.0	-10.6	-13.6	-9.1	-19.7	-19.6	-28.4	-27.7	-35.7	-30.7	-18.2	-21.3
.630	-17.8	-14.3	-11.9	-14.3	-8.4	-17.4	-17.7	-24.7	-28.9	-32.8	-28.0	-17.8	-21.5
.800	-16.0	-12.6	-9.4	-10.9	-6.4	-15.4	-18.1	-24.2	-23.7	-41.5	-28.2	-16.5	-20.1
1.00	-14.3	-11.1	-6.9	-7.0	-4.8	-16.5	-21.6	-28.9	-19.6	-25.9	-25.6	-20.8	-17.7
1.25	-10.5	-9.9	-3.6	-2.0	-2.8	-17.7	-17.2	-14.0	-11.8	-13.5	-13.8	-15.6	-13.1
1.60	-2.1	-10.3	1.2	5.0	2.3	-1.0	-2.5	-1.2	-1.3	-3.3	-3.3	-5.4	-6.3
2.00	-14.4	-25.8	-9.4	-4.1	-5.8	-7.4	-6.8	-9.6	-8.6	-12.2	-13.4	-15.4	-16.1
2.50	-14.6	-26.7	-13.7	-9.7	-10.4	-10.1	-12.0	-14.9	-13.3	-17.2	-20.3	-20.8	-21.5
3.15	-14.1	-28.9	-12.4	-9.8	-10.6	-8.5	-11.2	-14.4	-16.5	-19.1	-20.3	-22.7	-26.4
4.00	-5.8	-23.9	-5.0	-2.8	-2.2	-0.1	-3.9	-5.3	-9.2	-9.8	-10.3	-9.7	-14.3
5.00	-10.0	-30.1	-12.9	-7.3	-8.8	-5.6	-5.2	-8.2	-8.9	-12.9	-15.2	-16.3	-22.6
6.30	-14.9	-30.7	-11.1	-6.9	-8.3	-6.1	-4.9	-12.5	-18.0	-19.3	-16.8	-19.0	-22.3
8.00	-18.6	-31.3	-21.6	-16.2	-17.3	-12.7	-13.4	-23.8	-28.4	-23.8	-24.9	-25.7	-27.5
10.0	-18.7	-36.5	-19.1	-16.4	-16.9	-15.4	-11.8	-16.7	-22.6	-23.6	-22.2	-26.2	-27.0
12.5	-18.0	-32.0	-20.9	-22.4	-17.0	-16.0	-11.8	-15.6	-16.0	-17.6	-20.3	-22.8	-24.1
16.0	-23.4	-38.8	-21.9	-19.9	-19.8	-26.9	-20.7	-17.8	-21.4	-20.6	-27.1	-30.7	-32.1
20.0	-22.4	-34.0	-22.9	-22.3	-19.8	-19.0	-24.1	-19.5	-23.0	-18.1	-24.5	-29.5	-29.5
25.0	-24.0	-44.3	-33.0	-29.1	-24.8	-19.4	-22.1	-20.4	-23.6	-23.5	-32.3	-31.0	-35.6
31.5	-22.9	-43.0	-32.5	-21.8	-23.7	-18.5	-19.3	-18.4	-22.2	-22.4	-27.9	-31.5	-30.3
40.0	-22.9	-37.8	-29.8	-23.2	-25.4	-19.1	-16.7	-19.4	-20.1	-27.0	-28.4	-31.3	-31.8
50.0	-25.8	-38.3	-29.2	-27.6	-30.6	-18.6	-23.3	-23.6	-28.1	-29.8	-32.5	-35.6	-33.6
63.0	-27.0	-41.3	-38.2	-34.4	-35.4	-16.1	-33.3	-31.8	-38.1	-36.2	-38.3	-44.2	-42.4
	OPTF$_i$ ← NOSPL$_i$ →												
	32.6	-18.4	-11.7	-10.7	-11.1	-12.3	-13.4	-16.3	-17.6	-20.2	-21.4	-20.8	-21.9

1/3 OCTAVE NTC (dB) WITH RESPECT TO INCIDENT SPL (NTC_i)

$M_{J_1} = 0.8$ $M_{J_2} = 1.2$ T_{R_1} = AMBIENT $T_{R_2} = 600$ K

MULTICHUTE NOZZLE (RUN NO = 157)

EMISSION ANGLE (RELATIVE TO JET EXHAUST) REFERENCED TO NOZZLE EXIT (DEGREES)

FREQ KHZ	PTF_i	60.	70.	80.
.250	14.6	25.8	7.6	8.5
.315	-7.6	3.6	-14.4	-13.1
.400	-19.6	-8.7	-24.0	-20.6
.500	-21.6	-10.7	-26.7	-23.6
.630	-24.1	-12.8	-30.0	-28.9
.800	-23.4	-12.1	-27.3	-27.8
1.00	-21.8	-10.6	-24.0	-25.5
1.25	-19.2	-8.0	-19.7	-21.9
1.60	-15.1	-4.3	-14.2	-16.9
2.00	-8.9	1.6	-6.9	-10.1
2.50	-12.0	-1.8	-8.9	-12.3
3.15	-25.1	-10.4	-16.3	-19.9
4.00	-22.1	-12.6	-17.5	-21.3
5.00	-10.6	-7.6	-11.7	-15.6
6.30	-11.1	-1.5	-4.4	-8.5
8.00	-13.1	-5.0	-6.4	-11.0
10.0	-14.5	-6.5	-7.2	-15.3
12.5	-14.0	-3.5	-13.1	-17.7
16.0	-14.6	-3.8	-22.5	-16.7
20.0	-17.7	-9.4	-18.9	-10.7
25.0	-18.7	-8.5	-17.2	-19.1
31.5	-22.6	-13.4	-23.1	-18.5
40.0	-29.5	-22.1	-23.4	-24.7
50.0	-24.0	-17.5	-16.7	-20.0
63.0	-31.5	-24.4	-23.2	-28.5

DATA FOR THE REMAINING ANGLES NOT ANALYZED DUE TO JET NOISE CONTAMINATION

$OPTF_i$	← $NOSPL_i$ →		
19.6	-7.2	-14.8	-18.1

REF. COAXIAL NOZZLE (RUN NO =176)

EMISSION ANGLE (RELATIVE TO JET EXHAUST) REFERENCED TO NOZZLE EXIT (DEGREES)

FREQ KHZ	PTF_i	50.
.250	-4.4	7.3
.315	-6.0	5.8
.400	-22.2	-10.5
.500	-11.9	-0.2
.630	-9.1	2.7
.800	-11.8	0.0
1.00	-13.3	-1.5
1.25	-13.2	-1.4
1.60	-9.7	2.0
2.00	-1.9	9.8
2.50	-2.0	9.2
3.15	-15.2	-3.5
4.00	-20.6	-9.1
5.00	-23.7	-11.9
6.30	-11.6	0.2
8.00	-20.7	-9.0
10.0	-21.1	-9.3
12.5	-20.8	-8.9
16.0	-20.8	-9.1
20.0	-24.8	-13.1
25.0	-21.4	-9.7
31.5	-28.5	-17.2
40.0	-25.6	-13.9
50.0	-30.0	-24.2
63.0	-34.9	-23.1

DATA FOR THE REMAINING ANGLES NOT ANALYZED DUE TO JET NOISE CONTAMINATION

$OPTF_i$	← $NOSPL_i$ →
22.5	-4.1

1/3 OCTAVE NTC (dB) WITH RESPECT TO INCIDENT SPL (NTC_i)

M_{J_1} = 0.8 M_{J_2} = 0.9 T_{R_1} =AMBIENT T_{R_2} = 900 K

MULTICHUTE NOZZLE (RUN NO = 159)

EMISSION ANGLE (RELATIVE TO JET EXHAUST) REFERENCED TO NOZZLE EXIT (DEGREES)

FREQ KHZ	PTF_i	20.	30.	40.	50.	60.	70.	80.	90.	100.	110.
.250	-5.9	2.7	-3.9	-5.3	-5.3	0.3	-7.2	-9.9	-5.6	-7.4	-10.4
.315	-15.7	-7.2	-13.3	-15.1	-14.6	-9.5	-16.4	-19.8	-16.5	-17.4	-20.3
.400	-26.9	-21.8	-21.4	-27.9	-21.9	-23.0	-23.4	-33.5	-31.3	-35.3	-35.1
.500	-27.0	-26.1	-24.5	-29.1	-23.1	-23.7	-23.2	-30.6	-26.2	-30.7	-34.5
.630	-27.0	-18.9	-32.9	-30.3	-24.2	-24.3	-22.9	-28.9	-24.1	-28.7	-34.0
.800	-22.9	-14.7	-27.5	-25.8	-18.7	-20.2	-18.5	-25.2	-23.3	-26.8	-33.2
1.00	-13.8	-8.4	-20.0	-18.7	-5.4	-14.5	-13.5	-21.2	-22.7	-23.7	-32.4
1.25	-11.2	-7.0	-16.9	-15.6	-2.2	-14.3	-14.7	-22.5	-30.0	-23.7	-34.2
1.60	-14.1	-8.8	-16.9	-15.0	-5.6	-17.6	-16.1	-19.7	-26.4	-22.7	-31.3
2.00	-8.4	-4.3	-16.9	-8.1	+0.7	-10.6	-5.9	-10.8	-18.2	-17.6	-24.4
2.50	6.7	8.3	2.8	6.0	14.2	7.8	9.0	3.7	-3.9	-8.3	-5.1
3.15	-7.4	-6.9	-12.1	-7.2	+0.7	-2.9	-5.4	-11.8	-20.2	-15.9	-14.0
4.00	-13.2	-14.0	-20.6	-14.3	-7.8	-7.1	-10.8	-18.7	-18.3	-18.9	-20.2
5.00	-17.4	-15.9	-22.6	-20.1	-14.2	-16.3	-15.3	-15.2	-19.9	-22.7	-30.0
6.30	-7.7	-4.9	-9.8	-12.2	-7.8	-0.2	-2.3	-6.6	-12.8	-12.4	-15.3
8.00	-7.5	-8.0	-14.9	-11.8	-8.3	-3.7	1.1	-7.5	-13.6	-16.0	-21.3
10.0	-2.0	-1.4	-2.7	-4.2	+3.9	6.5	3.5	-2.8	-12.3	-6.0	-11.9
12.5	-4.2	1.0	-1.7	2.2	+4.3	2.2	-1.4	-12.4	-10.4	-10.0	-11.5
16.0	-9.9	-6.2	-14.6	-10.9	-9.8	-2.4	-4.1	-14.7	-15.9	-13.7	-14.7
20.0	-11.9	-4.8	-15.5	-11.2	-11.2	-5.3	-7.5	-13.1	-16.3	-15.6	-14.9
25.0	-6.1	3.1	-15.3	-8.5	-2.2	-3.4	-2.0	-8.6	-12.6	-11.7	-11.7
31.5	-5.2	-0.1	-12.3	-6.3	+1.2	-2.0	0.2	-5.2	-11.7	-8.3	-12.3
40.0	-6.1	-2.9	-16.4	-13.8	-0.8	-0.7	-3.0	-8.8	-13.3	-11.5	-9.0
50.0	-12.3	-16.2	-15.5	-20.7	-7.8	-6.0	-10.3	-8.8	-18.6	-17.4	-15.4
63.0	-19.7	-15.9	-23.0	-22.4	-14.7	-18.7	-14.8	-21.2	-26.5	-18.6	-22.6

$OPTF_i$	← $NOSPL_i$ →								
24.4	-9.4	-15.6	-13.3	-8.1	-7.1	-8.8	-14.4	-18.0	-18.4	-20.5

REF. COAXIAL NOZZLE (RUN NO =177)

EMISSION ANGLE (RELATIVE TO JET EXHAUST) REFERENCED TO NOZZLE EXIT (DEGREES)

FREQ KHZ	PTF_i	70.
.250	-0.7	1.2
.315	-11.2	-0.3
.400	-24.9	-14.0
.500	-17.2	-6.3
.630	-13.7	-2.9
.800	-14.4	-3.5
1.00	-14.9	-4.0
1.25	-15.4	-4.5
1.60	-15.9	-5.0
2.00	-16.7	-4.8
2.50	-13.4	-2.5
3.15	-16.9	-6.0
4.00	-19.8	-8.6
5.00	-21.8	-10.9
6.30	-15.4	-4.6
8.00	-14.6	-3.8
10.0	-22.0	-11.2
12.5	-11.6	-0.8
16.0	-21.2	-10.3
20.0	-22.5	-11.6
25.0	-10.9	0.0
31.5	-14.4	-3.5
40.0	-14.3	-3.4
50.0	-22.2	-11.3
63.0	-27.7	-16.9

DATA FOR THE REMAINING ANGLES NOT ANALYZED DUE TO JET NOISE CONTAMINATION

$OPTF_i$	← $NOSPL_i$ →
22.2	-5.7

1/3 OCTAVE NTC (dB) WITH RESPECT TO INCIDENT SPL (NTC_i)

$M_{J_1} = 0.8$ $M_{J_2} = 0.9$ $T_{R_1} = 450\,K$ $T_{R_2} = 600\,K$

MULTICHUTE NOZZLE (RUN NO = 160)

FREQ KHZ	EMISSION ANGLE (RELATIVE TO JET EXHAUST) REFERENCED TO NOZZLE EXIT (DEGREES)											
	PTF_i	10.	20.	30.	40.	50.	60.	70.	80.	90.	100.	110.	120.
.250	-6.2	-11.5	3.2	-6.0	-9.8	-13.8	0.0	-12.2	-6.6	-6.7	-9.9	-8.9	-6.8
.315	-11.3	-7.4	-1.4	-16.7	-12.8	-17.7	-4.9	-16.2	-12.0	-12.1	-14.1	-14.4	-12.2
.400	-17.8	-6.5	-7.7	-15.1	-14.8	-21.3	-12.3	-20.3	-28.1	-29.2	-18.5	-47.2	-28.7
.500	-17.8	-5.9	-9.3	-16.6	-15.1	-19.3	-14.3	-20.8	-21.9	-23.5	-19.7	-28.0	-23.0
.630	-18.4	-8.2	-12.9	-20.2	-15.4	-17.8	-21.2	-21.6	-18.9	-20.6	-22.3	-21.4	-20.1
.800	-18.1	-8.6	-11.2	-24.0	-12.9	-14.4	-18.2	-19.6	-20.0	-21.1	-22.2	-21.6	-20.3
1.00	-16.5	-10.6	-9.0	-18.2	-9.5	-13.1	-14.7	-16.9	-23.5	-22.4	-23.1	-22.9	-20.5
1.25	-14.9	-13.2	-8.3	-7.9	-7.1	-16.2	-11.7	-14.5	-20.6	-21.6	-25.7	-27.1	-22.5
1.60	-12.9	-20.1	-12.7	-5.0	-9.4	-8.5	-10.6	-12.0	-14.1	-17.0	-20.7	-26.6	-23.1
2.00	-6.9	-18.5	-17.9	-3.1	-7.1	0.6	-5.9	-8.9	-9.6	-11.6	-17.7	-20.1	-15.0
2.50	-4.8	-21.4	-19.3	-7.5	-4.3	2.8	-3.0	-4.1	-7.4	-10.2	-17.6	-18.0	-14.9
3.15	-12.8	-34.1	-22.9	-18.6	-12.9	-8.5	-9.6	-13.7	-15.5	-19.0	-18.8	-18.4	-20.2
4.00	-16.0	-37.5	-25.9	-20.8	-17.5	-8.9	-12.2	-18.3	-18.7	-18.8	-22.6	-24.9	-28.1
5.00	-12.9	-39.5	-20.2	-16.4	-14.3	-6.6	-8.7	-12.9	-11.6	-15.6	-23.9	-27.8	-26.3
6.30	-4.1	-33.7	-10.0	-7.0	-4.2	0.7	-0.5	-0.4	-1.3	-8.2	-14.6	-17.1	-18.6
8.00	-13.2	-36.1	-14.0	-13.2	-9.8	-7.1	-10.9	-11.4	-17.2	-21.1	-20.4	-20.3	-27.2
10.0	-15.1	-34.4	-18.7	-14.6	-13.7	-10.9	-8.1	-15.1	-17.6	-18.6	-23.1	-27.3	-23.0
12.5	-4.1	-24.2	-5.5	-1.5	-1.1	0.6	2.0	-6.0	-7.9	-9.7	-12.9	-15.7	-15.7
16.0	-14.5	-36.1	-15.8	-11.9	-15.9	-6.8	-2.9	-8.2	-11.1	-15.5	-24.0	-22.0	-25.3
20.0	-12.7	-33.5	-16.9	-9.4	-15.4	-10.3	-5.0	-8.7	-18.0	-15.2	-20.4	-18.3	-21.4
25.0	-11.4	-30.4	-23.0	-9.5	-14.9	-8.8	-4.4	-6.4	-13.4	-16.4	-17.5	-18.3	-20.4
31.5	-14.1	-34.3	-15.9	-7.7	-20.8	-10.7	-9.0	-11.9	-14.6	-14.1	-25.5	-18.5	-22.0
40.0	-16.6	-36.8	-22.7	-17.0	-18.2	-11.8	-10.9	-15.0	-14.2	-19.9	-21.9	-22.8	-25.0
50.0	-18.5	-29.8	-18.4	-15.9	-22.6	-15.0	-14.6	-19.5	-13.5	-17.7	-26.1	-22.5	-24.0
63.0	-21.6	-27.2	-16.6	-16.0	-24.8	-19.5	-17.7	-21.2	-19.1	-23.7	-21.0	-27.2	-27.7

$OPTF_i$ ← $NOSPL_i$ →

24.2 -13.1 -9.4 -13.1 -13.1 -7.7 -8.2 -12.7 -13.6 -16.1 -19.1 -19.6 -18.8

REF. COAXIAL NOZZLE (RUN NO =179)

FREQ KHZ	EMISSION ANGLE (RELATIVE TO JET EXHAUST) REFERENCED TO NOZZLE EXIT (DEGREES)				
	PTF_i	60.	70.	80.	90.
.250	-10.5	-9.4	-10.8	-11.4	-10.4
.315	-15.1	-5.1	-14.9	-15.8	-15.2
.400	-26.9	-18.5	-21.2	-24.3	-32.9
.500	-24.8	-16.7	-22.3	-19.7	-24.4
.630	-22.7	-14.8	-24.7	-16.5	-20.6
.800	-20.8	-12.3	-21.5	-15.9	-18.0
1.00	-18.4	-9.2	-19.3	-16.7	-14.8
1.25	-17.2	-6.9	-17.1	-26.5	-14.0
1.60	-12.9	-2.7	-10.4	-19.3	-12.0
2.00	-3.2	5.7	1.8	-4.4	-2.6
2.50	-8.9	-1.2	-3.3	-6.3	-8.0
3.15	-15.3	-6.3	-10.6	-13.9	-17.9
4.00	-18.7	-9.8	-13.9	-17.8	-19.2
5.00	-14.0	-5.2	-9.1	-13.4	-14.6
6.30	-10.3	-1.9	-5.2	-8.7	-9.5
8.00	-19.4	-13.8	-12.6	-19.6	-15.5
10.0	-12.1	-3.1	-9.8	-8.0	-13.7
12.5	-17.8	-7.7	-14.3	-16.1	-18.4
16.0	-19.3	-14.1	-13.6	-17.2	-13.8
20.0	-18.7	-12.7	-12.6	-17.5	-13.9
25.0	-13.3	-7.6	-6.5	-10.8	-10.7
31.5	-19.4	-14.7	-12.5	-19.7	-14.0
40.0	-17.5	-12.4	-10.5	-13.2	-14.1
50.0	-26.3	-22.2	-20.7	-22.2	-21.4
63.0	-34.8	-27.7	-22.2	-27.6	-27.0

$OPTF_i$ ← $NOSPL_i$ →

22.8 -7.8 -12.6 -15.1 -15.7

DATA FOR THE REMAINING ANGLES NOT ANALYZED DUE TO JET NOISE CONTAMINATION

1/3 OCTAVE NTC (dB) WITH RESPECT TO INCIDENT SPL (NTC_i)

$M_{J_1} = 0.8$ $M_{J_2} = 0.9$ $T_{R_1} = 675$ $T_{R_2} = 900\,K$

MULTICHUTE NOZZLE (RUN NO = 161)

EMISSION ANGLE (RELATIVE TO JET EXHAUST) REFERENCED TO NOZZLE EXIT (DEGREES)

FREQ KHZ	PTF_i	50.	60.	70.	80.	90.	100.	110.	120.
.250	-16.2	-15.4	-8.1	-17.9	-20.0	-13.7	-16.0	-17.5	-17.6
.315	-16.6	-15.2	-8.3	-18.1	-19.9	-14.5	-16.6	-17.8	-18.3
.400	-18.5	-14.3	-9.4	-21.6	-19.5	-34.8	-22.5	-20.0	-27.4
.500	-16.7	-13.9	-8.4	-21.7	-19.1	-15.0	-16.5	-19.8	-20.4
.630	-11.5	-12.9	-4.5	-22.4	-17.0	-6.2	-7.6	-18.6	-12.5
.800	-11.6	-11.1	-3.0	-21.2	-16.9	-6.4	-10.8	-17.9	-16.1
1.00	-14.3	-8.9	-0.9	-19.9	-16.6	-5.9	-15.1	-17.4	-21.5
1.25	-8.7	-2.3	3.9	-14.1	-15.8	-3.0	-16.6	-14.1	-14.8
1.60	-6.8	-0.9	0.3	-8.7	-11.2	-9.6	-8.3	-12.4	-9.9
2.00	-7.9	-2.8	-7.8	-3.0	-5.6	-10.0	-6.0	-14.6	-12.0
2.50	-4.5	-2.4	0.9	1.3	-1.9	-5.0	-6.7	-11.6	-7.6
3.15	-11.2	-9.9	-5.6	-4.6	-11.0	-13.3	-13.9	-11.9	-14.2
4.00	-14.8	-13.4	-10.2	-8.6	-17.2	-12.3	-13.9	-15.2	-23.5
5.00	-17.5	-15.2	-14.1	-11.8	-16.8	-14.2	-16.3	-24.7	-29.4
6.30	-11.3	-7.7	-6.3	-6.2	-9.4	-9.7	-20.2	-17.4	-19.8
8.00	-9.2	-6.9	-4.7	-2.4	-5.9	-7.5	-19.7	-19.4	-25.4
10.0	-5.3	-3.2	-5.9	-3.7	-11.1	-4.5	-17.9	-16.8	-18.3
12.5	-6.4	-11.8	-2.2	3.5	-7.8	-7.6	-14.6	-15.7	-17.9
16.0	-11.5	-7.7	-6.6	-7.0	-10.9	-9.6	-14.4	-16.6	-18.9
20.0	-8.1	-5.3	-3.0	-2.7	-6.6	-6.1	-13.1	-10.3	-18.3
25.0	-2.3	3.9	0.3	0.2	-3.8	-1.6	-8.2	-2.9	-11.9
31.5	-2.6	0.1	-3.4	-0.0	2.3	1.6	-2.6	-3.0	-11.6
40.0	-5.6	-3.9	-3.6	-0.6	-4.3	-1.3	-5.6	-6.3	-11.5
50.0	-13.0	-15.6	-8.6	-8.7	-7.7	-14.3	-10.0	-11.8	-15.4
63.0	-16.1	-11.8	-15.6	-9.6	-16.7	-11.0	-9.7	-17.6	-22.8

$OPTF_i$ ← $NOSPL_i$ →

23.4 -11.2 -8.1 -9.0 -13.6 -11.8 -15.3 -17.2 -19.4

REF. COAXIAL NOZZLE (RUN NO = 178)

EMISSION ANGLE (RELATIVE TO JET EXHAUST) REFERENCED TO NOZZLE EXIT (DEGREES)

FREQ KHZ	PTF_i	60.	70.	80.
.250	-9.1	-6.6	-2.1	-13.9
.315	-9.3	-6.8	-2.1	-14.0
.400	-14.4	-3.1	-2.1	-15.4
.500	-15.7	-6.1	-9.9	-18.7
.630	-18.6	-6.9	-22.7	-19.7
.800	-16.1	-5.0	-20.2	-17.4
1.00	-13.1	-1.9	-17.6	-15.5
1.25	-9.7	1.8	-15.1	-15.2
1.60	-7.6	3.8	-14.8	-17.3
2.00	-6.6	2.8	-13.7	-0.6
2.50	1.8	11.6	-1.2	5.6
3.15	-4.8	5.1	-3.2	-0.8
4.00	-14.3	-6.1	-9.4	-10.0
5.00	-18.5	-11.8	-12.9	-12.5
6.30	-13.0	-8.9	-6.2	-11.4
8.00	-15.8	-9.1	-8.5	-8.9
10.0	-14.4	-6.3	-9.3	-9.0
12.5	-5.1	4.6	-1.7	-4.8
16.0	-15.6	-7.4	-11.4	-12.0
20.0	-14.8	-1.6	-6.1	-9.4
25.0	-8.0	2.2	-8.9	-5.0
31.5	-11.1	-2.9	-6.2	-9.1
40.0	-8.0	2.0	-6.5	-8.6
50.0	-19.4	-10.0	-15.4	-17.1
63.0	-22.1	-13.4	-15.8	-20.2

DATA FOR THE REMAINING ANGLES NOT ANALYZED DUE TO JET NOISE CONTAMINATION

$OPTF_i$ ← $NOSPL_i$ →

26.8 -3.4 -7.2 -10.3

1/3 OCTAVE NTC (dB) WITH RESPECT TO INCIDENT SPL (NTC_i)

$M_{J_1} = 0.8$ $M_{J_2} = 0.9$ T_{R_1} = AMBIENT $T_{R_2} = 600$ K

MULTICHUTE NOZZLE (RUN NO = 162)

FREQ KHZ	EMISSION ANGLE (RELATIVE TO JET EXHAUST) REFERENCED TO NOZZLE EXIT (DEGREES)									
	PTF_i	30.	40.	50.	60.	70.	80.	90.	100.	110.	120.
.250	-19.0	-12.6	-7.6	-10.4	-1.4	-11.8	-14.4	-10.9	-11.8	-15.1	-11.1
.315	-14.4	-17.1	-11.5	-15.0	-5.9	-16.1	-17.9	-16.5	-16.4	-19.5	-15.7
.400	-25.4	-30.7	-17.6	-31.2	-18.2	-25.2	-22.6	-46.1	-32.6	-30.3	-33.1
.500	-25.1	-26.9	-19.6	-23.8	-18.9	-26.1	-23.1	-25.5	-27.3	-31.6	-27.7
.630	-24.7	-24.1	-27.1	-20.5	-20.2	-27.6	-24.1	-21.8	-24.4	-34.4	-24.7
.800	-24.1	-19.7	-26.4	-19.7	-21.0	-26.5	-22.3	-22.9	-24.9	-32.9	-24.1
1.00	-23.3	-14.6	-21.5	-19.9	-23.6	-26.8	-20.8	-26.2	-26.8	-31.9	-23.6
1.25	-19.4	-9.5	-13.6	-15.5	-20.4	-27.9	-21.9	-23.5	-30.0	-29.7	-24.7
1.60	-12.8	-9.0	-8.7	-6.0	-10.8	-14.8	-15.6	-14.1	-19.0	-26.0	-23.8
2.00	-6.4	-8.0	-4.0	1.1	-4.8	-6.9	-6.8	-9.3	-14.5	-18.4	-15.2
2.50	-1.0	-12.8	-9.8	-3.4	-8.2	-9.6	-11.6	-15.8	-20.6	-16.6	-17.0
3.15	-15.2	-21.6	-18.0	-8.6	-10.1	-14.2	-16.9	-16.7	-20.1	-21.0	-21.3
4.00	-17.3	-27.7	-20.4	-10.6	-12.0	-19.1	-20.5	-20.2	-22.5	-25.2	-28.8
5.00	-13.1	-22.8	-18.4	-5.7	-10.1	-14.3	-13.7	-16.4	-23.4	-26.4	-25.7
6.30	-2.9	-11.7	-4.7	3.4	-0.7	1.1	-3.0	-11.5	-19.9	-18.8	-15.2
8.00	-14.7	-20.7	-14.5	-9.8	-8.7	-9.6	-21.1	-28.1	-25.6	-23.6	-31.2
10.0	-11.9	-16.4	-9.8	-10.5	-2.8	-8.7	-23.4	-24.4	-23.0	-25.6	-22.0
12.5	-9.8	-12.1	-7.4	-6.0	-2.1	-7.1	-14.0	-12.5	-20.4	-15.6	-20.6
16.0	-13.9	-21.8	-21.3	-11.1	-4.6	-13.1	-18.4	-22.7	-22.2	-23.4	-23.7
20.0	-13.5	-19.9	-15.0	-11.2	-4.9	-11.6	-17.7	-18.6	-19.6	-21.1	-22.0
25.0	-9.7	-16.2	-14.5	-6.7	-1.4	-9.1	-12.4	-15.3	-15.8	-18.9	-13.7
31.5	-11.9	-16.2	-21.8	-7.3	-4.8	-10.4	-16.8	-15.4	-16.9	-18.1	-22.0
40.0	-14.3	-15.1	-14.9	-10.7	-0.7	-10.4	-12.5	-10.8	-14.2	-15.4	-17.7
50.0	-18.0	-19.6	-21.9	-16.6	-10.2	-15.7	-15.9	-18.1	-21.9	-20.8	-23.7
63.0	-22.1	-22.0	-28.3	-23.7	-14.8	-18.3	-25.2	-20.4	-21.4	-25.9	-29.7

$OPTF_i$ ← $NOSPL_i$ →

22.9 -18.3 -14.4 -8.6 -8.1 -13.3 -16.8 -17.7 -19.5 -22.1 -20.2

REF. COAXIAL NOZZLE (RUN NO = 175)

FREQ KHZ	EMISSION ANGLE (RELATIVE TO JET EXHAUST) REFERENCED TO NOZZLE EXIT (DEGREES)									
	PTF_i	30.	40.	50.	60.	70.	80.	90.	100.	110.	120.
.250	-9.4	-1.8	-2.3	-10.4	-4.4	-5.5	-19.7	-16.2	-16.1	-15.0	-18.7
.315	-14.1	-2.5	-3.2	-8.6	-6.0	-7.5	-21.4	-18.1	-17.3	-17.0	-20.5
.400	-12.8	-5.8	-5.2	-7.0	-11.5	-21.5	-27.2	-26.6	-20.5	-27.4	-28.5
.500	-15.3	-9.4	-9.4	-8.9	-15.7	-18.7	-26.0	-24.8	-20.2	-23.2	-24.9
.630	-16.9	-12.3	-14.0	-9.9	-20.1	-14.5	-25.5	-24.2	-20.0	-22.2	-24.0
.800	-14.4	-8.6	-11.6	-7.1	-17.2	-14.0	-23.3	-23.4	-19.0	-23.1	-22.5
1.00	-12.8	-4.6	-8.8	-4.8	-14.1	-14.3	-21.8	-22.7	-17.6	-25.4	-20.7
1.25	-9.9	-0.9	-5.6	-3.7	-10.9	-17.8	-18.6	-21.4	-15.6	-25.0	-19.0
1.60	-7.9	2.3	-2.4	-4.9	-7.3	-18.6	-10.6	-16.8	-12.5	-16.8	-16.1
2.00	-1.2	8.0	4.3	1.0	0.7	-5.8	-0.6	-6.8	-6.7	-7.8	-8.9
2.50	-3.8	3.5	1.7	-1.5	0.1	-6.0	-2.6	-6.4	-11.9	-8.5	-12.8
3.15	-13.7	-9.8	-8.5	-14.4	-8.1	-10.9	-12.4	-12.4	-23.1	-18.1	-27.4
4.00	-16.9	-18.7	-15.2	-13.8	-10.8	-13.2	-15.7	-17.7	-21.9	-25.4	-35.6
5.00	-14.8	-24.6	-15.1	-12.0	-6.8	-10.3	-18.0	-17.0	-17.6	-23.0	-22.5
6.30	-7.1	-9.0	-11.4	-7.0	-0.2	-4.3	-5.6	-3.7	-11.8	-11.8	-13.3
8.00	-15.6	-19.8	-12.4	-11.6	-8.9	-13.7	-20.7	-18.4	-25.4	-25.0	-26.1
10.0	-12.3	-14.5	-13.0	-15.3	-2.9	-7.3	-16.2	-20.4	-20.9	-23.1	-19.6
12.5	-11.9	-8.9	-9.0	-9.2	-5.6	-8.1	-12.7	-16.6	-16.0	-24.2	-23.0
16.0	-11.8	-9.7	-10.0	-9.6	-2.8	-10.5	-18.1	-12.0	-17.4	-13.6	-21.7
20.0	-18.5	-19.0	-26.0	-18.0	-8.7	-17.4	-19.8	-19.6	-28.0	-29.3	-29.5
25.0	-16.8	-19.6	-21.1	-17.9	-7.7	-13.0	-17.2	-21.7	-23.9	-28.5	-31.8
31.5	-17.2	-17.8	-26.7	-18.1	-8.1	-15.6	-18.2	-24.2	-27.1	-26.2	-29.0
40.0	-18.5	-18.6	-29.9	-20.4	-8.8	-16.3	-17.6	-21.2	-24.0	-28.3	-29.7
50.0	-22.4	-19.4	-31.1	-22.5	-12.7	-27.3	-18.5	-26.7	-29.7	-29.9	-34.4
63.0	-28.7	-28.7	-36.6	-29.7	-21.8	-26.3	-32.7	-33.9	-27.5	-35.1	-37.2

$OPTF_i$ ← $NOSPL_i$ →

25.4 -7.1 -8.8 -10.5 -8.2 -11.2 -15.4 -16.3 -19.1 -20.3 -22.8

APPENDIX D

NOMENCLATURE

A	cross-sectional area of the duct
c	speed of sound
D	diameter
f	frequency
h	annulus width
I	acoustic intensity
k	wave number, $2\pi f/c$
L	protrusion of primary exit beyond the fan exit
NTC (≡NTF)	nozzle transmission coefficient (≡nozzle transfer function)
M	Mach number
p	acoustic pressure amplitude
P	static pressure
PTF	power transfer function
R	radius
R_m	polar arc radius
t	time
T	temperature
u	particle velocity
V	mean velocity
W	acoustic power
x	axial coordinate

λ	wave length
ρ	density
σ	reflection coefficient amplitude
θ	far-field measurement angle (degrees) with the jet axis
ϕ	convergence angle of the nozzle

Subscripts

0	relating to the ambient
1	relating to the primary jet
2	relating to the fan jet
c	relating to the conical nozzle
D	relating to the duct
DL	relating to the daisy lobe nozzle
e	relating to the exit conditions
f	relating to the far-field
i	relating to the incident wave
J	relating to the fully-expanded jet condition
r	relating to the reflected signal
R	relating to the reservoir conditions
t	relating to the transmitted signal
T	relating to the free-jet

REFERENCES

1.1 R. K. Matta et al.: G.E. Core Engine Noise Investigation. FAA Report RD-77-3, February 1977.

1.2 B. Lowrie: Rolls Royce Core Engine Noise Compared with Various Prediction Schemes. Presented at DOT/FAA Jet Noise/Core Noise Status Review, February 1977.

1.3 P. D. Dean, M. Salikuddin, K. K. Ahuja, H. E. Plumblee, and P. Mungur: "Studies of the Acoustic Transmission Characteristics of Coaxial Nozzles with Inverted Velocity Profiles". NASA CR-159698, 1979.

1.4 U. von Glahn: "Acoustic Considerations of Flight Effects on Jet Noise Suppressor Nozzles", NASA Technical Memorandum 81377, 1980.

1.5 P. R. Knott et al: "Acoustic Tests of Duct-Buring Turbofan Jet Noise Simulation". Final Report by G. E. For NASA Contract NAS3-18008. 1978.

1.6 W. T. Rowe, E. S. Johnson and R. A. McKinnon: "Technology Status of Jet Noise Suppression Concepts for Advanced Supersonic Transports". AIAA Paper 77-833, 1977.

1.7 "Cooperative Wind Tunnel Tests of Douglas Advanced Supersonic Technology Jet Noise Suppressor", NASA Contractor Report 158996, 1978.

1.8 M. Salikuddin, P. D. Dean, H. E. Plumblee, and K. K. Ahuja: "An Impulse Test Technique with Application to Acoustic Measurements". AIAA 5th Aeroacoustics Conference, AIAA Paper 79-0679, Seattle, Washington, March 12-14, 1979.

1.9 H. Levine, J. Schwinger: "On the Radiation of Sound from an Unflanged Circular Pipe". Physical Review, 73 (1948), Feb. 15, pp. 383-406.

2.1 H. E. Plumblee (Editor): "A Study of the Effects of Forward Velocity on Turbulent Jet Mixing Noise". NASA CR-2702, 1975.

2.2 K. K. Ahuja, B. J. Tester, and H. K. Tanna: "The Free Jet as a Simulator of Forward Velocity Effects on Jet Noise", NASA CR-3056, 1978.

2.3 H. E. Plumblee (Editor): "A Progress Report on Studies of Jet Noise Generation and Radiation, Turbulence Structure and Laser Velocimetry," AFAPL-TR-74-24, 1974.

2.4 H. K. Tanna: "An Experimental Study of Jet Noise, Part I: Turbulent Mixing Noise." J. Sound Vib., 50(3), p. 405-428, 1977.

2.5 H. K. Tanna: "An Experimental Study of Jet Noise, Part II: Shock Associated Noise." J. Sound Vib., 50(3), p. 429-444, 1977.

2.6 H. K. Tanna, B. J. Tester, and J. C. Lau: "The Noise and Flow Characteristics of Inverted-Profile Coannular Jets." NASA CR-158995, 1979.

2.7 R. H. Burrin, and H. K. Tanna: The Lockheed-Georgia Coannular Jet Research Facility. Lockheed Report LG77ER0243.

2.8 P. D. Dean, M. Salikuddin, K. K. Ahuja, H. E. Plumblee, and P. Mungur: "Studies of the Acoustic Transmission Characteristics of Coaxial Nozzles with Inverted Velocity Profiles". NASA CR-159698, 1979.

2.9 W. T. Rowe, E. S. Johnson and R. A. McKinnon: "Technology Status of Jet Noise Suppression Concepts for Advanced Supersonic Transports." AIAA Paper 77-833 , 1977.

2.10 "Cooperative Wind Tunnel Tests of Douglas Advanced Supersonic Technology Jet Noise Suppressor", NASA Contractor Report 158996, 1978.

2.11 P. R. Knott et al: "Acoustic Tests of Duct-Buring Turbofan Jet Noise Simulation". Final Report by G. E. For NASA Contract NAS3-18008, 1978.

2.12 F. D. Shields and H. E. Bass: "Atmospheric Absorption of High Frequency Noise and Application to Fractional-Octave Bands." NASA CR-2760, 1977.

2.13 D. I. Blokhintsev: "*Acoustics of a Nonhomogeneous Moving Medium* (Gostekhizdat)". Translated in Tech. Memo NACA, Wash. 1399 (1956).

3.1 C. Imelmann: "Einfluß der Strömung auf den Schalldurchgang durch Rohrmündungen" (Influence of Flow on the Sound Transmission Through Orifices). Diplomarbeit, Technische, Universität Berline, Institut fur Technische Akustik, 1978.

3.2 M. Salikuddin and H. E. Plumblee: "Low Frequency Sound Absorption of Orifice Plates, Perforated Plates and Nozzles," AIAA Paper 80-0991. 1980.

3.3 D. W. Bechert: "Sound Absorption Casued by Vorticity Shedding Demonstrated with a Jet Flow, AIAA 5th Aeroacoustics Conference, AIAA Paper 79-0571, Seattle, Washington, March 12-14, 1979.

3.4 P. H. Morse: *Vibration and Sound*, McGraw-Hill, 2nd Ed., 1948.

3.5 M. J. Lighthill "*Waves in Fluids*", Cambridge University Press, 1978.

3.6 M. Abrishman: "Effect of Flow on the Acoustic Impedance of a Duct Exit", Spectral Dynamics Research Corporation Paper.

3.7 M. Salikuddin, P. D. Dean, H. E. Plumblee and K. K. Ahuja: "An Impulse Test Technique with Application to Acoustic Measurements." AIAA 5th Aeroacoustics Conference, AIAA Paper 79-0679, Seattle, Washington, March 12-14, 1979.

3.8 H. Levine and J. Schwinger: "On the Radiation of Sound from an Unflanged Circular Pipe". Physical Review, 73 (1948), Feb. 15, pp. 383-406.

3.9 D. Bechert, U. Michel and E. Pfizenmaier: "Experiments on the Transmission of Sound Through Jets". AIAA 4th Aeroacoustics Conference, Atlanta, Ga., Oct. 3-5, 1977, AIAA-Paper 77-1278. Synopsis published in AIAA-J. 16,9 (1978), pp. 873-874.

3.10 K. K. Ahuja, B. J. Tester, and H. K. Tanna: "The Free Jet as a Simulator of Forward Velocity Effects on Jet Noise," NASA CR-3056, 1978.

3.11 J. Stone: "On the Effects of Flight on Jet Engine Exhaust Noise". NASA TMX-1819, Nov. 1975.

3.12 R. A. Pinker and W. D. Bryce: "The Radiation of Plane-Wave Duct Noise from a Jet Exhaust, Statically and in Flight". AIAA Paper 76-581.

4.1 P. D. Dean, M. Salikuddin, K. K. Ahuja, H. E. Plumblee, and P. Mungur: "Studies of the Acoustic Transmission Characteristics of Coaxial Nozzles with Inverted Velocity Profiles". NASA CR-159698, 1979.

5.1 P. D. Dean, M. Salikuddin, K. K. Ahuja, H. E. Plumblee, Jr., and P. Mungur: "Studies of the Acoustic Transmission Characteristics of Coaxial Nozzles with Inverted Velocity Profiles". NASA CR-159698, 1979.

5.2 Charles R. Trimble: "What is Signal Averaging". Hewlett-Packard Journal, April 1968.

6.1 C. J. Moore: "The Role of Shear-Layer Instability Waves in Jet Exhaust Noise". J. Fluid Mech. 80 (1977), pp. 321-367.

6.2 D. Bechert, E. Pfizenmaier: "On the Amplification of Broadband Jet Noise by a Pure Tone Excitation". J. Sound & Vib. 43 (1975), pp. 581-487.

6.3 P. R. Gliebe: "Diagnostic Evaluation of Jet Noise Suppression Mechanisms," AIAA Paper 79-0674, Mar. 1979.

6.4 D. R. Regan and W. C. Meecham: "Multitube Turbojet Noise-Suppression Studies using Cross-Correlation Techniques". J. Acoust Soc. Am. 63 (6), 1978.

6.5 W. T. Rowe, E. S. Johnson and R. A. McKinnon: "Technology Status of Jet Noise Suppression Concepts for Advanced Supersonic Transports". AIAA Paper 77-833, 1977.

6.6 U. von Glahn: "Acoustic Considerations of Flight Effects on Jet Noise Suppressor Nozzles" NASA Technical Memorandum 81377, 1980.

6.7 K. K. Ahuja, B. J. Tester, and H. K. Tanna: "The Free Jet as a Simulator of Forward Velocity Effects on Jet Noise, " NASA CR-3056, 1978.

6.8 K. K. Ahuja: "Noise Studies of Cold and Heated Model Jets at Supersonic and High Subsonic Speeds with Particular Reference to Noise Reduction". Ph.D Thesis, Mechanical Engrg., Syracuse University, June 1976.

6.9 P. K. Bhutiani: "Investigations of the Flow and Radiated Noise from Coaxial Jets to Study: (a) The effect of Heating One of the Jets, (b) The Role of Lip Thickness on Noise Suppression". Ph. D. Thesis, Mech. Engrg., Syracuse University, 1976.

1. Report No.	2. Government Accession No.	3. Recipient's Catalog No.
NASA CR- 165133		

4. Title and Subtitle	5. Report Date
A STUDY OF THE ACOUSTIC TRANSMISSION CHARACTERISTICS OF SUPPRESSOR NOZZLES	June 1980
	6. Performing Organization Code
7. Author(s)	8. Performing Organization Report No.
K. K. Ahuja, M. Salikuddin, R. H. Burrin and H. E. Plumblee, Jr.	
9. Performing Organization Name and Address	10. Work Unit No.
Lockheed-Georgia Company Marietta, Georgia 30063	11. Contract or Grant No. NAS3-20797
12. Sponsoring Agency Name and Address	13. Type of Report and Period Covered
National Aeronautics and Space Administration Washington, D. C. 20546	Contract Report
	14. Sponsoring Agency Code

15. Supplementary Notes

Project Manager, E. A. Krejsa, V/STOL and Noise Division, NASA-Lewis Research Center, Cleveland, Ohio.
Lockheed Program Manager, H. E. Plumblee, Jr.

16. Abstract

An impulse test technique developed in Phase 1 of this program was used to study the internal noise radiation characteristics for two mechanical suppressor nozzles, namely, a single stream 12-lobe 24-tube suppressor nozzle and a dual stream 36-chute suppressor nozzle. An equivalent single round conical nozzle and an equivalent coannular nozzle system were also tested to provide a reference for the two suppressors. This technique utilizes a high voltage spark discharge as a noise source within the test duct and enables one to separate the incident, reflected and transmitted signals in the time domain. These signals are then Fourier transformed to obtain various transmission parameters, in particular, the nozzle transmission coefficient (NTC) and the power transfer function (PTF). These transmission parameters for the 12-lobe, 24-tube suppressor nozzle and the reference conical nozzle are presented as a function of jet Mach number, duct Mach number polar angle and temperature. Effects of simulated forward flight are also considered for this nozzle. For the dual stream, 36-chute suppressor, the NTC and PTF are presented as a function of velocity ratios and temperature ratios. Where possible data for the equivalent coaxial nozzle is also presented. As a by-product of this work, data on jet-mixing noise and broad-band amplification was also available. Typical results describing the jet noise suppression by these suppressors are, therefore, presented. A new technique using signal recovery and an electro-acoustic driver, developed to improve the single-shot spark discharge method, has also been discussed. Many of the results described here are new and are not amenable to immediate explanations. Due to the interesting nature of these results and their usefulness, the transmission data has been included in this report as an appendix.

17. Key Words (Suggested by Author(s))	18. Distribution Statement
Acoustic Measurements, Acoustic Sources, Duct Acoustics, Electric Spark, Engine Noise, Internal Noise, Inverted Velocity and Temperature Coaxial Jets, Impulse Noise, Refraction Daisy lobe nozzle, Multi-chute suppressor Nozzle, Signal averaging, Broadband amplification, Jet Noise, low frequency absorption	Unclassified - Unlimited STAR Category 71

19. Security Classif. (of this report)	20. Security Classif. (of this page)	21. No. of Pages	22. Price*
UNCLASSIFIED	UNCLASSIFIED		

*For sale by the National Technical Information Service, Springfield, Virginia 22161